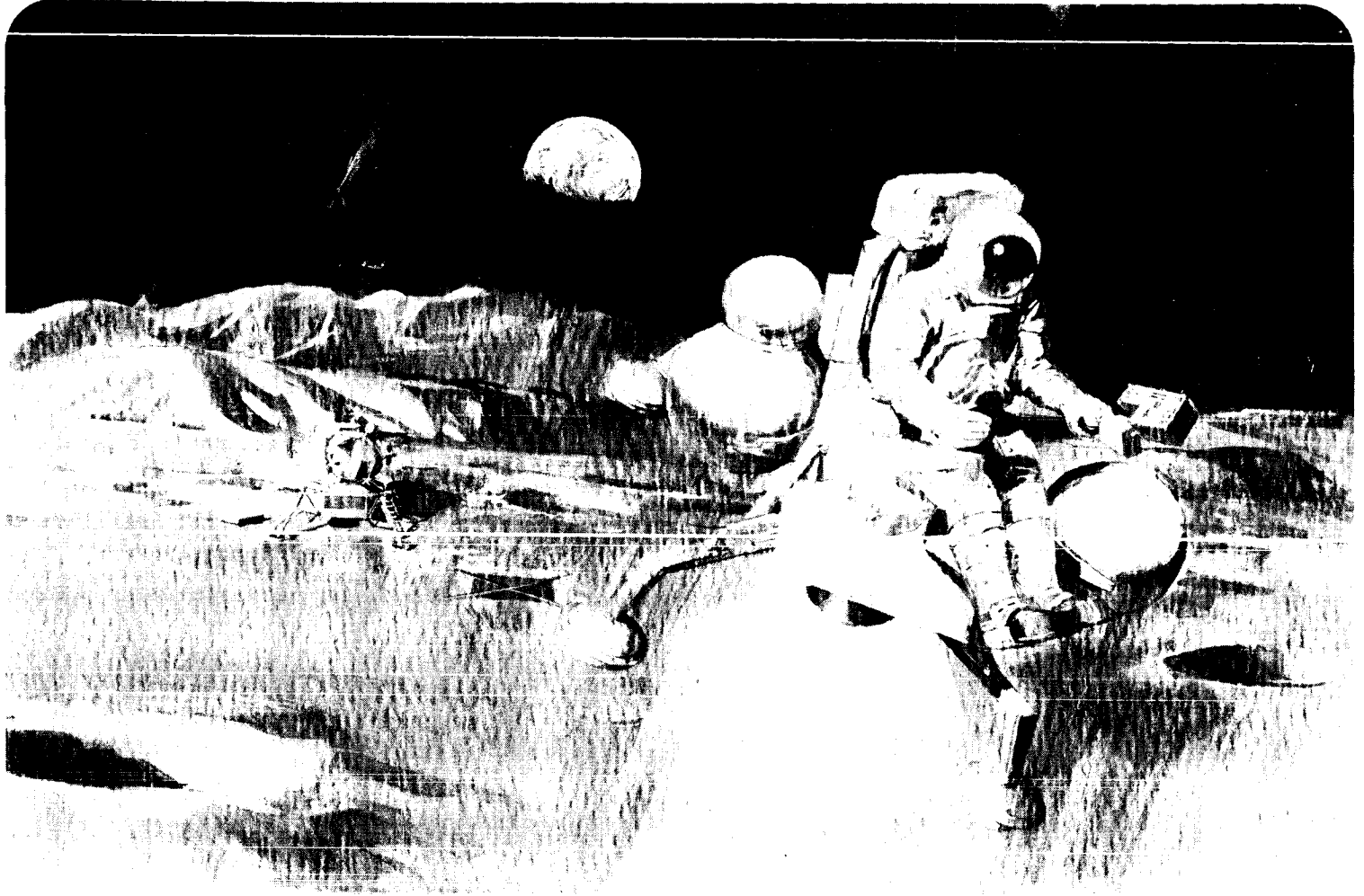


CASE FILE  
COPY

N69-38205  
NASA CR-101920

SD 69-419-4



Study of **ONE-MAN LUNAR FLYING VEHICLE**  
**FINAL REPORT**

---

Volume IV  
Configuration Design



Space Division  
North American Rockwell

NASA CR 101920

SD 69-419-4

STUDY OF ONE-MAN LUNAR FLYING VEHICLE  
FINAL REPORT

VOLUME IV  
CONFIGURATION DESIGN

Contract NAS9-9045

31 August 1969

## FOREWORD

This document presents the details of the design trade-offs leading to the preliminary design of the one-man lunar flying vehicle. This work was accomplished under the One-Man Lunar Flying Vehicle Contract (NAS9-9045), conducted by the North American Rockwell Space Division for the National Aeronautics and Space Administration Manned Spacecraft Center, Houston, Texas. An appendix to this volume is submitted under separate cover. Other volumes to this report are:

- Volume 1. Summary
- Volume 2. Mission Analysis
- Volume 3. Subsystem Studies
- Volume 5. Preliminary Design and Specifications
- Volume 6. Training and Resources Plans

PRECEDING PAGE BLANK NOT FILMED.

TECHNICAL REPORT INDEX/ABSTRACT

|  |  |   |  |  |  |   |  |
|--|--|---|--|--|--|---|--|
| ACCESSION NUMBER   |  |   |  | DOCUMENT SECURITY CLASSIFICATION<br>UNCLASSIFIED |  |   |  |
| TITLE OF DOCUMENT<br>STUDY OF ONE-MAN LUNAR FLYING VEHICLE - FINAL REPORT: VOLUME 1 - SUMMARY; VOLUME 2 - MISSION ANALYSIS; VOLUME 3 - SUBSYSTEM STUDIES; VOLUME 4 - CONFIGURATION DESIGN; VOLUME 5 - PRELIMINARY DESIGN AND SPECIFICATIONS; VOLUME 6 - TRAINING AND RESOURCES PLANS |  |   |  |  |  | LIBRARY USE ONLY                              |  |
| AUTHOR(S)  |  |   |  |  |  |   |  |
| CODE<br>NAJ65231   |  | ORIGINATING AGENCY AND OTHER SOURCES<br>NORTH AMERICAN ROCKWELL, SPACE DIVISION |  |  |  | DOCUMENT NUMBER<br>SD 69-419-1,-2,-3,-4,-5,-6 |  |
| PUBLICATION DATE<br>31AUG69  |  |   |  | CONTRACT NUMBER<br>NAS9-9045                     |  |   |  |
| DESCRIPTIVE TERMS<br>*ONE-MAN LUNAR FLYING VEHICLE, *CONTROL SYSTEMS, *PROPULSION SYSTEMS, *TRAJECTORIES, *DESIGN, *TRAINING, *RESOURCES, *MISSION ANALYSIS  |  |   |  |  |  |   |  |

|  |
|--|
| <p>ABSTRACT</p> <p>THE PRIMARY OBJECTIVES OF THIS STUDY WERE TO OPTIMIZE THE DESIGN AND TO DEVELOP SYSTEM SPECIFICATIONS OF THE LUNAR FLYING VEHICLE. THE SCOPE ENCOMPASSED PARAMETRIC INVESTIGATIONS, CONCEPT GENERATION, AND EVALUATION EFFORT FOR THE DEFINITION OF A RECOMMENDED CONCEPT; PRODUCTION OF A PRELIMINARY DESIGN AND DEVELOPMENT OF SYSTEMS SPECIFICATIONS OF THE RECOMMENDED CONCEPT; AND DEFINITION OF RESOURCES AND CREW TRAINING PLANS. IN ADDITION TO GENERATION OF THE LFV DESIGN, THE SCOPE OF THE STUDY INCLUDED LUNAR MODULE INTEGRATION, FLIGHT SUIT INTERFACE STUDIES, AND DEFINITION OF GROUND SUPPORT EQUIPMENT FOR EARTH AND LUNAR OPERATIONS.</p> <p>AS A RESULT OF PARAMETRIC STUDIES CONDUCTED DURING THE FIRST PHASE OF THIS EFFORT, A CONCEPT WAS SELECTED WHICH HAS THE FOLLOWING CHARACTERISTICS: (1) STABILITY-AUGMENTED CONTROL, (2) FOUR GIMBALED ENGINES WHICH ARE CLUSTERED BENEATH THE VEHICLE, (3) A SEATED PILOT POSITION, AND (4) AN INTEGRAL X-FRAME LANDING GEAR WITH 6 HYDRAULIC ATTENUATORS. THIS VEHICLE IS CAPABLE OF CARRYING A 370-LB PAYLOAD IN ADDITION TO THE PILOT. THE DRY WEIGHT OF THE VEHICLE IS 304 LB. WHEN LOADED WITH 300 POUNDS OF LM DESCENT STAGE PROPELLANTS, THE VEHICLE CAN OPERATE WITH A 4.6 NAUTICAL MILE RADIUS WITH NO PAYLOAD.</p> |
|--|

## CONTENTS

|   | Page |
|---|------|
| INTRODUCTION . . . . .                                      | 1    |
| BASELINE VEHICLE . . . . .                                  | 3    |
| General Arrangement . . . . .                               | 3    |
| Parametric Phase Concepts . . . . .                         | 3    |
| Preliminary Design Optimization . . . . .                   | 23   |
| Description of Preliminary Design Configuration . . . . .   | 47   |
| Preliminary Design Mass Properties/Geometric Data . . . . . | 65   |
| Human Factors . . . . .                                     | 67   |
| Design Criteria . . . . .                                   | 67   |
| Impact Tolerance and Restraint Design . . . . .             | 91   |
| Mockup Tests . . . . .                                      | 97   |
| Reliability . . . . .                                       | 113  |
| Design Objective of Reliability Study . . . . .             | 113  |
| General Considerations . . . . .                            | 114  |
| Reliability Logic . . . . .                                 | 125  |
| Reliability Growth . . . . .                                | 138  |
| Two Engine - Four Engine Comparison . . . . .               | 146  |
| Landing Gear . . . . .                                      | 151  |
| Requirements . . . . .                                      | 151  |
| Concept Development . . . . .                               | 157  |
| Design Optimization . . . . .                               | 160  |
| Attenuator Design . . . . .                                 | 168  |
| Structure . . . . .   | 174  |
| Parametric Phase . . . . .                                  | 174  |
| Application of Boron Composites . . . . .                   | 175  |
| Conceptual Design . . . . .                                 | 177  |
| Preliminary Design Structural Analysis . . . . .            | 177  |
| Structural Design Loads . . . . .                           | 179  |
| Environments . . . . .                                      | 181  |
| Loading Distribution . . . . .                              | 181  |
| Stress Analysis . . . . .                                   | 185  |
| Payload Integration . . . . .                               | 193  |
| Conceptual Studies . . . . .                                | 193  |
| Preliminary Design . . . . .                                | 198  |
| Payload Capability . . . . .                                | 201  |



|   | Page |
|---|------|
| Lunar Module Integration . . . . .          | 201  |
| Lunar Support Equipment . . . . .           | 214  |
| Lunar Debris Control . . . . .              | 216  |
| Weight and Balance Equipment . . . . .      | 217  |
| Preliminary Design . . . . .                | 217  |
| Mass Properties Summary . . . . .           | 220  |
| Pulse-Modulated Thruster Concept . . . . .  | 224  |
| R4D Engine Characteristics . . . . .        | 224  |
| Pulsed-Thruster Concepts . . . . .          | 226  |
| Engine-Induced Vibration . . . . .          | 231  |
| Control System Characteristics . . . . .    | 241  |
| Flight Performance . . . . .                | 252  |
| MODIFIED VEHICLE OPTIONS . . . . .          | 255  |
| 100-Pound Maximum Payload Vehicle . . . . . | 255  |
| Earthshine Operations Vehicle . . . . .     | 255  |
| Escape-to-Orbit Vehicle . . . . .           | 257  |
| REFERENCE . . . . .                         | 261  |

ILLUSTRATIONS

| Figure |   | Page |
|--------|---|------|
| 1      | Study Logic, Configuration Design - Phase One . . . . .   | 4    |
| 2      | Initial Control Configuration of Lunar Flying Vehicle<br>(Drawing 2030-27) . . . . .                    | 7    |
| 3      | Recessed Platform Study Configuration 2<br>(Drawing 2230-2) . . . . .                                   | 11   |
| 4      | Recessed Platform Study Configuration<br>(Drawing 2230-1) . . . . .                                     | 13   |
| 5      | Minimum Payload Concept . . . . .   | 15   |
| 6      | Seated Pilot, Four-Tank, Parallel Feed Alternative<br>Vehicle Configuration (Drawing 2230-7) . . . . .  | 17   |
| 7      | Seated Pilot, Four Tank, Leg-Frame Gear Alternative<br>Vehicle Configuration (Drawing 2230-8) . . . . . | 19   |
| 8      | Leg Geometry . . . . .  | 22   |
| 9      | C. G. -Pivoted Engines Alternative Vehicle Configuration<br>(Drawing 2230-9) . . . . .                  | 25   |
| 10     | Four-Engine, Eight Actuator Installation Study<br>Configuration (Drawing 2230-10) . . . . .             | 27   |
| 11     | Four-Engine, Sliding Plate Canted Engine Installation<br>(Drawing 2230-13) . . . . .                    | 29   |
| 12     | Seated Pilot, Single Gimballed Engine Vehicle<br>Configuration (Drawing 2230-14) . . . . .              | 31   |
| 13     | Seated Pilot, Long Radius Gimbal Vehicle Configuration<br>(Drawing 2230-4) . . . . .                    | 33   |
| 14     | Four-Engine Sliding Plate, Zero Cant Angle Vehicle<br>Configuration (Drawing 2230-16) . . . . .         | 35   |
| 15     | In-Line Sliding Plate Four-Engine Installation<br>Configuration (Drawing 2230-19) . . . . .             | 37   |
| 16     | Study Logic, Configuration Design - Phase Two . . . . .   | 39   |
| 17     | Phase Two Control Configuration of Lunar Flying<br>Vehicle (Drawing 2230-18) . . . . .                  | 41   |
| 18     | Preliminary Design Engine-Installation<br>(Drawing 2230-21A) . . . . .                                  | 43   |
| 19     | Preliminary Design General Arrangement<br>(Drawing 2230-23) . . . . .                                   | 45   |
| 20     | Seat and Instrument Panel Assembly<br>(Drawing 2230-20C) . . . . .                                      | 49   |
| 21     | Preliminary Design Stowage Arrangement<br>(Drawing 2230-24) . . . . .                                   | 51   |

| Figure |  | Page |
|--------|--|------|
| 22     | Preliminary Design Structure and Landing Gear<br>(Drawing 2230-25) . . . . .                     | 53   |
| 23     | Propellant Tank Installation (Drawing 2230-26A) . . . . .  | 55   |
| 24     | Preliminary Design Attenuator (Drawing 2230-27) . . . . .  | 57   |
| 25     | Propulsion Schematic (Drawing 2230-101C) . . . . .   | 59   |
| 26     | Preliminary Design Propellant Tank<br>(Drawing 2230-102A) . . . . .                              | 61   |
| 27     | Instrumentation, Control, and Power Subsystem<br>Diagram (Drawing 2230-104) . . . . .            | 63   |
| 28     | Control Layout of Crewman Dimensions and Block II<br>Apollo Suit (Drawing V36-960030) . . . . .  | 71   |
| 29     | Standing-Position Dimensions . . . . .   | 75   |
| 30     | Recommended Angles for LFV Pilot's Seat . . . . .  | 77   |
| 31     | Maximum Viewing Angles, Eye Rotation Only, Vertical<br>Motion in Sagittal Plane . . . . .        | 81   |
| 32     | Maximum Viewing Angles, Head Rotation Only,<br>Vertical Motion in Sagittal Plane . . . . .       | 82   |
| 33     | Maximum Viewing Angles, Eye and Head Rotation,<br>Vertical Motion in Sagittal Plane . . . . .    | 83   |
| 34     | Relatively Unrestrained Pilot . . . . .  | 92   |
| 35     | Closely Restrained Pilot, Seated . . . . .   | 93   |
| 36     | Longitudinal Impact Tolerance, Standing Position . . . . .                                       | 94   |
| 37     | Idealized Unrestrained Pilot Attenuation . . . . .   | 98   |
| 38     | LFV Configuration A With Components in Flight<br>Position . . . . .                              | 101  |
| 39     | LFV Configuration B With Components in Stowage<br>Position . . . . .                             | 103  |
| 40     | LFV Configuration A Showing Test Subject Attempting<br>Ingress . . . . .                         | 104  |
| 41     | LFV Configuration B Showing Test Subject's Approach<br>for Seat Entry . . . . .                  | 106  |
| 42     | LFV Configuration A With Seat Tilted Forward to<br>Improve Forward and Downward Vision . . . . . | 108  |
| 43     | LFV Configuration A Modified by Removal of Footrest<br>Platform and Seat Rotation . . . . .      | 109  |
| 44     | LFV Configuration B Incorporating All Modifications . . . . .                                    | 110  |
| 45     | Mission Success for LFV Configuration 1, Rule A . . . . .  | 115  |
| 46     | Mission Success for LFV Configuration 2, Rule A . . . . .  | 116  |
| 47     | Mission Success for LFV Configuration 3, Rule A . . . . .  | 117  |
| 48     | Crew Safety for LFV Configuration 1, Rule A . . . . .  | 118  |
| 49     | Crew Safety for LFV Configuration 2, Rule A . . . . .  | 119  |
| 50     | Crew Safety for LFV Configuration 3, Rule A . . . . .  | 120  |
| 51     | Mission Reliability Sequence for LFV Configurations 1<br>and 2 . . . . .                         | 121  |





| Figure |   | Page |
|--------|---|------|
| 52     | Successful-Path Diagram, Mission Crew Safety . . . . .  | 126  |
| 53     | Successful-Path Diagram, Sorties 1 Through 4<br>Crew Safety . . . . .                           | 127  |
| 54     | Successful-Path Diagram, Sortie 5 Crew Safety . . . . .   | 129  |
| 55     | Eight-Actuator Mission Logic . . . . .  | 134  |
| 56     | Four, Two-in-a-Can Actuator Mission Logic . . . . .   | 135  |
| 57     | Four, Two-in-a-Can Actuator Crew Safety Logic . . . . .   | 136  |
| 58     | Crew Safety Logic for Sliding Plate Configuration . . . . .                                     | 137  |
| 59     | Cumulative Reliability Point Estimate . . . . .   | 143  |
| 60     | Mean Life Growth Level . . . . .  | 144  |
| 61     | Engine Valve Redundancy . . . . .   | 150  |
| 62     | Landing Performance Data From Visual Simulation,<br>Three-Axis Stability Augmentation . . . . . | 153  |
| 63     | Landing Performance Data From Visual Simulation<br>Hardware and Neutral C. G. . . . .           | 154  |
| 64     | Toppling Stability . . . . .  | 156  |
| 65     | Cutoff Height Capability . . . . .  | 158  |
| 66     | Footpad and Horizontal Attenuator Assembly . . . . .  | 159  |
| 67     | Landing Gear Concepts . . . . .   | 161  |
| 68     | Leg Frame Gear for Seated-Pilot Vehicle<br>Configuration . . . . .                              | 163  |
| 69     | Landing Gear Capability . . . . .   | 166  |
| 70     | Dynamics Program Coordinate System . . . . .  | 169  |
| 71     | B-58 Escape Capsule Metal-Deformation Attenuator . . . . .                                      | 171  |
| 72     | Metal-Deformation Energy Absorber Concept . . . . .   | 172  |
| 73     | Surveyor Fluid-Spring Attenuator . . . . .  | 173  |
| 74     | Leg-Shear Force Diagram . . . . .   | 183  |
| 75     | Leg Bending Moment Diagram . . . . .  | 184  |
| 76     | Shear and Bending Moment for Tank Crossbeam . . . . .   | 186  |
| 77     | Shear and Bending Moment for Load Pan Crossbeam . . . . .                                       | 187  |
| 78     | Leg Cross Section . . . . .   | 189  |
| 79     | Payload Study Logic . . . . .   | 194  |
| 80     | Payload Variations Studied (Drawing 2230-11) . . . . .  | 195  |
| 81     | Fixed Load Pan Variations (Drawing 2230-12) . . . . .   | 199  |
| 82     | Payload Capability Envelope . . . . .   | 202  |
| 83     | ELM, Roving Vehicle Interface Definition . . . . .  | 203  |
| 84     | Stowing Arrangement, Initial Control Vehicle<br>Configuration (Drawing 2230-3A) . . . . .       | 205  |
| 85     | 100-Pound Maximum Payload Vehicle Configuration<br>(Drawing 2230-15) . . . . .                  | 209  |
| 86     | Simplified, Fixed Component Vehicle Configuration<br>(Drawing 2230-17) . . . . .                | 211  |
| 87     | Propellant Servicing Configuration . . . . .  | 215  |

| Figure |   | Page |
|--------|---|------|
| 88     | Takeoff Mat Coverage Pattern . . . . .  | 218  |
| 89     | Weights of Candidate Mat Materials . . . . .  | 219  |
| 90     | Pulse-Width Modulated Performance - R4D . . . . .   | 225  |
| 91     | Tilting-Platform, Pulsed-Thruster Concept . . . . .   | 227  |
| 92     | Level-Platform, Pulsed-Thruster Concept . . . . .   | 229  |
| 93     | LFV Pulsed Thruster, Body Frame Schematic . . . . .   | 233  |
| 94     | Engine and Mass Data for LFV Pulsed Thruster . . . . .  | 234  |
| 95     | LFV Pulsed Thruster, Fluctuation of Life Forces<br>With Staggered Ignition of Four Engines . . . . .                        | 237  |
| 96     | LFV Pulsed Thruster, Fluctuation of Life Forces<br>With Staggered Ignition of Paired Engines . . . . .                      | 238  |
| 97     | LFV Pulsed Thruster, Fluctuation of Life Forces<br>With Staggered Ignition of Individual Engines . . . . .                  | 239  |
| 98     | LFV Pulsed Thruster Fluctuation of Life and Forward<br>Thrust Forces With Staggered Ignition of Paired<br>Engines . . . . . | 240  |
| 99     | Control System for Pulsed LFV . . . . .   | 242  |
| 100    | Engine Geometry for Pulsed LFV, Eight Engines . . . . .   | 243  |
| 101    | Translational Dynamics . . . . .  | 244  |
| 102    | Translational Dynamics and Propellant Consumption . . . . .   | 245  |
| 103    | Rotational Dynamics, Body Attitude in Radians . . . . .   | 246  |
| 104    | Rotational Dynamics, Body Rates in RPS . . . . .  | 247  |
| 105    | Limit Cycle Amplitudes, Body Rates in RPS . . . . .   | 248  |
| 106    | Limit Cycle Amplitudes, Body Attitude in Radians . . . . .  | 249  |
| 107    | Effect of C. G. Error on Limit Cycle Amplitudes, Body<br>Rates in RPS . . . . .   | 250  |
| 108    | Effect of C. G. Error on Limit Cycle Amplitudes, Body<br>Attitude in Radians . . . . .                                      | 251  |
| 109    | Escape-to-Orbit Vehicle Configuration . . . . .   | 259  |

TABLES

| Table |  | Page |
|-------|--|------|
| 1     | Two-Tank/Four-Tank Weight Comparison . . . . .   | 21   |
| 2     | Preliminary Design Configuration Control<br>Characteristics . . . . .                  | 66   |
| 3     | Supplementary Anthropometric Data for A7L Suit . . . . .                               | 73   |
| 4     | Recommended Joint Angles - Standing Position . . . . .                                 | 76   |
| 5     | Summary of Voluntary Tolerances to Vertical Impact . . . . .                           | 94   |
| 6     | Pilot Accelerations - Current Design Limits . . . . .                                  | 99   |
| 7     | Mockup Seat and Astronaut Body Angles . . . . .  | 111  |
| 8     | Control Configuration Comparison (Rule A) . . . . .                                    | 122  |
| 9     | Mission Continuation Risks - Crew Losses Due to<br>Multiple Failures . . . . .         | 124  |
| 10    | Typical In-Phase Logic - Four-Engine Configuration<br>(ARMM Program Logic) . . . . .   | 131  |
| 11    | Typical In-Phase Logic - Single-Engine Configuration<br>(ARMM Program Logic) . . . . . | 132  |
| 12    | Component Failure Rates . . . . .  | 139  |
| 13    | Rocket Engine Failure Modes (Reference 20) . . . . .                                   | 140  |
| 14    | Failure Mode Analysis of "Two-in-a-Can" Actuator<br>Configuration . . . . .            | 141  |
| 15    | Sliding Plate Failure Mode Analysis . . . . .  | 142  |
| 16    | Two-Engine Configuration Components . . . . .  | 147  |
| 17    | Two-Engine Configuration Failure Probabilities . . . . .                               | 148  |
| 18    | Reliability Criteria Comparison . . . . .  | 149  |
| 19    | Worst-Case Landing Displacement . . . . .  | 167  |
| 20    | Representative LFV Payloads . . . . .  | 197  |
| 21    | Vehicle Weight and Balance . . . . .   | 220  |
| 22    | Vehicle Inertias ( Slug Ft <sup>2</sup> ) . . . . .                                    | 221  |
| 23    | Vehicle Summary Weight Statement, Baseline<br>Configuration . . . . .                  | 222  |
| 24    | Lunar Flying Vehicle Flight Elements Summary Weight<br>Statement . . . . .             | 223  |
| 25    | Marquardt R4D Engine Characteristics . . . . .   | 226  |
| 26    | Vibration Isolation Versus Engine-Operation Mode . . . . .                             | 235  |
| 27    | Flight Performance Comparisons . . . . .   | 254  |
| 28    | Weight Reduction, 100-Pound Maximum Payload Vehicle . . . . .                          | 256  |

## INTRODUCTION

~~This volume of SD69-419 covers~~ the general subjects of configuration <sup>inc. p. 5</sup> design and design integration of the lunar flying vehicle (LFV). The results of the landing gear subsystem, structure, and payload integration design studies are included. Design integration aspects covered include human factors, reliability, mass properties, and lunar support equipment. All of these subjects are treated in detail as part of the design of the baseline vehicle. Vehicle options involving modification of the baseline vehicle are covered separately. These options include a version that has a maximum payload capability of 100 pounds, as opposed to 370 pounds for the baseline vehicle; a vehicle modified for earthshine operations instead of the baseline daylight operations; and a vehicle capable of escape to lunar orbit with two crew members. An alternate design for the baseline mission using available engines in a pulsed mode is also described.

## BASELINE VEHICLE

### GENERAL ARRANGEMENT

This section discusses the configuration (general form) of the vehicle and its major subsystems and structural elements. The relationship of the vehicle form to the conclusions of the functional studies is described by first considering the parametric phase of conceptual design development, and finally the preliminary design phase, or optimized general arrangement design development.

#### Parametric Phase Concepts

Although the emphasis in this report is on the work performed under contract, considerable concept development had been accomplished prior to the initiation of this study. The precontract work consisted of the exploration of a broad range of concepts and was most useful in showing the interactions involved in integrating configurations in which the number of propellant tanks, engines, type of control, and landing gear arrangement were varied. To indicate the nature and extent of the precontract concept development, a representative selection of these drawings is included as Appendix C.

#### Conceptual Design Approach

The primary factors influencing general vehicle arrangement are LM stowing, operational and mission constraints, and the functional/installation requirements of the various subsystem concepts considered. The method used to satisfy these many requirements and the sequence of work are shown in the logic diagram of Figure 1. The study was initiated by issuing a control configuration, which consisted of a design drawing and a descriptive definition of the characteristics of the baseline design point. As the study progressed and significant changes accumulated, the control configuration was updated. As concepts were developed, mass properties and reliability characteristics were assessed, permitting configuration concept screening, and finally, selection. As described in other sections of this report, certain areas were handled separately as subassemblies to permit focusing of reliability and/or weight comparisons. Among these were the engine/control mechanization studies, and the comparison of landing gear alternatives.

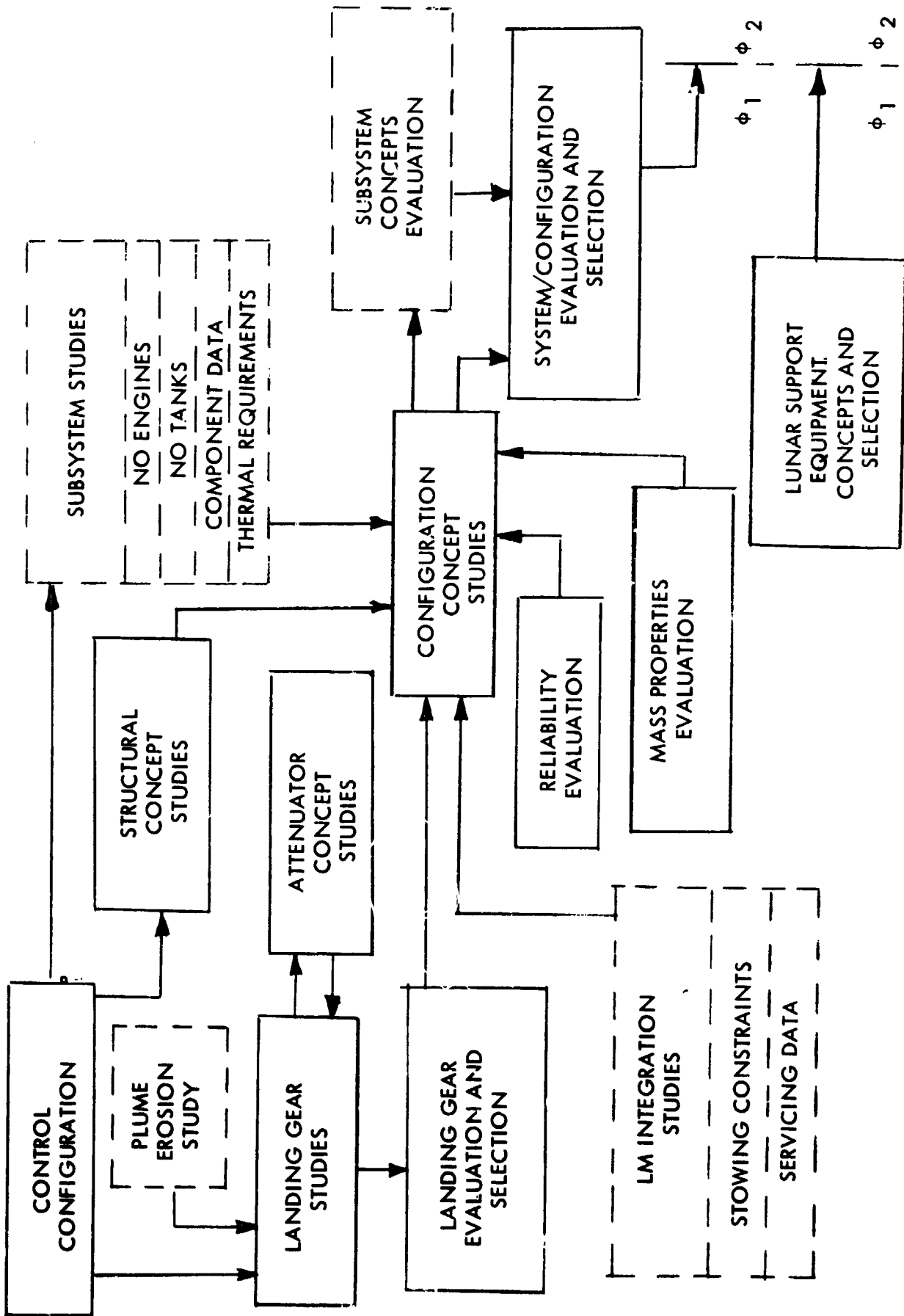
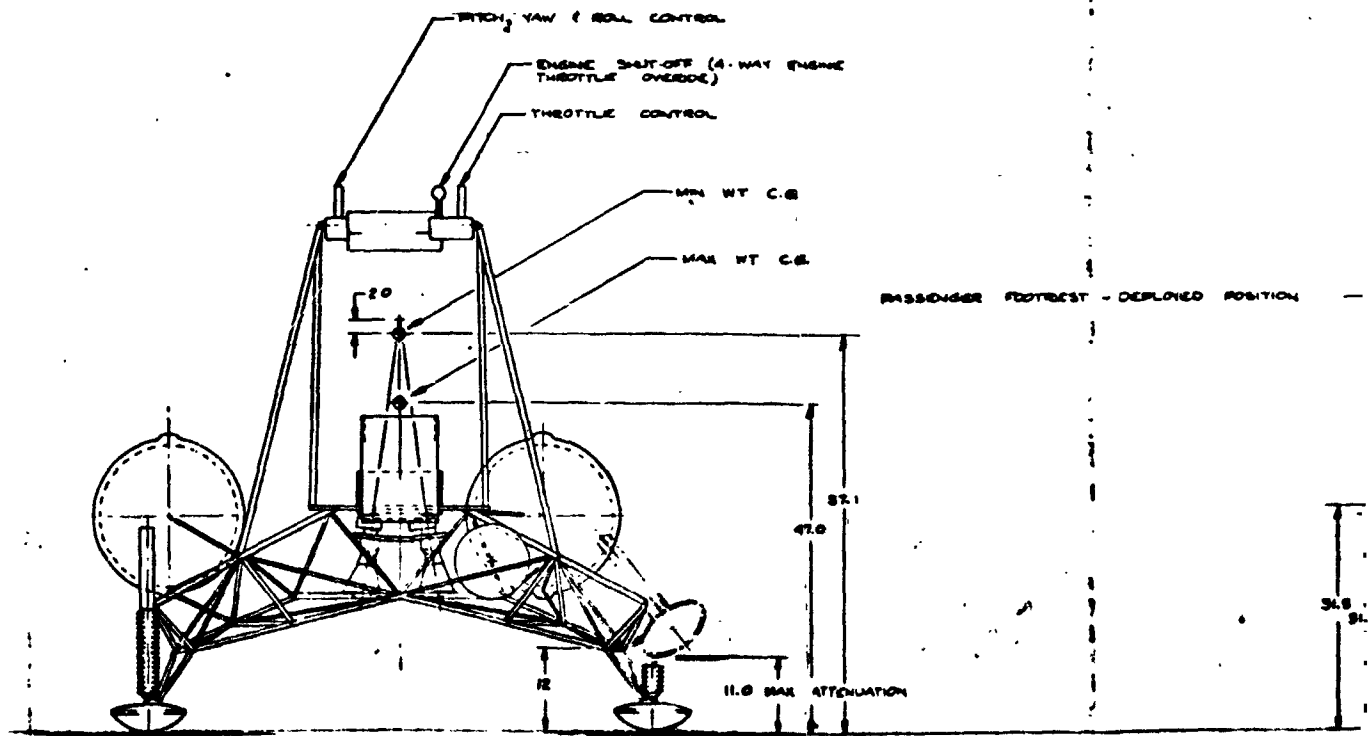


Figure 1. Study Logic, Configuration Design - Phase One

## Concept Evolution

The initial control configuration is illustrated in Figure 2. It represents the results of the precontract activity and incorporates two spherical propellant tanks, four gimballed engines in a central cluster, stability-augmented control utilizing electromechanical actuators, and a landing gear featuring at-pad attenuators. The position of the pilot in this design is unrestrained and standing. In compliance with a contract provision that was removed near the midpoint of the study, the vehicle incorporated provisions to carry a rescued astronaut in a reclining position. The characteristics of this basepoint design are described in more detail as follows:

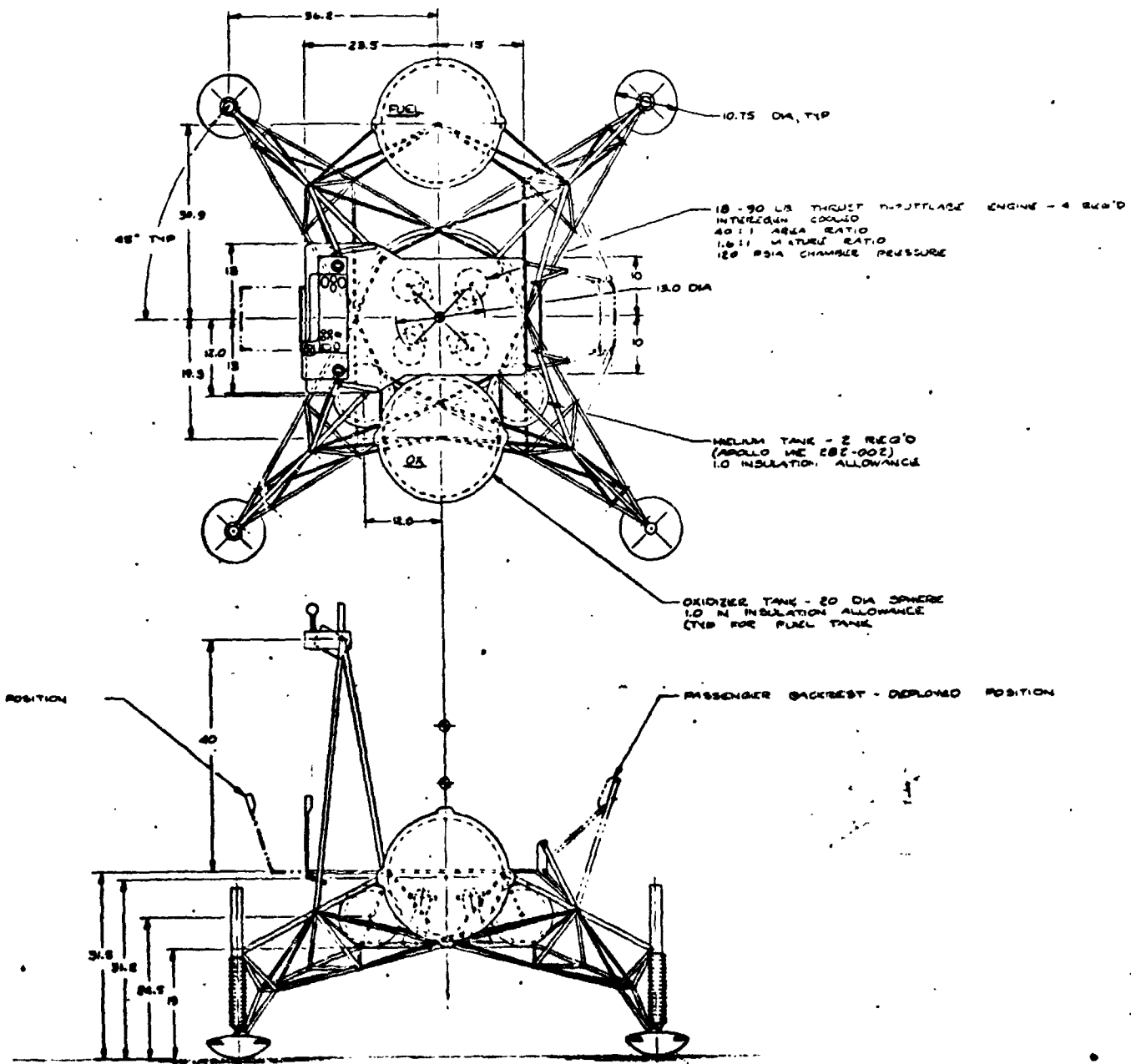
1. Two 20-inch diameter, modified Gemini spherical propellant tanks
2. Two Apollo SM RCS pressurant vessels
3. LM descent stage residual propellant, Aerozine 50/N<sub>2</sub>O<sub>4</sub> at a mixture ratio of 1.6
4. Four engines with throttling from 18 to 90 pounds thrust, area ratio of 40, 120 psia chamber pressure
5. Engines gimballed individually for redundant pitch, yaw, and roll control
6. Stability-augmented control, electromechanical actuators
7. Truss-designed LFV body structure
8. Four-leg, nonattenuating truss struts, omnidirectional landing capability
9. Attenuation at each pad with a hydraulic attenuator for vertical velocity and an internal spring attenuator for lateral velocity
10. Landing criteria of 20 degrees tipover safety margin, 6 feet per second (fps) vertical velocity, 2 fps horizontal velocity, 3 degrees per second (deg/sec) attitude rate, 10-degree initial attitude, 10-degree ground slope, 8 g maximum vertical deceleration, rock impact (no sliding)
11. Eight-inch minimum ground clearance
12. Two LFV's per LM landing which can be removed, deployed, transferred to takeoff site, and fueled by one astronaut with



ADJUST FRAME



REPRODUCIBILITY OF THE ORIGINAL PAGE IS POOR.

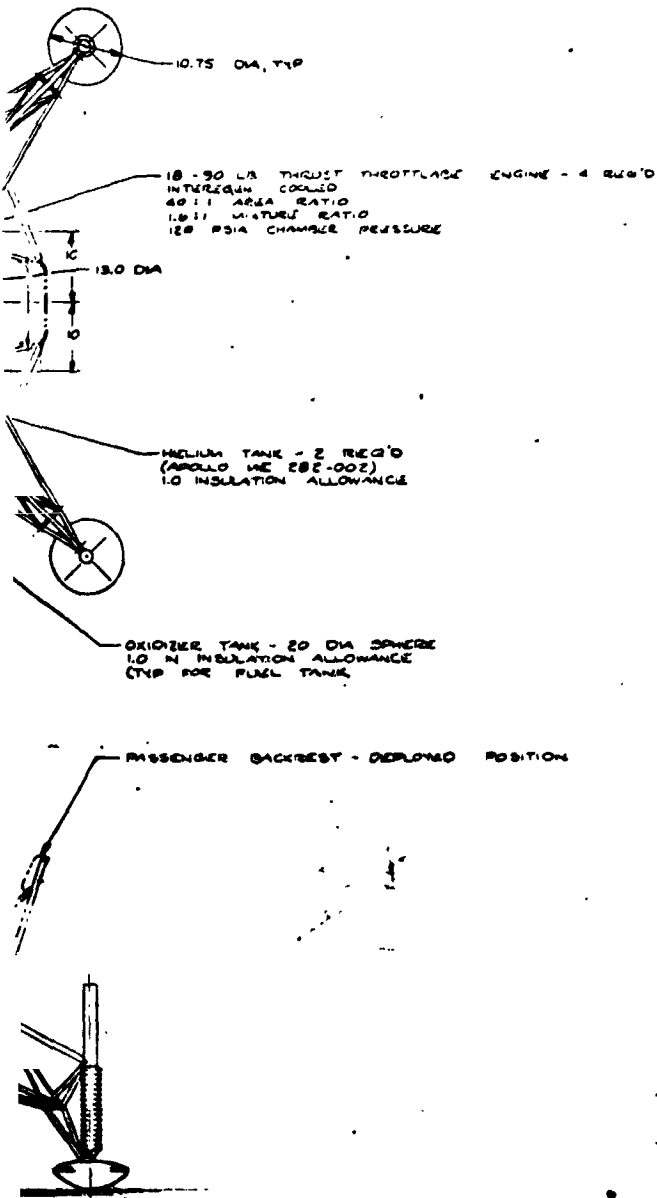


|          |      |
|----------|------|
| REV      | DATE |
| 1/6      | 1/68 |
| LUNAR    |      |
| 4-ENGINE |      |

Figure 2. . Initial Control Configuration (Drawing 2030-

FOLDCOM FRAM

FOLDCOM FRAM PRECEDING PAGE BLANK



|           |                |                    |   |         |
|-----------|----------------|--------------------|---|---------|
| REV<br>No | DATE<br>0-3-68 | BY<br>J. W. HARRIS | DESCRIPTION<br>LUNAR FLYING UNIT -<br>4-ENGINE, 2-TANK, AUTOMATIC CONTROL | 2030-27 |
|-----------|----------------|--------------------|---|---------|

Figure 2. . Initial Control Configuration of Lunar Flying Vehicle  
(Drawing 2030-27)

REDUCE TO 11 INCHES

minimum hazard to the astronaut and with minimum needs for time and physical exertion by the astronaut

13. Payload capability of 370 pounds of scientific equipment, disabled astronaut, or additional propellant
14. Pilot in an unrestrained standing position

To improve the baseline design, the factors receiving emphasis in the beginning of the study were weight reduction, reduction of center of gravity (c. g.) height to improve toppling stability with a given landing gear spread, and stowability.

Several studies were conducted to lower the c. g. height. One of these involved a recessed-deck concept. As shown in Figure 3, this design was treated parametrically with passenger position, engine quantity, arrangement, and gimbal angle being varied for each concept so that the characteristics of the design with respect to engine cant angle, tank centerline spacing, c. g. location, gear spread, and pilot foot placement could be determined. All of the concepts considered reduced the c. g. height from 57.1 inches to approximately 49 inches, with proportional reductions in gear footprint and with improved stowability. Concept B-7 of Figure 3 was selected after evaluation, since it offered the best pilot foot placement, the lowest engine spacing, the least engine cant angle, and the lowest tank centerline spacing. This concept was then developed more fully as shown in Figure 4.

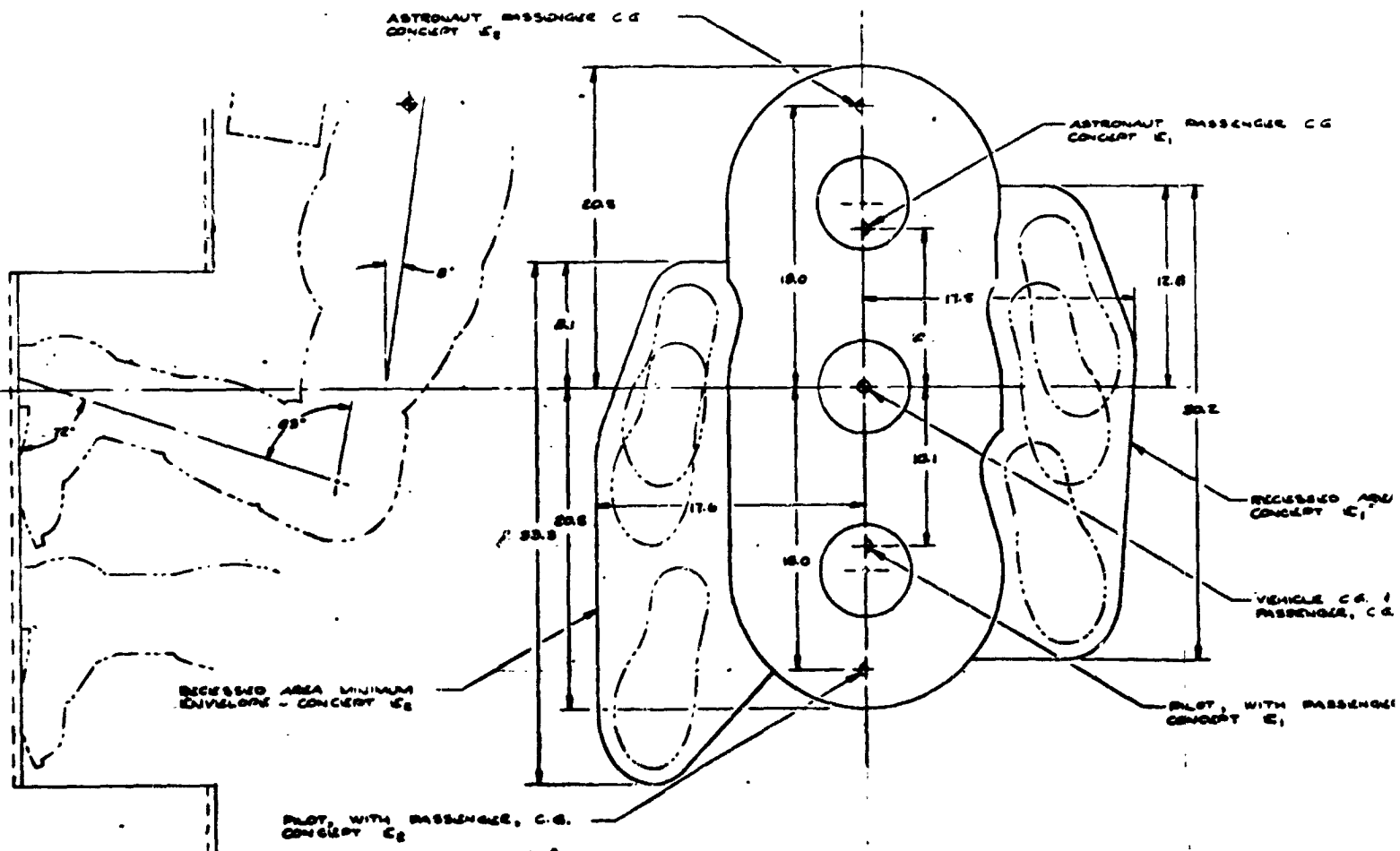
Another concept developed to lower the c. g. is shown in Figure 5. This concept is based on a requirement that the vehicle always carry a minimum payload of at least 130 pounds. This permits the pilot to be located at a low elevation (by moving him away from the vehicle centerline) and still maintain balance.

Both of the concepts described for lowering the c. g. with a standing pilot involved serious compromises. The recessed-deck design required engines to be spaced so far outboard that rotational moments induced upon loss of an engine would be excessively high. This would adversely affect the ability to recover that is needed to attain the reliability advantage of engine-out capability. The minimum-payload concept also incurred a serious compromise in the restriction on operational capability.

The need to reduce c. g. height was finally removed by a change in the control configuration concept to a seated pilot design. As described in another section of this volume, this change was a result of other factors, most important of which was the low g-tolerance level of the pilot in the standing position. However, a beneficial result of the change was lowering

| CONFIG | RESSECT POSITION               | CONCEPT        | ENGINE QUANTITY | ENGINE ARRANGEMENT | BRAKE ANGLE (S DEG) | ENGINE & BRACING DA (IN) | MAX ENGINE ANGLE TO C.S. (DEG) | TANK & BRACING (IN) | VEL. & LOCATION (M. ABOVE GLD.) |          | GEAR RESTRAINT DA (IN) |          | PULT MAX. FOOT SPREAD (IN) |      |
|--------|--------------------------------|----------------|-----------------|--------------------|---------------------|--------------------------|--------------------------------|---------------------|---------------------------------|----------|------------------------|----------|----------------------------|------|
|        |                                |                |                 |                    |                     |                          |                                |                     | MIN. WT.                        | MAX. WT. | MIN. WT.               | MAX. WT. |                            |      |
| A      | PRONE<br>720°/4 13°            | A <sub>1</sub> | 1               | N.A.               | N.A.                |                          |                                |                     |                                 |          |                        |          | N.A.                       |      |
|        |                                | A <sub>2</sub> | 3               | IN-LINE, PITCH     | N.A.                |                          |                                |                     |                                 |          |                        |          |                            | N.A. |
|        |                                | A <sub>3</sub> | 3               | IN-LINE, ROLL      | N.A.                |                          |                                |                     |                                 |          |                        |          |                            | N.A. |
|        |                                | A <sub>4</sub> | 3               | 120°, AFT          | 10                  | 22.0                     | 63                             | 54.9                | 49.0                            | 39.0     | 27.9                   | -        |                            | 19.5 |
|        |                                | A <sub>5</sub> | 3               | 120°, FWD          | 10                  | 22.0                     | 63                             | 54.9                | 49.0                            | 39.0     | 27.9                   | -        |                            | 19.5 |
|        |                                | A <sub>6</sub> | 4               | PITCH/ROLL         | 10                  | 70.7                     | 62                             | 141.6               | 49.0                            | 39.0     | 27.9                   | -        |                            | 19.5 |
|        |                                | A <sub>7</sub> | 4               | 45°                | 10                  | 39.6                     | 65                             | 34.9                | 49.0                            | 39.0     | 27.9                   | -        |                            | 19.5 |
|        |                                | A <sub>8</sub> | 4               | 45°                | 0                   | 39.6                     | 65                             | 34.9                | 49.0                            | 39.0     | 27.9                   | -        |                            | 19.5 |
| B      | VERTICAL<br>93°                | B <sub>1</sub> | 1               | N.A.               | N.A.                |                          |                                |                     |                                 |          |                        |          |                            | N.A. |
|        |                                | B <sub>2</sub> | 3               | IN-LINE, PITCH     | N.A.                |                          |                                |                     |                                 |          |                        |          |                            | N.A. |
|        |                                | B <sub>3</sub> | 3               | IN-LINE, ROLL      | N.A.                |                          |                                |                     |                                 |          |                        |          |                            | N.A. |
|        |                                | B <sub>4</sub> | 3               | 120°, AFT          | 10                  | 42.1                     | 36                             | 22.1                | 49.9                            | 49.4     | 29.5                   | -        |                            | 6.8  |
|        |                                | B <sub>5</sub> | 3               | 120°, FWD          | 10                  | 42.1                     | 36                             | 22.1                | 49.9                            | 49.4     | 29.5                   | -        |                            | 6.8  |
|        |                                | B <sub>6</sub> | 4               | PITCH/ROLL         | 10                  | 44.1                     | 36                             | 21.2                | 49.9                            | 49.4     | 29.5                   | -        |                            | 6.8  |
|        |                                | B <sub>7</sub> | 4               | 45°                | 10                  | 44.1                     | 36                             | 21.2                | 49.9                            | 49.4     | 29.5                   | -        |                            | 6.8  |
|        |                                | B <sub>8</sub> | 4               | 45°                | 0                   | 44.1                     | 36                             | 21.2                | 49.9                            | 49.4     | 29.5                   | -        |                            | 6.8  |
| C      | VERTICAL<br>99°                | C <sub>1</sub> | 1               | N.A.               | 10                  | N.A.                     | N.A.                           | 102.0               | 41.3                            | 49.3     | -                      | 22.4     | 25.0                       |      |
|        |                                | C <sub>2</sub> | 1               | N.A.               | 0                   | N.A.                     | N.A.                           | 70.5                | 44.2                            | 49.3     | -                      | 22.4     | 22.3                       |      |
| D      | VERTICAL, 93°<br>VERTICAL, 93° | D <sub>1</sub> | 4               | 45°                | 10                  | 12.0                     | 13                             | 77.4                | 42.1                            | 49.2     | -                      | 22.2     | 21.5                       |      |
|        |                                | D <sub>2</sub> | 4               | PITCH/ROLL         | 0                   | 12.0                     | 13                             | 22.6                | 47.2                            | 49.3     | -                      | 22.4     | 22.9                       |      |
| E      | VERTICAL, 93°<br>SITTING, 8°   | E <sub>1</sub> | 3               | IN-LINE, ROLL      | 10                  | 23.4                     | 21                             | 60.9                | 42.0                            | 42.1     | -                      | 22.0     | 22.9                       |      |
|        |                                | E <sub>2</sub> | 3               | IN-LINE, ROLL      | 0                   | 23.4                     | 21                             | 67.8                | 42.0                            | 42.4     | -                      | -        | 24.0                       |      |
| BRIDGE | SITTING, 61°                   | -              | 4               | 45°                | 10                  | 12.0                     | 13                             | 22.2                | 27.1                            | 47.0     | 102.4                  | -        | 19.5                       |      |

WELDOUT FRAME



**CONFIGURATION E**  
 3-DIGIT, M-LINE, OPTIMIZATION

FOLDOUT FRAME

PASSENGER C.G.

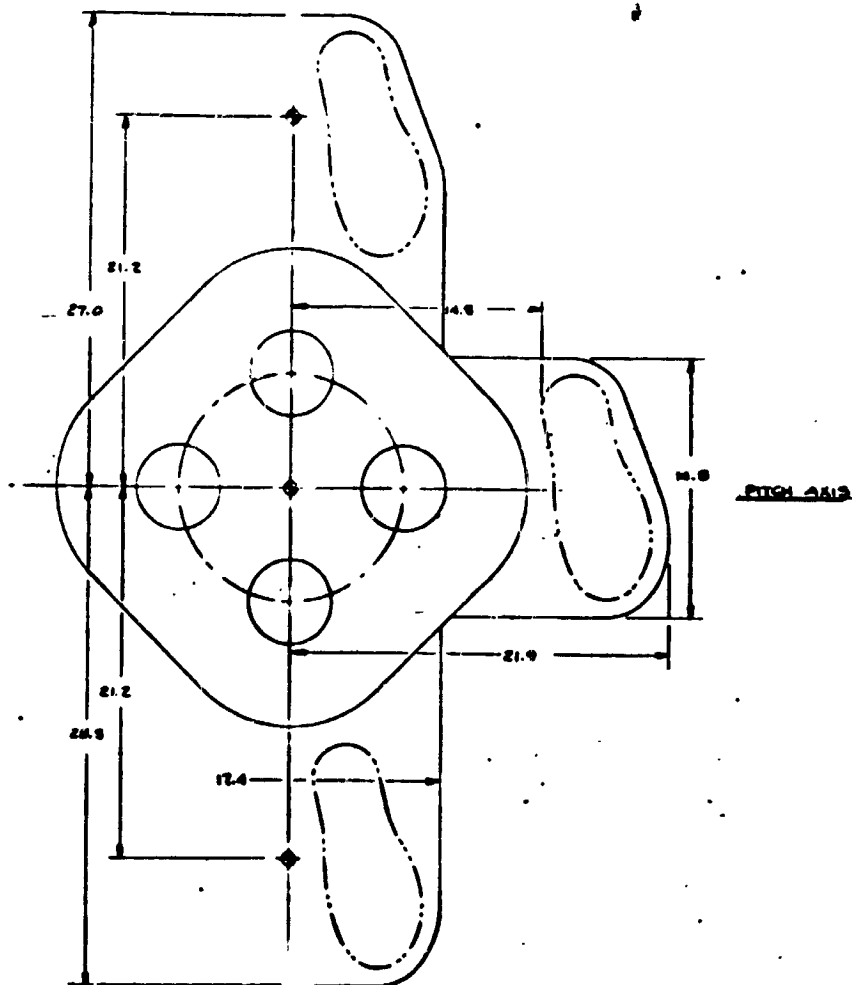
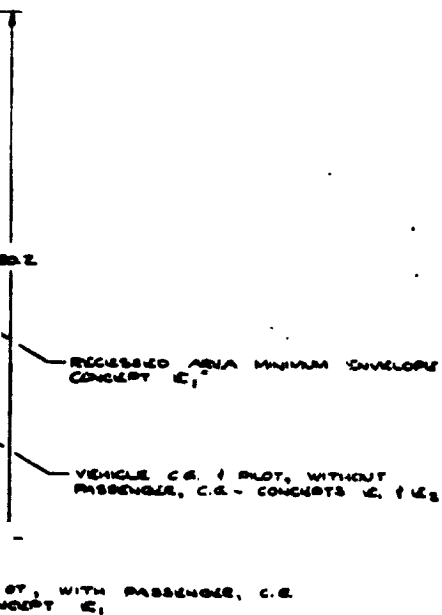
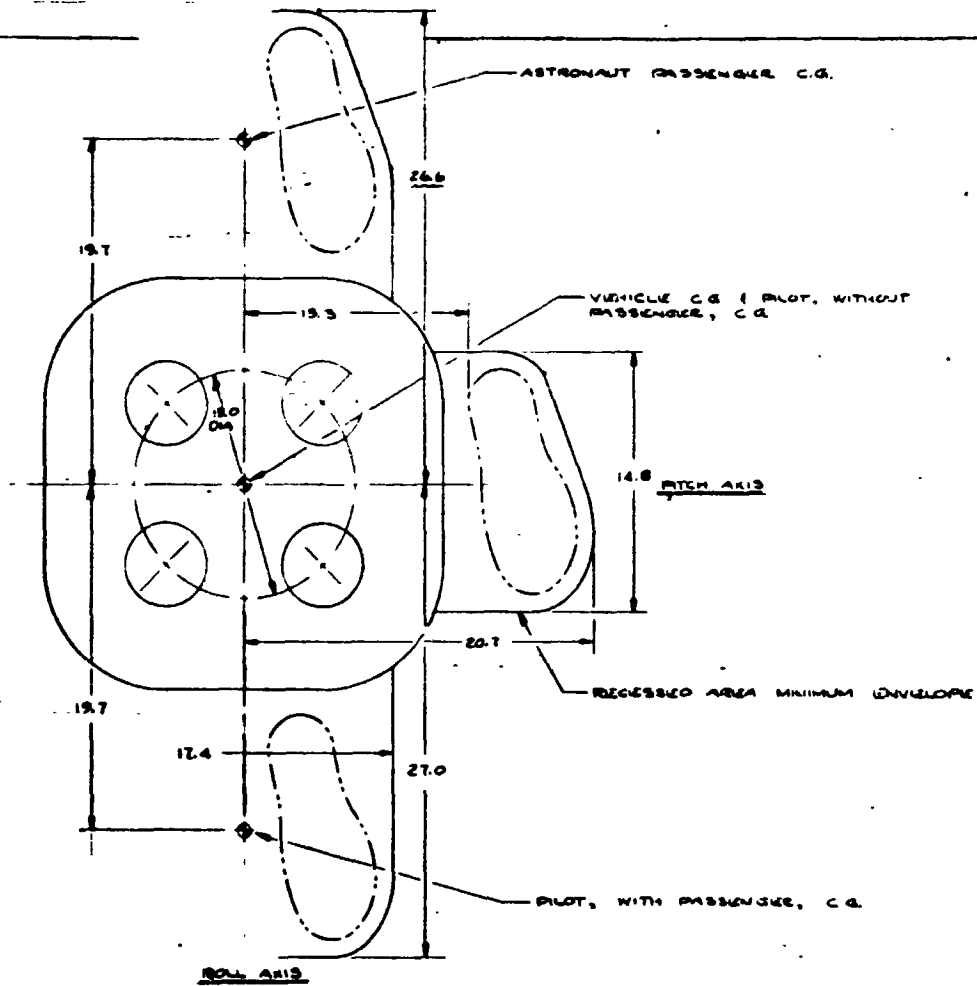


FIG. 4A13

CONFIGURATION  $C_2$   
4. ENGINE, IN-LINE, OPTIMIZATION  
CRITICAL TO  $C_1$ , ACCEPT AS NOTED

FOLDOUT FRAME



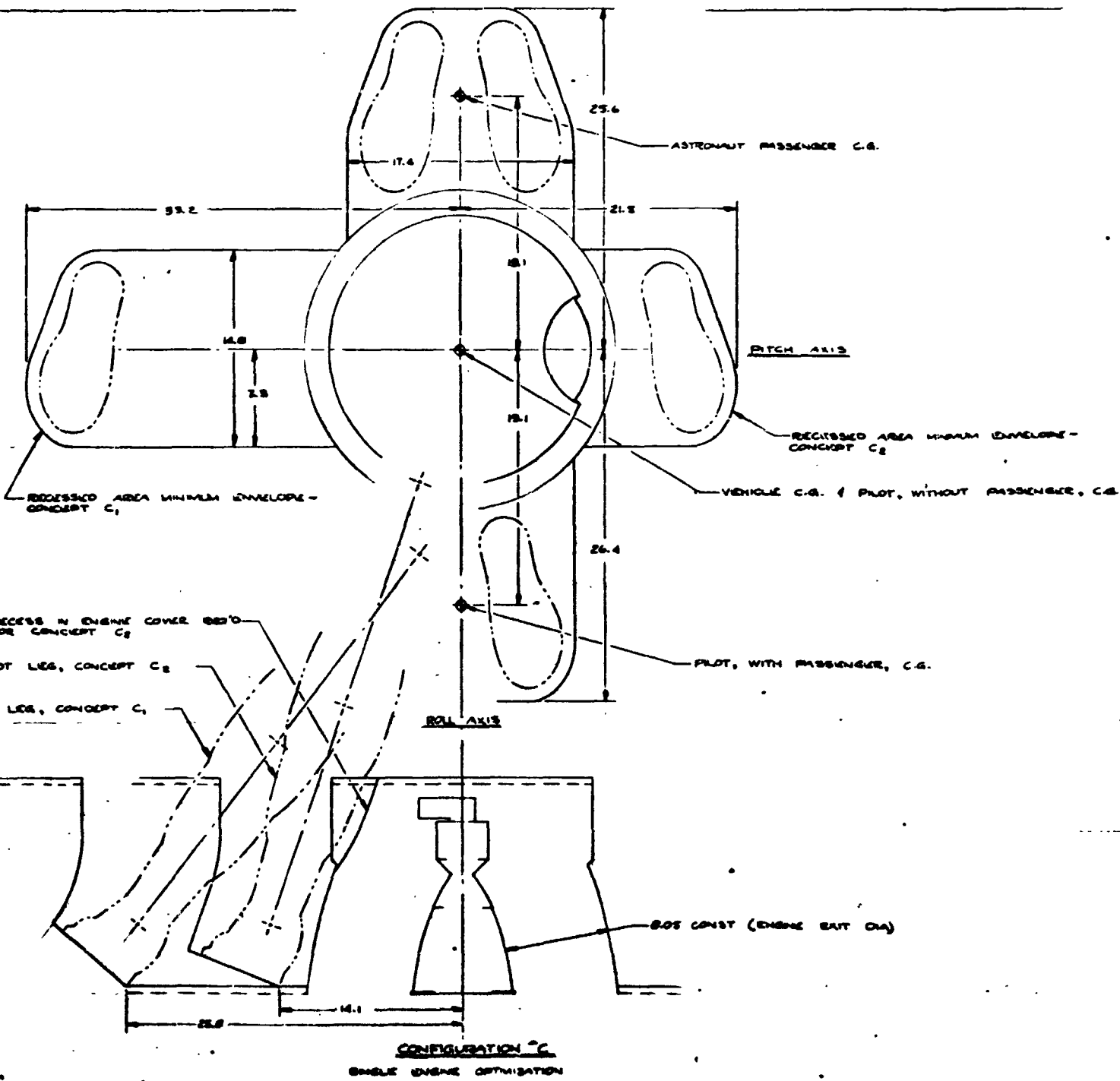
RECESS IN END FOR CONCEPT

PILOT LEG, CONC

PILOT LEG, CONDEF

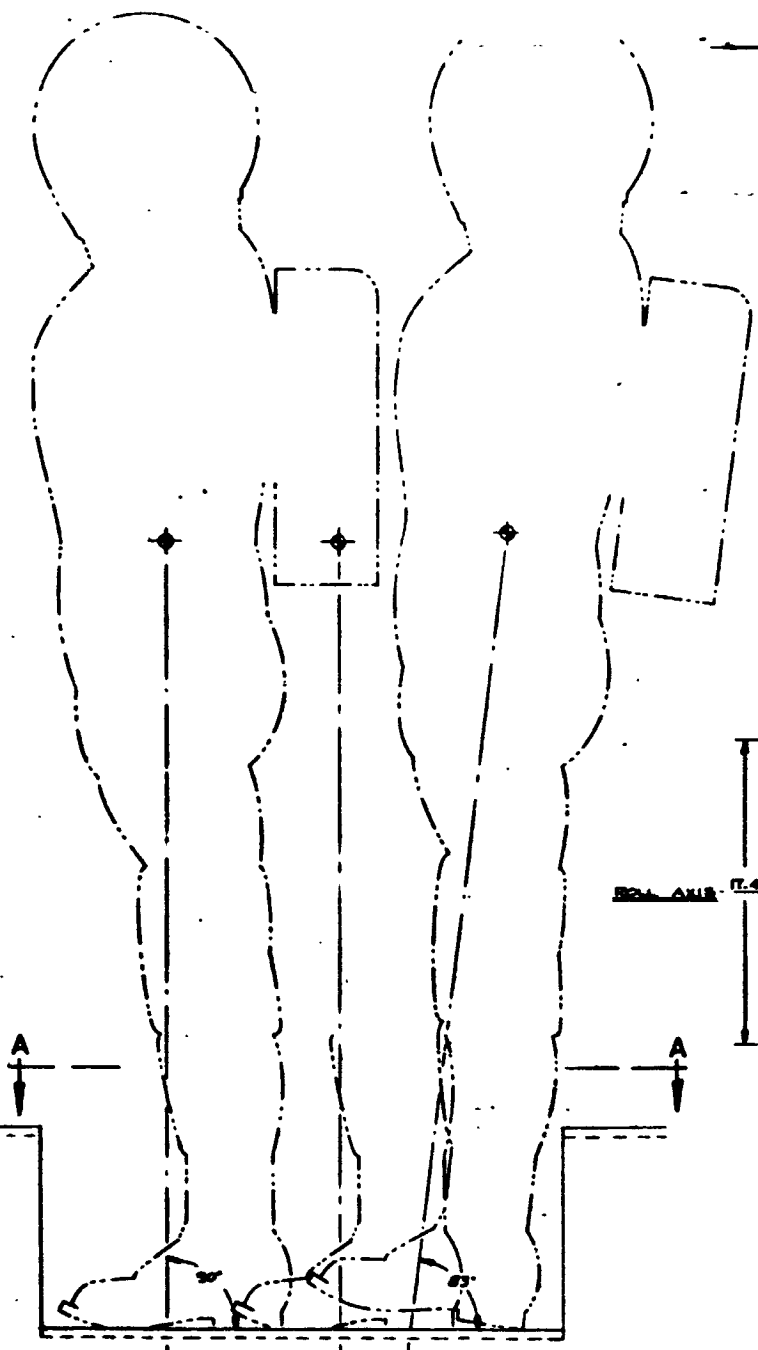
CONFIGURATION D.  
4-ENGINE, 45°, OPTIMIZATION

FOLDOUT FRAME

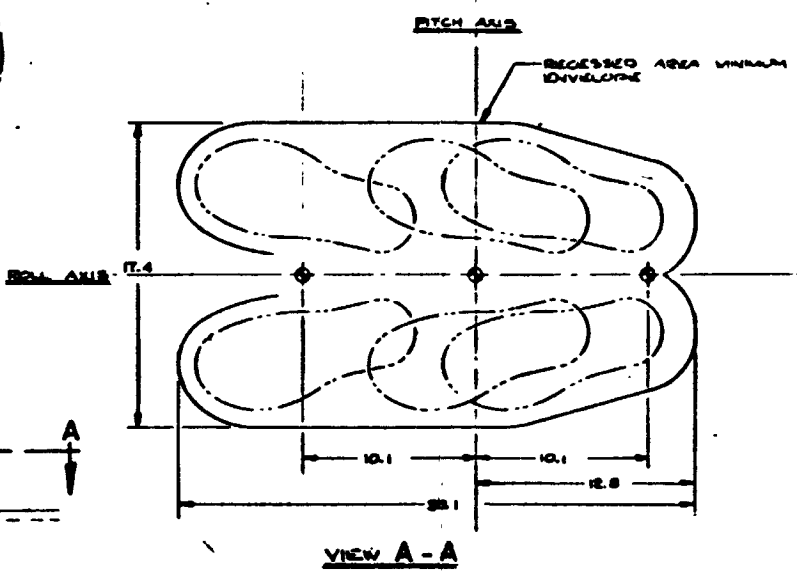


FOLDOUT FRAME





CONFIGURATION B  
 ASTRONAUT RESIDENCE IN VERTICAL  
 POSITION



FOLDOUT FRAME

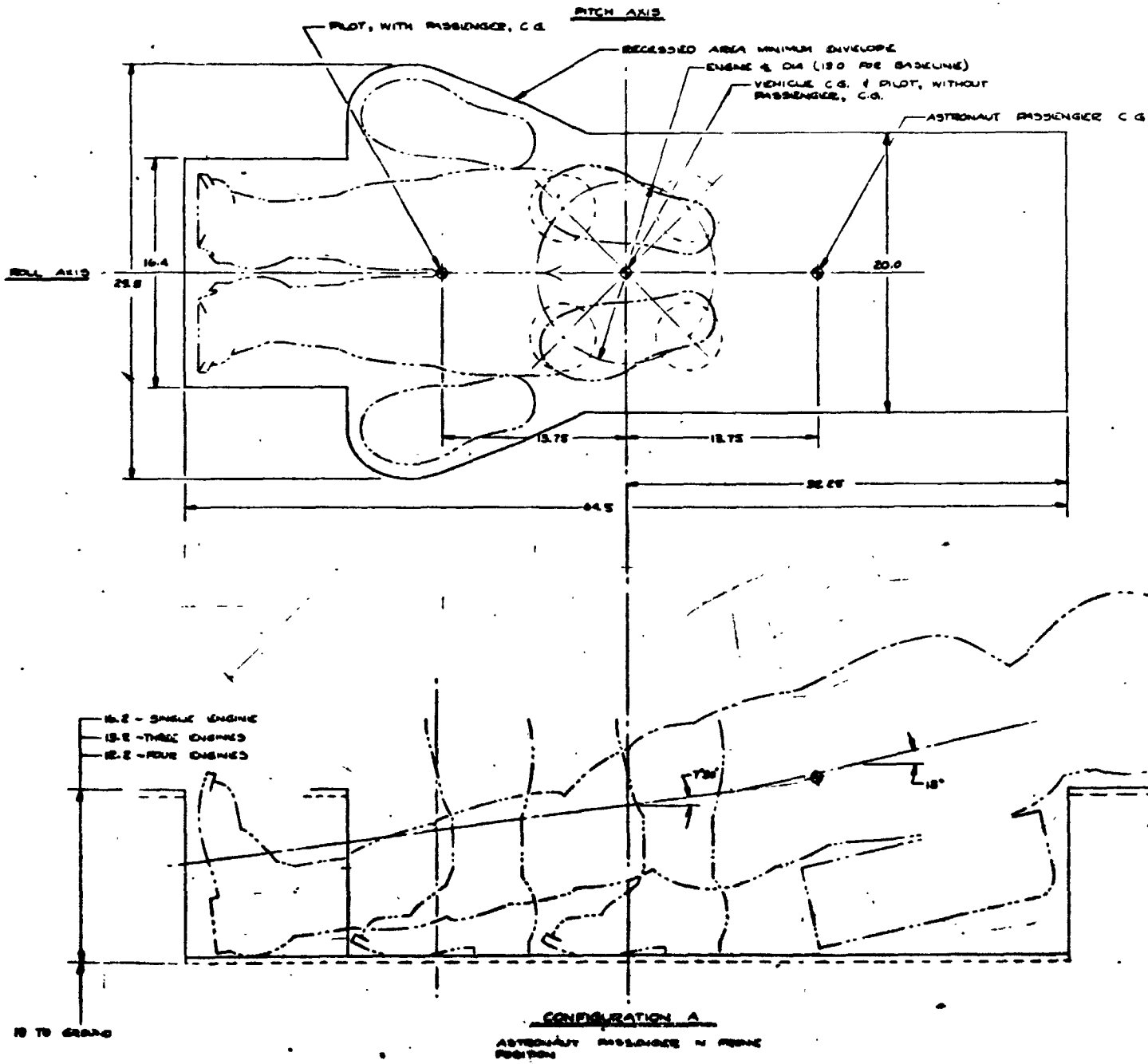


Figure 3. Re

FOLDOUT FRAME

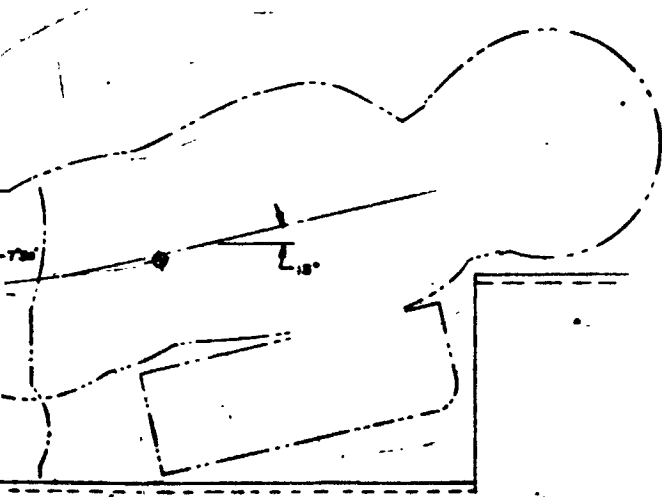
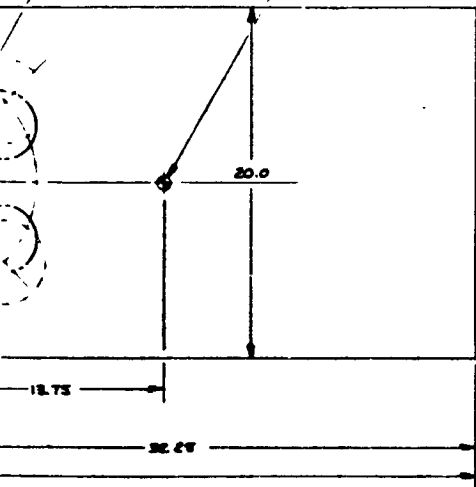
FOLDOUT FRAME

PREC FOLDOUT FRAME



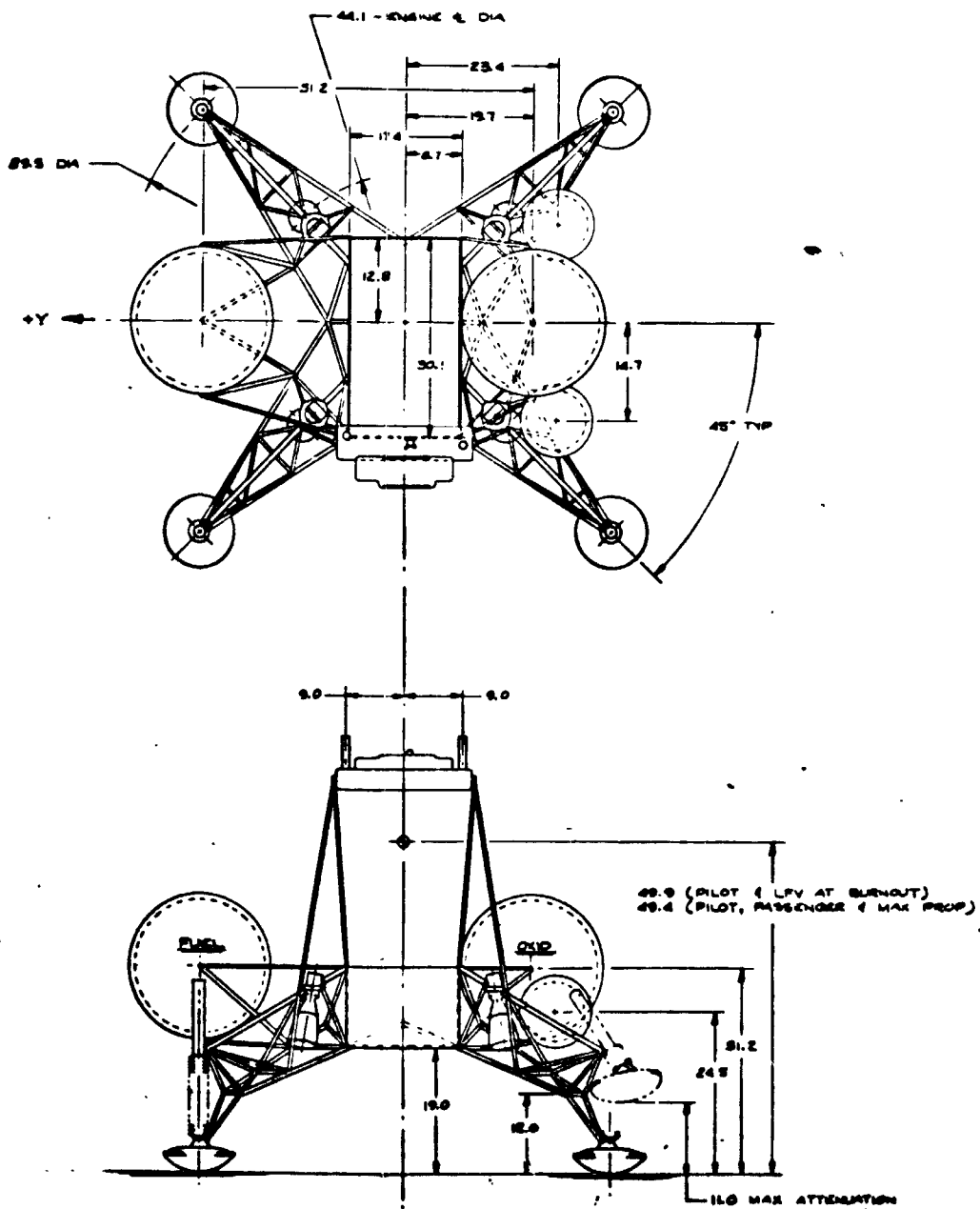
Space Division  
North American Rockwell

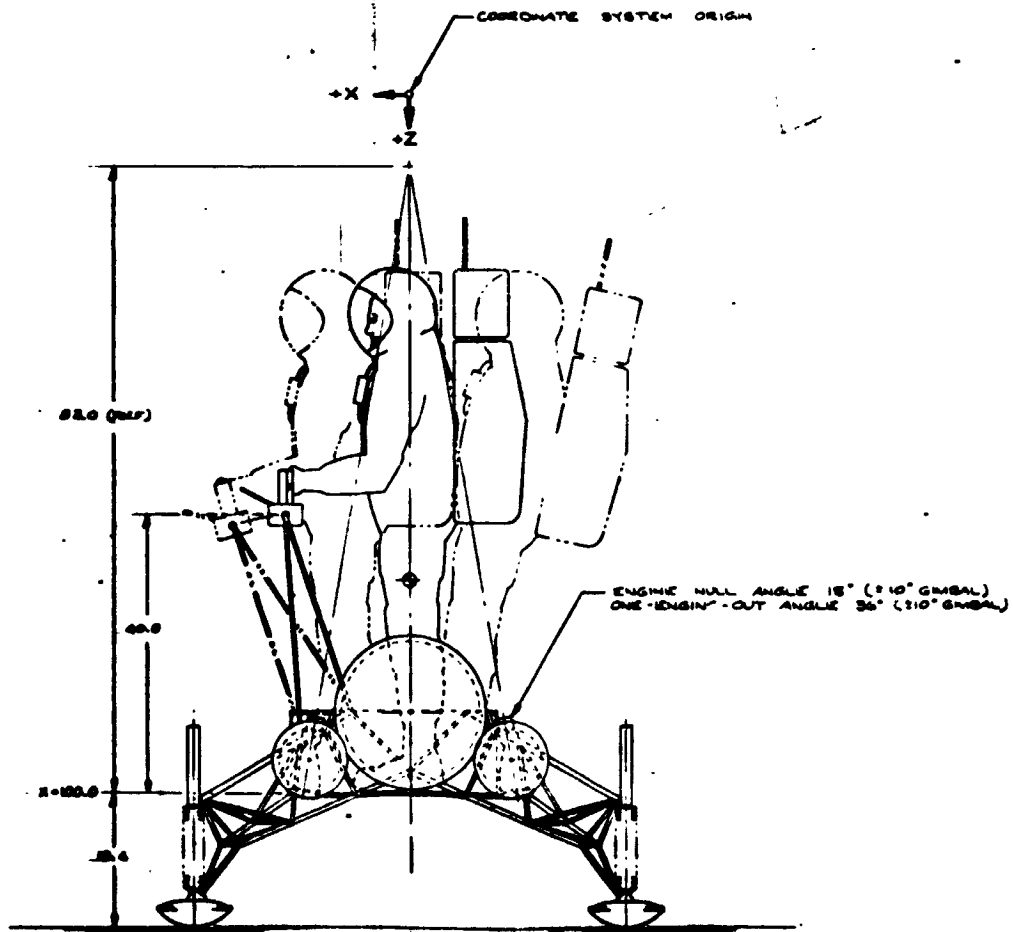
MINIMUM ENVELOPE  
ENGINE & OX (180 FOR BASELINE)  
VEHICLE C.G. & PILOT, WITHOUT  
PASSENGER, C.G.  
ASTRONAUT PASSENGER C.G.



|     |      |    |     |  |
|-----|------|----|-----|--|
| REV | DATE | BY | APP | DESCRIPTION  |
| 1/4 |      |    |     | ONE-MAN LRV -<br>RETRACTED PLATFORM INVESTIGATION,<br>VEHICLE, ENGINE & ASTRONAUT<br>POSITIONS |
|     |      |    |     | 2230-2   |

Figure 3. Retracted Platform Study Configuration 2 (Drawing 2230-2)





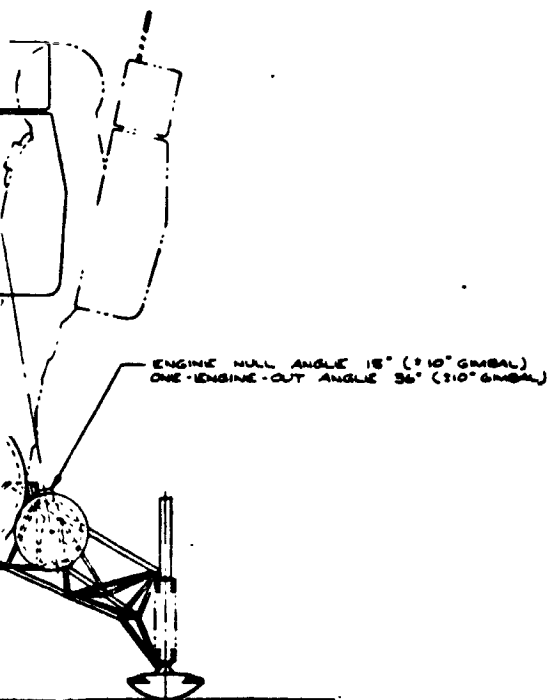
|                                   |          |
|-----------------------------------|----------|
| No                                | 88472-NS |
|                                   | 1-3-63   |
| ONE-MAN CONTROL CONF. REQUIRED BY |          |

Figure 4. Recessed Platform Study Configuration

FOLDOUT FRAME

FOLDOUT FRAME

— COORDINATE SYSTEM ORIGIN



|   |            |        |        |
|---|------------|--------|--------|
| 40  | REVISIONS  | DATE   | 2230-1 |
|   | REV 1-3-65 | 1-3-65 |        |
| ONE-MAN LFV -<br>CONTROL CONFIGURATION ALT.,<br>RECESSED PLATFORM |            |        |        |

Figure 4. Recessed Platform Study Configuration 1 (Drawing 2230-1)

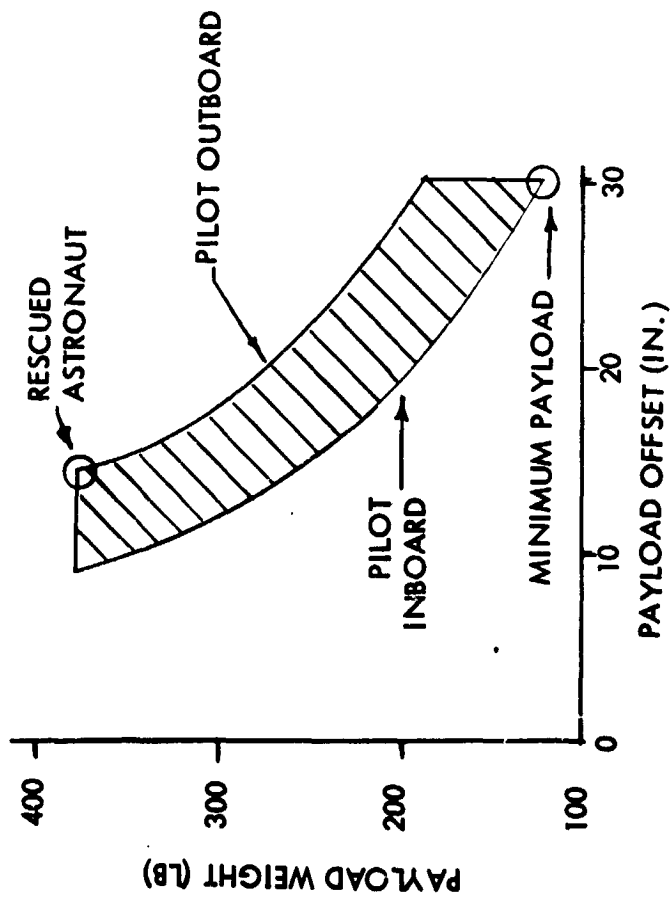
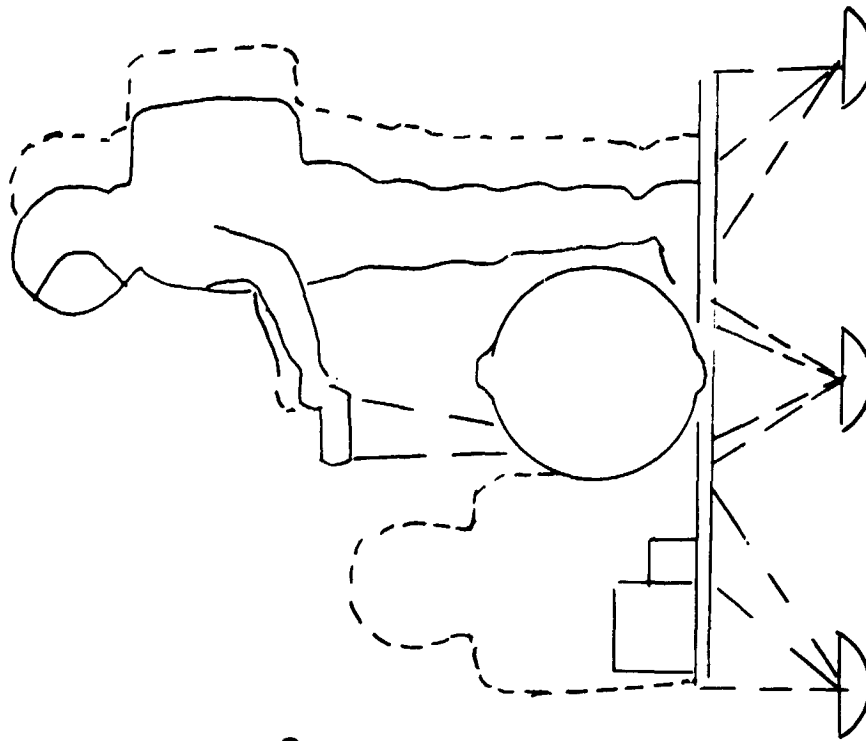


Figure 5. Minimum Payload Concept

of the c. g. to a point where no further reduction was necessary. A subsequent change to the NASA requirements, which eliminated the provision for carrying a rescued astronaut, permitted the c. g. to be lowered even further. However, even if that provision were reinstated as a requirement, the increased c. g. height would not be considered excessive. The primary result would be an increase in the allowable minimum vertical velocity condition for toppling stability.

A subsequent important change in the selected concept involved the change to an integral leg frame gear from an independent at-pad attenuated truss type of gear. The basis for this change is described in this volume in the section on landing gear.

An examination of the factors affecting selection of engine mixture ratio revealed that a change to a mixture ratio of 1.5 from the previous value of 1.6 was in order. The change incurred a loss of approximately 3 seconds in specific impulse but had no adverse effect on the development status of available hardware. The lower mixture ratio decreases tank centerline spacing, which improves LM stowing dimensions - and more important, the change is consistent with the most probable value of LM residual propellant mixture ratio, as noted in Reference 1.

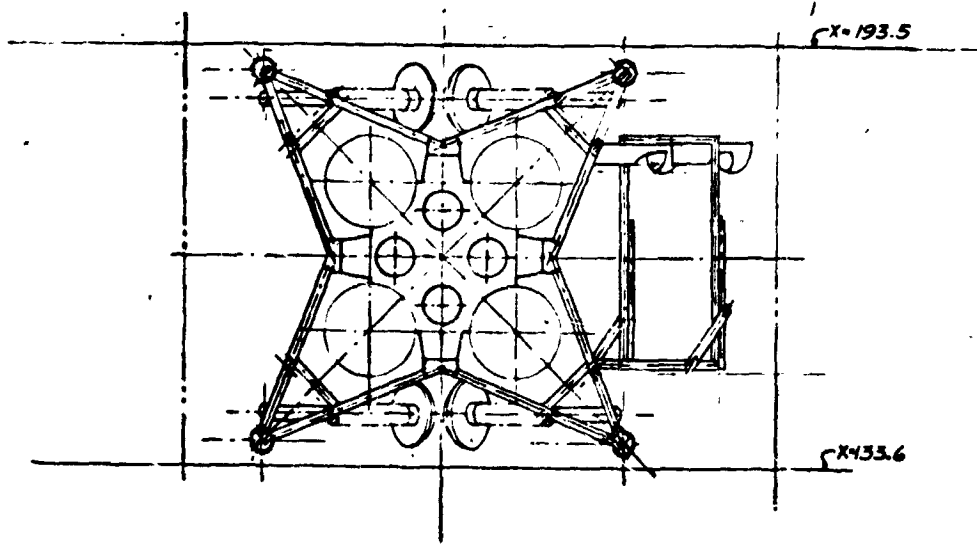
Two other configuration alternatives were seriously considered in the conceptual phase of the general arrangement study. However, these did not result in changes to the design, since the choices used in the initial control configuration were maintained. One of these was a four-tank parallel-feed design which, being more compact, indicated a potential advantage for LM stowing. Development of this concept is illustrated in Figures 6 and 7. The advantages of the four-tank design did not, however, outweigh its disadvantages. As described in the propulsion section of Volume 3, the concept involves comparatively more propulsion development activity. It is also heavier by 21.6 pounds (see Table 1). Finally, its stowing advantage is not required, since the two-tank design ultimately evolved to a configuration having acceptable stowing characteristics.

The other concept seriously considered, but not selected, was a landing gear incorporating three legs instead of four. On first consideration it appears that three legs would be lighter than four legs by a considerable margin; however, referring to Figure 8, it may be seen from the geometry that this effect is offset by the increased length of the three leg members. This additional length adds weight in two ways: through sheer length, and through the increased bending moment due to the increased length. The net result for the same minimum toppling radius of the inscribed circle is that the three-leg design is 5.4 pounds heavier. Other factors considered in this trade study were: the three-leg design has lower leg rigidity, giving a greater spring effect; the surface conformity of the four-leg design is



LM RCS ENGINE

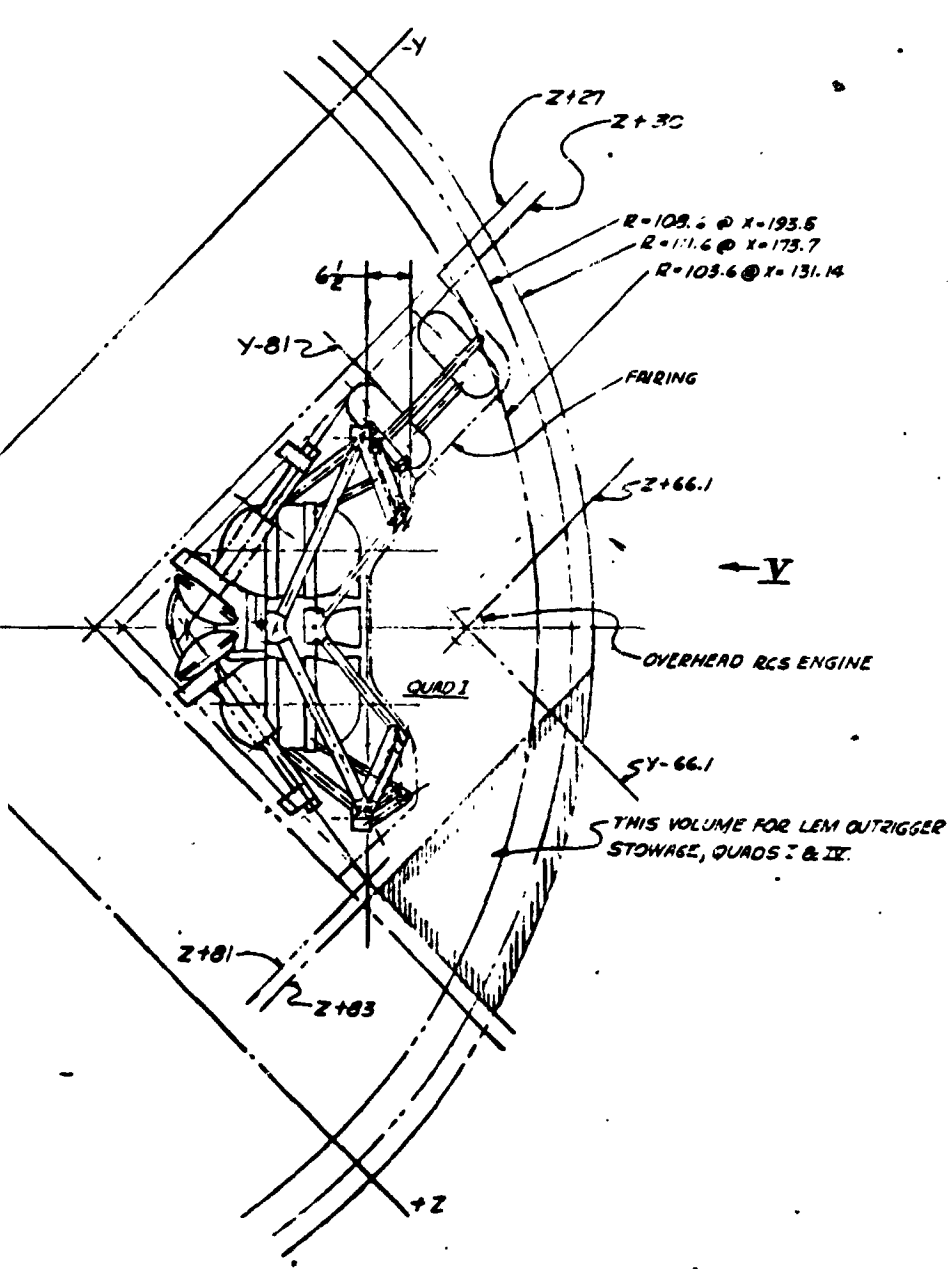
X-238.594



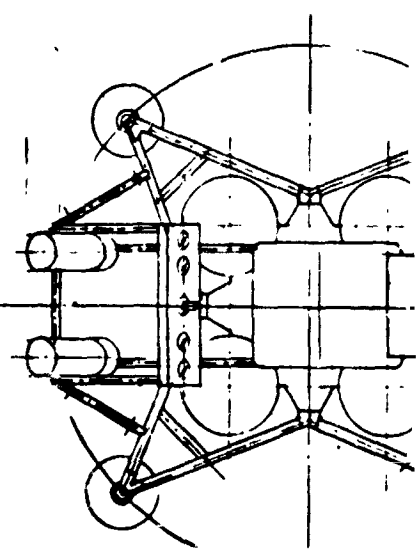
VIEW AT V (ROTATED)

STOW

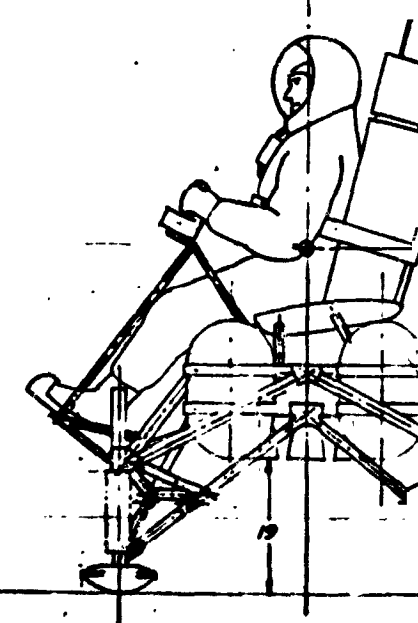
FOLDOUT FRAME .



STOWED CONFIGURATION-ONE MAN



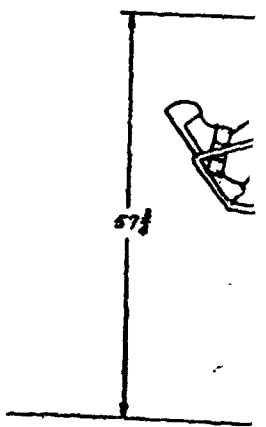
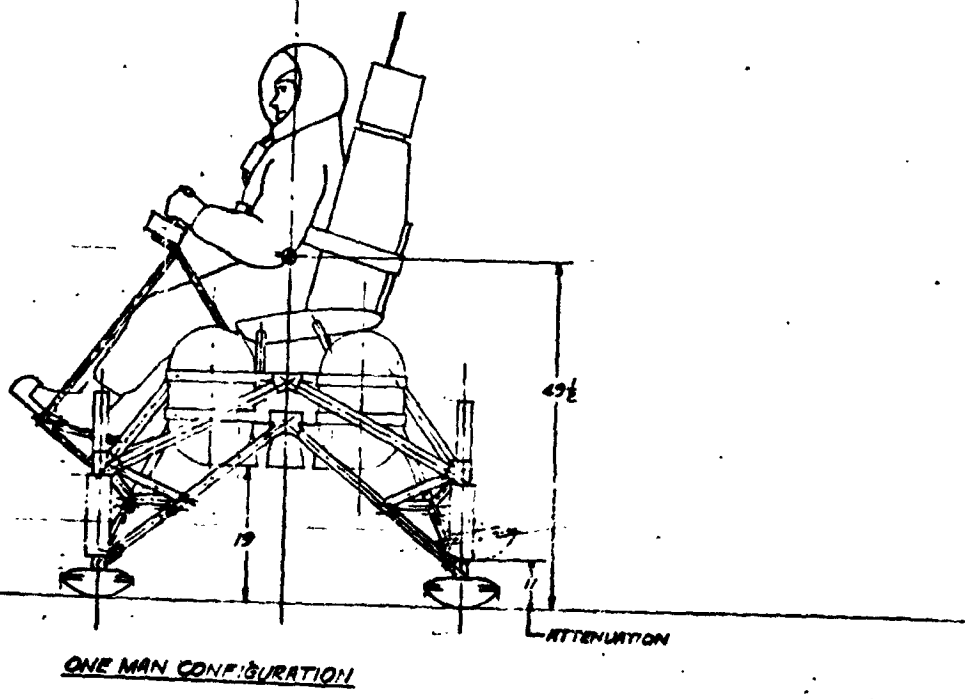
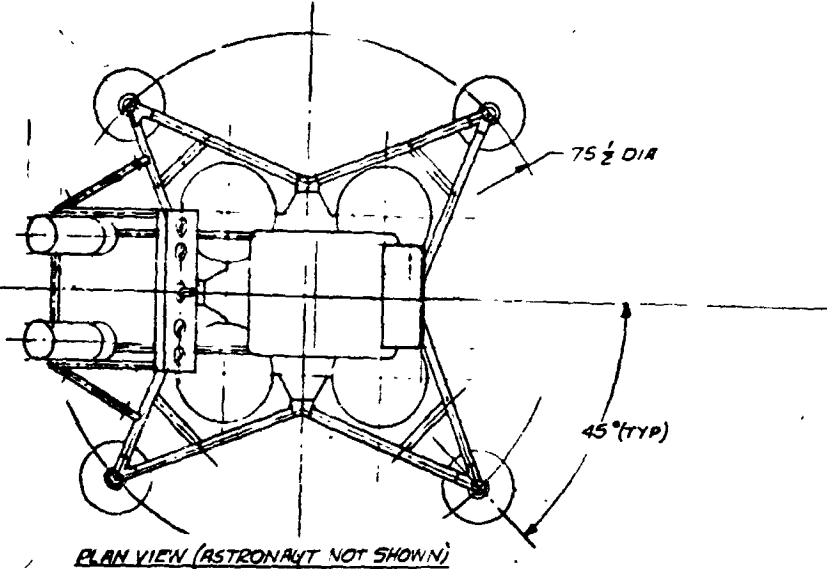
PLAN VIEW (ASTRONOMY NOT SH)



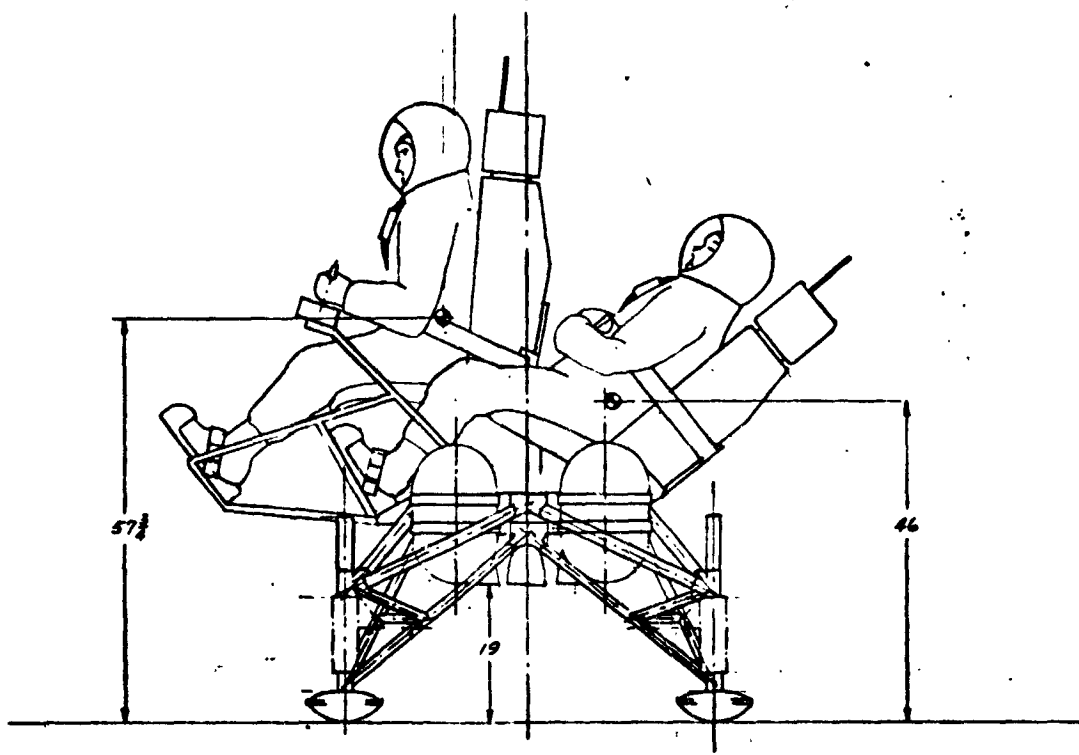
ONE MAN CONFIGURATION

FORWARD FRAMES

FORWARD FRAMES

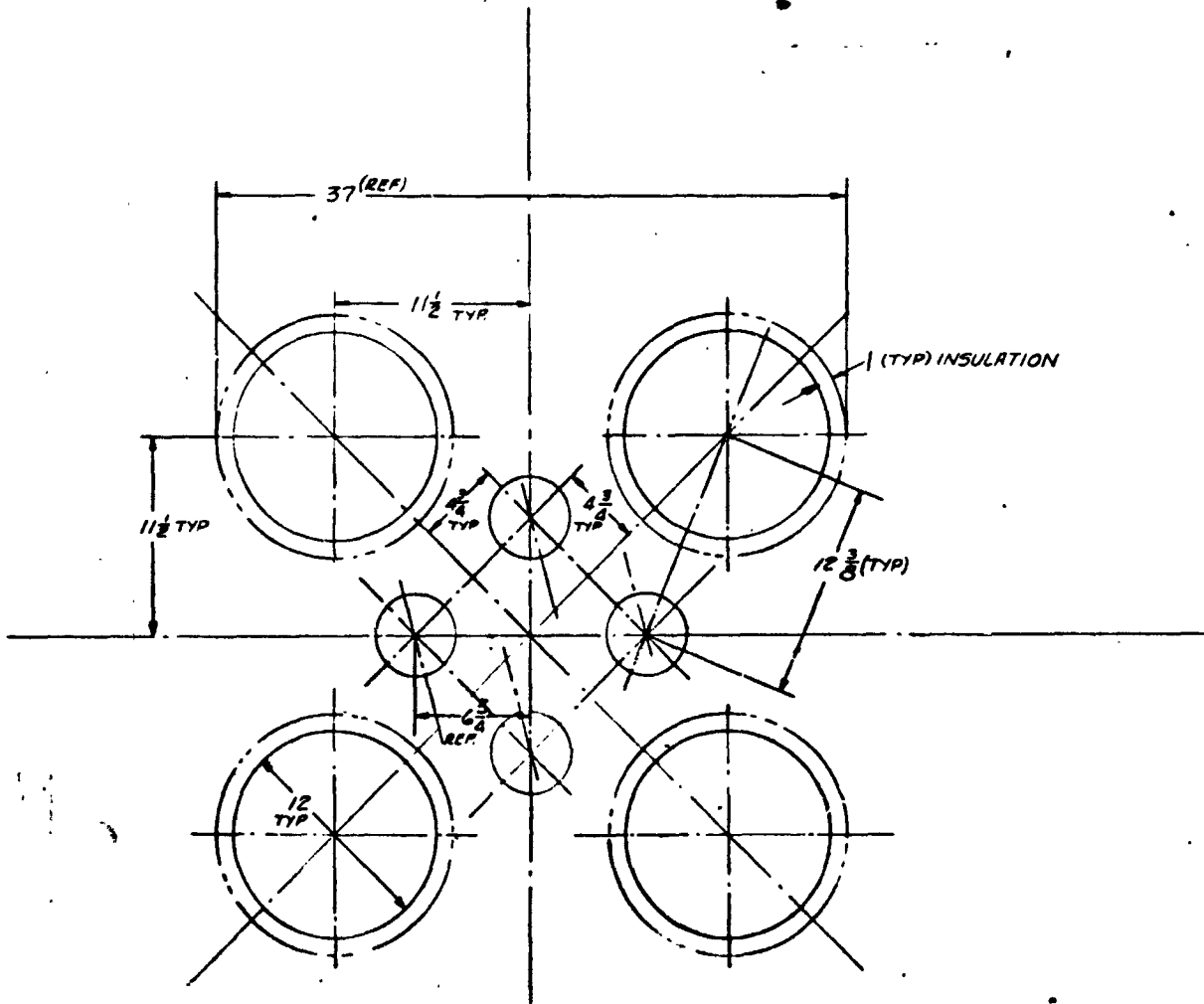


WELDOUT FRAME



TWO MAN (RESCUE) CONFIGURATION

**BOLDOUT FRAME**

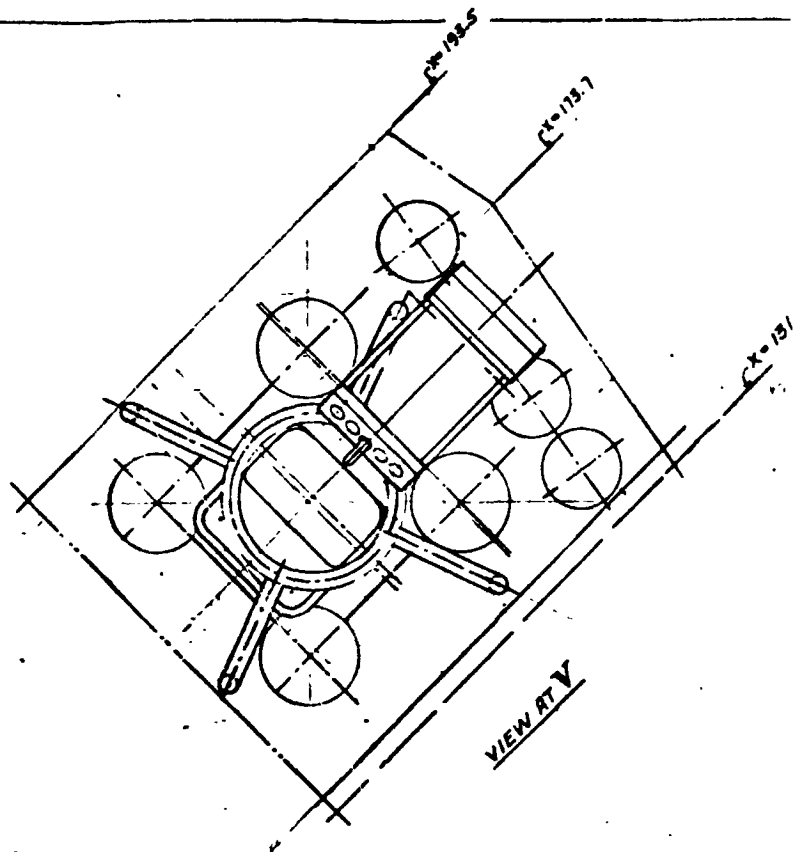


ENGINE/TANK ARRANGEMENT

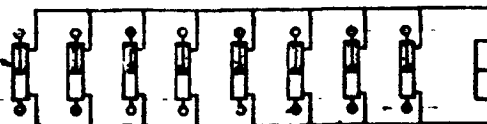
SCALE 1/4

|   |             |      |                                  |
|---|-------------|------|----------------------------------|
| REV   | NO. 2230-7  | DATE |                                  |
| 1/10  | REV. 1-1-67 | BY   | JOHN J. GIBSON, GENERAL ENGINEER |
| 4   | REV. 1-1-67 | BY   | JOHN J. GIBSON, GENERAL ENGINEER |
| * ONE MAN L.F.V.<br>CONTROL CONFIGURATION ALTERNATE<br>SEATED PILOT, 4-TANK |             |      | 2230-7                           |
|   |             |      | SHEET 1 OF 1                     |

Figure 6. Seated Pilot, Four-Tank, Parallel Feed Alternative Vehicle Configuration (Drawing 2230-7)



ACTUATOR - DBL. ACTING,  
 SPRING CENTERED,  
 8-REQD

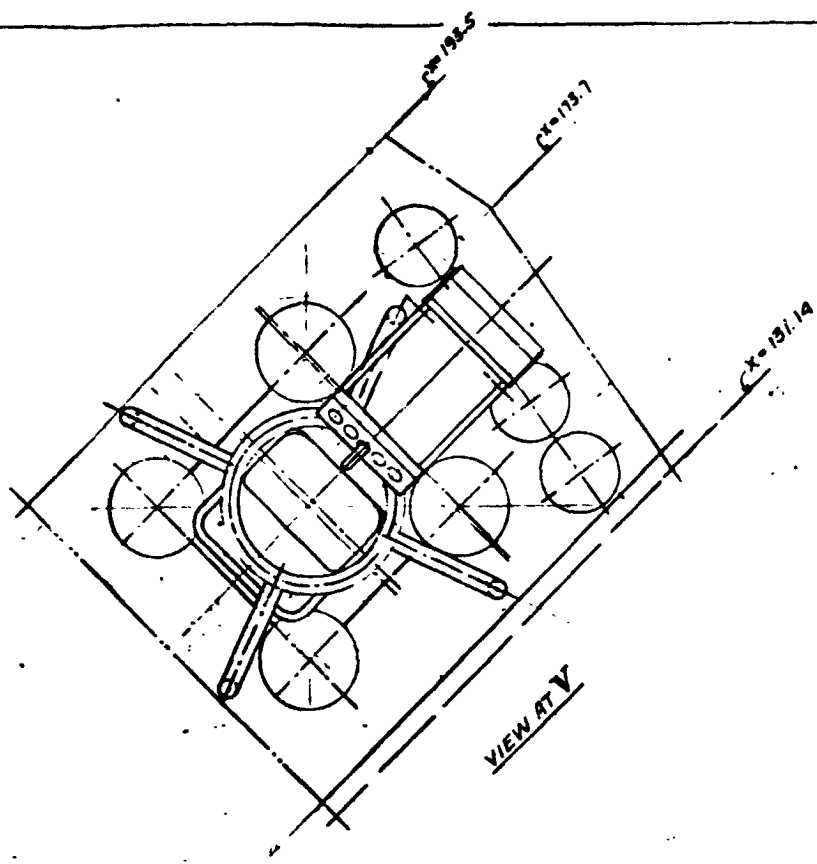


CENTRAL ATTENUATOR -  
 VARIABLE ORIFICE,  
 DBL. ACTING

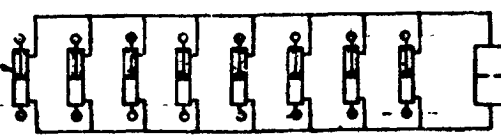
SCHEMATIC DIAGRAM - CENTRAL ATTENUATOR SYSTEM

FOLDOUT FRAME

FOLDOUT FRAME



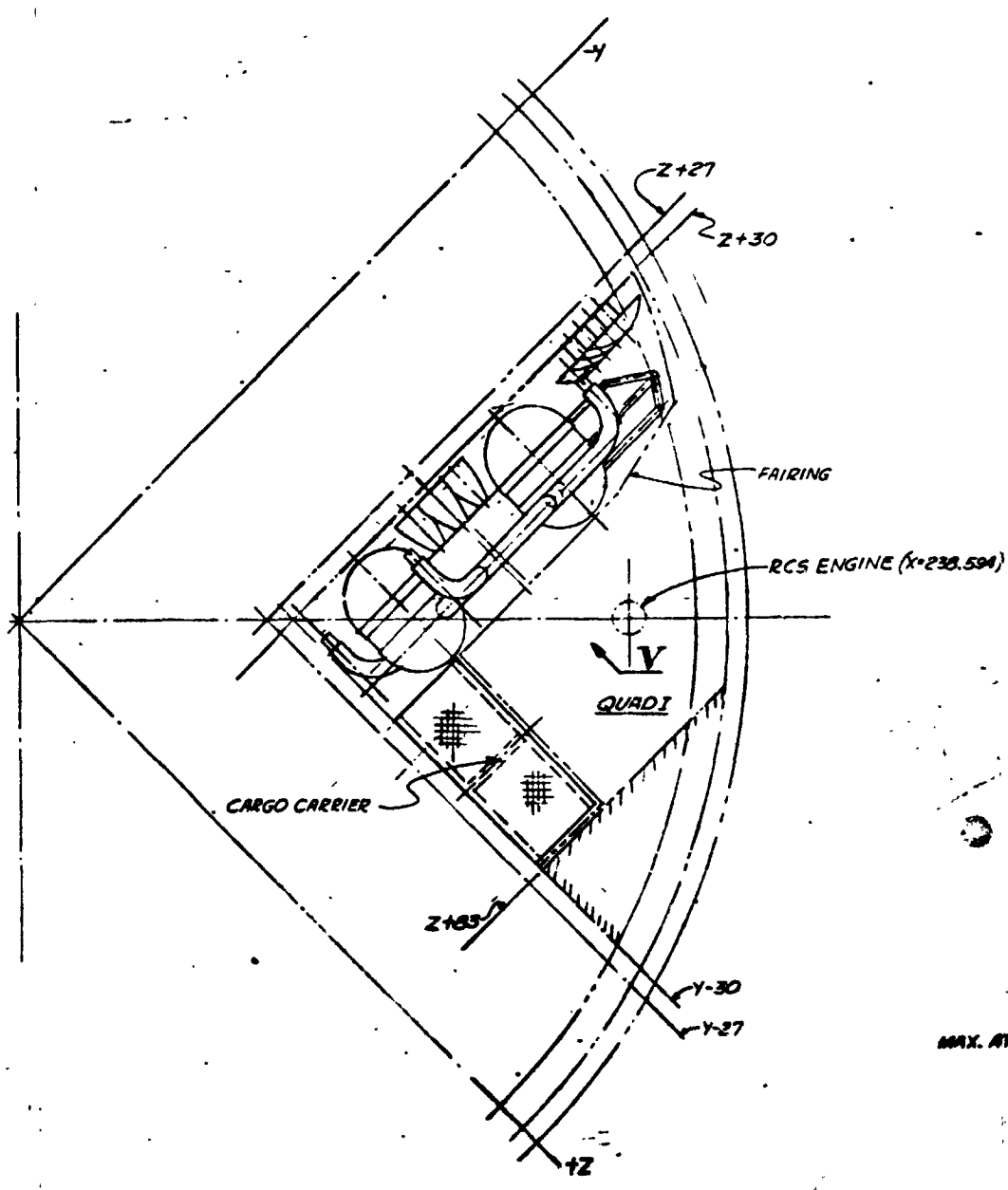
ACTUATOR - DBL. ACTING,  
SPRING CENTERED,  
8-REQD



CENTRAL ATTENUATOR -  
VARIABLE ORIFICE,  
DBL. ACTING

SCHEMATIC DIAGRAM - CENTRAL ATTENUATOR SYSTEM

FOLDOUT FRAME

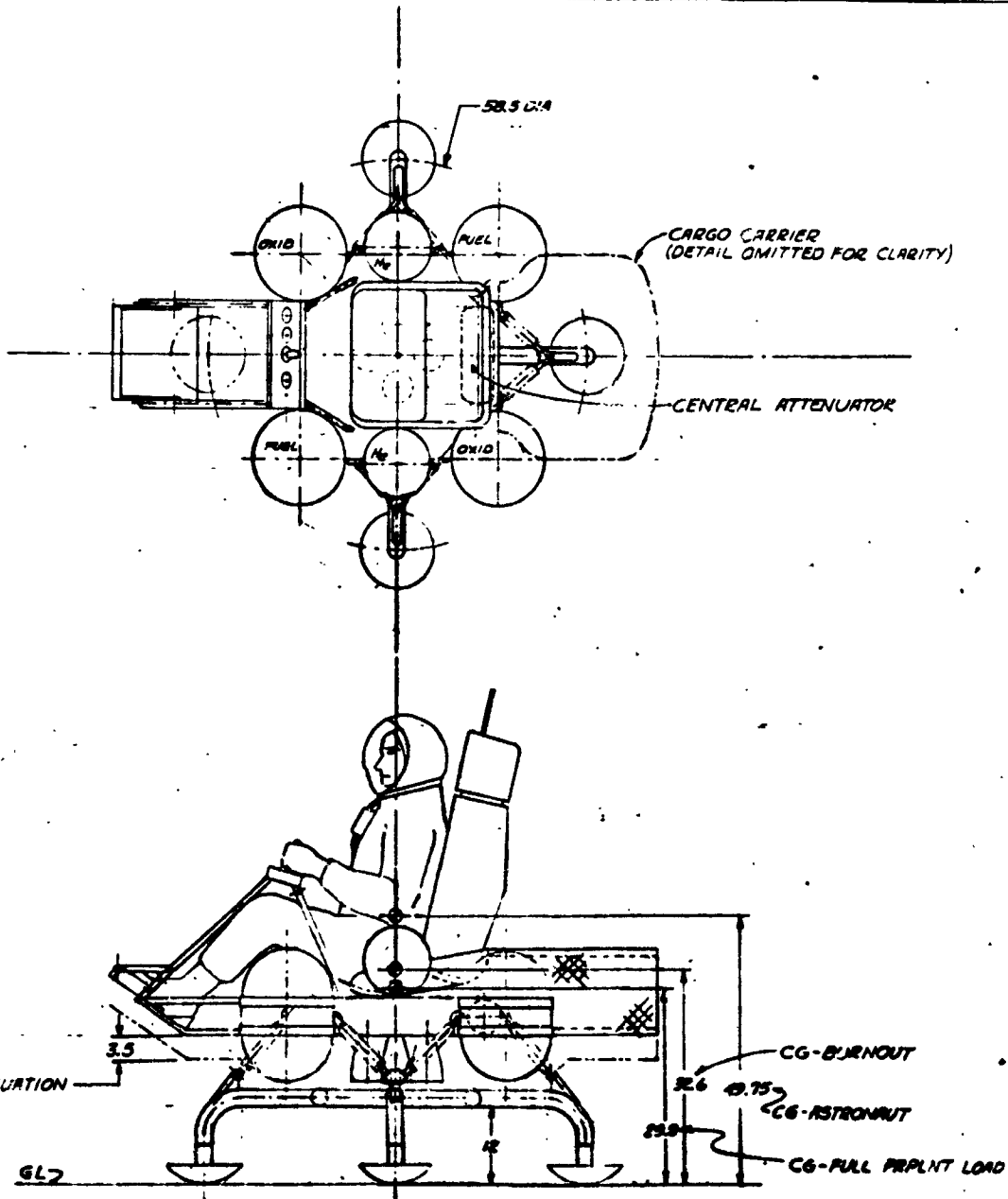


MAX. ATTENUATION

6L2

FOLDOUT FRAME





ENGINE (X-230.594)

|    |        |   |              |
|----|--------|---|--------------|
| NO | 2-7148 | ONE MAN LRV<br>CONTROL CONFIGURATION ALTERNATE<br>SEATED PILOT, 4-YANK<br>CENTRAL ATTENUATORS | 2230-8       |
|    |        |   | SHEET 1 OF 1 |

Figure 7. Seated Pilot, Four Tank, Log-Frame Gear Alternative Vehicle Configuration (Drawing 2230-8)



Table 1. Two-Tank/Four-Tank Weight Comparison

| Group                           | Two-Tank Weight<br>(lb) | Four-Tank Weight<br>(lb) |
|---------------------------------|-------------------------|--------------------------|
| Body structure                  | 17.9                    | 20.0                     |
| Environmental protection        | 10.0                    | 11.8                     |
| Landing gear                    | 42.3                    | 42.3                     |
| Main propulsion                 | 92.2                    | 105.6                    |
| Power source                    | 0.7                     | 0.7                      |
| Guidance and navigation         | 7.0                     | 7.0                      |
| Crew station controls and panel | 15.0                    | 15.0                     |
| Contingency                     | 2.9                     | 2.9                      |
| Total*                          | <u>188.0</u>            | <u>205.3</u>             |
| Delta Weight                    | --                      | 17.3                     |
| Growth                          | --                      | 4.3                      |
| Total delta weight              |                         | <u>21.6</u>              |
| Residuals                       | 21.7                    | 24.7                     |
| *Initial baseline data          |                         |                          |

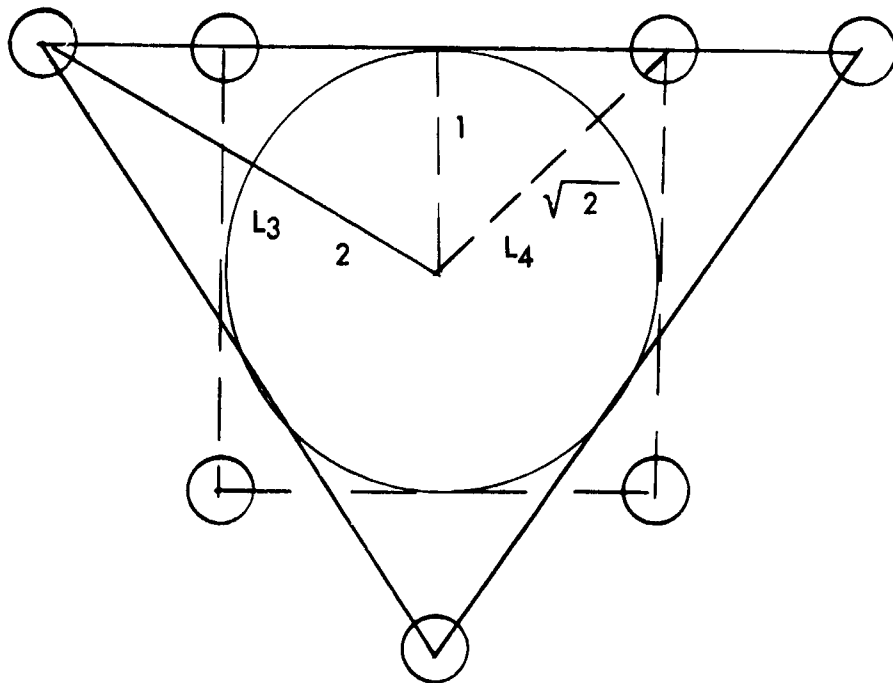


Figure 8. Leg Geometry



inferior but is of minor importance, since this effect applies only to an extremely hard surface; and the shorter four-leg design can be stowed in place on the LM, whereas the three-leg design required disassembly or folding.

During the conceptual phase, studies of payload accommodation provisions also affected the general arrangement to a degree. A complete discussion of this is contained in the section of this volume entitled "Payload Integration."

#### Subsystem Concept Installation Studies

As subsystem concept requirement definitions were developed, installation drawings were prepared to determine if their effect on the general arrangement would be of significance in the evaluation. In some cases, the concept was treated as a subsystem installation, and in others, a general arrangement layout was developed to assess the overall effect. Particularly important installation studies were those involving engine/control concepts. These are illustrated in Figures 9 through 15 and include long-radius gimbal designs, sliding-plate engine thrust vector control designs, and single-engine designs. None of these concepts displaced the initial control configuration concept as a selected version; however, the installation layouts were utilized to develop data for the engine/control concept evaluations described in another section of this report.

#### Preliminary Design Optimization

At the completion of the first phase, selected configuration characteristics included the following: stability-augmented control, four engines; seated and restrained astronaut; four-leg, integral leg frame landing gear; and two spherical propellant tanks. Unresolved issues that were to be examined as preliminary design optimizations were: payload arrangement and further definition of payload requirements, and the mechanization of four-engine thrust vector control. The mechanization study was made necessary by the fact that reliability advantages of the four-engine concept depended on engine-out capability, and this required detailed examination to establish that the mechanization arrangement could, in fact, give the redundancy assumed.

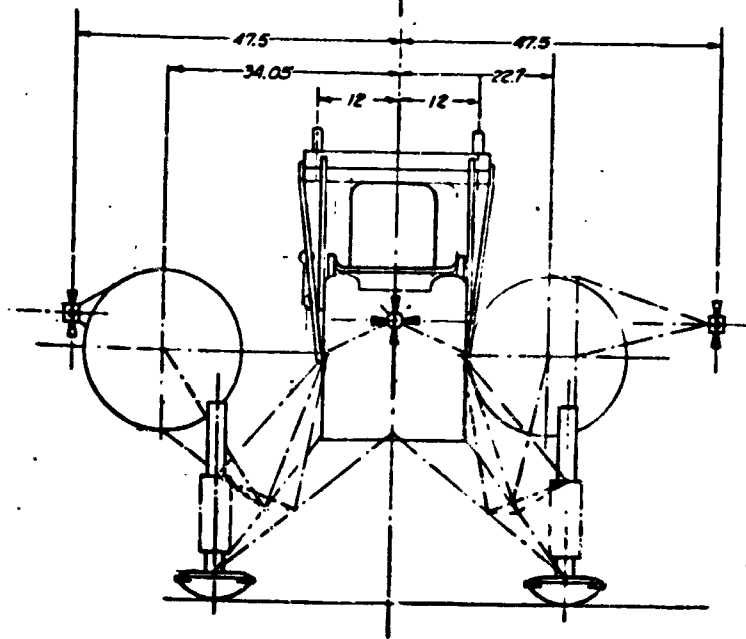
#### Approach

The study elements and sequence of effort for the second phase of configuration design are shown in the logic diagram of Figure 16. Subsystem optimization of engine control mechanization considered three designs in depth. Configuration optimization involved making adjustments in vehicle arrangement, geometries, clearances, and the height of the pilot and the

LOCUS OF CONTROLLABLE SEAT MOTION

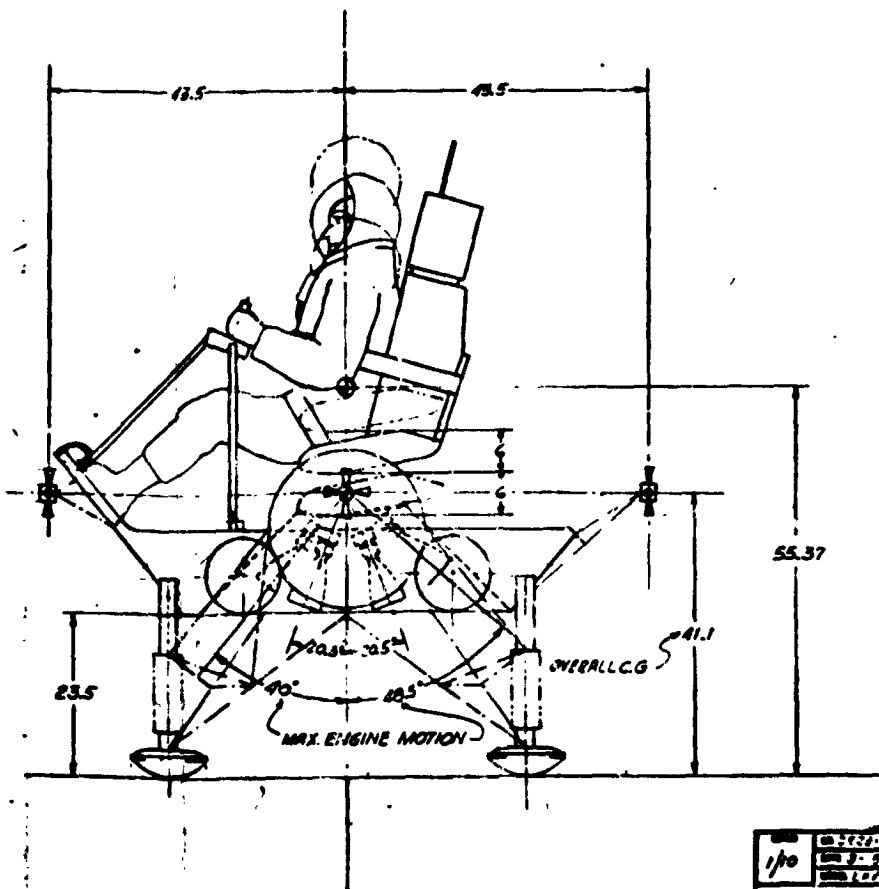
73.7 DIA

SEAT MOTION CONTROL HANDLE  
(PROVIDES PITCH & ROLL CONTROL  
BACKUP MODE)



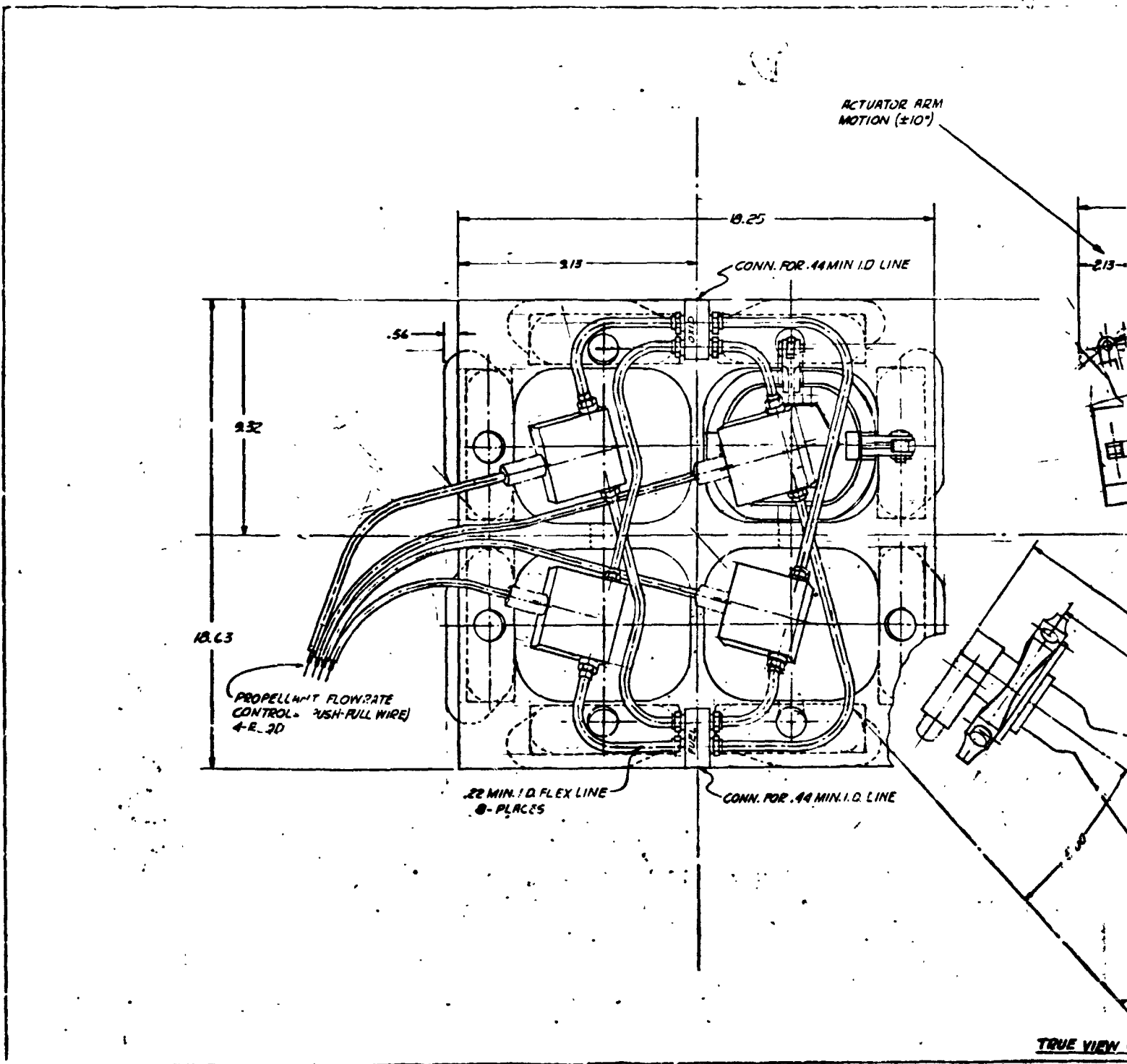
FOLDCUT FRAME

FOLDCUT FRAME



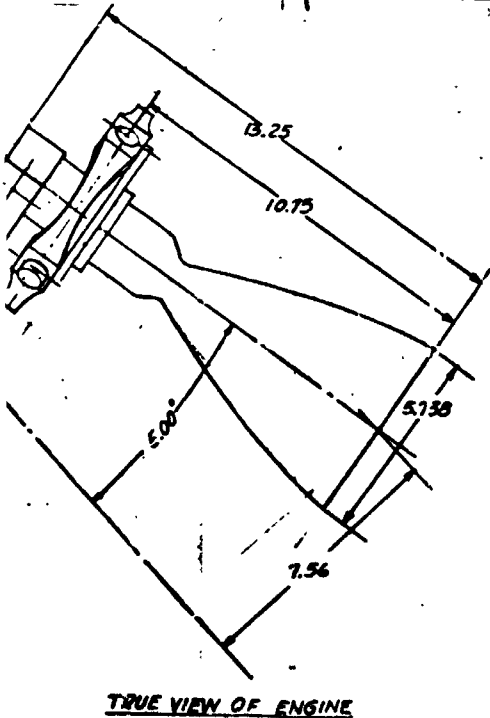
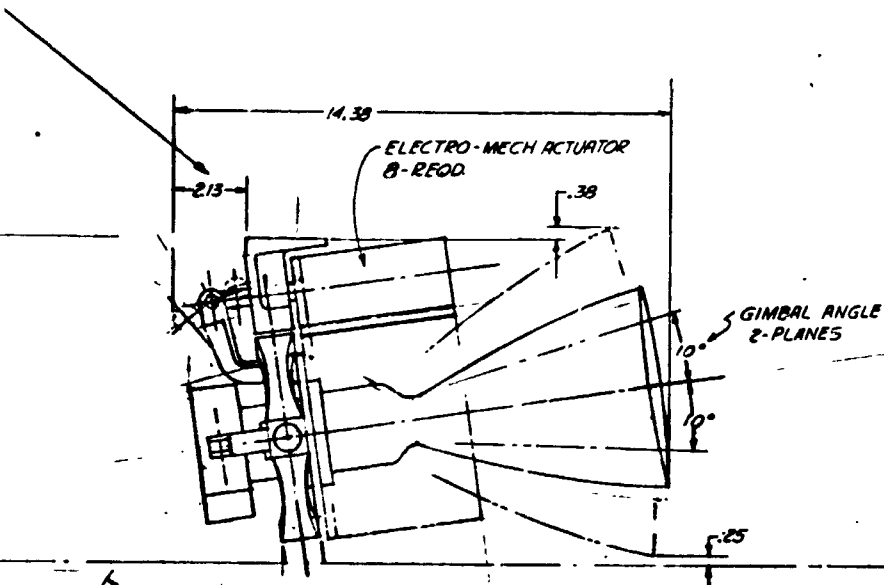
|  |             |   |              |
|--|-------------|---|--------------|
| 1/0  | 2230-9-28   | DATE CHANGED                            |              |
|  | REV. 2-9-62 | SPACE DIVISION TECHNICAL CONTROL CENTER |              |
|  | REV. 1-67   | 3000 WILSON AVENUE, CANON, CALIFORNIA   |              |
| ONE MAN LFV<br>CONTROL CONFIGURATION ALTERNATE<br>C.G. PIVOTED ENGINES |             |   | 2230-9       |
|  |             |   | Sheet 1 of 1 |

Figure 9. C.G. -Pivoted Engines Alternative Vehicle Configuration  
(Drawing 2230-9)



WELDED FRAME

IT FRAME



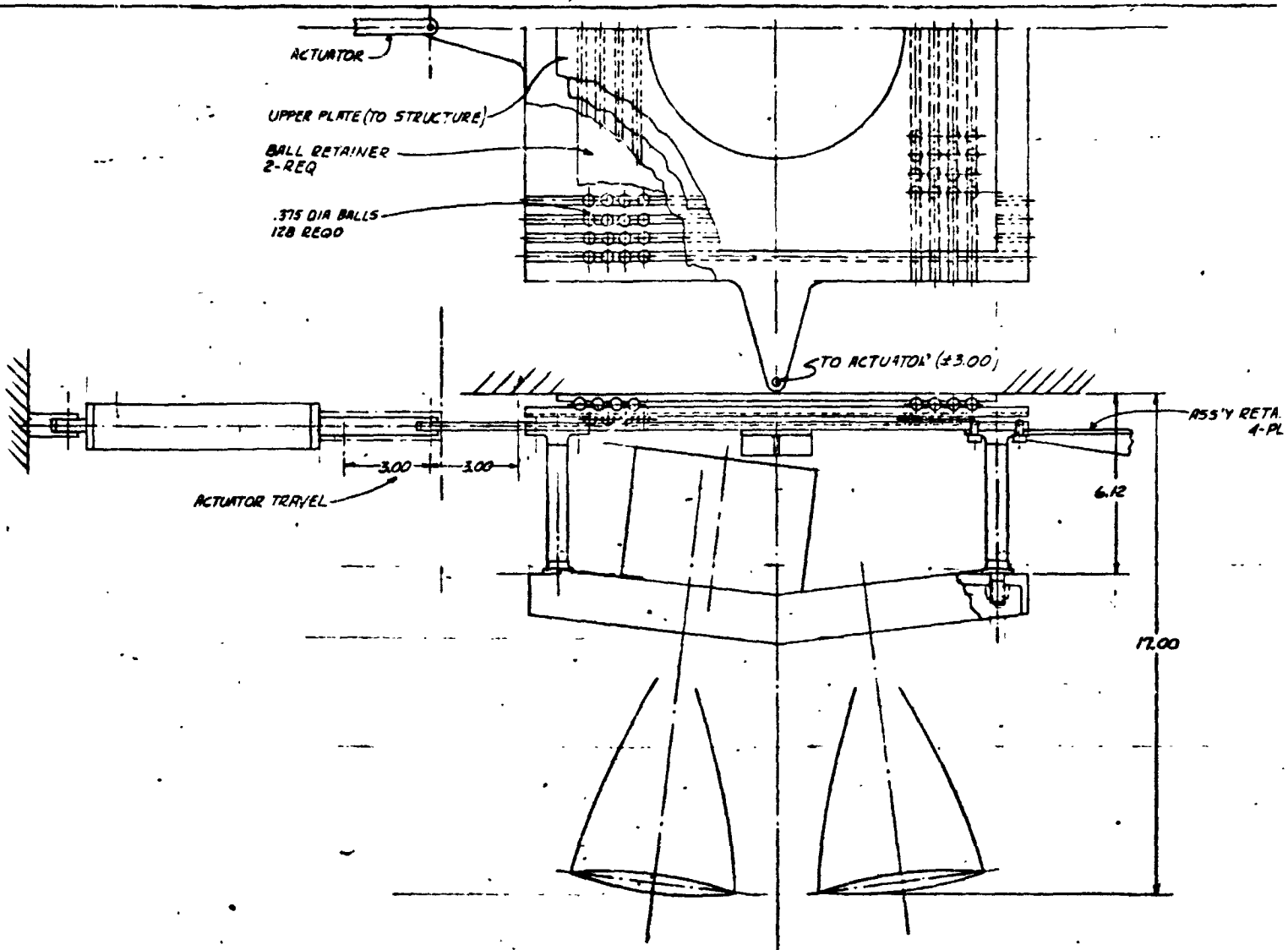
**SPECIFICATIONS:**

ENGINE: MARQUARDT MODEL R4D  
 NOMINAL THRUST 100 LBS.  
 CHAMBER PRESSURE 100 PSIA  
 MIXTURE RATIO 15-1  
 PROPELLANTS A-50 & N<sub>2</sub>O<sub>4</sub>  
 SPECIFIC IMPULSE 293 SECS  
 EXPANSION RATIO 40:1

|   |              |      |              |
|---|--------------|------|--------------|
| 1/8   | BY DESIGNER  | DATE | 2230-10      |
|   | DATE 5-25-69 | BY   |              |
| ONE MAN LFV<br>CONTROL CONFIGURATION<br>ENGINE INSTALLATION |              |      | SHEET 1 OF 1 |

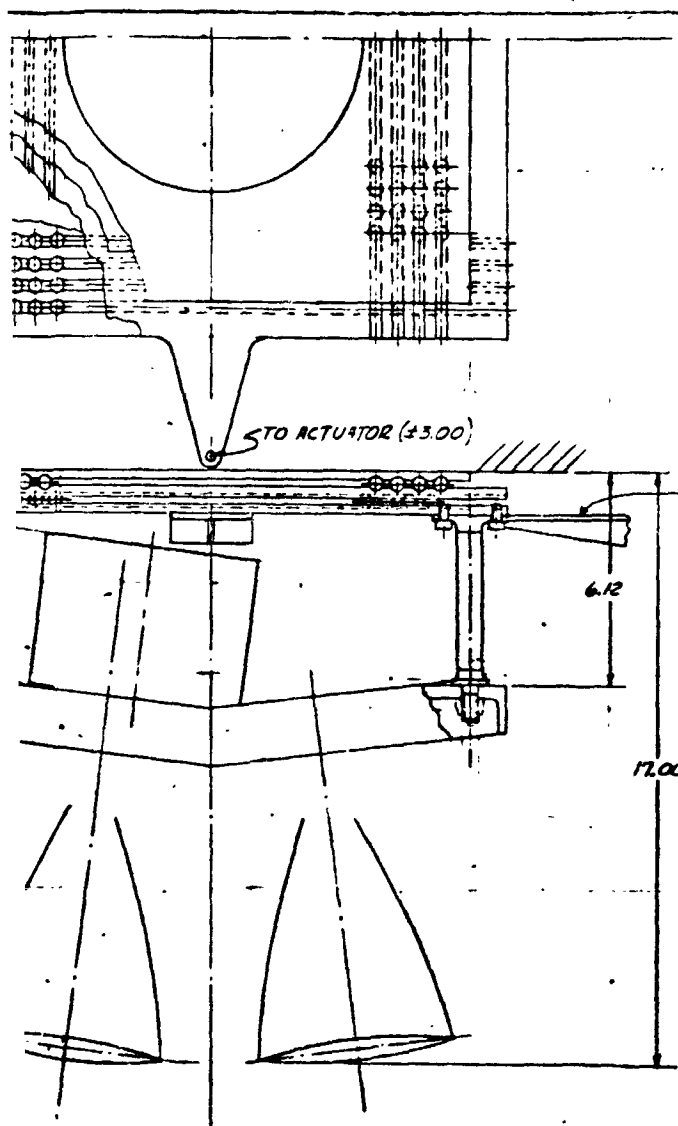
Figure 10. Four-Engine, Eight Actuator Installation Study Configuration (Drawing 2230-10)



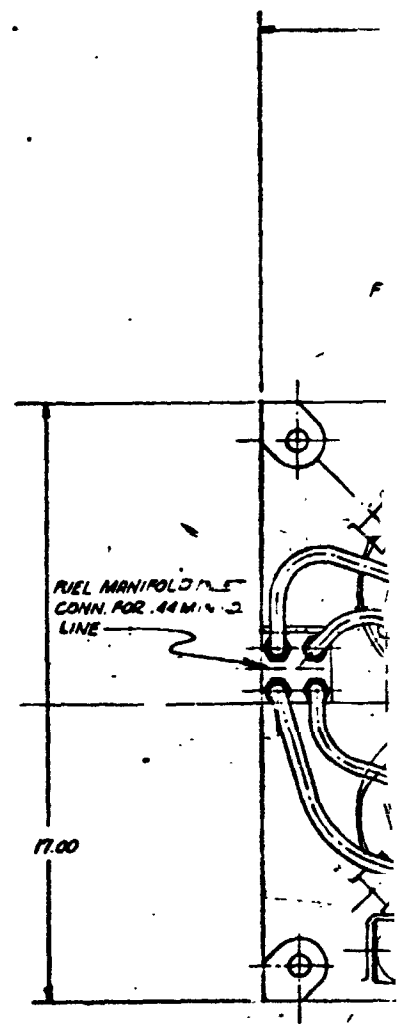


FOLDOUT FRAME

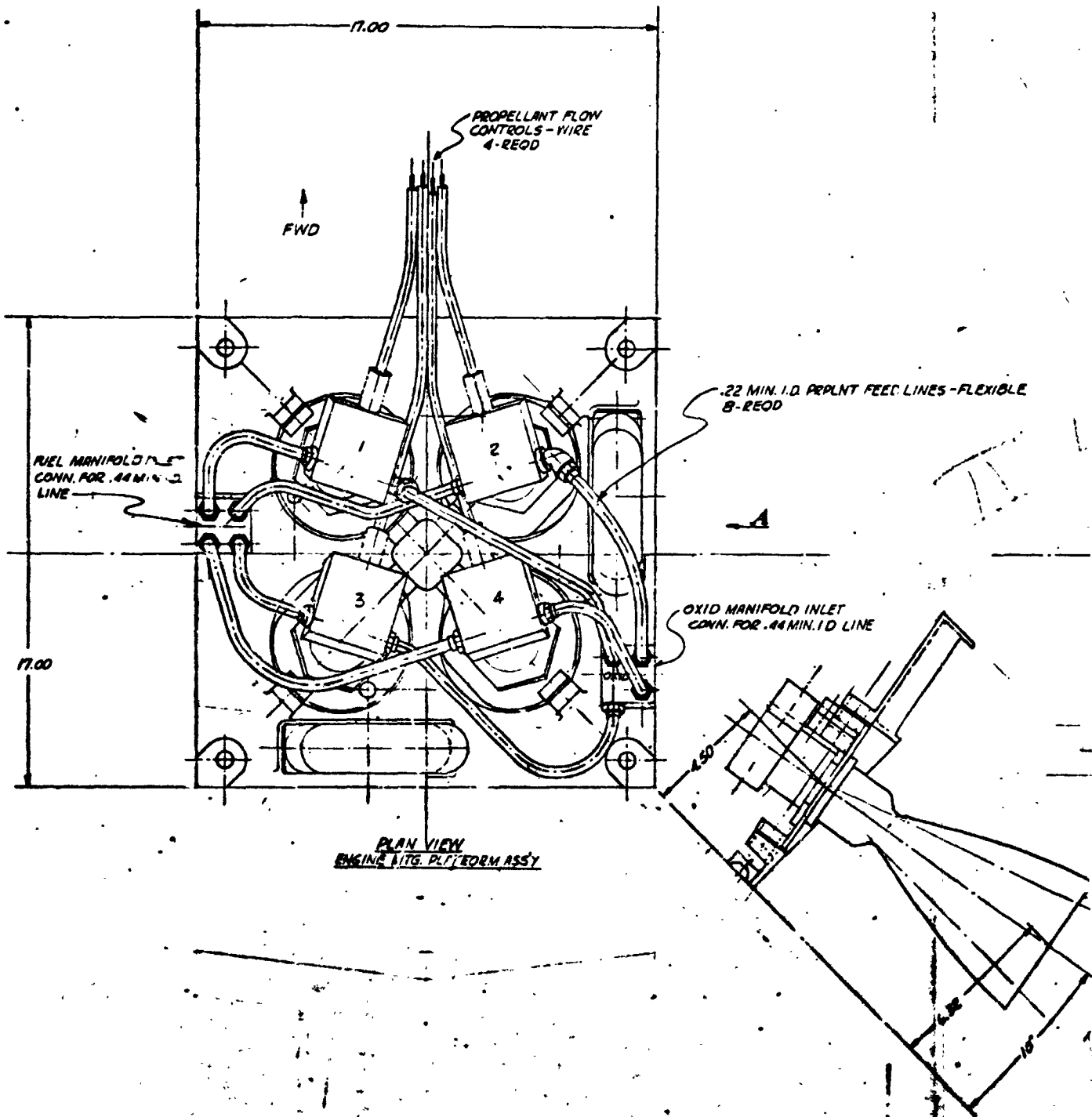
FOLDOUT FRAME



ASS'Y RETAINER (TO STRUCTURE)  
4-PLACES

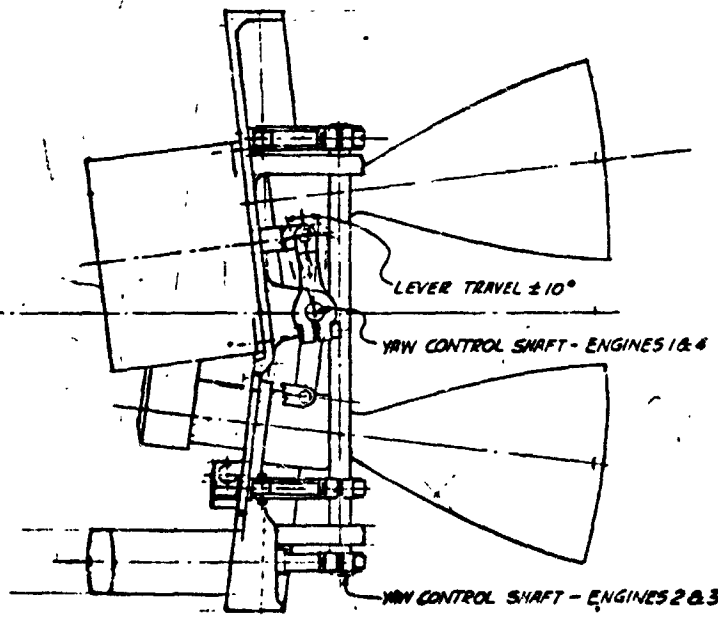


FRAME



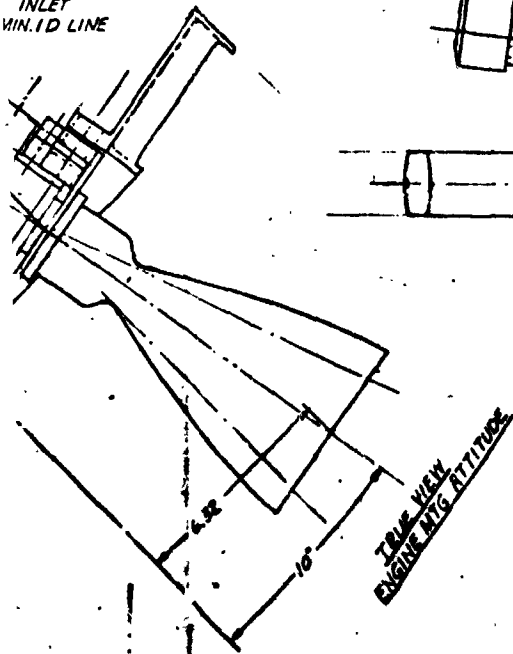
D. PROPLNT FEED LINES - FLEXIBLE

INLET  
MIN. I.D. LINE



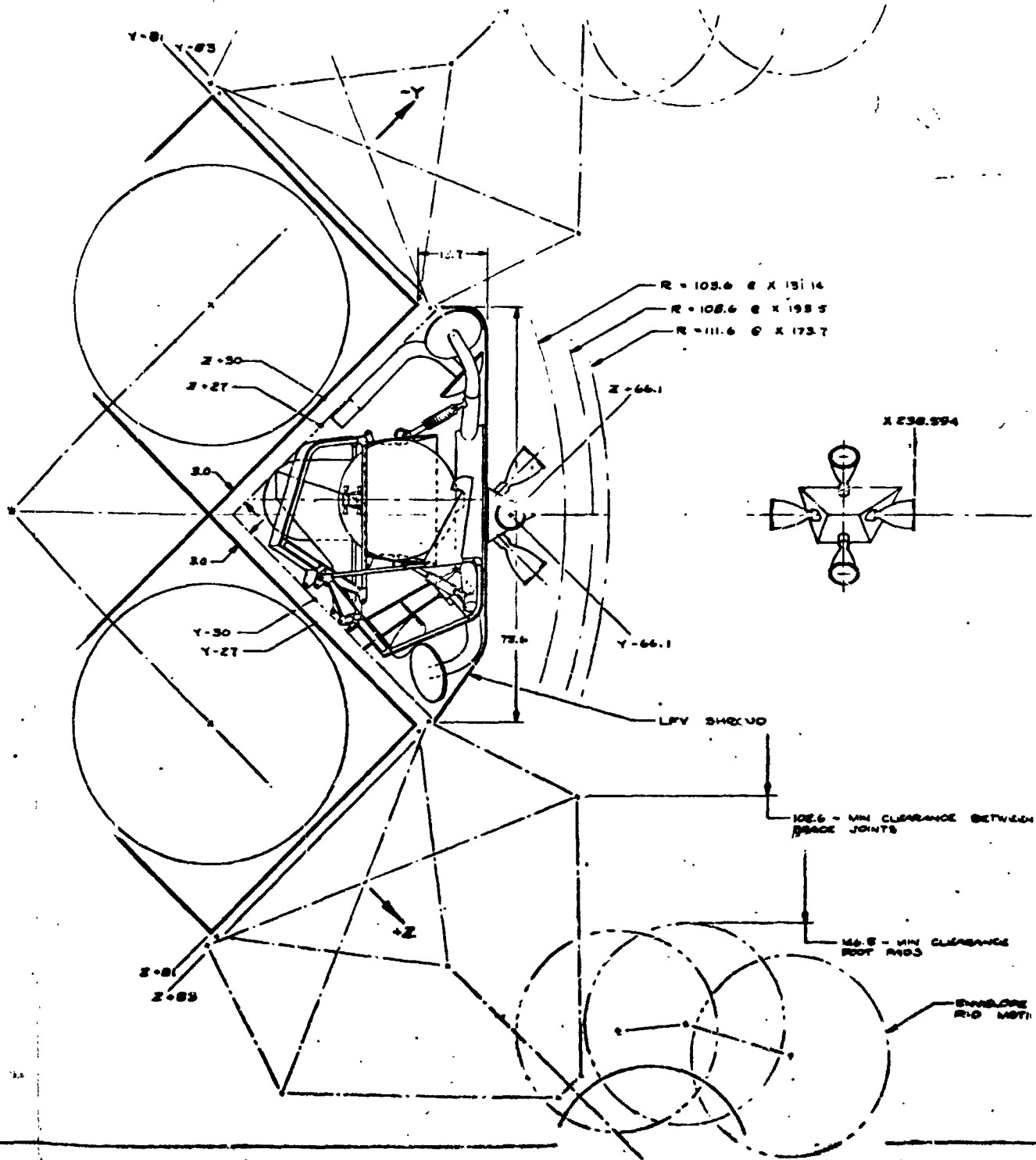
PARTIAL VIEW  
SHOWING YAW CONTROL MECHANISM

**SPECIFICATIONS:**  
 ENGINE: MARQUARDT MODEL 24D  
 NOMINAL THRUST 100 LBS.  
 CHAMBER PRESSURE 100 PSIA  
 MIXTURE RATIO 1.5-1  
 PROPELLANT A-SDB 1404  
 SPECIFIC IMPULSE 293 SECS.  
 EXPANSION RATIO 40:1

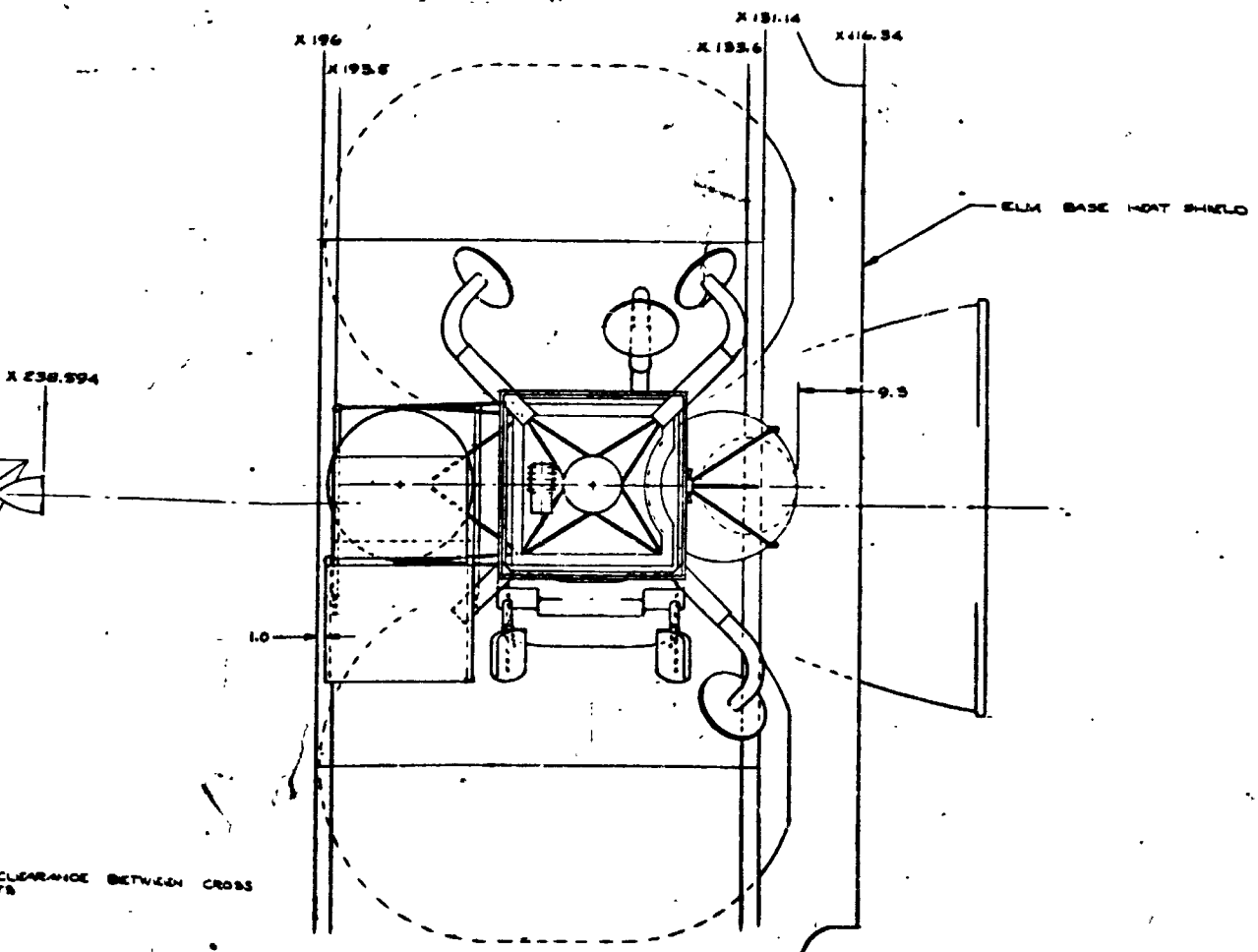


|   |            |                         |
|---|------------|-------------------------|
| 1/8   | DATE CHG'D | 2230-13                 |
| ONE-MAN LRV<br>CONTROL CONFIGURATION ALTERNATE<br>ENGINE INSTALLATION |            | 2230-13<br>SHEET 1 OF 1 |

Figure 11. Four-Engine, Sliding Plate Canted Engine Installation  
(Drawing 2230-13)

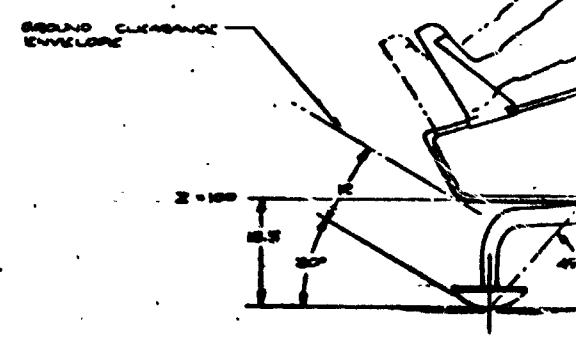
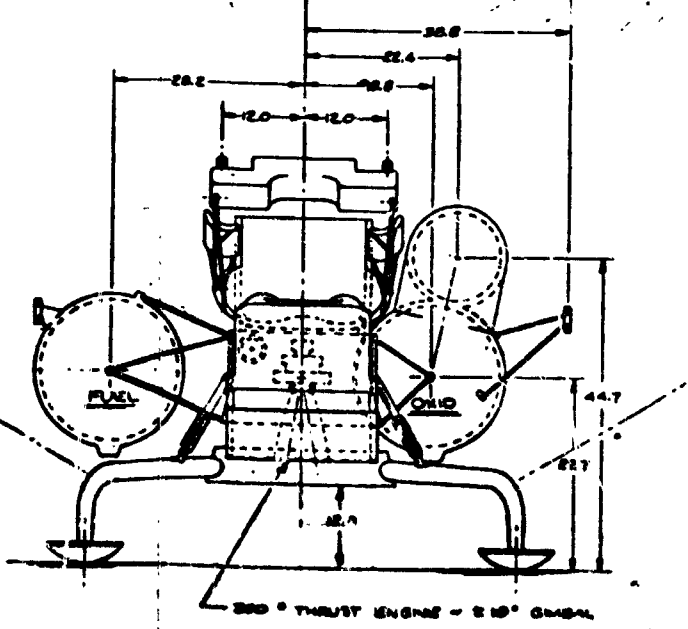
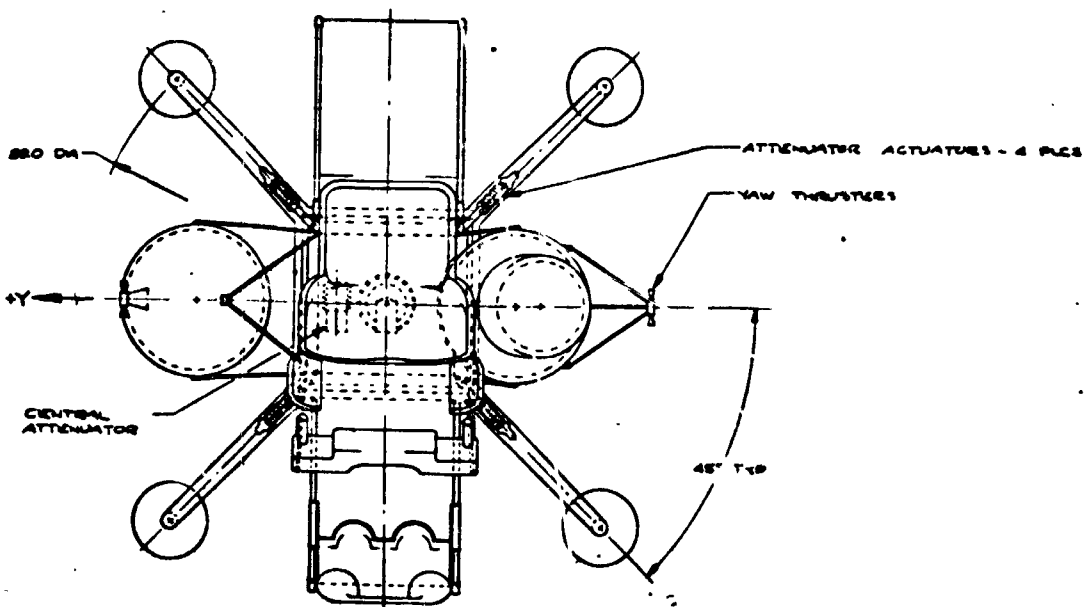


FOLDOUT FRAME



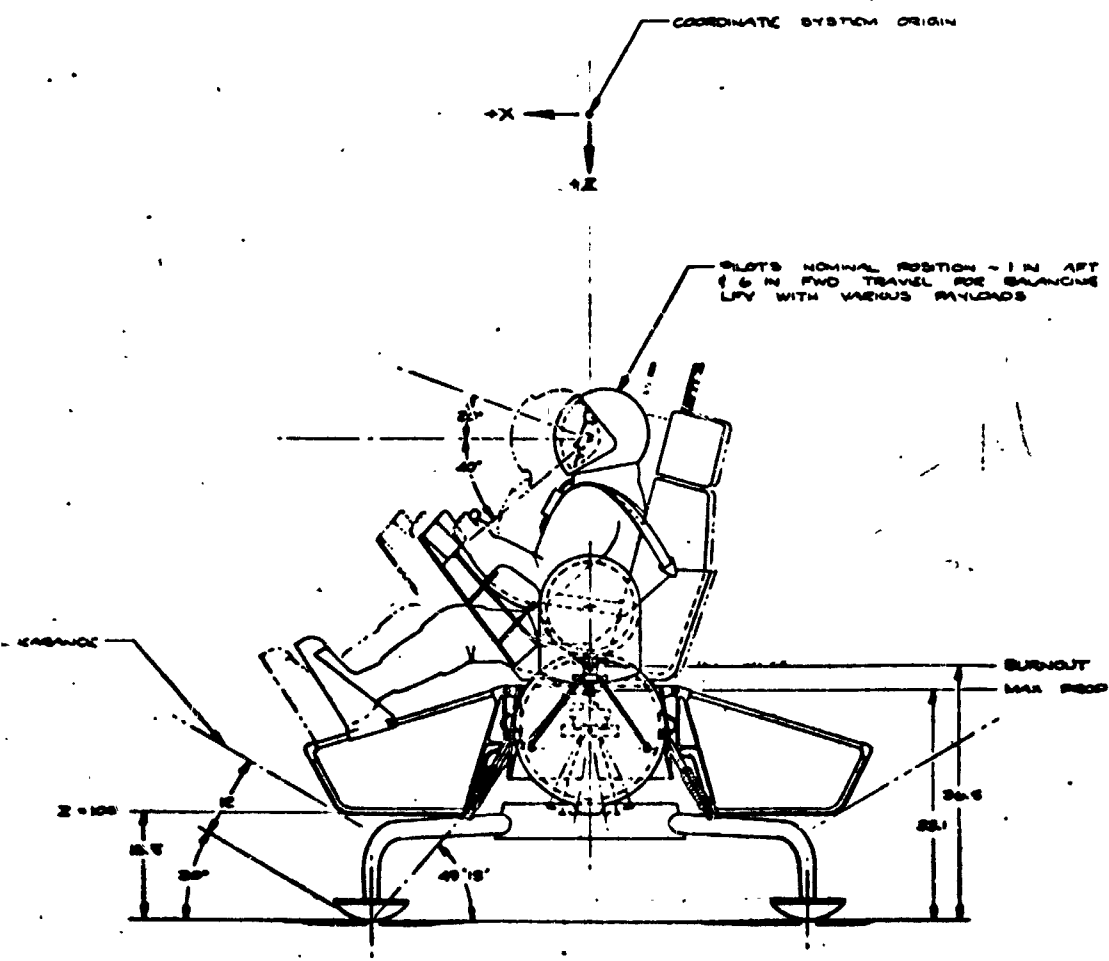
FOLDOUT FRAME

FOLDOUT FRAME



FOURTH FRAME

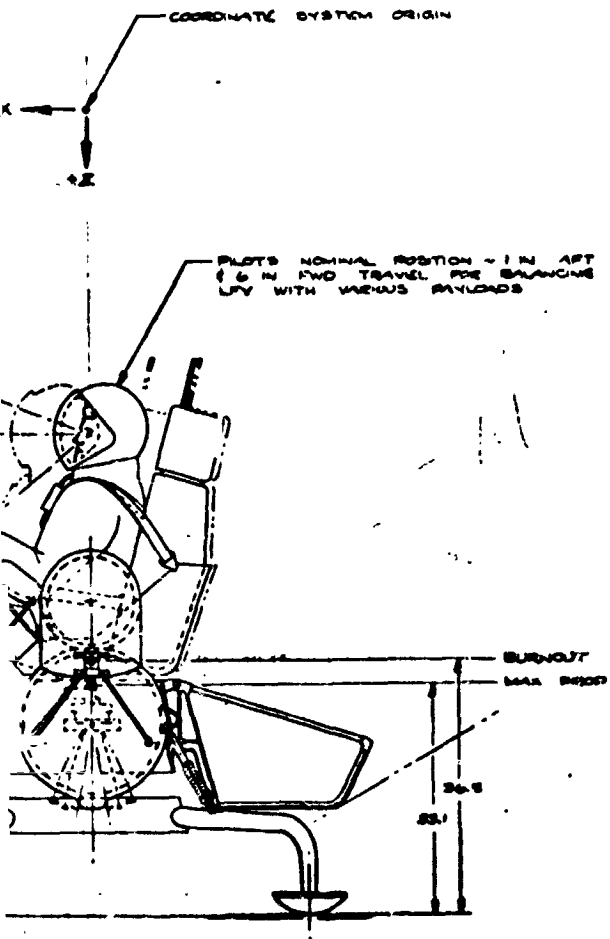
PAGE



|    |         |  |
|----|---------|--|
| 10 | 2230-14 | ONE MAN LFV -<br>CONTROL CONFIGURATION A<br>EMULE ENGINE, GIMBALED |
|----|---------|--|

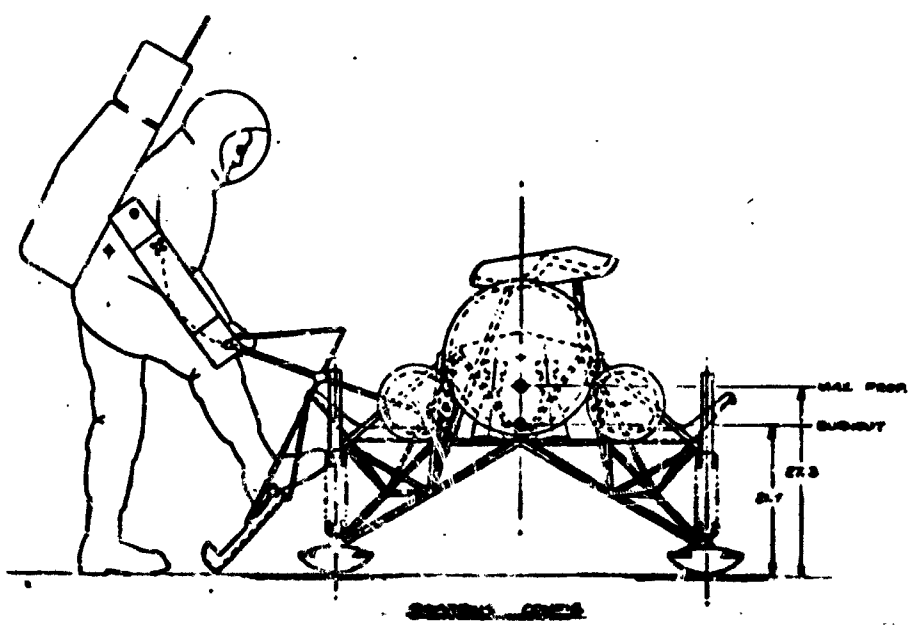
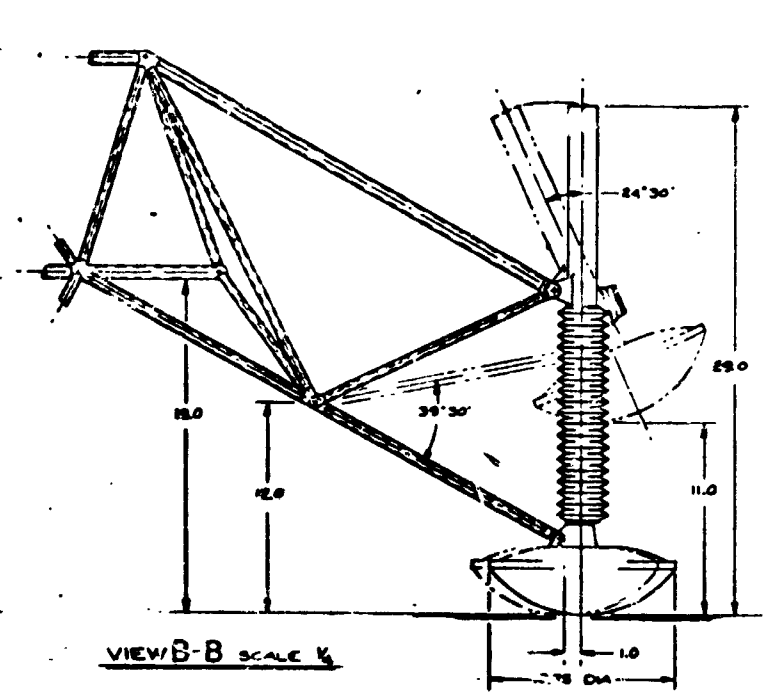
Figure 12. Seated Pilot, Single Gimbal Engine Veh  
(Drawing 2230-14)



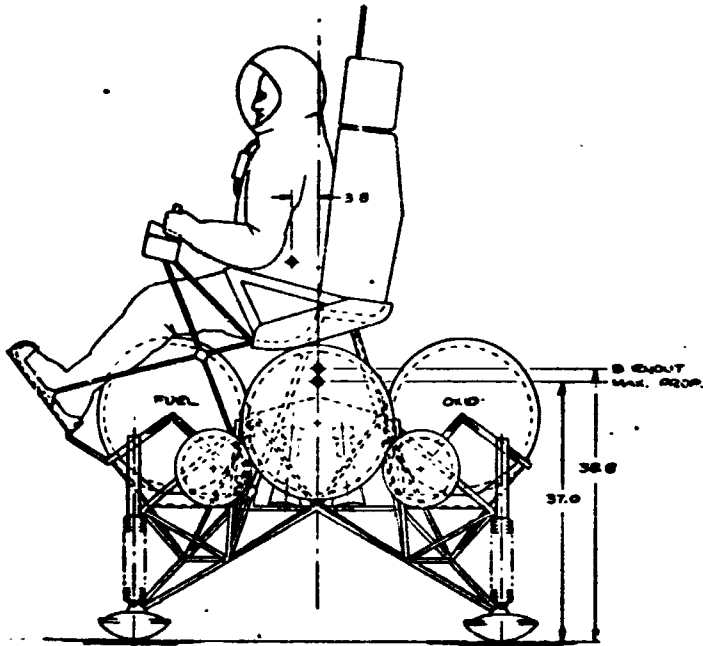


|   |     |          |   |
|---|-----|----------|---|
| NO  | REV | DATE     | DESCRIPTION   |
| 1/6   | 1   | 10/24/67 | INITIAL DESIGN CONCEPT DEVELOPMENT<br>FOR J-1 ENGINE, SINGLE ENGINE, GIMBALED |
| ONE-MAN LPV -<br>CONTROL CONFIGURATION ALT -<br>SINGLE ENGINE, GIMBALED |     |          | 2230-14   |

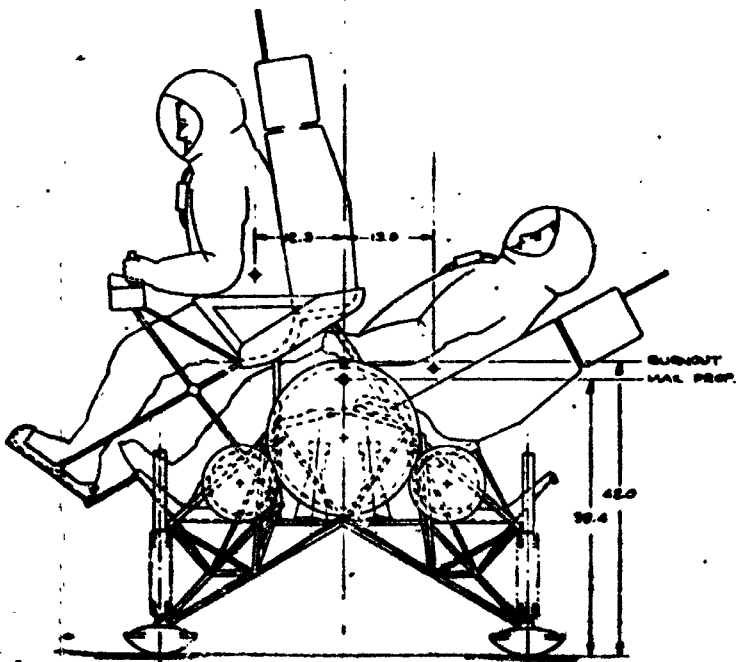
Figure 12. Seated Pilot, Single Gimbaled Engine Vehicle Configuration  
(Drawing 2230-14)



FOLDOUT FRAME



PROPELLANT RINLOAD CONFIG.



ANTICIPAT. RINLOAD CONFIG.

L0 - MAX. C.G. OFFSET  
 & MAX. VERTICAL C.G.  
 E0 - MAX. C.G. OFFSET  
 VECTOR & MAX. VERTICAL

E1 - MAX. C.G. OFFSET  
 VECTOR & MIN. VERTICAL  
 L1 - MAX. C.G. OFFSET  
 & MIN. VERTICAL C.G.

PITCH & ROLL CONTROL

CAVITY MAY BE FILLED WITH  
 VISCOUS FLUID TO PROVIDE  
 VEHICLE DAMPING

FLEXIBLE DUST BOOT

SELF TO GROUND

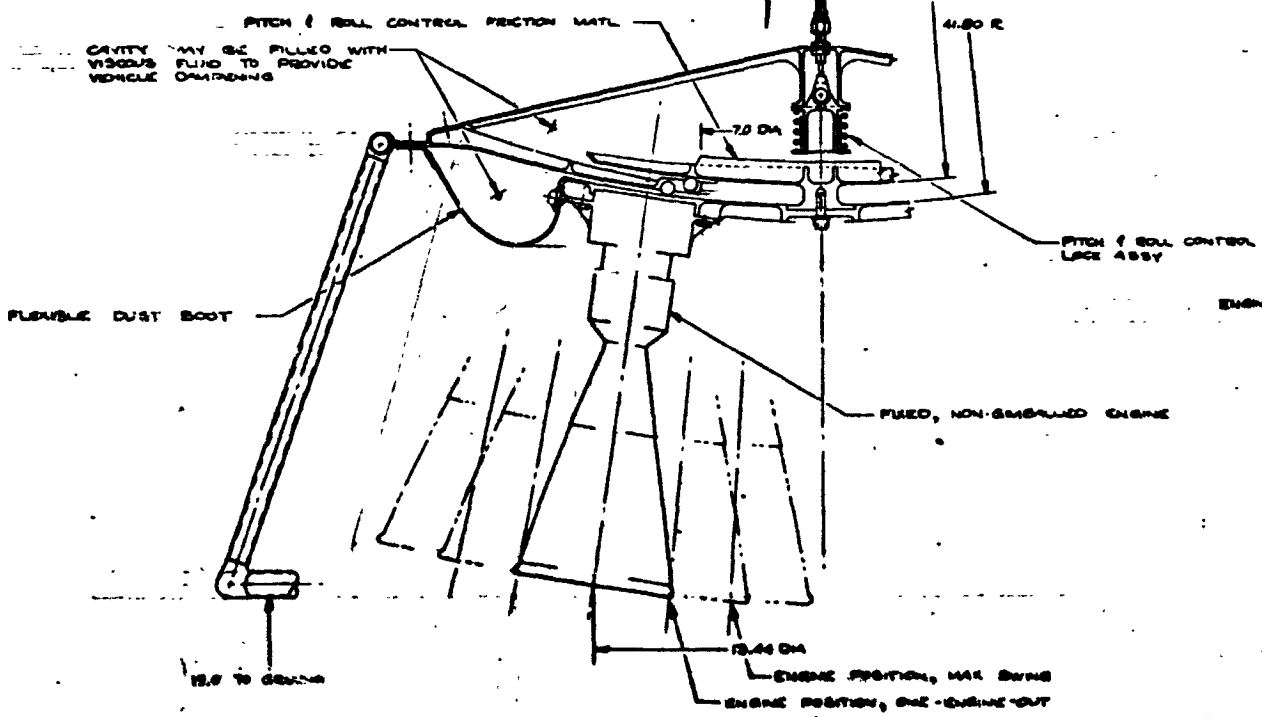
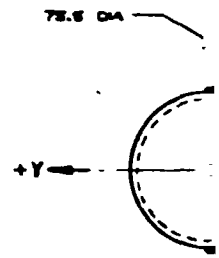
FORGOUT FRAME

ONE-ENGINE-OUT THRUST VECTOR  
 NORMAL THRUST VECTOR

10 - MAX. C.G. OFFSET WITH ONE-ENGINE-OUT & MAX VERTICAL C.G.  
 20 - MAX. C.G. OFFSET WITH NORMAL THRUST VECTOR & MAX VERTICAL C.G.  
 27 - MAX. C.G. OFFSET WITH NORMAL THRUST VECTOR & MIN VERTICAL C.G.  
 18 - MAX. C.G. OFFSET WITH ONE-ENGINE-OUT & MIN VERTICAL C.G.

MAX VERTICAL C.G. (PILOT ONLY AT BURNDOUT OR PILOT & PASSENGER AT BURNDOUT)  
 MIN VERTICAL C.G. (PILOT WITH PROP PAYLOAD & FULL VEHICLE PROP)

PITCH & ROLL CONTROL ASSY - MECHANISM TO LOCK ASSY. ACTIVATION LOCKS ENGINE ASSY TO VEHICLE; CHANGES IN VEHICLE ATTITUDE THEN PRODUCED BY KINESTHETIC CONTROL OF PILOT. AFTER NEW ATTITUDE IS ACHIEVED ASSY IS UNLOCKED & VEHICLE IS UNDER PENULTIMATE STABILITY FLIGHT.



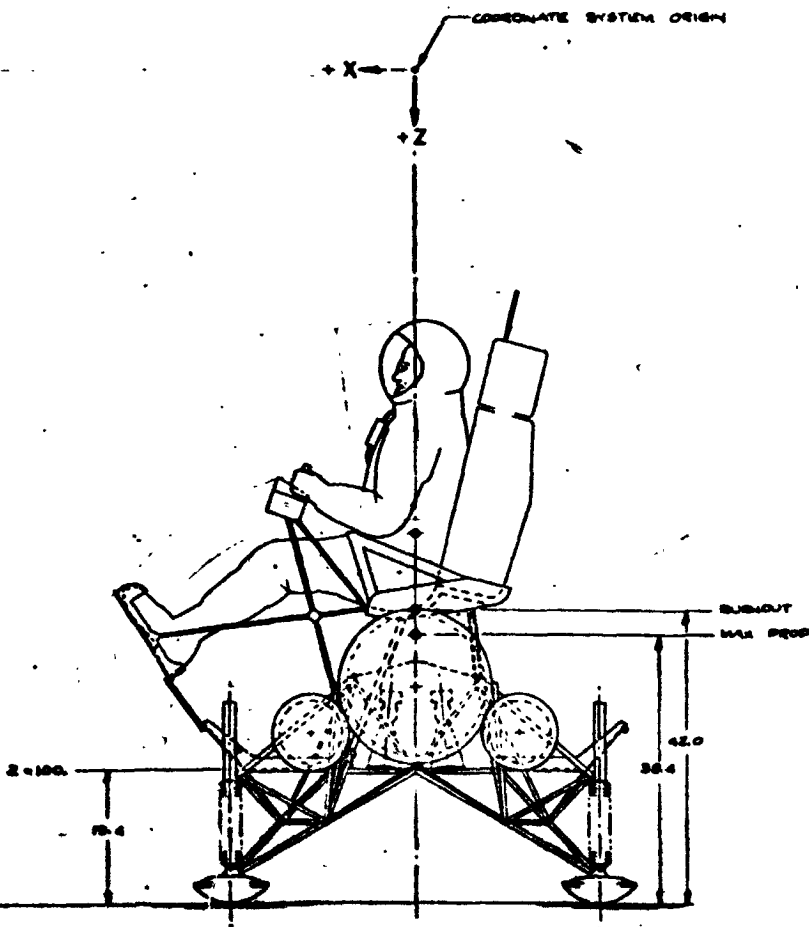
VIEW A-A SCALE 1/2



FOLDOUT FRAME

FOLDOUT FRAME





|              |            |      |
|--------------|------------|------|
| REV          | BY         | DATE |
| No 1         | W. E. 19-7 | 1957 |
| REV          | BY         | DATE |
| ONE - M      |            |      |
| ENTRICAL COM |            |      |
| POSTED       |            |      |

Figure 1b. Seated Pilot, Long Radius Gim  
(Drawing 2230-4)

- 33, 74 -

FOLDOUT FRAME

FOLDOUT FRAME



Space Division  
North American Rockwell

SYSTEM ORIGIN



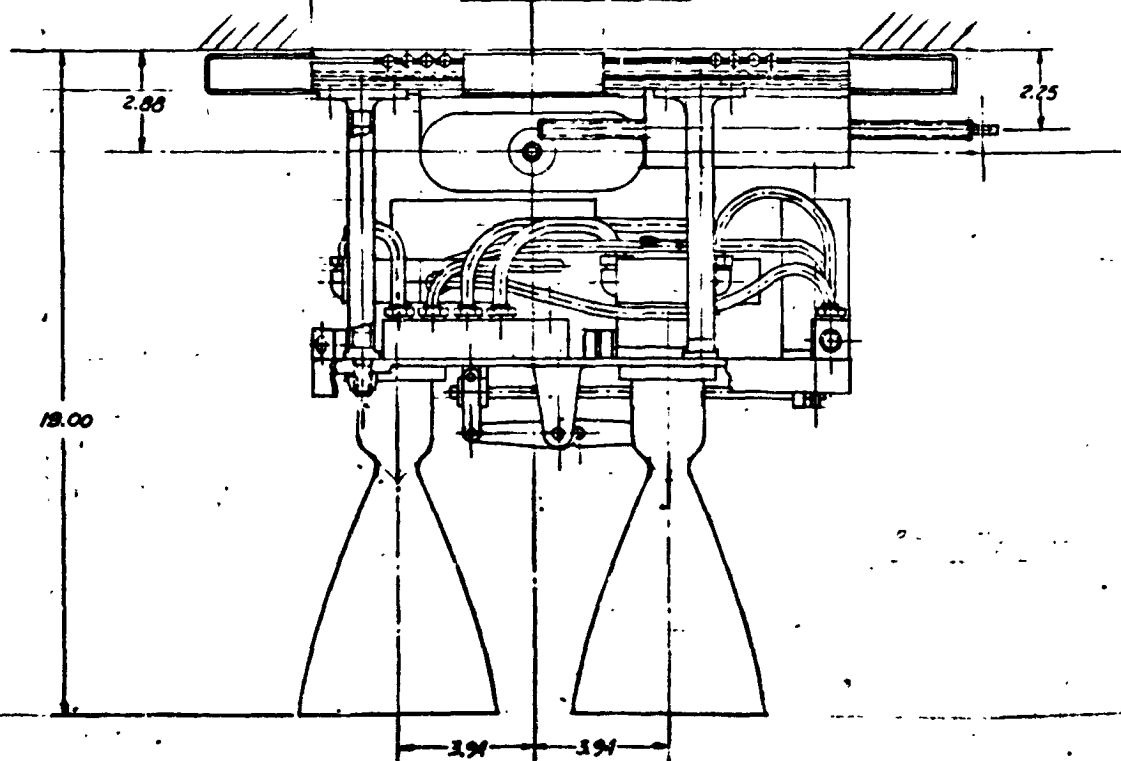
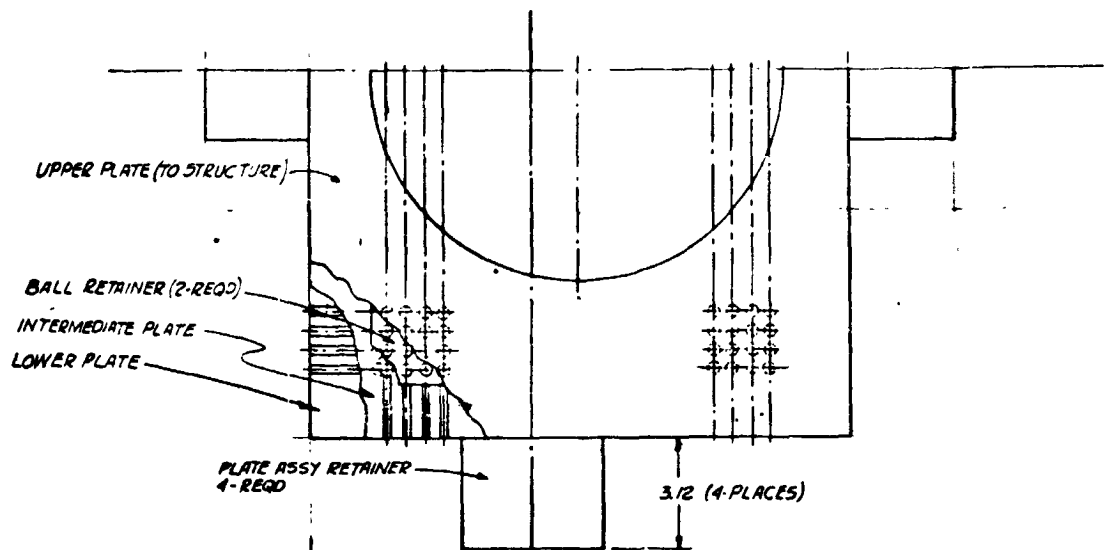
|   |                       |                         |        |
|---|-----------------------|-------------------------|--------|
| REV<br>No 1   | BY<br>DATE<br>2-19-69 | CHKD<br>DATE<br>2-19-69 | 2230-4 |
| ONE - MAN LFV -<br>CONTROL CONFIGURATION A-T-1<br>SEATED PILOT & TENDON'S STABILITY |                       |                         |        |

Figure 13. Seated Pilot, Long Radius Gimbal Vehicle Configuration  
(Drawing 2230-4)

- 33, 34 -

SD 69-419-4

FOLDOUT FRAME



FOLDOUT FRAME



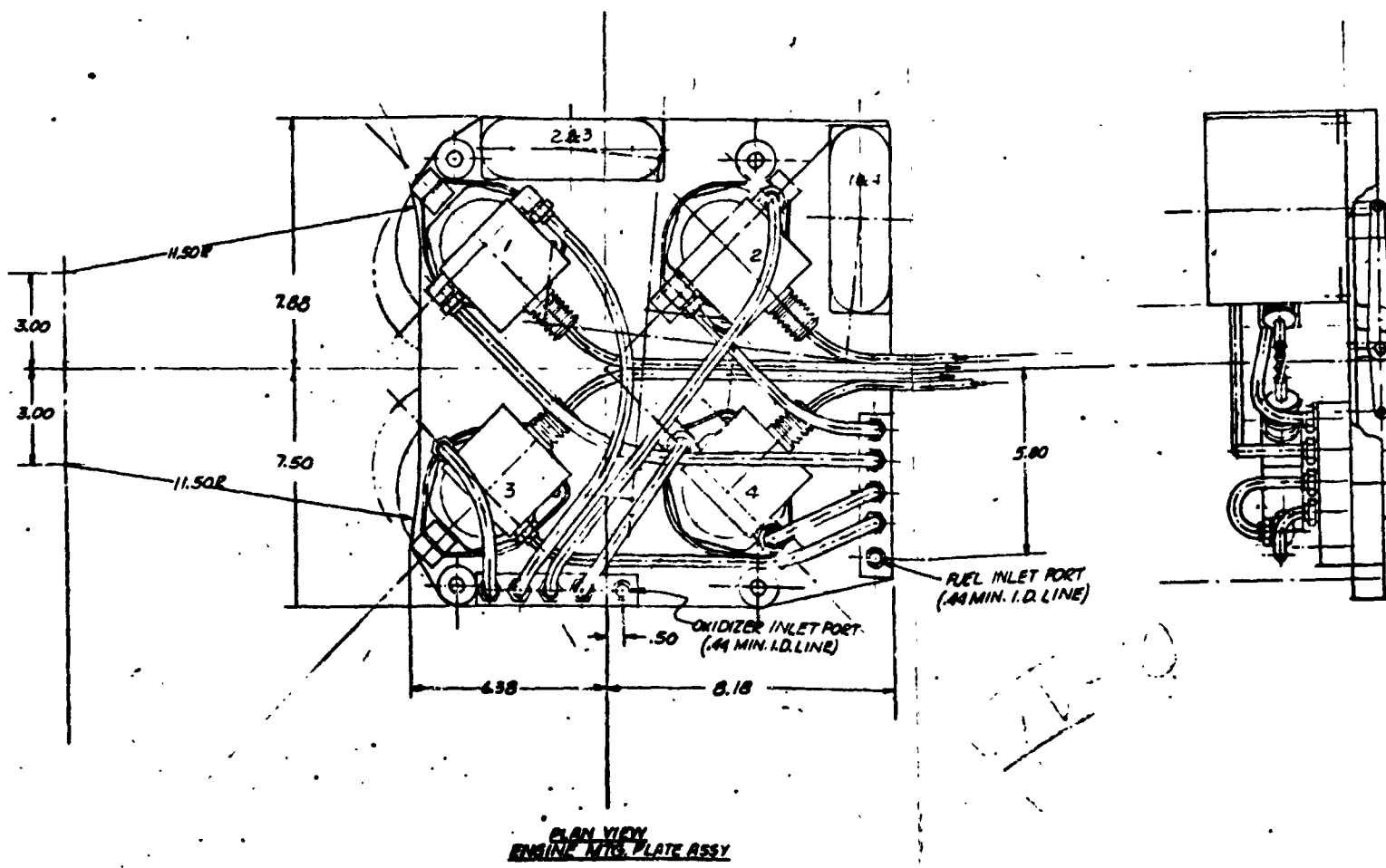


Figure 14. Four-Engine Configuration

FOLDOUT FRAME

FOLDOUT

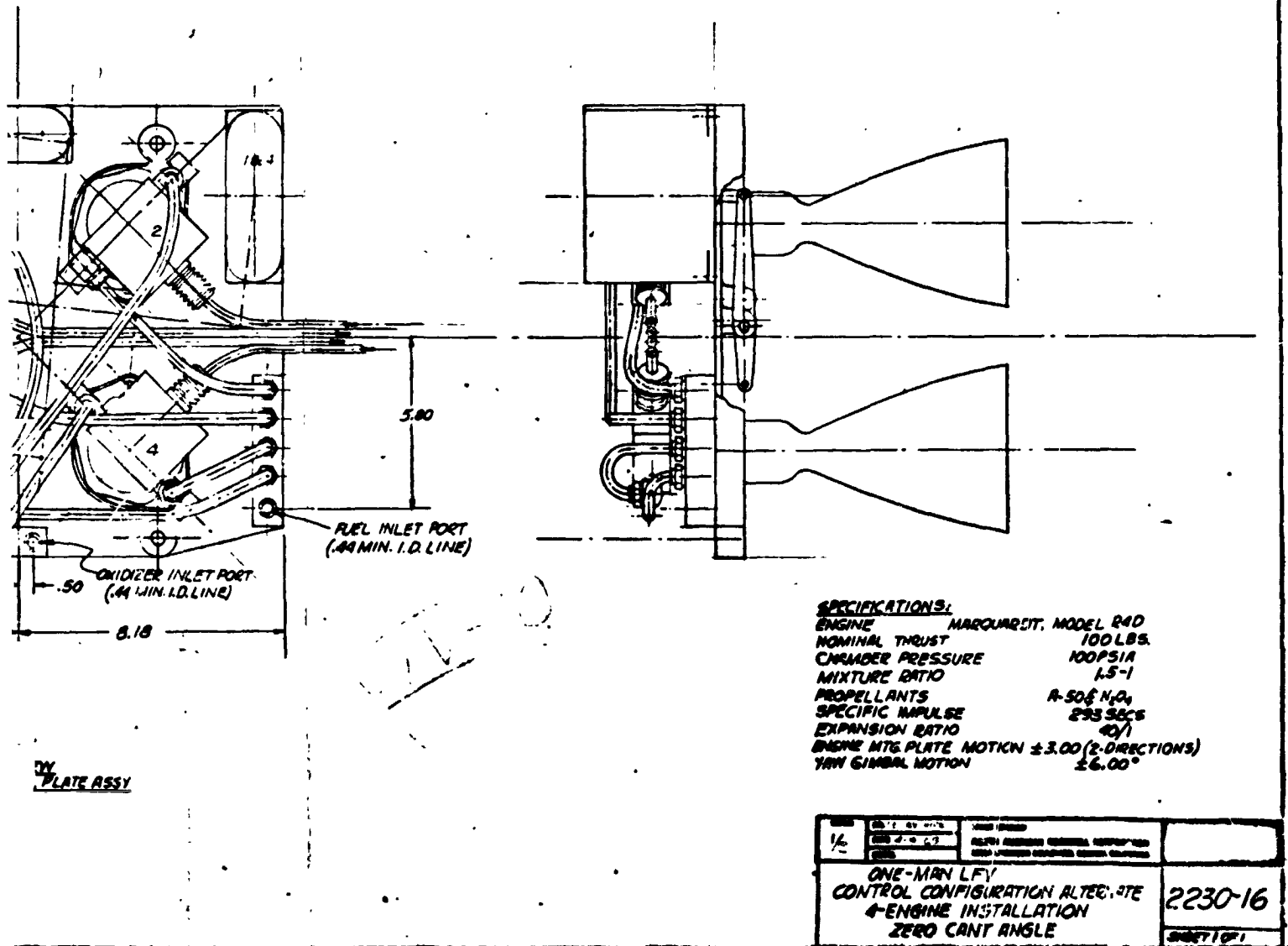
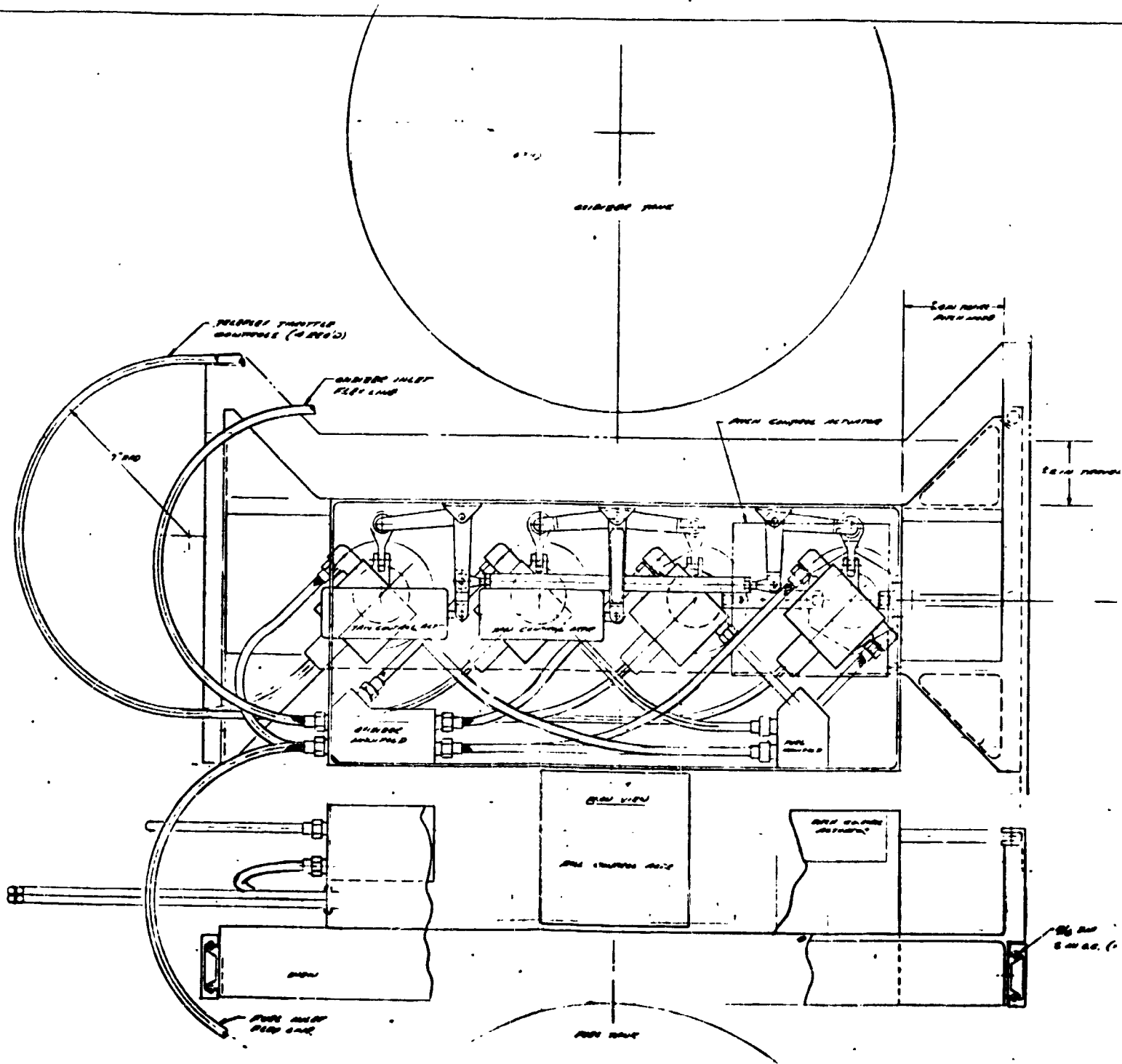
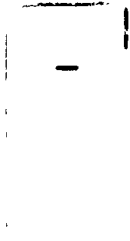
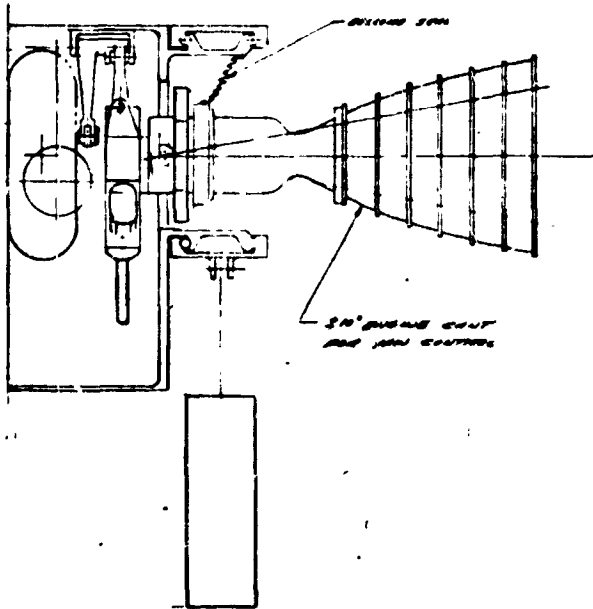


Figure 14. Four-Engine Sliding Plate, Zero Cant Angle Vehicle Configuration (Drawing 2230-16)





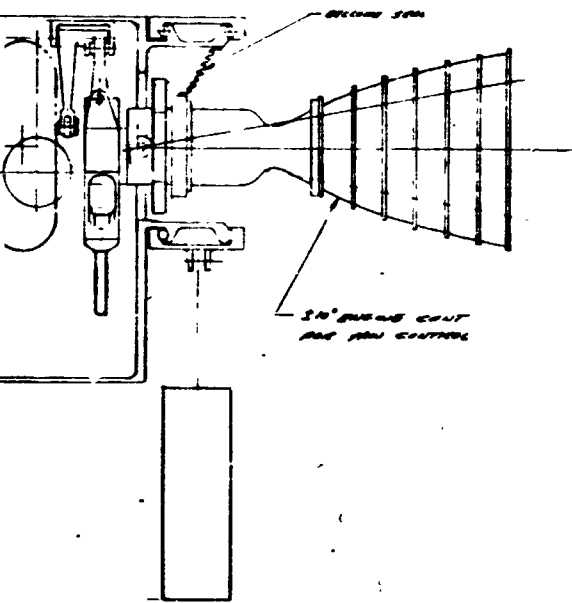
2.5 IN. THROU IN. DIA. HOLES



1/2 IN. DIA. BALLS  
5 IN. O.C. (FIVE BALL SPACING)

|      |   |         |
|------|---|---------|
| REV. | DESCRIPTION                             | DATE    |
| 1    | ISSUED FOR PRODUCTION                   | 10/1/50 |
| 2    | REVISED TO SHOW 1/2 IN. DIA. BALLS      | 10/1/50 |
| 3    | REVISED TO SHOW 5 IN. O.C. BALL SPACING | 10/1/50 |

Figure 15. In-Line Sliding Plate Four-Engine In.  
(Drawing 2230-19)



|                                  |          |            |    |
|----------------------------------|----------|------------|----|
| REV<br>A                         | REV. NO. | DATE       | BY |
|                                  | 0-11-69  | 0-11-69    |    |
| DRAWN BY                         |          | CHECKED BY |    |
| GAS PERM. LEV. - EXHAUST SYSTEMS |          | 2230-19    |    |
| 4 IN. LONG - SLIDING PLATE       |          |            |    |

Figure 15. In-Line Sliding Plate Four-Engine Installation Configuration  
(Drawing 2230-19)

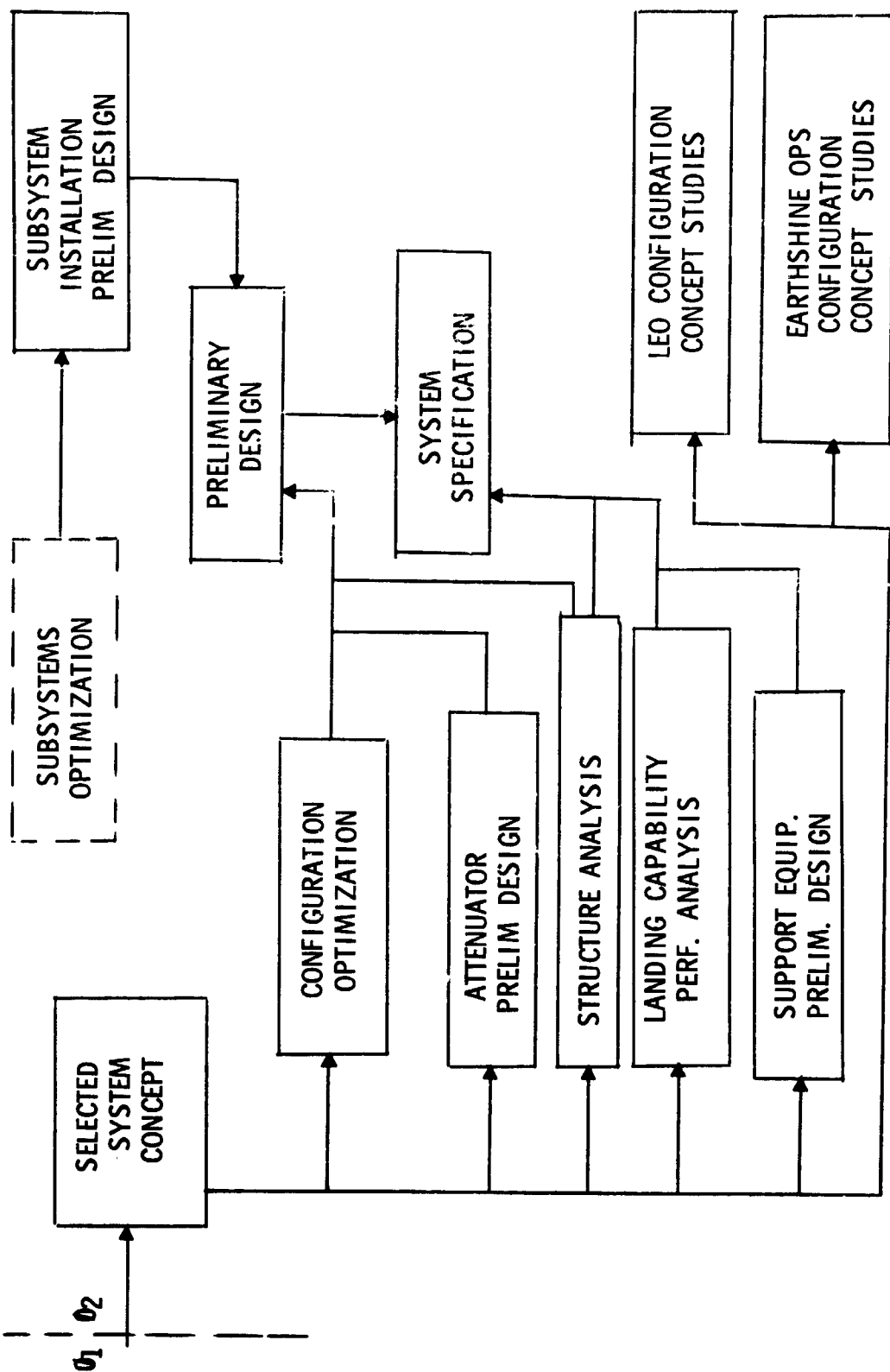


Figure 16. Study Logic, Configuration Design - Phase Two

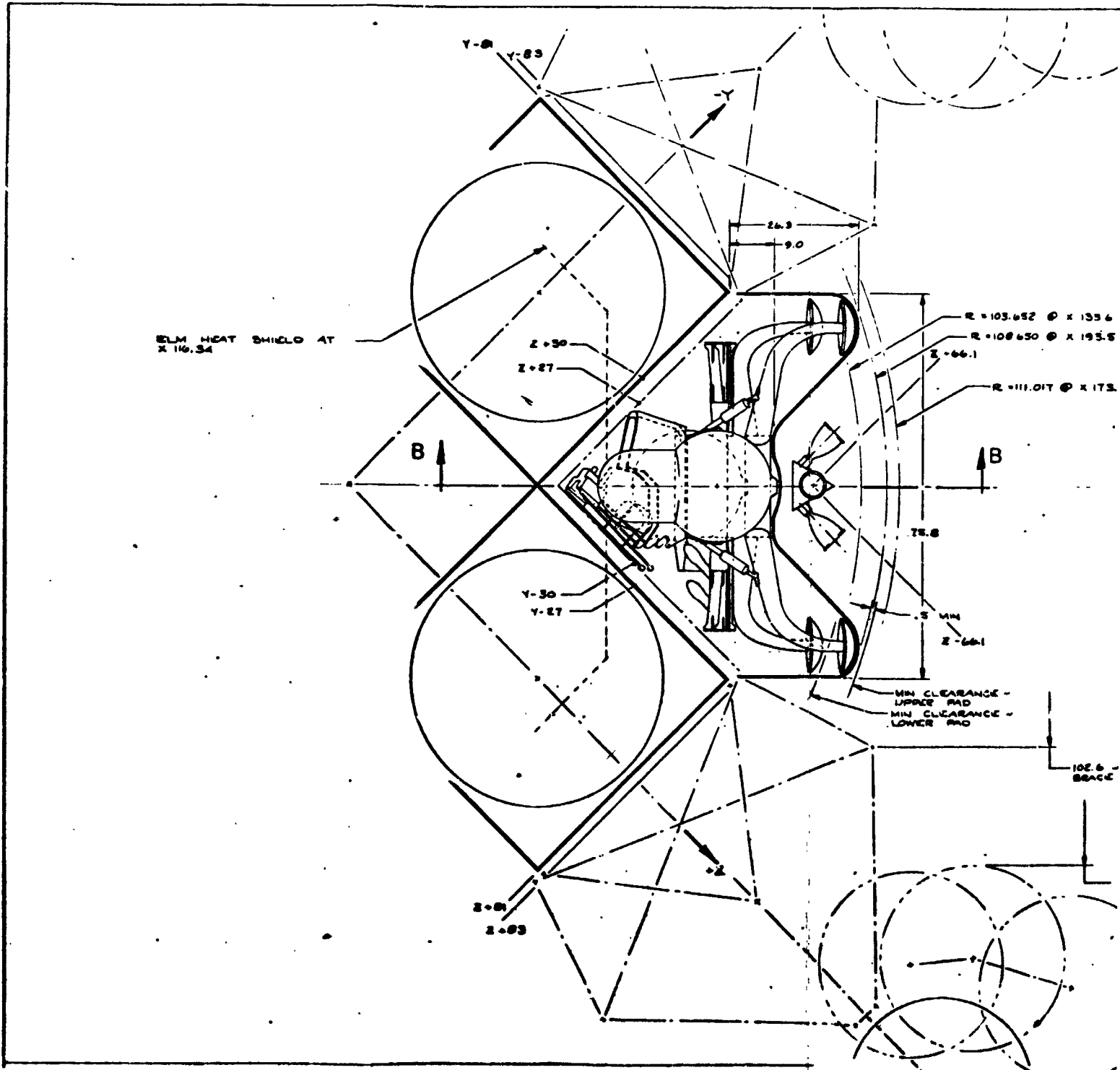
portable life support system (PLSS) in order to best satisfy conflicting requirements. A preliminary landing gear design was developed to permit better dimensional definition of the configuration. Dimensional improvements also followed as more definitive information was obtained from subsystem optimization studies.

#### Preliminary Design Evolution

The first significant change in the selected configuration during the preliminary design phase involved rotating the pilot and the load pans 45 degrees with respect to each other to improve visibility and payload bulk capability at the forward load pan. The change also considerably enhanced ingress/egress ease for the pilot. This concept is illustrated in Figure 17.

The next significant change resulted from the engine/control mechanization study. The selection (described in the subsystems portion of Volume 3 and in this volume under "Reliability") incorporated a two-axis gimbal for each engine and eight actuators, one for each axis of each engine. Definition and sizing of engines and actuators resulted in the engine sub-assembly installation drawing of Figure 18. The engines are mounted to the landing gear leg-frame. Previous designs had utilized legs attached to a box structure around an engine compartment supported by the vehicle body. Detailed dimensional layouts revealed that the stack-up of attenuation motion and gimbal travel allowances gave insufficient room for the box structure without increasing tank spacing and correspondingly increasing stowing dimensions. A more compact design was obtained by mounting the engines on the leg frame. At the same time the leg structure was changed from the box to a cruciform shape at a weight saving of 8 to 12 pounds. The change also eliminated direct plume impingement and improved the engine radiation window. The leg-mounted location involved shock accelerations of 15 to 20 g maximum on landing, but small shock mounts are utilized to reduce this value to 6 to 12 g, an acceptable value for engine compartment hardware. Engines, gimbal bearings, flexible lines, and cables normally accommodate shocks of this level. The actuators can also readily accept this requirement, but design and test criteria must be made compatible.

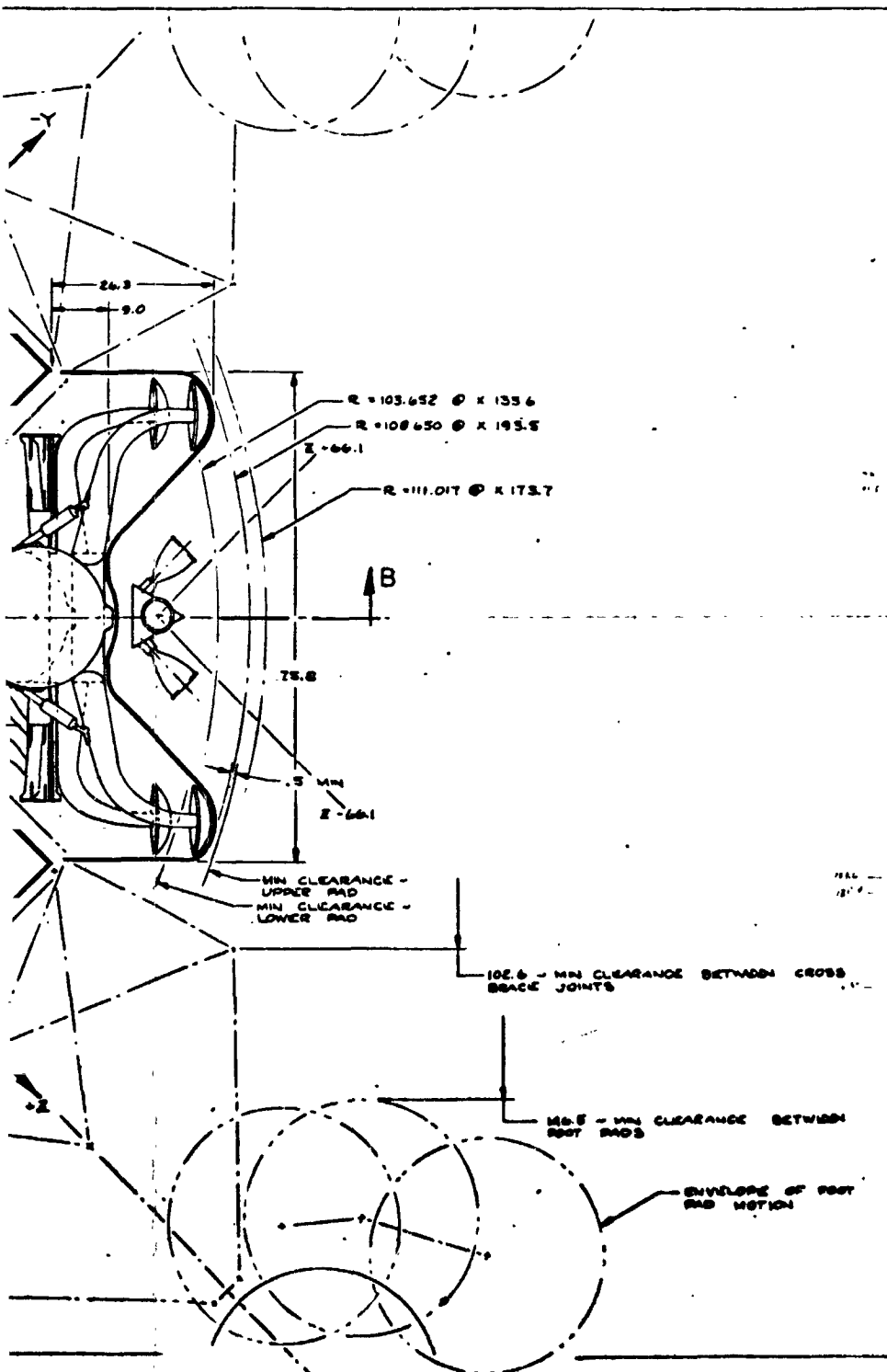
The preceding design data, together with final landing gear capability analysis and attenuation motion definition, permitted the final dimensional characteristics of the configuration to be developed (Figure 19). The end result is a completely acceptable general arrangement design which involves no serious compromises of the many factors influencing vehicle configuration. It is considered, however, that improvements could be made in the weight of the structure and in fabrication complexity. It is also anticipated that a reduction of tank centerline spacing to lessen the stowing envelope could be achieved by a second iteration of the design process.



FOLDOUT FRAME



X 298.594



X 196  
X 102.5

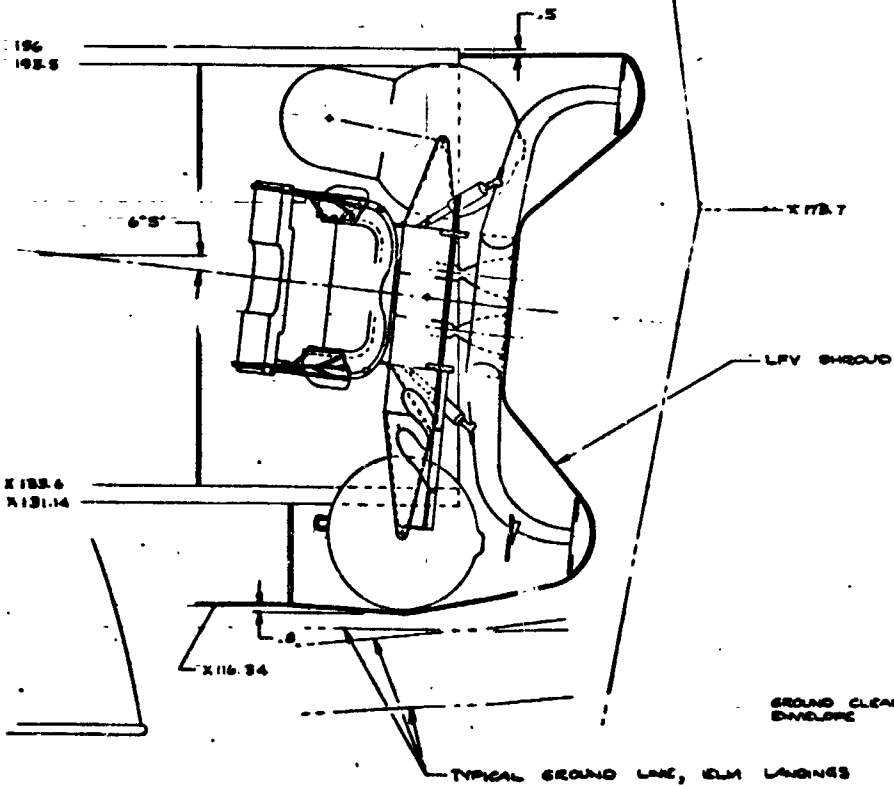
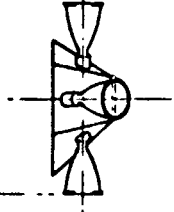
X 135.6  
X 131.14

X 116.34

SECTION B-B

FOLDOUT FRAME.

X 238.594



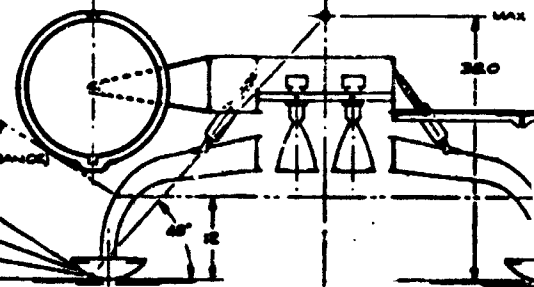
SECTION B-B

GROUND CLEARANCE ENVELOPE

TYPICAL GROUND LINE, ICLM LAININGS

12" (MAX WINDS RETURN)

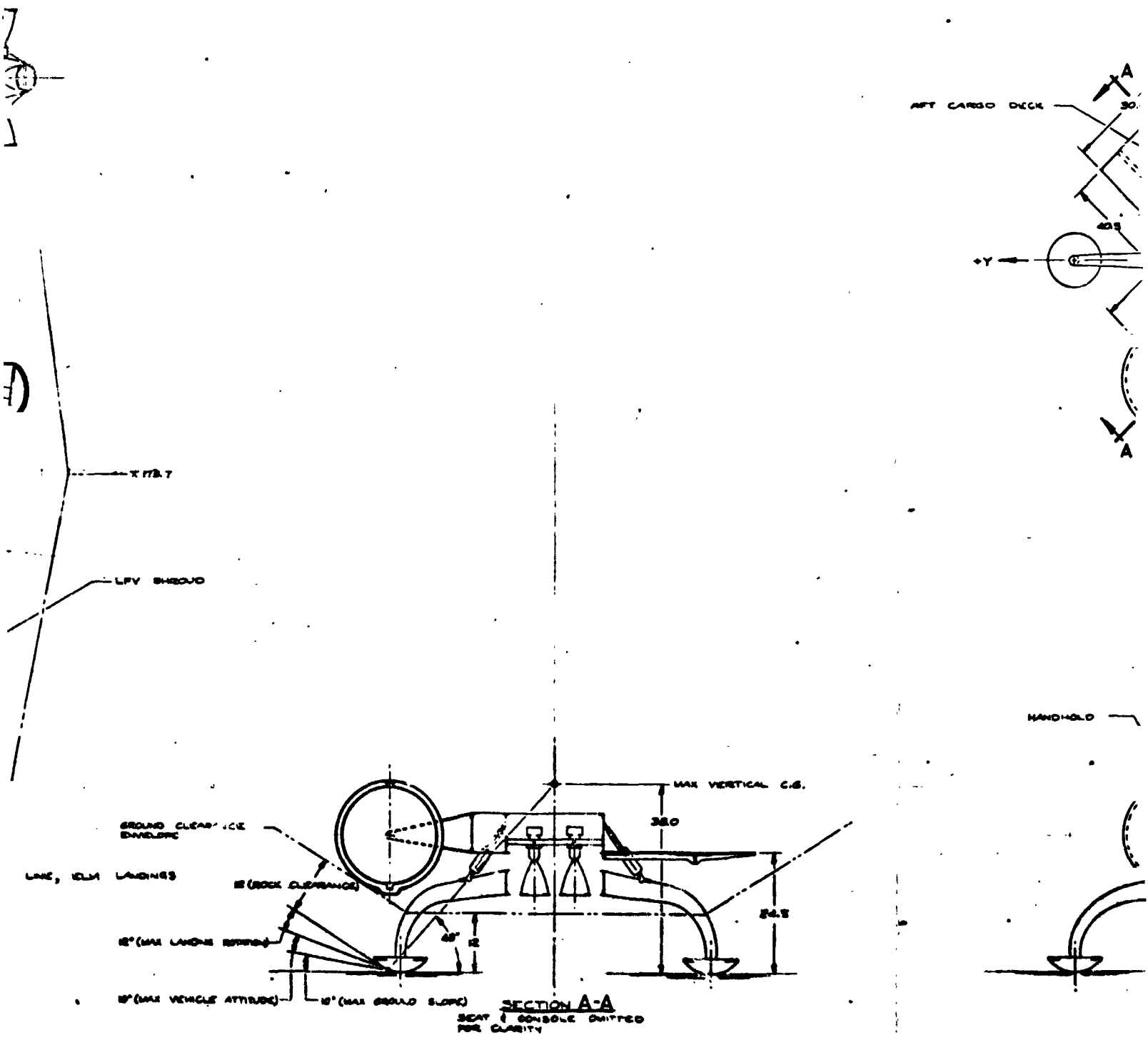
12" (MAX VEHICLE ATTITUDE)



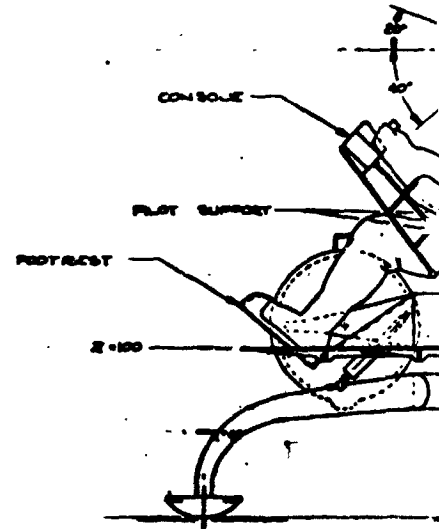
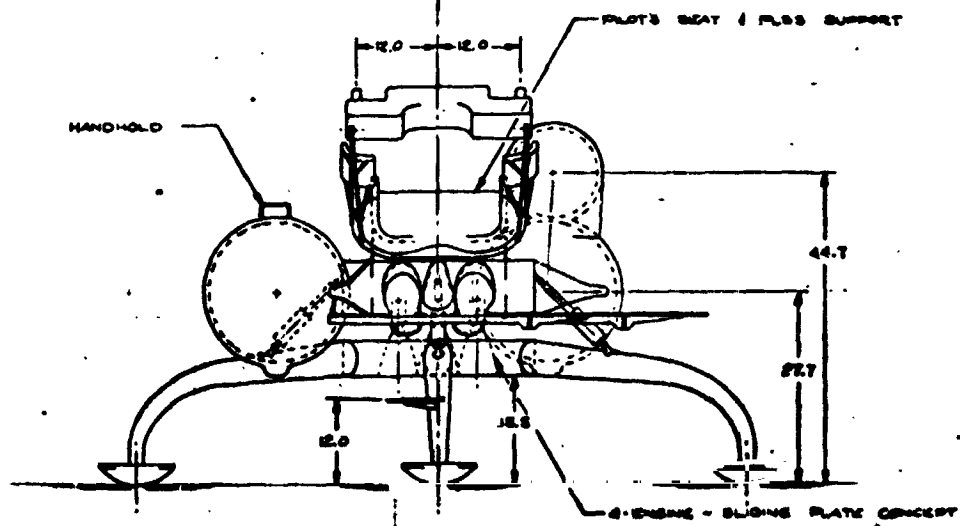
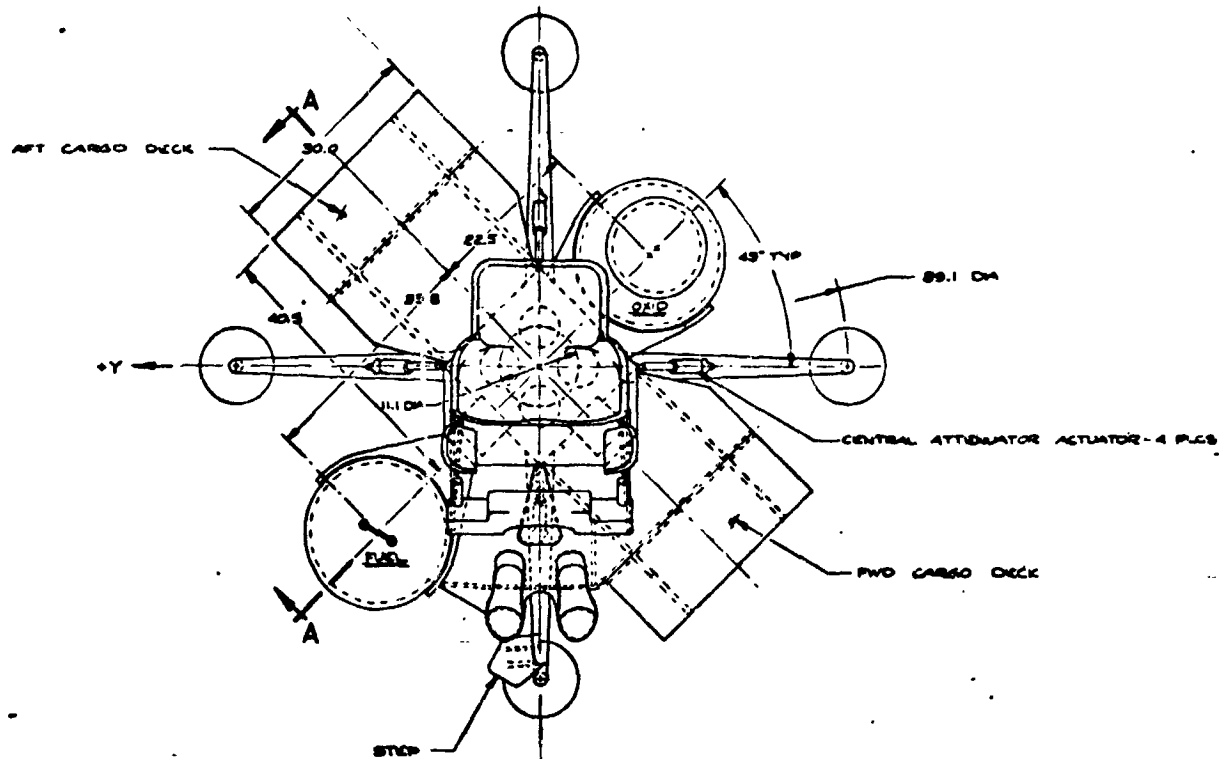
SECTION A-A  
SEAT & CONSOLE DOTTED FOR CLARITY

FOLDOUT FRAME.

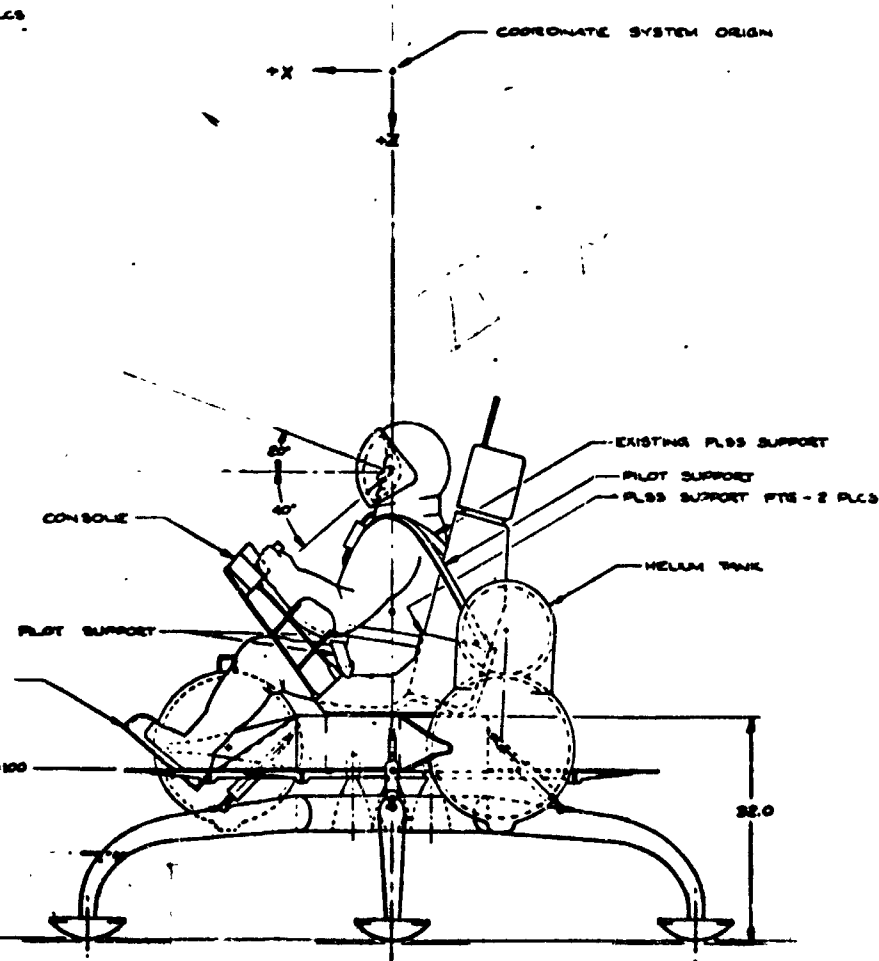
FOLDOUT FRAME



FOLDOUT FRAME

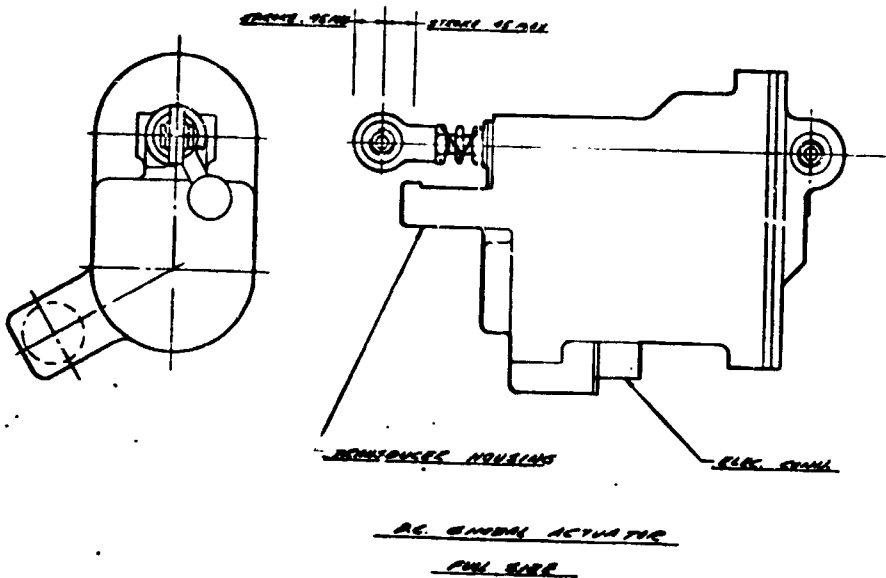


FOLDOUT FRAME



|                                   |              |  |         |
|-----------------------------------|--------------|--|---------|
| 6                                 | REVISED      | ONE ITEM   | 2230-18 |
|                                   | REV 2 (8-63) | SPACE AMERICA GENERAL CORPORATION<br>1000 AIRPORT DRIVE, GARDEN CITY, CALIFORNIA |         |
| ONE-MAN LTV -<br>SELECTED CONCEPT |              |  | 2230-18 |

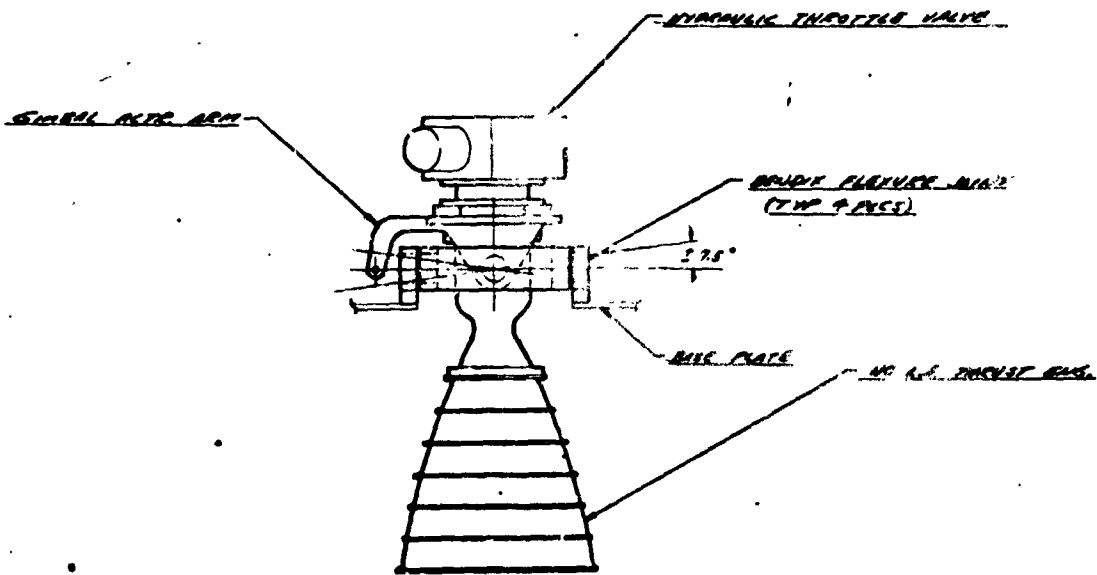
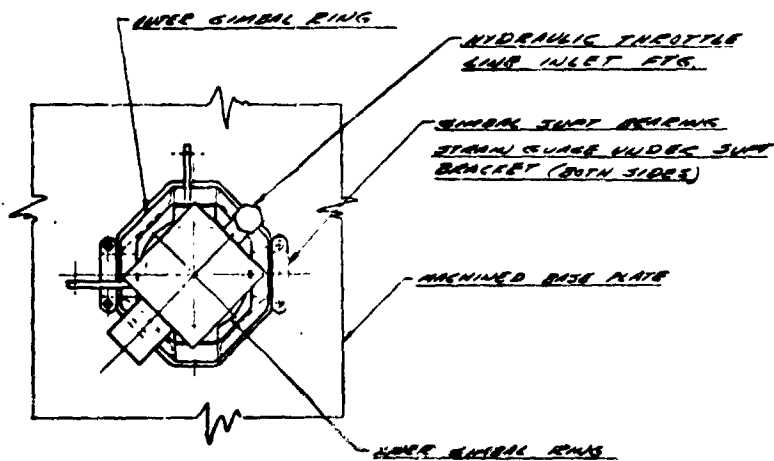
Figure 17. Phase Two Control Configuration of Lunar Flying Vehicle  
(Drawing 2230-18)



GENERAL ACT. ARM

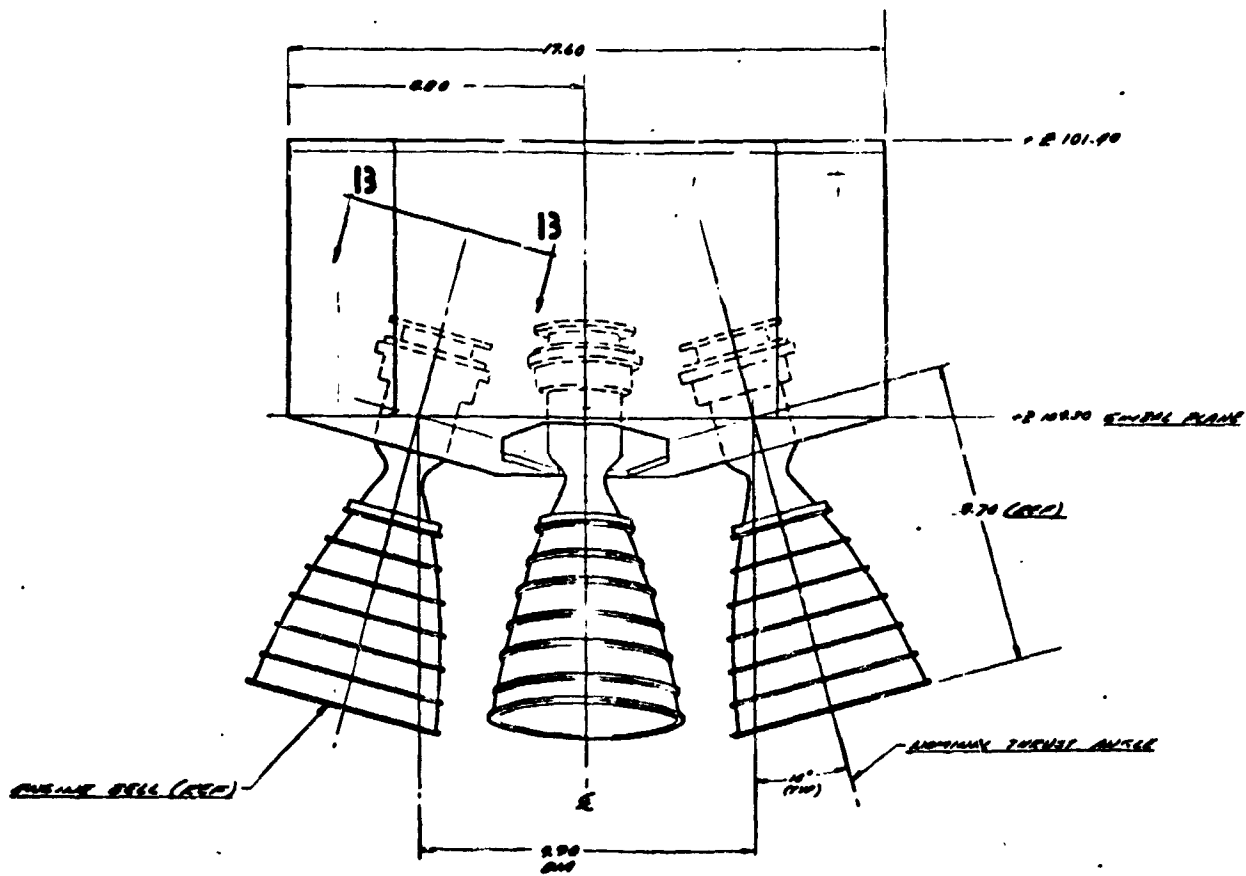
FOLDOUT FRAME

FOLDOUT FRAME



FINISH: 250

VIEW 13-13  
 DRAWING OF GIMBAL ASSEMBLY & DETAIL

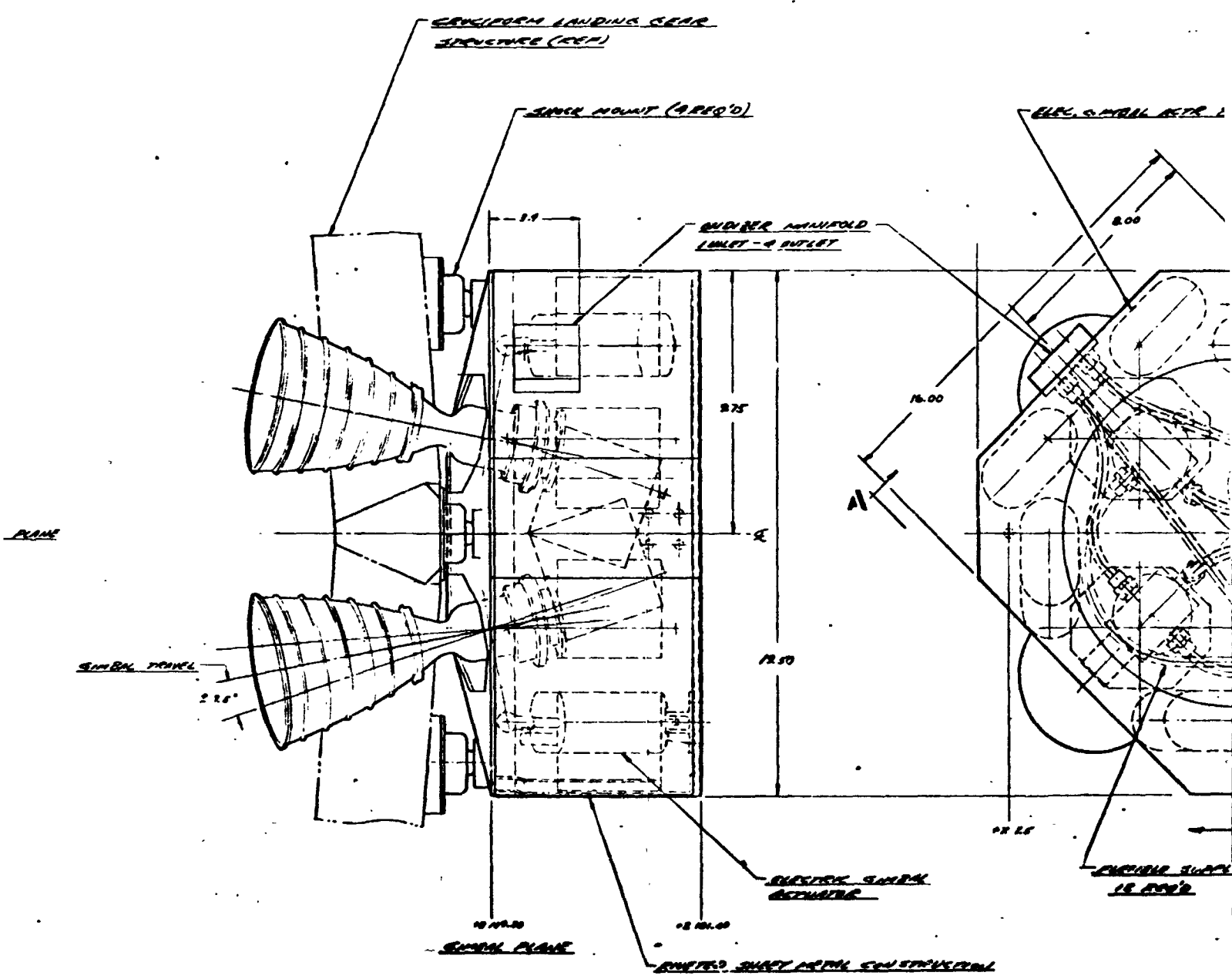


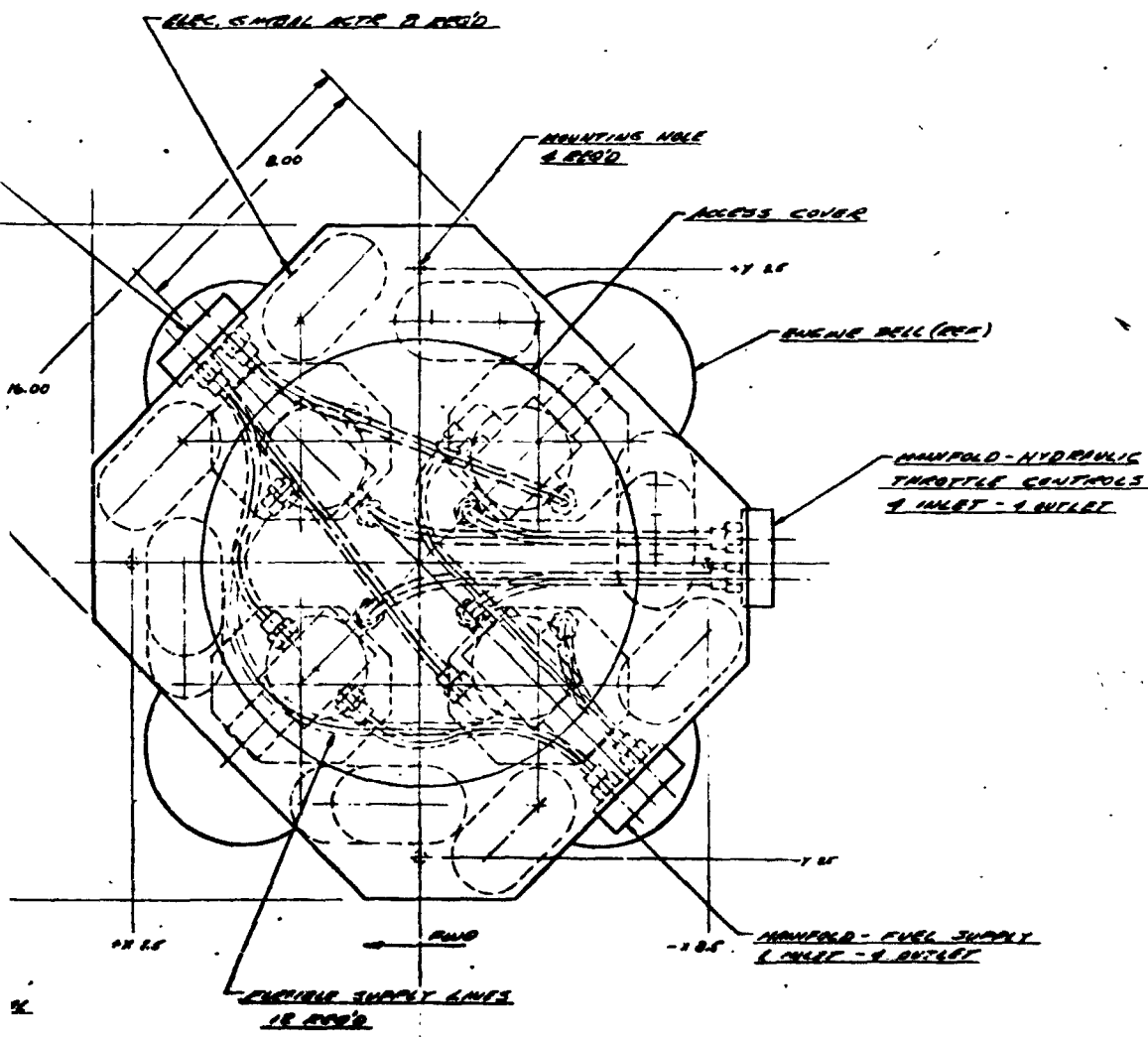
SECTION A-A

FOLDOUT FRAME

FOLDOUT FRAME







*ENGINE SPECI  
ENGINE: (NOTE)  
INCLUDE THE  
CHAMBER FOR  
FUTURE ENT.  
PROPPELLANT  
SPECIFIC AND  
EXPANSION P*

*NOTE: CRISWELL MODEL 512 JETWAY 1  
PURPOSE OF ILLUSTRATION ONLY*

**Figure 18. Preliminary**

**FOLDOUT FRAME**

**FOLDOUT FRAME**



Space Division  
North American Rockwell

- BELL (200)

- MANIFOLD - HYDRAULIC  
THROTTLE CONTROLS  
4 INLET - 4 OUTLET

| <u>ENGINE SPECIFICATIONS</u> |                                      |
|------------------------------|--------------------------------------|
| ENGINE: (NONE)               |                                      |
| MAXIMUM THRUST               | 105 LBS                              |
| CHAMBER PRESS                | 100 PSIA (MIN)                       |
| MIXTURE RATIO                | 1.5:1                                |
| PROPULSANTS                  | A-50 / H <sub>2</sub> O <sub>2</sub> |
| SPECIFIC IMPULSE             | 293 SECS (MIN)                       |
| EXPANSION RATIO              | 40:1 (MIN)                           |

- FUEL SUPPLY  
- 4 OUTLET

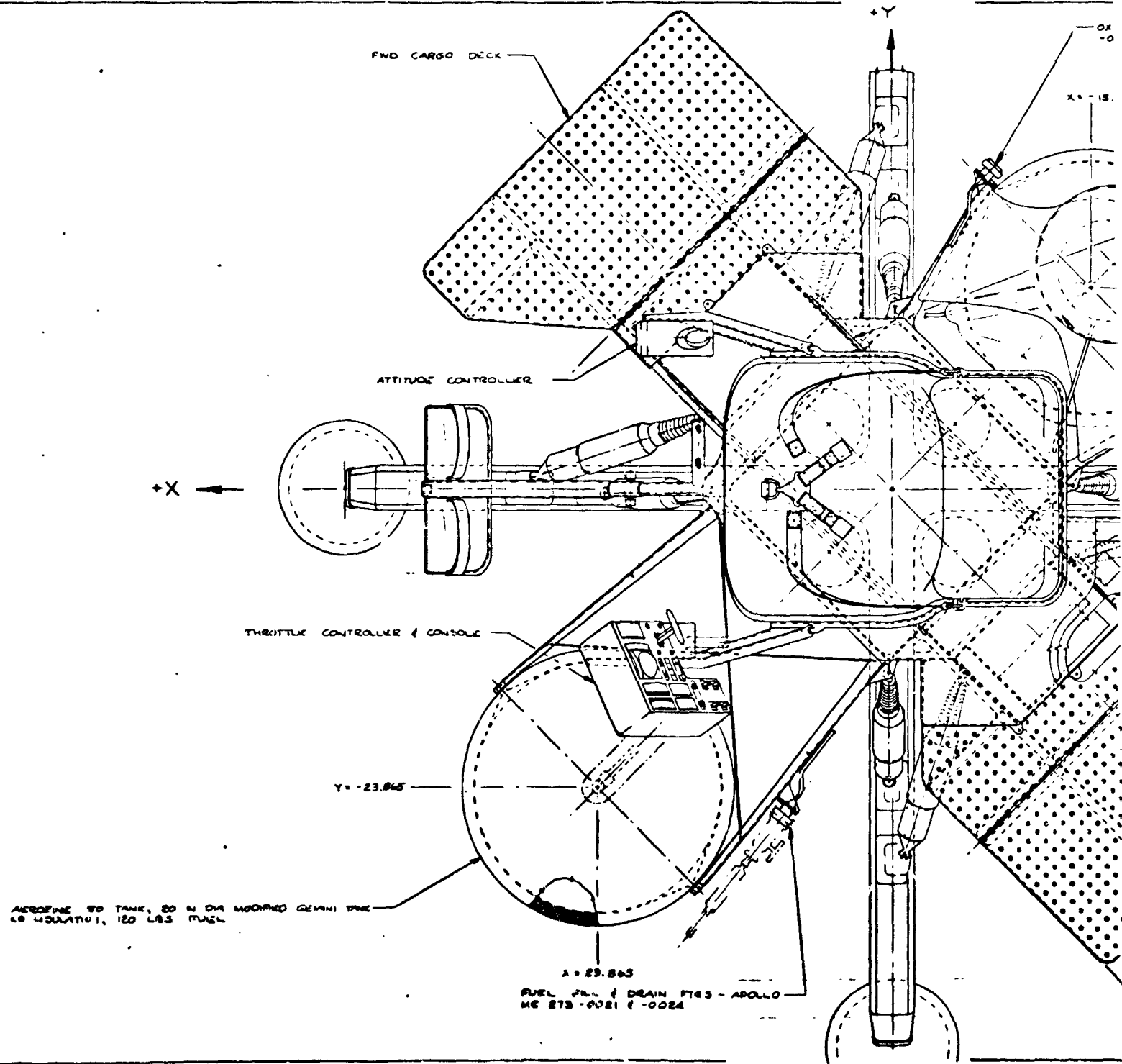
NOTE: PRELIMINARY MODEL AND JETTING FOR  
PURPOSE OF ILLUSTRATION ONLY

A 6-25-69 CUN *LV*

|   |              |              |          |
|---|--------------|--------------|----------|
| NO. 2230-21A  | DATE 6-25-69 | ISSUE NUMBER | 2230-21A |
| REV. 1  | DATE         | DESCRIPTION  |          |
| ONE NEW LTV - ONE NEW JETTING,<br>4 CHAMBERED BUSINES<br>SELECTED CONCEPT |              |              |          |

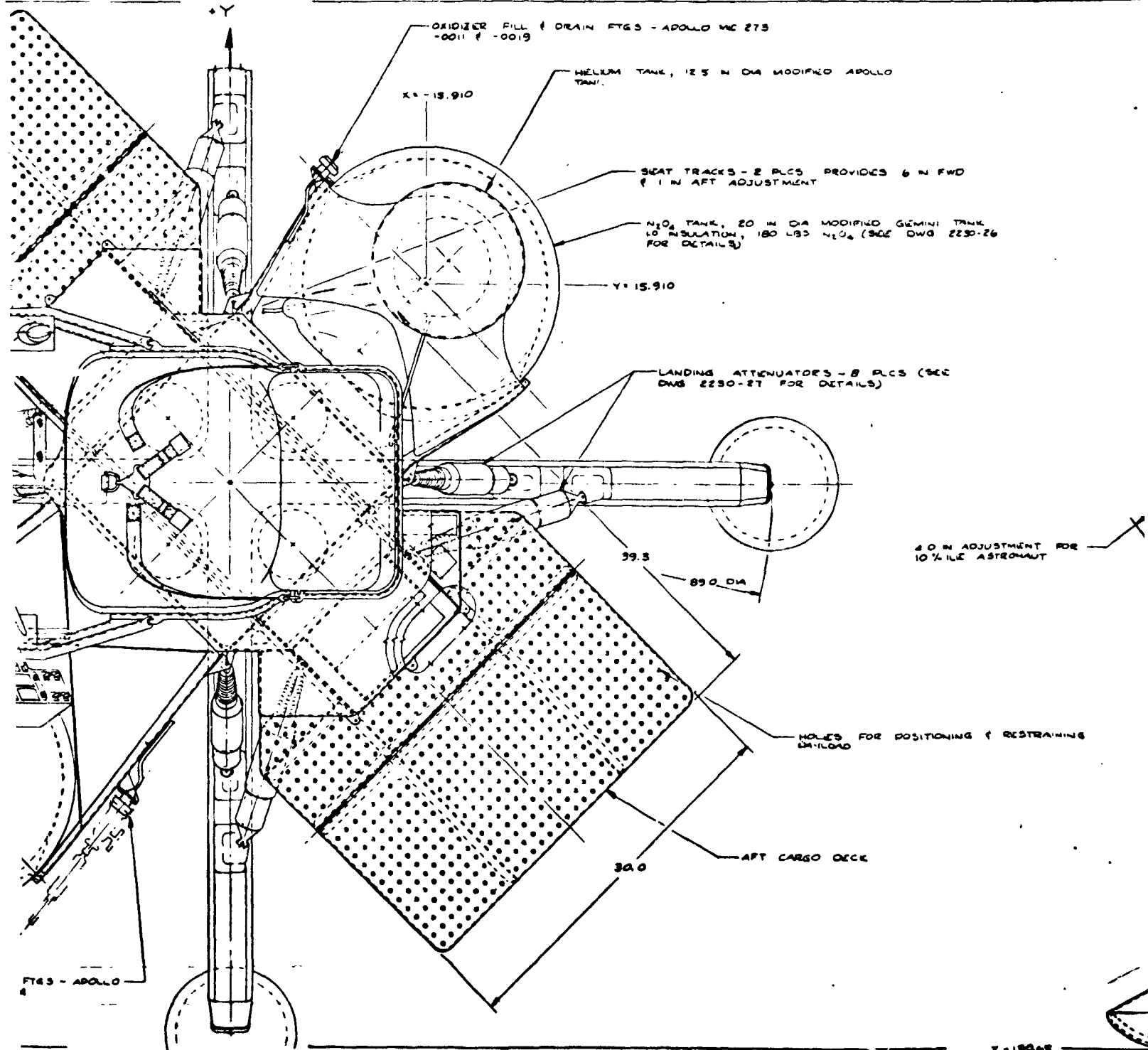
Figure 18. Preliminary Design Engine-Installation (Drawing 2230-21A)

FOLDOUT FRAME

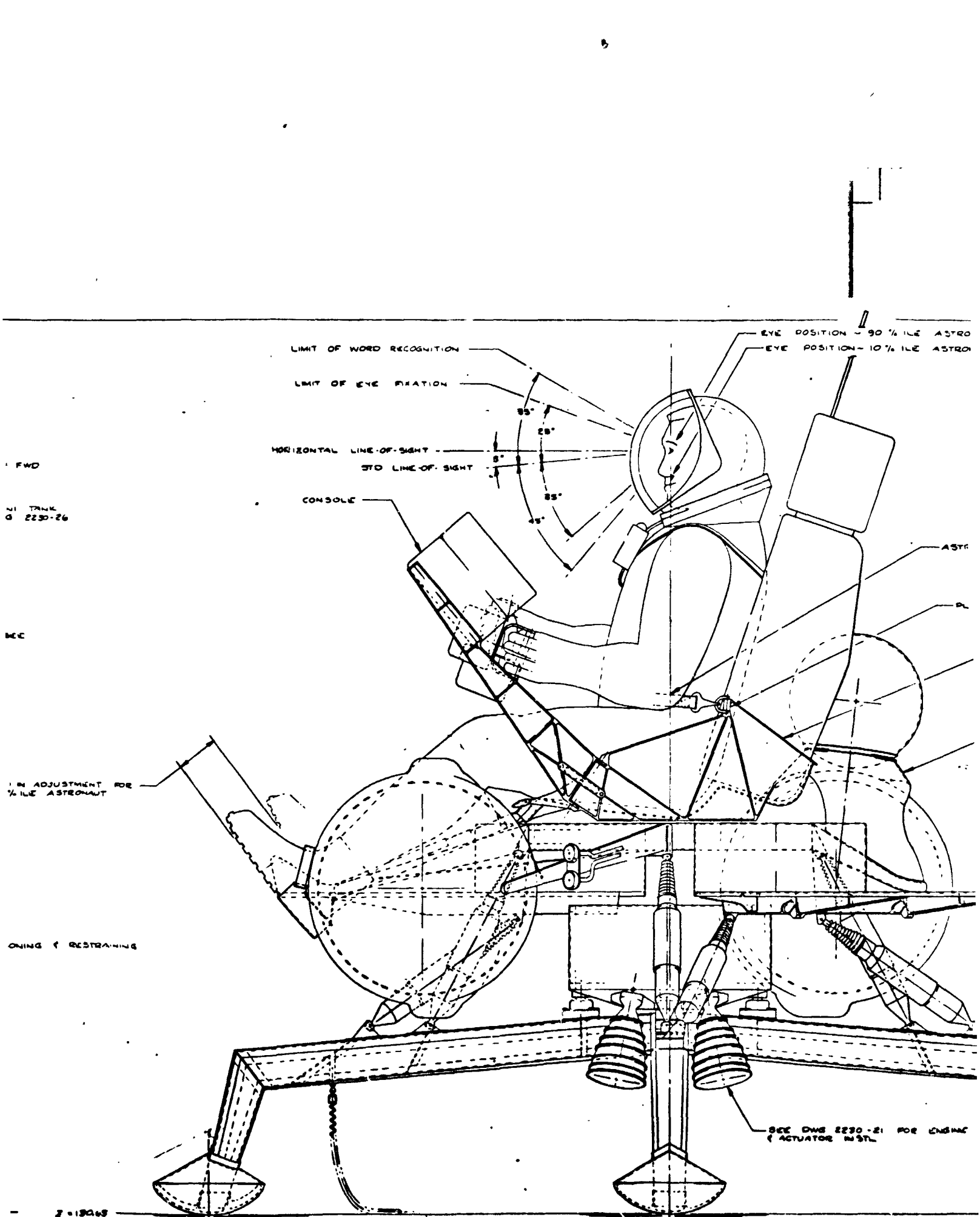


FOLDOUT FRAME

FOLDOUT



FOLDOUT FRAME



FOLDOUT FRAME

UPSIZE P.  
BLOW UP CA

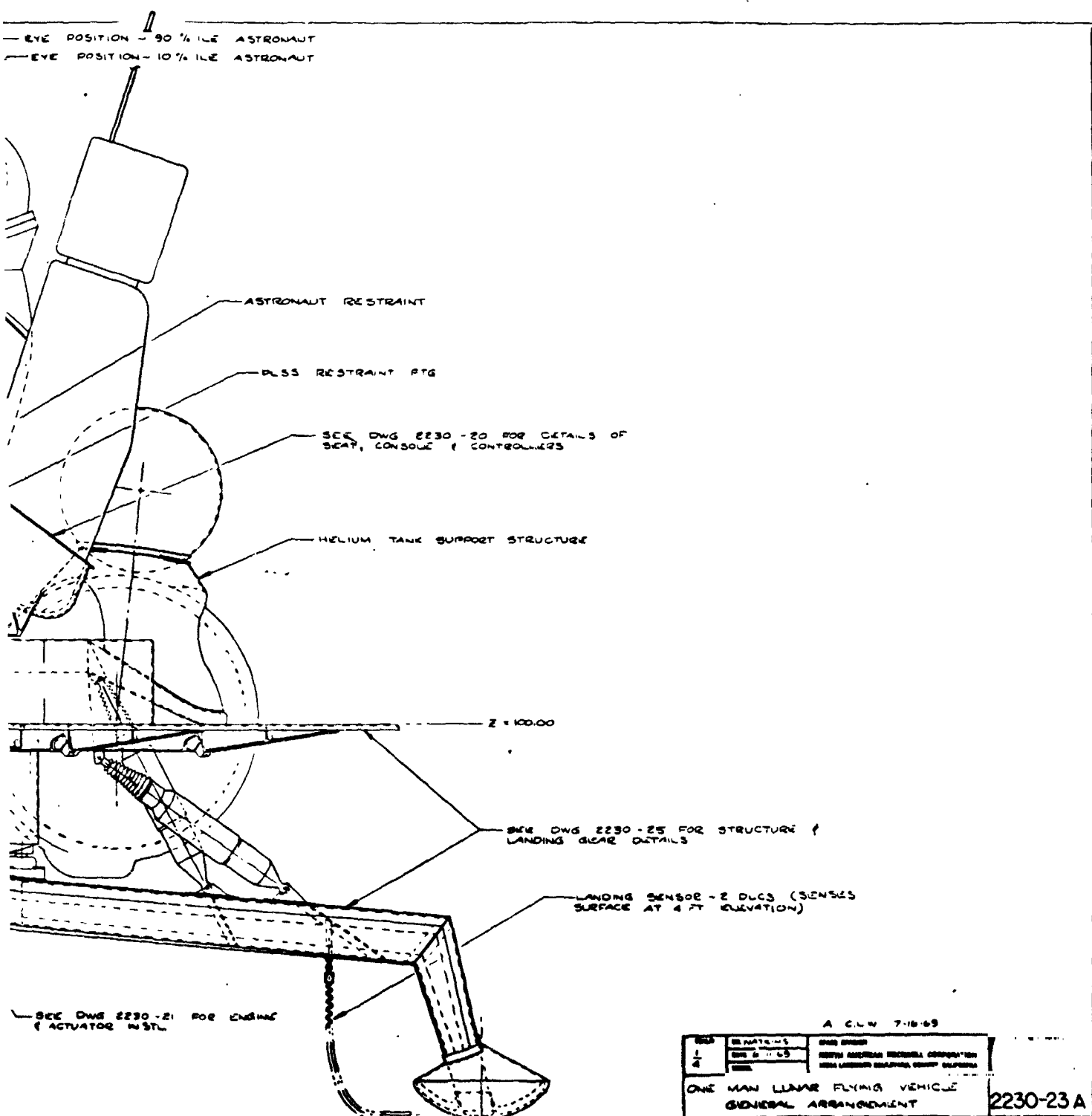


Figure 19. Preliminary Design General Arrangement (Drawing 2230-23)

Descriptions of other factors influencing the arrangement of pilot provisions, load pans, and landing gear attenuators are contained in the related sections of this volume.

### Description of Preliminary Design Configuration

The general characteristics of the vehicle are illustrated in Figures 18 through 27. The pilot is seated and restrained; two propellant tanks are used, with the fuel tank located further outboard to maintain the propellant c. g. on the vehicle centerline; four engines are located in a central cluster and mounted on the four-leg cruciform landing gear; and the upper body structure is supported from the landing gear by eight attenuators, four inclined vertically on axis to take care of vertical velocity and pitch and roll, and four skewed to resist yaw couples. The pilot gains access by moving backward while straddling the forward landing gear until reaching the seat. Entry into the seat is aided by both foot and hand supports. The payload decks are skewed 45 degrees from the forward direction to provide for better visibility and access. One helium tank is mounted on the oxidizer tank support. Two ground sensors are attached to the vehicle landing gear to signal surface contact for correct timing of engine cutoff. The sensors consist of flexible rods that actuate a switch which controls panel lights.

Details of the primary structure and landing gear are illustrated in Figure 22. The design utilizes beams to support the primary loads from the upper box frame, which is supported on the lower cruciform landing gear structure by the eight attenuators. The upper frame is sheeted top and bottom. Two cantilever beams, integrally stiffened, provide the support for each of the two propellant tanks. Two additional beams are utilized to support each of the two cargo decks. The cargo is supported by the cargo deck skin. Since the cargo decks must be folded 45 degrees for stowing, a hinge and lock are required. The pilot seat, backpack support, console, and footrest form an integral assembly (see Figure 20) that is supported by the central structure through seat translation tracks.

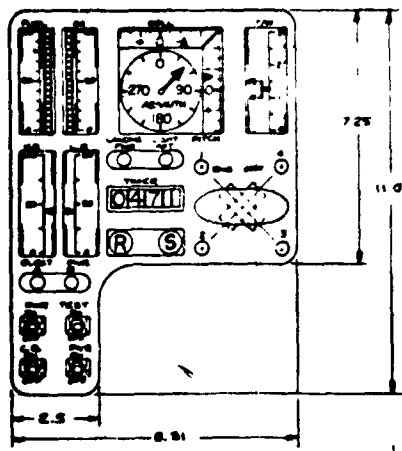
The four landing pads are integrally stiffened components rigidly attached to the cruciform structure that forms the four landing legs. Skin-stringer design was employed for the cruciform structure after other concepts were investigated. The triangular cross section provides two compression caps and a single tension cap with internal bulkheads located to stabilize the member and provide load-spreading capability at points of concentrated load.

Preliminary design selection of material indicates the use of 7075 aluminum throughout most of the upper and lower structures. The propellant tanks are 6AL-4VA titanium. The seat assembly is integrally stiffened, molded fiberglass. To balance the fore and aft payload disparities that may

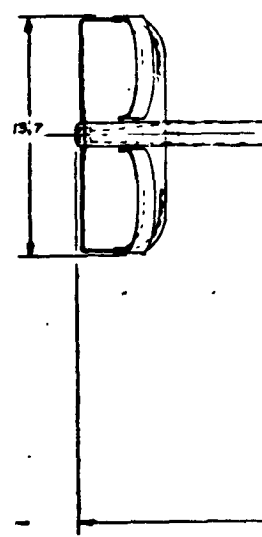


ATTITUDE CONTROLLER - MODIFIED APPROX.  
INC 301-017E

DEPLOYMENT HANDLE



DISPLAY PANEL - SCALE 1/2

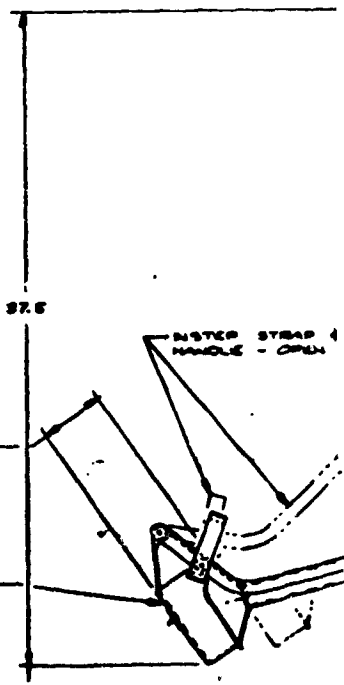


37.5

4.0 - FOOT RESTRAINT ADJUSTMENT FOR  
10% TO 80% G

FOOT RESTRAINT

INSTR STRAP  
HANDLE - OPEN



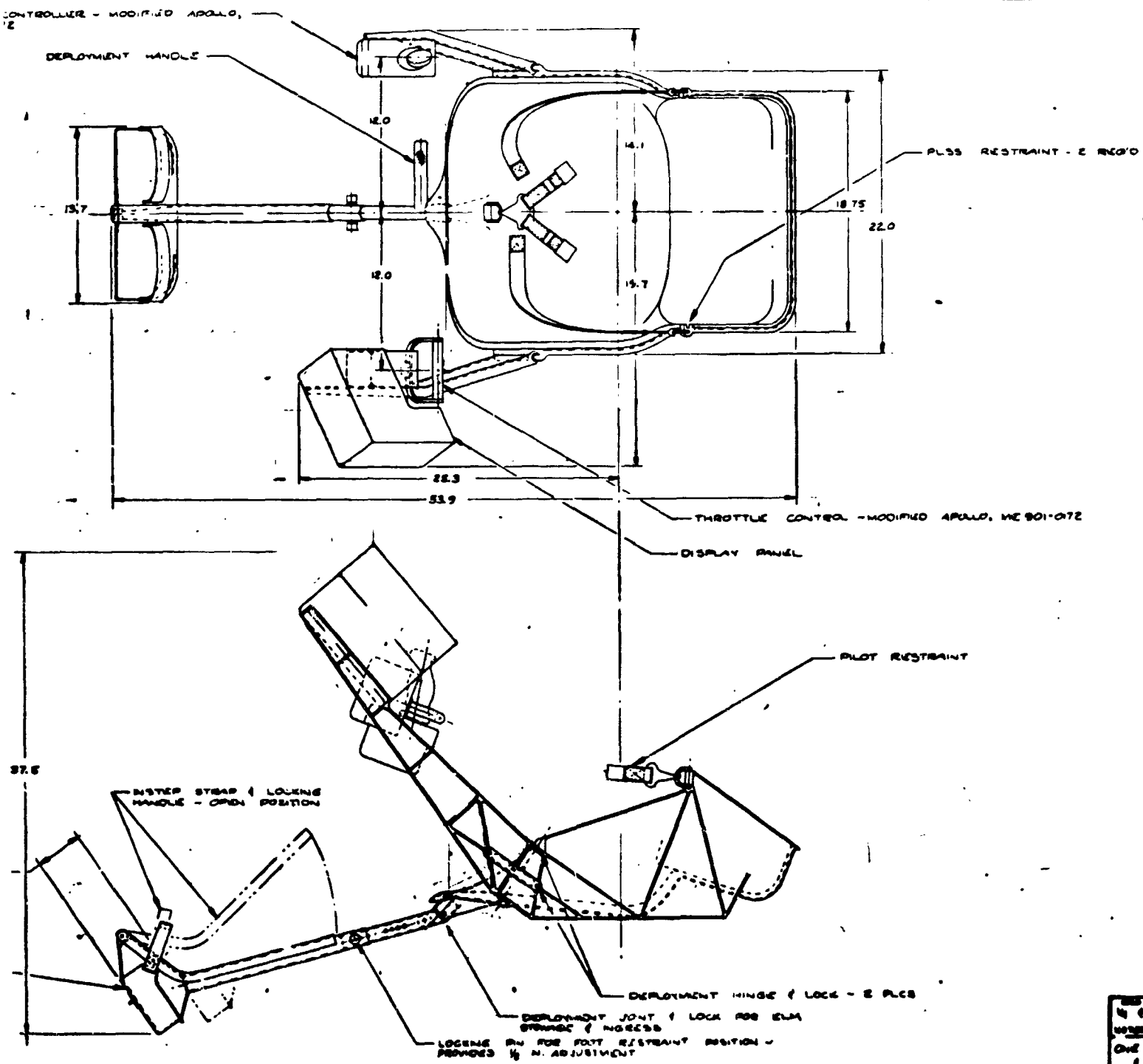


Figure 20. Seat and Instrument Panel Asse

PRECEDING PAGE BLANK NOT FILMED. 49, 50 -

FOLDOUT FRAME

FOLDOUT FRAME

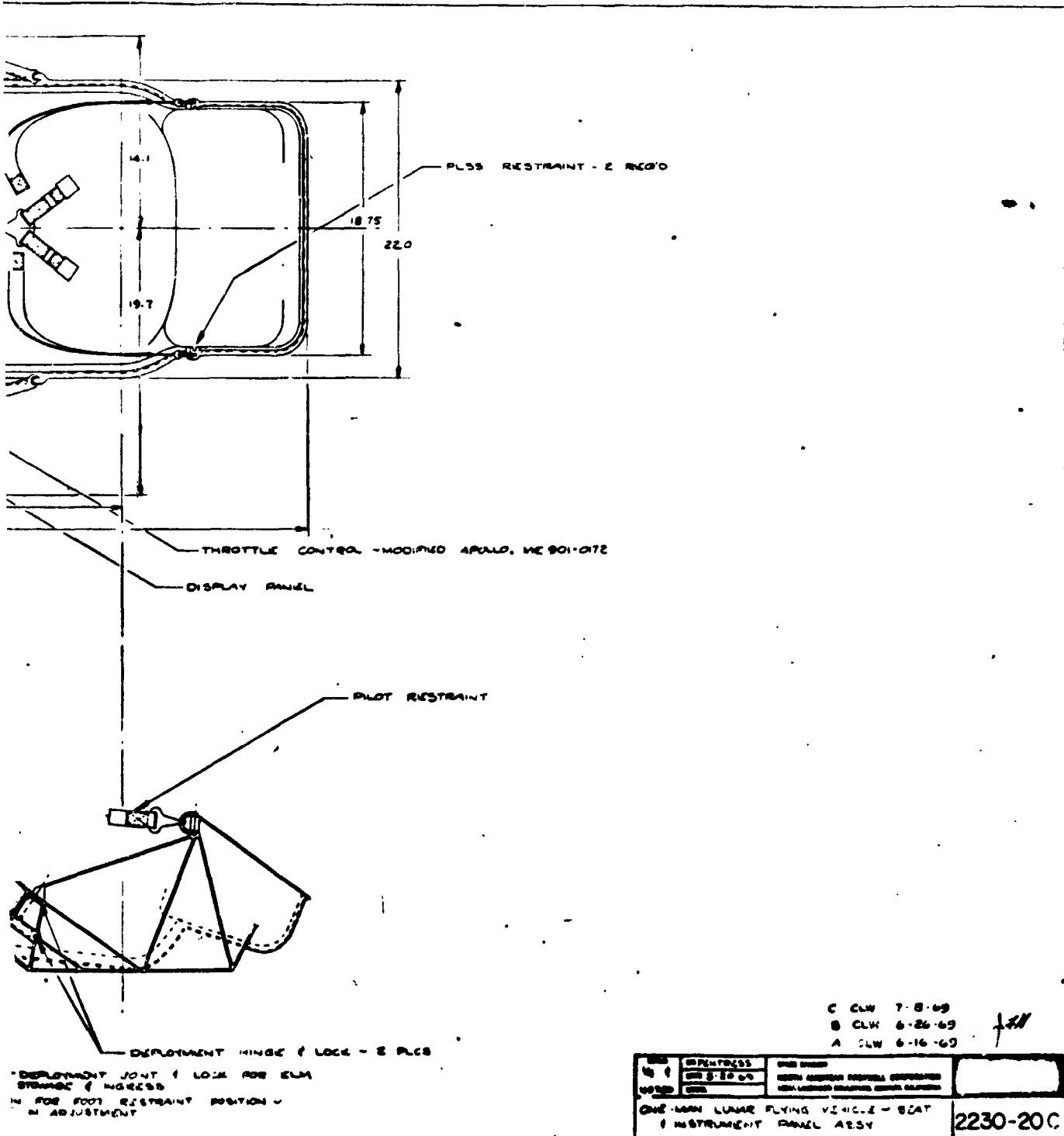
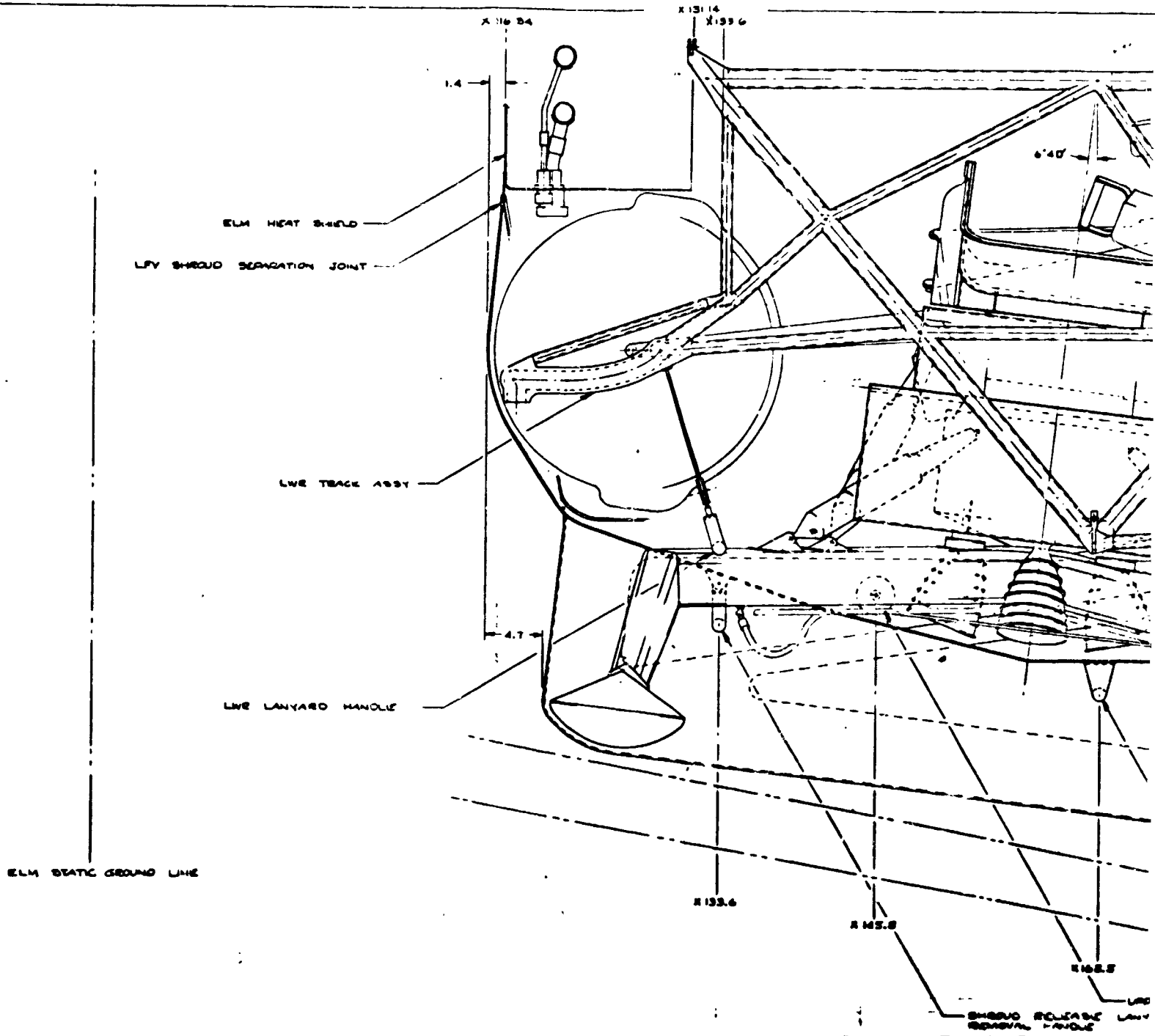


Figure 20. Seat and Instrument Panel Assembly (Drawing 2230-20C)

PRECEDING PAGE BLANK NOT FILMED. 49, 50 -

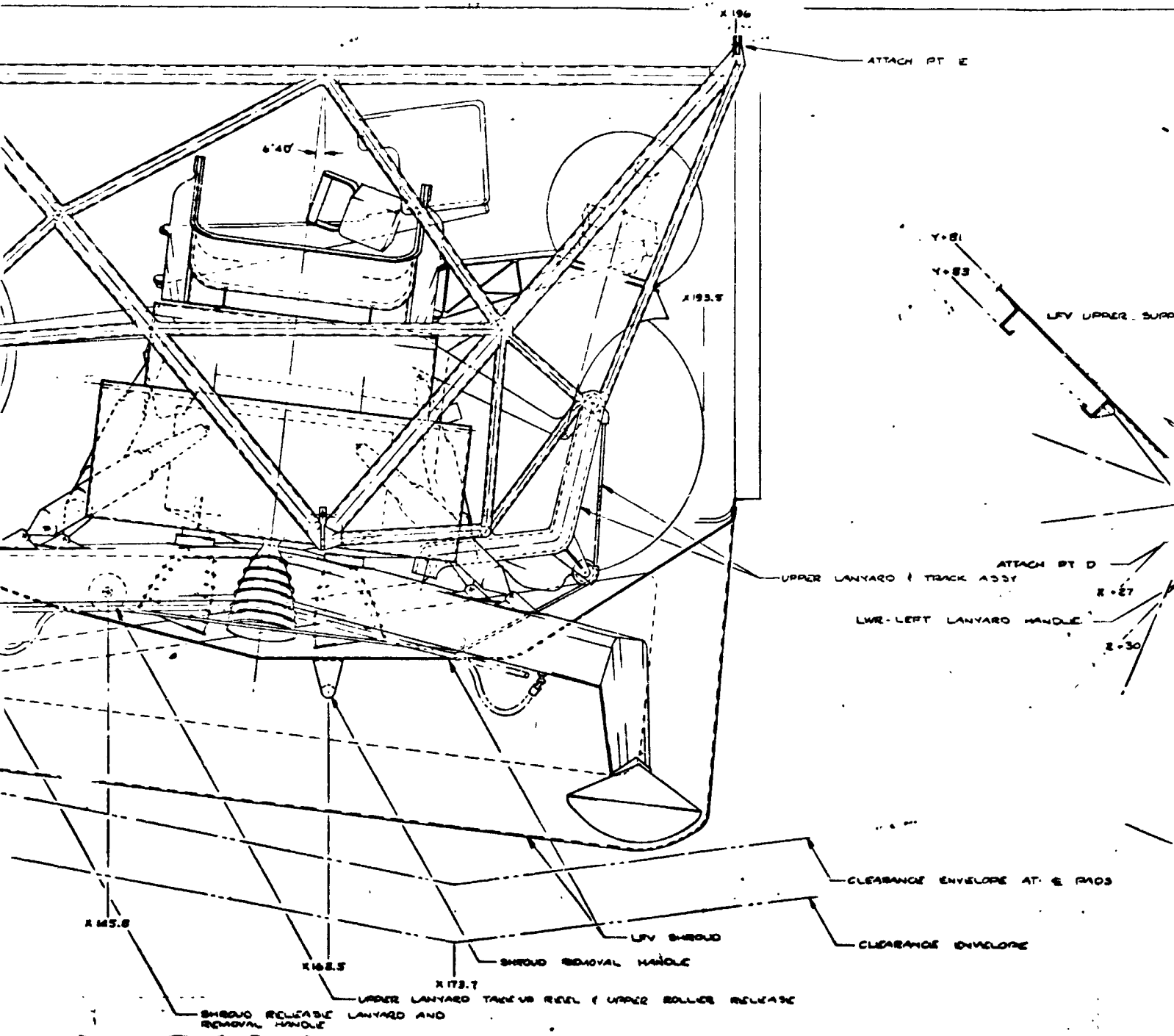
FOLDOUT FRAME

SD 69-419-4

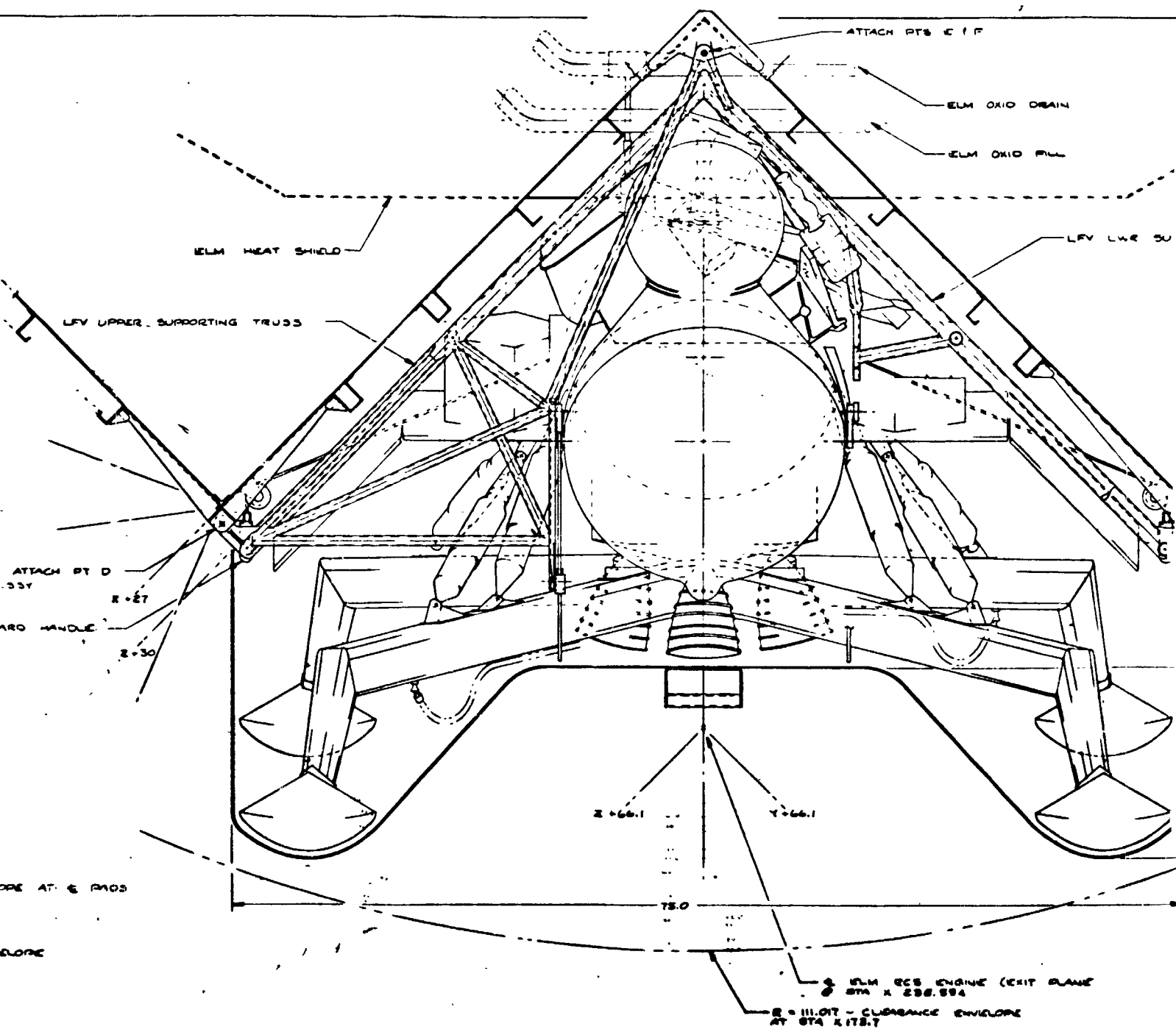


FOLDOUT FRAME

FOLDOUT



FOLDOUT FRAME



FOLDOUT FRAME

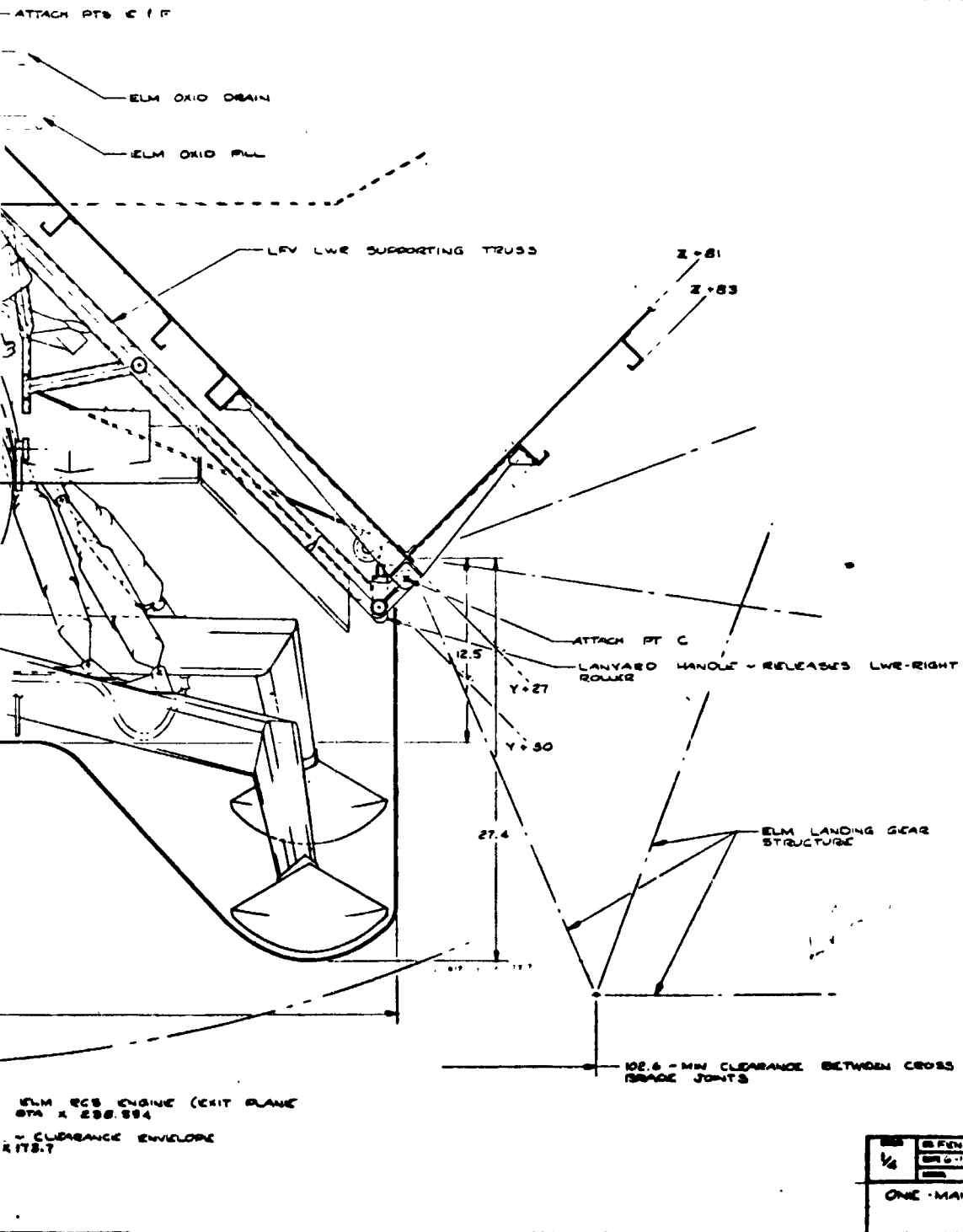
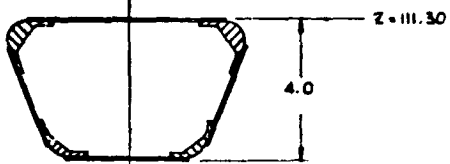
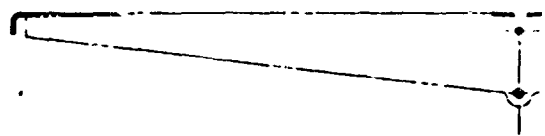
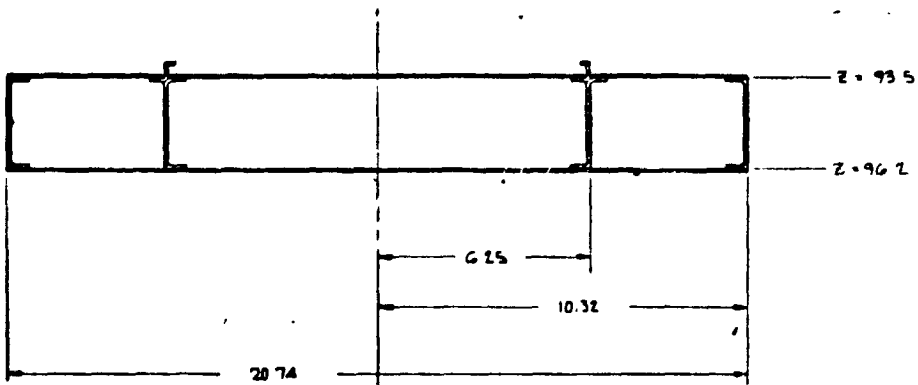
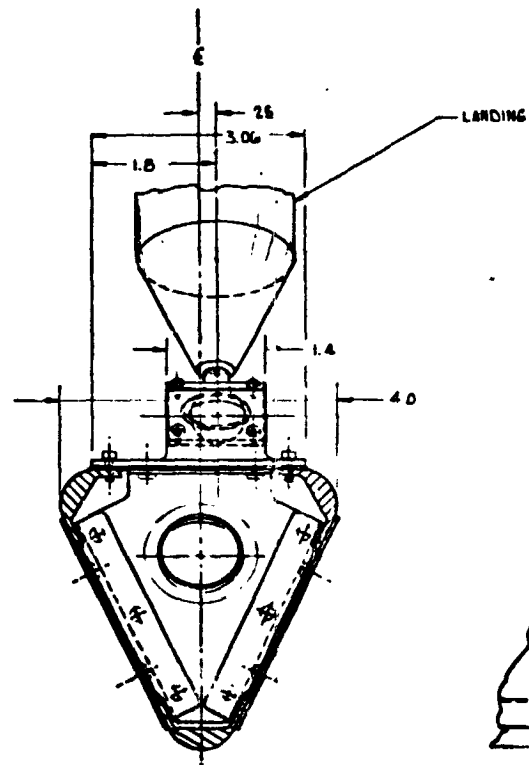


Figure 21. Preliminary Design Stowage Arrangement (Drawing 2230-24)

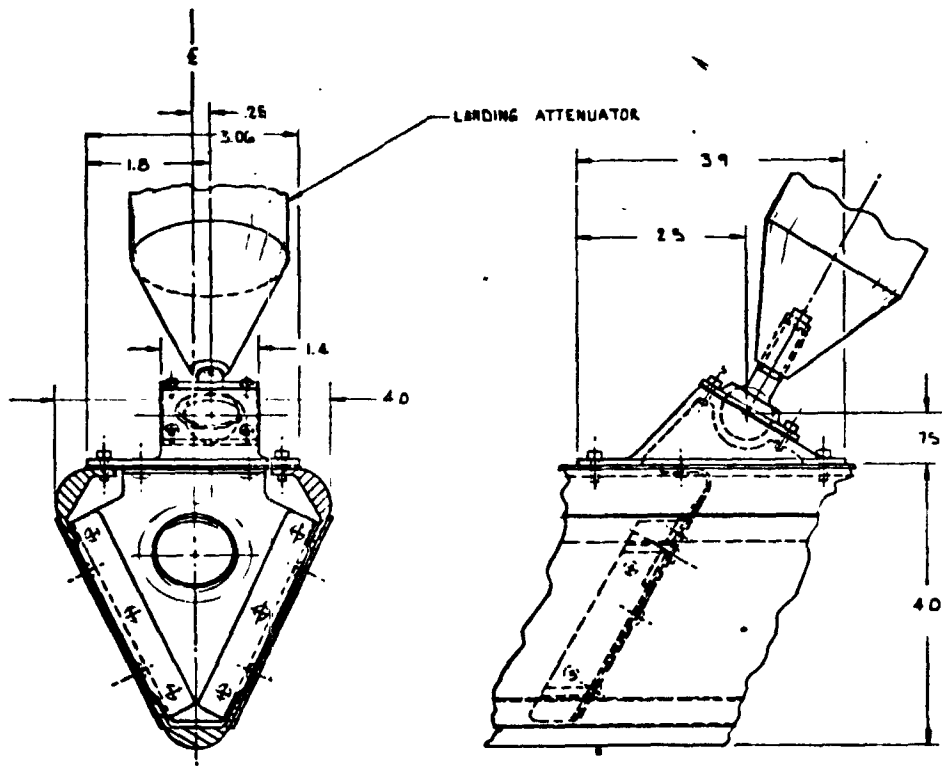
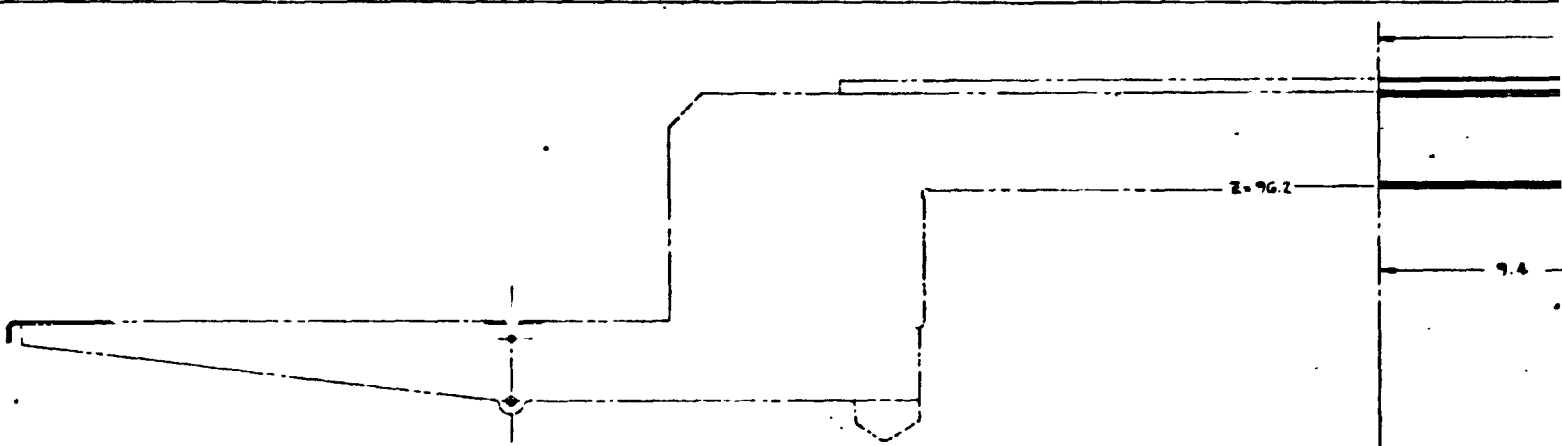


SECTION B - B  
SCALE: HALF

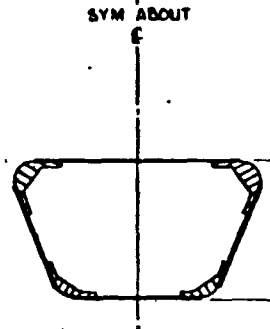


VIEW C  
SCALE: FULL

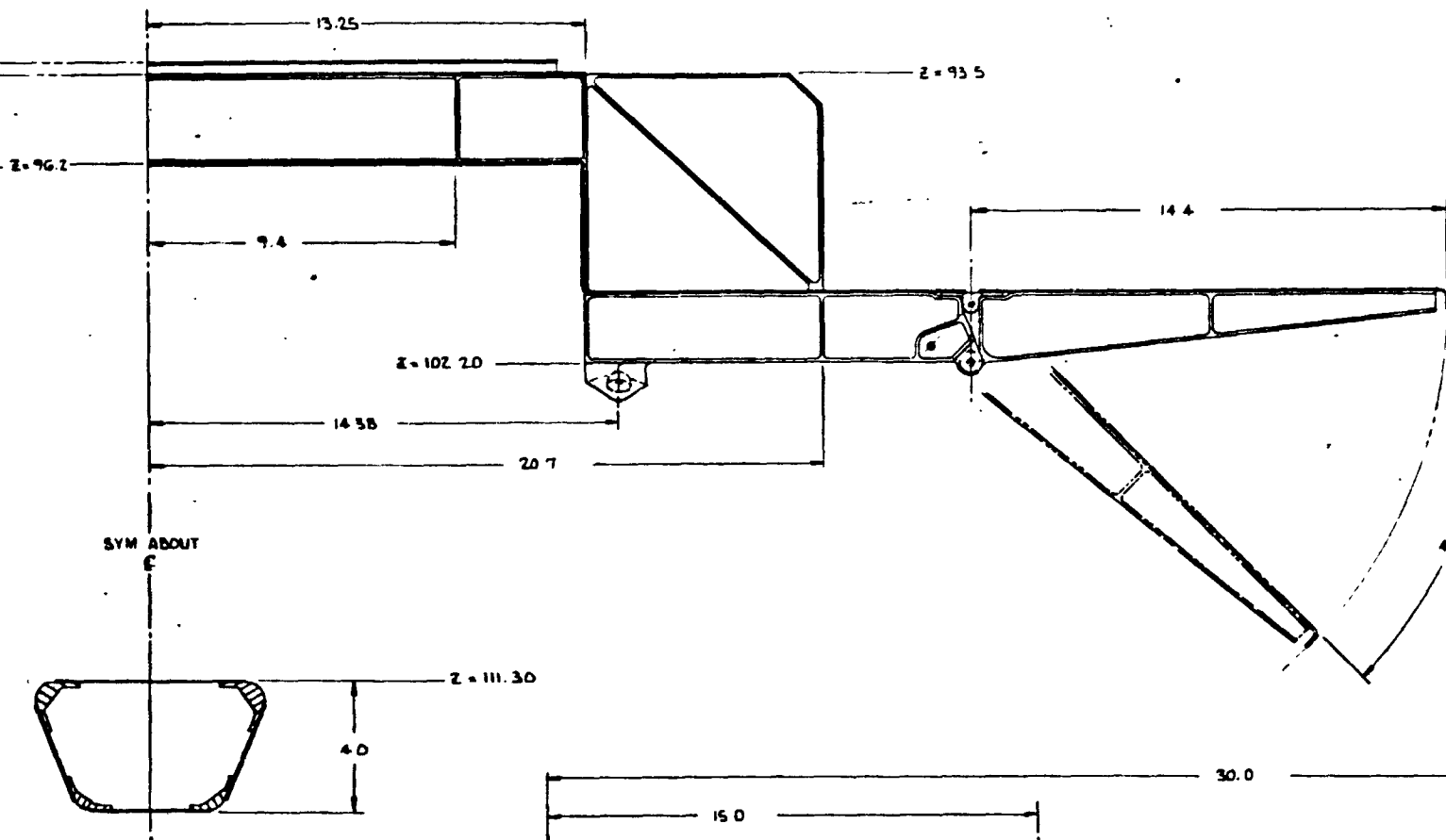




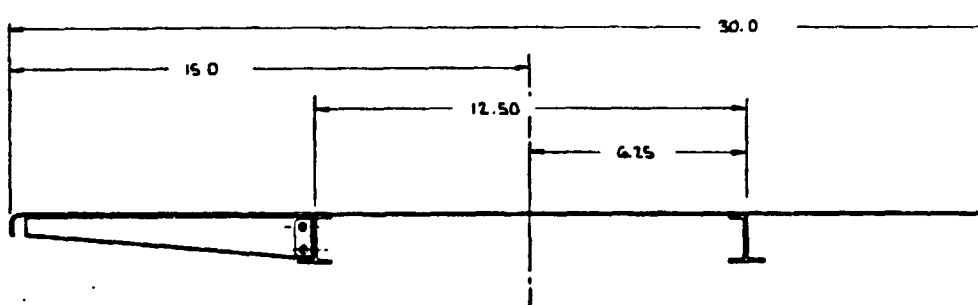
VIEW C  
SCALE: FULL



SECTION A-A  
SCALE: HALF

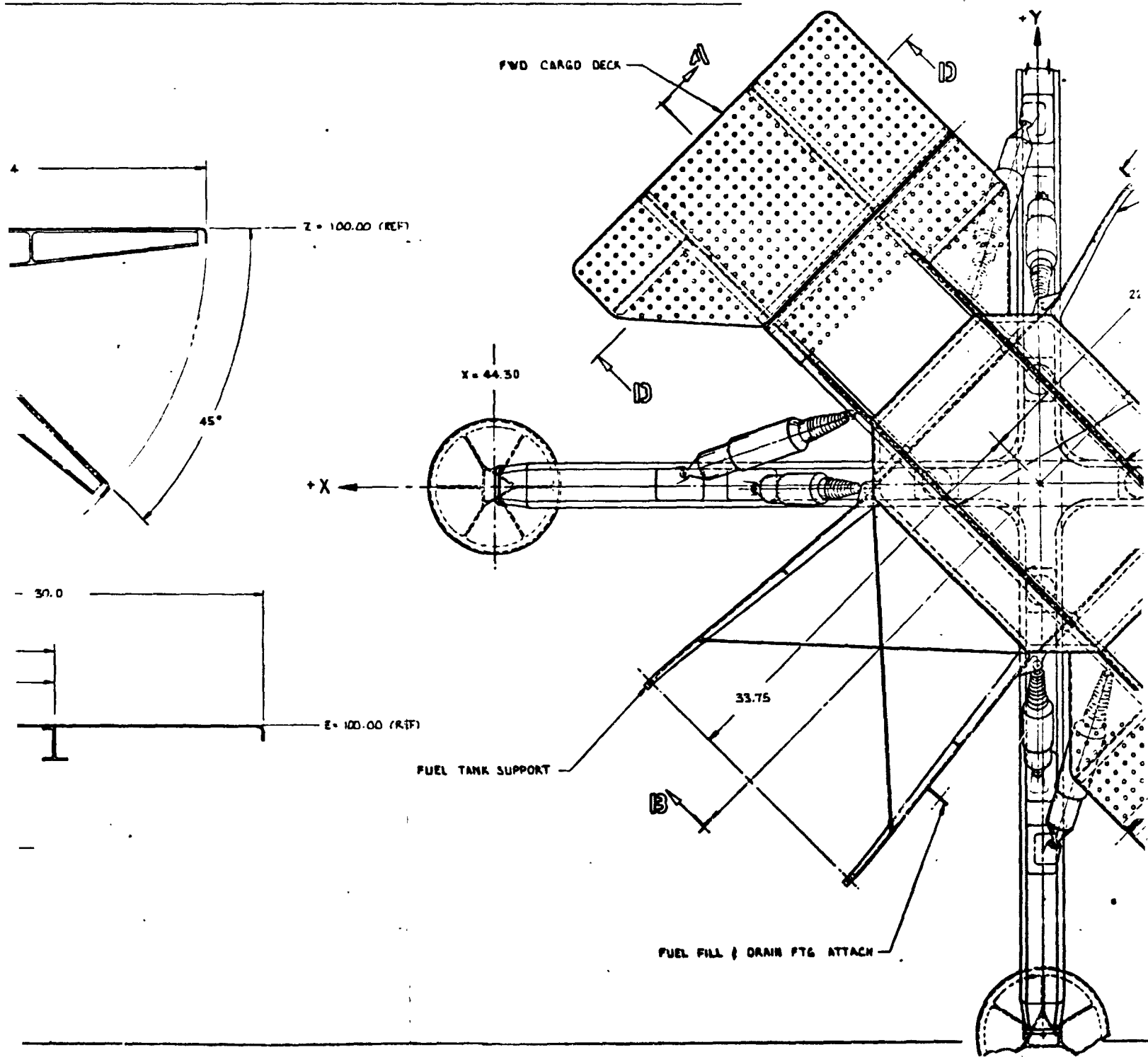


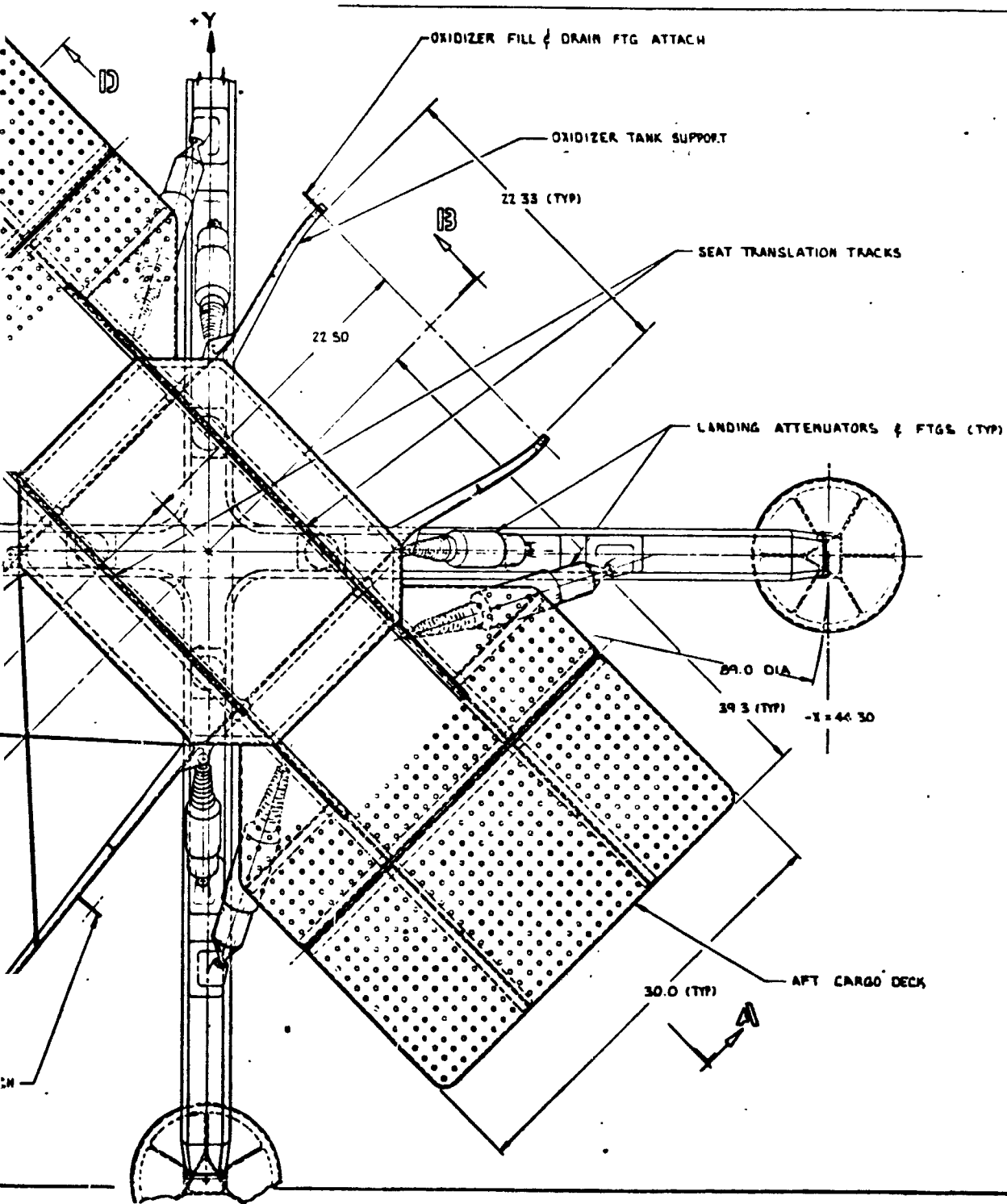
SECTION A-A  
SCALE: HALF



SECTION D-D  
SCALE: HALF

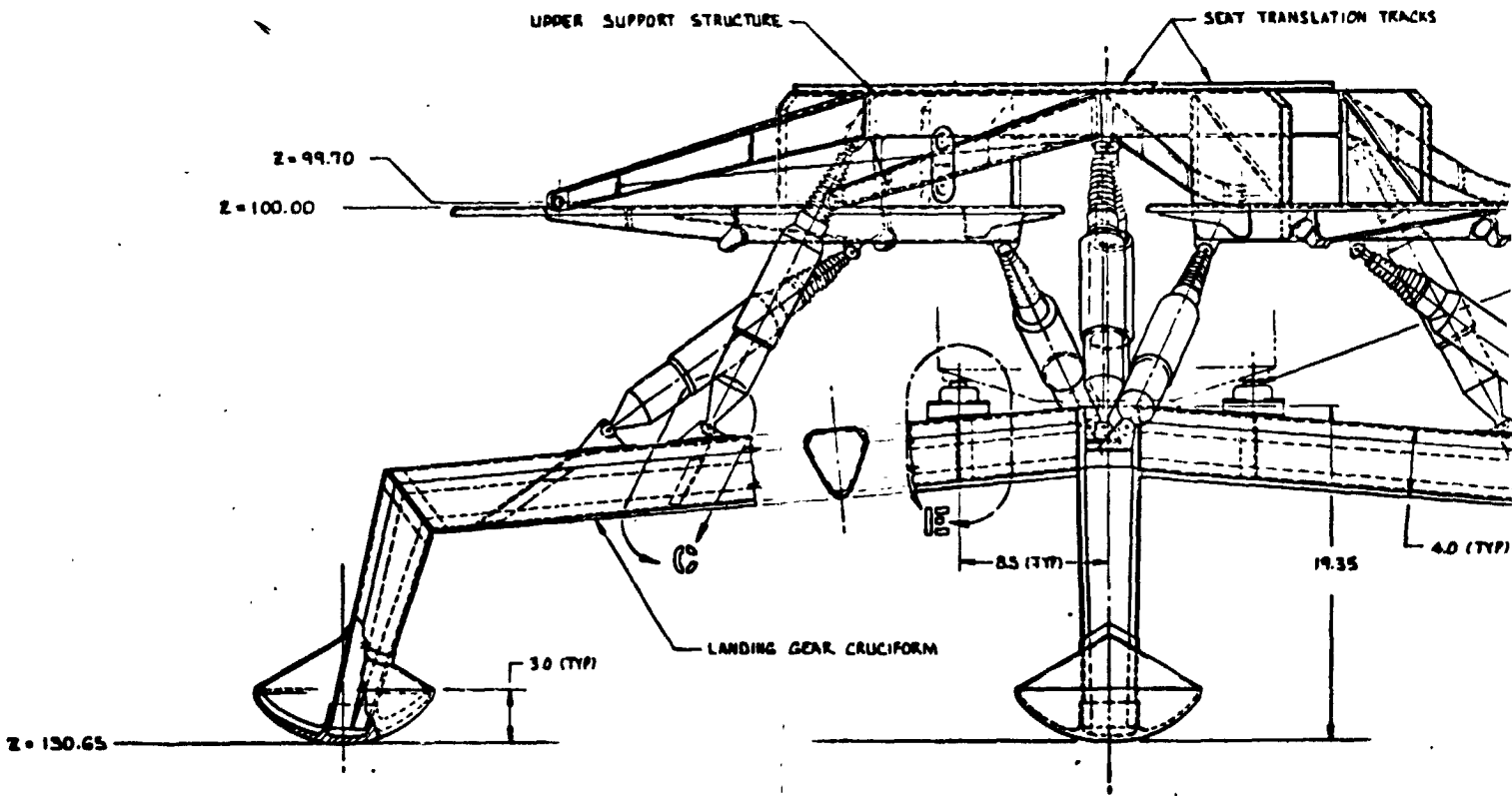
FOLDOUT FRAME

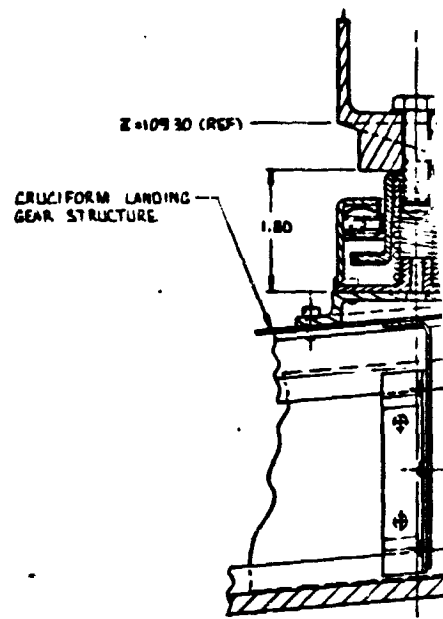
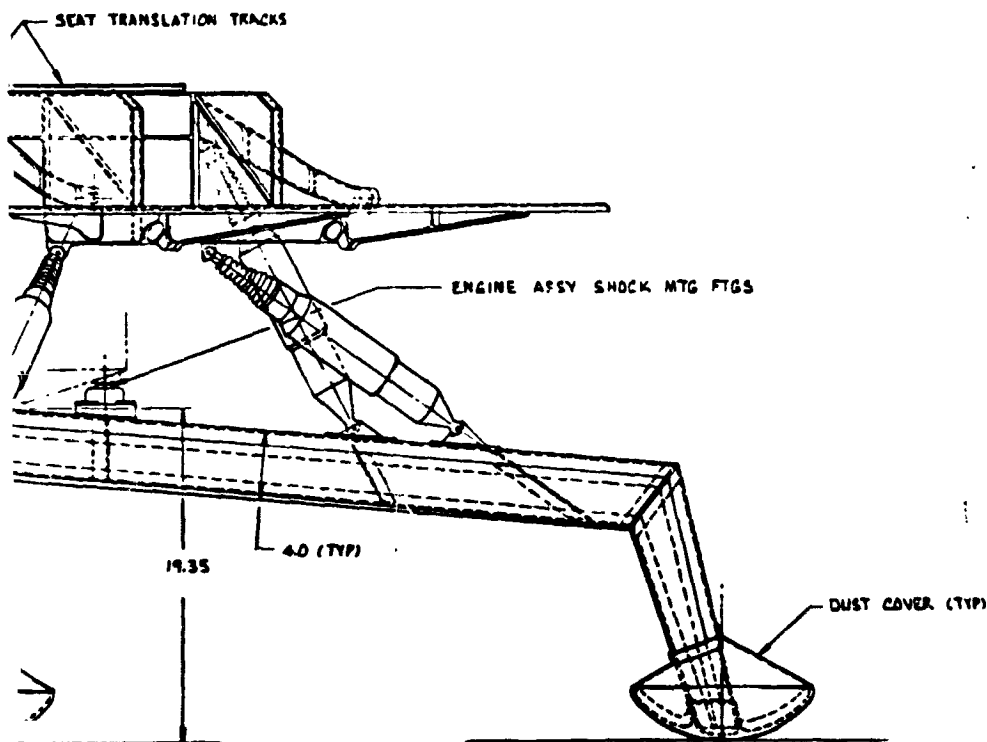




FOLDOUT FRAME

FOLDOUT FRAME





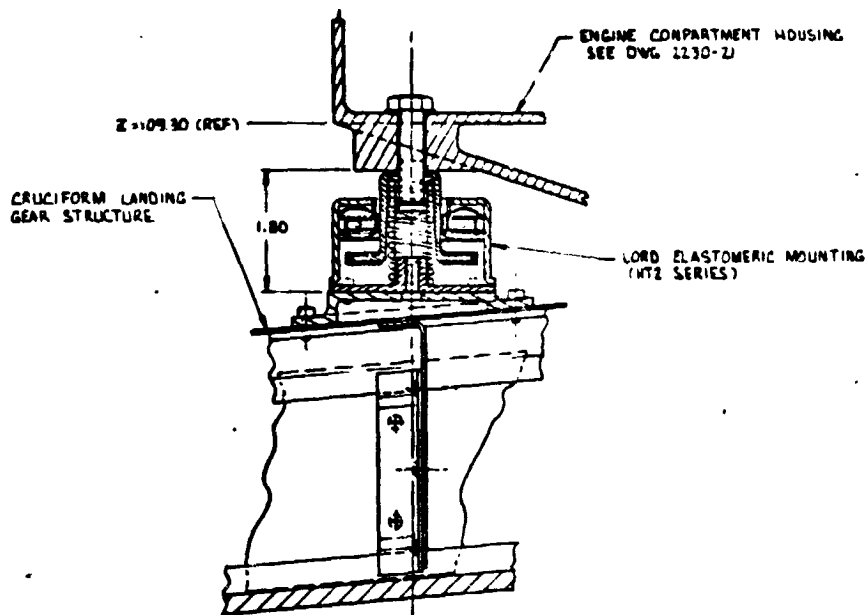
SECTION  
SCALE

Figure 22, Prelimin

FOLDOUT FRAME

FOLDOUT FRAME

UPSIZE PAGEMAT - 120% KEYLINE IMAGE AREA  
BLOW UP CALLOUTS 120% - REDUCE TO 50% OF ORIGINAL



SECTION **D/E**  
SCALE: FULL

DUST COVER (TYP)

REVISION CHANGE 7-22-69

|   |                       |                      |          |
|---|-----------------------|----------------------|----------|
| DATE<br>7/22/69   | BY<br>J. J. [unclear] | CHKD BY<br>[unclear] | 2230-25A |
| ONE MAN LUNAR FLIGHT<br>STRUCTURE & LANDING GEAR ASSEMBLY |                       |                      |          |

Figure 22. Preliminary Design Structure and Landing Gear.  
(Drawing 2230-25)

FOLDOUT FRAME

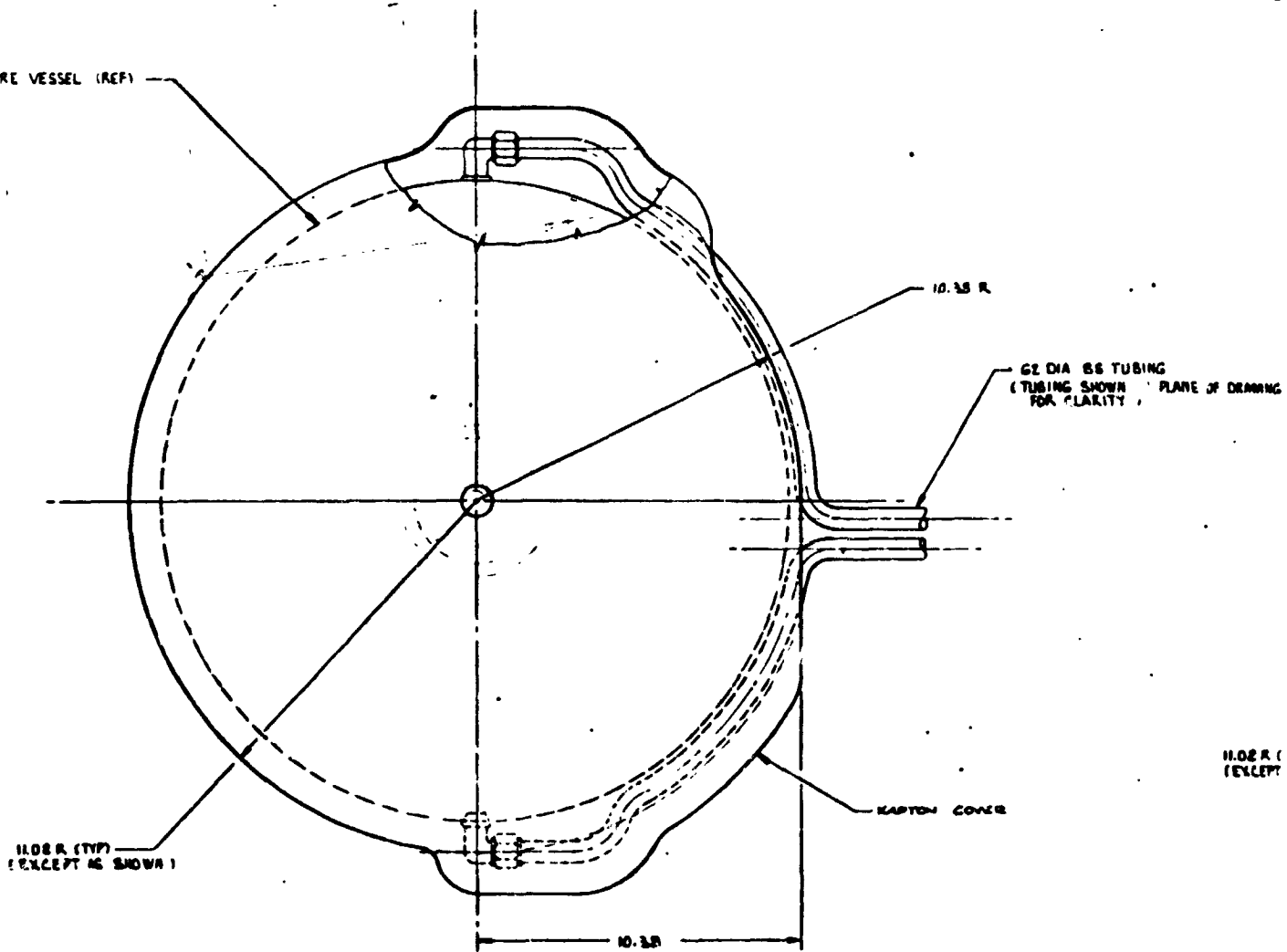
- 53, 54 -

SD 69-419-4

UPSIZE Pagemat - 120% KEYLINE IMAGE AREA  
BLOW UP CALLOUTS 120% - REDUCE TO 83% OF ORIGINAL

PLEASE MAKE CORRECTIONS ON TISSUE OVERLAYS  
OR READING COPY IF AVAILABLE

2230-105 PRESSURE VESSEL (REF)



11.02 R (EXCEPT AS SHOWN)

10.35 R

62 DIA SS TUBING  
(TUBING SHOWN IN PLANE OF DRAWING  
FOR CLARITY)

KARTON COVER

11.02 R  
(EXCEPT

10.35

N<sub>2</sub>O<sub>4</sub> TANK

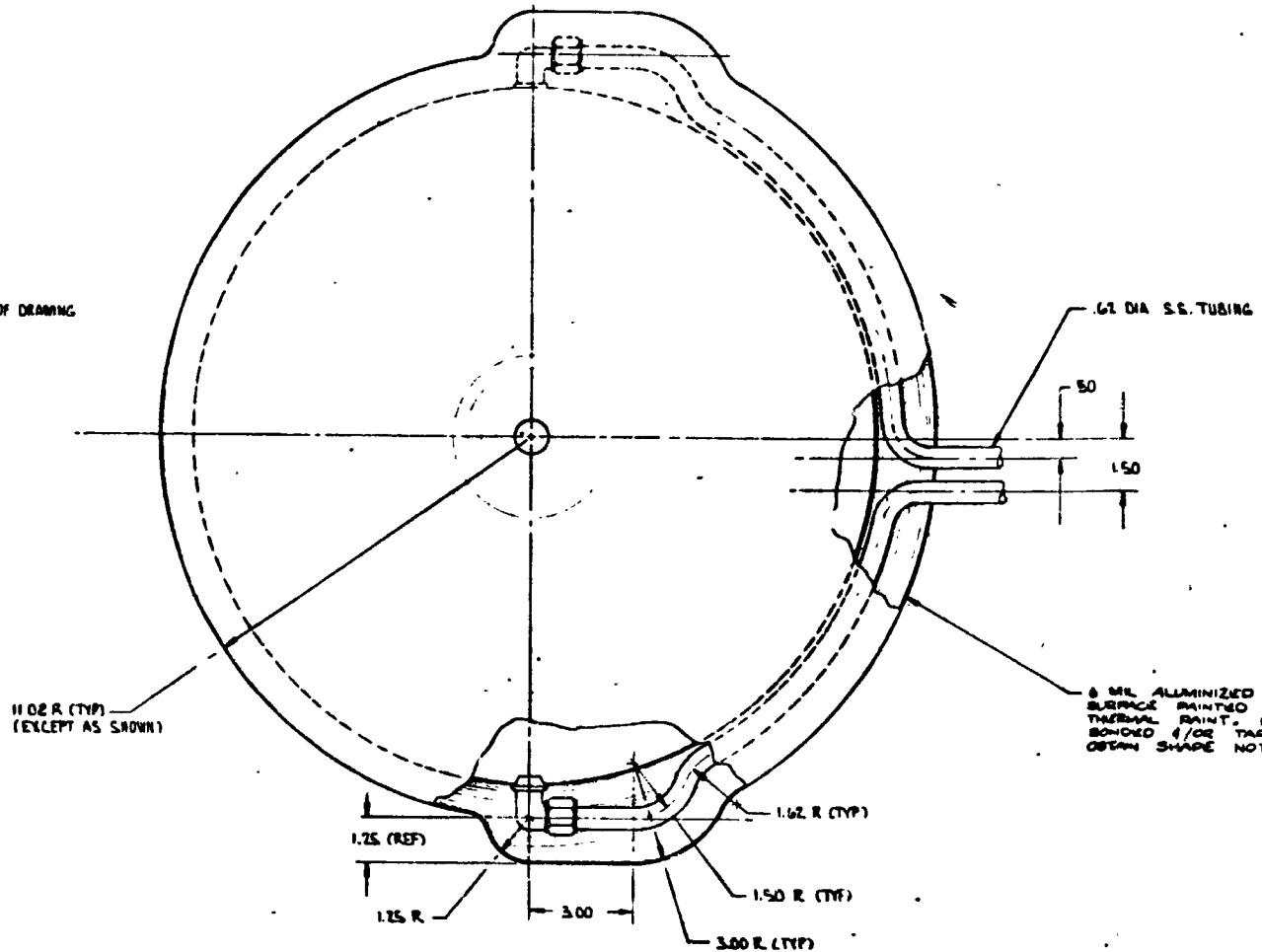
(IDENTICAL TO AEROLINE 50 TANK EXCEPT AS SHOWN)

FOLDOUT FRAME

FOLDOUT FRAM

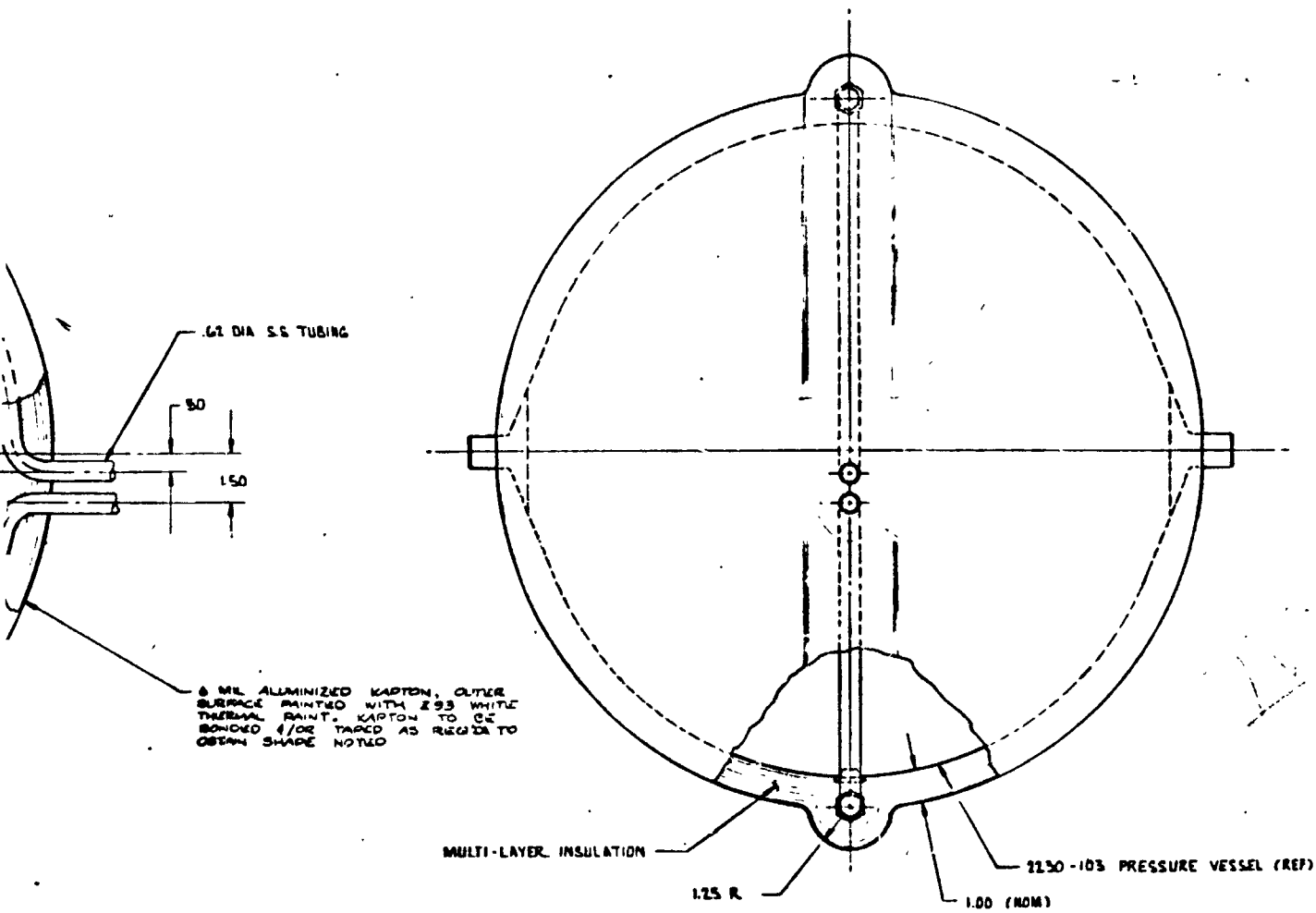


.62 DIA S.S. TUBING  
(TUBING SHOWN IN PLANE OF DRAWING  
FOR CLARITY)



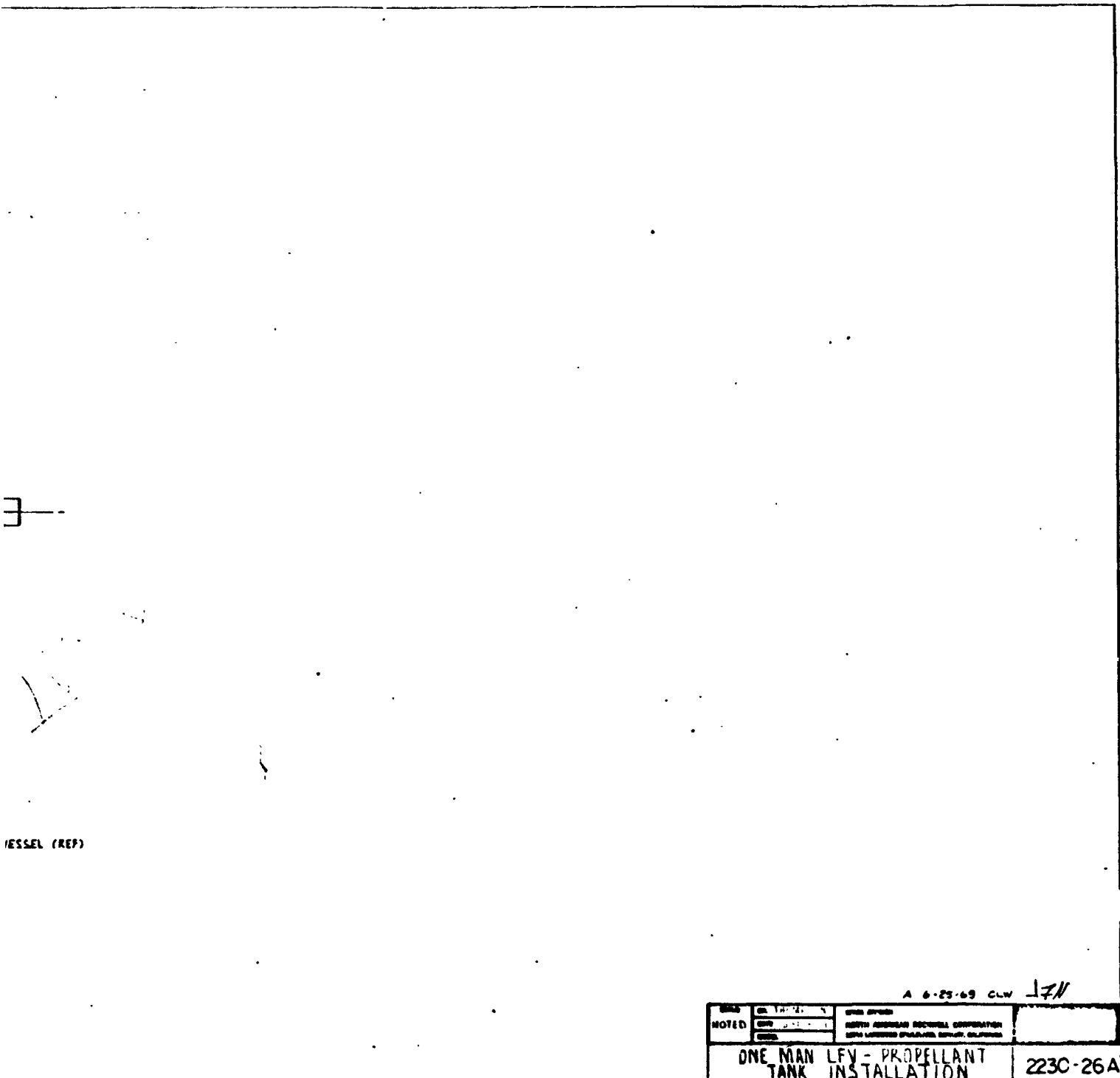
AEROZINE 50 TANK

FOLE-OUT FRAME



AEROZINE 50 TANK

FOLDOUT FRAME

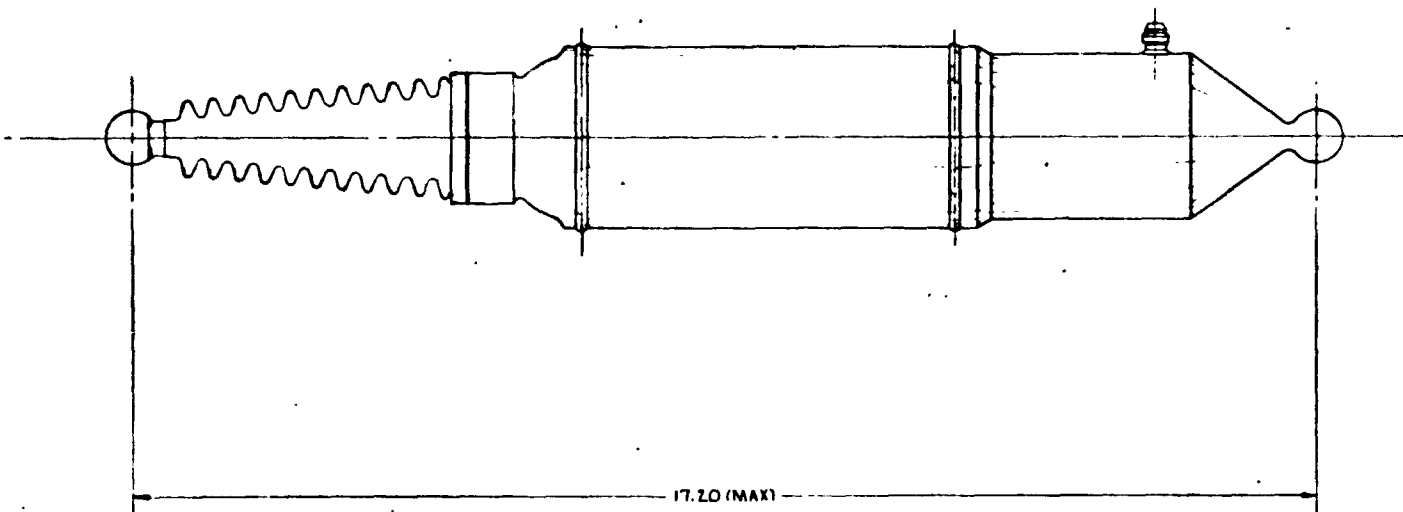


VESSEL (REF)

A 6-25-69 CLW JFV

|  |    |       |          |
|--|----|-------|----------|
| DATE   | BY | APP'D |          |
| NOTED  |    |       |          |
| NORTH AMERICAN ROCKWELL CORPORATION<br>4800 LANTANA DRIVE, CANON, CALIFORNIA |    |       |          |
| ONE MAN LFV - PROPELLANT<br>TANK INSTALLATION                                |    |       | 2230-26A |

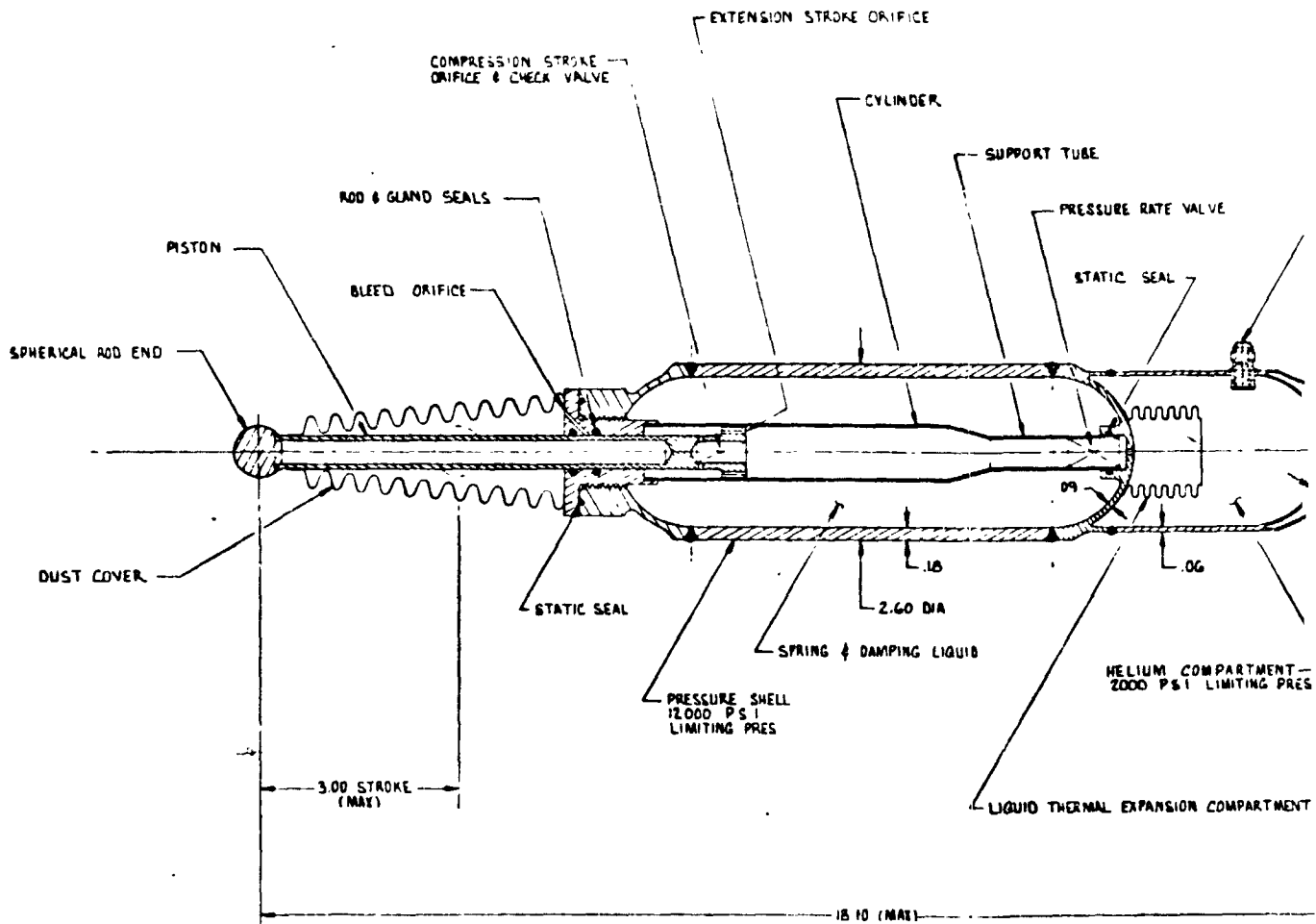
Figure 23. Propellant Tank Installation (Drawing 2230-26A)



ATTENUATOR - TYPE I

( IDENTICAL TO TYPE II EXCEPT AS SHOWN )  
SCALE: FULL

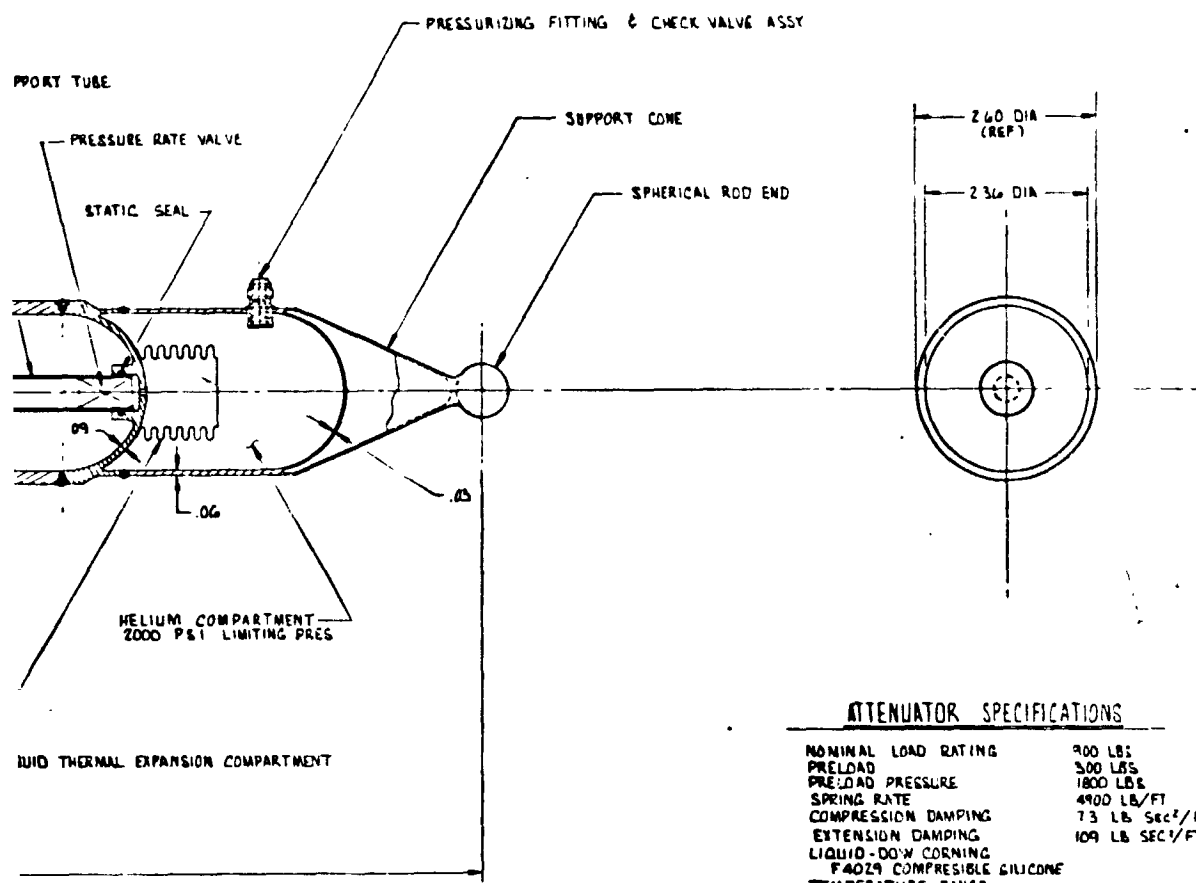
FOLDOUT FRAME



**ATTENUATOR - TYPE II**

SCALE: FULL

BOLDOUT DRAW



**ATTENUATOR SPECIFICATIONS**

|                             |  |
|-----------------------------|--|
| NOMINAL LOAD RATING         | 900 LBS                                  |
| PRELOAD                     | 500 LBS                                  |
| PRELOAD PRESSURE            | 1800 LBS                                 |
| SPRING RATE                 | 4900 LB/FT                               |
| COMPRESSION DAMPING         | 73 LB SEC <sup>2</sup> /FT <sup>2</sup>  |
| EXTENSION DAMPING           | 109 LB SEC <sup>2</sup> /FT <sup>2</sup> |
| LIQUID-DOWN CORNING         |  |
| F4029 COMPRESSIBLE SILICONE |  |
| TEMPERATURE RANGE           |  |
| STORAGE                     | -65° TO 195° F                           |
| OPERATING                   | 0° TO 125° F                             |
| RATED LIFE                  | 200 CYCLES                               |

Fig

FOLDOUR FRAME



REQUIREMENTS

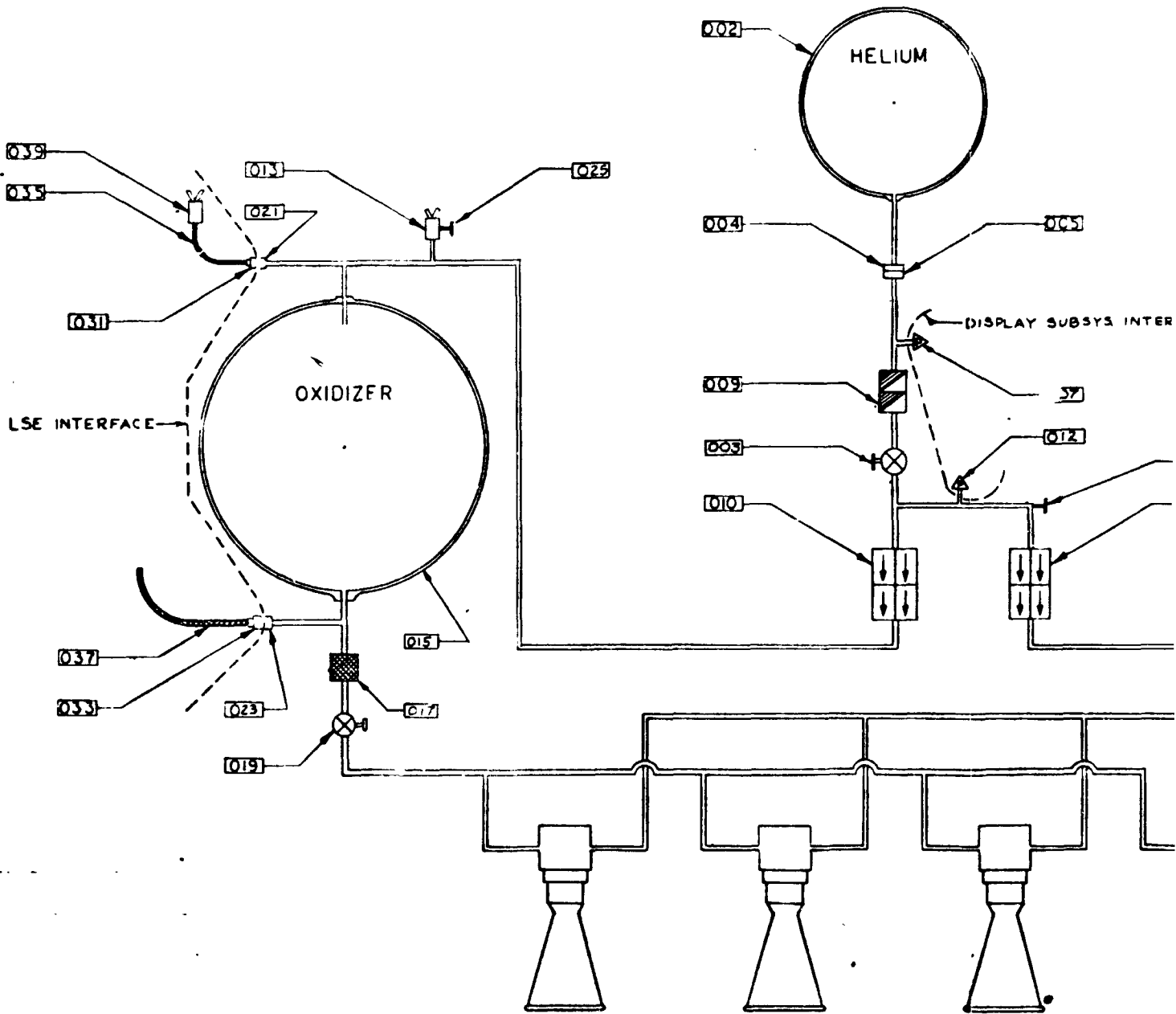
- 900 LBS
- 300 LBS
- 1800 LBS
- 4900 LB/FT
- 73 LB SEC<sup>2</sup>/FT<sup>2</sup>
- 109 LB SEC<sup>2</sup>/FT<sup>2</sup>

ENVIRONMENT

- 65° TO 195° F
- 0° TO 125° F
- 200 CYCLES

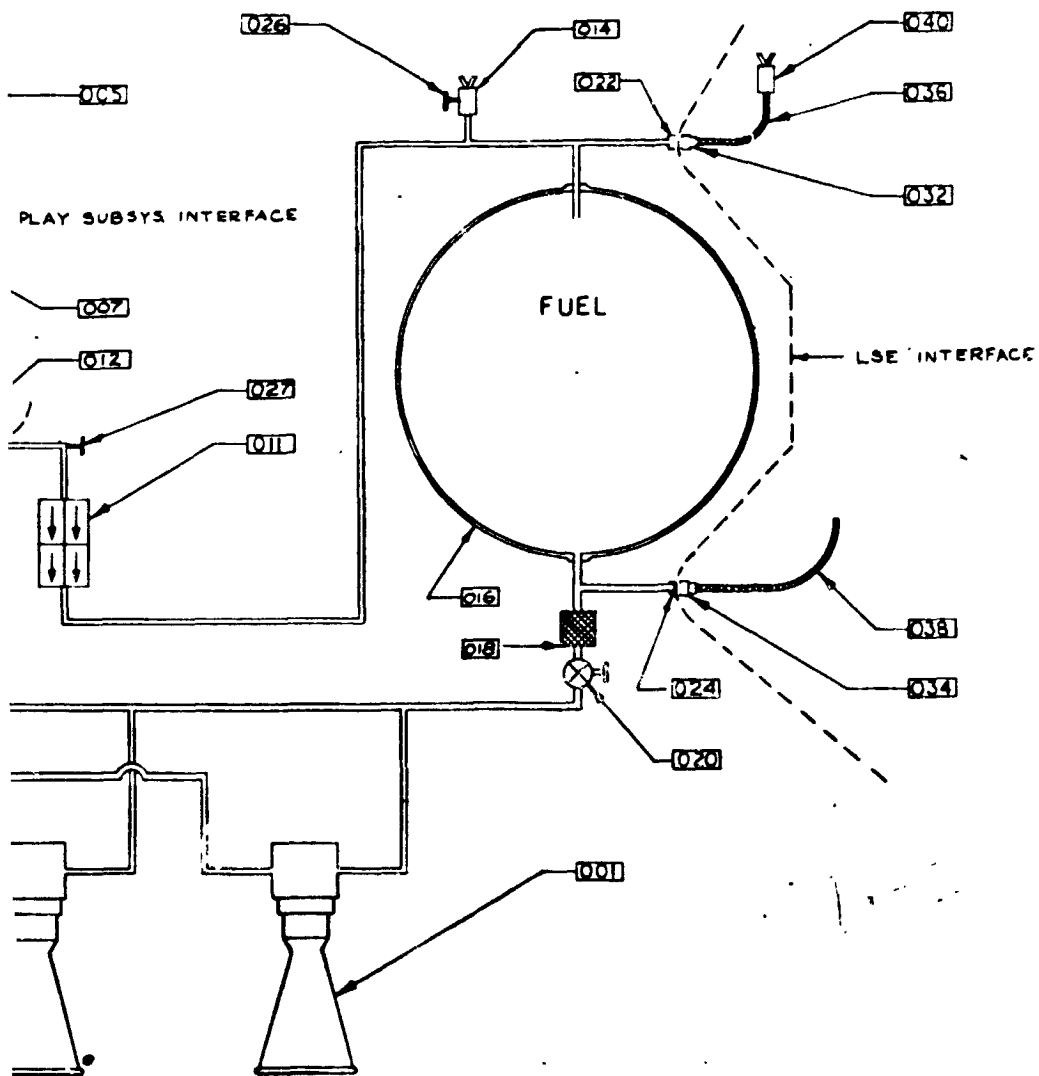
|  |      |    |         |
|--|------|----|---------|
| REV  | DATE | BY | APP'D   |
| FULL   |      |    |         |
| NORTH AMERICAN ROCKWELL CORPORATION<br>4801 LINDSEY BLVD., CANON, CALIFORNIA |      |    |         |
| ONE MAN LFV ATTENUATOR CONCEPT   |      |    | 2230-27 |

Figure 24. Preliminary Design Attenuator (Drawing 2230-27)



FOLDOUT FRAME





① REDESIGN FOR PRESSURE AND SPACE QUALIFICATION  
 ② REDESIGN TO NEW SYSTEM AND REDESIGNATION MAY BE  
 NOTE: UNLESS OTHERWISE SPEC

FOLDCUT FRAME

FOLDCUT



| REVISIONS |   |
|-----------|---|
| A         | DELETED VLV ITEM 006<br>RELOCATED VLV ITEM 003<br>A. J. Beck<br>4-2-69  |
| B         | DELETED ONE AND RELOCATED<br>OTHER PRESS SENSOR ITEM 012.<br>S. J. Beck<br>5-14-69  |
| C         | ADDED TEST POINT CPLGS ITEMS<br>025, 026, 027.<br>INDICATED LSE AND DISPLAY<br>SUBSYSTEM INTERFACES<br>S. J. Beck<br>6-5-69 |

| PART NO | QTY | DESCRIPTION                 | APOLLO PART NO     |
|---------|-----|-----------------------------|--------------------|
| 040     | 1   | VENT RELIEF, FUEL           | NEW PART           |
| 039     | 1   | VENT RELIEF, OXID           | NEW PART           |
| 038     | 1   | FILL HOSE, FUEL             | NEW PART           |
| 037     | 1   | FILL HOSE, OXID.            | NEW PART           |
| 036     | 1   | VENT HOSE, FUEL             | NEW PART           |
| 035     | 1   | VENT HOSE, OXID             | NEW PART           |
| 034     | 1   | FILL COUPLING, FUEL 1/2 IN  | ME 273-0021-0001   |
| 033     | 1   | FILL COUPLING, OXID 1/2 IN  | ME 273-0022-0001   |
| 032     | 1   | VENT COUPLING, FUEL 1/2 IN  | ME 273-0023-0001   |
| 031     | 1   | VENT COUPLING, OXID 1/2 IN  | ME 273-0024-0001   |
| 012     | 1   | PRESS SENSOR, HEL. RES.     |                    |
| 007     | 1   | PRESS SENSOR, HEL. HIGH     |                    |
| 029     | 1   | FILL COUPLING, FUEL 1/4 IN  | ME 273-0021-0001   |
| 023     | 1   | FILL COUPLING, OXID 1/4 IN  | ME 273-0022-0001   |
| 020     | 1   | MANUAL VALVE, FUEL          | NEW PART           |
| 019     | 1   | MANUAL VALVE, OXID.         | NEW PART           |
| 018     | 1   | FILTER, FUEL                | ME 284-0039 TYPE   |
| 017     | 1   | FILTER, OXID                | ME 284-0039 TYPE   |
| 027     | 1   | TEST POINT COUPLING, HELIUM | ME 184-0024-0001   |
| 026     | 1   | TEST POINT COUPLING, FUEL   | ME 184-0025-0001   |
| 025     | 1   | TEST POINT COUPLING, OXID   | ME 184-0026-0001   |
| 022     | 1   | VENT COUPLING, FUEL 1/2 IN  | ME 273-0023-0001   |
| 021     | 1   | VENT COUPLING, OXID 1/2 IN  | ME 273-0024-0001   |
| 014     | 1   | RELIEF VALVE, FUEL          | ME 284-0042-0001   |
| 013     | 1   | RELIEF VALVE, OXID          | ME 284-0043-0001   |
| 011     | 1   | CHECK VALVE A, FUEL         | ME 284-0044-0001   |
| 010     | 1   | CHECK VALVE ASSY, OXID      | ME 284-0045-0001   |
| 009     | 1   | PRESSURE REGULATOR          | ME 284-0046-0001   |
| 008     | 1   | HELIUM COUPLING, 1/4 IN     | ME 273-0010-0001   |
| 005     | 1   | MANUAL VALVE, HELIUM        | NEW PART           |
| 004     | 1   | HELIUM COUPLING TANK 1/2    | ME 273-0011-0001   |
| 003     | 1   | HELIUM VESSEL               | ME 282-0051-0001   |
| 016     | 1   | TANK, FUEL                  | MADE FROM 20 SEMIN |
| 015     | 1   | TANK, OXID                  | OAMS TANK SHELL    |
| 001     | 0   | ENGINE AND S VBLE           | NEW PART           |
| PART NO | QTY | DESCRIPTION                 | APOLLO PART NO     |

LIST OF MATERIALS

|     |          |        |    |
|-----|----------|--------|----|
| REV | REV. NO. | DATE   | BY |
|     | 1        | 4-2-69 | SA |

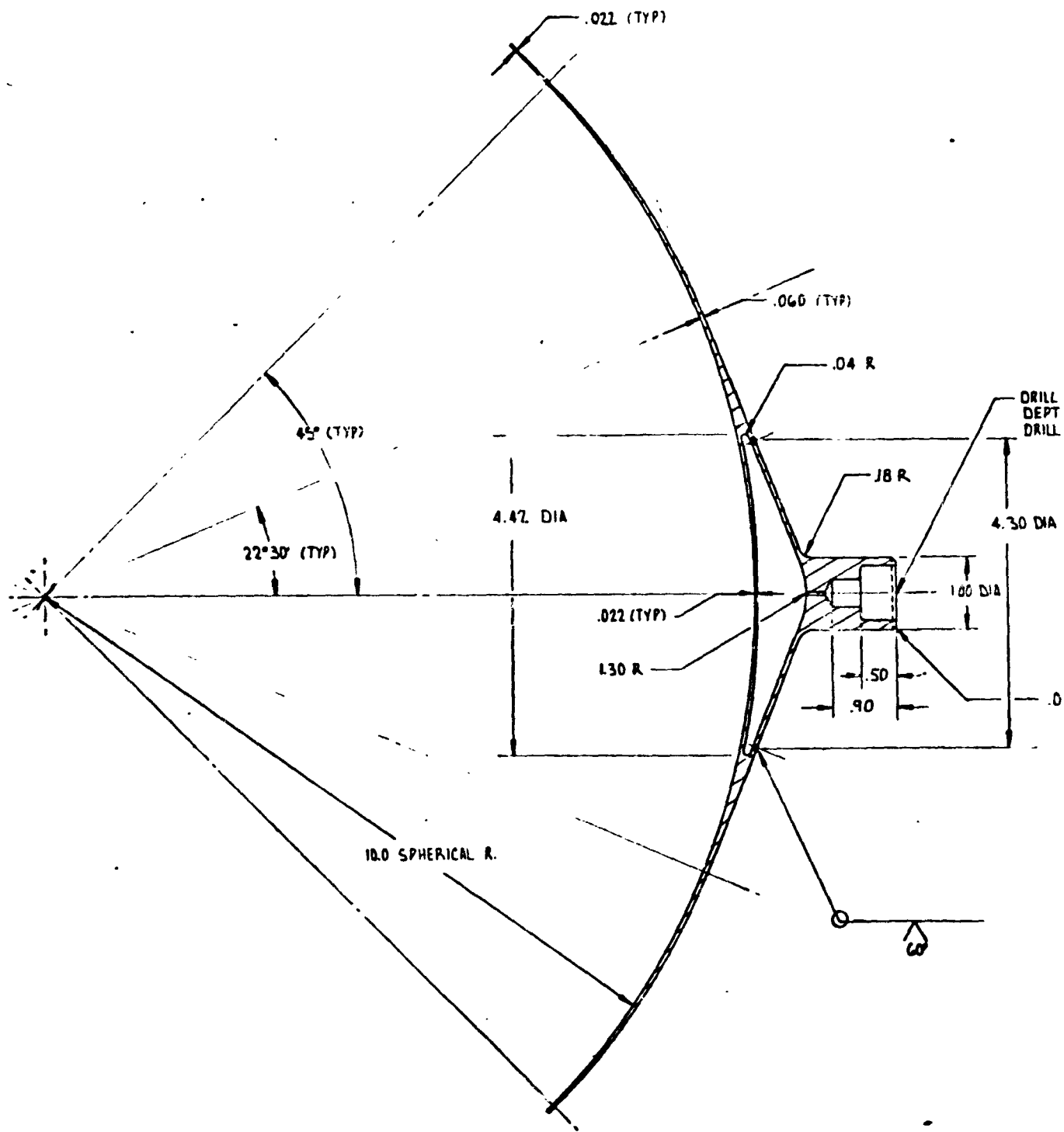
LUNAR FLYING VEHICLE,  
PROPULSION SUBSYSTEM  
SCHEMATIC


2230-101C

SHEET 1 OF 3

- ① REDESIGN FOR PRESSURE SUIT USE AND SPACE QUALIFICATION REQUIRED
  - ② REDESIGN TO NEW SYSTEM PRESSURE AND REDESIGNATION MAY BE REQUIRED.
- NOTE: UNLESS OTHERWISE SPECIFIED

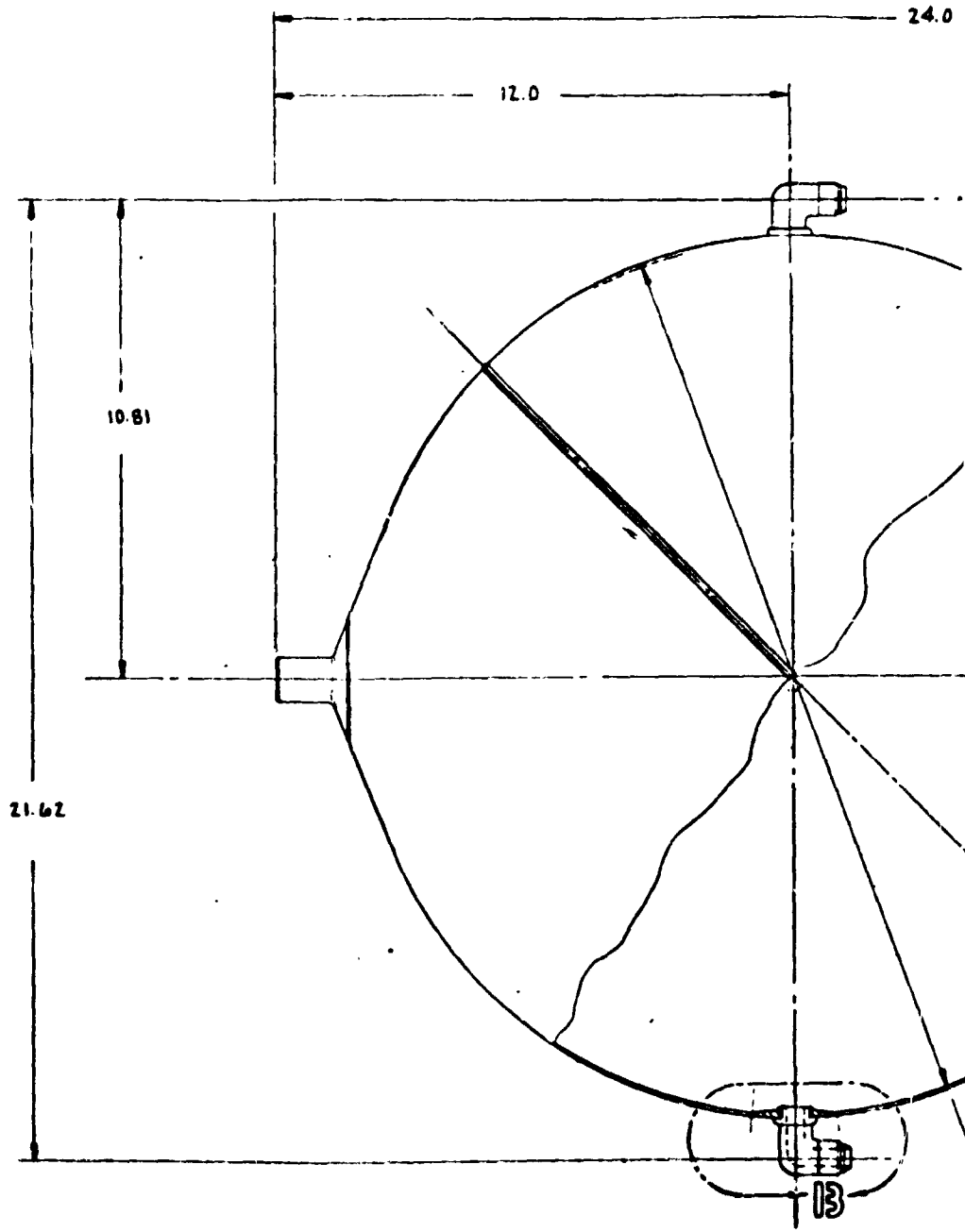
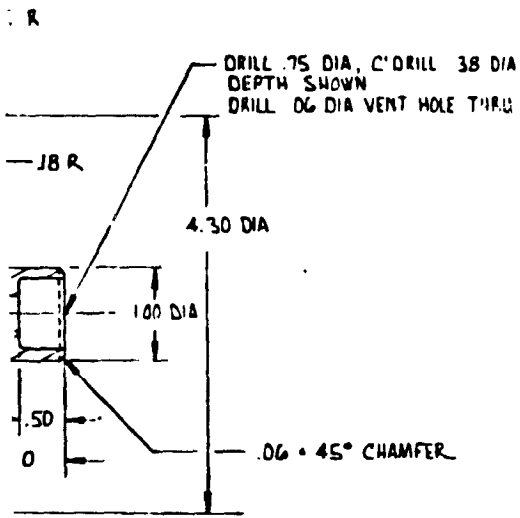
Figure 25. Propulsion Schematic (Drawing 2230-101C)



VIEW   
 SCALE: FULL

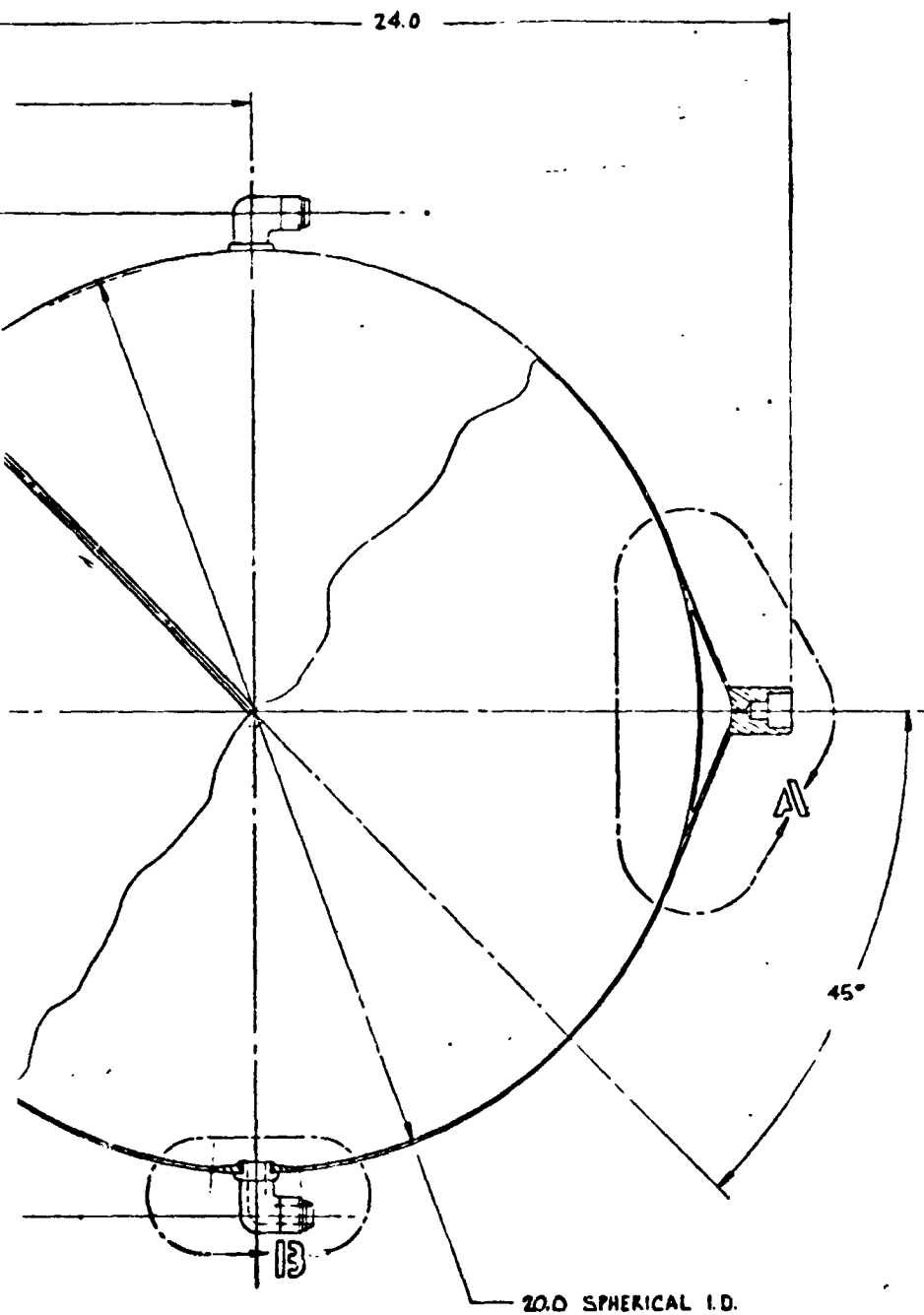
FOLDOUT FRAME

FOLDOUT FRAME



**LFV PROPELLANT TANK**  
 SCALE: HALF SIZE

FOLIOUT FRAME

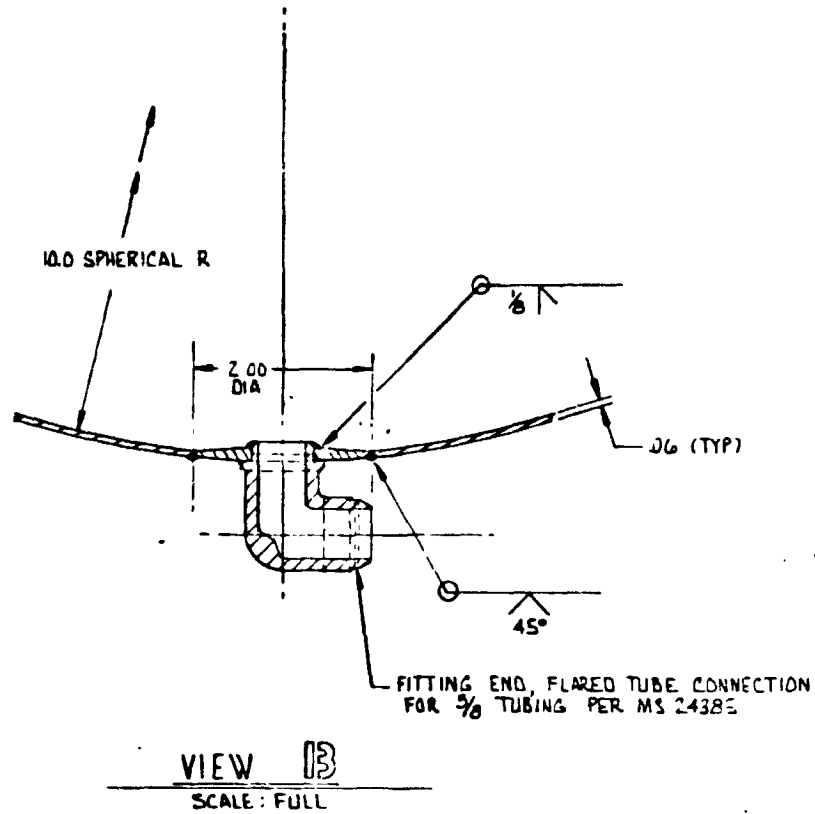


**LFV PROPELLANT TANK**  
 SCALE: HALF SIZE

**Figure 26. Preliminary**

FOLDOUT FRAME

FOLDOUT FRAME



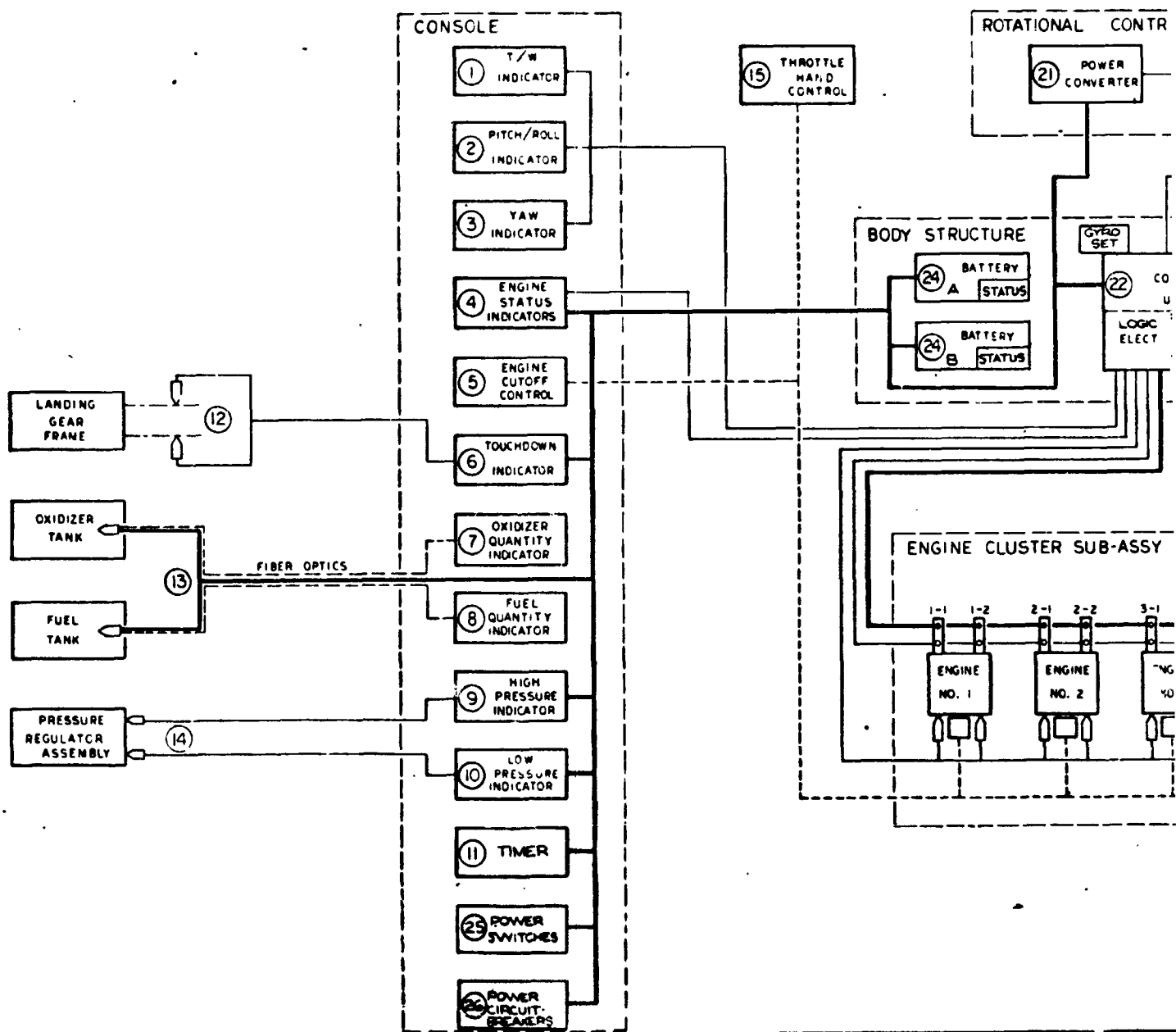
A 6-25-69 *[Signature]*

|   |              |   |               |
|---|--------------|---|---------------|
| SCALE                                     | DR. THOMPSON | SPACE DIVISION                            |               |
| NOTED                                     | DATE 6-15-69 | NORTH AMERICAN ROCKWELL CORPORATION       |               |
|   |              | 12254 LARWOOD BULFARD, BOUNTY, CALIFORNIA |               |
| LFV PROPELLANT TANK<br>PRELIMINARY DESIGN |              |   | 2230-103<br>A |

Figure 26. Preliminary Design Propellant Tank (Drawing 2230-102A)

FOLDOUT FRAME

# LFV INSTRUMENTATION/CONTROL/P. SUBSYSTEM DIAGRAM



CONTROL / POWER  
DIAGRAM

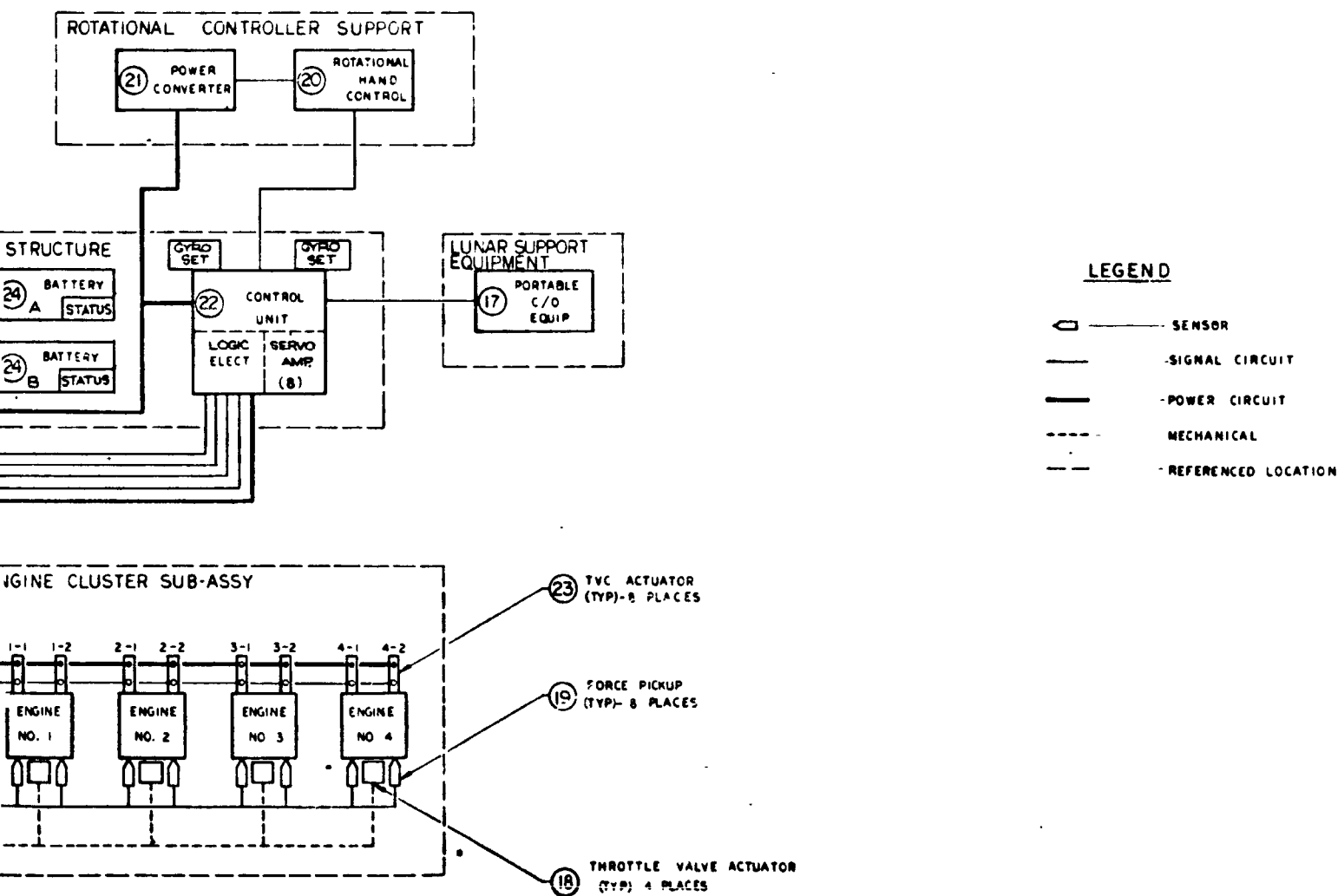


Figure 27. Instrumentation  
(Draw

FOLDOUT FRAME




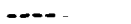

FOLDOUT FRAME





Space Division  
North American Rockwell

**LEGEND**

-  SENSOR
-  SIGNAL CIRCUIT
-  POWER CIRCUIT
-  MECHANICAL
-  REFERENCED LOCATION

R  
S

ES

ALVE ACTUATOR  
CES

6-8-68  
7/1/69


|   |  |                            |  |
|---|--|----------------------------|--|
|  | DESIGNED BY<br>THOMAS W. S. N.                           | DRAWN BY<br>G. S. T. S. J. | NORTH AMERICAN ROCKWELL CORPORATION<br>4814 LINDSEY BLVD., CANOGA PARK, CALIF. 91304 |
|   | LRV INSTRUMENTATION - CONTROL<br>POWER SUBSYSTEM DIAGRAM |                            |  |

Figure 27. Instrumentation, Control, and Power Subsystem Diagram  
(Drawing 2230-104)

occur, the seat assembly translates 7 inches (+6, -1) along the axis of the load pans. To aid ingress and egress, the display panel and throttle control are positioned on the left-hand support, and the attitude controller on the right hand. This structure is also integrally stiffened and is hinged for stowage. Displays are provided to monitor vehicle attitude and azimuth, thrust-to-weight ratio, tank pressures and quantities, engine failure and shutdown, electrical power status and control and time. The display panel is positioned to maximize the pilot's visibility of both the panel and the lunar surface.

The four engines are installed at a cant angle of 15 degrees to the vehicle centerline (see Figure 18). Each engine has a two-axis gimbal providing 7-1/2 degrees of rotation in each plane. Bendix flexural pivots and eight electromechanical actuators are also part of the assembly. The throttling bipropellant valve is actuated, in the concept illustrated, by a hydraulic system. However, in the selected design, cables are used.

Installation of the propellant tanks is illustrated in Figure 23. The tank is a modified Gemini tank of 20-inch inside diameter, trunnion-mounted at two places. Propellant fill and engine supply passages are routed through the lower boss. The upper boss is utilized for both propellant overflow and venting during filling, and for pressurization during firing. Tank internals include capillary screens for baffles and outage minimization. These are installed prior to welding the girth of the tank. Allowance has been made for 1 inch of insulation with an outer cover of aluminized Kapton and with a final coat of white thermal paint.

The preliminary design of the attenuator is illustrated in Figure 24. As described in the section on landing gear, it utilizes the design principles of the Surveyor attenuator and is cycleable for repeated landings. It also has a high preload (approximately 600 pounds) which, besides providing the proper landing load-stroke curve, resists the engine thrust and prevents any motion of the c. g. with respect to the engine mount during flight

Additional subsystem preliminary design definition is illustrated in Figures 25 through 27.

#### Preliminary Design Mass Properties/Geometric Data

Several LFV design and performance properties are a function of the geometric arrangement and mass properties (c. g. location, inertias, etc.). Throughout this report, some of these properties have been described on the basis of nominal or preliminary configurations. To update this information, Table 2 presents these important characteristics as computed from the final preliminary design point geometric and mass properties data.

Table 2. Preliminary Design Configuration Control Characteristics<sup>1</sup>

| Vehicle Loading Condition |            | Hover Thrust Angular Acceleration (= rad/sec <sup>2</sup> ) |                      | Vehicle Attitude Inclination at Hover ( $\pm$ deg pitch or roll) |                      | Landing Attitude Limit Delta from Nominal (deg pitch or roll) <sup>2</sup> |
|---------------------------|------------|---|----------------------|--|----------------------|--|
| Payload                   | Propellant | With Engine <sup>3,4</sup> Failed                           | With Actuator Failed | With Engine <sup>3</sup> Failed                                  | With Actuator Failed |  |
| None                      | Full       | 0.36  | 0.15                 | 5.2  | 0                    | -1.1   |
|                           | Burnout    | 0.45  | 0.19                 | 4.3  | 0                    | +1.7   |
| 100 pounds                | Full       | 0.34  | 0.14                 | 5.3  | 0                    | -1.1   |
|                           | Burnout    | 0.41  | 0.17                 | 4.5  | 0                    | +1.0   |
| 370 pounds                | Full       | 0.31  | 0.13                 | 5.6  | 0                    | -1.7   |
|                           | Burnout    | 0.37  | 0.15                 | 5.0  | 0                    | -0.2   |

<sup>1</sup> Design properties taken from mass properties (Tables 21 and 22) and general arrangements of Figure 19.

<sup>2</sup> Attitude limits for landing capability in Figure 69 are modified by algebraic addition of deltas shown in this table.

<sup>3</sup> Small angle approximations used.

<sup>4</sup> Acceleration shown is in pitch. Roll value is slightly higher.

## HUMAN FACTORS

The basic objectives of the human factors efforts were to establish feasibility limits and to develop design criteria to ensure compatibility of the LFV system for operation by a space-suited crewman. Mockup testing utilizing a subject in a pressurized suit was also performed to verify and modify requirements.

### Design Criteria

Design criteria development was based upon mission and task analysis, extrapolation from Apollo experience, and literature review.

### Crew Task Descriptions

To form a design criteria basis for the crew tasks of removing the LFV from the LM and performing preflight and flight operations, a brief analysis was performed. The coverage of these activities is indicated by the following abbreviated task outline:

1. Unstow LFV
  - a. Release shroud fasteners
  - b. Remove shroud and stow
  - c. Deploy LFV lowering device
  - d. Release LFV tiedown restraints
  - e. Lower LFV to surface
2. Assemble LFV
  - a. Install loose equipment
  - b. Deploy and secure control/display assemblies
  - c. Connect electrical cables
3. Deploy LFV for launch
  - a. Set up landing mat
  - b. Install handling equipment

- c. Move LFV to launch site
- d. Position LFV on landing mat
- 4. Service LFV
  - a. Deploy servicing hoses
  - b. Simulate tank fill
  - c. Disconnect and stow hoses
  - d. Install helium tank
  - e. Install payload
- 5. Ingress to LFV
  - a. Ascend to platform
  - b. Enter seat
  - c. Unstow and fasten restraints
- 6. Flight maneuvers
  - a. Actuate throttle
  - b. Actuate attitude controller in pitch, roll, and yaw
  - c. Read and interpret instruments
- 7. Egress from LFV
  - a. Unfasten and stow restraints
  - b. Exit from seat
  - c. Descend to surface
  - d. Deploy launching mat

8. Deploy scientific payload
  - a. Unstow payload components
  - b. Set up scientific equipment

Consideration of these activities led to selection of those critical ones which would benefit from mockup tests and would require human engineering recommendations for design. The most critical problems appeared to relate to the basic flight operations and involve the crew body position and vehicle configuration interface with the astronaut wearing the extravehicular mobility unit (EMU). Next most important were the problems of loading, unloading, boarding, and egressing from the vehicle while wearing the EMU. Last were the problems of removal from the LM, fueling, checkout, and launch/landing mat deployment.

#### Astronaut Suit Requirements

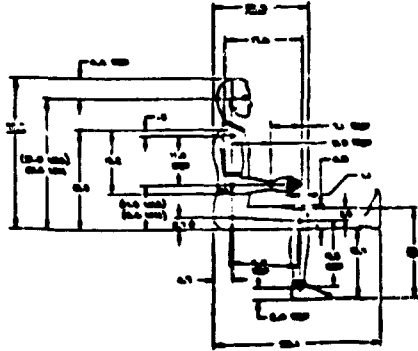
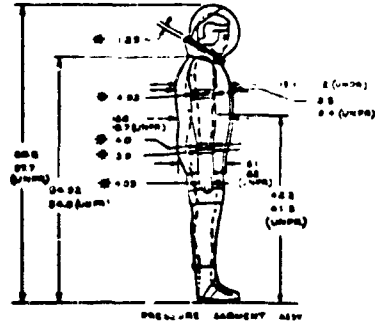
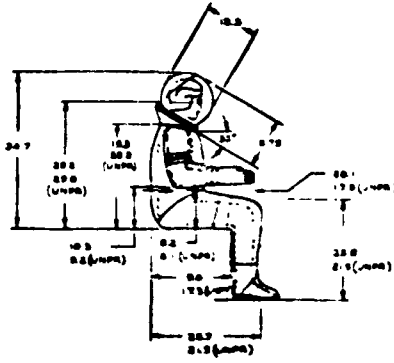
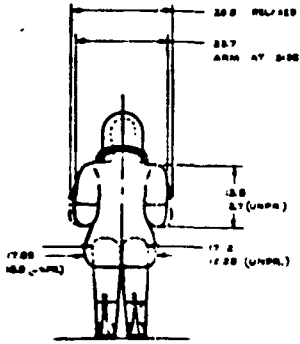
The basic problems studied in this area dealt with required physical size and shape of the vehicle body support system and pilot flight control and display systems. Included were anthropometric characteristics, suit and portable life support weight and bulk, and reach and vision capabilities of the suited pilot.

#### Astronaut Anthropometry

The crew size limits were assumed to be basically the same as for Apollo crewmen. The limits of 10th and 90th percentiles apply for eight major body dimensions. These percentiles are based upon a 1950 Air Force survey of flying personnel (Reference 2). Figure 28 shows standard anthropometric standing and seated positions for a "large" crewman (90th to 95th percentiles) and a "small" crewman (10th to 5th percentiles). Clothing conditions shown are for the man clothed in a constant-wear garment and in a space suit with dimensions approximating the International Latex Corporation Model A5L. For LFV design, the suit dimensional criteria were revised to conform to the latest estimates for the A7L models for critical areas such as the gloves, lunar overshoes, and helmet. These data, listed in Table 3, were obtained through a series of telephone conversations with NASA Crew Systems Division personnel and from dimensional drawings received from International Latex Corporation.

Two basically different body positions were investigated: standing and sitting. The standing position was considered to be required for the kinesthetic control mode, which was one of the control system approaches at the inception of the study. Experience regarding human engineering and

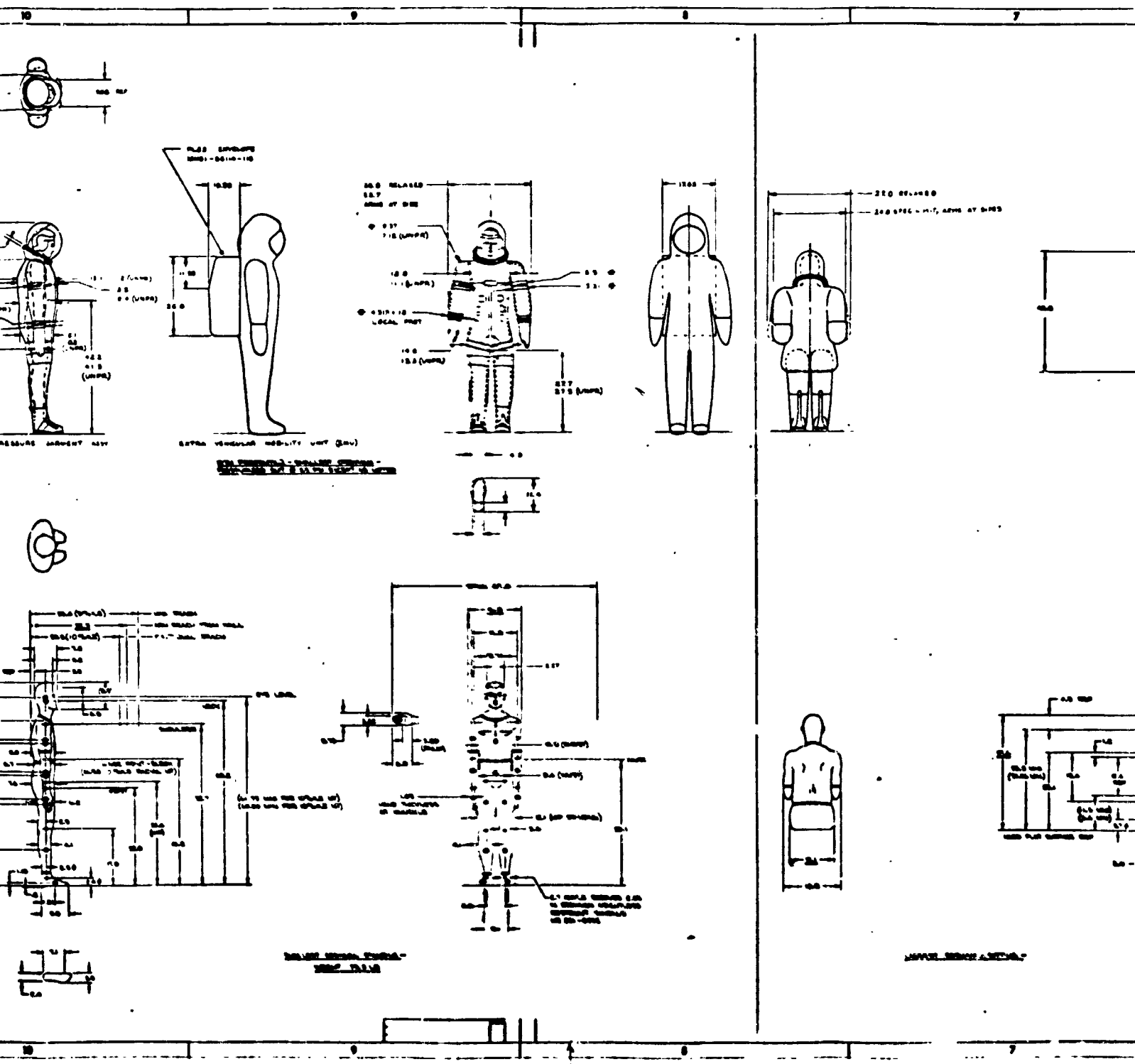
AP 470



FRAME STRUCTURE

FOLDOUT FRAME

FOLDOUT FRAME



FOLDOUT FRAME

FOLDOUT FRAME







Table 3. Supplementary Anthropometric Data for A7L Suit

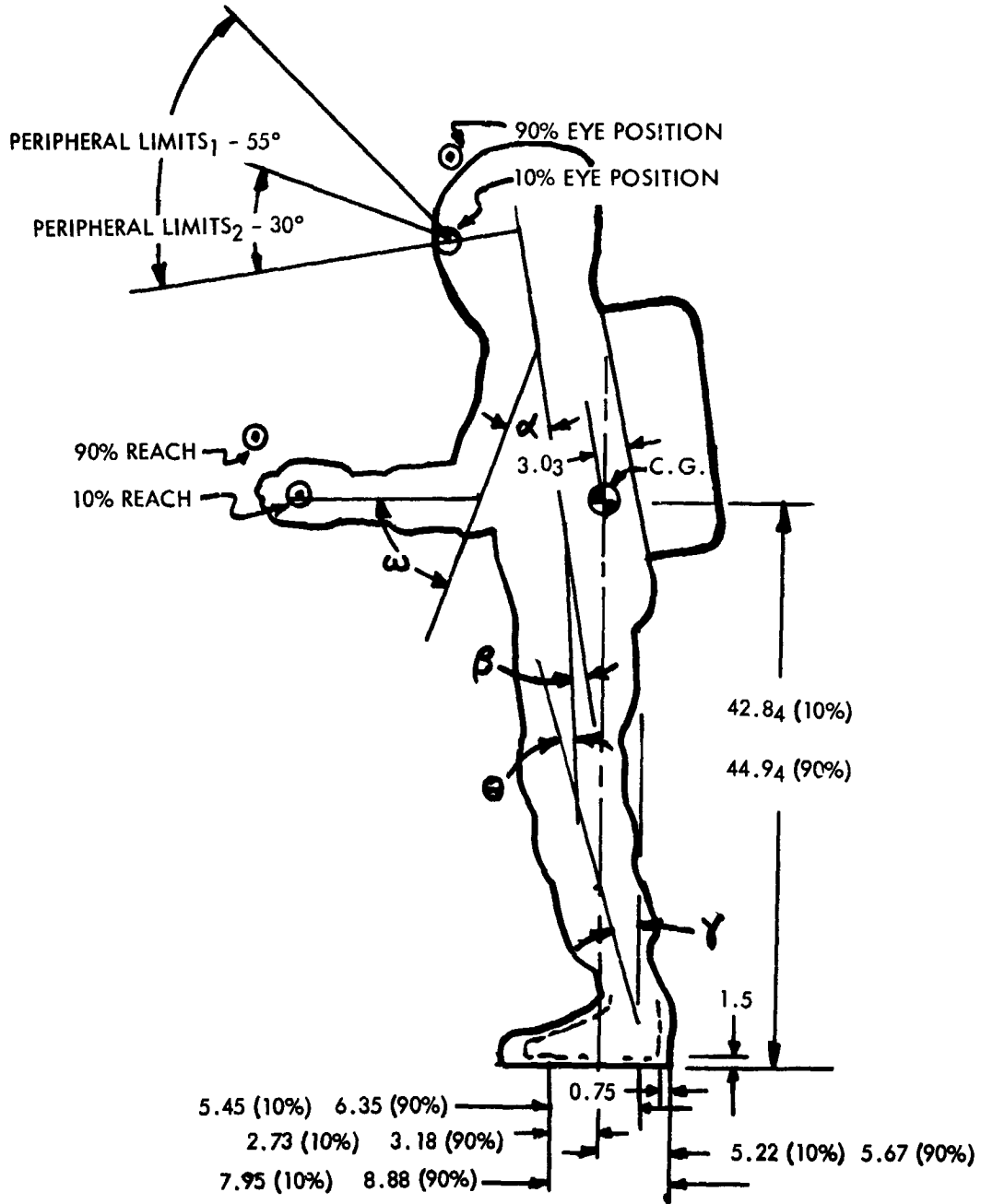
| Dimension Name             | Suit Condition          | Dimension in Inches                  |                 |                |                 |
|----------------------------|-------------------------|--------------------------------------|-----------------|----------------|-----------------|
|                            |                         | Body Position                        |                 |                |                 |
|                            |                         | Seated                               |                 | Standing       |                 |
|                            |                         | 5th Percentile                       | 95th Percentile | 5th Percentile | 95th Percentile |
| Seat width                 | Vented                  | 15.3                                 | 18.0            | 13.0           | 15.3            |
|                            | Pressurized             | 15.4                                 | 18.1            | 15.6           | 17.9            |
| Elbow-to-Elbow breadth     | Vented                  | 20 - 24                              |                 |                |                 |
|                            | Pressurized             | 28 - 29                              |                 |                |                 |
| Shoulder breadth           | Pressurized             | 26                                   |                 |                |                 |
| Knee-to-knee breadth       | Pressurized             | 18                                   |                 |                |                 |
| PGA boot thickness         | Vented                  | 0.25 Sole<br>0.50 Heel<br>0.75 Total |                 |                |                 |
| Lunar overshoe             |                         | Large                                |                 | Medium         |                 |
| Length                     |                         | 14-1/8                               |                 | 13             |                 |
| Width                      |                         | 6-1/8                                |                 | 6              |                 |
| Total height, extended     |                         | 8                                    |                 | 8              |                 |
| Minimum height, folded     |                         | 3-1/2                                |                 | 3-1/2          |                 |
| EVA gloves                 | Pressurized (3.75 psid) |                                      |                 |                |                 |
| Circumference              |                         | 11.2                                 |                 |                |                 |
| Finger diameter            |                         | 1.0 each                             |                 |                |                 |
| Width - fingers only       |                         | 4.2                                  |                 |                |                 |
| Width - including thumb    |                         | 4.5                                  |                 |                |                 |
| Finger length              |                         | 3.25                                 |                 |                |                 |
| Length - overall           |                         | 17.0                                 |                 |                |                 |
| Length to wrist disconnect |                         | 10.5                                 |                 |                |                 |

anthropometric criteria for standing pilot positions is very limited because of the small number of vehicles using this position. Information related to vehicle operation while wearing a backpack in the lunar environment is even more limited. In consequence, criteria were derived or estimated for acceptable body angles, tolerance of g forces, restraint systems, visibility, and controller positions. Review of NASA contractor reports and photographs, discussion with NASA personnel, and the experience of North American Rockwell Life Sciences personnel were combined to produce the estimated standing body position described in Figure 29 and Table 4. Problems of provisions for body movement during landing are discussed in a following paragraph.

The following ground rules for a standing body position were used in deriving the design criteria.

1. The astronaut/backpack c. g. shall be located on a vertical line passing through the midpoint between the heel and ball of the foot, which is the center of support for combined astronaut/backpack mass.
2. For all except kinesthetic control designs, astronaut body movements, including head and arm movements, shall be minimized to avoid undesirable disturbances to the system.
3. Astronaut head and eye orientation shall be such as to optimize forward vision with a minimum of unnecessary head movements.
4. Astronaut knees shall be bent slightly to facilitate weight shifts as required for any kinesthetic stability and control designs. Such knee bending shall be minimized to avoid unnecessary muscle strain in supporting the weight and acceleration loads involved.
5. Hip and shoulder movements, which tend to be the most limited by suit design characteristics, shall be kept to a minimum, i. e., the posture shall be compatible, to the extent possible, with the design characteristics of the suit.
6. The lower arm shall be approximately horizontal to the platform of the LFV.

The seated position was adopted following a careful analysis of human tolerance to expected landing impacts and consequent design requirements for body support, c. g. location, and landing gear sizing.



- NOTES:  
 1 EYE MOVEMENT - NO HEAD MOVEMENT  
 2 NO EYE MOVEMENT  
 3 ADJUSTED FOR ARMS EXTENDED  
 4 ALLOWANCE FOR FOOT SEPARATION - 18 IN.

Figure 29. Standing-Position Dimensions

Table 4. Recommended Joint Angles - Standing Position

| Hinge Point |             | Desired Angle (deg) | Comfortable Range (deg) |
|-------------|-------------|---------------------|-------------------------|
| Symbol      | Body Sector |                     |                         |
| $\alpha$    | Shoulder    | 25                  | 10 to 40                |
| $\omega$    | Elbow       | 70                  | 10 to 90                |
| $\beta$     | Hip         | 5                   | 0 to 20                 |
| $\theta$    | Knee        | 10                  | 0 to 30                 |
| $\gamma$    | Ankle       | As required         | +20 to -15              |

A great deal of data have been gathered regarding design requirements for human comfort and efficiency in seated positions for shirtsleeve and unpressurized suit conditions. However, very little has been done with respect to men wearing pressurized suits of the type used in Apollo. In particular, the problems of PLSS support and the suit/PLSS interface for high-g conditions have not been explored. Spacesuit mobility data from specifications have often not been realizable in actual experience, particularly with suits that were not designed specifically to fit the available subjects. Therefore, the approach to preparation of design criteria must be cautious and supported by mockup testing to determine if the proposed criteria are valid.

The preliminary crew position data for design were as shown in Figure 30. The most optimistic estimate shown was Angle C between the back and thigh. Previous in-house mobility testing with the A5L (Reference 3) indicated that this angle could be closed to 90 degrees with difficulty, yet suit specification data indicated that an angle of 65 degrees is possible (Reference 4). A more conservative open angle than that shown in Figure 30 would have been used, but the seat pan angle appeared minimum for an actual seated position, and increasing the back pan aft tilt would decrease visibility due to helmet rise and limited torso adjustment capability.

Further discussion concerning each angle is given in the Subsections below. The angles described are not human body joint angles, but refer to the structural elements of the seat. Angle designations refer to Figure 30.

DEGREES

- A 15
- B 3 TO 5
- C 100 TO 102
- D 110
- E 90

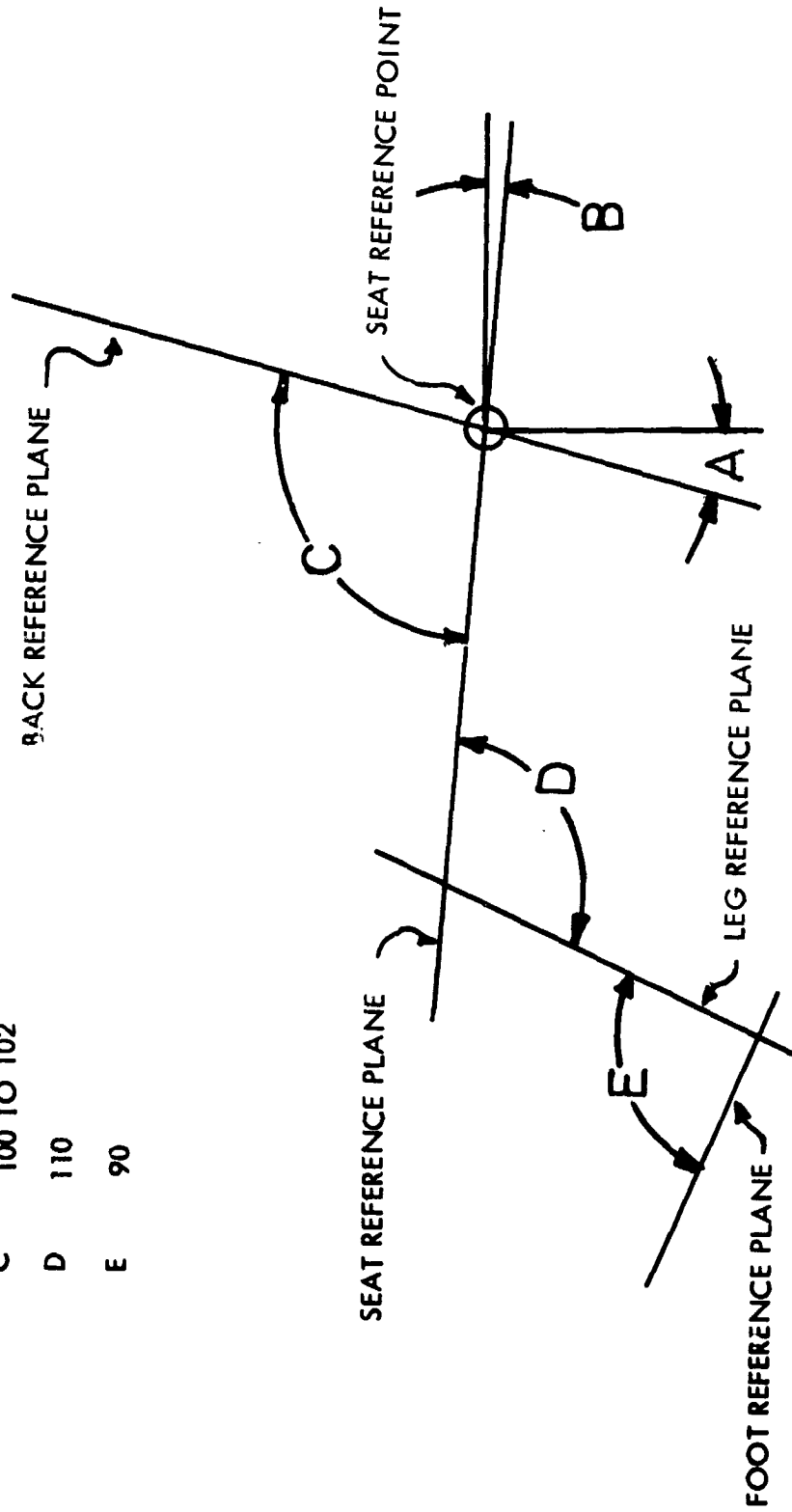


Figure 30. Recommended Angles for LFV Pilot's Seat

Back Reference Plane (A). The normal range of values for the back reference plane is from 15 through 23 degrees from the vertical, varying with different types of seating. Although a 23-degree angle is considered optimum for comfort, 15 degrees may be more compatible with the forward and downward vision requirements associated with the vehicle attitudes peculiar to the LFV mission. The 15-degree angle for the back reference plane is therefore regarded as acceptable.

Seat Reference Plane (B). The normal angle for the seat reference plane for various types of seating ranges between 3 and 10 degrees from the horizontal. An angle between 3 and 5 degrees is recommended in this case, in order to avoid, as much as possible, hip angles that would result in excessive suit compression and difficulties in mounting.

Seat Reference Plane to Back Reference Plane (C). The normal range for this angle, which establishes the hip angle, is from 95 to 108 degrees. Given the A and B angles recommended above, however, this angle will be between 100 and 102 degrees. The hip angle is critical to ease of mounting and pilot comfort, and may indirectly affect other critical variables because of excessive suit compression if the mobility characteristics of the suit are incompatible with the angle selected.

Although mobility tests of the A7L suit have been accomplished, results are not yet available. Preliminary data suggests that the angle selected will be compatible with the measured hip joint mobility. This characteristic, however, should receive empirical evaluation in a mockup.

Seat Reference Plane to Leg Reference Plane (D). A 110-degree angle is the most comfortable and is recommended. The minimum acceptable angle is 90 degrees and the maximum is 140 degrees. A lower leg pan is not required if the feet are restrained, as they should be.

Leg Reference Plane to Foot Reference Plane (E). This angle should be approximately 90 degrees. The footrest should have sufficient adjustment capability to accommodate upper and lower leg dimensions from the 10th to the 90th percentiles.

The angles specified above describe conventional pilot seating, which is generally to be preferred. The conventional configuration provides effective body support in high-acceleration environments as well as the most efficient support for the PLSS. It also provides a basis for an efficient restraint system, which should include foot restraints, thigh and lap straps, and possibly upper torso restraints.



## Visor Visibility

Astronaut visibility in the extravehicular visor assembly (EVVA) is an important factor because it affects the pilot's ability to maintain flight control. In particular, the vertical viewing angles are critical due to the high angle (45 degrees) of pitch required by the trajectory. Unfortunately, few valid test data are available. The International Latex Corporation has informally reported visual test data for the pressure garment assembly (PGA) helmet without the EVVA installed. These data relate only to the vertical and lateral limits of peripheral vision, not to viewing angles suitable for instrument heading and critical flight attitude information. Therefore, an analysis of vertical viewing angles was undertaken based on available data relating to head position and mobility in the pressurized PGA, the configuration of the EVVA, and viewing angle and visual field data (from standard human factors data sources). This analysis was based on the following assumptions and considerations:

1. Eye and head positions. The "at rest" position of the eyes with respect to the helmet was established on the basis of limited dimensional information provided in Reference 5. These dimensions were derived from measurements of a subject (having generally 50th-percentile body dimensions), wearing a pressurized A7L PGA with TMG. The arc of movement of the eye resulting from dorsal and ventral flexion of the neck generally conforms to that described in Reference 6. The head dimensions employed were derived from the 50th-percentile norms tabulated in Reference 7.
2. Orientation of the head. The "at rest" orientation of the longitudinal axis of the head in the midsagittal plane is assumed to be at the normal carrying angle of 5 degrees ventral (negative) rotation from the vertical. This places the standard line of sight, to which measurement of viewing angles and the visual field in the midsagittal plane are generally referred, at an angle 5 degrees below the horizontal. The carrying angle of 5 degrees is assumed for both the seated and the standing positions.
3. Head mobility. The values employed in the analysis for neck flexion limits of a subject wearing the pressurized PGA were derived from test data of Reference 8. The values of interest were: ventral (negative) flexion, 30 degrees; dorsal (positive) flexion, 46 degrees (angular displacement measured from the vertical). These values represent substantial constraints imposed by the PGA helmet, since the values for an unencumbered subject are, on the average, 60 degrees and 61 degrees, respectively. It should be emphasized that the values utilized are based

on measurements of a single subject and may be subject to revision upon receipt of more data. Such revision, however, could only have a significant effect on downward viewing angles, since intrusion of the EVVA into the visual field is the limiting factor in upward viewing angles.

4. EVVA characteristics. Data significant to the analysis concerning the extravehicular visor assembly were derived from Reference 9.
5. Restraint system. It appears that the requirements for body support and restraint, as well as c.g. alignment requirements, will effectively prevent flexion of the upper body in support of visual tasks associated with control of the LFV. The use of trunk flexion to improve viewing angles has not, therefore, been considered in the analysis.

The results of this analysis are shown in Figures 31, 32, and 33.

In Figure 31, the maximum vertical viewing angles available with eye rotation only (no head movement) are shown, measured from the standard line of sight. It will be observed that the latter is displaced 5 degrees downward from the horizontal because of the normal carrying angle of the head. The eye position for a horizontal line of sight (with the longitudinal axis of the head rotated to the vertical) is also shown, in the event a horizontal or vertical reference is desired. In such a case, the limits shown would be rotated 5 degrees upward. It will be seen that the visor assembly has no effect on viewing angles available through eye rotation, and in fact, places no constraints whatever on the visual field in the midsagittal plane, although the limits of peripheral vision are not shown. The limits of eye rotation were derived from Reference 10.

The maximum viewing angles available with head rotation only (no eye rotation) are shown in Figure 32, measured from both the standard line of sight and the horizontal line of sight. The values for angular displacement from the horizontal line of sight correspond precisely with the measured limits for sagittal neck flexion (in the PGA) provided in Reference 8. It will be seen that the visor assembly intrudes substantially into the upper field of view at maximum dorsal neck flexion, although it does not limit eye fixation in the absence of eye rotation.

In Figure 33, the maximum viewing angles available with a combination of head and eye rotation are shown, measured from both the standard line of sight and the horizontal line of sight. In this case, the maximum viewing angle upward is substantially limited by intrusion of the visor

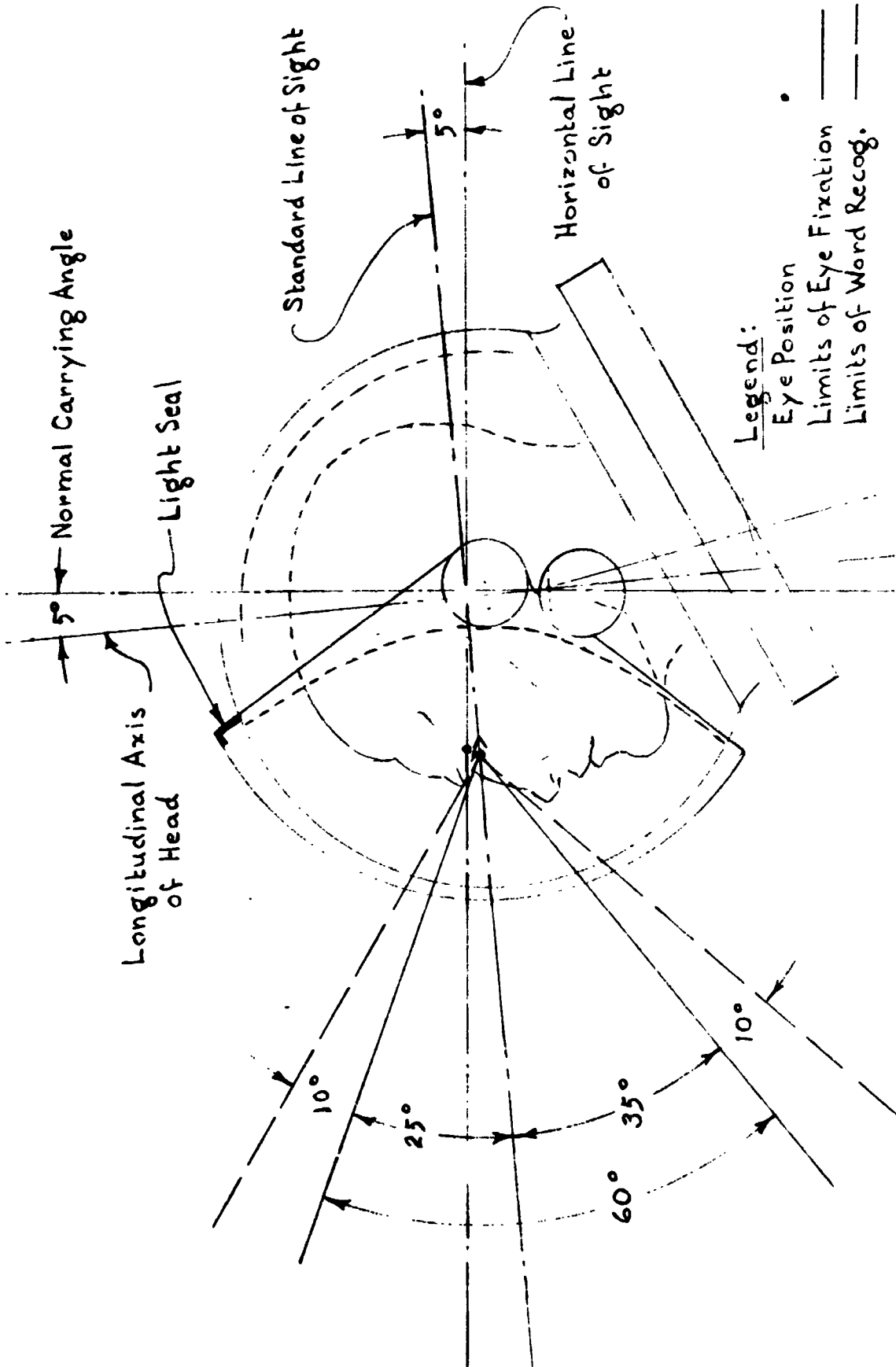


Figure 31. Maximum Viewing Angles, Eye Rotation Only,  
Vertical Motion in Sagittal Plane

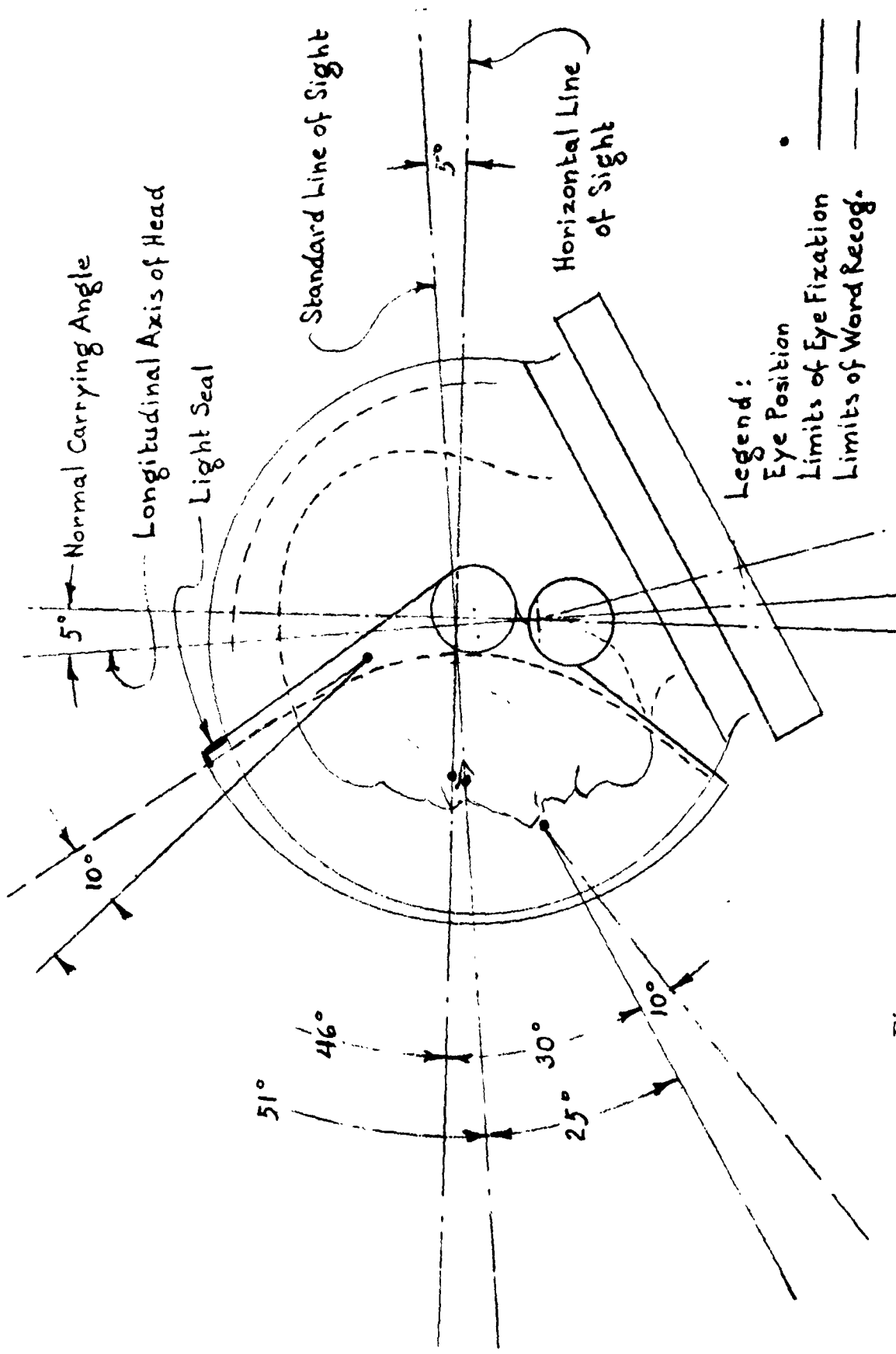


Figure 32. Maximum Viewing Angles, Head Rotation Only,  
Vertical Motion in Sagittal Plane

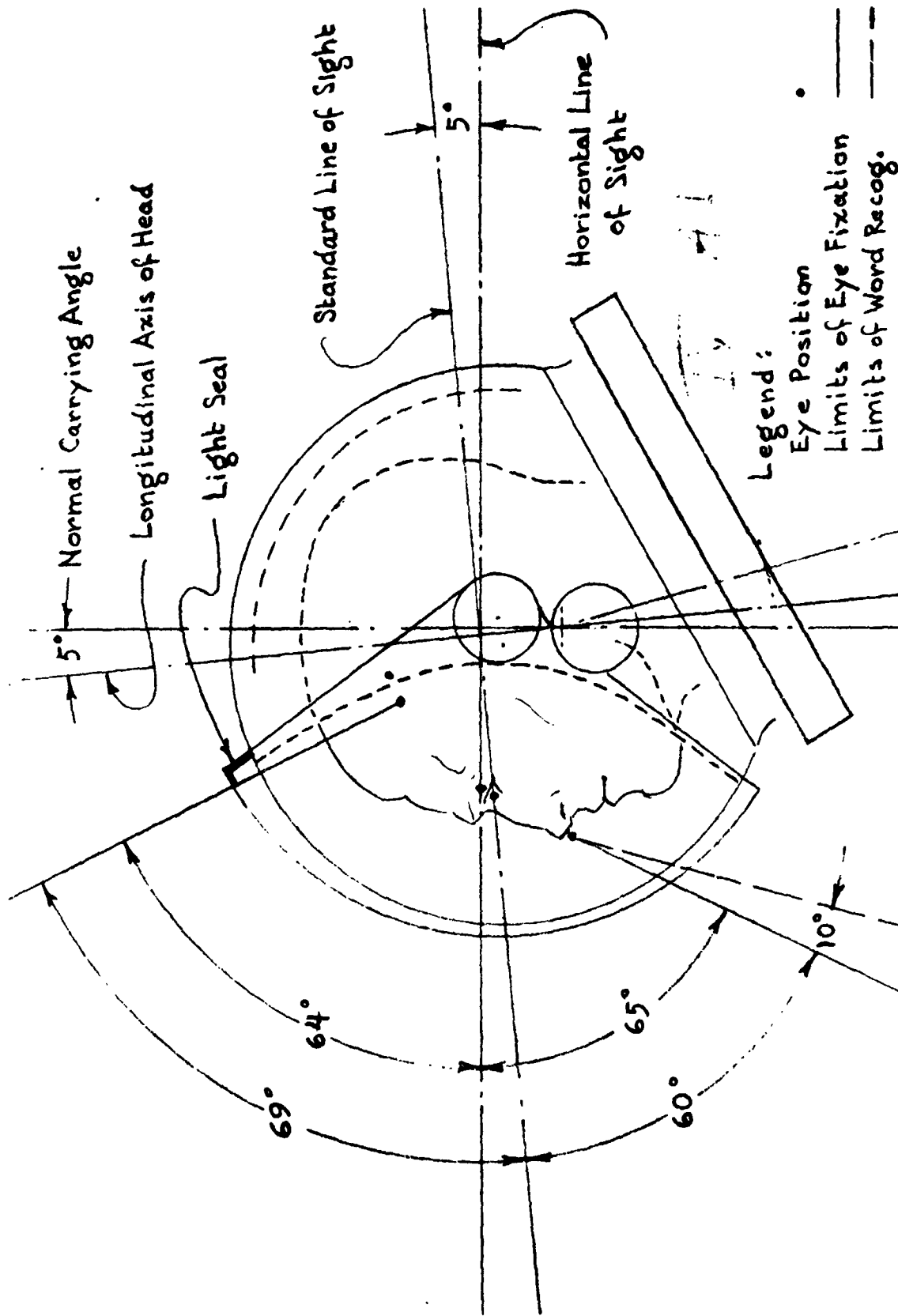


Figure 33. Maximum Viewing Angles, Eye and Head Rotation, Vertical Motion in Sagittal Plane

assembly into the field of view. Downward viewing angles are limited by the restrictions on head mobility imposed by the PGA helmet. It should be observed that the maximum upward viewing angle shown in Figure 33 is not achieved by maximum dorsal neck flexion, but by extreme eye rotation combined with neck flexion considerably less than maximum.

### Panel and Controller Arrangements

Based on the above anthropometric and visibility considerations, general recommendations for arrangement of the display panel and flight controller handles were developed. Emphasis was given to compatibility and standardization with Apollo CSM/lunar module control systems. This approach was requested by astronauts who were interviewed concerning the control/display system for the LFV. It was also recognized, however, that the flight regime and normal crew suit restrictions are considerably different in the LFV than in the LM, so that some compromises might be necessary.

The right-hand controller for nonkinesthetic control is essentially the same as the rotational controller for the Apollo CSM, as regards range of motion, orientation of handle, and maximum force range. It is expected that proportional control and a smaller deadband will be required for control in such close proximity to lunar terrain. (See discussion of simulation test results.)

The left-hand (throttle) control, which determines power application, is somewhat different from the command module or lunar module. It is not a translation control as such, although vertical and horizontal translation rates are affected by its use. It is strictly an engine throttle. For optimum analogous movement convention, it should move upward and downward parallel to the average engine thrust line. Other common throttle conventions involve fore-aft motion. However, in the LFV, it is possible such movement could be difficult to effect and accurately control as a result of suit mobility decrements, and that it could lead to control difficulties from the effects of varying acceleration forces during flight. A rotary motion around the long axis of the handle (motorcycle throttle concept) has been used during flight tests and simulation studies. This design is based on the concept that most acceleration forces will cause loads perpendicular to the handle axis, no matter what its orientation. Horizontal and vertical axis orientations have been tried. The major problem, when the rotation is about the handle axis, is the relative lack of sensitivity of the control, since such wrist motion in the suit is limited to approximately 100 to 115 degrees. For A7L space suit operations, a handle that rotates about an axis through the length of the forearm is easiest to operate, since the suit resistance is low at the wrist ring, there is no return force to overcome, and full pronation-supination arm movement (approximately 180 degrees) is available. Such a throttle device, compatible with these directions, could be provided.

However, this would be an unusual, nonstandard convention for power control motion and could result in training problems and lack of pilot acceptance. Consequently, the results of the current study are inconclusive. It appears that several methods would be feasible, but a series of dynamic flight test simulations and consensus of astronaut pilot opinion will be required to establish the final design.

Engine starting and cutoff controls are also related to the throttle design. The landing impact forces are high enough to require that there be a handle for the pilot's hands to grip to prevent falling. The controller handles are a logical choice, since he is gripping them for flight operations, and need not risk removing them. However, inadvertent power application and rotational commands due to the landing impact are hazards if the power on-off control is a part of the range of motion of the throttle. A separate on-off control switch closely adjacent to the throttle handle is one possibility. Automatic cutoff by a sensor device on the legs is another possible approach. A thorough review of failure modes is necessary as one step in selection of such a system. Experience with the Apollo command module guidance system suggests that a button control or switch, closely adjacent to the throttle (perhaps a thumb switch on the handle), could be safely operated by the astronaut if it were properly located.

The spacing between controls should be greater than for Apollo command module (CM) controls. There are no elbow and shoulder clearance limitations, and in the pressurized A7L suit, the upper arm is more comfortable when slightly akimbo. Based on present data on suits, a spacing range of 24 to 30 inches is recommended. The average spread is then 27 inches. The comments of the subject in a recent NASA drop test indicate that 24 inches is too small, and that a spread of about 28 inches would be preferable. Statistical test data from a representative group of astronauts wearing the pressurized suit will be required to achieve any greater degree of confidence in criteria for control spacing.

#### Suit Mobility

Two basic areas of suit mobility are of concern in the LFV project. These are requirements and capabilities for LFV handling during lunar ground operations, and restraint design and g-tolerance. A third area, rescue of a stranded pilot using a second vehicle, was considered initially but was later deleted by NASA.

Experience with persons in pressurized suits during the Apollo and astronaut maneuvering unit (AMU) programs, and operation in simulated and actual low-gravity conditions, have indicated a need for special design provisions for lunar deployment of the LFV. Among the major problems to be



overcome are those dealing with ingress and egress. These problems are, for the most part, attributable to characteristics of the pressurized extra-vehicular mobility unit that seriously degrade human sensor and motor performance. Performance effects include decreased mobility and body segment flexibility, decreased manipulative capability, decreased proprioceptive feedback effectiveness, decreased tactual sensitivity, and decreased visual capability. Each of these effects will be significant to the performance of one or more ingress/egress task elements and will require consideration in the elements of LFV design that relate to ingress/egress operations. The design considerations relative to ingress/egress task elements, as affected by the performance characteristics of the suited astronaut, are discussed below.

Ascent To and Descent From LFV Platform. Under 1-g (earth) conditions, climbing is reported to be one of the more difficult operations to perform for an astronaut encumbered with a pressurized EMU. This difficulty may be attributed primarily to the mobility restrictions imposed by the pressurized suit, the high energy expenditure involved in flexing the joints of the suit, the unfamiliar mass distribution and weight of the EMU assembly, and the postural instability associated with these conditions. Simulation experiments as well as theory give reason to believe that the act of climbing or jumping upward will be considerably easier in the 1/6-g lunar environment. However, assurance of safe ascent to (and descent from) the LFV pilot station, if the station is not near ground level, requires provision of some carefully located steps to facilitate climbing and descending — and more importantly, the provision of conveniently located handholds or other devices for stabilization of the upper body.

Steps or platforms should be designed with generous dimensions to accommodate the dimensions of the lunar overshoes worn by the astronaut and allow for reduced precision of foot placement or possible entanglement (the latter is particularly important in 1/6-g because of greatly reduced traction). The vertical rise between rungs or threads should be 9 to 10 inches when simple leg raising is to be used. Greater vertical spacing will require additional level surface area to accommodate inaccuracies in body placement. Level surfaces at the platform level are necessary to assure standing and maneuvering safety. (Inclined surfaces will be difficult for the suited astronaut.) Handholds for ascending to each step or platform should be provided at points no higher than shoulder height, and within easy reach of the astronaut during ascent and descent. During climbing motions, a forward lean angle of 10 to 20 degrees is expected, and this should be taken into account in locating handholds. The critical characteristics of the handhold design should generally conform to those shown in North American Rockwell Drawing LS-0698, except that the interior longitudinal clearance dimension should be not less than 4-1/2 inches in order to accommodate



the extravehicular glove. A vertical orientation is recommended, and there is some evidence that an oval or rectangular cross section would be helpful in prevention of inadvertent body rotation. Examples of acceptable Apollo extravehicular activity (EVA) handholds are noted on North American Rockwell Drawing F01-100525. It is possible that structural elements of the vehicle could serve as handholds if the desired characteristics were present.

Access for Seat Entry or Exit. The control/display panel, situated for flight in front of the pilot, will block entry to or exit from the seat. It must, therefore, be pivoted or hinged so that it may be deployed to one side for entry and exit, securely latched in the closed position, and detented or latched in the open position. The design of the latching devices must be compatible with the gross manipulative capabilities of the suited astronaut wearing the (pressurized) EV gloves, and the latch locations should be such as to be easily seen, reached, and manipulated by the astronaut from the seated position. A design alternative is provision of an offset panel that would permit direct access to the seat. This might be advantageous for forward and downward vision during the landing approach, although it would be less desirable for instrument reading and checking purposes. The relative advantages of the design alternatives warrant study in mockups and simulation exercises in the course of system development.

Seat Entry. Experience with ASMU docking, doffing/donning exercises, and a number of Apollo studies indicates that PLSS support structure and proper alignment of the PLSS for entry into the seat may constitute considerable problems. These arise partly because of suit constraints on mobility and visual capability, reduced proprioceptive feedback effectiveness, and the variable relationship between the principal axes of the PLSS and the suited astronaut (this relationship varies not only between astronauts, but also from moment to moment for the same astronaut).

Unassisted backward docking maneuvers are, of course, difficult under any circumstances, because of the limitations on visual control inherent in such tasks. In order to alleviate this problem, the design of the PLSS support structure could provide adequate lead-in guides for automatic alignment of the PLSS. Visual alignment capability is nearly mandatory.

A further seat entry problem may be encountered in achievement of sufficient suit flexure at the hip for a secure seated position. Information received informally from the A7L suit manufacturer indicates that the suit mobility characteristics are adequate for this purpose, but an official test report has not been received to support this conclusion. A mockup evaluation of the suit hip flexure characteristics is, therefore, in order.

Restraint System Stowage and Fastening. Apollo experience has shown that retrieval and positioning of restraint system components is quite tedious and difficult if the components are not within the astronaut's field of view. This problem is caused by suit constraints on mobility, reduced tactual sensitivity, and reduced manipulative capability. The design of the LFV restraints system must provide for stowage of strap components within the visual field of the seated astronaut, stowage devices within convenient reach distance from the seated position, convenient attach points for restraint installation, and component handling characteristics compatible with the manipulative characteristics of the extravehicular (EV) gloves. Apollo couch restraints may not meet this criteria, since they were not designed for operation with EV gloves.

A special problem with upper torso restraint is presented by the LFV system because of the PLSS. Shoulder straps from LFV structure points do not appear to be practical because they must pass around the PLSS. Such a design, which will permit slippage and slack to develop, appears impractical. Also, chest straps would interfere with the gas connection hardware and hoses mounted on the front of the suit. The most obvious alternative is to provide a restraint for the PLSS, which would, in turn, restrain the upper torso of the astronaut. The design of such a restraint should permit automatic latching or securing, with a convenient and reliable manual release. It is possible that the stowage attach points mounted on either side of the PLSS could be utilized as restraint system attach points, but the feasibility of their use for such a purpose would have to be evaluated. Such a system would afford a further benefit in preventing rebound of the PLSS upon landing impact (the PLSS is free to move upward for a short distance under normal circumstances).

Vehicle Transport Deployment and Servicing. The problem of moving the LFV from the vicinity of the LM to the launch area and performing fueling and checkout activities are significant human factors areas for which some general requirements have been developed.

Transport of the LFV from the LM to the servicing/takeoff area will cover a distance of 40 feet. It is expected that this can normally be done by one crew member, who would simply drag the vehicle over the surface. The crewman weighs 20 percent more than the vehicle, and the traction of his feet should greatly exceed the friction of the landing pads. As on earth, his shoes would penetrate and bear on the soil at an angle, provided the surface is not inordinately hard. The curved pads, on the other hand, would tend to "surf," with only a light soil pressure opposing the motion. If the two lead pads were lifted free, the resisting force would have a component which would add to the crewman's weight and aid traction.

At this time, the use of auxiliary wheels or sleds is not considered necessary. The floatation area of two landing pads exceeds the shoe bearing area by about 60 percent. Hand grips placed at a convenient height and to permit unobstructed leg motion should be provided on one of the load pans or on an auxiliary drawbar to permit dragging the LFV while the two lead pads are lifted above the surface. Mockup tests are needed to establish the best location. The transport concept described is based on current knowledge of the lunar surface. Prior to final design, additional information to be obtained from Apollo lunar landings should be considered.

Deployment of a landing mat for protection against rocks, sand, and dust ejected by the rocket engine blast is also affected by mobility. It is expected that this problem will be overcome by an easily erectable fabric-stiffening framework arrangement. The detailed design of such a blast protective device has not yet been pursued. Inflatable tubes integral with the fabric, shade roller dispensers, or mechanical tubular frameworks are possible methods for deployment. The basic need is to permit the placement of the protective material under the LFV without requiring stooping or crawling on the lunar surface by the astronaut. Ground stakes should be inserted from a standing position, by the use of an extension tool.

Propellant servicing operations will require large valve and connector handles and generously proportioned guides to accommodate the gross motions of the astronaut in the pressurized garment. Design of these mechanisms will need to incorporate special safety provisions to assure that no propellant vapors impinge directly upon the suit.

Design of the devices for removal of the LFV from the LM will require single-point, lanyard-operated latches and hoists that may be reached from the ground.

#### Environment Analysis

Primary concerns of the human factors environmental analysis for the LFV system were lighting, thermal input from the vehicle, exhaust gas impingement, solar radiation thermal effects, propellant toxicity protection, and the limited work capacity of the pressure-suited astronauts.

Of these problems, the most pertinent and unusual new conditions imposed by the LFV are the exhaust gas effects and the fuel toxicity problems.

Exhaust Gas Thermal Effects. The primary problems of exhaust gases in the majority of LFV configurations studied relate to near-ground operations. The exhaust location below the pilot assures that no direct impingement on the pilot's suit will occur at altitude. Effects at low altitudes depend on

reflected plume geometry. Present configurations provide protection from all but a very low-density zone by the placement of payloads, tanks, and structure to the sides and around the pilot. It is expected that the normal thermal resistance properties of the suit will be sufficient.

Propellant Toxicity. Hazards of propellant spillage and toxic engine exhaust products are recognized as a potentially serious problem for the LFV system. A recent NASA report describes the severe damage to suit materials which is possible from immersion in various rocket fuels (Reference 18). It was noted, however, that the outer suit layer provides good protection against such damage, except possibly at the sewn seams and joints. The main problem appears to be the highly toxic nature of the materials. If the material clings to the suit, some of it may be brought back into the LM at the end of an EVA period. In the confined LM air space, only an extremely minute amount could be permitted. The threshold limit value for the oxidizer is 5 parts per million (ppm) expressed as nitrogen dioxide or 2.5 ppm expressed as nitrogen tetroxide. The fuel, hydrazine, has a threshold limit value of 1 ppm and the UDMH value is 0.5 ppm.

The mechanism for toxic material transport into the LM requires further extensive study. At present it is not clear just how severe the problem is. The model assumed at present, which will require considerable analysis to quantify, has the following characteristics:

1. Propellant vapors are vented during servicing at a distance of approximately 10 feet from the crew member.
2. Exhaust products are ejected beneath the LFV.
3. Leakage is not a significant source of vapors.
4. Transport through lunar space over these distances is diffuse molecular flow at average molecular velocities of about 0.5 km/sec.
5. After engine shutdown and after completion of servicing, contaminating vapor is no longer present in the space surrounding the crewmen (hard vacuum). The near-equilibrium condition for the suit will then be reached in a few minutes. This condition will, at least, involve an amount of adsorbed contaminant gas corresponding to the temperature and pressure of surrounding space, and the nature of the adsorbent and the adsorbate. At the worst, there will be some gas-phase contaminants which are trapped or venting over a period of time. No liquid is assumed to be present. The temperature effect is such as to decrease the amount of adsorbent with increasing temperature.

6. Upon reentering the LM, if the temperature of the suit is lowered, the adsorbed contaminant would not tend to leave the suit, and vice versa.

A propellant-handling coverall suit is one possible solution if the problem is found to be severe. However, consideration of the operational problems of donning and doffing such a suit outside the LM while wearing a fully pressurized suit makes this approach very nearly impractical. It may be adequate to doff the coverall after depressuring the suit within the LM and then discard it overboard, depending on the time/temperature effects which control the amount of vapor released inside the LM. Further analysis and vacuum tests with the suit and the gases are needed to resolve these questions.

#### Impact Tolerance and Restraint Design

One of the most critical human factors questions affecting design is the problem of human tolerance to landing impact forces (g-tolerance). The specific problem involved the comparison of capabilities of a standing and sitting astronaut, restrained and unrestrained, and wearing the pressurized EMU, including the PLSS backpack. These positions are illustrated in Figures 34 and 35.

Investigation of the human tolerance limits elicited very little directly useful data and none for the exact conditions specified. However, a few related data points were obtained from human engineering handbooks (Reference 12), and studies performed by the Federal Aviation Administration (References 13 and 14) and the U. S. Navy (Reference 15). Motion picture records and analyses of impact tests performed by Grumman Aircraft Engineering Corporation on pilot subjects in a LM standing position without backpack were also reviewed. In addition, impact tests were recently performed by NASA using a subject wearing a pressurized suit with backpack.

The data from the FAA studies on a man in shirtsleeves (no pack) are summarized in Table 5. A spring-mounted platform was used for body support. The basic conclusions were that very high-g, short-term impacts at the foot level are acceptable for a standing man as long as the shoulder g level is less than 10. The severe pain in chest, stomach, small of back, hips, top of head, and lesser pains in arches, back of legs, ankles, heels, and throat at 10 g indicate the g levels should be no more than 7 to 8 for an operational vehicle. It should be noted also that body movement down to a squatting position followed the impacts with flexed knees. Such movement is unacceptable for a standing astronaut in the LFV. Comparison of human body effective weight supported by the legs with effective suit and PLSS-OPS weight supported by the legs indicates a maximum tolerance of 4 g for the

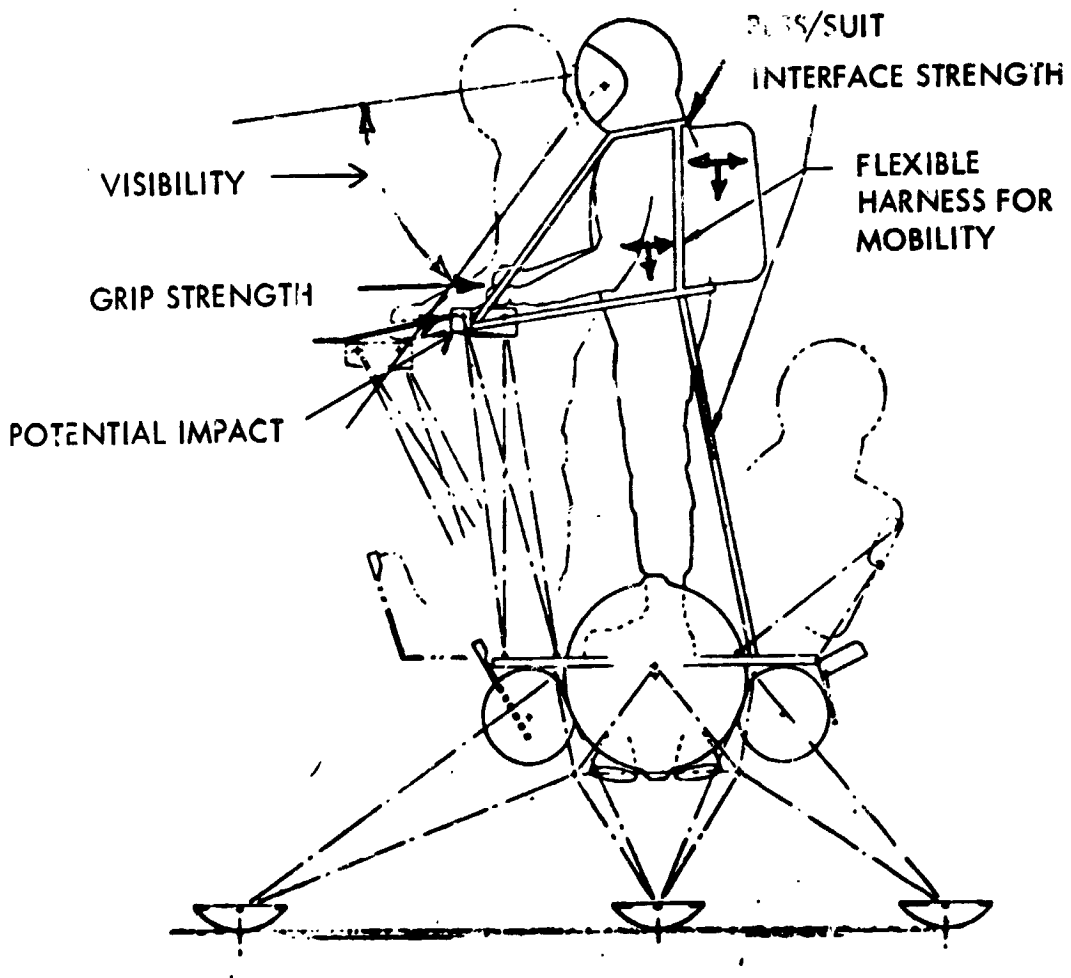


Figure 34. Relatively Unrestrained Pilot

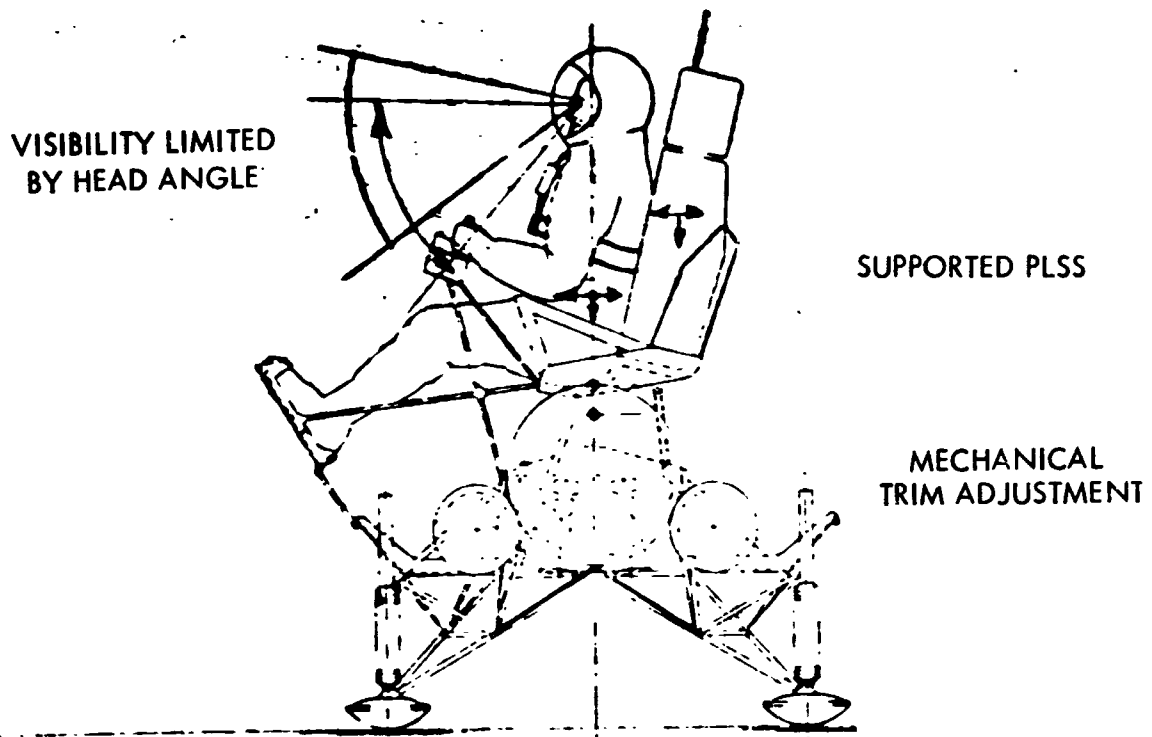


Figure 35. Closely Restrained Pilot, Seated

**Table 5. Summary of Voluntary Tolerances to Vertical Impact**

| Body Position   | Maximum Voluntary Tolerance as Measured at Shoulder Level |               |                                |        | Loading Applied at Point of Impact |                    |             | Physiological Symptoms | Transmission (Impact-Shoulder) |                   |  |
|---|---|---------------|--------------------------------|--------|------------------------------------|--------------------|-------------|------------------------|--------------------------------|-------------------|--|
|   | Peak g  | Onset (g/sec) | Duration of Deceleration (sec) | Peak g | Onset (g/sec)                      | Duration of Impact | Attenuation |                        | Time (sec)                     | Velocity (ft/sec) |  |
| Standing, knees locked  | 10  | 666           | 0.04                           | 65     | 10,000                             | 0.008              | 6.5         | 0.003                  | 1,000                          |                   |  |
| Seated in rigid chair   | 10  | 625           | 0.057                          | 95     | 19,000                             | 0.0075             | 9.5         | 0.0035                 | 410                            |                   |  |
| Standing, legs flexing  | *7  | 583           | 0.16                           | 230    | 50,000                             | 0.0075             | 36          | 0.02                   | 250                            |                   |  |
| Squatting   | 5   | 250           | 0.30                           | 133    | 26,600                             | 0.0075             | 29          | 0.03                   | 83                             |                   |  |
| Seated in chair equipped with Stafoam                             | *9  | 250           | 0.12                           | 230    | 44,000                             | 0.0065             | 25          | 0.024                  | 166                            |                   |  |
| *Not maximum tolerance - test limited by height of drop mechanism |   |               |                                |        |                                    |                    |             |                        |                                |                   |  |



suited man in terms of leg muscle strength, based upon the 8-g tolerance limit.

Other tests by the FAA involved subjects in shirtsleeves wearing weighted backpacks who were dropped at various speeds to earth. Pertinent results are shown in Figure 36, which is a graph of backpack weight acceptable versus velocity change. Acceleration measurements were not made. A comparison with the range of suited astronaut weights and the LFV impact velocity possible with the LFV potential energy at maximum design engine cutoff height is also shown in Figure 36. It is clear from this graph that there is considerable danger of pilot injury from landing impact due to the weight of the PLSS. Possible protection of the man due to suit stiffness is not shown. Note that these data are only for a vertical drop and do not include lateral or transverse effects.

Discussion of these problems with NASA prompted a limited series of NASA tests involving a subject in the pressurized suit and backpack (Reference 11). Two shock conditions tested were approximately 3 g for 220 milliseconds and 8 g for 40 milliseconds, exerted at the subjects' feet. The subject's comments indicated that the impact caused "no real sensation" other than surprise. . . that neither case is particularly severe, in fact they are relatively easy. . . no physical injury or discomfort was experienced during the drops." These and other comments indicated the pressurized suit relieved the PLSS load from the subject, and only a small bruise at the top of the left buttock was noticed about 48 hours later. However, the subject was unable to maintain an adequately stable body position during the impact. The motion picture records showed backward toppling. A 10-inch tether, used to limit vertical excursion, was observed to become taut in Case I, whereas an 18-inch tether did not become taut in a later, similar test. A 12-inch tether in Case II (8 g) did not become taut. North American Rockwell personnel observing the film concluded that the two cases imposed accelerations exceeding the values that would be acceptable for LFV operation.

The element of surprise is a considerable factor in this problem. Human reaction time is such that it would be very difficult for a pilot to make use of the available strength in his legs until the impact was nearly completed. Reference 12 gives a reaction time for touch (probably hand) of 0.16 second and longer for sight (0.2 second). "It takes about 20 percent longer to respond with the feet than with the hands" (Reference 12). For nonideal conditions, such reactions may be much longer.

The series of tests of impact on a suited subject simulating LM landing conditions indicated that the ability of the crewman to withstand shocks combining lateral and vertical motion was much less than for simple vertical impact in the sense that gross head, shoulder, and knee movements result

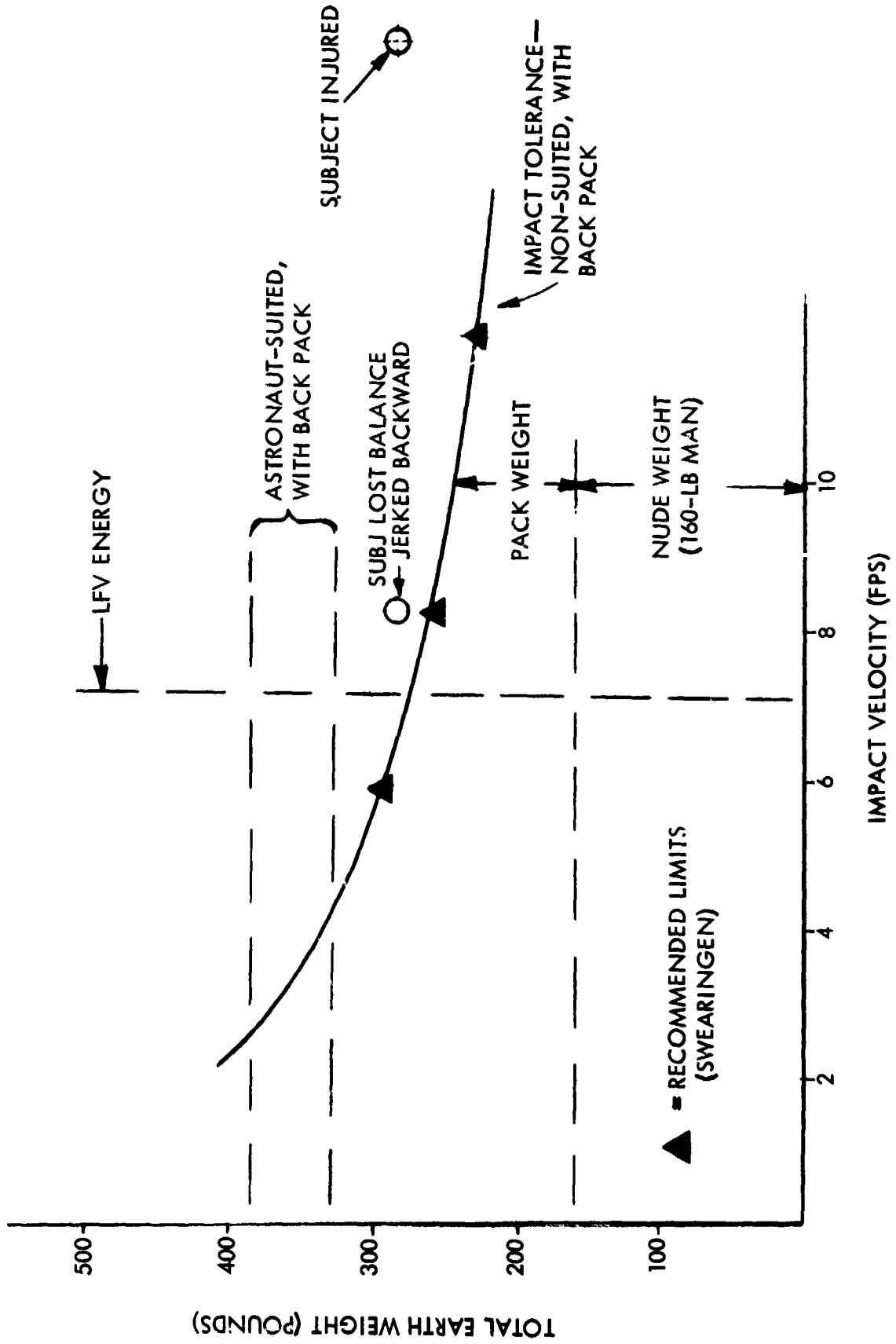


Figure 36. Longitudinal Impact Tolerance, Standing Position

(References 16 and 17). As regards pain effects, none of the subjects felt their tolerance limit was reached, though peak levels reached 10 to 11 g (a maximum of 6.9 g is reported in Reference 16).

An idealized representation of some of the factors involved in human impact tolerance is shown in Figure 37. The critical parameters in this analysis are velocity and relative motion. The relative motion of the pilot's shoulder in terms of velocity and distance are shown in comparison to the platform (LFV) velocity and its deflection (landing gear stroke) as a function of time (attenuation interval) and the g level of the pilot and platform. It is seen that absolute shoulder velocity change (decrement) lags the platform velocity due to the reaction time of the subject, and that his velocity change (slope of the curve) is less than that of the platform due to attenuation by the legs, etc. However, the velocity change lasts longer. This analysis indicated that a reaction time of more than 0.2 second gave excessive knee bending (up to 15 inches) for the standing pilot unless the landing gear reduced the vertical g loading to less than 3. This simplified kinematic analysis thus verified the observation of the drop tests.

From these investigations of space suit and human tolerance, acceptable g-tolerance design limits for standing and seated positions were derived and used in the design of the landing gear. These design factors are summarized in Table 6.

### Mockup Tests

#### Objectives

The general objectives initially established for the LFV mockup tests were to demonstrate the compatibility of the vehicle's design features with the anthropometric characteristics and performance capabilities of the pressure-suited astronaut in the execution of lunar surface operations, to assess the utility of analytical crew station data developed in the course of design, and to evaluate preliminary design solutions to potential crew performance problems identified during the design studies. Thorough fulfillment of these objectives would, of course, require the provision of complex mockup hardware (involving a large number of test articles), test facilities and equipment, and test conditions for an extensive experimental evaluation of all anticipated LFV lunar surface operations. These operations would include removal of the vehicle from its stowed position on the LM, installation of loose equipment, deployment of the vehicle and auxiliary equipment, simulated servicing, payload stowage and deployment, and ingress/egress. In addition, a number of test subjects representative of the range of physical characteristics of the astronaut population, each equipped with appropriately sized EMU's, would be required. The implementation of such

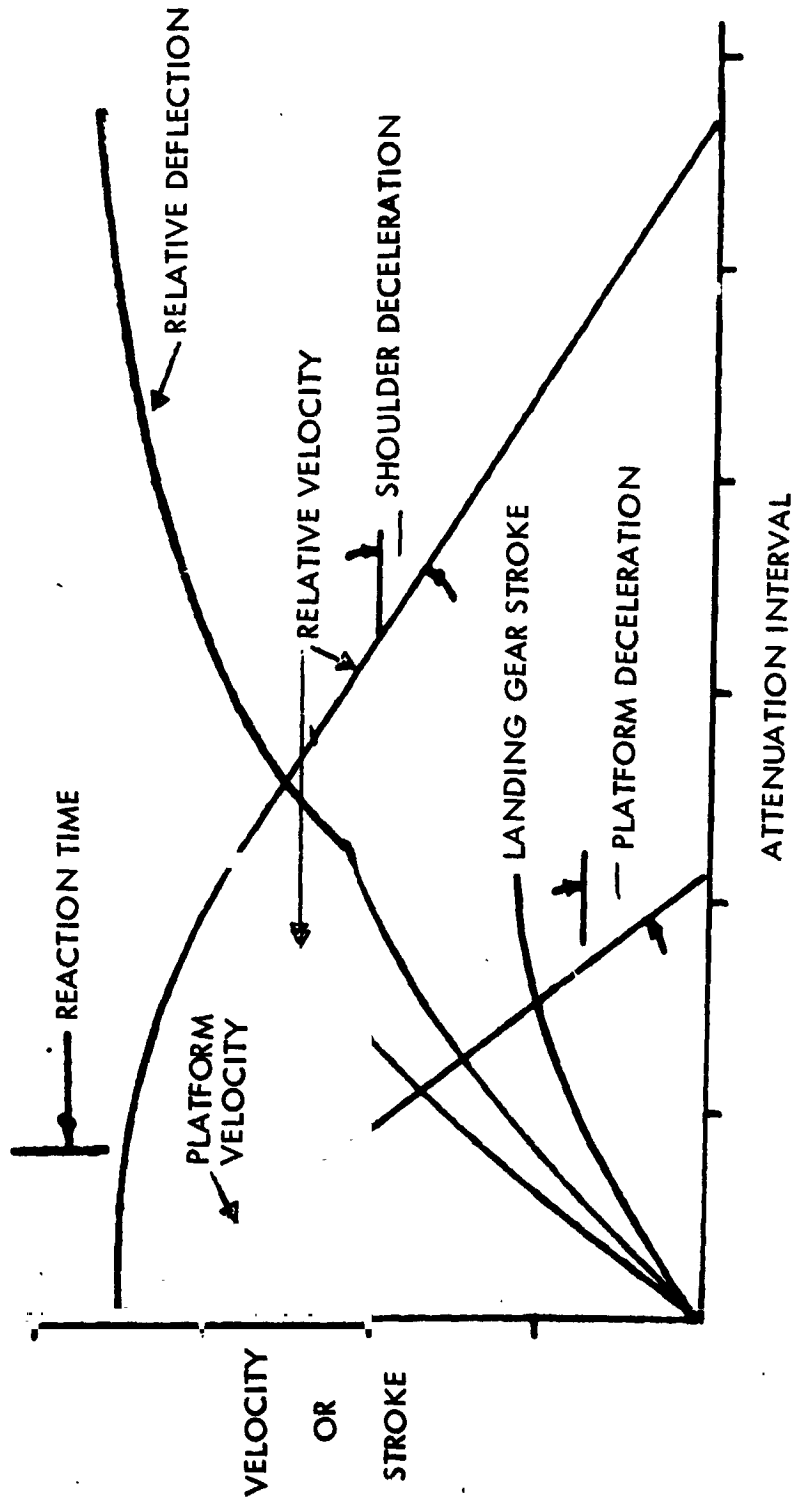


Figure 37. Idealized Unrestrained Pilot Attenuation

Table 6. Pilot Accelerations - Current Design Limits

| Subject Condition     | Controlling Factor                     | Normal g |          | Lateral g |          | Relative Motion (inches) |
|-----------------------|--|----------|----------|-----------|----------|--------------------------|
|                       |  | Platform | Shoulder | Platform  | Shoulder |                          |
| Unrestrained standing | Grip/arms (grip aid) (60-lb PLSS pull) | --       | --       | 1.0       | 0.5      | 8.4                      |
|                       | PLSS/suit interface                    | --       | 2 +      | --        | 2 +      | --                       |
|                       | Knee deflection                        | 3        | 2        | --        | --       | 8 to 15*                 |
| Closely restrained    | Design                                 | 3        | 2        | 1         | 0.5      | --                       |
|                       | Head motion                            | 8        | 8        | 4         | 4        | 0                        |
|                       | Spine (with local attenuation)         | 8        | 2        | --        | --       | 3.0                      |
|                       | PLSS/suit interface                    | 8        | 8        | 8         | 8        | 0                        |
|                       | Design                                 | 8        | 8        | 4         | 4        | --                       |
| *excessive deflection |  |          |          |           |          |                          |

an extensive test program, although ultimately necessary for final design of a system such as the LFV, was not feasible within the scope of this program. Accordingly, a much more modest test program limited to the most important objectives (study of vehicle ingress and egress operations and evaluation of vehicle/astronaut physical interfaces) was implemented.

#### Test Conditions and Procedures

The LFV mockup testing was carried out in the North American Rockwell Space Division mockup display area, which is equipped with suit pressurization and breathing air equipment, communications equipment, and a suit donning and removal room. The EMU worn by the test subject during all testing was provided by NASA MSC Crew Systems and included an A5L PGA modified to an A6L configuration, an integrated thermal meteoroid garment, an extravehicular visor assembly, lunar boots, a communications carrier, and an uncharged PLSS and OPS. A remote control unit was also provided but could not be utilized because of the absence of attachment hardware on the suit. A constant-wear garment was available in the North American Rockwell suit facility. All testing was performed under normal earth gravity with normal room lighting and ambient atmospheric conditions. One test subject was selected for compatibility of body dimensions with the available PGA from a group of Space Division pilots experienced in pressure-suited operations. Familiarization and practice operations were carried out in shirtsleeves and vented-suit conditions. Documented operations were performed in the pressurized mode, at 3.75 psig, using air for breathing gas.

The design of the mockup test article was based on a configuration developed early in the preliminary design phase. With the exception of some movable components, the mockup was essentially nonfunctional. Two configurations (designated Configurations A and B) were evaluated in the test series. The basic configuration (A) was utilized in the initial testing and incorporated the crew station features established in the design studies. In the second configuration, crew station features were modified on the basis of the initial test results.

Configuration A, illustrated in Figure 38, provided a pilot's station of essentially conventional design with respect to ingress/egress operations and body segment angular positions. This station design was based largely on A7L suit mobility specifications and mobility test data provided informally by the suit manufacturer. Special features of the mockup design included capability for rotation of the seat about a vertical axis through the approximate center; forward rotation of the seat about a hinge line beneath and slightly to the rear of the forward edge of the seat pan; hinged control/display arms which could be deployed inboard to the stowage position, outboard to a position approximately perpendicular to the sides of the seat,

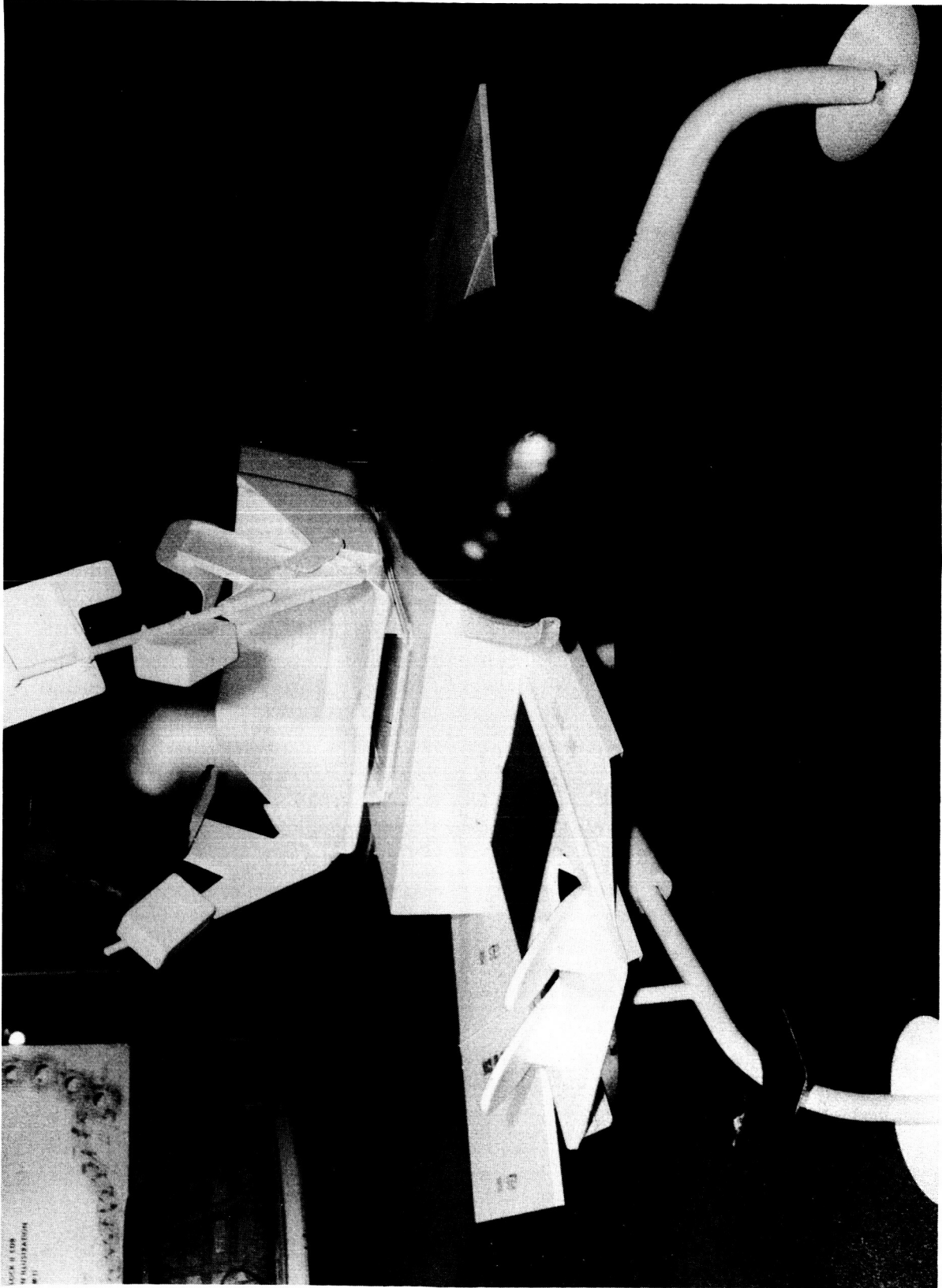


Figure 38. LFV Configuration A With Components in Flight Position

700-04-37A

LOCK 8 FOR  
RE-ILLUSTRATION  
#11

and latched in flight position; cargo shelves hinged for stowage and deployment; a removable helium tank cover; and controller assemblies adjustable for test subject forearm length. The ingress procedure established for Configuration A involved ascent to the platform in front of the seat by means of a step on the landing gear strut, aided by a handle mounted on the fuel tank and a handhold on the control display arm (mounted on the seat). After reaching the platform, the suited subject executed a 180-degree body rotation to achieve alignment for backward seat entry, and lowered himself into the seat with the control/display arms providing grasping points for support. The egress procedure was the reverse of the ingress procedure.

Configuration B, illustrated in Figure 39, differs from the basic configuration only in the design characteristics of the pilot station. The changes included removal of the platform with integral footrest, removal of the step from the landing gear strut, removal of the handle from the fuel tank, provision of an adjustable crossbar on the strut to representing a footrest, forward rotation of the pilot seat 15 degrees about its hinge line, provision of a lap strap in the stowage provisions, removal of the armrests from the controller/display arms, relocation of the controllers to a position about 4 inches outboard of their original position, and provision of stops on the controller arms to arrest outboard deployment of the arms 30 degrees from the flight position. The ingress procedure involved straddling the landing gear strut with the legs spread to clear the footrest, backing up to the seat, verifying proper body alignment, partially entering the seat with slight upward and backward motion, and achieving a secure seated position by placing the feet on the footrest and applying a pushing force with the legs. Egress consisted of lowering the legs from the footrests, sliding forward and down to make contact with the surface, with the legs straddling the landing strut, and walking forward with the legs spread to clear the footrest.

#### Results and Conclusions

In general, the results of the mockup test series showed that the mobility characteristics of the EMU provided for the tests were not compatible with some of the design features of Configuration A (the initial configuration), particularly those affecting ingress and egress operations. The postural instability associated with the mass distribution properties of the suit-backpack combination, together with the limited mobility of the pressurized subject, involved a considerable risk of loss of balance and body support in gaining access to the seat and descending to the surface. The problem experienced by the subject during these operations is vividly illustrated in Figure 40. This condition results primarily from inadequacies in the location and characteristics of the handhold provisions and the steps. The



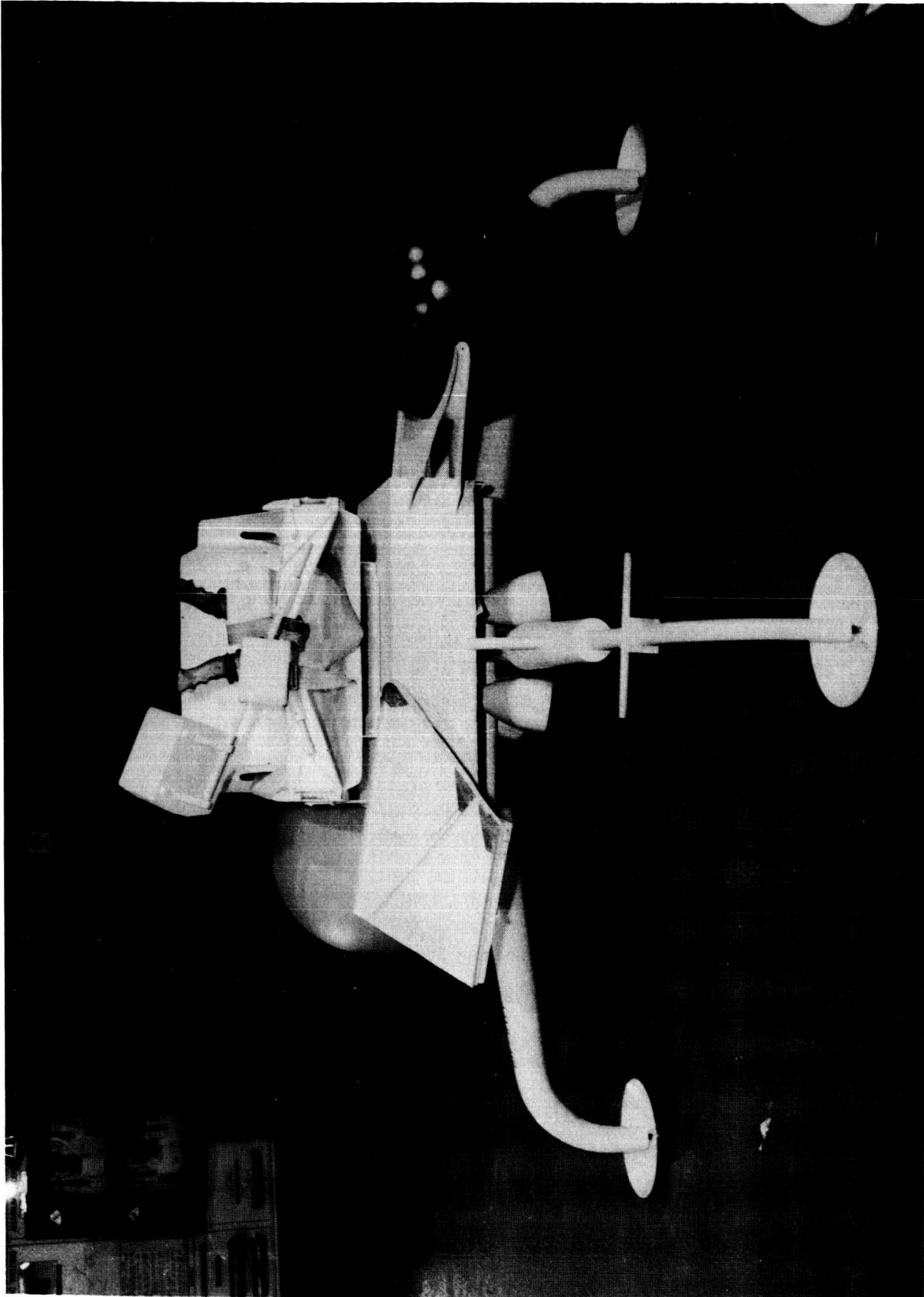
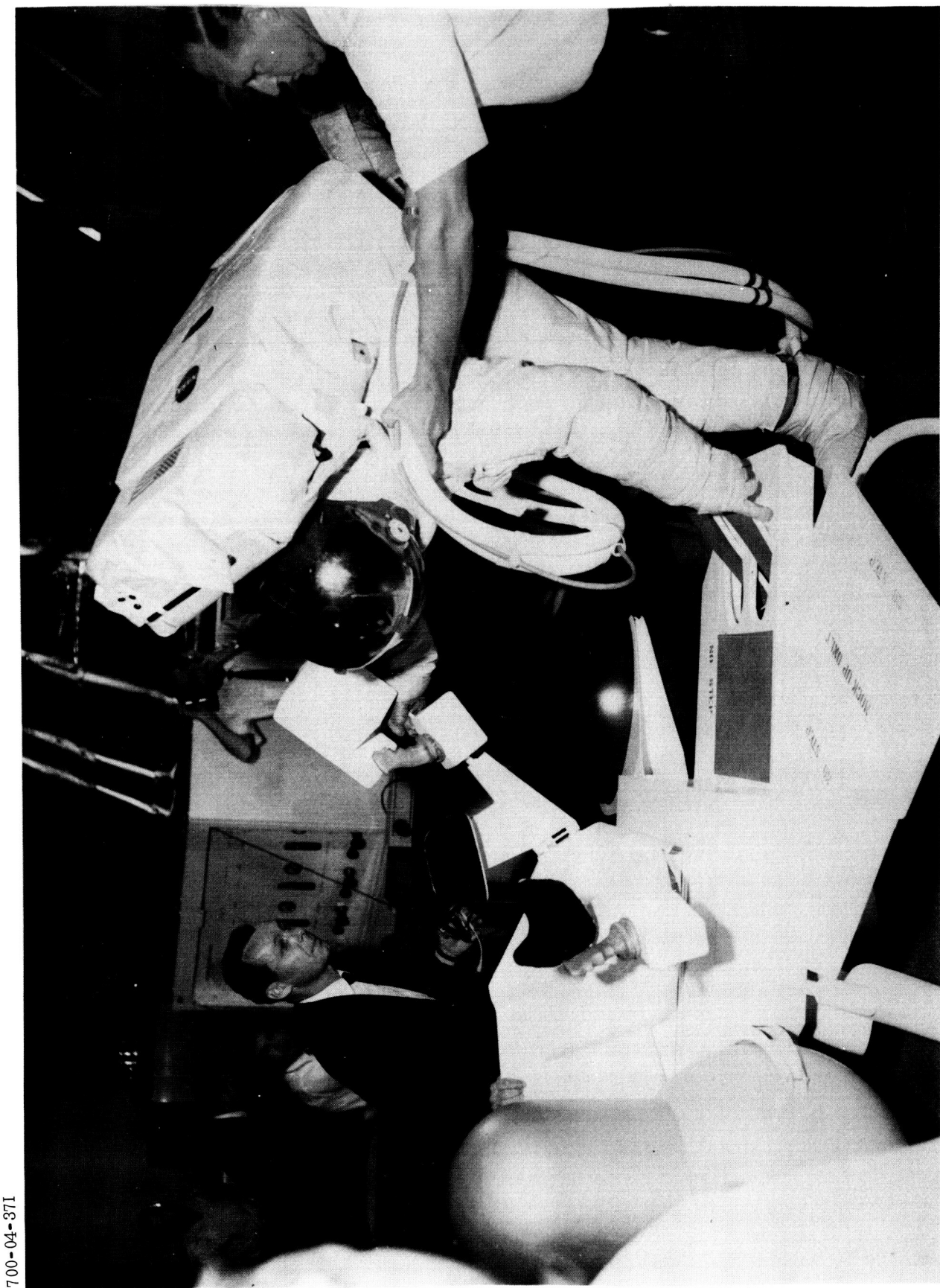


Figure 39. LFV Configuration B With Components in Stowage Position

7008-04-126A



700-04-871

Figure 40. LFV Configuration A Showing Test Subject Attempting Ingress

handholds were intended to provide the necessary body support and maintenance of body stability during ingress/egress operations. The mockup step spacing required a degree of knee flexure difficult for the pressurized subject to achieve. The difficulties described certainly could be substantially reduced by provision of a handrail system and additional steps, but this type of corrective action could not entirely eliminate the risk, would involve additional weight, and would present design problems associated with stowage provisions and interference with deployment of the controller arms. A simpler solution, and one which eliminates the risks described, is offered by Configuration B, which provides for direct access to the seat and required a minimum of handhold provisions. In Figure 41, the test subject is shown in a backward approach to the seat and has reached the point where he is initiating a sliding entry into the seat. It will be observed that a small ramp has been provided to facilitate seat entry by raising the body slightly. This feature was not necessary for the test subject, who has generally 90th-percentile body dimensions, but will be necessary for smaller subjects, who would have some difficulty with seat entry and exit with the seat at its present height. Such a mechanism would also assure subjects of a correct approach and seat entry if the vehicle is resting on a lunar surface with uneven or rough contours. The device could be integrated into the vehicle in such a way as to provide a shield against rocket plume and debris for the lower legs and could also be mechanized to swing up into position for use as a footrest and restraint. Further tests and development will be necessary to establish the seat entry requirements and to integrate these requirements into the vehicle design.

One of the more important elements of the seat entry maneuver requiring further study is the insertion of the PLSS into its support (in the event a support is required). It was observed in the course of testing that if the subject was not precisely aligned, the PLSS would impinge upon the top edge of the seat bucket sides or against the offset between the side of the seat and the side of the PLSS receptacle. Either case effectively blocked insertion of the PLSS into its support until the test subject realigned his body position to the correct orientation. A more gradual lead-in offset would facilitate this maneuver, but it appears that a folding mirror mounted on a controller arm for visual control of the maneuver may be necessary to assure proper body alignment.

As pointed out above, the pilot station characteristics of Configuration A conform generally to conventional pilot seat criteria relating to seat reference plane angles, as will be seen by reference to Figure 41. The mobility characteristics of the suit utilized in the tests were found to be compatible with this design, as anticipated on the basis of suit mobility data obtained for the design studies. The hip angle (102 degrees) associated with this design, however, resulted in suit compression which forced the front of the helmet upward, seriously degrading the visual field and viewing angles

7008-04-126C

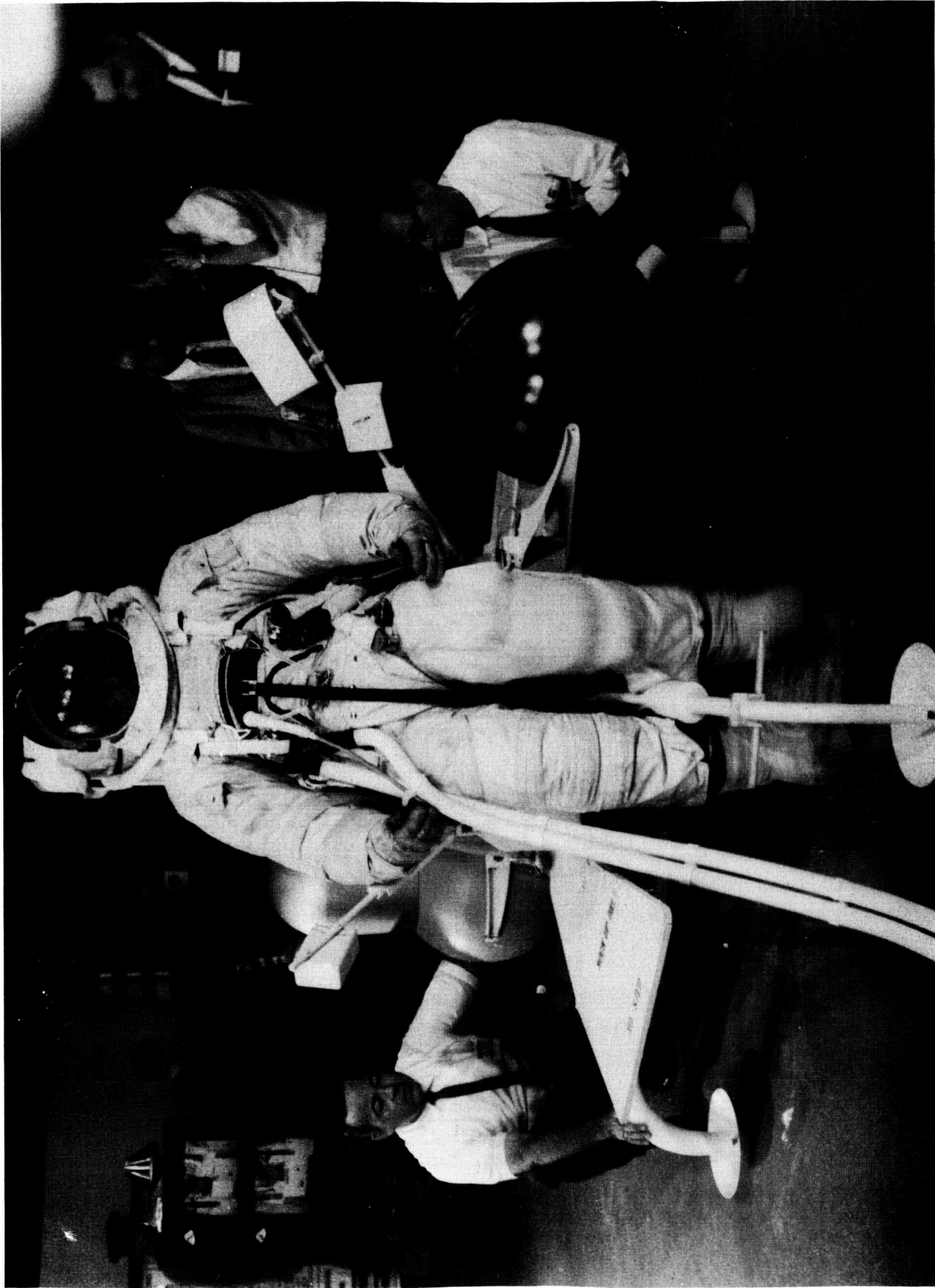


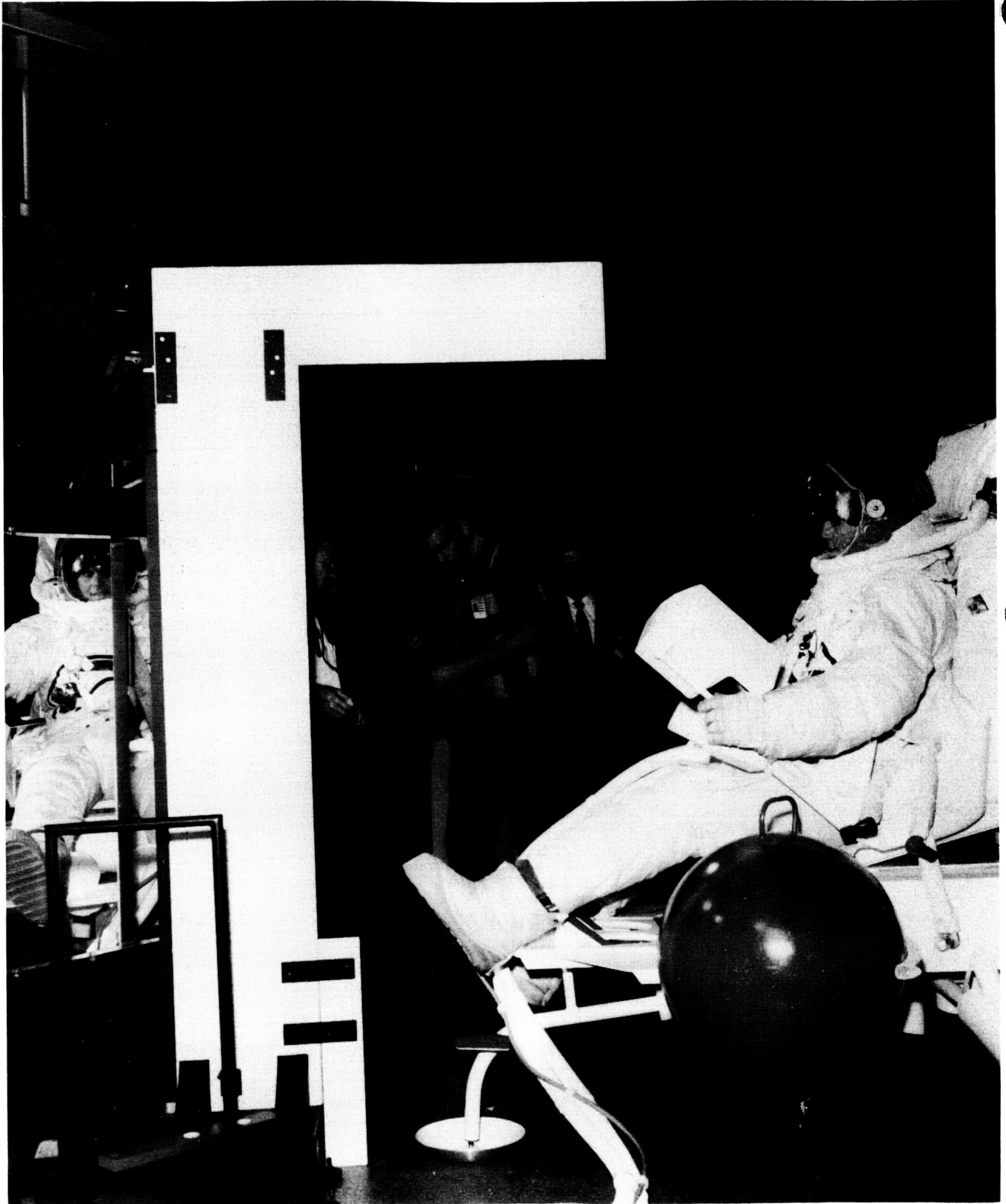
Figure 41. LFV Configuration B Showing Test Subject's Approach for Seat Entry

available to the test subject. This condition was corrected by adjustment of the front tiedown strap, which pulled the front of the helmet neck ring downward, restoring normal visual capability in the midsagittal plane. Upon descent from the vehicle, however, the tiedown strap adjustment made for the seated position forced the subject into a head-down position, so that adequate vision for the erect position could not be achieved. A further adjustment of the front tiedown strap was necessary to correct this condition. Neither of these adjustments could be accomplished by the test subject; assistance from another person was required.

It is clear from the foregoing that in the type of space suit used for this test, there is a fundamental incompatibility between sitting and standing postural adjustments. For comfort and visibility in the seated position, the tiedown strap must be tightened to permit an efficient helmet attitude when the subject is leaning back into his seat at an angle which can adequately support his PLSS and upper torso. For the standing position, however, the strap must be loosened, as the mass distribution of the suit-backpack combination required a forward leaning of the upper body to place the combined center of gravity forward over the feet. Current suit designs apparently make adjustment of the front tiedown strap very difficult when the suit is pressurized. Therefore, a compromise position for the strap may be necessary. Such a compromise strap adjustment, however, is incompatible with the visual requirements for the seated position in Configuration A, and it was necessary to tilt the seat forward as shown in Figure 42, rotating the upper body into a more upright position to improve visual capabilities for both the seated and standing positions. This measure did not completely correct the visual problem, and it also forced an excessive knee flexure for insertion of the feet into the footrest. A comfortable position for the legs could only be achieved by extending the feet beyond the footrest. The footrest platform assembly was therefore removed, and a temporary footrest was installed on the landing gear strut, as shown in Figure 43. This modification had the effect of opening the hip angle, thereby correcting the visual problem and providing a comfortable position for the subject's feet. It should be pointed out, however, that many of these difficulties may have been caused by an inadequate fitting of the suit.

In Configuration B, the forward tilt of the seat was firmly fixed, and an adjustable footrest was provided on the landing gear strut. These features are illustrated in Figure 44. The body segment angles associated with this modification sequence are shown in Table 7. Further design and test effort will be necessary to develop the footrest for adequate support and restraint of the feet.

A logical consequence of the evolution of the pilot's station into the B configuration was a tendency of the test subject to slide forward on the seat pan, even though he was restrained by a suitably deployed lap belt. This effect is primarily attributable to the downward seat pan angle of approximately 7 degrees, which results from the forward rotation of the seat.



700-04-87C

Figure 42. LFV Configuration A With Seat Tilted Forward to Improve Forward and Downward Vision

700-04-37D

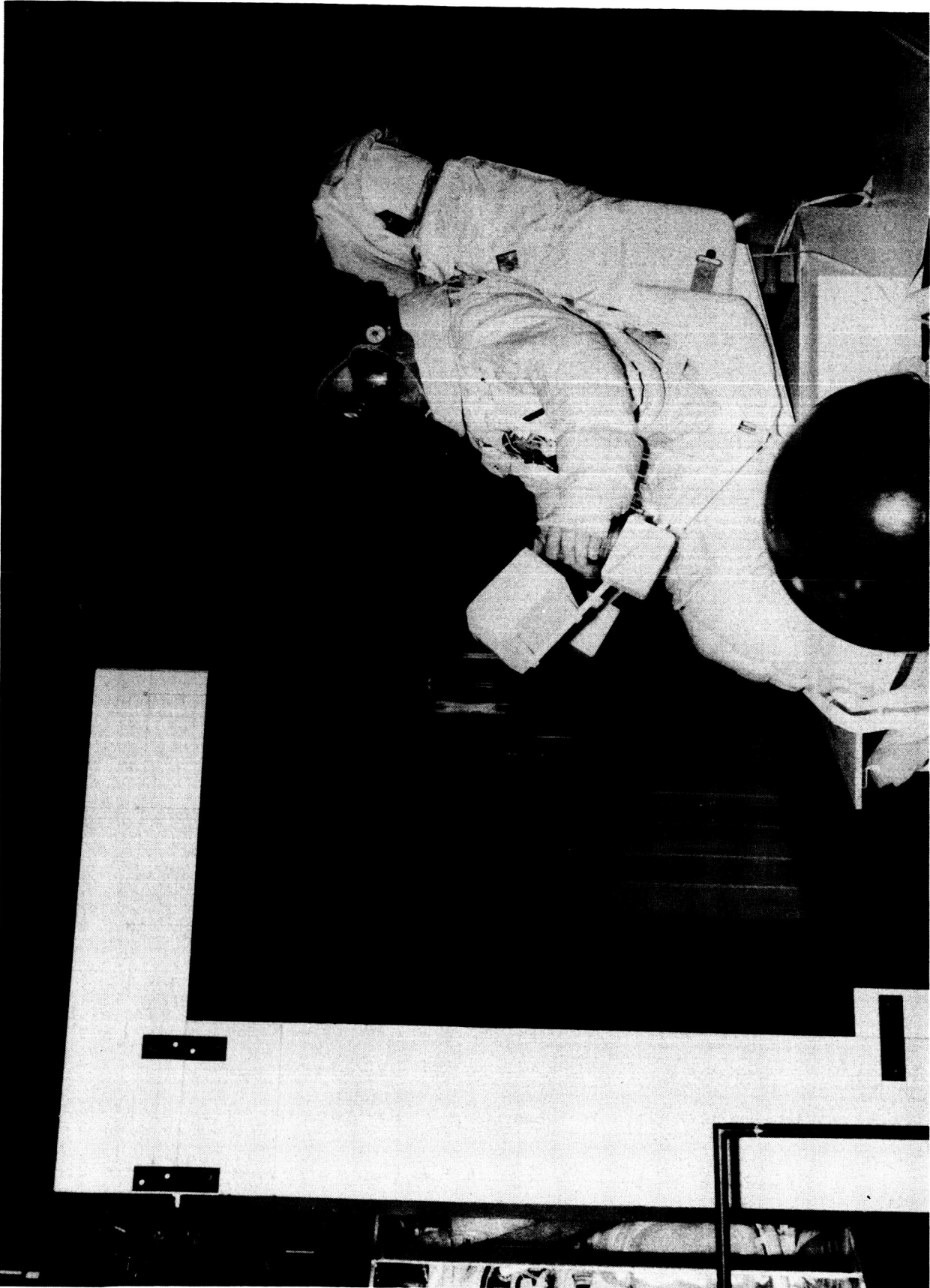


Figure 43. LfV Configuration A Modified by Removal of  
Footrest Platform and Seat Rotation

7008-04-126B

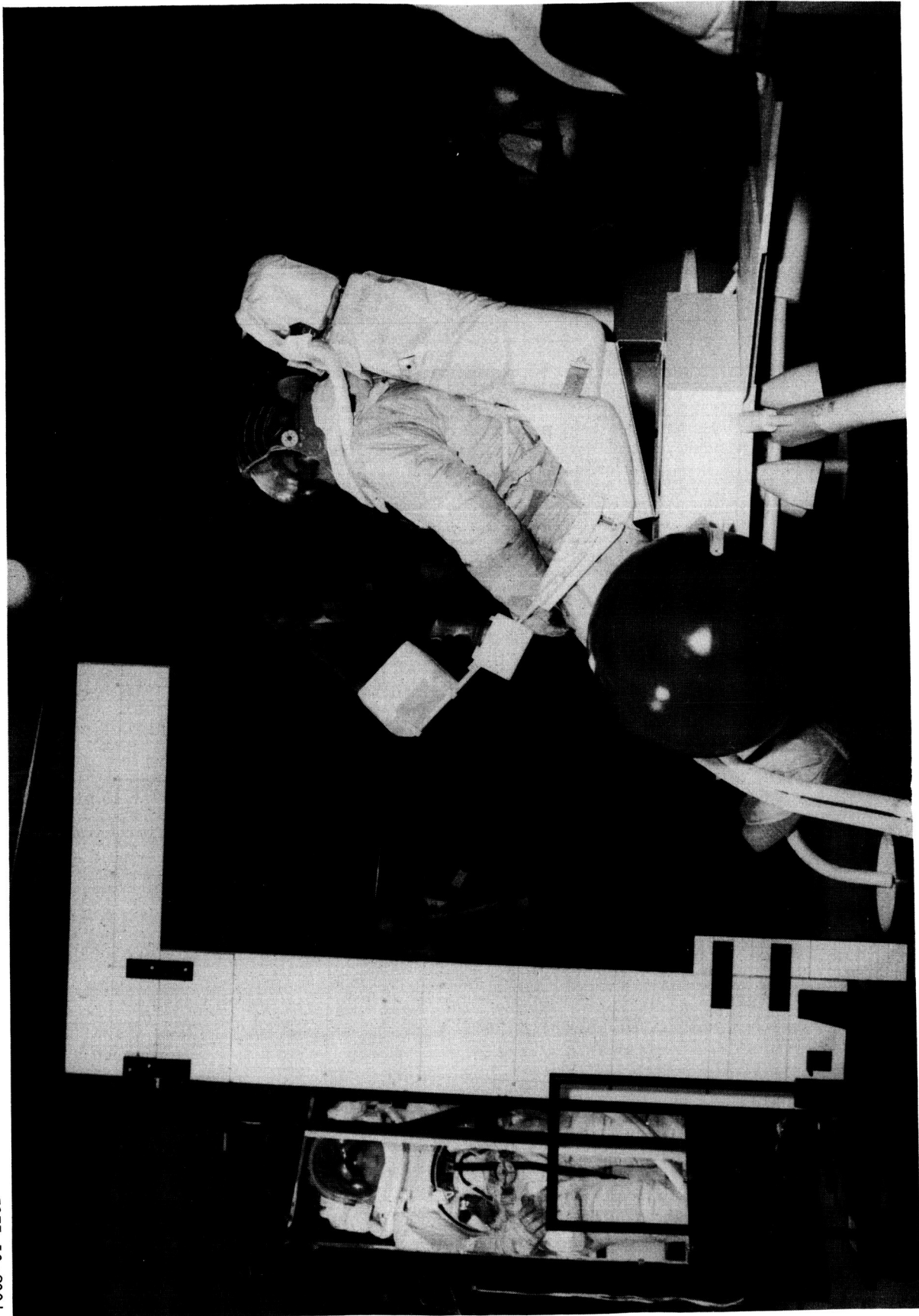


Figure 44. LFV Configuration B Incorporating All Modifications



**Table 7. Mockup Seat and Astronaut Body Angles**

| Observed Side View Angles*  | 6/16/69   |   | 6/19/69  |
|---|---|---|--|
|   | Configuration A<br>MOD 1<br>(Tilted<br>Seat)<br>(deg) | Configuration A<br>MOD 2<br>(Footrest Plat-<br>form Removed)<br>(deg) | Configuration B<br>(Adjustable<br>Footrest)<br>(deg) |
| Back angle (PLSS front)<br>from vertical, aft.  | 10 (P)  | 14 (P)  | 12.5 (P)   |
| Mockup seat, tilt, forward<br>(above horizontal)  | 14.5 (P)  | 15 (P)  | 14.5 (P)   |
|   | 15 (M)  | 15 (P)  | 15 (M)   |
| Mockup seat back angle resulting:<br>(from vertical, backtilt)                                    | 6.5 (P)   | 7 (P)   | 5.5 (P)  |
| Apparent mockup deck<br>angle from vertical   | 90 (P)<br>(Horizontal)                                | 90 (P)<br>(Horizontal)  | 90 (P)<br>(Horizontal)                               |
| Apparent mean thigh angle<br>below horizontal<br>Sagevection**                                    | 11 (P)  | 11.5 (P)  | 37.5 (P)   |
|   | 67 (P)  | 63.5 (P)  | 40.0 (P)   |
| Apparent mean lower leg angle below<br>horizontal<br>from vertical front of foot<br>Sagevection** | 45 (P)  | 71 (P)  | 54 (P)   |
|   | 45 (P)  | 16 (P)  | 36 (P)   |
|   | 35 (P)  | 4 (P)   | 27 (P)   |
| Apparent mean upper arm angle from<br>vertical, aft of elbow<br>Sagevection**                     | (Hands not<br>on control-<br>lers in photo)           | 19 (P)<br>5 (P)   | (Hands not<br>on control-<br>lers in photo)          |
|   |   | 10 (P)<br>65 (P)  |  |
| Apparent lower arm above<br>horizontal (elbow above waist)<br>Sagevection**                       |   |   |  |

\* (P) = Photographic measurement, (M) = Measurement on mockup

\*\* Sagevection is a space-suit mobility term coined to assure accurate technical meaning for limb position rotation with respect to the upper body. It is the angle of rotational movement forward and upward from the frontal reference plane midway through the subject's torso as seen from the side. Each major body segment is conceived as having a vector through its long axis, pointing outward from the torso (except the head). All vectors point downward to a starting (zero-degree) position when subject is standing "at attention."

Another factor contributing to the effect is that the normal back angle assumed by the subject did not conform to the angle of the PLSS support (which was very nearly vertical) because the tilt of the seat forced the subject forward in the seat. This effect would be a serious problem during landing impact at anticipated loads, but it can readily be corrected by installation of thigh restraints (which were not incorporated into the mockup, although they are provided by the vehicle design), deepening the seat pan and PLSS support, and modifying the back angle of the support.

The design also provides for upper torso restraint in the form of shoulder straps, but the need for such a restraint was questioned by the test subject during the test series. The subject felt that suit compression effects would limit forward pitch of the upper torso under landing loads, and these effects were verified during the tests by introducing forward transverse forces at the back of the PLSS. This was not a realistic simulation of landing impact effect, however, and dynamic testing at design impact loads will be necessary to verify the safety of a restraint system design that does not provide for upper torso restraint. In the absence of test data, it must be assumed that the safety of the pilot during landing impact will require the provision of an upper torso restraint.

One feature of the pilot station design which presented an unexpected problem during the tests was the provision of armrests on the controller arms. It was anticipated that the armrests would contribute to the comfort and support of the subject, but it was observed that they interfered substantially with deployment of the controller arms from the outboard position to the flight position, as well as the latching operation, and the test subject reported that they were too constraining. Since they are probably not necessary for body support during landing impact under the g-loading conditions anticipated, the armrests were removed in Configuration B. This facilitated retrieval of the controller arms from the outboard position, but it was also found necessary to limit the outboard position to 30 degrees by installation of mechanical stop in order to achieve efficient operation. This position provided sufficient clearance for seat entry and reduced reach distance for retrieval and deployment of the arms.

Fore and aft adjustment and vertical position of the throttle and attitude controllers were found to be comfortable and efficient for the test subject, but because of an error in fabrication, the controllers were displaced inboard from their design positions. The controllers were relocated to positions which were reported to be comfortable by the test subject (approximately 13-1/2 inches from the centerline of the seat). The position and orientation of the display panel were found to be satisfactory, but a minor change in configuration was necessary in order to improve the clearance between the throttle and the lower edge of the panel.

## RELIABILITY

### Design Objective of Reliability Study

Reliability methods and evaluation were applied to both phases of system and subsystem design as a pervasive standard. The most compelling reason for this approach is the fact that all lunar surface operations are hazardous, and a utilitarian vehicle (the nature and extent of its use are somewhat optional or discretionary) like the LFV will simply not be used if it compounds or increases the hazards significantly. This rational indicates that the emphasis should be placed on crew safety wherever there is a trade between crew safety and mission success. As indicated by the results of the design selection process, this emphasis was, in fact, applied.

The most important reliability principle applied was that of minimizing single-point failures that involved hardware with low unit reliability. The most notable example of that type of hardware on the LFV is the engine cluster. As an illustration, a design using two outboard engines represents two single-point failures. The loss of either engine in flight or on the ground beyond walk-back range results in the loss of a crew member, and the probability of crew loss is twice the probability of failure of a single engine. If the single-point failures were minimized to one - a single-engine design - crew loss probability would be reduced by a factor of two. Further improvement is also possible by using redundancy or backup elements to minimize single-point failures to zero. The recommended four-engine design is an example, since it is designed to be operable with one engine failed.

The achievement of true redundancy in a design can only be verified at the detailed mechanization level. This is because the interactions between redundant elements often involves a common failure cause. It is in this area that much of the study effort, in design as well as reliability evaluation, was expended - particularly with respect to the engines, gimbal actuators, power, stability and control system (SCS) components, and circuitry as combined subsystems. The study demonstrated that the desired redundancy was achievable without excessive weight penalty or other serious design compromises. It should be noted that reliability engineering was used only as an important design technique. The reliability values developed were essentially relative or comparative, and no attempt was made to develop absolute measures of LFV reliability that could be used to predict operational values.

## General Considerations

### Procedure

Reliability and safety evaluation of several LFV configuration alternatives was completed for the purpose of initial comparison and selection. The precontract analysis was updated and expanded to include more alternatives with a more detailed mission model and configuration set. Hardware reliability estimates were based on similarity to previously constructed space vehicle components and were modified by relative environmental severity. Relationships among phases in the five sortie missions and the single LFV component interactions were modeled by conditional, sequential logic, as well as by in-phase reliability logic from which mathematical models were derived. Sortie calculations were made by an automatic computer program called the abort automatic mathematical model (AARMM), and combination into a five-sortie mission was accomplished by a desk-type calculator. The mission was aborted after detection of any failure (Rule A). Additional evaluations of the control mode only and the checkout location were made from a mission model consisting of a single time phase of total mission length.

### Configuration Reliability Comparison

Comparison of reliabilities among the several configurations shows a complex mission success and crew safety relationship for varying rocket engine and gimbal actuator reliabilities. Figures 45 through 50 illustrate these variations over the practical reliability ranges and indicate that a single-engine configuration has higher mission success probability but lower crew safety than the multiple, redundant-engine configuration. The eight-actuator case is the only configuration that has complete actuator and engine redundancy, and that case exhibits the highest crew safety over all practical engine reliabilities.

Figure 51 illustrates another way to compare configurations, i. e., mission sortie number versus probability of success. The same conclusions as before are reached, with the additional information of comparison at each sequential time phase.

### Control Method Reliability Comparison

Control evaluation was performed on three configurations: eight single gimbal actuators; four two-in-a-can gimbal actuators; and sliding plate with two two-in-a-can actuators and two single-motor actuators. Table 8 indicates that the four two-in-a-can actuator configuration is the most reliable for crew safety under the assumption that failure detection and switching could be accomplished with a risk of 0.005 (i. e., five failures

NOTES: FOUR ENGINES AND  
EIGHT ACTUATORS

ACTUATOR RELIABILITY  $\left\{ \begin{array}{l} A_4 = 1.0 \\ A_3 = 0.999 \end{array} \right.$

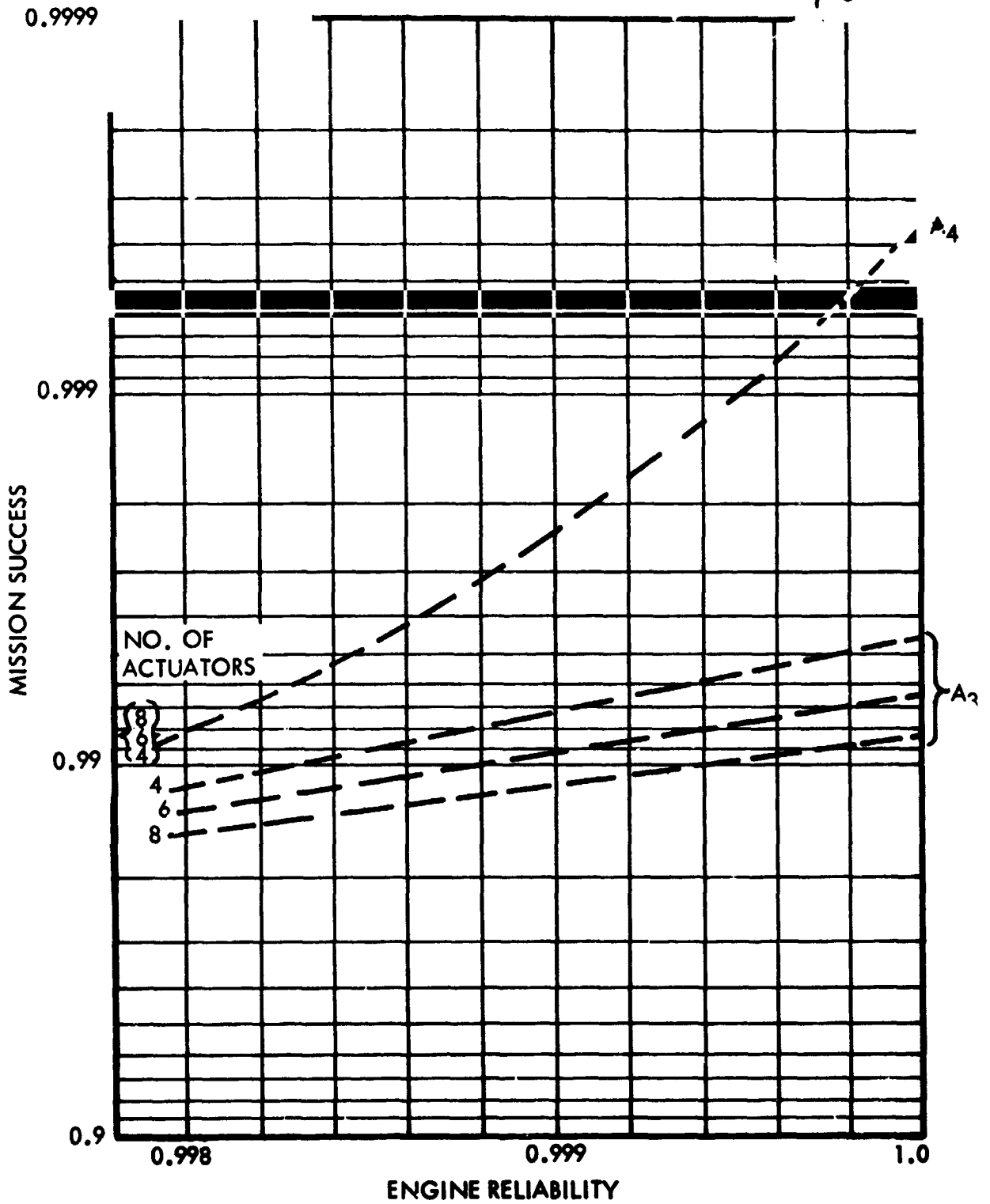


Figure 45. Mission Success for LFV Configuration 1, Rule A

NOTES:  
SINGLE LIFT ENGINE  
2 ACTUATORS, AND  
4 RCS ENGINES  
ACTUATOR {  $A_4 = 1.0$   
RELIABILITY {  $A_3 = 0.999$

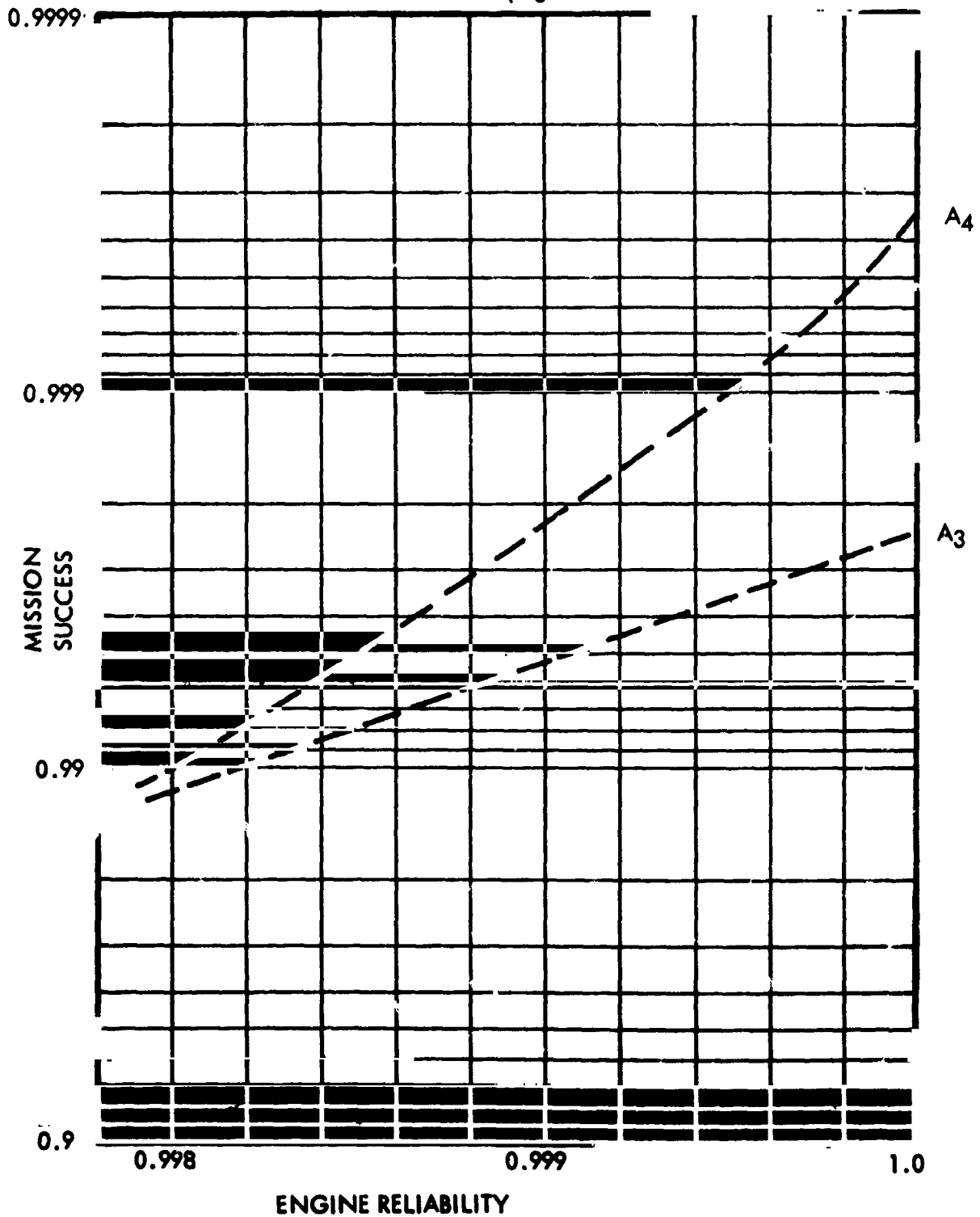


Figure 46. Mission Success for LEV Configuration 2, Rule A

NOTE:  
SINGLE LIFT ENGINE AND  
TWELVE RCS ENGINES

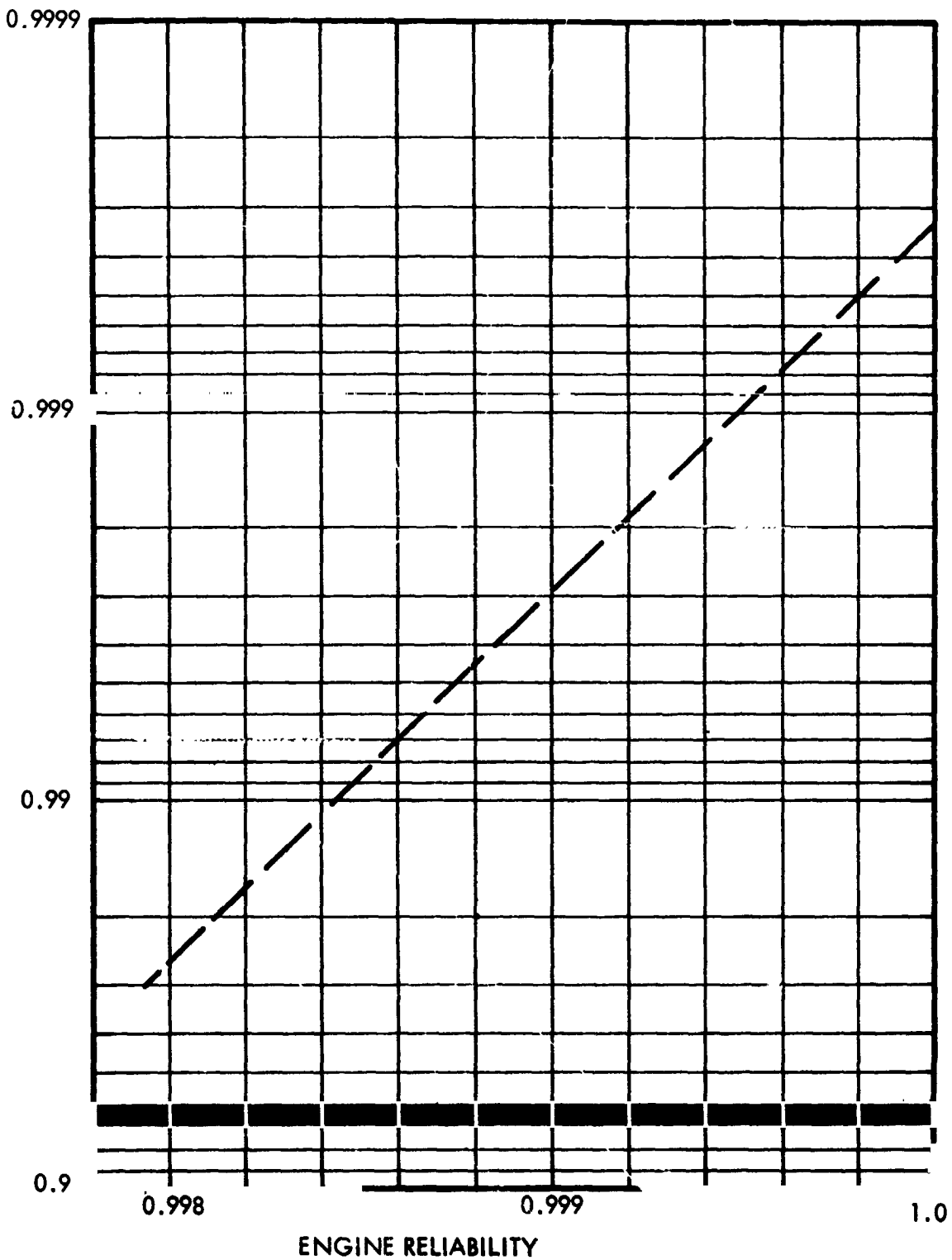


Fig re 47. Mission Success for LFV Configuration 3, Rule A

NOTES:  
SINGLE ENGINE  
AND 4 ACTUATORS  
ACTUATOR RELIABILITY  $\left\{ \begin{array}{l} A_4 = 1.0 \\ A_3 = 0.999 \end{array} \right.$

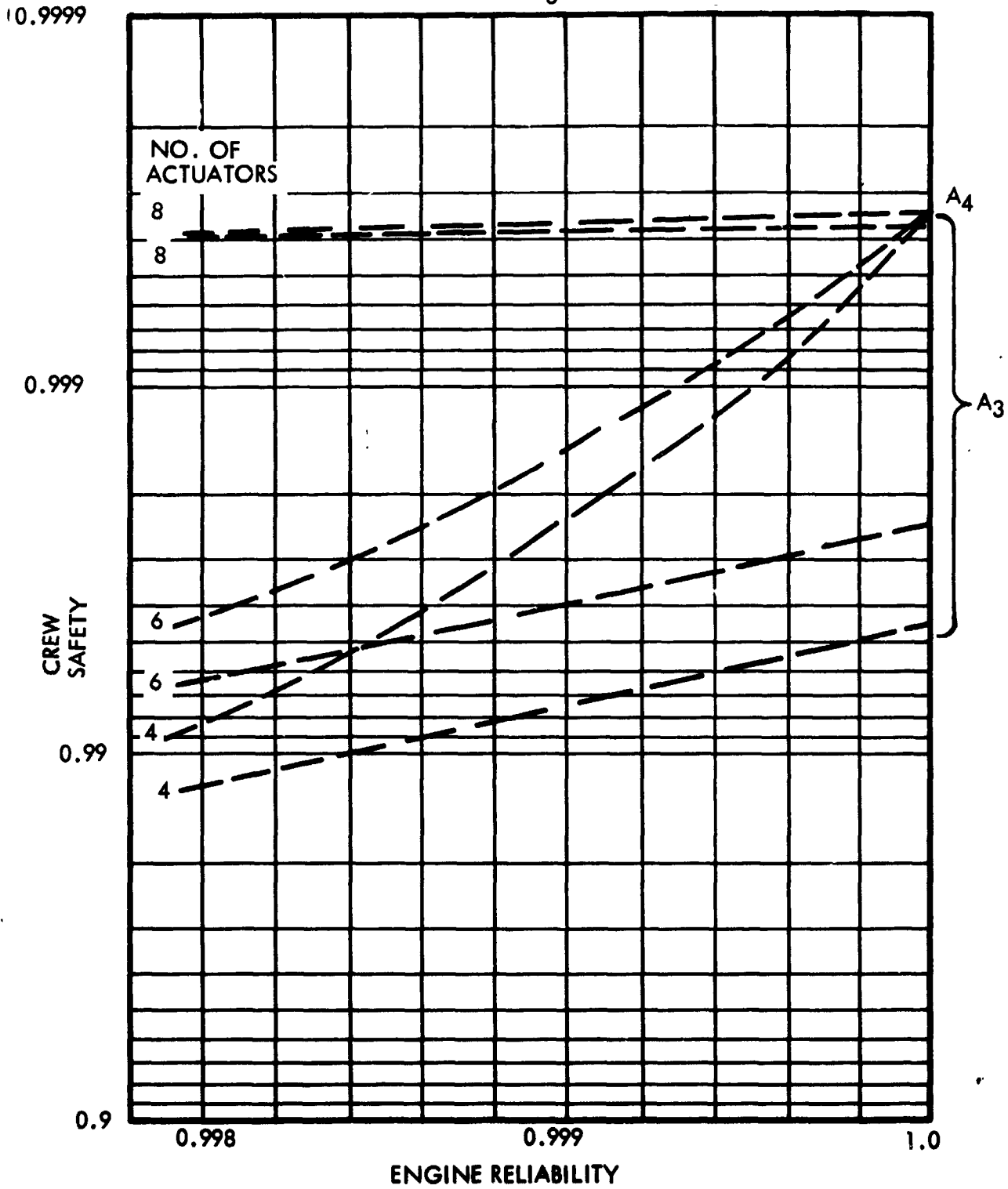


Figure 48. Crew Safety for LFV Configuration 1, Rule A



NOTES:  
SINGLE LIFT ENGINE,  
TWO ACTUATORS, AND  
FOUR RCS ENGINES  
ACTUATOR  $A_4 = 1.0$   
RELIABILITY  $A_3 = 0.999$

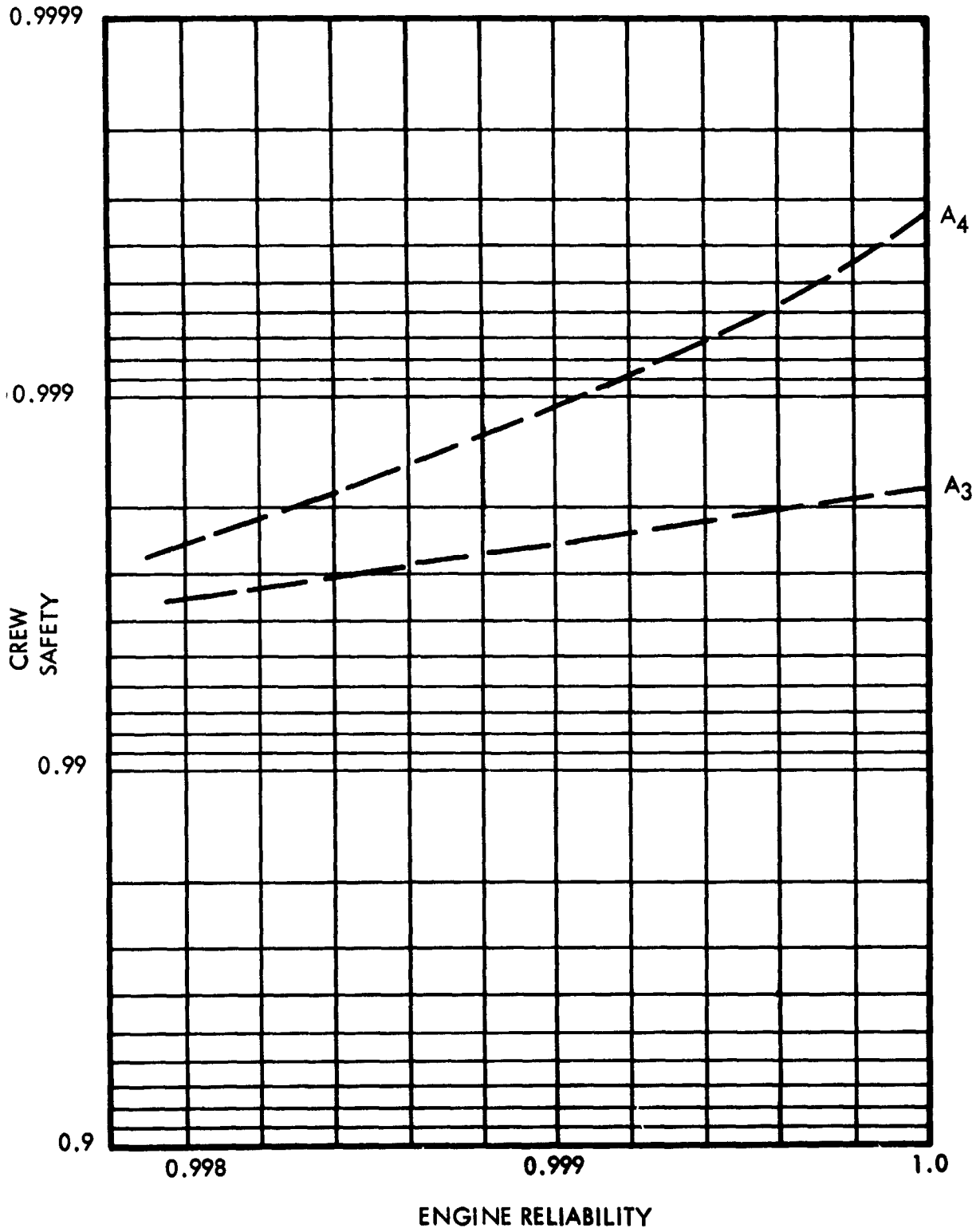


Figure 49. Crew Safety for LFV Configuration 2, Rule A

SINGLE LIFT ENGINE AND  
TWELVE RCS ENGINES

NOTE:

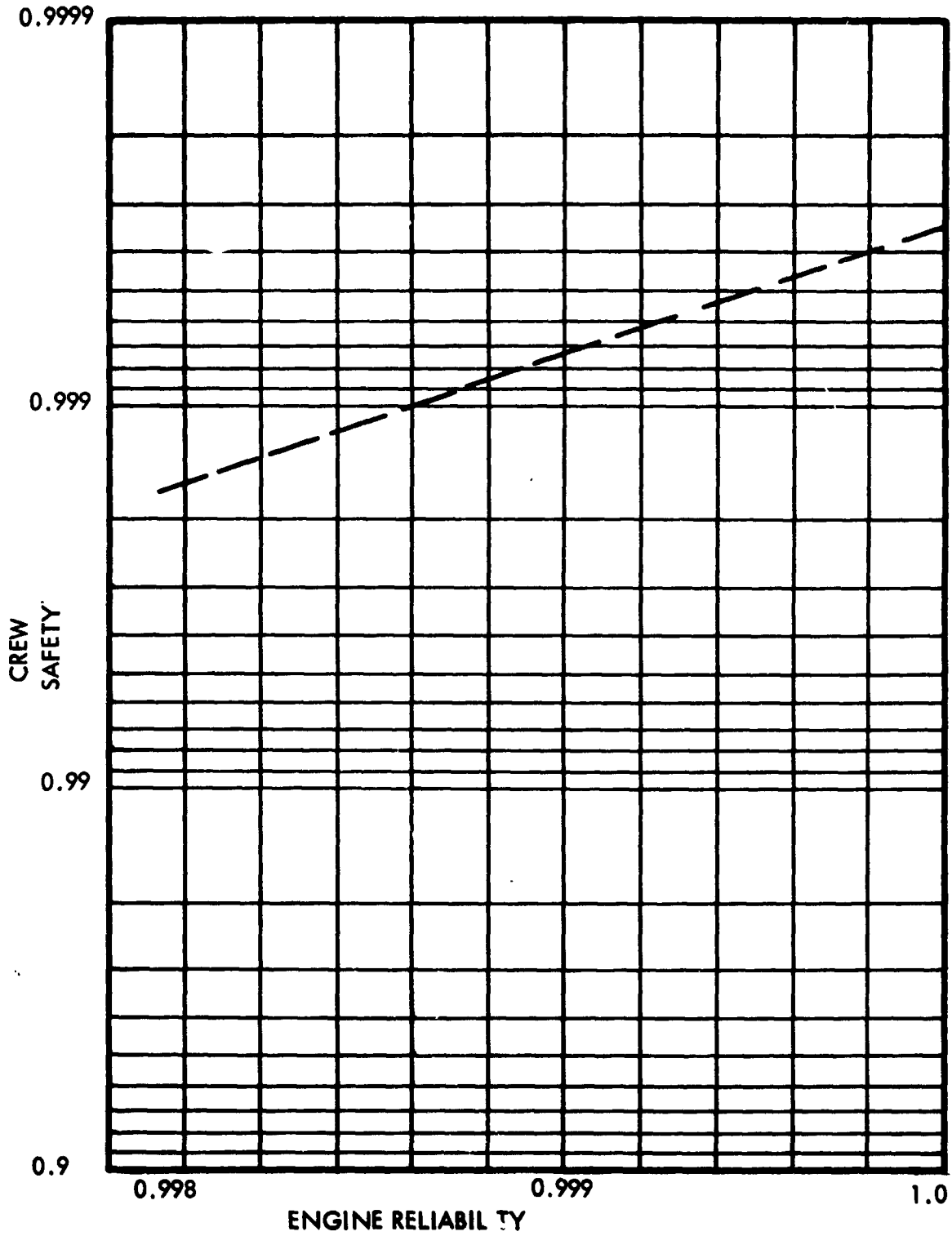


Figure 50. Crew Safety for LFV Configuration 3, Rule A

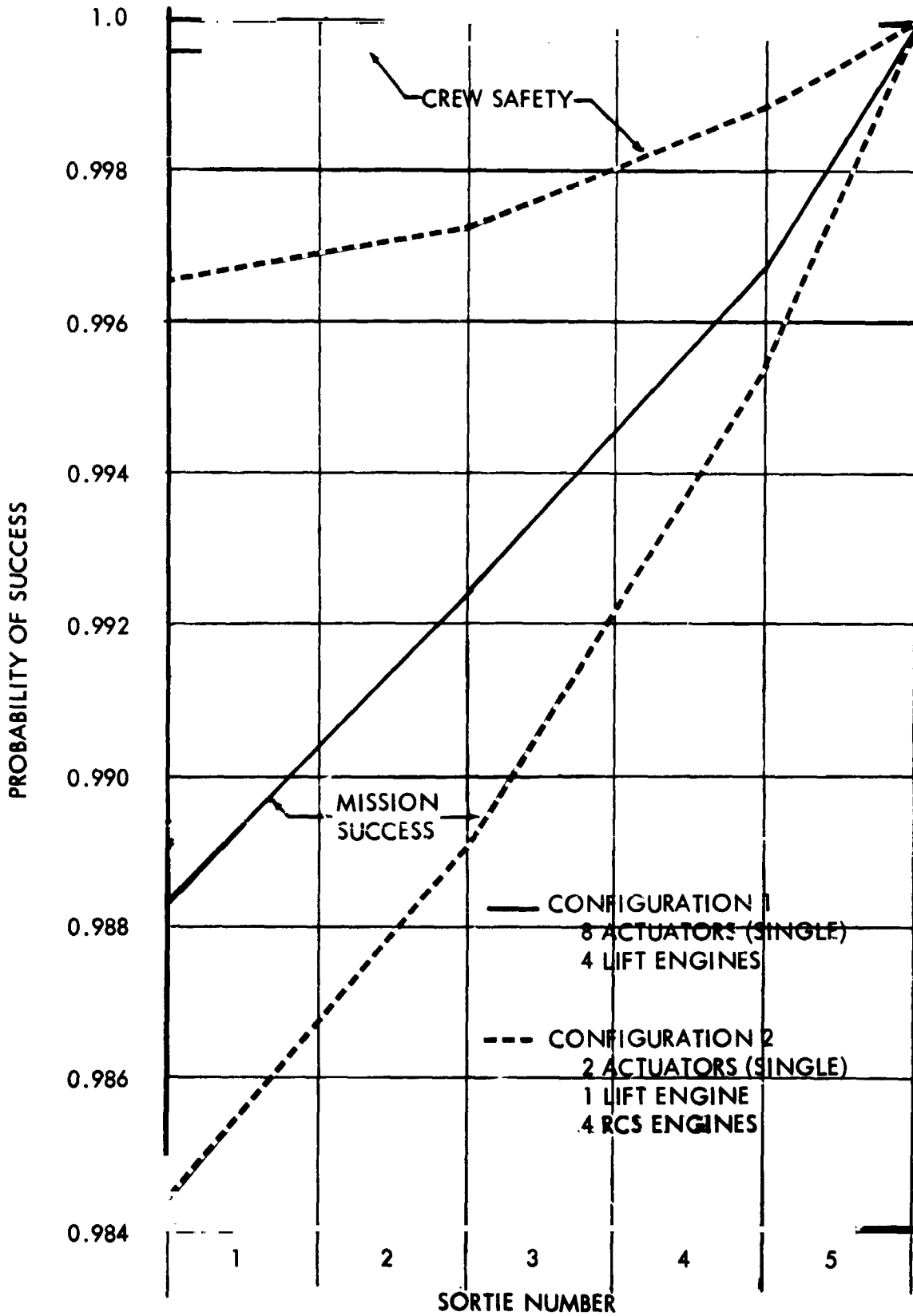


Figure 51. Mission Reliability Sequence for LFV Configurations 1 and 2

Table 8. Control Configuration Comparison  
 (Rule A)

| Configuration  | Mission Success * | Crew Safety * |
|--|-------------------|---------------|
| Eight actuators  | 0.992028          | 0.999972      |
| Four two-in-a-can actuators                                  |                   |               |
| Single-motor block or series item switching                  | 0.996006          | 0.9999998     |
| Four-motor block switching on single failure                 | 0.996006          | 0.999986      |
| Sliding plate  |                   |               |
| Single-motor block switching                                 |                   |               |
| Yaw loose (failure is fatal)                                 | 0.997003          | 0.999028      |
| Series items (loose failure is fatal)                        | 0.997003          | 0.999899      |
| Two-motor block switching on single failure (pitch and roll) |                   |               |
| Yaw loose (failure is fatal)                                 | 0.997003          | 0.999026      |
| Series items loose (failure is fatal)                        | 0.997003          | 0.999897      |
| *Computed on actuator failure only                           |                   |               |

per thousand missions). Any degradation of this value due to physical response capabilities of the astronaut would restructure the comparison toward the eight-actuator configuration. In the eight-actuator configuration, detection and switching is more of a convenience than a necessity because LFV operational capability is retained for any single actuator failure. The sliding plate method is not preferred because crew safety is lowered by actuator considerations as well as by the additional complexity of plates, ball bearings, plate assembly retainers, and linkages.

## Checkout Location Study

Checkout locations were studied by using computer results for Sortie 5 (triangular sortie) and selection of those failure combinations that would cause crew loss after a failure went undetected (i. e., equivalent to the mission continuation operational mode). Table 9 indicates that in-flight and remote landing site discovery of failures has a very small effect on crew safety. For this reason, checkout at the LM is acceptable.

## System Reliability Criteria

Two system reliability criteria are recommended for use in evaluating the capabilities of the LFV:

1. Mission success: LFV hardware probability of completing the anticipated mission sequence successfully
2. Crew safety: probability of no crew loss due to LFV equipment failure

Each of these criteria has a slightly different composition under each of two rules:

1. Rule A is defined as abort after one failure in flight or on lunar surface.
  - a. Mission success includes all components operating successfully over the entire mission, or a failure occurring that was not detected, and the mission being completed.
  - b. Crew safety includes mission success and all failures, detections, and safe abort sequences.
2. Rule B is defined as mission continuation whenever possible after one failure.
  - a. Mission success includes the employment of all possible means toward successful completion of the mission sequence.
  - b. Crew safety includes mission success and those failures which result in an inability to leave the LM or which occur within walk-back range.

Table 9. Mission Continuation Risks - Crew Losses  
Due to Multiple Failures

|   |
|---|
| Configuration 1 (four engines and eight actuators)  |
| $5 \times 10^{-6}$ /Sortie 5 for nonabort mode<br><br>$3 \times 10^{-6}$ /Sortie 5 for abort mode<br><br><hr style="width: 20%; margin-left: 0;"/> $2 \times 10^{-6}$ /Sortie 5 for nonabort penalty<br><br>$\frac{2 \times 10^{-6}}{130 \times 10^{-6}} \times 100 = 1.5\%$ /Sortie 5 for nonabort penalty<br>in % of total crew loss  |
| Configuration 2 (one lift engine, two actuators, and four reaction control engines)   |
| $2 \times 10^{-6}$ /Sortie 5 for nonabort mode<br><br>$1 \times 10^{-6}$ /Sortie 5 for abort mode<br><br><hr style="width: 20%; margin-left: 0;"/> $1 \times 10^{-6}$ /Sortie 5 for nonabort penalty<br><br>$\frac{1 \times 10^{-6}}{1130 \times 10^{-6}} \times 100 = 0.1\%$ /Sortie 5 for nonabort penalty<br>in % of total crew loss |

Precontract goals were that mission success and crew safety be 0.99 and 0.9999, respectively. The more detailed evaluation conducted under this contract has substantiated the mission success goal under Rule A. Figures 45 through 50 clearly indicate that the initial reliability estimates are very near these goals, and all mission success curves lie above the goal for some reasonable engine reliability values. Crew safety did not fare as well, since no configuration met this goal due to conservative component reliability estimates for propellant supply and control electronics. When further details on these subsystems are available, a more definitive evaluation can be made. In the meantime, a reasonable crew safety comparison can be made at 0.999, which can be met by all configurations

but with increasing difficulty by the single-engine and nonredundant actuator cases. Under Rule B, mission success increases toward the crew safety limit, so that 0.999 becomes a better means for comparison. The degradation of crew safety under Rule A to crew safety under Rule B is very small, as indicated by the checkout location study above, so the comparison can be made at 0.999 again. It must be noted that these numerical goals do not include probability of the astronaut to maneuver, to detect failures, to recover control after a failure, or to return to the LM by walking.

### Reliability Logic

#### Mission Sequence

The reference mission timeline was used to model the mission in logical alternate paths. Figure 52 shows the successful path diagram for the entire mission, beginning with liftoff from earth and ending with the triangular sortie (Sortie 5). Abort is necessary after every detectable failure and is successful by any possible means for return to the LM.

Logic diagrams were constructed for each sortie (Figures 53 and 54). These models are all very similar in construction because each considers the sequential nature of mission phases and abort decisions; i.e., the mission must be successful for the preceding phases in order to reach any given phase. Any abort from a preceding phase precludes the attempt of any succeeding phase. Logic for the criterion of mission success is included in Figures 52, 53, and 54 as completely successful operation (the top path in each). The first two phases in Figure 52, quiescent storage and assembly, were common to all configurations and were not included in the comparison numerics. The walk-back shown in Figures 52 and 53 is a particular case of successful return to the LM. Successful return to the LM under Rule A covers all abort means during a flight to or from the LM. Successful return to the LM under Rule B covers all abort means from remote mission operations. All configurations were required to complete all five sorties according to the same logic.

#### In-Phase Logic

Each configuration required its own reliability logic within each time phase because of different component failure effects; e.g., for crew safety, a single engine is not redundant, and four engines are successful if any three are successful. Rather than depict each time phase of each configuration in a standard reliability logic diagram, tables of conditional criticality and dependency were prepared. These were sufficient for describing the logic input to the computer program discussed in a succeeding section. Two typical pages are shown in Tables 10 and 11 for the four-engine and

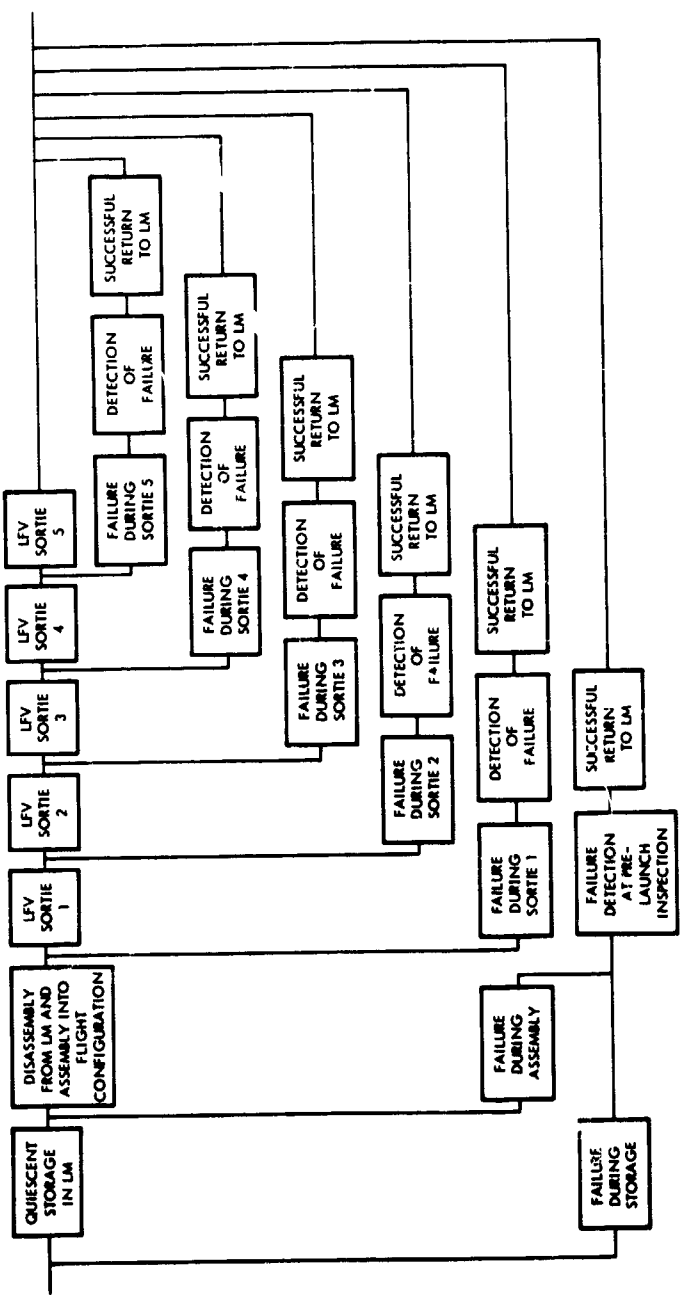


Figure 52. Successful-Path Diagram, Mission Crew Safety



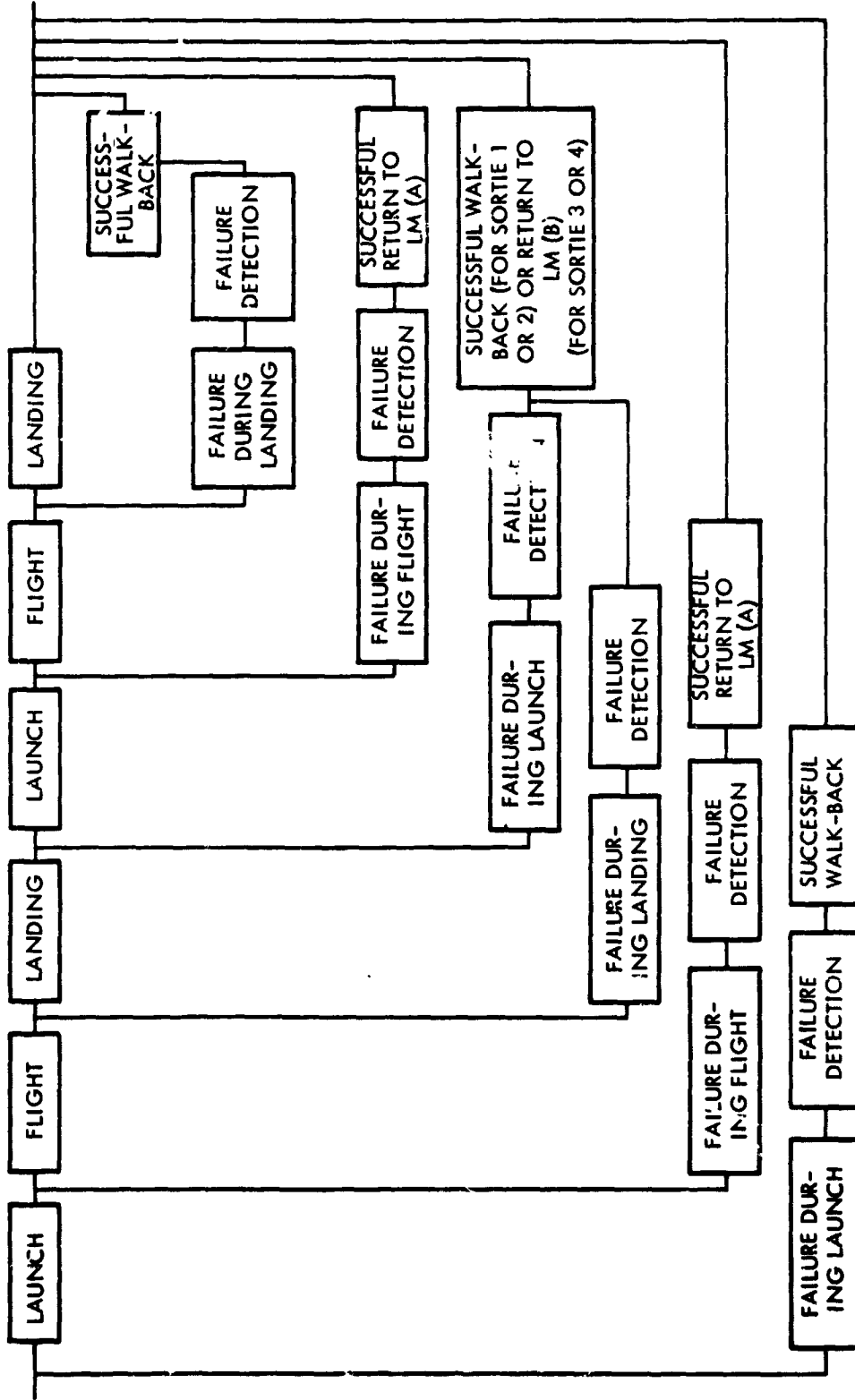
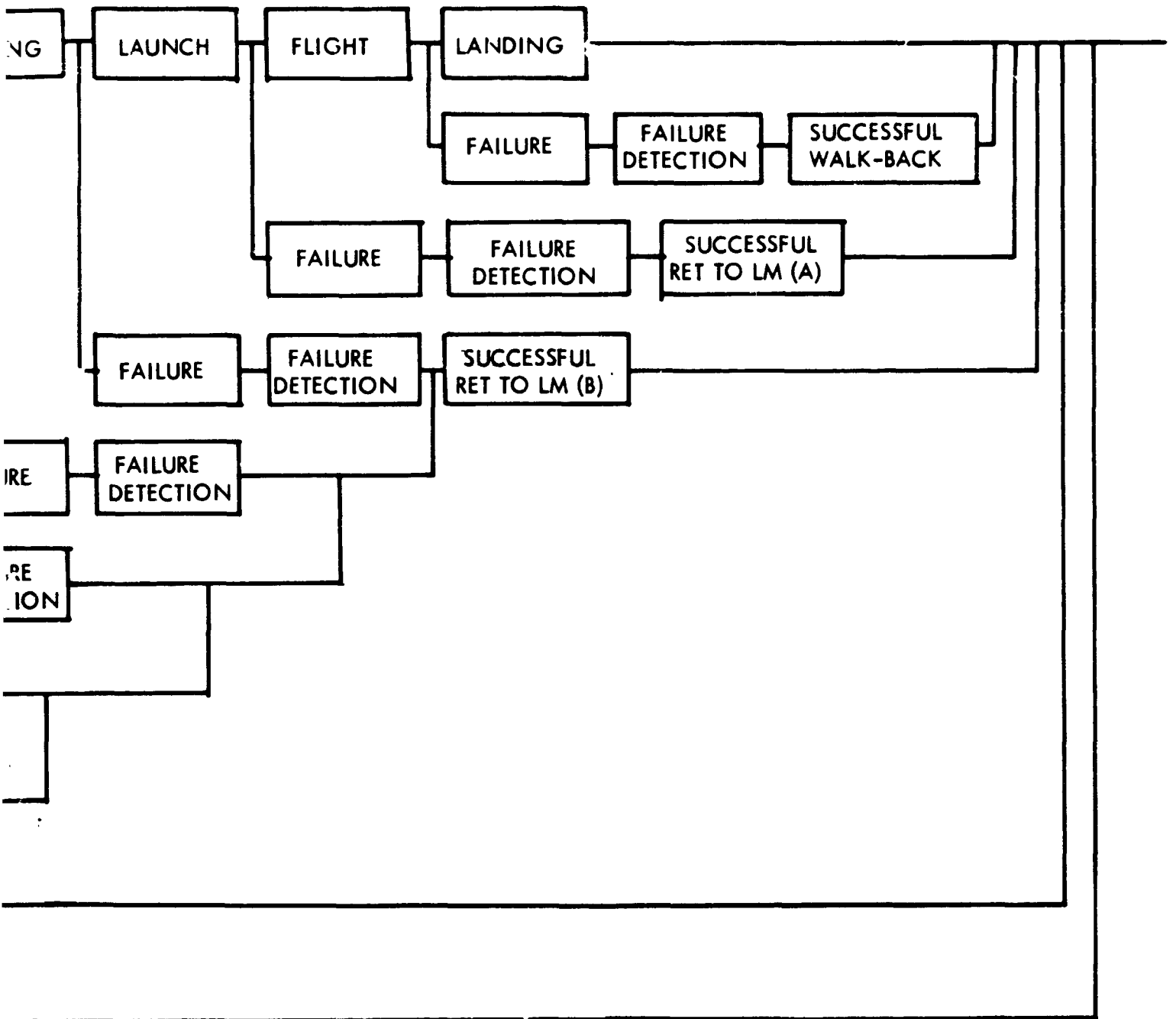


Figure 53. Successful-Path Diagram, Sorties 1 Through 4 Crew Safety





PRECEDING PAGE BLANK NOT FILMED.

Figure 54. Successful-Path Diagram, Sortie 5 Crew Safety

**Table 10. Typical In-Phase Logic - Four-Engine Configuration  
 (ARM PROGRAM LOGIC)**

| Configuration 1<br>(4 Engines), Rule A<br>Component | Failure<br>Rate<br>x10 <sup>-6</sup> /hour | Criticality |                  |                  |       | Abort            |       | Depend-<br>ency<br>Components |
|---|--|-------------|------------------|------------------|-------|------------------|-------|-------------------------------|
|   |  | Alone       | Combination      |                  | Alone | Combina-<br>tion |       |                               |
|   |  |             | Time Phase       | Abort            |       |                  |       |                               |
| 1.2 ENGINE 1 - FAILURE MODE: CEASE TO OPERATE       |  |             |                  |                  |       |                  |       |                               |
| Phase 1.1, 2.1                                      | 26060                                      | 0           | 0                | 0                | 0     | 0                | 1 (M) | 1.6, 3.2                      |
| 1.2, 2.2  | 2606                                       | 0           | 1 (M $\bar{E}$ ) | 1 (M $\bar{E}$ ) | 0     | 0                | 1 (M) | 1.6, 3.2                      |
| 1.3, 2.3  | 26060                                      | 0           | 0                | 0                | 0     | 0                | 1 (M) | 1.6, 3.2                      |
| 1.4, 2.4  | 26060                                      | 0           | 0                | 0                | 0     | 0                | 1 (M) | 1.6, 3.2                      |
| 1.5, 2.5  | 2606                                       | 0           | 1 (M $\bar{E}$ ) | 1 (M $\bar{E}$ ) | 0     | 0                | 1 (M) | 1.6, 3.2                      |
| 1.6, 2.6  | 26060                                      | 0           | 0                | 0                | 0     | 0                | 1 (M) | 1.6, 3.2                      |
| Phase 3.1, 4.1                                      | 26060                                      | 0           | 0                | 0                | 0     | 0                | 1 (M) | 1.6, 3.2                      |
| 3.2, 4.2  | 2606                                       | 0           | 1 (M $\bar{E}$ ) | 1 (M $\bar{E}$ ) | 0     | 0                | 1 (M) | 1.6, 3.2                      |
| 3.3, 4.3  | 26060                                      | 0           | 1 (M $\bar{E}$ ) | 1 (M $\bar{E}$ ) | 0     | 0                | 1 (M) | 1.6, 3.2                      |
| 3.4, 4.4  | 26060                                      | 0           | 1 (M $\bar{E}$ ) | 1 (M $\bar{E}$ ) | 0     | 0                | 1 (M) | 1.6, 3.2                      |
| 3.5, 4.5  | 2606                                       | 0           | 1 (M $\bar{E}$ ) | 1 (M $\bar{E}$ ) | 0     | 0                | 1 (M) | 1.6, 3.2                      |
| 3.6, 4.6  | 26060                                      | 0           | 0                | 0                | 0     | 0                | 1 (M) | 1.6, 3.2                      |
| Phase 5.1   | 26060                                      | 0           | 0                | 0                | 0     | 0                | 1 (M) | 1.6, 3.2                      |
| 5.2   | 2606                                       | 0           | 1 (M $\bar{E}$ ) | 1 (M $\bar{E}$ ) | 0     | 0                | 1 (M) | 1.6, 3.2                      |
| 5.3   | 26060                                      | 0           | 1 (M $\bar{E}$ ) | 1 (M $\bar{E}$ ) | 0     | 0                | 1 (M) | 1.6, 3.2                      |
| 5.4   | 26060                                      | 0           | 1 (M $\bar{E}$ ) | 1 (M $\bar{E}$ ) | 0     | 0                | 1 (M) | 1.6, 3.2                      |
| 5.5   | 2606                                       | 0           | 1 (M $\bar{E}$ ) | 1 (M $\bar{E}$ ) | 0     | 0                | 1 (M) | 1.6, 3.2                      |
| 5.6   | 26060                                      | 0           | 1 (M $\bar{E}$ ) | 1 (M $\bar{E}$ ) | 0     | 0                | 1 (M) | 1.6, 3.2                      |
| 5.7   | 26060                                      | 0           | 1 (M $\bar{E}$ ) | 1 (M $\bar{E}$ ) | 0     | 0                | 1 (M) | 1.6, 3.2                      |
| 5.8   | 2606                                       | 0           | 1 (M $\bar{E}$ ) | 1 (M $\bar{E}$ ) | 0     | 0                | 1 (M) | 1.6, 3.2                      |
| 5.9   | 26060                                      | 0           | 0                | 0                | 0     | 0                | 1 (M) | 1.6, 3.2                      |

0  $\triangleq$  Not applicable  
 1  $\triangleq$  Applicable  
 M  $\triangleq$  Failure detection  
 E  $\triangleq$  Any other engine

**Table 11. Typical In-Phase Logic - Single-Engine Configuration  
(ARMM PROGRAM LOGIC)**

| Configuration 2<br>(1 Engine), Rule A<br>Component   | Failure<br>Rate<br>$\times 10^{-6}$ /hour | Criticality |             |       |       | Abort       |       | Dependency    |
|--|---|-------------|-------------|-------|-------|-------------|-------|---------------|
|  |   | Alone       | Combination |       | Alone | Combination |       |               |
|  |   |             | Time Phase  | Abort |       |             |       |               |
| 1.2 ENGINE - FAILURE MODE: CEASE TO OPERATE  |   |             |             |       |       |             |       |               |
| Phase 1.1, 2.1   | 26060                                     | 0           | 0           | 0     | 0     | 0           | 1 (M) | 1.3, 3.2, 3.3 |
| 1.2, 2.2   | 2606                                      | 1           | 0           | 0     | 0     | 0           | 0     | 0             |
| 1.3, 2.3   | 26060                                     | 0           | 0           | 0     | 0     | 0           | 1 (M) | 1.3, 3.2, 3.3 |
| 1.4, 2.4   | 26060                                     | 0           | 0           | 0     | 0     | 0           | 1 (M) | 1.3, 3.2, 3.3 |
| 1.5, 2.5   | 2606                                      | 1           | 0           | 0     | 0     | 0           | 0     | 0             |
| 1.6, 2.6   | 26060                                     | 0           | 0           | 0     | 0     | 0           | 1 (M) | 1.3, 3.2, 3.3 |
| Phase 3.1, 4.1   | 26060                                     | 0           | 0           | 0     | 0     | 0           | 1 (M) | 1.3, 3.2, 3.3 |
| 3.2, 4.2   | 2606                                      | 1           | 0           | 0     | 0     | 0           | 0     | 0             |
| 3.3, 4.3   | 26060                                     | 1           | 0           | 0     | 0     | 0           | 0     | 0             |
| 3.4, 4.4   | 26060                                     | 1           | 0           | 0     | 0     | 0           | 0     | 0             |
| 3.5, 4.5   | 2606                                      | 1           | 0           | 0     | 0     | 0           | 0     | 0             |
| 3.6, 4.6   | 26060                                     | 0           | 0           | 0     | 0     | 0           | 1 (M) | 1.3, 3.2, 3.3 |
| Phase 5.1  | 26060                                     | 0           | 0           | 0     | 0     | 0           | 1 (M) | 1.3, 3.2, 3.3 |
| 5.2  | 2606                                      | 1           | 0           | 0     | 0     | 0           | 0     | 0             |
| 5.3  | 26060                                     | 1           | 0           | 0     | 0     | 0           | 0     | 0             |
| 5.4  | 26060                                     | 1           | 0           | 0     | 0     | 0           | 0     | 0             |
| 5.5  | 2606                                      | 1           | 0           | 0     | 0     | 0           | 0     | 0             |
| 5.6  | 26060                                     | 1           | 0           | 0     | 0     | 0           | 0     | 0             |
| 5.7  | 26060                                     | 1           | 0           | 0     | 0     | 0           | 0     | 0             |
| 5.8  | 2606                                      | 1           | 0           | 0     | 0     | 0           | 0     | 0             |
| 5.9  | 26060                                     | 0           | 0           | 0     | 0     | 0           | 1 (M) | 1.3, 3.2, 3.3 |
| <p>0 <math>\triangleq</math> Not applicable<br/>           1 <math>\triangleq</math> Applicable<br/>           M <math>\triangleq</math> Failure detection</p> |   |             |             |       |       |             |       |               |

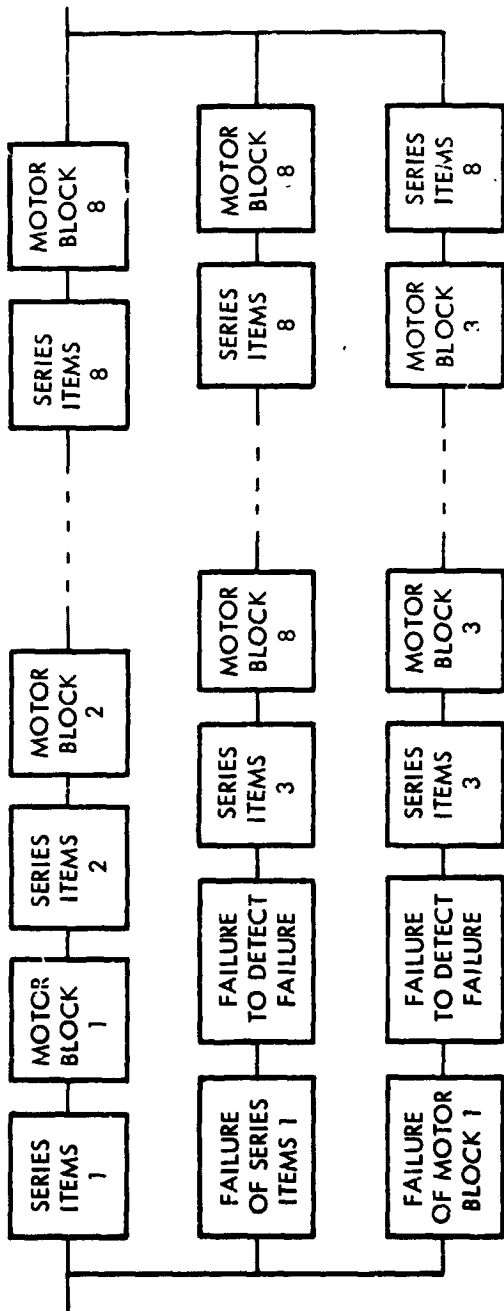
single-engine configurations, respectively. For the failure mode of ceasing to operate, the differences between Tables 10 and 11 clearly illustrate the configuration differences; e. g., engine failure is immediately critical for flight and remote site failures in Table 11 and is critical only in combinations of two additional failures in the time phase, or one additional failure during abort in Table 10. Hardware configurations were those of the Phase 2 control configuration (Figure 17).

#### Control Method Comparison Logic

Comparison among three control methods required additional logic consisting of the differences. Simulation of the complete mission and configuration was not feasible within the project time constraints, since comparison was the only objective and since the common portions probably make only small differences. The single actuator is divided into series items (end connections, ball screw, and gears), motor block (motor, electrical plug, wiring, and magnetic clutch), and failure detection and switching (rate transducer measurement and astronaut compensation). Figure 55 shows the logic used for mission success and crew safety for eight-actuator control of four engines; i. e., essentially all success for mission success, and any three out of four sets of two actuators each for crew safety. Figure 56 presents the logic for the four two-in-a-can actuator control of four engines where the motor block is made redundant in each actuator (i. e., single-motor block switching). The other operating mode for this configuration which allows simpler switching is to switch all four motor blocks on detection of single-motor block or series-items failure. Mission success logic does not change, and Figure 57 shows the crew safety logic, in which the number of alternate paths is reduced because of the multiple switching. The sliding plate logic requires consideration of not only single and double switching, but also the effects of loose failure of the yaw actuators. Mission success is again effectively all items working successfully for the entire mission. A composite logic diagram, Figure 58, shows crew safety for all modes of operation.

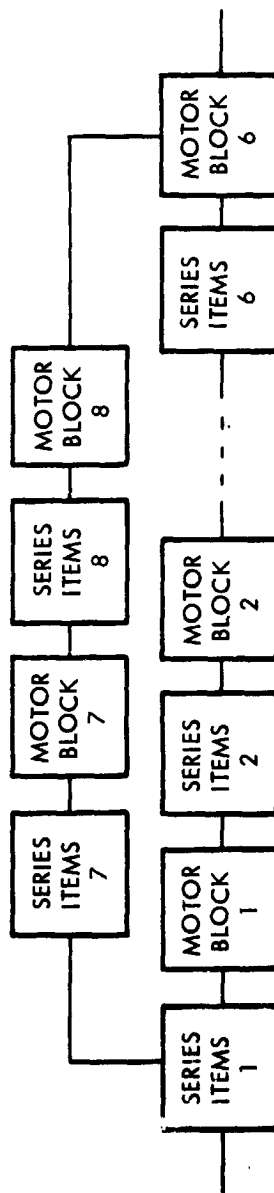
#### Estimated Hardware Reliabilities

Estimation of reliability capabilities for specific hardware items is always difficult, with the difficulty compounded when details of items are not defined. Such things as hermetic sealing, vacuum lubrication, safety margin, expected environment, operating modes, and partial redundancies cause wide swings in the final reliability of equipment. When these factors are not defined, the estimate must be based on past experience on similar items in similar environments, with the expectation that the initial estimate will be utilized in determining the detailed design. This interaction between reliability requirement analysis and detailed design is necessary for optimum



MISSION SUCCESS (SUCCESSFUL PATH DIAGRAM)

ANY 3 OUT OF 4 SETS OF ACTUATORS



CREW SAFETY (RELIABILITY LOGIC DIAGRAM)

Figure 55. Eight-Actuator Mission Logic

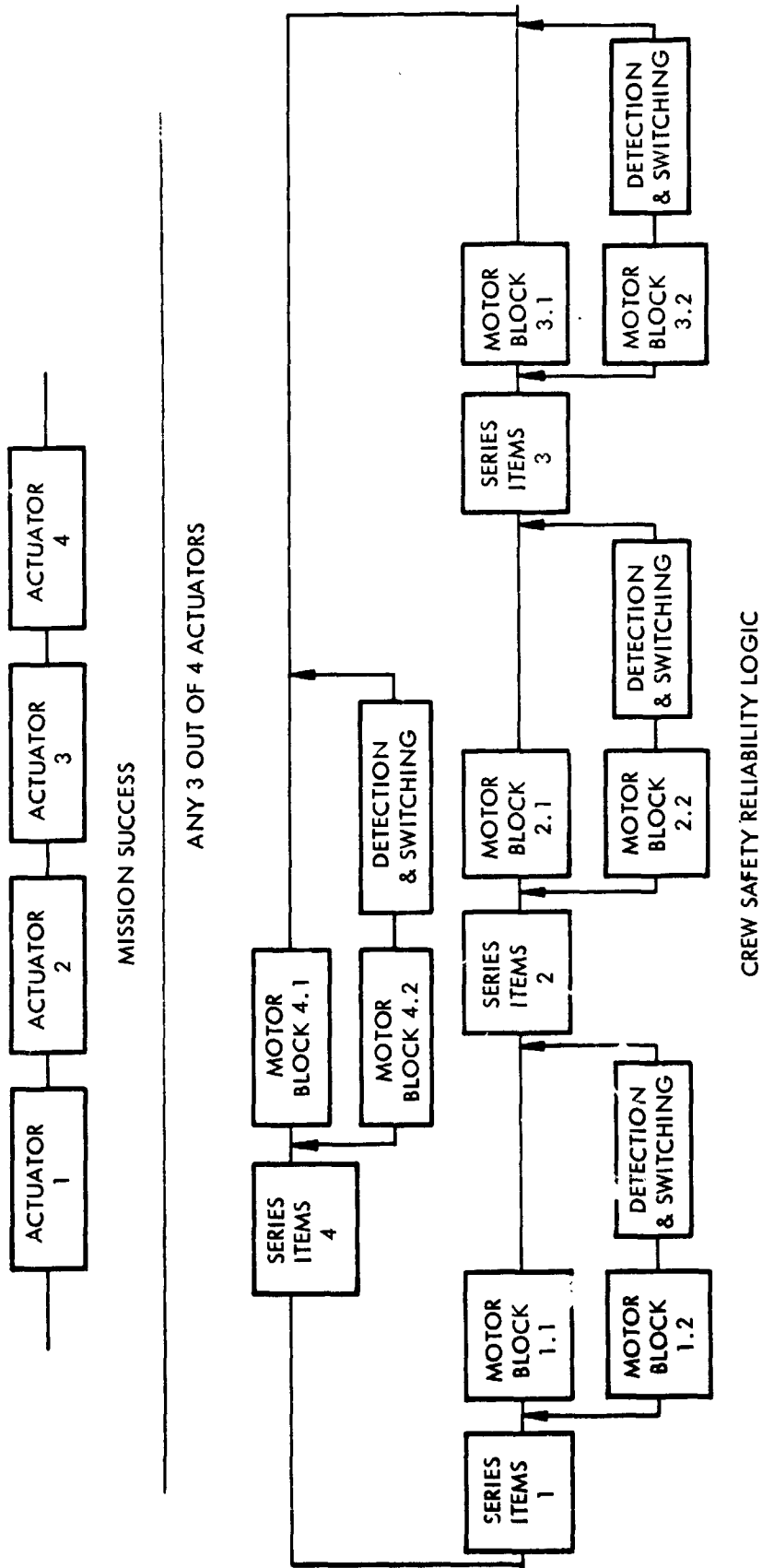


Figure 56. Four, Two-in-a-Can Actuator Mission Logic



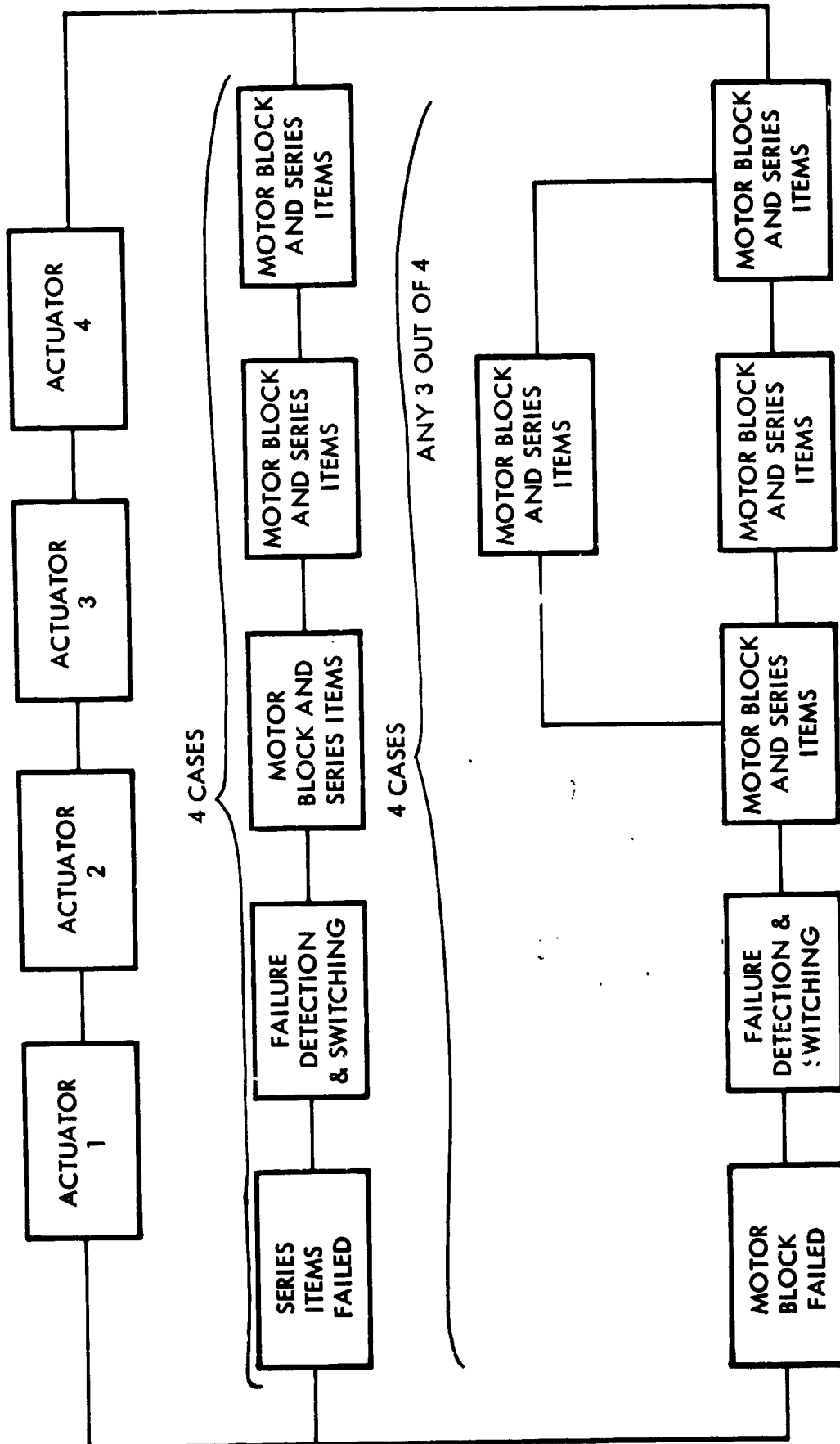


Figure 57. Four, Two-in-a-Can Actuator Crew Safety Logic

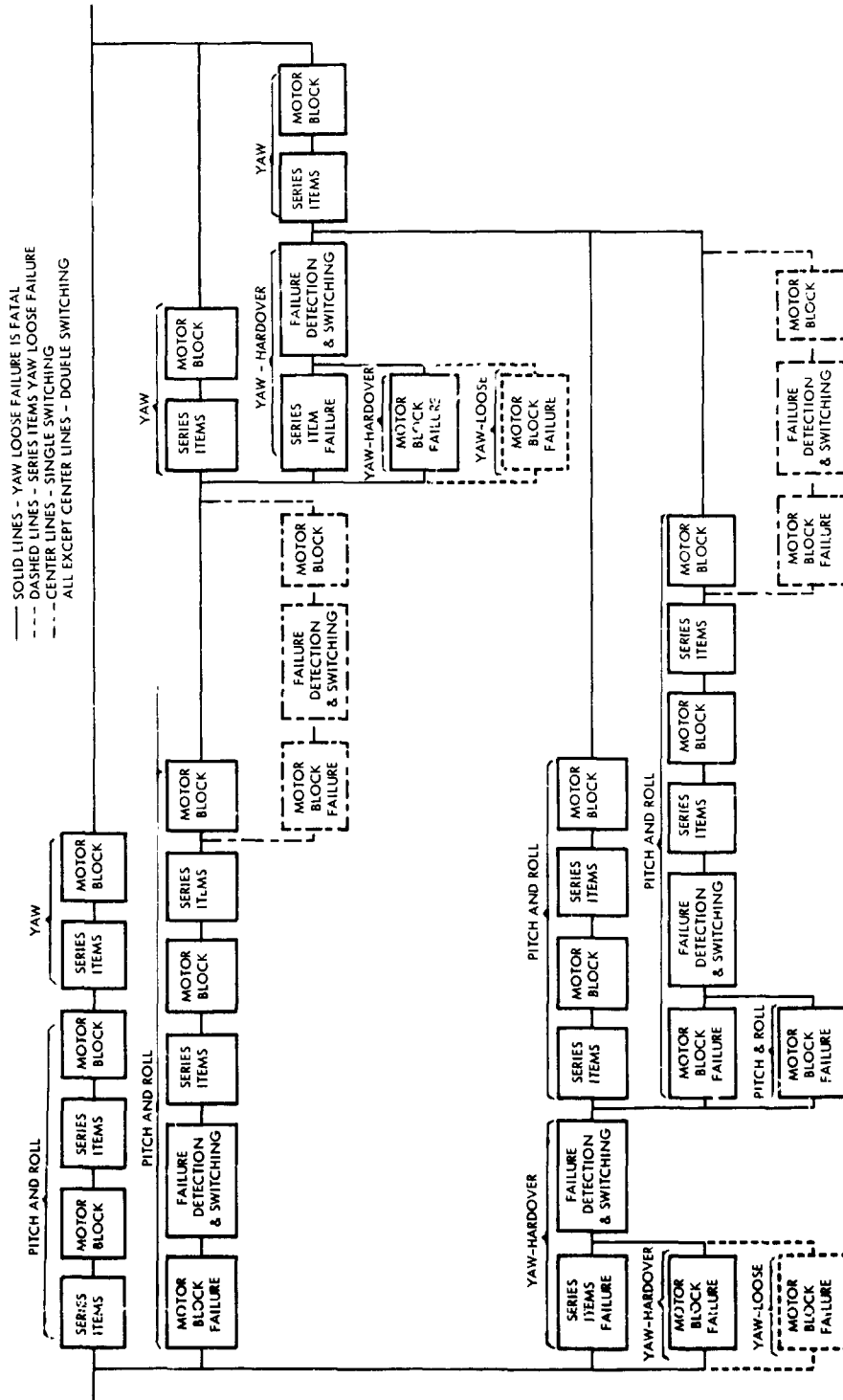


Figure 58. Crew Safety Logic for Sliding Plate Configuration

cost, schedule, and performance in the approach. Absolute reliability level is not essential to the initial analysis as long as the numerical values are indicative of final values and preserve a relative ranking, because comparisons among configurations can then be made. The reliability logic should be indicative of the expected mission and configuration capabilities, and the numerical reliability values can be point-estimated or region-estimated for synthesis into mission criteria. Table 12 shows the failure rates applied to the hardware level needed in the reliability analysis, and the sources of these rates.

Failure modes were detailed in only a few cases in a qualitative way. Tables 13, 14, and 15 give examples of the detail considered necessary for this portion of the study for three components: rocket engine, two-in-a-can actuator, and sliding plate.

Numerical evaluation of the reliability of the sliding plate is extremely difficult because design details are the controlling factor. Large margins and vacuum protection would alleviate many of the anticipated problems but would raise the spectres of excessive weight and cost. A weak point in the design is the means of retaining the plates in vertical position for freedom of movement without losing the ball bearings or allowing shock on engine start. Again, detailed design could overcome this, but at the expense of additional complexity.

### Reliability Growth

Reliability increase with development effort has been discussed at length in several publications, and many models have been suggested. Each organization has a model which seems to fit its data best; however, the general shape of the reliability growth curves is the same. This disagreement and agreement are shown by two curves in Figure 59 for reliability prediction of the same Rocketdyne engine (H-1) by North American Rockwell/Rocketdyne and GE/Tempo. Even though Rocketdyne is much more optimistic, the shapes of the curves are essentially the same, with number of tests as a measure of effort. Using the exponential growth model, the single characteristic, mean life, was calculated from the basic data. Figure 60 shows the many resulting curves to be widespread but very nearly linear, with a mathematical model as follows:

$$R \triangleq e^{\frac{-1}{ML}}$$

$$ML \triangleq \text{mean life} = kn$$

Table 12. Component Failure Rates

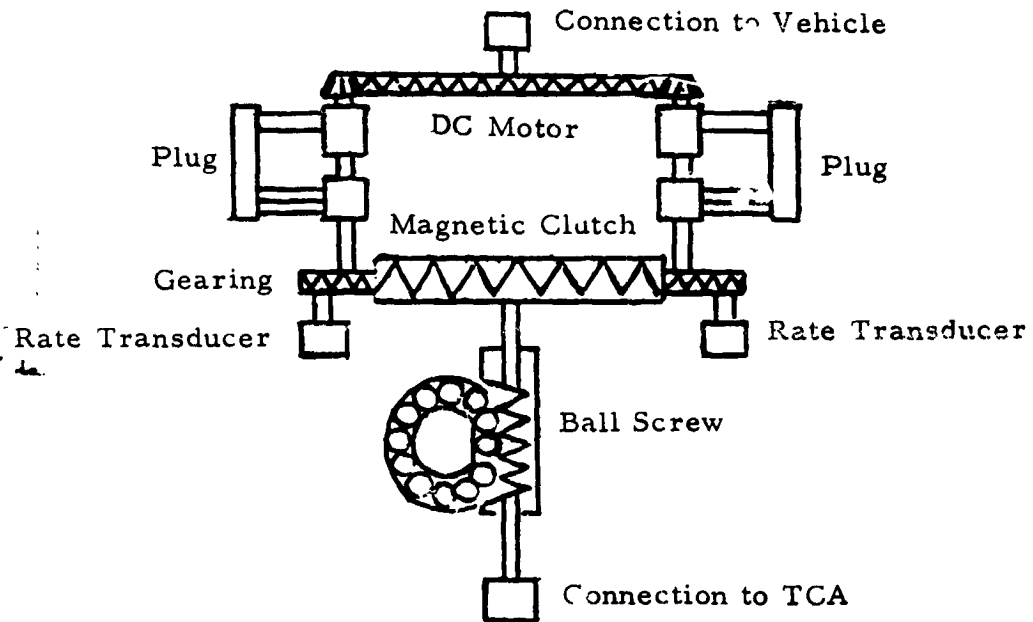
| Component                     | Failure Mode                                      | Failure Rate<br>(10 <sup>6</sup> hr) | Source   |
|-------------------------------|---|--------------------------------------|--|
| Failure detection measurement | Failure to detect failure                         | 10,000                               | Apollo and expected LFV instrumentation and astronaut capability   |
| Power supply                  | Failure to supply electrical power                | 20                                   | Apollo and expected LFV design   |
| Control electronics           | Failure to provide proper attitude control signal | 208                                  | Apollo and expected LFV design   |
| Structure                     | Breakage  | 1                                    | Expected LFV design margins  |
| Mechanical systems            | Failure to function                               | 200                                  | AVCO and expected LFV design margins   |
| Propellant supply system      | Failure to supply propellant                      | 500                                  | Apollo service module reaction control system propellant supply modified by LFV environment  |
| Rocket engine                 | Cease to operate                                  |                                      | Allocated by Apollo experience from generic estimate of 0.998 per mission from engine data from Marquardt, Rocketdyne, Aerojet, and GE |
|                               | Start   | 26,060                               |  |
|                               | Steady state                                      | 2,606                                |  |
|                               | Catastrophic failure                              | 26                                   |  |
| Control Actuator              | Fail to operate                                   | 1,826                                | Allocated by Apollo experience from generic estimate of 0.999 per mission from Autonetics  |
|                               | Hard over   | 183                                  |  |
| Motor block                   | Fail to operate                                   | 1,940                                |  |
|                               | Hard over   | 194                                  |  |
|                               | Loose   | 1,746                                |  |
| Series items                  | Fail to operate                                   | 60                                   |  |
|                               | Hard over   | 6                                    |  |
|                               | Loose   | 54                                   |  |

Table 13. Rocket Engine Failure Modes (Reference 20)

| Subassemblies                              | Failure Mode                                   | Percentage Weight Factor ( $W_i$ ) | Allocated Reliability Goal |
|--|--|------------------------------------|----------------------------|
| Fuel flow control orifice and retainer     | Out of calibration                             | 0*                                 | 0.99999+ *                 |
| Fuel valve                                 | Open, closed, and leakage                      | 0.3060                             | 0.99908                    |
| Oxidizer flow control orifice and retainer | Out of calibration                             | 0                                  | 0.99999+                   |
| Oxidizer valve                             | Open, closed, and leakage                      | 0.3553                             | 0.99893                    |
| Fuel sealing hardware                      | Leakage  | 0.0136                             | 0.99996                    |
| Oxidizer sealing hardware                  | Leakage  | 0.0264                             | 0.99992                    |
| Injector head assembly                     | Burned injector holes or abnormal flow pattern | 0.2300                             | 0.99931                    |
| Combustion gas sealing and attach hardware | Leakage and breakage                           | 0.0105                             | 0.99997                    |
| Thrust chamber hardware                    | Hot spots, leakage, and explosion              | 0.0528                             | 0.99983                    |

\*Percentage weight factors for the orifice and retainers was less than 0.0001 and consequently were considered as zero.

Table 14. Failure Mode Analysis of "Two-in-a-Can"  
Actuator Configuration



|   |   |
|---|---|
| Plug: short - excessive current - fuse overload protection            | Redundant                               |
| Open  | Redundant                               |
| DC motor: short - excessive current - fuse overload protection        | Redundant                               |
| Open  | Redundant                               |
| Binding - excessive current - fuse overload protection                | Redundant                               |
| Magnetic clutch: short - excessive current - fuse overload protection | Redundant                               |
| Open  | Redundant                               |
| Leakage   | Redundant                               |
| Gearing: binding  | no gimbal capability                    |
| Free movement   | no gimbal capability                    |
| Rate transducer: open or short  | reduced control capability<br>Redundant |
| Ball screw: binding   | No gimbal capability                    |
| Free movement   | No gimbal capability                    |
| End connection: binding   | No gimbal capability                    |
| Separation  | No gimbal capability                    |

Table 15. Sliding Plate Failure Mode Analysis

| Component               | Failure Mode   | Requirements  |
|-------------------------|--|---|
| Upper plate             | Warping (Temperature or load)  | Sufficient margin<br>Close tolerances   |
| Intermediate plate      | Warping (temperature or load)  | Sufficient margin<br>Close tolerances   |
| Lower plate             | Warping (temperature or load)  | Sufficient margin<br>Close tolerances   |
| Upper ball retainer     | Warping (temperature and vacuum)<br>Excessive drag, low-friction material<br>Outgassing (vacuum), loss of physical properties, bearing seizure |   |
| Lower ball retainer     | Warping (temperature and vacuum)<br>Excessive drag, low-friction material<br>Outgassing (vacuum), loss of physical properties, bearing seizure |   |
| Upper ball bearings     | Vacuum welding, bearing seizure<br>Binding, contamination or corrosion<br>Brinnelling, shock of engine start                                   |   |
| Lower ball bearings     | Vacuum welding, bearing seizure<br>Binding, contamination or corrosion<br>Brinnelling of races, shock of start                                 |   |
| Plate assembly retainer | Too loose, bearings out of races<br>Too tight, excessive friction to movement  | Close tolerances<br>Sufficient margin   |
| Linkage                 | Breakage<br><br>Vacuum Welding, bearing seizure (10 bearings for yaw).   | Close tolerances and sufficient margin, especially for single point failure links (cause two engines to flap) |

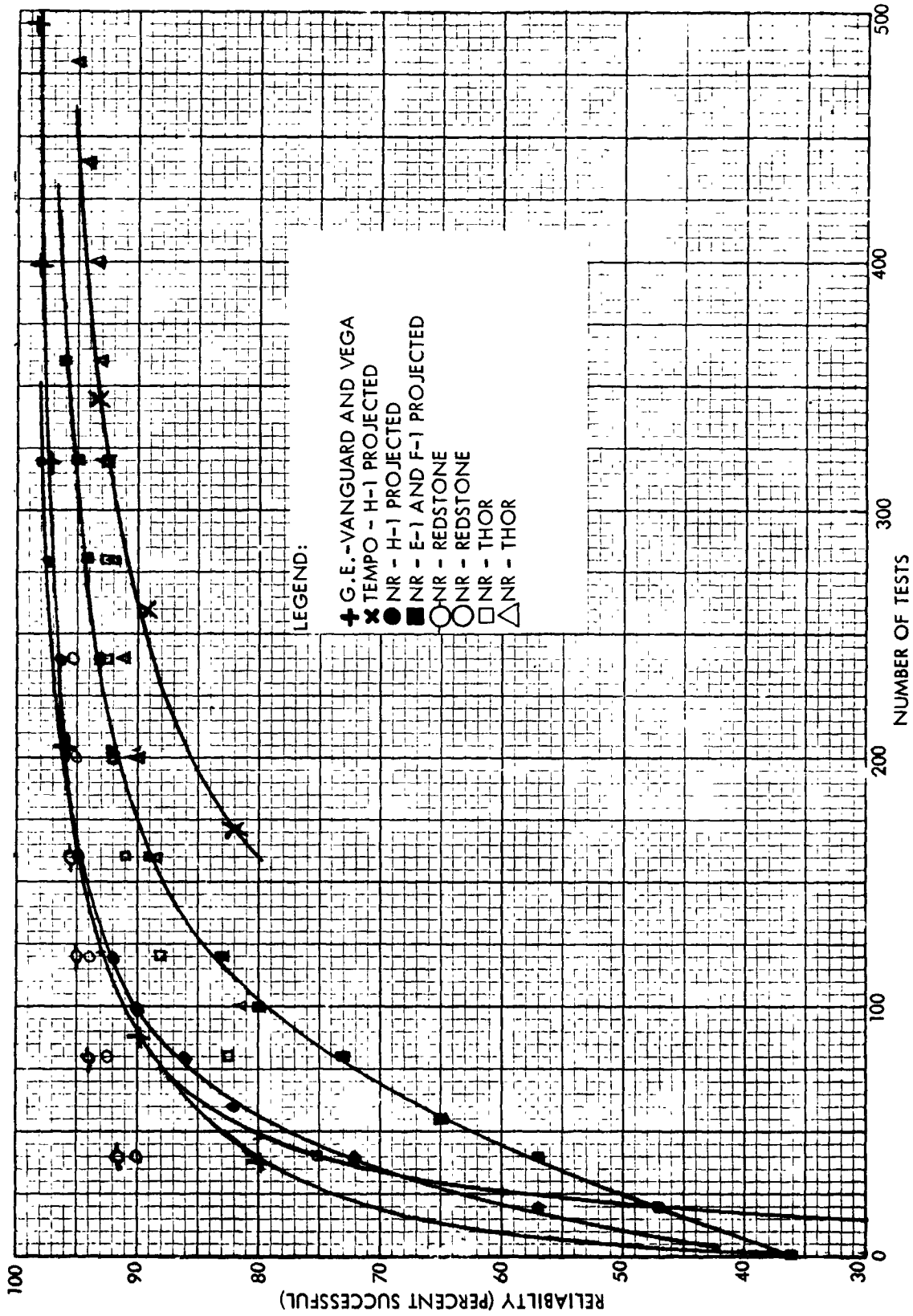
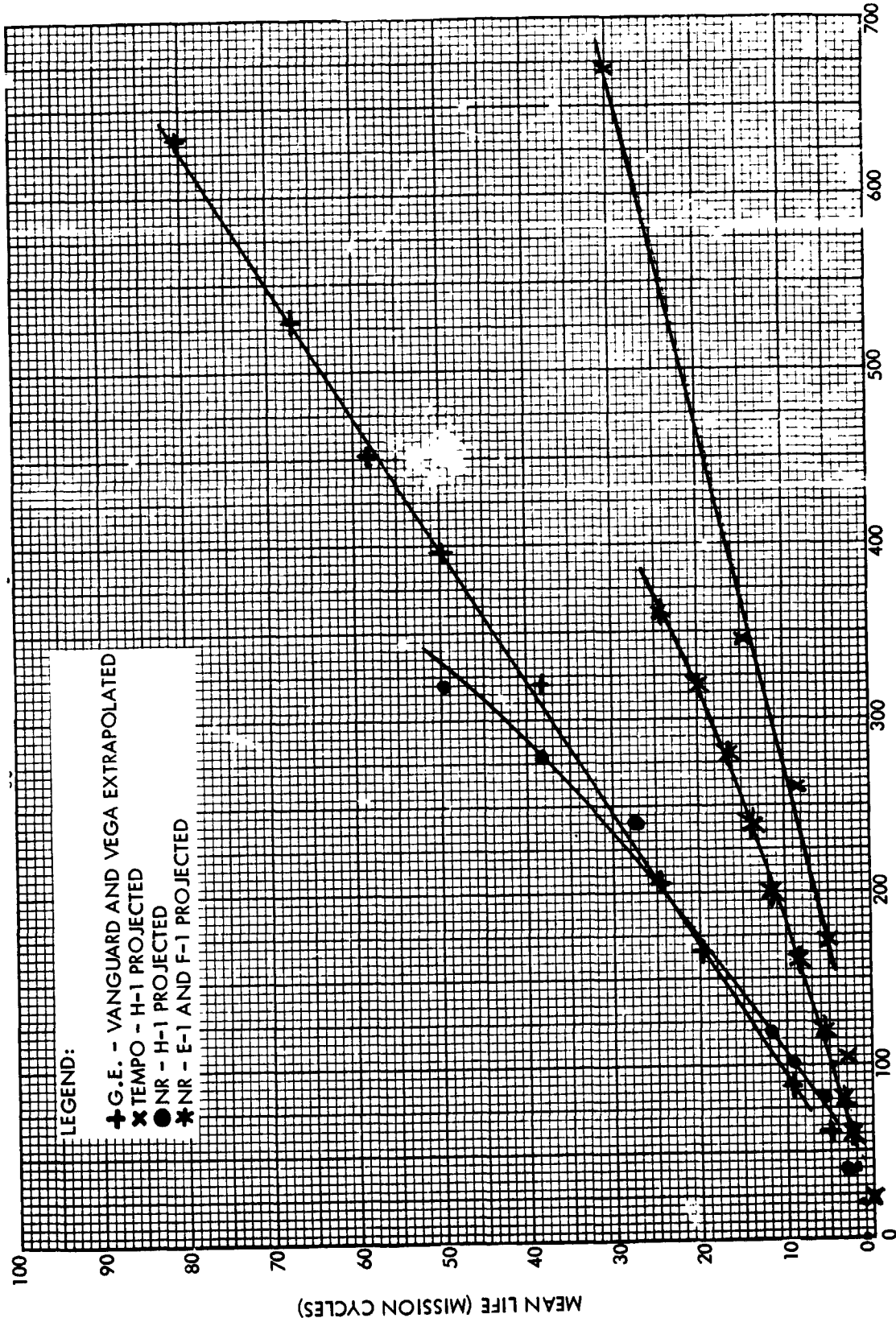


Figure 59. Cumulative Reliability Point Estimate





NUMBER OF DEVELOPMENT TESTS  
Figure 60. Mean Life Growth Model

$\Delta$   $\equiv$  number of successful runs  
number of failures

k  $\Delta$   $\equiv$  empirical constant

n  $\Delta$   $\equiv$  number of test runs

Pratt & Whitney, GE, and North American Rockwell data indicate that a reasonable empirical value for k for a turbopumped rocket engine is:

$$k = \begin{cases} \frac{30}{245} = 0.12245 \\ \frac{50}{396} = 0.12626 = 0.125 = \frac{1}{8} \\ \frac{80.5}{632} = 0.12737 \end{cases}$$

Since the failures are approximately equally distributed between turbopump and chamber assembly, the chamber assembly empirical constant is 1/4. The duration of test runs is dependent on the reliability growth because the early failures will not permit in full-duration runs. Therefore, the average run time will be less than the full mission duration. For only a few test runs, (100), the average will be about 72 percent.

| Cumulative Number of Test Runs | Expected Cumulative Number of Failures | Expected Percentage Successful | Expected ML | Expected R |
|--------------------------------|--|--------------------------------|-------------|------------|
| 100                            | 28                                     | 72                             | 25          | 0.96       |
| 200                            | 34                                     | 83                             | 50          | 0.98       |
| 400                            | 40                                     | 90                             | 100         | 0.99       |
| 800                            | 46                                     | 94                             | 200         | 0.995      |
| 1600                           | 52                                     | 96.8                           | 400         | 0.9975     |
| 2000                           | 54                                     | 97.3                           | 500         | 0.998      |

If the hardware already has an initial reliability, the total number of test runs is reduced; e. g., if the initial reliability were 0.98 and the final desired reliability were 0.99, the number of expected development test runs is 400-200 = 200. This model places a premium on design activities and the utilization of already developed hardware, since the total number of development tests can be decreased drastically by either of these two



expedients. It is obvious that extremely high reliabilities are difficult to reach, because the model essentially assumes that failure modes are found by test before they can be fixed. The model also assumes an infinite number of possible failure modes which are discovered and fixed as they occur in test, but succeeding failure modes have lower failure rates and are harder to find. Increasing insight into rocket chamber assembly failure modes, overstress testing for tolerance investigation, and the provision of adequate margin for each failure mode assist in increasing initial reliability.

Particular test plans which emphasize failure modes with high failure rates are more productive than others which call for full duration on every test run; e.g., since start and shutdown have higher failure rates than steady-state operation, many tests consisting of start, stop, and very short steady state would improve assembly reliability with less total duration. For the case of the start failures equal to all others combined, and a full-duration test cost of ten times a start/shutdown test, minimum cost occurs when three start/shutdown tests are run for every full-duration test (one start/shutdown test includes all expected starts per mission). For the reliability goal of 0.998, 3300 start/shutdown tests and 1100 full-duration tests are projected. If all the full-duration tests were successful, the reliability goal of 0.998 would be proven with a binomial sequential statistical confidence of 90 percent. Further reduction in number of tests can be made if partly developed engines are used; for example, for the Marquardt engine (where start tests are already completed), 800 full-duration tests are expected to be sufficient.

#### Two Engine-Four Engine Configuration Comparison

Gross comparison of the nonredundant two-engine configuration with the four-engine selected configuration has been completed. The objectives were to investigate means for improving the two-engine valve and gimbal actuator reliabilities, to compute the reliability criteria, and to compare the results with the selected design. Many design features of the two-engine configuration were assumed (Table 16), and failure rates were allocated to each component failure mode (Table 17) according to North American Rockwell Space Division experience, in only that degree of detail necessary to illustrate the differences between configurations.

The four-engine configuration remained higher in crew safety but lower in mission success than all two-engine configuration improvements evaluated (Table 18). Crew safety is higher because of the ability to make more components redundant (i. e., all except the catastrophic failure of the thrust chambers). The two-engine configuration can use redundant start valves and gimbal actuator motor blocks, but gimbal actuator series items and throttle valve redundancy would entail substantial development and

improvement in the state of the art. Mission success is lower because of the larger number of components and the rule of aborting on a single failure. It is apparent from Table 18 that as the number of modifications to the two-engine design is increased, crew safety rises only slightly but mission success drops severely. Increasing the configuration spectrum to include even more redundancy should result in the same trends.

Table 16. Two-Engine Configuration Components

| Component       | Considerations  |
|-----------------|---|
| Propulsion      | <p>Propellant feed system equivalent to four-engine design</p> <p>Two rocket engines providing all functions of variable lift, pitch, roll, and yaw. Each engine has one fuel start valve, one oxidizer start valve, one injector, and one chamber that are equivalent to four-engine design.</p> |
| Control         | <p>Stability augmentation (electronics) equivalent to four-engine design</p> <p>Two electrically operated gimbal actuators on each engine, equivalent to four-engine design</p>   |
| Structure       | Safety margins equivalent to four-engine design   |
| Power           | Batteries and distribution system equivalent to four-engine design  |
| Instrumentation | Detection of each failure equivalent to four-engine design  |
| Modification 1  | Each actuator is modified to include two motor blocks, with either single or multiple switching.  |
| Modification 2  | Engine start valves are made redundant for all modes, i. e., four series/parallel valves for each propellant.   |
| Modification 3  | Combination of Modifications 1 and 2  |

Table 17. Two-Engine Configuration Failure Probabilities

| Component               | Primary Failure Mode | Probability of Occurrence/LFV Mission | Comments  |
|-------------------------|----------------------|---------------------------------------|---|
| Propellant supply       | Leakage              | 0.000360                              | All failures considered critical to reliability criteria. Same numeric value as four-engine design. |
| Control electronics     | False signal         |                                       |   |
| Structure               | Breakage             |                                       |   |
| Power                   | Low voltage          |                                       |   |
| <b>Engine</b>           |                      |                                       |   |
| Oxidizer start valve    | Open                 | 0.000209                              | Allocated from Marquardt data and expectation of final engine reliability of 0.998                  |
|                         | Closed               | 0.000209                              |   |
| Fuel start valve        | Open                 | 0.000209                              |   |
|                         | Closed               | 0.000209                              |   |
| Oxidizer throttle valve | High                 | 0.000209                              |   |
|                         | Low                  | 0.000209                              |   |
| Fuel throttle valve     | High                 | 0.000209                              |   |
|                         | Low                  | 0.000209                              |   |
| Injector                | Poor combustion      | 0.000270                              |   |
| Chamber assembly        | Hot spot             | 0.000038                              |   |
|                         | Explosion            | 0.000020                              |   |
| <b>Gimbal Actuator</b>  |                      |                                       |   |
| Series items            | Breakage             | 0.000030                              | Allocated from Aerojet-General data and expectation of final actuator reliability of 0.999          |
| Motor block             | No power             | 0.000970                              |   |

Since throttling valve redundancy was a major factor in the low crew safety of the two-engine configuration, several alternatives were evaluated qualitatively. The TRW style of linked variable cavitating venturi and injector valve is unsuited for complete redundancy; i. e., the injector valve is embedded in the injector design to the extent that separation would involve a complete redevelopment and increase the complication in a

Table 18. Reliability Criteria Comparison

| Configuration   | Probability of Mission Success/<br>LFV Mission | Probability of Crew Safety/<br>LFV Mission |
|---|--|--|
| Two-engine design   |  |  |
| Nonredundant  | 0.993655                                       | 0.993655                                   |
| Modification 1: Two-in-a-can actuators  | 0.993655                                       | 0.993655                                   |
| Single-motor block switching  | 0.993655                                       | 0.995510                                   |
| Four-motor block switching  | 0.993655                                       | 0.995499                                   |
| Modification 2: engine start valve redundancy   | 0.986707                                       | 0.993302                                   |
| Modification 3: combination of modifications 1 and 2  |  |  |
| Single-motor block switching  | 0.986707                                       | 0.997147                                   |
| Four-motor block switching  | 0.986707                                       | 0.997136                                   |
| Four-engine design (computer results modified to be on the same gross terms as two-engine design) | 0.983762                                       | 0.999516                                   |

critical location. Other wide-range throttling means are equally difficult because of the rocket engine characteristic of high injector impedance (normally, pressure drop) for combustion stability. Narrow-range throttling can be accomplished by valves in the propellant lines (Figure 61). Including both engines, the number of valves is equal to that of the selected four-engine configuration, and alternate modes are provided for each valve failure. All valves could be operated normally open by providing enough electronics to allow parallel throttling valves to compensate for errors in the other (i. e., individual control of each throttling valve). Although this is promising, noncatastrophic injector and chamber failures, as well as gimbal actuator series items failures, are not compensated in the two-engine design. In other words, the added complexity has brought some benefits, but not as many as are inherent in the four-engine configuration.

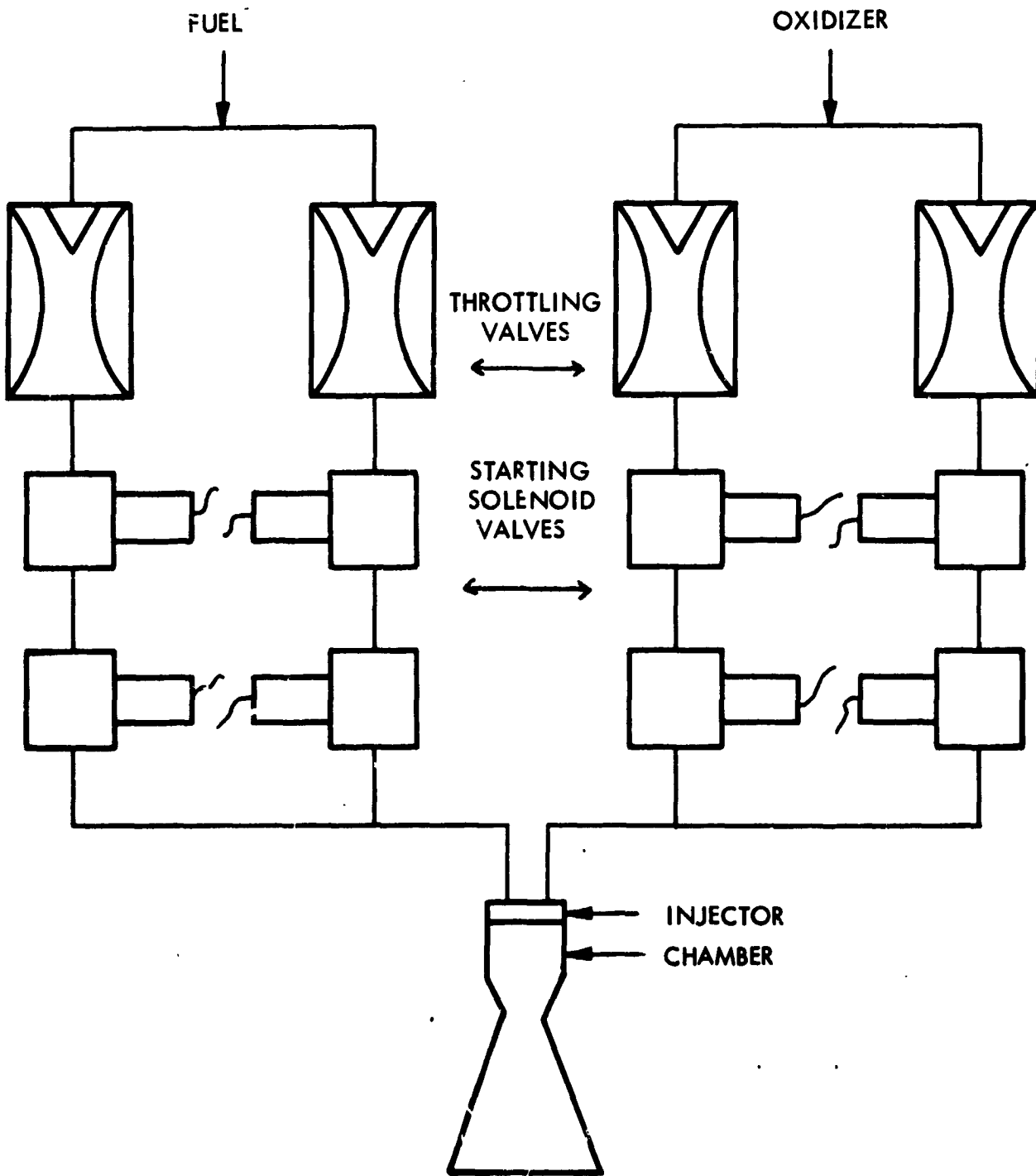


Figure 61. Engine Valve Redundancy

## LANDING GEAR

The landing gear design developed as a result of this study is considered to be relatively conservative, both with respect to its capability and the LFV design intended to match that capability. However, it is evident that if less stringent data on requirements are obtained, and as design optimization work becomes more precise, it will be quite simple to modify the design in the directions of less capability. On the other hand, an increase in capability from a fundamentally different design would be quite difficult. On this basis, it is expected that with future effort, the design weight allocation for the landing gear may be reduced.

As may be seen from the following discussion, the conservative approach was necessary because the requirements are relatively obscure. This results from the limited data on lunar surface characteristics and lack of experience in flight control for this type of vehicle.

### Requirements

#### Lurrain Character

The NASA Lunar Trafficability Model Working Group has assessed the nature of the lunar surface, primarily from the viewpoint of a Rover design requirement. Gross lunar topography, of course, is fairly well known. The nature of detailed topography and soil is somewhat indeterminate, however. The best data available come from Surveyor and Lunar Orbiter flights (see Reference 21). In this reference, the surface is classified by location into smooth mare, rough mare, hummocky upland, and rough upland. As would be expected, the data on soil properties come from Surveyor flights, but only one of these flights, Surveyor VII, was in the highlands (near the rim of Tycho). Reference 21 attempts to estimate the depth of the overlain soil, partly from Surveyor data but mostly by noting that blocky ejecta from a crater could only be thrown out if the soil layer had been penetrated. With this observation, the minimum size of craters with blocky ejecta is deduced to indicate the depth of the soil. Using this reasoning, the smooth mare and rough mare are considered to have a median thickness of the overlain soil of 6 and 3 meters, respectively. The report is somewhat ambiguous, since the two upland areas are noted at one point as having a median soil layer thickness of 5 meters. In another section, after first remarking that "since very little data is available" the layer can only be estimated, it states that, from Surveyor data, the layer is a few centimeters or deeper. With respect to local topography, the report states, "many of the rocks appear to be lying on the fine matrix, other seems to extend slightly below the matrix surface, and others are almost completely buried." Evidently not all small rocks are



frangible, since the report notes that a stress applied by the Surveyor soil mechanics surface sampler (SMSS) to break a rock was calculated at 290 psi.

After assessing this report's interpretation of lunar data, and including data from Surveyor pictures and reports, it was established that the only workable assumptions at the present time for design of the LFV landing gear would be that in some locations of interest to exploratory operations with the LFV, the soil layer may be thin and/or hard; and that hard rocks may be in contact with the landing gear at touchdown, either because of poor pilot visibility, because of the frequency of rock distribution, or because the rocks are hidden by a thin soil layer. It is apparent that other assumptions could be made, but not without limiting (at least in light of present knowledge) the design capability of the LFV to land in various areas of the moon. Apparently, the blocky-wall craters, the ejecta piled up in the center of craters, and similar phenomena are of interest for exploration.

With respect to slopes, there is a wide variation over the moon. A selection of 10-degree slope capability was made arbitrarily, with the assumption that this would permit most of the areas to be explored. It should be noted, however, that slope is not a strong influence on the landing gear design, as may be seen in the following discussions.

#### Perception and Control Limits

The initial conditions for landing -- angular and vertical velocities and free-fall heights -- are primarily governed by control system precision and the pilot's ability to operate the controls and observe the surface well enough to stay within the design initial conditions. It was noted in early precontract studies that if attempts were made to have landing conditions approach zero-zero, the propellant consumption would be excessive. Surveyor and LM have a similar trade between landing gear and propellant weight, but the use of the LFV for repeated landings within one mission magnifies the problem and tends to shift the optimum in the direction of proportionately heavier landing gear and even better control and precision at touchdown. If it is conceded that the control system by itself is sufficiently precise, then the limiting condition is the pilot and his ability to perceive the vehicle's motion and its relationship to the surface. The best sources of data in this area are the visual flight simulations performed by North American Rockwell concurrently with this study. The results of this simulation of achievable landing initial conditions are shown in Figures 62 and 63. Since the landing gear design process started before the simulations, the estimates of proper landing initial conditions from prior trade studies (intended to balance propellant weight against landing gear weight) were used as goals for the pilot. As noted in Figure 62, the design capability exceeds the mean value of the simulation results for every parameter -- with or without an engine

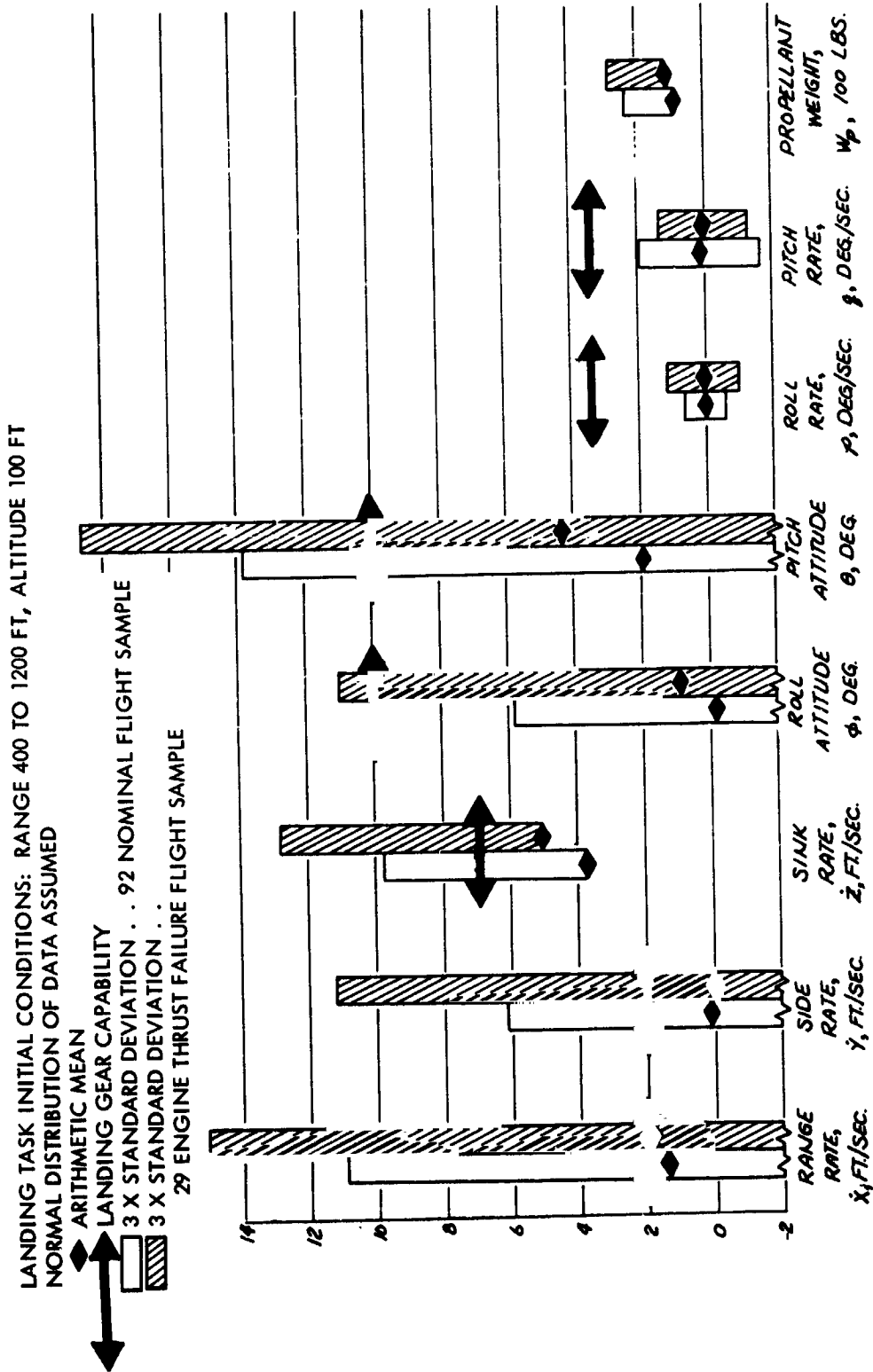


Figure 62. Landing Performance Data From Visual Simulation,  
Three-Axis Stability Augmentation

LANDING TASK INITIAL CONDITIONS: RANGE 400 TO 1200 FT, ALTITUDE 100 FT  
NORMAL DISTRIBUTION OF DATA ASSUMED

◆ ARITHMETIC MEAN

ALL FLIGHTS WITH YAW STABILITY AUGMENTED

3 X STANDARD DEVIATIONS:

□ 92 FLIGHT SAMPLE . . . STABILITY AUGMENTATION WITH GIMBAL BELOW CG

▨ 7 FLIGHT SAMPLE . . . HARDWARE WITH GIMBAL BELOW CG

▩ 6 FLIGHT SAMPLE . . . HARDWARE WITH GIMBAL ABOVE CG

▧ 28 FLIGHT SAMPLE . . . STABLE PLATFORM WITH NEUTRAL CG

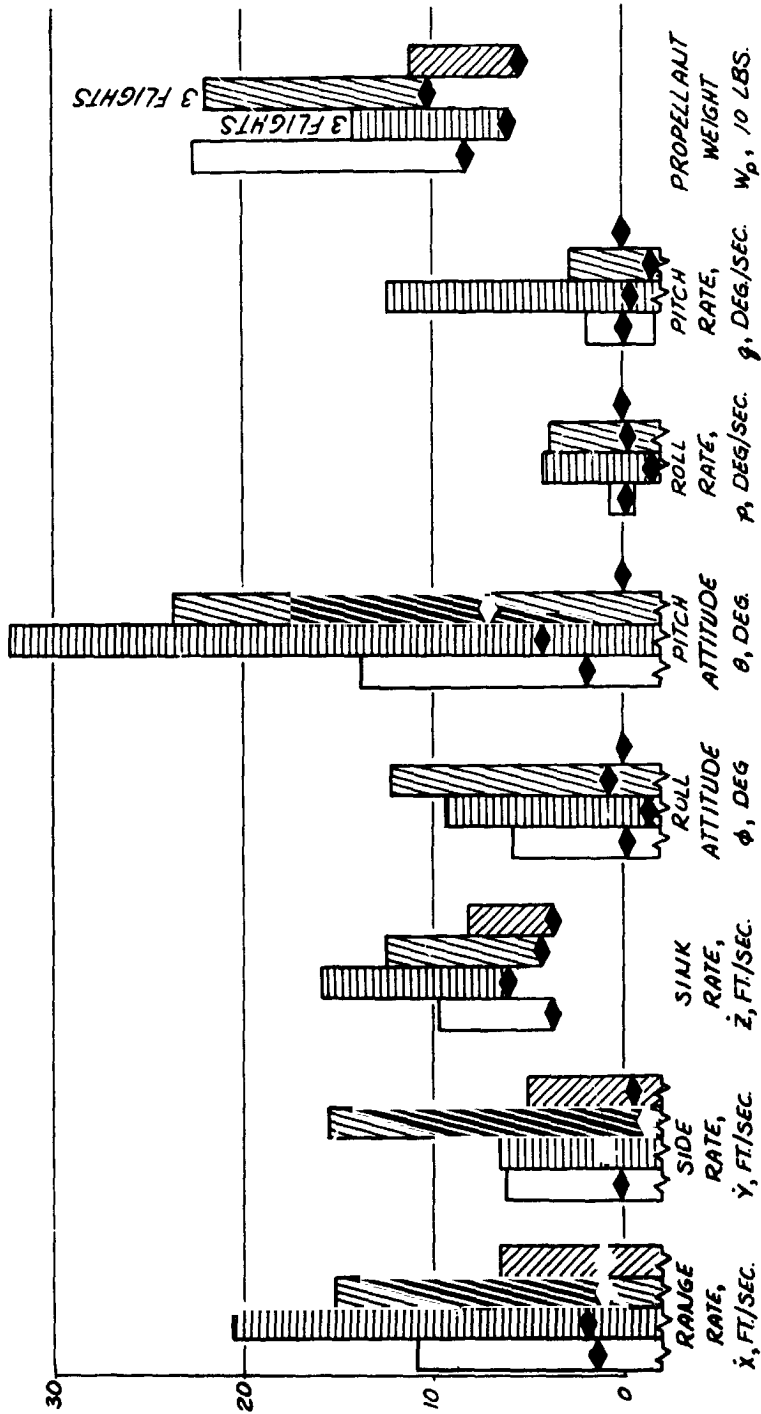


Figure 63. Landing Performance Data From Visual Simulation,  
Hardware and Neutral C.G.



failure. However, the  $3\sigma$  values in some cases, particularly the lateral and vertical velocities, exceed the design limits. It would be most desirable if the simulation showed no discrepancy between design conditions and pilot/control system capability, even at the  $3\sigma$  levels. However, it was concluded that with the simulation limitations that prevailed, probable performance in lunar operations with better visual cues and with ample training would be within the design limits of the landing gear. It is apparent, however, that there is no margin for imprecision in the control system itself (which would be present if stability augmentation were not used) (see Figure 63).

#### Pilot Attenuation

The primary purpose of the landing gear is to attenuate the landing shock to a level that is tolerable to the pilot. The attenuation requirements of the hardware are not the controlling condition. As described in the "Human Factors" section of this volume, these limits were established after study to be 2 g vertical and 1 g lateral for a standing unrestrained pilot, and 8 g vertical and 4 g lateral for a sitting or standing, closely restrained pilot. In order to prevent rebound, most of the mass must be attenuated and the energy dissipated, not merely stored temporarily in a spring. To attenuate only the pilot would leave a sizable unattenuated mass, and rebound would be excessive.

#### Toppling Stability

To prevent toppling, the gear spread must be wide enough to convert all horizontal kinetic energy to potential energy by rotation about locked pads. This assumes rock impact, or no sliding. The vertical velocity component resists this overturning. The design requirement used is 2 fps at zero vertical velocity (tripping into a slope) and is considered conservative. It assumes an initial touchdown pitch attitude of minus 10 degrees and a 20-degree stability margin. In terms of the angle ( $\alpha$ ) between the X-Y plane and a plane through two pads and the c. g., the gear spread requirement is shown in Figure 64 with vertical velocity and c. g. height as parameters.

#### Vehicle Integration

The preceding discussion would apply to any lunar flying vehicle. There are, however, several aspects of the particular design and its constraints which affect the landing gear. Most important is stowability. The landing gear is the part of the structure which forms the extremities of the vehicle, and as such it becomes the limiting envelope in LM stowing.

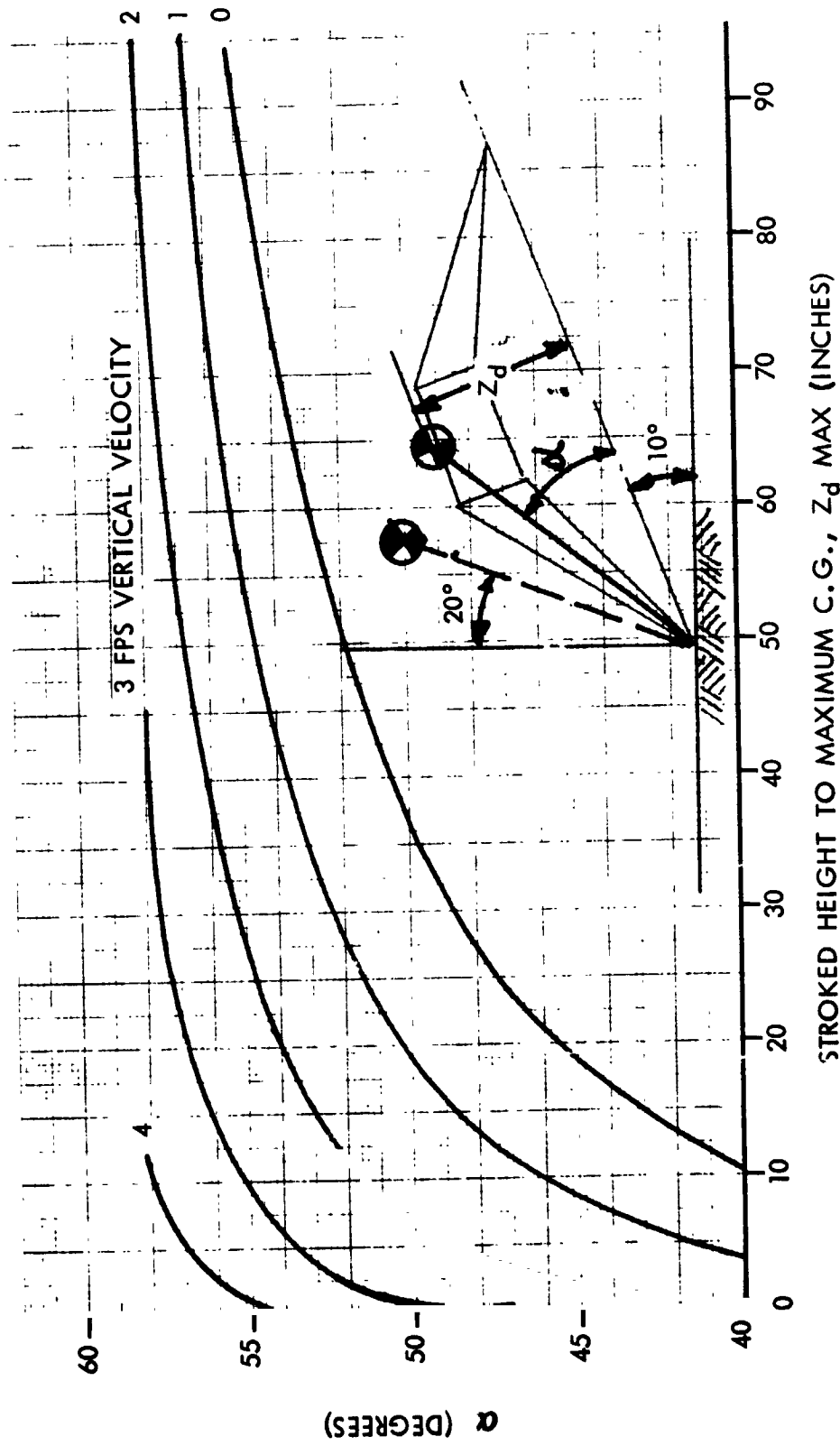


Figure 64. Toppling Stability

Early designs were forced to accept a compromise solution by folding or disassembly of the legs in order to fit the LM corner compartment. Fortunately, the c. g. of the final preliminary design was low enough to avoid this.

A second important aspect of vehicle integration considers the plume ejecta resulting from engine operation near the surface during landing. A study defining the characteristics of the plume and the ejecta is described in Volume 2. This study indicates that there can be, at levels lower than 50 to 60 inches, plume ejecta that might damage the vehicle. It is not clear that this problem could be solved by protecting the base of the vehicle. The engines themselves would be vulnerable, at least from secondary particles, and being radiation-cooled, are not readily protected. A more favorable solution, and one which accrues no weight penalty, was used. It utilizes an operational rule that the engine must cut off at a safe plume height. In the event that subsequent study or operational experience proves that the safe plume height is much lower, only operational practices need be changed, not the design of the vehicle. The concept does require that the limiting condition on vertical velocity be compatible with the free-fall height. Figure 65 illustrates the variation of free-fall height with initial velocity at cutoff and the landing gear capability boundaries. To aid the pilot in staying within the boundaries, surface contact sensors to indicate the appropriate altitude for cutoff are provided on the vehicle.

The vehicle also has a payload range of 0 to 370 pounds. This, coupled with the variation in propellant aboard, causes a 2-to-1 weight variation at touchdown that must be considered in the design of the landing gear.

A final aspect of this particular vehicle program to be considered in landing gear design is the requirement to use available hardware techniques and mature arts wherever possible.

#### Concept Development

The precontract studies resulted in development of the landing gear concept shown in Figure 2 and incorporated in the baseline configuration at the inception of the contract study. This landing gear depended on a spring attenuator in the footpad (see Figure 66) to resist all lateral energy components. It utilizes a damped spring with deflection capability limited to about an inch. The hydraulic attenuator, which takes the vertical component, is adequate. However, subsequent investigations revealed that the lateral component could exceed the initial horizontal velocity at cutoff by a considerable margin due to rotation of the vehicle. In fact, the lateral velocity component, (relative to the body axis system), initially at a 2-fps horizontal

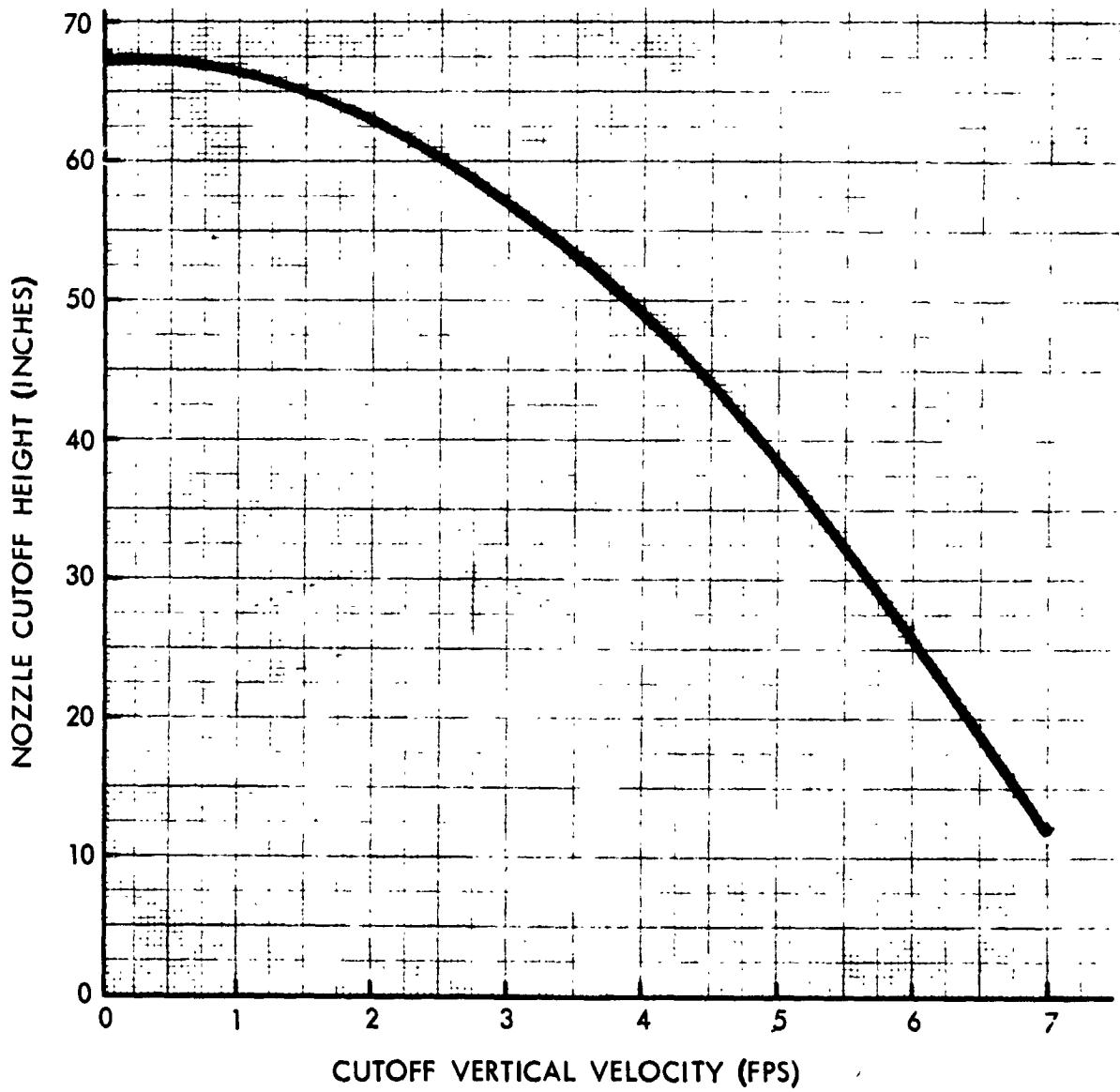


Figure 65. Cutoff Height Capability.

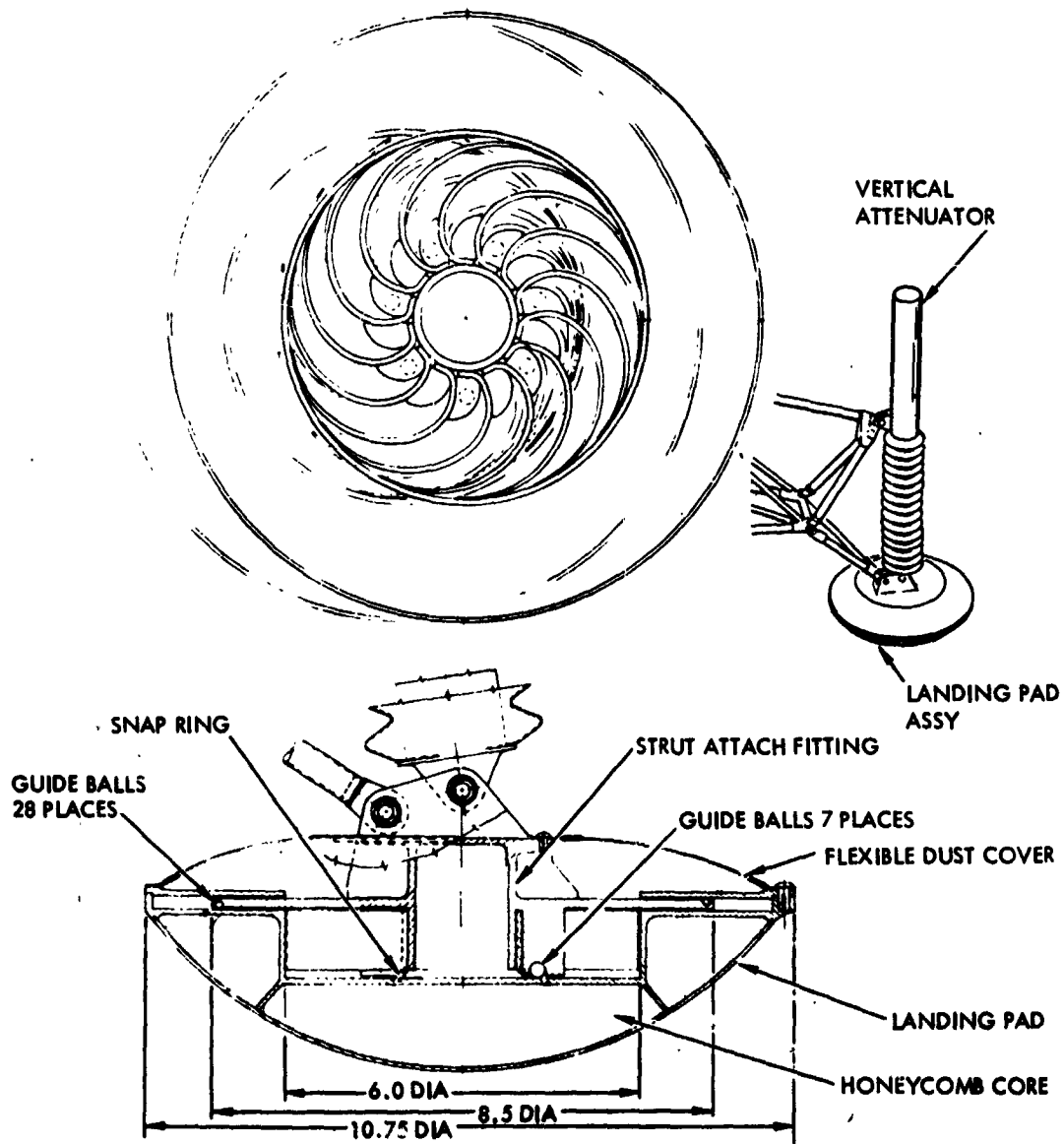


Figure 66. Footpad and Horizontal Attenuator Assembly



velocity at engine cutoff, can reach 3 to 4 fps at touchdown. This doubling of the lateral velocity increases the energy by a factor of 4, and the pad spring lateral attenuator concept became impractical purely from a weight standpoint.

Figure 67 presents the results of a study investigating several means of mechanizing the landing gear and integrating it with landing gear structure. This study utilizes the at-pad horizontal damped spring attenuator and was primarily an attempt to minimize the angular and lateral motion of the foot-pad during vertical attenuation.

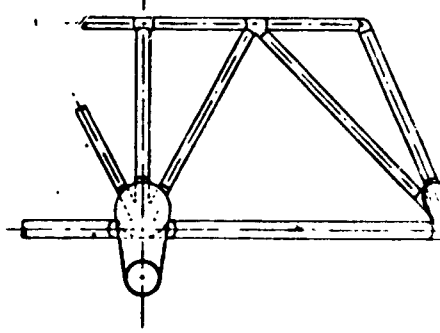
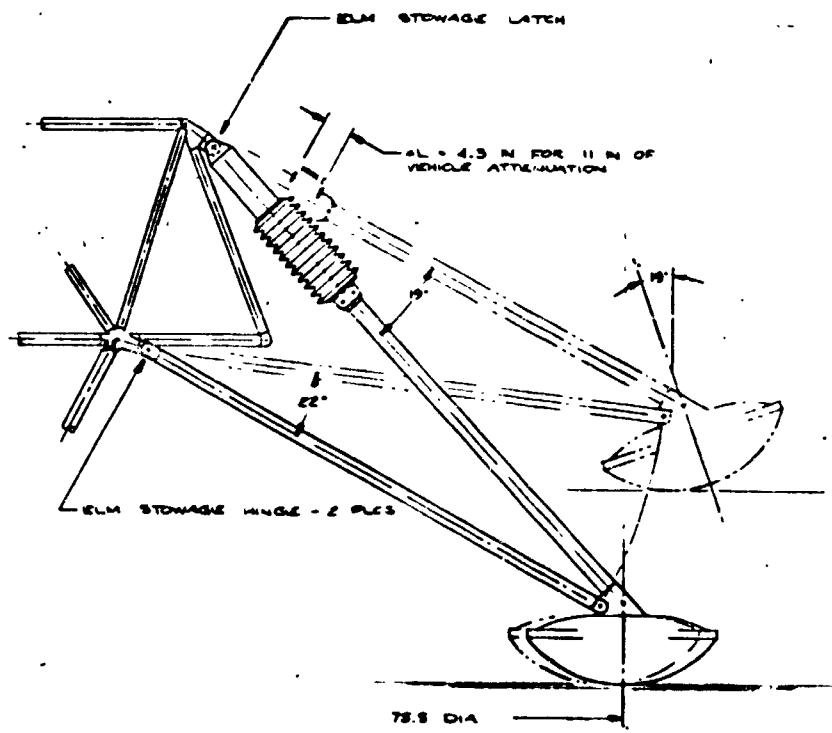
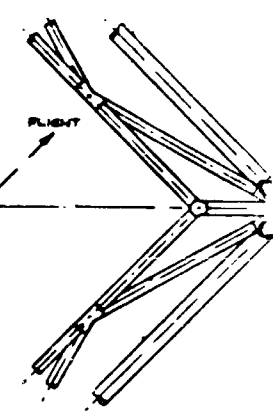
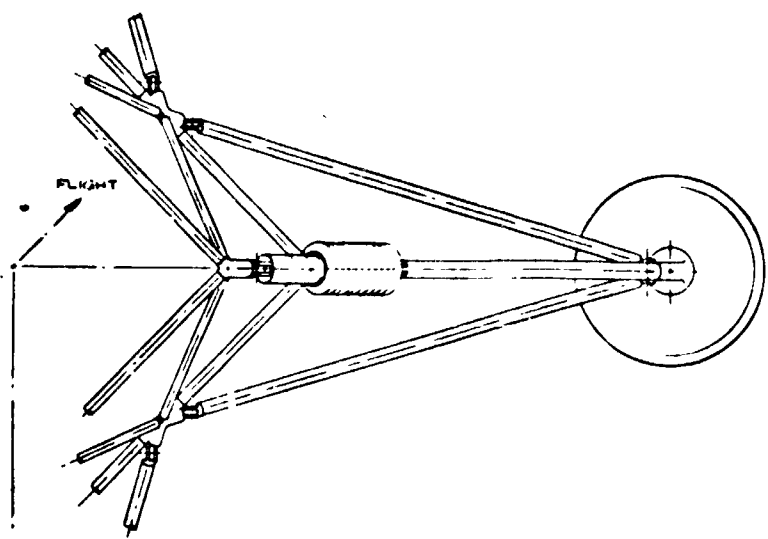
At this point in concept development, two important design problems were apparent. One was the need to develop a lightweight mechanism that would attenuate lateral velocity components and thus meet the requirement that the vehicle design attenuate hidden or unobserved rock impact (no sliding). The second serious problem was vaguely defined at the time as the desire to obtain a central attenuator. What was needed was a solution to the problem of independent landing legs wherein the energy is taken by any one or all of the legs. This gives rise to a multiplication factor (4 for a four-leg gear) on both stroke and acceleration attenuation level, depending on whether the vehicle is at the heavyweight stroke-limiting condition or the lightweight g-limiting condition.

Attempts at developing a mechanism for a central attenuator in which linkages were used from the legs to a central attenuator were not fruitful. All candidate designs were patently heavy, inasmuch as the leverage required introduces moments throughout the vehicle. For that reason, none of the designs were reduced to drawings.

The solution to both problems was obtained through the design shown in Figure 68. An early antecedent of this concept is the stagecoach suspension. It may not be optimum for large vehicles, but it is most suitable at the scale of a lunar flying vehicle. As may be seen in the figure, the effect of a central attenuator is essentially achieved, i. e. , all of the attenuators are acting in every landing condition, and there is no multiplication per se due to the number of pads in contact with the ground. Another way of expressing this is that, in any coordinate direction, rotational or linear, velocities are always taken by the same attenuator, and there is no superfluous set.

### Design Optimization

At the end of the conceptual phase, the concept of the integral leg-frame landing gear had been assumed to incorporate only four attenuators. It has been suggested that since the landing gear has six degrees of freedom, space mechanism principles require that it use at least six attenuators. However,

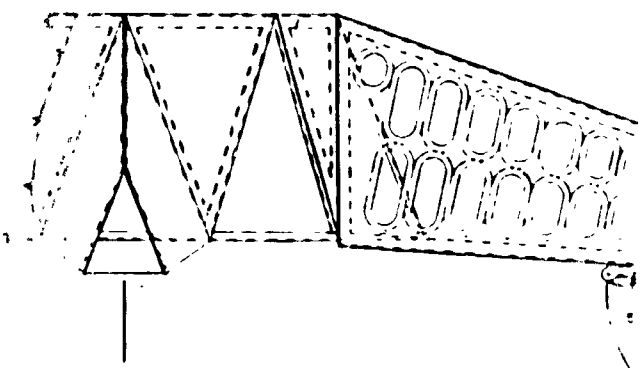
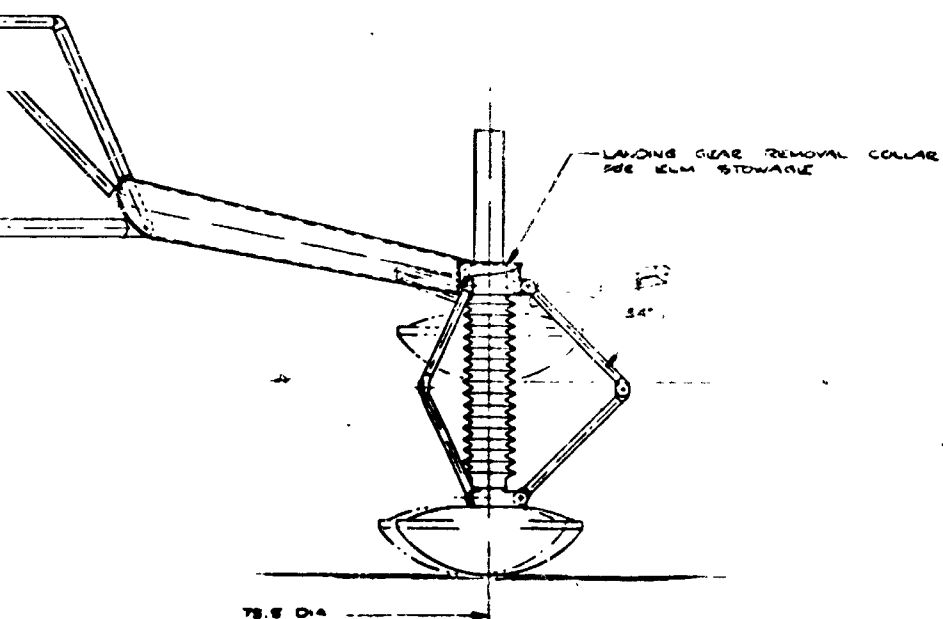
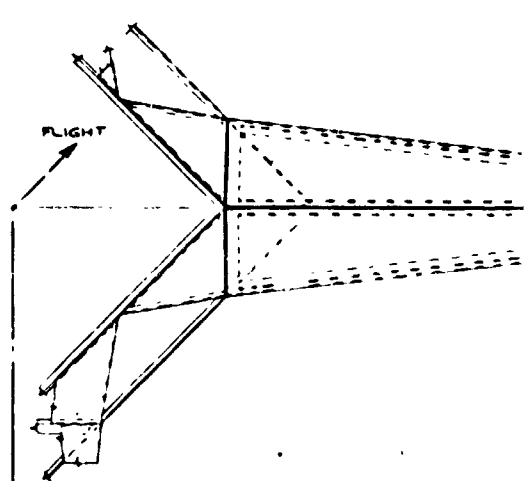
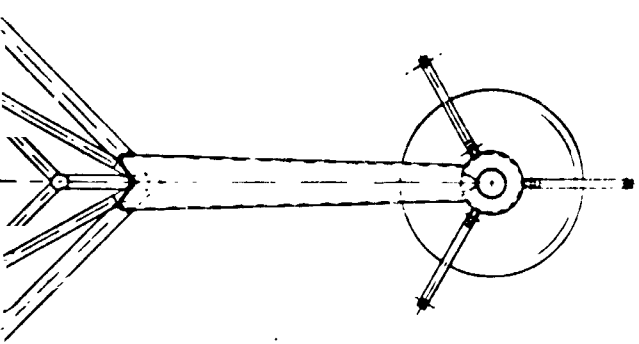


ALTERNATE A  
N-LINE COMPRESSION ATTENUATOR

ALTERNATE B  
SINGLE MEMBER ATTENUATOR, EXCEPT AS NOTED

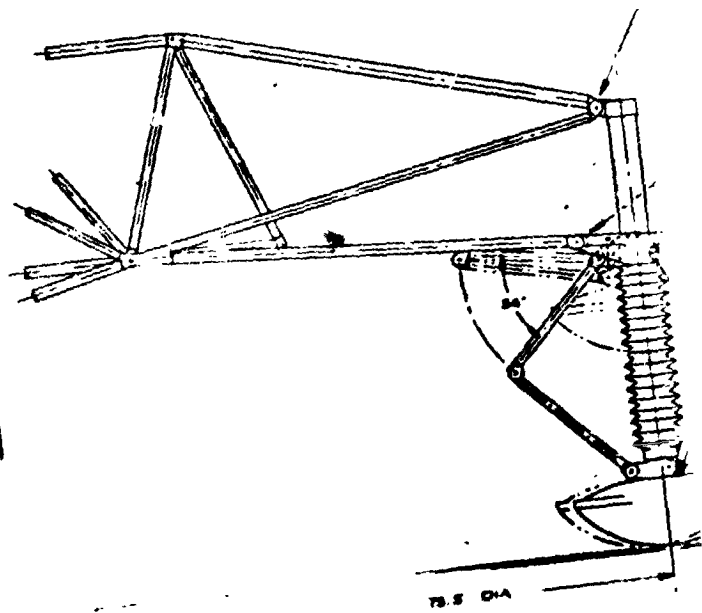
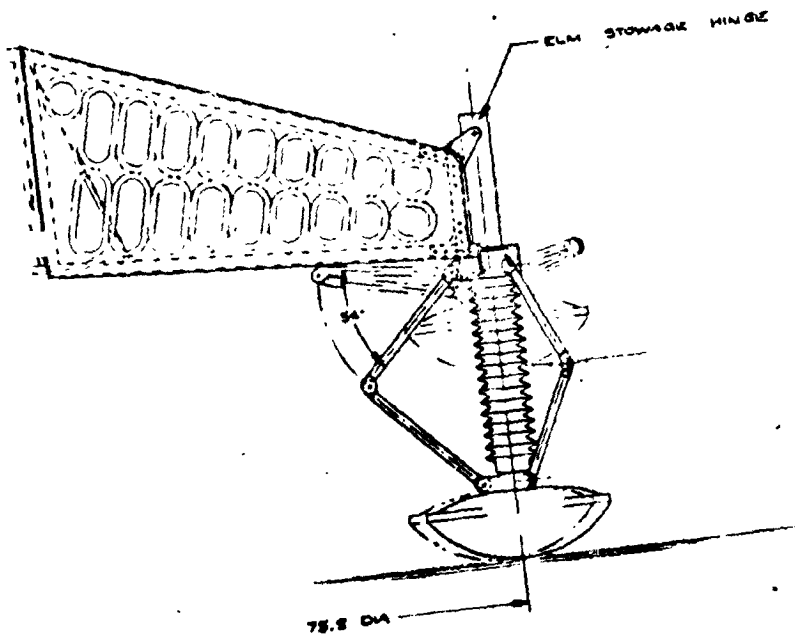
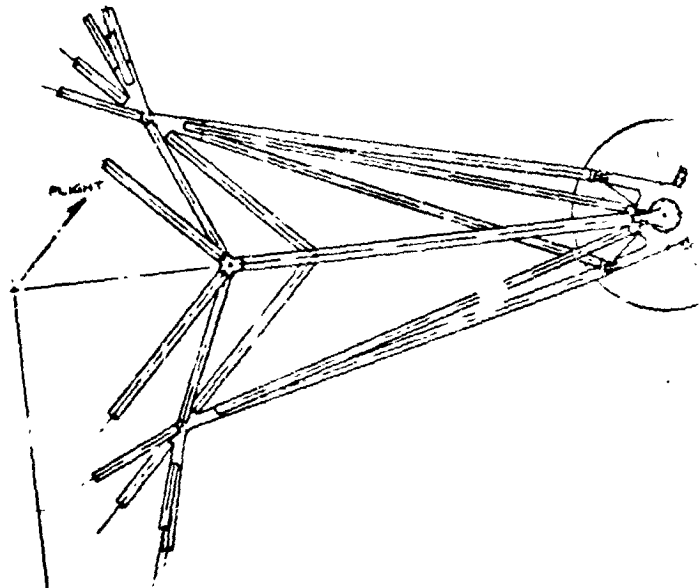
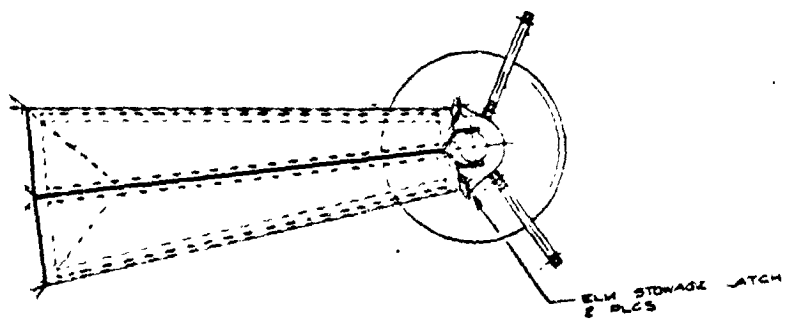
FOLDOUT FRAME

FOLDOUT FRAME



ALTERNATE "E"  
MEMBER STOUT. IDENTICAL TO  
"D" EXCEPT AS NOTED

ALTERNATE "E"  
DIAG. STRENGTH STOUT. IDENTICAL TO  
"D" EXCEPT AS NOTED

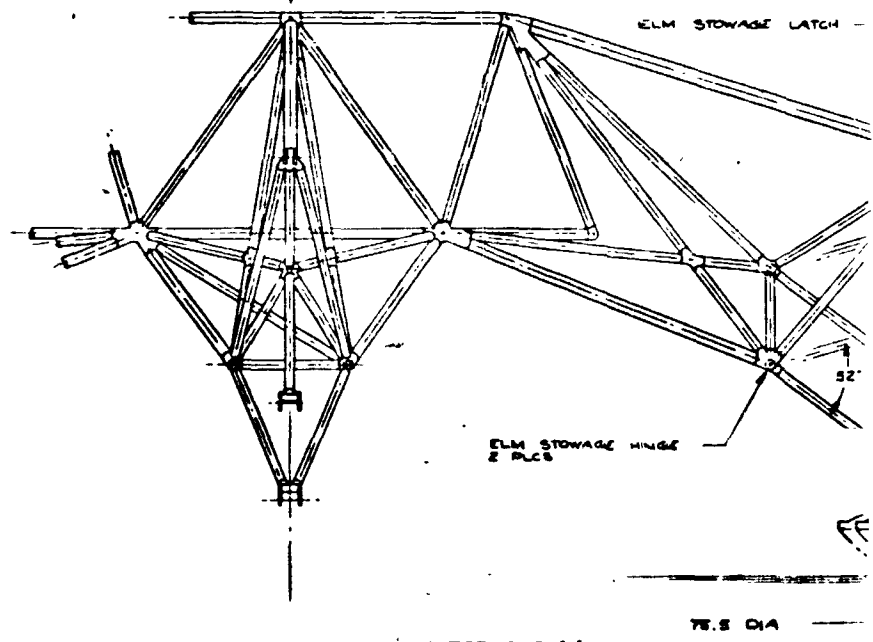
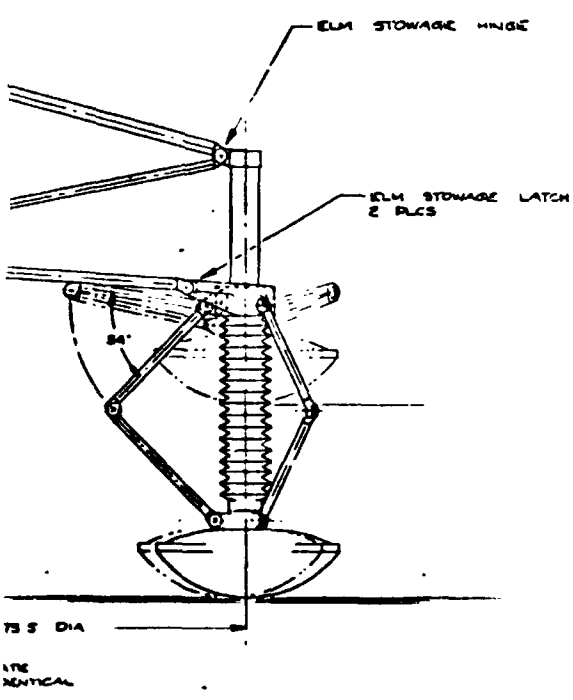
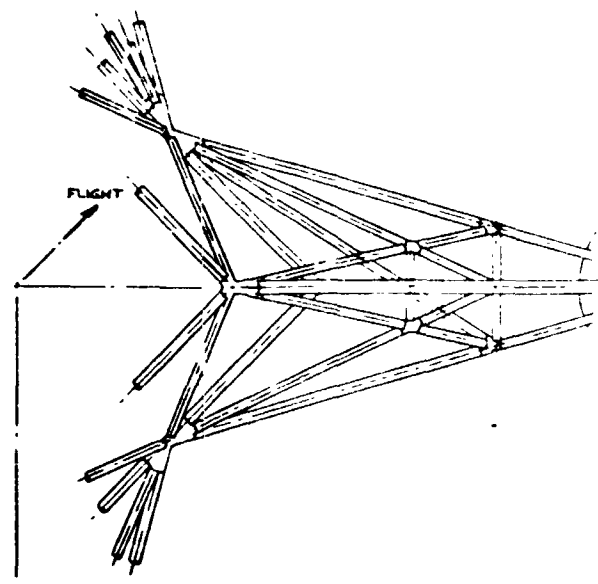
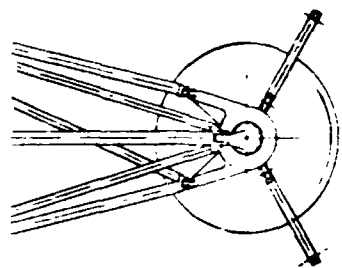


ALTERNATE TO  
FIG 27-10, IDENTICAL TO  
AS NOTED

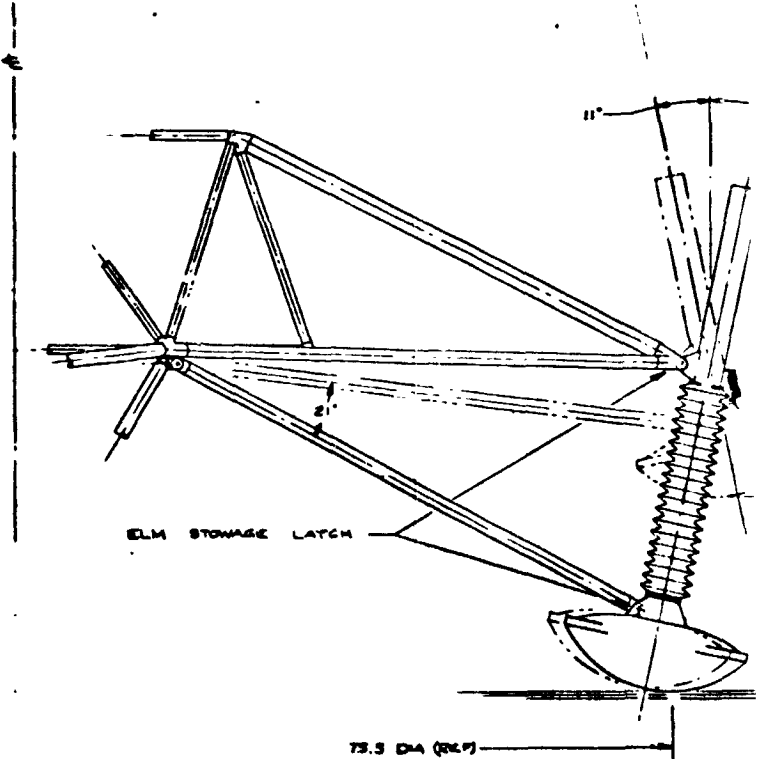
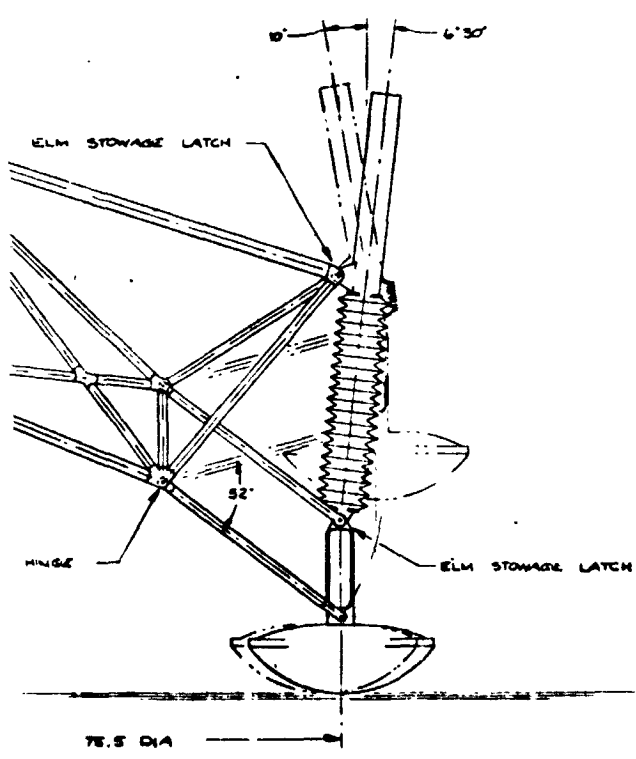
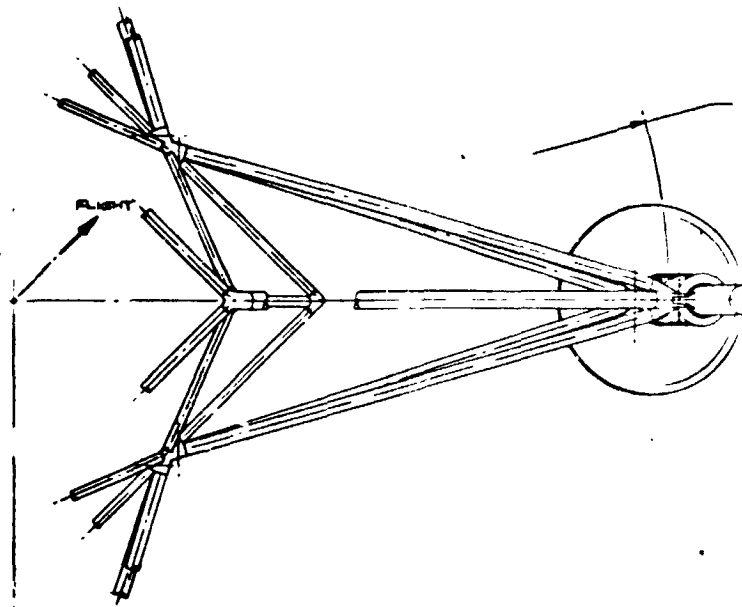
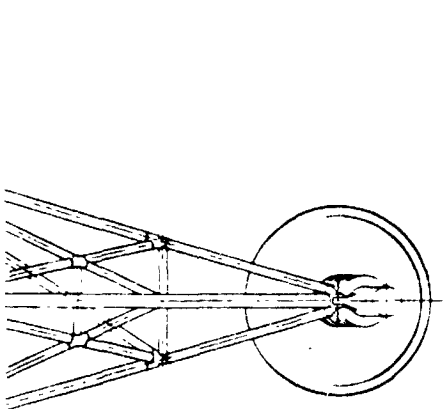
ALTERNATE TO  
FIG 27-10, IDENTICAL TO  
AS NOTED

FOLDOUT FRAME

FOLDOUT FRAME



ALTERNATE 'C'  
 A BAR LAGAGE TO MINIMIZE HORIZONTAL  
 TRANSLATION OF PNO. IDENTICAL TO 'A',  
 EXCEPT AS NOTED

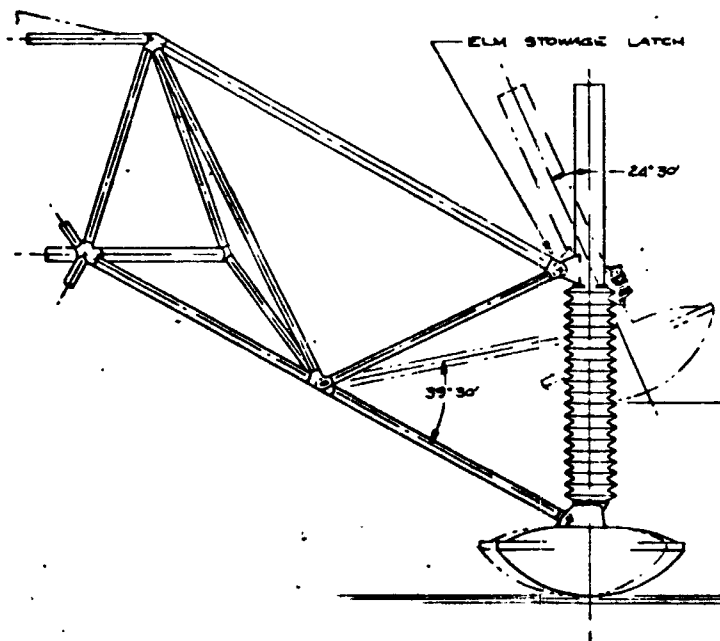
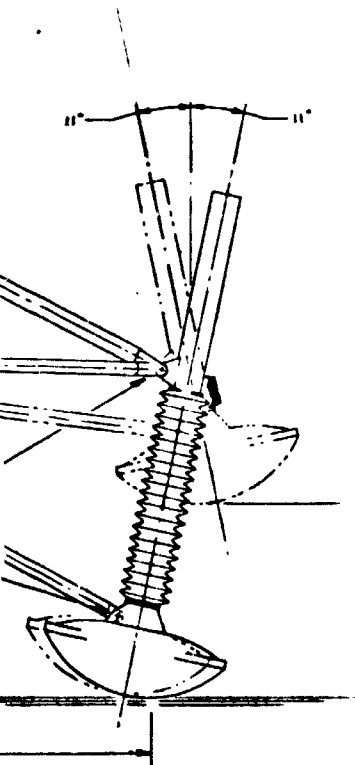
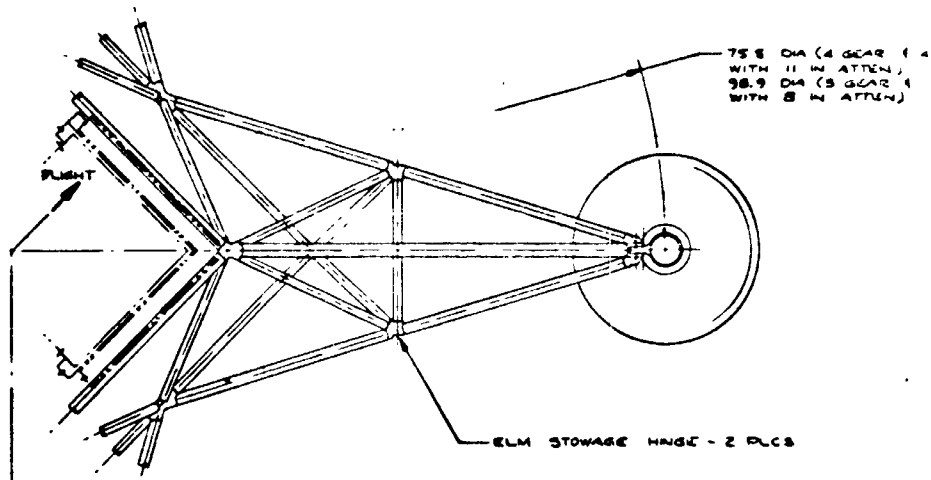
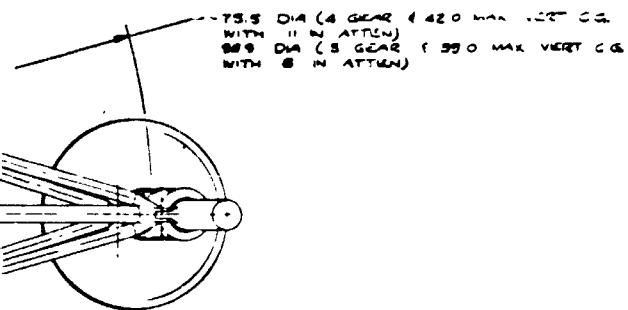


HORIZONTAL TO 'A'

ALTERNATE 'B'  
 MAXIMUM MEMBER TRUSS, IDENTICAL TO 'A';  
 EXCEPT AS NOTED

FOLDOUT FRAME

FOLDOUT FI



ALTERNATE A  
 SIMPLIFIED TRUSS FOR REDUCED FOOTPRINT  
 IDENTICAL TO CONTRA CONFIG, EXCEPT AS NOTED

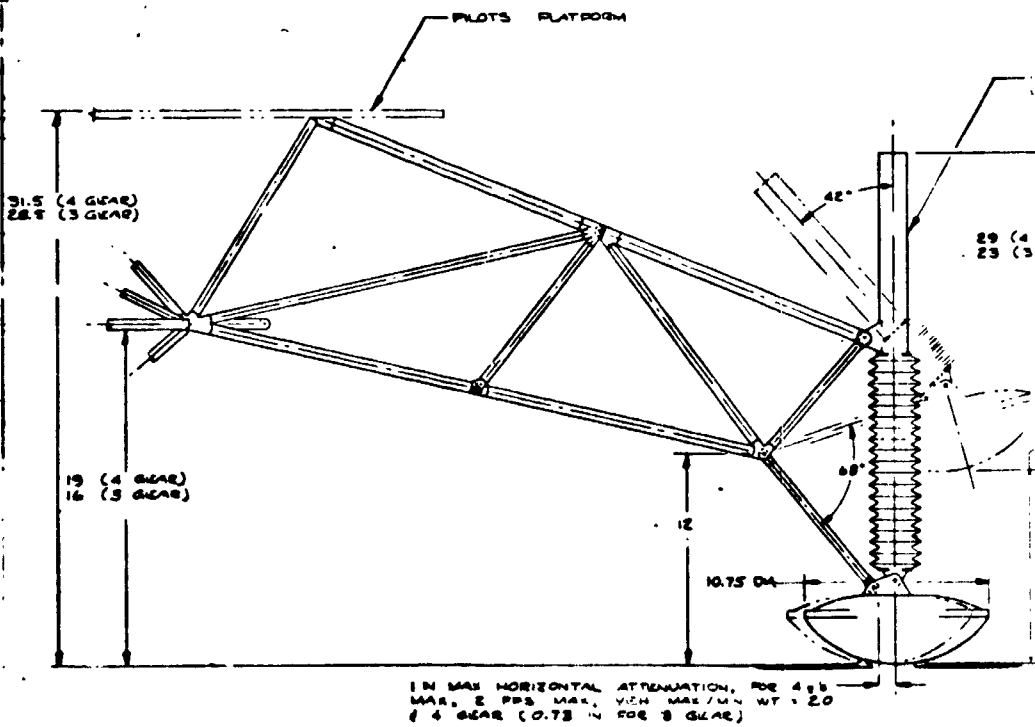
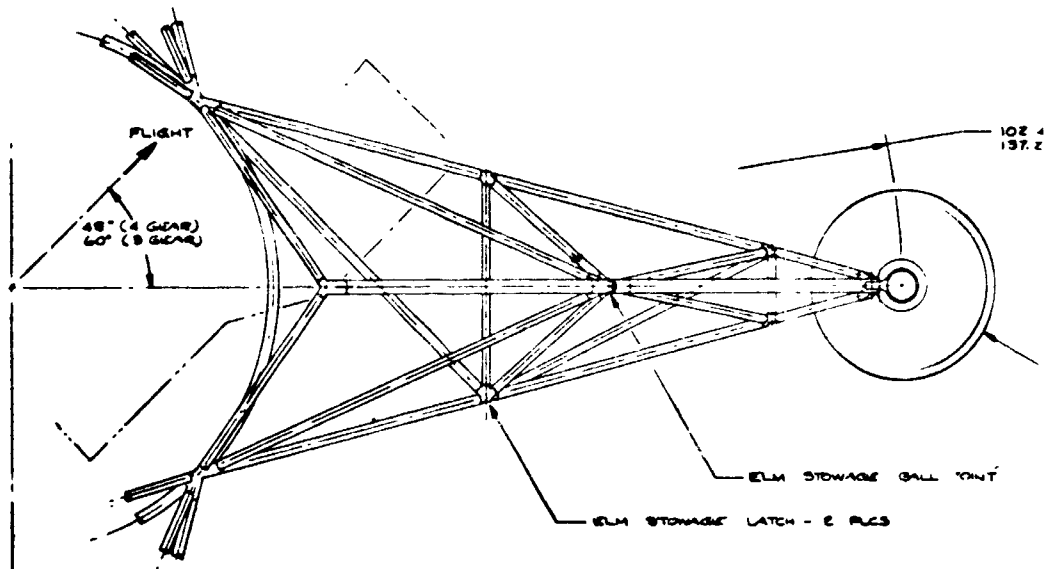
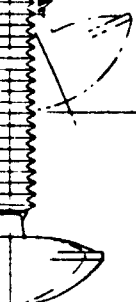
75.8 DIA (4 GEAR / 420 MAX VERT CG,  
WITH 11 IN ATTEN.)  
98.9 DIA (3 GEAR / 590 MAX VERT CG  
WITH 8 IN ATTEN.)



INDU - 2 PLCS

GE LATCH

24'30"



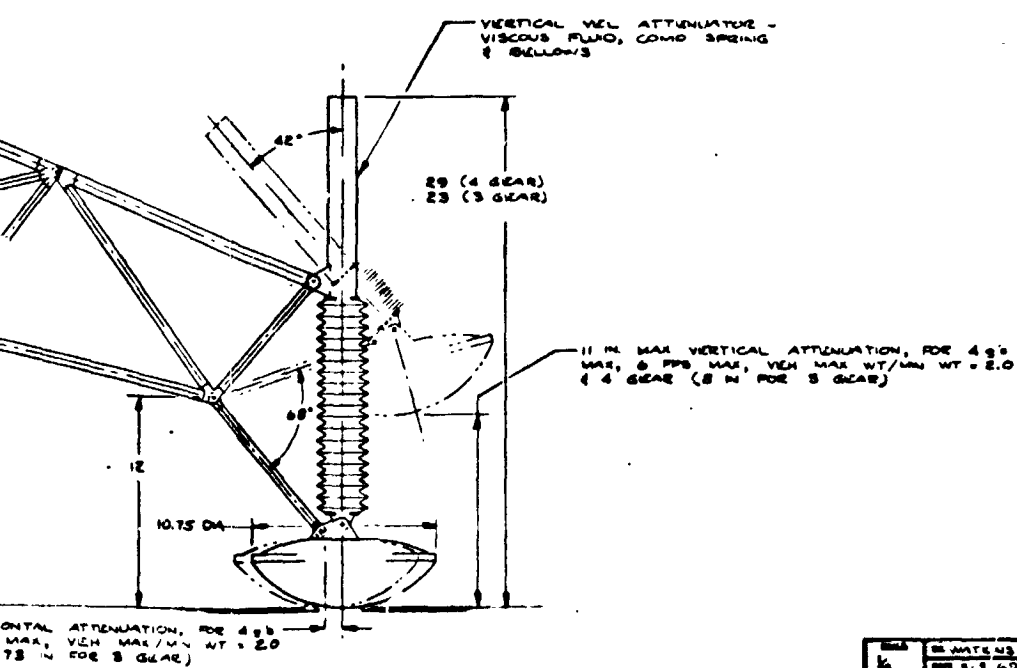
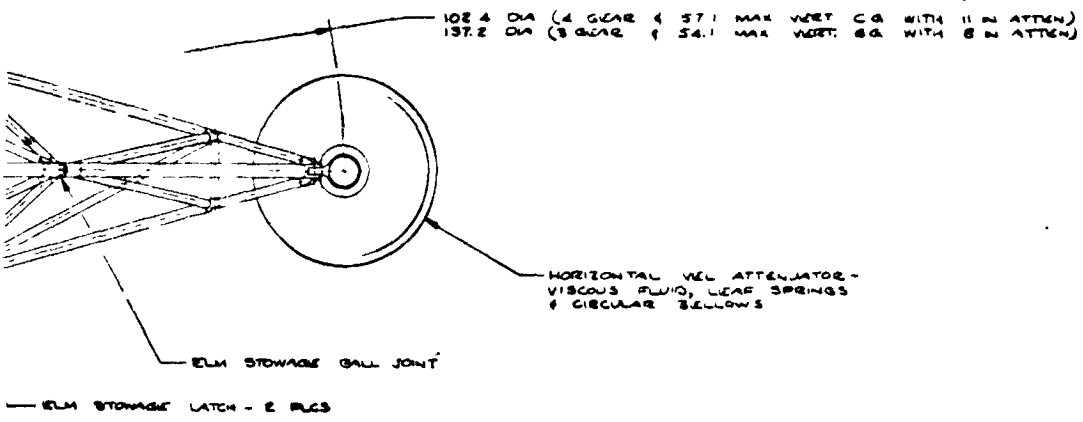
CONTROL CONFIGURATION

FOLDOUT FRAME

FOLDOUT

UPSIZE PAGEMAT - 120%  
BLOW UP CALLOUTS 120%





|  |          |  |        |
|--|----------|--|--------|
| REV  | REV DATE | BY   | CHKD   |
|  | 6        | 8-2-62   |        |
| TITLE  |          | DRAWN BY   |        |
| ONE-MAN LFV CONTROL CONFIGURATION ALTERNATE, LANDING GEAR STRUT CONCEPTS |          | NORTH AMERICAN ROCKWELL CORPORATION<br>1000 LO-RENO BLVD, CANON CITY, COLORADO |        |
|  |          |  | 2230-5 |

Figure 67. Landing Gear Concepts

- 161,162 -

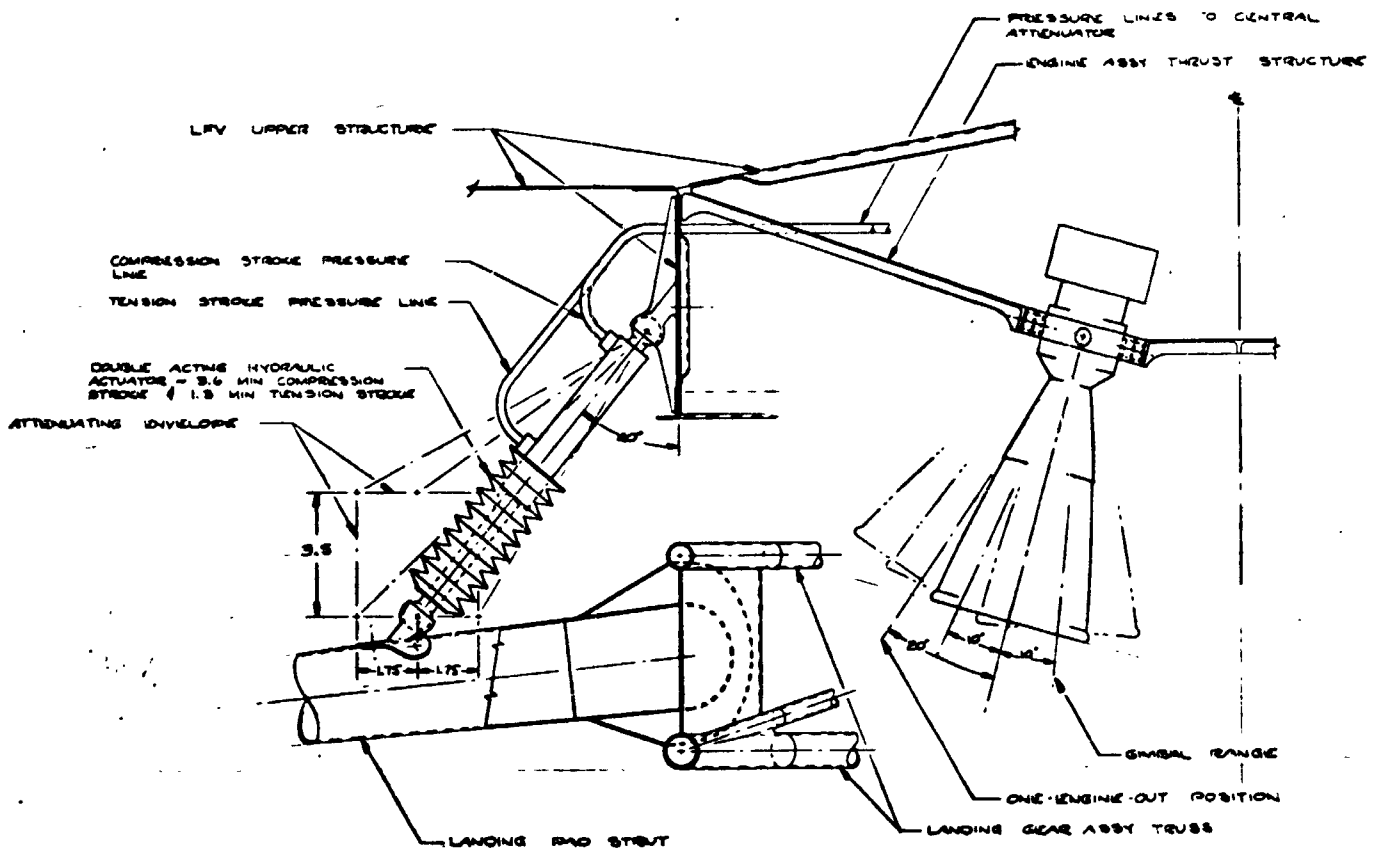
FRAME

FOLDOUT FRAME

SD 69-419-4

UPSIZE PAGEMAT - 120% KEYLINE IMAGE AREA  
BLOW UP CALLOUTS 120% - REDUCE TO 83% OF ORIGINAL

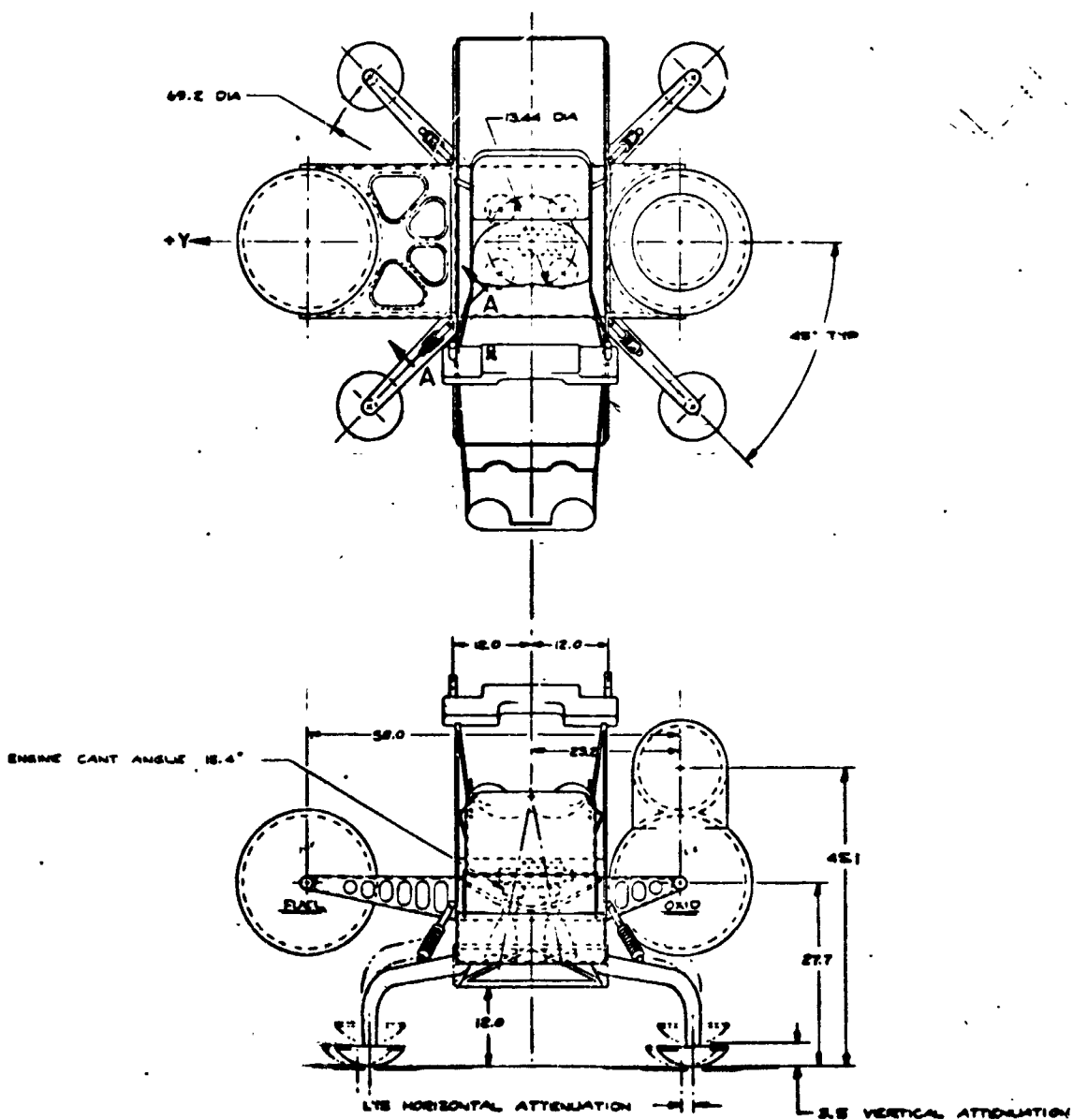
PLEASE MAKE CORRECTIONS ON TISSUE OVERLAYS,  
OR READING COPY IF AVAILABLE

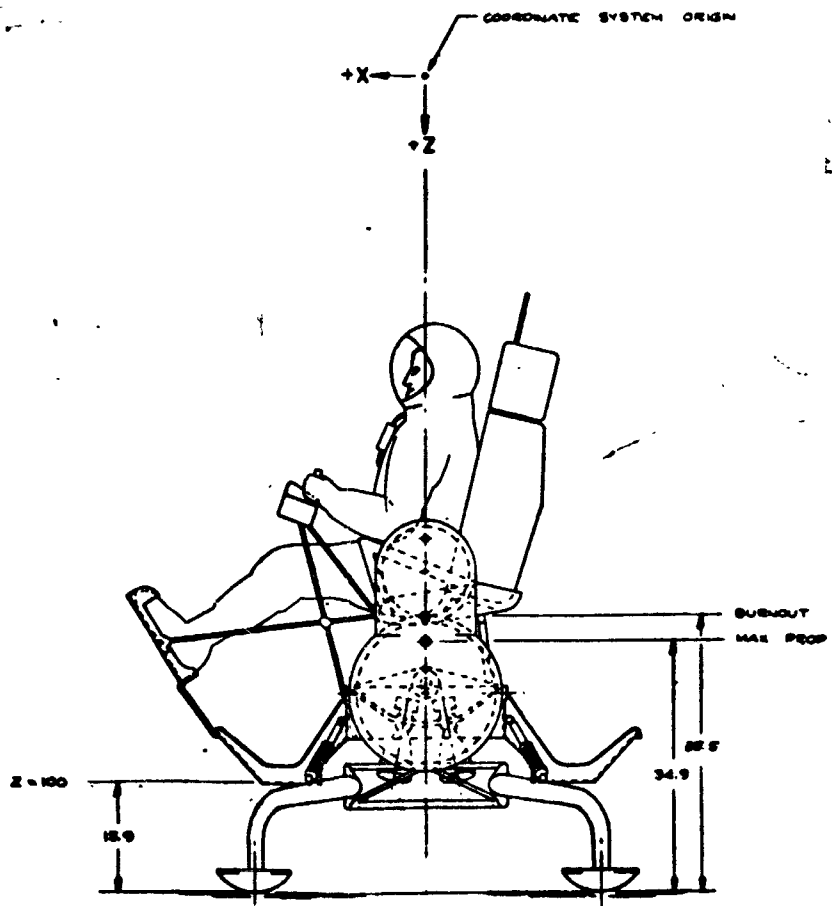


SECTION A-A SCALE 1/2

FOLDOUT FRAME

FOLDOUT FRAME





ATTENTION

|       |  |      |     |
|-------|--|------|-----|
| REV   | BY   | DATE | APP |
| 1     | ...  | ...  | ... |
| NOTES | ONE - MAN LP CONTROL CONFIGURATION SEATED PILOT CENTER |      |     |

Figure 68. Leg Frame Gear for Seated-Pilot V

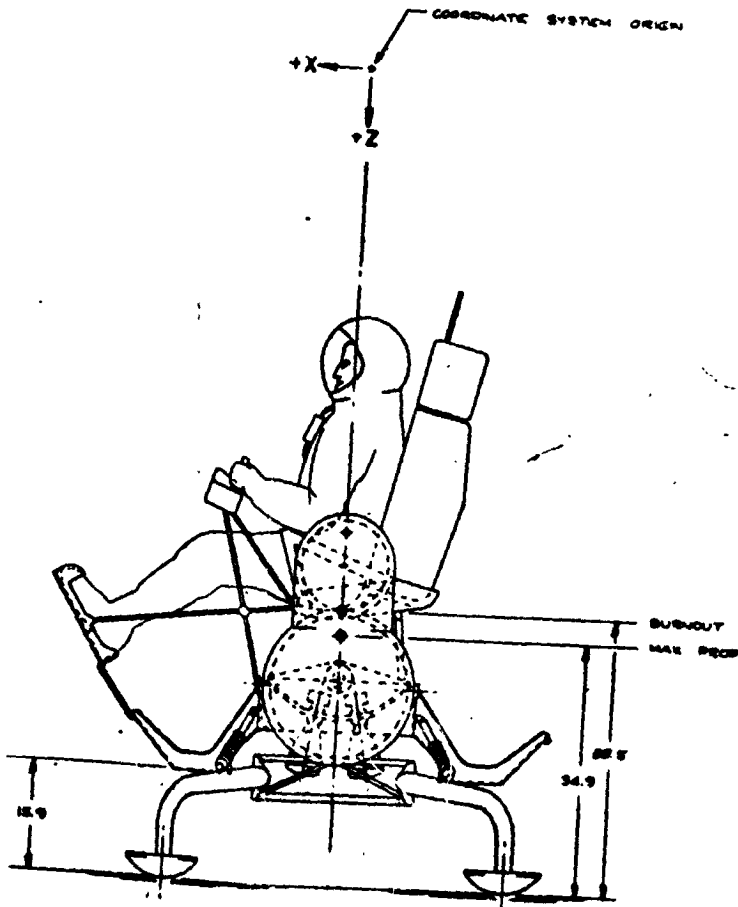
- 163,164 -

FOLDOUT FRAME

FOLDOUT FRAME

SD

UPSIZE PAGEMAT - 120% KEYLINE IMAGE AREA  
 BLOW UP CALLOUTS 120% - REDUCE TO 63% OF ORIGINAL



|     |          |        |  |
|-----|----------|--------|--|
| REV | BY       | DATE   | DESCRIPTION  |
| 1   | W. W. W. | 3-6-69 | ONE-MAN LFV - CONTROL CONFIGURATION ALT. SEATED PILOT & CENTRAL ATTENUATOR |
|     |          |        | 2230-6   |

Figure 68. Leg Frame Gear for Seated-Pilot Vehicle Configuration

- 163,164 -

FOLDOUT FRAME

SD 69-419-4

UPSIZE PAGEMAT - 120% KEYLINE IMAGE AREA  
BLOW UP CALLOUTS 120% - REDUCE TO 83% OF ORIGINAL

PLEASE MAKE CORRECTIONS ON TISSUE OVERLAY  
OR READING COPY IF AVAILABLE

in the design optimization study, a less elegant approach was used. This amounted simply to running the landing dynamics programs with various attenuator arrangements in an attempt to acquire stability over the large range of deflections involved at this energy level. The result was the determination that pin-ended, skewed struts could not be made stiff enough to satisfy both the g-load and platform displacement limits. Up to a certain point, the mechanism was capable of providing constrained motion, but after the angles between the attenuator and the body became obtuse, the arrangement was no longer kinematically correct. Several suggestions were made to restrain the struts in some manner that would effectively apply other mechanism principles. It is possible that this could work, but a very detailed investigation would be necessary to evaluate the additional hardware involved. Such restrained struts would experience excessive moments in most cases and probably would be quite heavy.

The use of six attenuators was proven, by a series of runs on the dynamics program, to be adequate. However, the attenuator pattern required three attach points to the cruciform type of landing gear. This geometry was not compatible with efficient structure, requiring excessive bridging to pick up the attenuator hard points. It was considered preferable to use eight attenuators, which gave a more satisfactory structure interface. This arrangement is shown in Figure 22. Two skewed struts are used per leg, one essentially for vertical and pitch and roll components, the other skewed in the lateral plane, primarily for yaw but also partially effective in the other coordinate directions. The yaw struts are arranged in opposing pairs. The final arrangement of the strut attach points was determined by iteration with the preliminary design layout and involved optimizing clearances with the tanks and the engines. Using this arrangement and the characteristic of the attenuator design that had been developed concurrently, several worst-case runs were made with the landing dynamics computer program. These runs established the anticipated loads, accelerations, attenuator strokes, and angular and linear displacements of the platform body relative to the leg frame and to the ground. The cases included verification of toppling stability as well. The runs indicate that the capability is within the limits defined by the approximate, closed-form analyses of Phase I displayed in Figure 69.

Table 19 shows the results of these cases with regard to relative motion of the body and the leg frame, and shows the general description of the initial conditions for each run. The results show a horizontal relative movement of 2.2 inches, a vertical movement of 2.3 inches or less, relative angular displacements of  $\pm 5$  degrees about the vertical axis, and a total horizontal inclined angle of 8 degrees between the platform and leg frame. The maximum stroke of the attenuator was 3 inches, using a strut payload of 141 pounds and a maximum strut force of about 1000 pounds. It

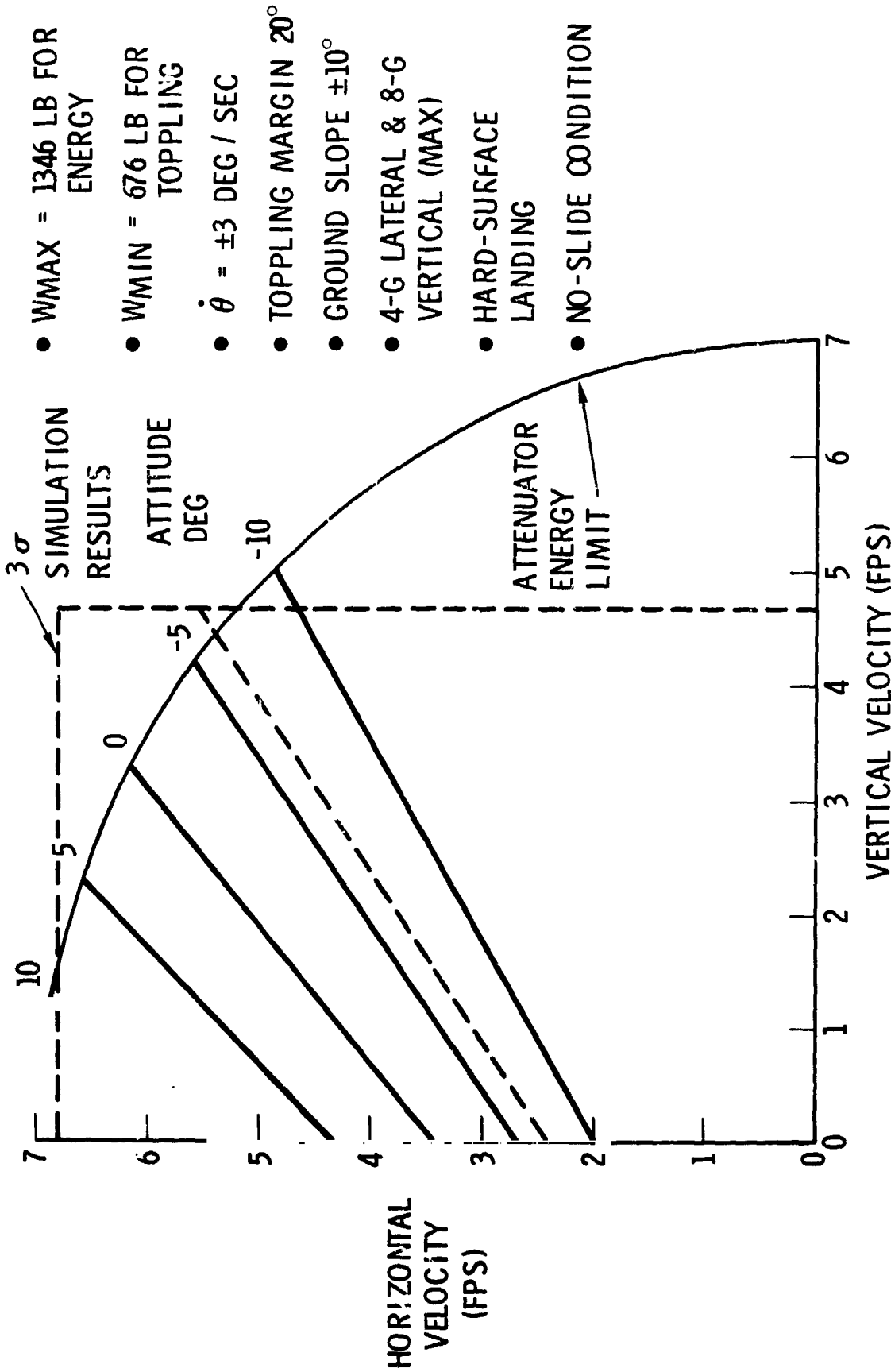


Figure 69. Landing Gear Capability

Table 19. Worst-Case Landing Displacement

| Case Description  | Initial Angle (deg) |        |        | Body/Leg Frame Maximum Relative Displacement |              |      |      |               |              |              | Impacting Leg |           |
|---|---------------------|--------|--------|--|--------------|------|------|---------------|--------------|--------------|---------------|-----------|
|   | Yaw                 | i Axis | j Axis | Slope (i Axis)                               | Linear (in.) |      |      | Angular (deg) |              |              |               |           |
|   |                     |        |        |  | k            | i    | j    | k Axis        | i Axis       | j Axis       |               | i-j Plane |
| Case 1<br>Nose down<br>Up slope   | -135                | 7.0    | -7.1   | 10   | -2.0         | -1.3 | -1.8 | -5.0          | -7.0         | -4.0         | 7.2           | 3         |
| Case 2<br>Nose up<br>Down slope   | 45                  | 7.0    | -7.1   | -10  | -2.2         | 1.0  | 1.9  | +3.0<br>-2.0  | 8.0          | 8.0          | 8.0           | 3         |
| Case 3<br>Nose up<br>Down slope<br>Strut 8 failed   | 45                  | 7.0    | -7.1   | -10  | -3.4         | 1.7  | 2.0  | 3.5<br>-2.5   | 11.0<br>-2.0 | 11.5<br>-1.5 | 12.3          | 1 & 3     |
| Case 4<br>Rolled left<br>Nose down<br>Slope up to left  | 90                  | -7.1   | 7.1    | 10   | -1.4         | 1.0  | 0.6  | 3.5<br>-2.0   | -5.0         | 5.0          | 7.0           | 3         |
| <b>General Conditions</b><br>Vertical velocity, 6 fps<br>Horizontal velocity, 3.5 fps<br>Soil pressure, 18 psi<br>Leg stiffness, 1,250 lb/in., all directions<br>Mass, 1,320 pounds<br>Hydraulic attenuator |                     |        |        |  |              |      |      |               |              |              |               |           |



was subsequently determined that the actual stiffness of the leg frame was lower than anticipated, which would permit a stiffer attenuator. For this reason, the results shown are somewhat conservative, and if the improved attenuator were part of the input, the results would be even more favorable. It is also probable that the entire load stroke curve of the attenuator could be improved by reshaping it to a much higher preload and a higher maximum load without exceeding the design acceleration.

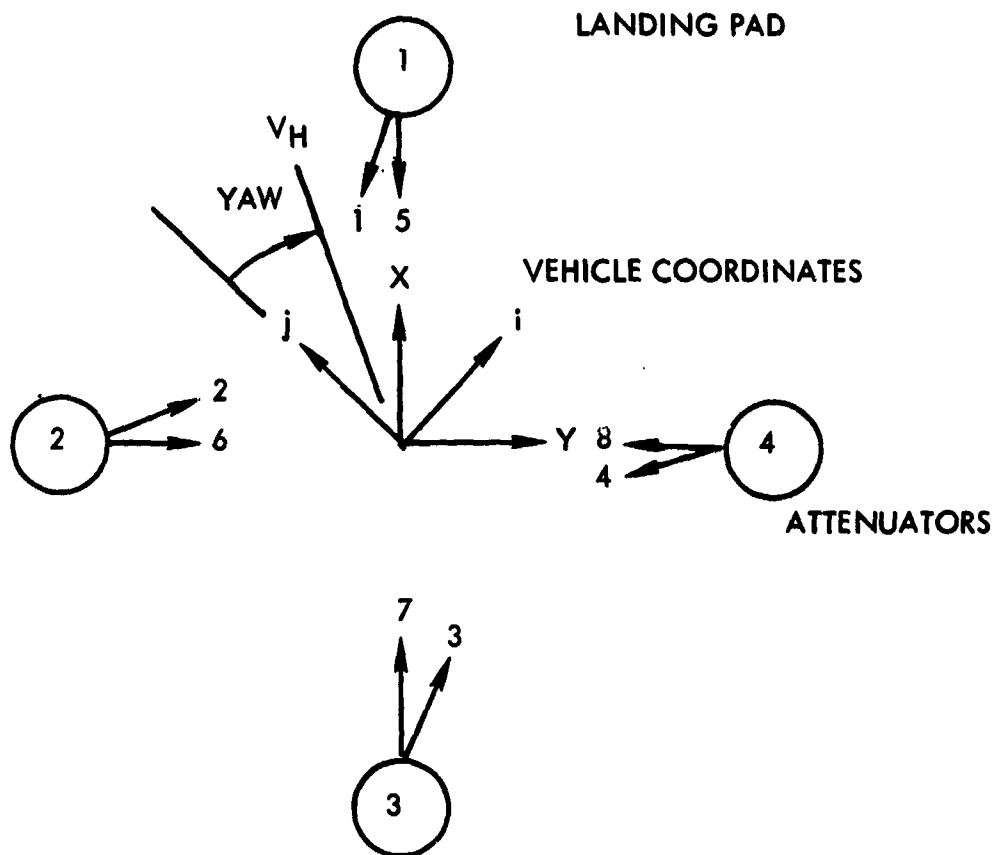
CRT plots resulting from the runs are contained in Appendix B. These plots show, besides the relative motions of Table 19, the accelerations, strut strokes, and motion with respect to the ground. In all cases, the first leg contacting the ground is assumed to impact a rock. The nose-up conditions are into a downhill slope, and the nose-down conditions are into a uphill slope. Figure 70 shows the coordinate system used on the printout and relates it to the coordinate system of the vehicle.

### Attenuator Design

#### Concept Development

Initial attenuator concept analyses covered a wide range of possible devices. All of these are force- and velocity-limited attenuators, and their efficiency for the application depends on how close they approximate a constant-force displacement (load-stroke curve at the velocity of interest). An ideal attenuator, of course, would be one that is g-limited, but such a device undoubtedly would incorporate sensors of a type that would add complexity and reduce reliability. Types originally considered included friction, cyclic deformation, inelastic deformation, and hydraulic. Springs alone were not considered, since the requirement of the attenuator is to ultimately (within a few cycles at most) absorb the kinetic energy of the vehicle (otherwise the rebound condition will be severe).

Internal friction or damping is utilized in the spring footpad attenuator of Figure 65. As noted in the preceding discussion, this device has extremely limited energy capabilities. The bicycle brake type of friction device was eliminated as having inherently low energy capacity per unit weight. Cyclic deformation types of attenuators were reviewed, and the "rolling ring" concept, at one time in development for the Apollo crew couch strut, was studied. This device was finally assessed as temperature-sensitive and somewhat heavy for this application. The most study emphasis was placed on the remaining two devices, inelastic deformation and hydraulic.



LEGEND

- $i$  = PRINTOUT Y
- $j$  = PRINTOUT Z
- $k$  = PRINTOUT X = -VEHICLE Z

Figure 70. Dynamics Program Coordinate System

The inelastic deformation type was studied by first reviewing an extensive patent and literature file on the subject. Most of the file concerned crushable honeycomb devices which were not considered suitable for the multiple-landing requirement of the LFV because they were bulky. The most compact and the highest in potential specific energy capability were found in devices such as the fragmenting tube, which utilized metal deformation. The field of candidates in this area was finally narrowed to one that had been thoroughly developed. This was the so called "flowerpot" concept illustrated in Figure 71. This concept was developed by Stanley Aviation and used on the B-58 airplane capsule as an attenuator. It is considered to have reproducible performance, high energy capacity per pound, and is relatively insensitive to thermal changes. Since the shear force, even for a small metal cross section, is very high, it was determined that a force multiplier was necessary to apply this concept to the LFV. A mechanism was also needed to recycle the unit for each successive landing. A method of doing this hydraulically is shown in Figure 72. One version shown is a central energy absorber type, actuated by hydraulic fluid from hydraulic pistons mounted at the attenuation point. The other version has the strut piston directly attached to the energy absorber. The force is multiplied hydraulically. In both cases, a gas spring actuates return fluid through a Surveyor-type rate-sensitive valve to re-extend the legs in preparation for the next landing. In this way, the insert would be progressively shortened by deformation at each landing. The insert was designed for up to five landings, after which it would be replaced.

Throughout the conceptual phase, the baseline configuration was a hydraulic attenuator of the Surveyor type. Review of the Surveyor design (Figure 73) showed that it is not particularly temperature-sensitive. It has a design operating range of 0 to 125 F. This was considered acceptable for the LFV environment and installation.

The conceptual phase was concluded by selecting the Surveyor hydraulic attenuator. The metal deformation type, though it has high potential, was not selected because extensive verification testing and development would be necessary to provide the principle, whereas, the hydraulic type has already been proven.

#### Attenuator Preliminary Design

The desired load stroke curve for the attenuator was established by an iterative technique using the landing dynamics program and the preliminary design landing gear arrangement. This gave an approximate desired characteristic. A short computer program was then written and incorporated into equations for the damping and spring effects of the attenuator, using the data from Dow Corning on the Surveyor Type F4029

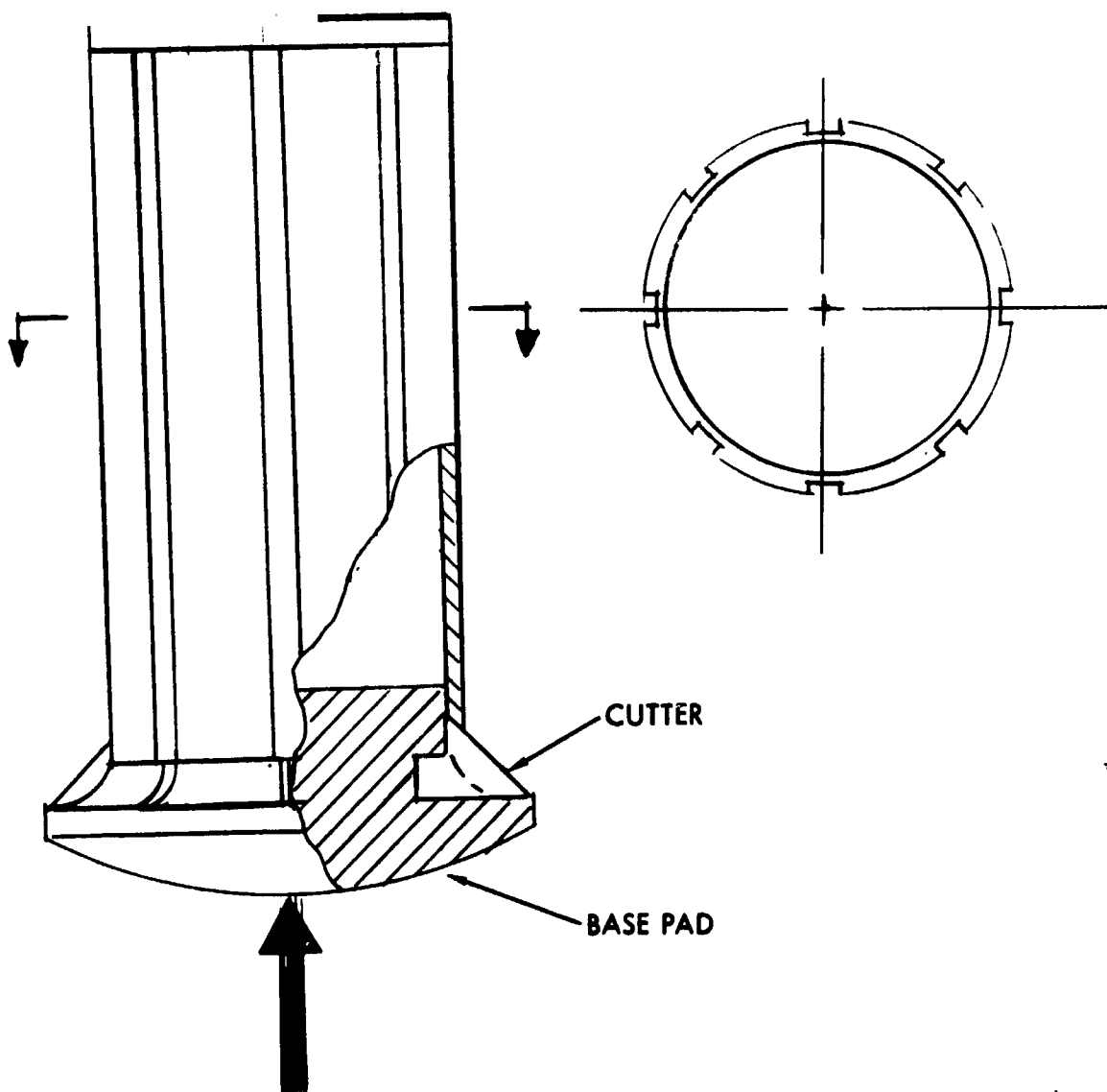


Figure 71. B-58 Escape Capsule Metal-Deformation Attenuator.

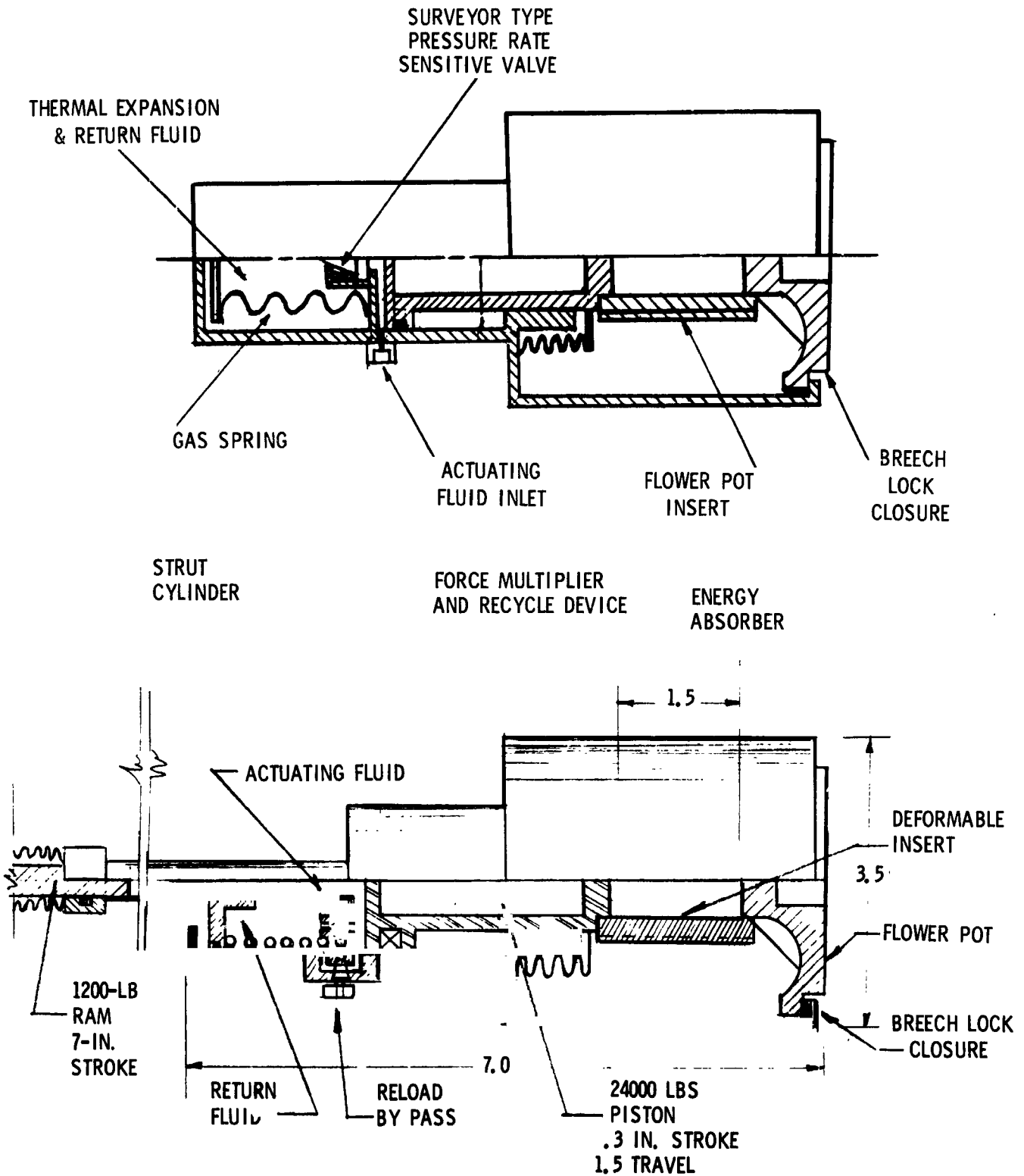
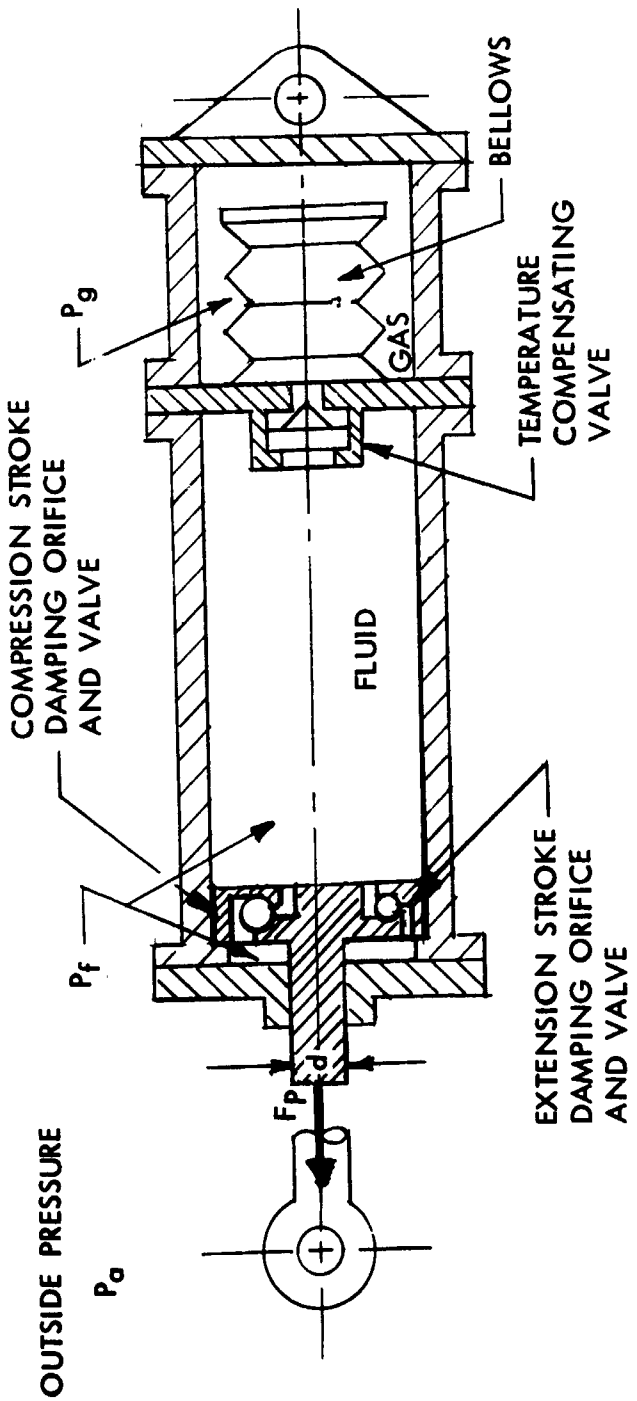


Figure 72. Metal-Deformation Energy Absorber Concept



IN EXTENDED POSITION {

FLUID PRESSURE =  $P_f$  = GAS PRESSURE =  $P_g$

SPRING FORCE (PRELOAD)  $F_p = (P_1 - P_0) \frac{2}{4} W$

IN STROKED POSITION, THE TEMPERATURE COMPENSATION VALVE IS CLOSED AND THE SPRING FORCE IS INCREASED, BECAUSE OF COMPRESSION OF THE FLUID (ENTERING OF PISTON ROD). A DAMPING RESISTANCE IS ALSO ENCOUNTERED, DEPENDING ON THE FLUID AND ORIFICE CHARACTERISTICS AND LINEARLY PROPORTIONAL TO THE SQUARE OF THE STROKING VELOCITY.

FROM: "THE SURVEYOR SHOCK ABSORBER" PAPER BY F. B. SPERLING, JPL, 3RD AEROSPACE MECHANISM SYMPOSIUM, 1968.

Figure 73. Surveyor Fluid-Spring Attenuator

compressible silicon fluid. From these equations, the actual load stroke curve of the attenuator was developed, along with piston and orifice sizes and liquid volume requirements. These values determined the basic characteristics of the design shown in Figure 24. The design uses 6Al-4Va titanium for the pressure shell. Preload is obtained by pressurizing the gas compartment to approximately 2000 psi. This pressure is transmitted to the stainless bellows and through the rate-sensitive Surveyor-type valve to the liquid compartment. This pressure acting over the area of the piston rod develops the preload force. It also is the force which re-extends the rod after landing. During motion of the piston, the liquid flows through the damping orifices, and energy is dissipated as heat. The compression stroke orifice, which is the larger, contains a check valve so that it is not actuated on the extension stroke. The extension stroke orifice is small enough to not require a check valve, and the liquid flows in either direction through it with negligible effect on compression stroke damping. The spring effect of the unit is obtained by compression of the fluid by the amount of wetted rod volume at the bottom of the stroke. The maximum pressure obtained due to this effect is 12,000 psi. All of these pressure values are comparable to those used on the Surveyor design. It is also expected that the rate-sensitive valve and the check valve are of a size comparable to those used on the Surveyor, and similar hardware may be used. For repeated landings, the rate of heat dissipation may be a controlling factor in the duty cycle. This requires thermal analysis to determine the unit's heat rejection rate and temperature profile and the preload excursion range.

## STRUCTURE

This section describes the results of design and analysis of the LFV structure. It includes a discussion of the selection of structural materials as well as of the methods chosen for framing LFV primary structure.

### Parametric Phase

Initial studies of the LFV design indicated no requirement to depart from conventional spacecraft materials. Most of the structure can advantageously use 6061-T6 or 7575-T6 aluminum in built-up sections. If necessary, highly stressed areas can utilize titanium 6Al-4Va to save weight. Fiberglass (polyimide or phenolic) is to be used in deep-formed sections such as the seat. To enclose externally applied multilayer insulation on areas such as the propellant tank, heat-formed and/or gore-fitted sections of 6-mil aluminized Kapton are to be used. The covering will be seamed and conformed with Kapton/silicone pressure-sensitive adhesive tape and then painted with white thermal paint. Helium vessels will be protected with an epoxy coat (as used on Apollo) with a final coat of white thermal paint.

### Application of Boron Composites

A preliminary investigation of the potential of boron composites-- epoxy or metal matrix--had the following objectives:

1. To reduce the weight of the structure
2. To simplify the structure by going to a single-member leg
3. To reduce the stowage envelope of the LFV

As these objectives require a substantial design effort, the potentials of boron composites and North American Rockwell capabilities with these materials were reviewed.

Generally, for conventional construction, the substitution of boron composites for aluminum structures yields an approximate weight saving ranging from 15 to 30 percent of the weight of the aluminum structure. This percentage increases when the structure is redesigned specifically to take advantage of boron composite properties. On the other hand, if the aluminum structure is controlled by a minimum-gauge requirement, the potential gain in the use of boron is reduced.

The material cost is relatively high. For the boron-epoxy the cost per pound, including fabrication, is \$500.00. The cost for boron-aluminum is at least twice that of boron-epoxy, or \$1000 per pound. However, the cost must be compared to the cost per pound of payload.

No damage due to outgassing of a boron-epoxy structure is predicted for exposure to a lunar environment up to one year. Good erosion resistance has been demonstrated in aircraft application of boron-epoxy in flight tests through rainstorms and hail.

It is not anticipated that scheduling and cost requirements would depart much from those for an all-aluminum structure.

The North American Rockwell Space Division Materials and Processes organization has been engaged over the past two years in the development of boron composites from the standpoint of structural efficiency, design, and manufacturing. The overall objectives consisted of:

1. Extending material properties definition into the cryogenic regime
2. Defining application areas for future space hardware
3. Design, fabrication, and test of a demonstration article



The demonstration article consisted of a cylindrical, tension-compression cryogenic strut for a nuclear flight stage and is presently under test. The lead time for ordering material required was six to eight weeks.

To assess what gains, if any, the application of boron-epoxy would afford the LFV, a cursory investigation of the truss defined in the baseline design was conducted.

The applied loads at the attenuator pad were based on an upper limit of 8.0 g on the astronaut. This condition occurs when the LFV is at minimum weight during a four-point landing.

For a weight of 601 pounds, one pad reaction is 1202 pounds. The compressive load in the truss upper member is 1700 pounds (Ultimate UFS - 1.5). For a pin-ended column length of 21.0 inches, the minimum  $I = 0.0076 \text{ in.}^4$  for aluminum. The dimensions of an aluminum tube to match the  $I$  are  $3/4$  inch outside diameter,  $t_w = 0.058$  inch, area =  $0.1261 \text{ in.}^2$ ; 1 inch outside diameter,  $t_w = 0.020$  inch, area =  $0.0624 \text{ in.}^2$ ; or 1.2 inch outside diameter,  $t_w = 0.012$  inch, area =  $0.0423 \text{ in.}^2$ .

The 1.2 inch outside diameter is limiting because of wall thickness and cross-sectional area (block compression and local buckling). The equivalent  $I$  in boron-epoxy will be

$$I = \frac{0.0076}{3} = 0.0025 \text{ in.}^4$$

Assuming a minimum of two layers, or 0.010 inch, the column radius is  $R = 0.43$  inch, or a diameter of  $7/8$  inch.

The cross-sectional area consistent with this diameter is

$$A_x = \pi \times \frac{7}{8} \times 0.01 = 0.0275 \text{ in.}^2$$

or a stress of

$$\sigma_A = \frac{1700}{0.0275} = 62000 \text{ psi}$$

One additional wrap will be required in the hoop direction to stabilize the filaments. Cross-sectional area is therefore

$$A_B = 0.0275 \times 1.5 = 0.0412 \text{ in.}^2$$

Compared to the aluminum structure, weight reduction is at least equal to 32.6 percent for the 1.2 inch outside diameter and at the maximum (outside diameter = 3/4 inch), it is 77.5 percent.

An average weight reduction of 50 percent may be realized. Applied to a body weight of 18 pounds and a truss weight of 13 pounds, and subtracting 15 pounds of unaffected fittings, the weight-saving improvement has a maximum potential of 8 pounds.

For tension application, the reductions are even larger, since the strength/density ratio between boron-epoxy and aluminum alloy is approximately 3.5.

This preliminary investigation indicates that boron-epoxy can result in about 8 pounds of weight reduction. However, further investigations will be necessary to ascertain that this weight reduction is not offset by increased weight in the end fittings. Use on the LFV is not recommended unless weight becomes extremely critical.

### Conceptual Design

No normal structural analysis was required or prepared for the several designs developed in the parametric phase. However, mass properties estimates for each configuration were based on member/section spot-check sizing calculations for primary elements.

### Preliminary Design Structural Analysis

This subsection presents the results of initial structural analyses of the preliminary design configuration (Figure 19).

#### Vehicle Factors of Safety

All loadings generated for the LFV were increased proportionately by multiplying them by the following factors for the general structure and pressure vessels.

1. General structure
  - a. Yield factor of safety = 1.10 x limit load
  - b. Ultimate factor of safety = 1.5 x limit load

## 2. Pressure vessels

- a. Proof pressure = 1.5 x maximum operating pressure
- b. Yield pressure = 1.66 x maximum operating pressure
- c. Burst pressure = 2.0 x maximum operating pressure

The pressure vessel factors are higher than those used for Apollo to reflect the repeated use and landing requirements of the LFV. They comply with the manned aircraft standard for rocket propellant tanks given in Reference 22.

### Description of Structure

Structurally, the LFV shown in Figure 22 consists of two major components: the legs, or landing gear, and the hub, or carry-through structure. These two components are separate elements interconnected by the attenuators.

### Legs

There are four legs, each consisting of two segments of uneven length. The short leg is vertical and carries the landing pad at one extremity. The other end is rigidly attached to the longer segment, forming an angle a little larger than 90 degrees. The four legs are joined together to form a cruciform. The rocket engines are mounted in the cruciform, one in each quadrant.

The leg cross section is triangular. It was constrained to this shape (rather than to a circular one, for instance) by clearance requirements of the rocket engine nozzle. However, the triangle embodies the structural features required to match the applied loadings, i. e., bending about a horizontal axis, bending about a vertical axis, and torque about a lateral axis (normal to the horizontal one). The bending material is placed at three corners of the triangular cross section.

### Hub

This component is so named because it forms a center for the collection and dispersal of loading or forces. The propellant tanks and payload pans are cantilevered from it; the pilot's seat and its attached accessories (consoles, footrest, throttle, controls, etc.) roll in tracks directly connected to the upper surface of the hub. The load transfer from legs to hub and vice versa occurs at the eight attenuator attach points.

Ideally, the hub should consist of two pairs of crossbeams forming a square frame. Each pair of beams would extend out to pick up the propellant tanks and payload pans. Differential rotation between the legs and the hub would require sheeting the top and bottom surfaces of the central square frame to form a shear-resistant box. The depth of the beams can be constrained to 2.5 to 3.0 inches.

The hub design, as shown in Figure 22, utilizes, in general, the shape described above. It was adjusted to accommodate the location of the attenuators (which define a rectangular rather than a square frame) and the payload pans, which are not level with the top of the hub. The central frame has been sheeted top and bottom instead of being framed. For seat adjustment, it was elected to use guides attached to the top surface of the box. The alternate approach would utilize framing instead of sheeting so that the seat could roll in the existing carry-through beam channels.

#### Structural Design Loads

The LFV is subjected to a variety of loading environments which may be classified under two load headings relating to preactivation and operational use of the vehicle.

The preactivation environments encompass fabrication, handling, transportation, testing, loading aboard the LM, launch to orbit, injection into lunar orbit, deorbit, and moon landing. However, throughout this phase, the LFV, dry and unloaded, is at its minimum weight, and the resultant loads have only a local effect.

A definition of the loads and environments for the preactivation phase is given in the LFV system specification (Volume 5 of this report).

#### Post-Activation Environment

The operational loading spectrum of the LFV covers the bulk of the design conditions for the vehicle. However, the peak loading is controlled by the allowable human tolerances, which are discussed under "Human Factors" in this volume.

The results may be summarized as follows: the maximum normal (or "eyeballs down") and lateral ("eyeballs in, out, or side") accelerations (in earth g) must not exceed 8.0 and 4.0, respectively. The maximum design force of the attenuators is therefore based on the force required when the vehicle is at its lightest weight and when all attenuators are active. The stroke of the attenuators will, on the other hand, be determined at the maximum gross weight and for the most unfavorable combination of

vertical, horizontal, and rotational velocities. The resultant g forces in this case will be inversely proportional to the ratio of minimum to maximum vehicle weight. This ratio may be as low as 1/2. Because of this wide variation in deceleration, vehicle components will be subjected to their maximum loading at different gross weights. A summary of the design conditions used in the analysis of the components of the LFV is given in the following subsections.

### Legs

Two conditions have been defined, one yielding maximum bending moment for a load applied in the plane of the legs, the other yielding maximum bending moment for loads in and out of the plane of the legs and resulting in maximum torque and shear.

Condition 1. a. This condition involves maximum vertical velocity (at maximum or minimum weight) and zero horizontal and rotational rates and postulates an uneven landing surface permitting only two diagonally opposed legs to contact the ground.

Condition 1. b. This condition is the same as Condition 1. a, except that the forward velocity is maximum and normal to the plane of the impacting legs. The legs are prevented from sliding by rocks. The resulting movement is a rotational acceleration bringing the leading leg in contact with the ground. The initial leading leg ground clearance was defined as 2.0 inches.

### Hub or Carry-Through Structure

Each pair of crossbeams is defined for the maximum condition associated with the element they support, i. e. , the payload pans and tanks. The seat-and-accessories loading is applied close to the attenuators and results in relatively low bending moments in the crossbeams.

### Payload Pans

The design condition for the payload pans arises when the LFV is at minimum propellant weight and at maximum vertical velocity. The resultant deceleration is

$$n_{Z_{pp}} = \frac{700}{1000} \times 8.0 = 5.6 g$$

### Tank Supports

In this case, the payload pans are empty, and the propellant tanks are full. The resultant deceleration is

$$n_{Z_{TS}} = \frac{700}{1070} \times 8.0 = 5.23 \text{ g}$$

### Propellant Tanks

The propellant tanks are subjected to an internal pressure of 300 psig at maximum operating condition. To this pressure must be added the hydraulic head at the maximum acceleration of 5.23 g. However, this amounts to approximately 4.5 psi at the lowest point in the tank, or 1.5 percent of the working pressure. It has been neglected in the calculations.

### Environments

Two environments are associated with the design conditions described above: thermal and meteoroid. A third environment, (vacuum) has no appreciable effect on the structural materials used. It has, however, an impact on exposed moving parts which require dry lubrication to avoid cold welding.

The thermal effects on the structure of the LFV originate from direct or indirect solar radiation and/or from the rocket engine bell nozzle and plume. Thermal protection is provided to limit the upper structural temperatures to 200 F. Cold soak may drive the temperature down to -150 F. In the structural analyses, the upper temperature of 200 F has been used.

Meteoroid penetration may affect the propellant tank design. However, the thermal protection over these components is possibly sufficient to double as meteoroid protection. The definition of the meteoroid environment is contained in the system specification (Volume 5).

### Loading Distribution

The internal loading distribution for the leg and hub structure is generated below for the design conditions outlined under "Structural Design Loads".

The weights used in the derivation of the loading were kept constant to avoid the occasional change in the control weights. However, they are close enough to the final weight to ignore the effect on the results.

Maximum gross weight is 1370.0 pounds. Propellant weight is 300.0 pounds (oxidizer = 180.0, fuel = 120). Payload weight is 370.0 pounds, and burnout weight (no payload) is 700.0 pounds. Leg loading for Condition 1. a (two-point contact with the two legs in contact being diagonally opposite) assumes uneven terrain and flat landing at maximum vertical velocity.

The resultant maximum acceleration is 8.0 g vertical. The landing shock loads are over before attenuation reaches its maximum value. Reaction at each leg,  $R_c = (700 \times 8.0 \times 1.5)/2 = 4200$  pounds. The attenuated mass applies the loads at four places on the cruciform platform at the attenuators. For this condition, the innermost attenuator reacts most of the load.

The shear force diagram is given in Figure 74, and the bending moment is given in Figure 75. In addition to these loads, a torque is introduced due to the attenuator attach point offset relative to the section centroid. This torque is assumed to be wholly balanced across the center section by the opposite torque.

This condition has been simplified to ignore the relieving effect of the bending moment occurring at the knee of the leg due to fixity, as shown below.



For Condition 1. b (two-leg contact and rock impact), in addition to the vertical velocity, the vehicle also has maximum forward velocity and is restrained from sliding by the interposition of rocks. Because of design criteria, the forces horizontally must not exceed 4.0 g, and the load on the legs may be assumed to be half that of the vertical.

However, because the force is proportional to the deflection (a rotation of the leg about its axis), the full load will not be developed. Instead, rotation of the body will bring the leading or trailing leg in contact with the ground and relieve the horizontal force. A force of one-half, or 2.0 g, can be expected. The corresponding side force is 1050 pounds. This loading introduces a bending moment as well as a torque. The bending moment and shear force diagrams are given on Figures 75 and 74, respectively.

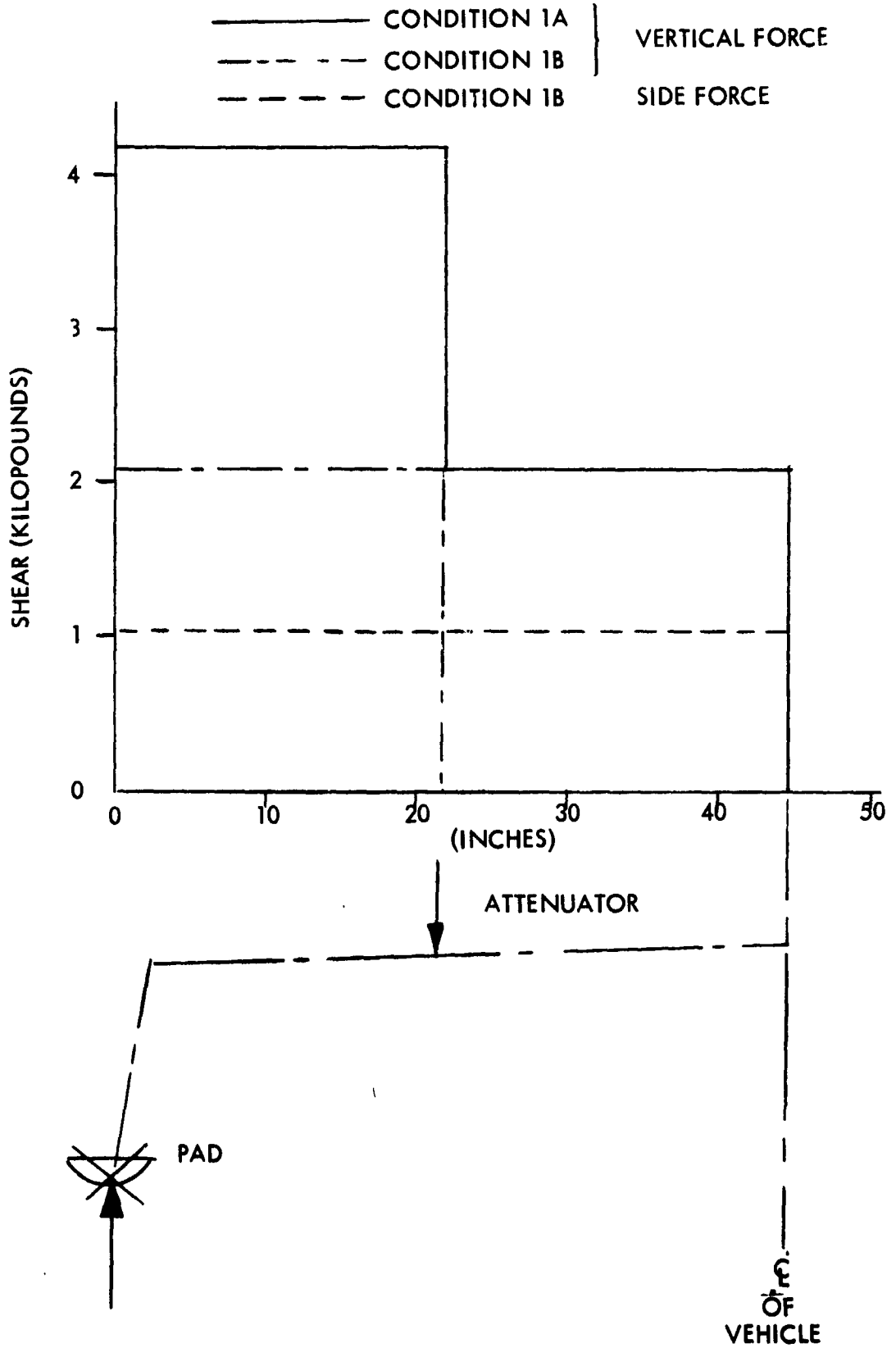


Figure 74. Leg-Shear Force Diagram



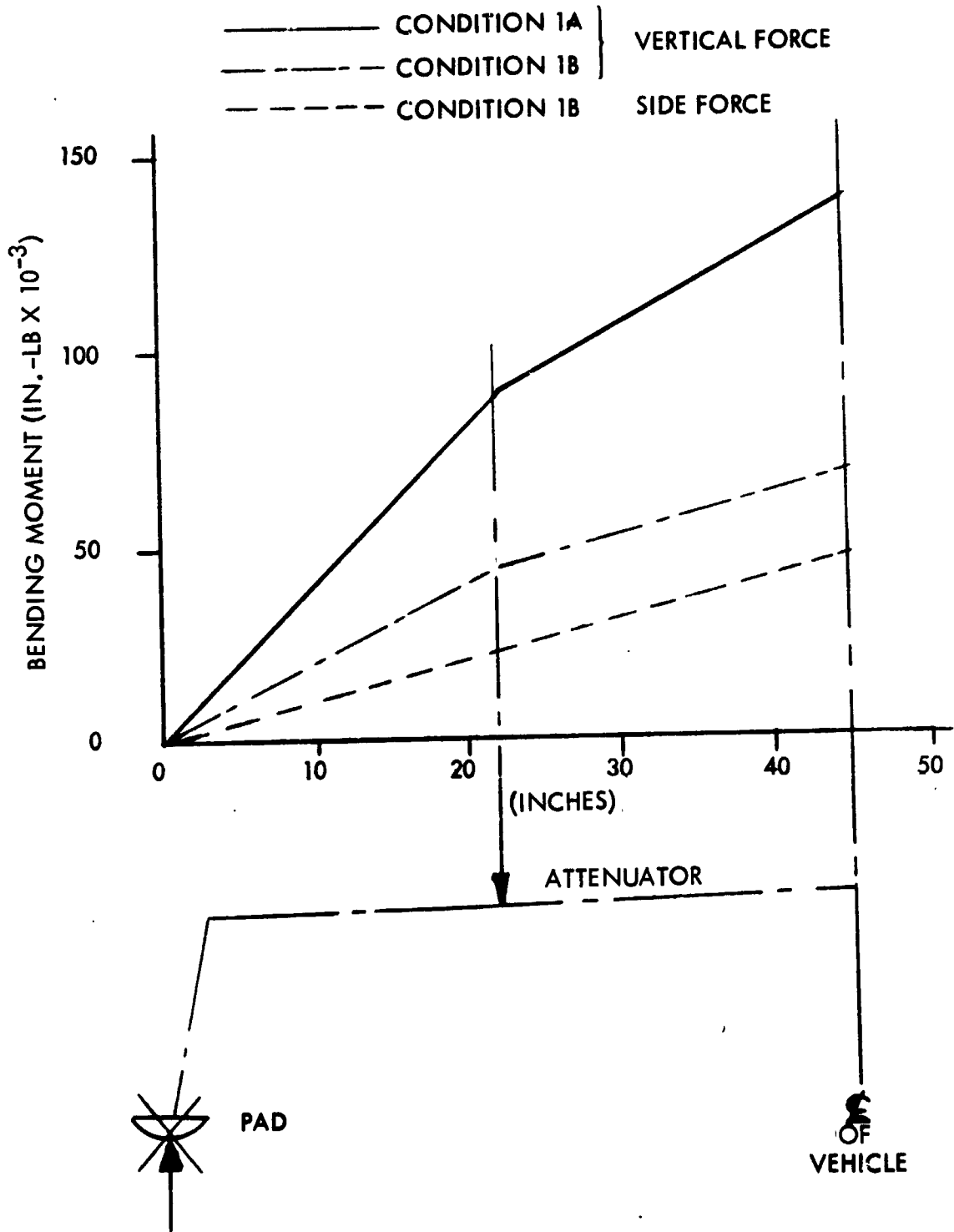


Figure 75. Leg Bending Moment Diagram

### Hub Loading

The hub loading, as described above, is the result of the payload pans and tanks, each alternately full and empty at their respective maximum accelerations. Each condition is analyzed below.

Tank Support Crossbeams. For this condition, the payload pans are empty, and the tanks are full. The reactions at each attenuator are equal.  $R_1 = R_2 = 703$  pounds. The shear and bending moment diagrams for each tank crossbeam are given in Figure 76.

Payload Pan Crossbeams. In this condition, the tanks are empty, and the payload pans are fully loaded. The reaction at each attenuator is  $R_1 = R_2 = 725$  pounds. The shear and bending moment diagrams for each load pan crossbeam are given in Figure 77.

### Tank Loading

The tanks are of the Gemini type and are 20.0 inches in diameter. The maximum operating pressure is 300.0 psig. The membrane loads are:

$$\text{At proof} \quad N_p = \frac{300 \times 1.5 \times 10}{2} = 2250 \text{ lb/in.}$$

$$\text{At yield} \quad N_y = \frac{300 \times 1.66 \times 10}{2} = 2500 \text{ lb/in.}$$

$$\text{At burst} \quad N_B = \frac{300 \times 2.0 \times 10}{2} = 3000 \text{ lb/in.}$$

The reactions at the trunnions due to the maximum vertical deceleration of  $n_z = 5.25$  for the oxidizer tank are

$$R_{ox} = \frac{200 \times 5.25 \times 2.0}{2} = 1060 \text{ pounds each}$$

Reactions for the fuel tank are

$$R_F = \frac{150 \times 5.25 \times 2.0}{2} = 787 \text{ pounds each}$$

### Stress Analysis

The following stress analysis was conducted for the major elements of the LFV (i. e., legs, hub, and tanks) based on the loading derived in the preceding subsection.

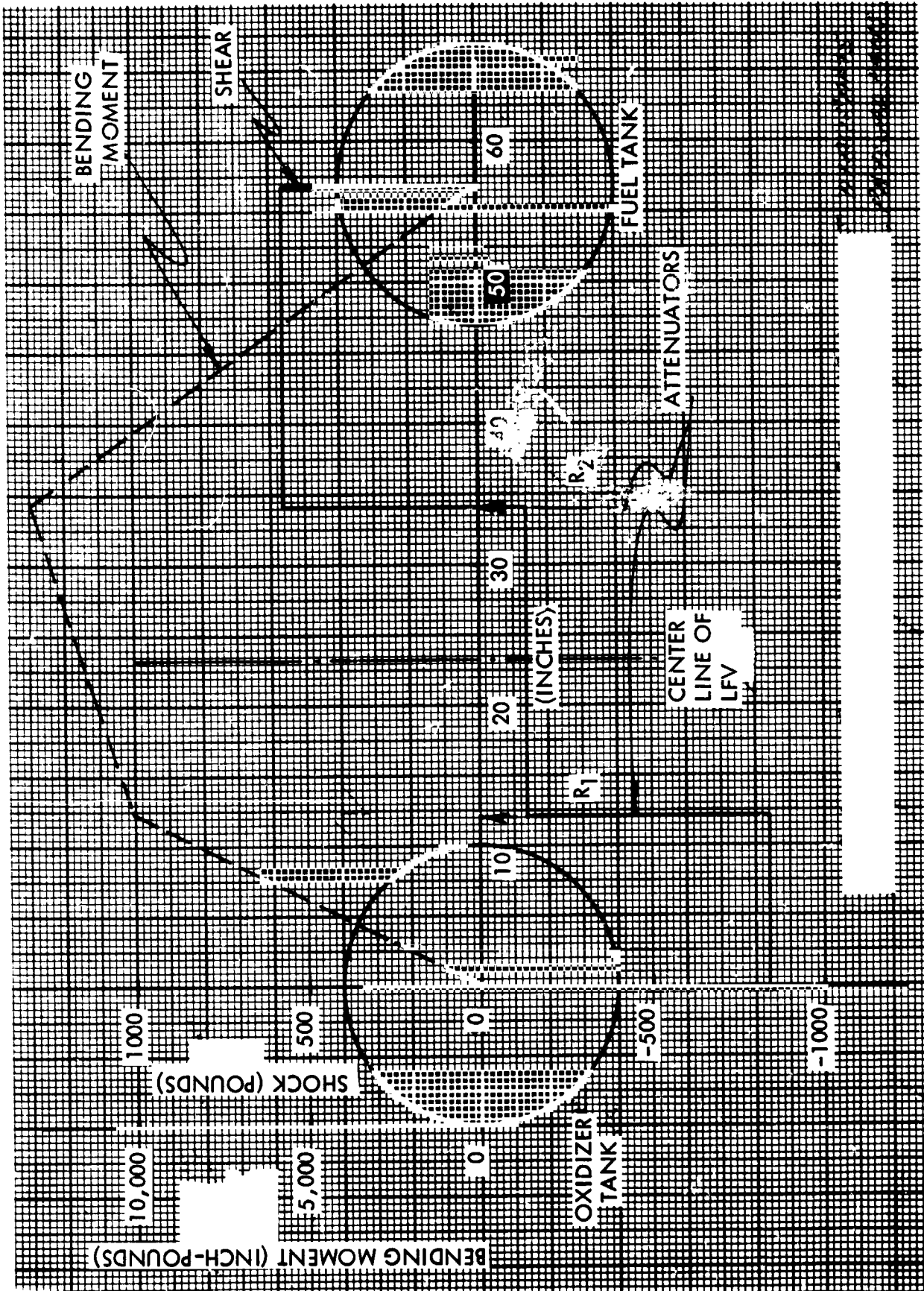


Figure 76. Shear and Bending Moment for Tank Crossbeam

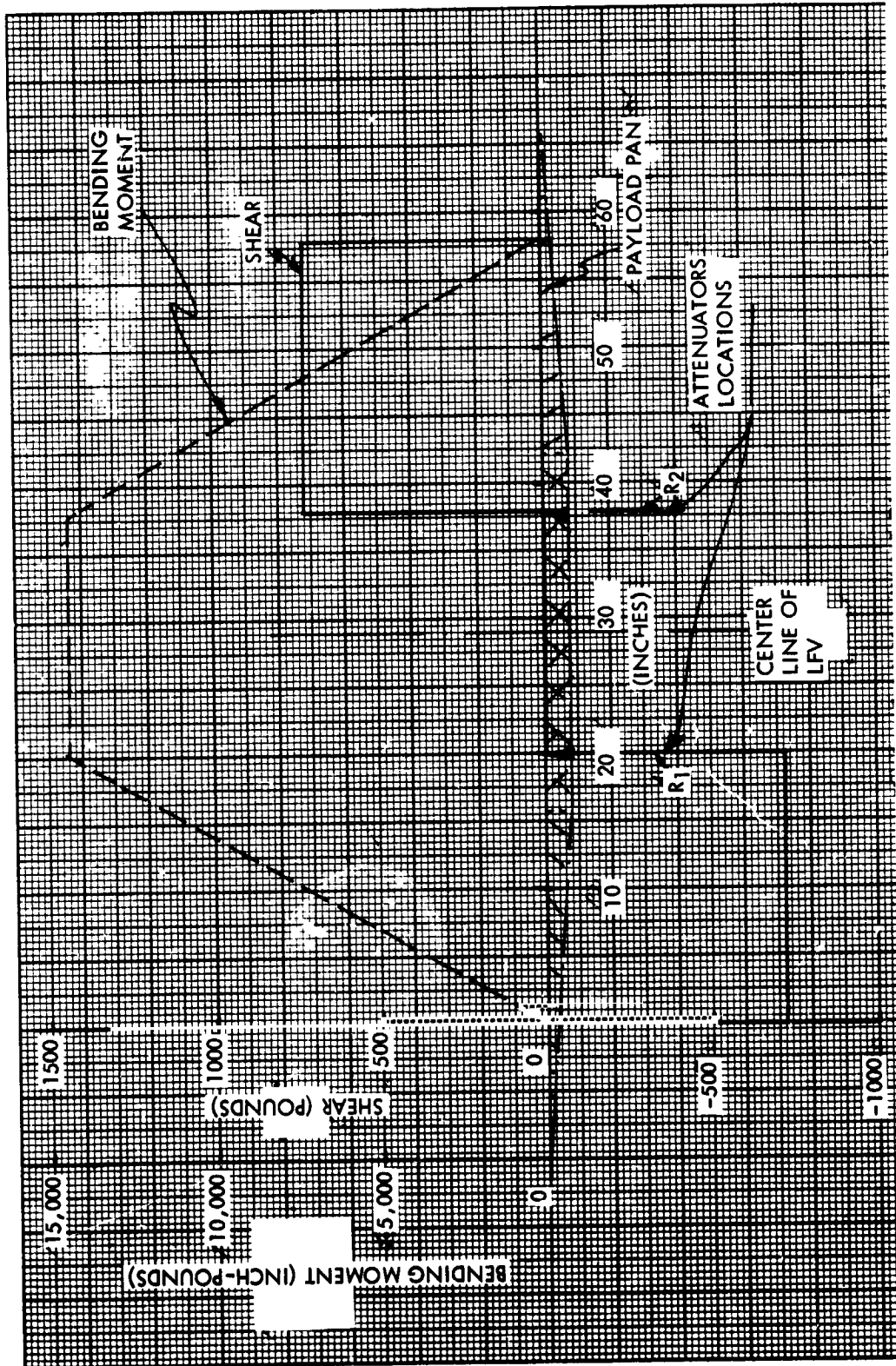


Figure 77. Shear and Bending Moment for Load Pan Crossbeam

Legs - Condition 1. a

The cross section of the leg was constrained by the tank clearance and engine geometry and is shown in Figure 78. The cap material is placed at the three corners of the triangular cross section.

Sizing of Cross Section. The distance  $h$  between centroids is approximately 3.7 inches. The load distribution, assuming that the area is concentrated at the centroids, is

$$P_v = \frac{M}{h} = \frac{138,600}{3.7} = 37,700 \text{ pounds}$$

The yield stress of the material at room temperature can be used at these large loads (for 7075-T6,  $\sigma_{cy} = 65,000$  psi, and  $\sigma_{tu} = 75,000$  psia). However, the temperature of the structure is assumed to reach 200 F, and the room temperature values must be degraded by 6 percent.

The tensile cross-sectional area,  $A_t$ , is given by

$$A_t = \frac{37,700 \times 1.06}{75,000} = 0.535 \text{ in.}^2$$

The compressive cross-sectional area,  $A_c$ , is given by

$$A_c = \frac{37,700 \times 1.06}{65,000} = 0.616 \text{ in.}^2$$

$A_c$  is divided equally between two caps, one at each corner of the base of the inverted triangle, or

$$A_{cl} = \frac{0.616}{2} = 0.308 \text{ in.}^2$$

Condition 1. b. The resultant bending moment is 47,200 in-lb, and the load/cap (at the base of the inverted triangle) is given by:

$$P_h = \frac{47,200}{2.9} = 16,300 \text{ pounds}$$

The net loading on one cap due to the combined bending is:

$$P_r = P_h + \frac{P_v}{2} = 16,300 + 18,850 = 35,150 \text{ pounds}$$

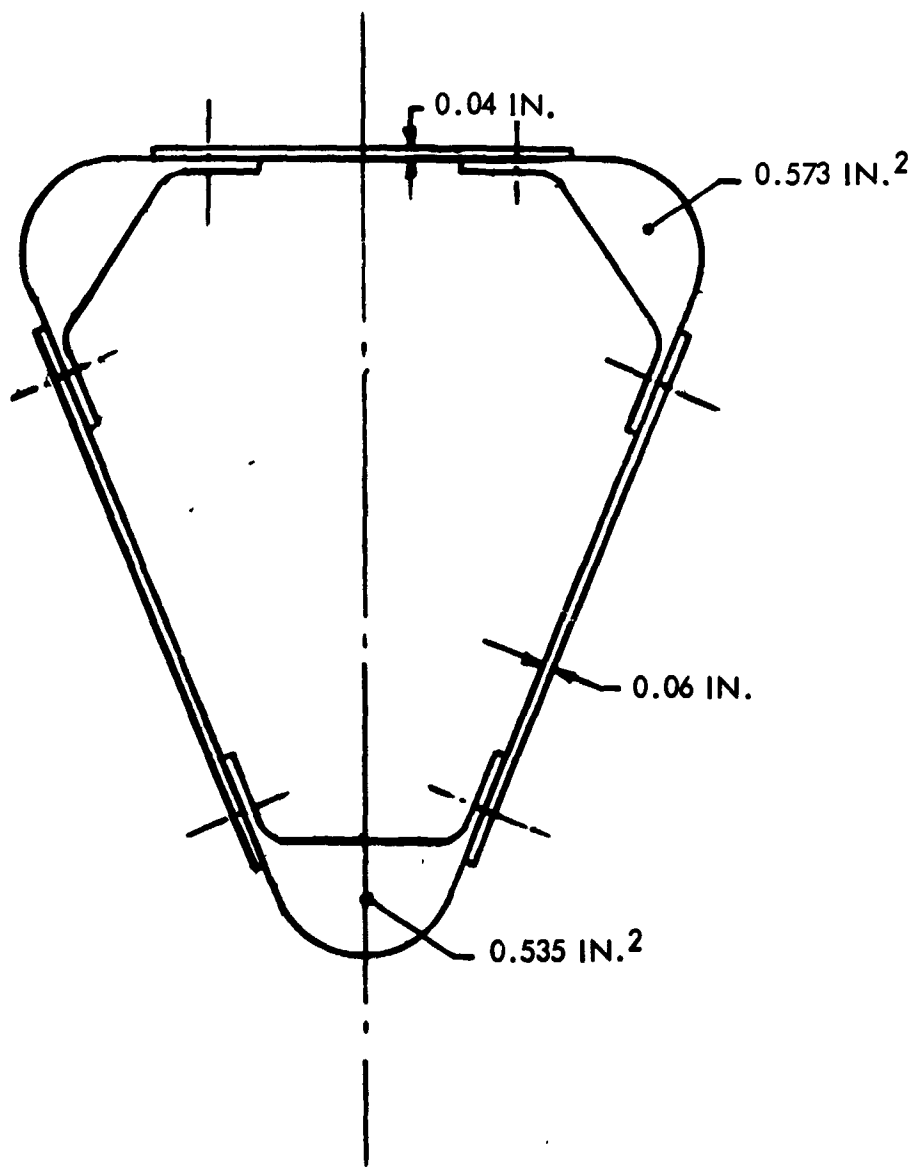


Figure 78 . Leg Cross Section

The cross-sectional area/cap is equal to

$$A_{c1} = \frac{35,150 \times 1.06}{65,000} = 0.573 \text{ in.}^2$$

The shear forces in the cross section are a combination of two shear forces and a torque. The torque is given by

$$T = 1050 \times 13.5 = 14,200 \text{ in. lb}$$

The cross-sectional area of the section is

$$A_{XS} = 2 \times 4.25 = 8.5 \text{ in.}^2$$

The shear flow due to torque is

$$q_T = \frac{14,200}{2 \times 8.5} = 835 \text{ lb/in.}$$

The shear flow due to lateral load is

$$q_{LT} = \frac{1050}{2 \times 1.7} = 310 \text{ lb/in.}$$

$$q_{LS} = \frac{1050}{2 \times 3.2} = 164 \text{ lb/in.}$$

The shear flow due to the vertical load is

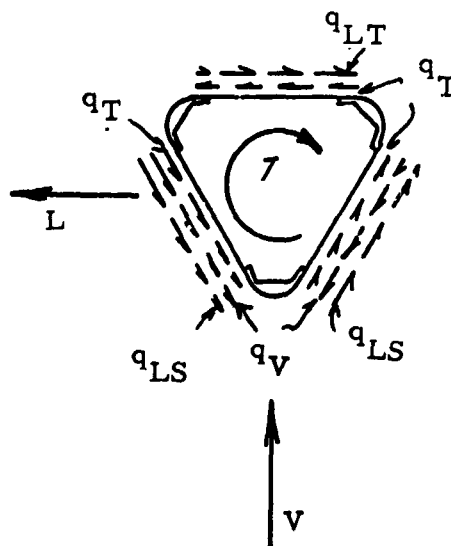
$$q_V = \frac{4200}{2 \times 2.5} = 840 \text{ lb/in.}$$

$$\therefore q_{MAX} = q_T + q_{LS} + q_V = 1839 \text{ lb/in.}$$

If material thickness is 0.06 inch, then the stress level is

$$= \frac{1839}{0.06} = 31,000 \text{ psi}$$

$$\tau_{all.} = 8 \times 10^7 \times \left(\frac{0.06}{2.5}\right)^2 = 46,000 \text{ psi}$$



The bending at the tip of the leg is due to the drag force in the plane of the leg frame. The maximum such force is equal to 2100 pounds. The resultant bending moment is

$$M_T = 2100 \times 13.5 = 28,400 \text{ in. -lb}$$

The material required to resist this moment is determined as for the root section:

$$P_{VT} = \frac{M_T}{h} = \frac{28,400}{3.7} = 7700 \text{ lbs}$$

Cap area required in compression (apex of triangle) is

$$A_{CT} = \frac{7700 \times 1.06}{65,000} = 0.125 \text{ in.}^2$$

Cap area required in tension is

$$A_{TT} = \frac{7700 \times 1.06}{2 \times 75,000} = 0.0545 \text{ in.}^2$$

#### Tank Support Crossbeams

The available depth of beams is 2.5 inches. Per support, the maximum bending moment is

$$M_{\text{max}} = 13,000 \text{ in. -lb}$$

The load per cap area is

$$P_{c \text{ max}} = \frac{M_{\text{max}}}{h_c} = \frac{13,000}{2.25} = 5800 \text{ pounds}$$

where  $h_c$  is the centroidal distance between caps.

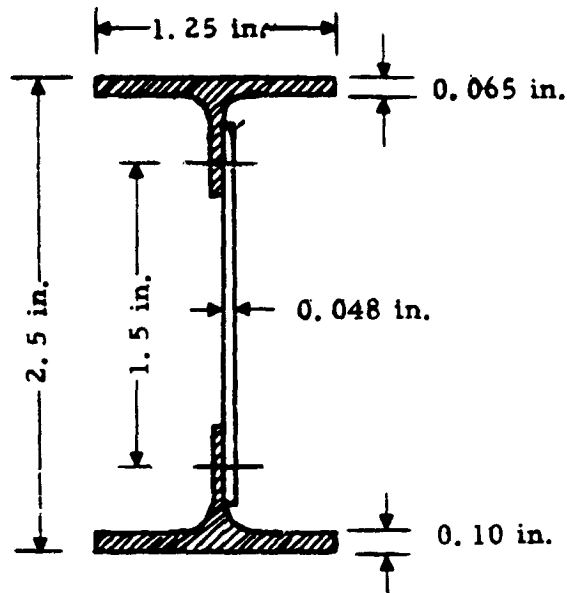
The cross-sectional material required in 7075-T6 aluminum is

$$A_{CT} = \frac{P_{c \text{ max}}}{\sigma_{\text{all.}}} = \frac{5800 \times 1.06}{75,000} = 0.0815 \text{ in.}^2$$



Compressive material is

$$A_{CC} = \frac{5800 \times 1.06}{48,000} = 0.128 \text{ in.}^2$$



Shear flow is

$$q_T = \frac{1680}{1.5} = 1120 \text{ lb/in.}$$

Shear stress is

$$\tau = \frac{1120}{0.048} = 23,400 \text{ psi}$$

Allowable shear stress is

$$\begin{aligned} \tau_{\text{all.}} &= K_S E \left(\frac{t}{B}\right)^2 \\ &= 5.3 \times 10^7 \times \left(\frac{0.048}{1.5}\right)^2 = 54,500 \text{ psi} \end{aligned}$$

This is not achievable because plasticity would modify this value downward. However, it indicates that a high allowable is achievable in excess of the 23,400 psi stress developed in the section.

#### Payload Pan Crossbeams

The loading in the crossbeams supporting the pans is very close to that for the tank, i. e., 14,450 in.-lb versus 13,000 in.-lb, or an 11 percent increase. The cross section as shown for the tank supports, including the sheeting effective width (not factored previously), is adequate for this application.

## PAYLOAD INTEGRATION

A mission requirement for the lunar flying vehicle is that it be capable of carrying up to 370 pounds of scientific payload. As noted in Figure 79, the logic diagram for the payload studies, it was also an initial mission requirement that a rescued astronaut be one of the payloads. This NASA requirement was later removed. The result of the payload characteristics definition study is shown in Table 20, which contains lists and describes representative scientific payloads supplied by NASA. In addition to the characteristics shown, it was established that each payload should be self-contained with respect to power, thermal protection, and structural integrity. The primary problem, then, for payload integration amounted to providing sufficient flexibility to accommodate the range of bulk densities, weights, and sizes of the various payloads and yet maintain vehicle balance during flight.

### Conceptual Studies

Comprehensive payload integration studies were initiated after primary vehicle characteristics, such as engine, tank, and landing gear placement, were established, since these depended on more fundamental requirements related to vehicle operability and safety. This approach was successful in that the final payload integration design did not result in compromising the fundamental requirements and characteristics of the vehicle. The primary interaction with vehicle design was with respect to pilot visibility and, as noted in the following discussion, this was ultimately solved without basic changes in the vehicle's general arrangement. Since the payload integration factors are essentially all geometric - involving weight and balance, pilot access, pilot visibility, and structural arrangement - most of the results of the study are illustrated in the drawing of Figure 80. As shown in the figure, a range of configurations covering a broad range of payload bulk characteristics were investigated. The study indicated that three concepts were basically acceptable. One involved load pans located above the tanks. Little or no seat movement for trim would be required if the payloads can be balanced. It is the simplest and the lightest structural arrangement for low-bulk payloads. It would, however, generally give a higher loaded c.g. for the vehicle.

A second concept utilized a fixed aft load pan (Configuration E, Figure 80). In order to obtain vehicle trim, the seat is movable forward, requiring 6 inches of movement for a 100-pound typical aft payload. This design was considered to be the lightest for moderate bulk at the 100-pound payload range. A third concept (Configuration A) moved the aft load pan and seat simultaneously. It was considered to be the most complex and heaviest, but had the greatest bulk capability. No concepts involving a forward load

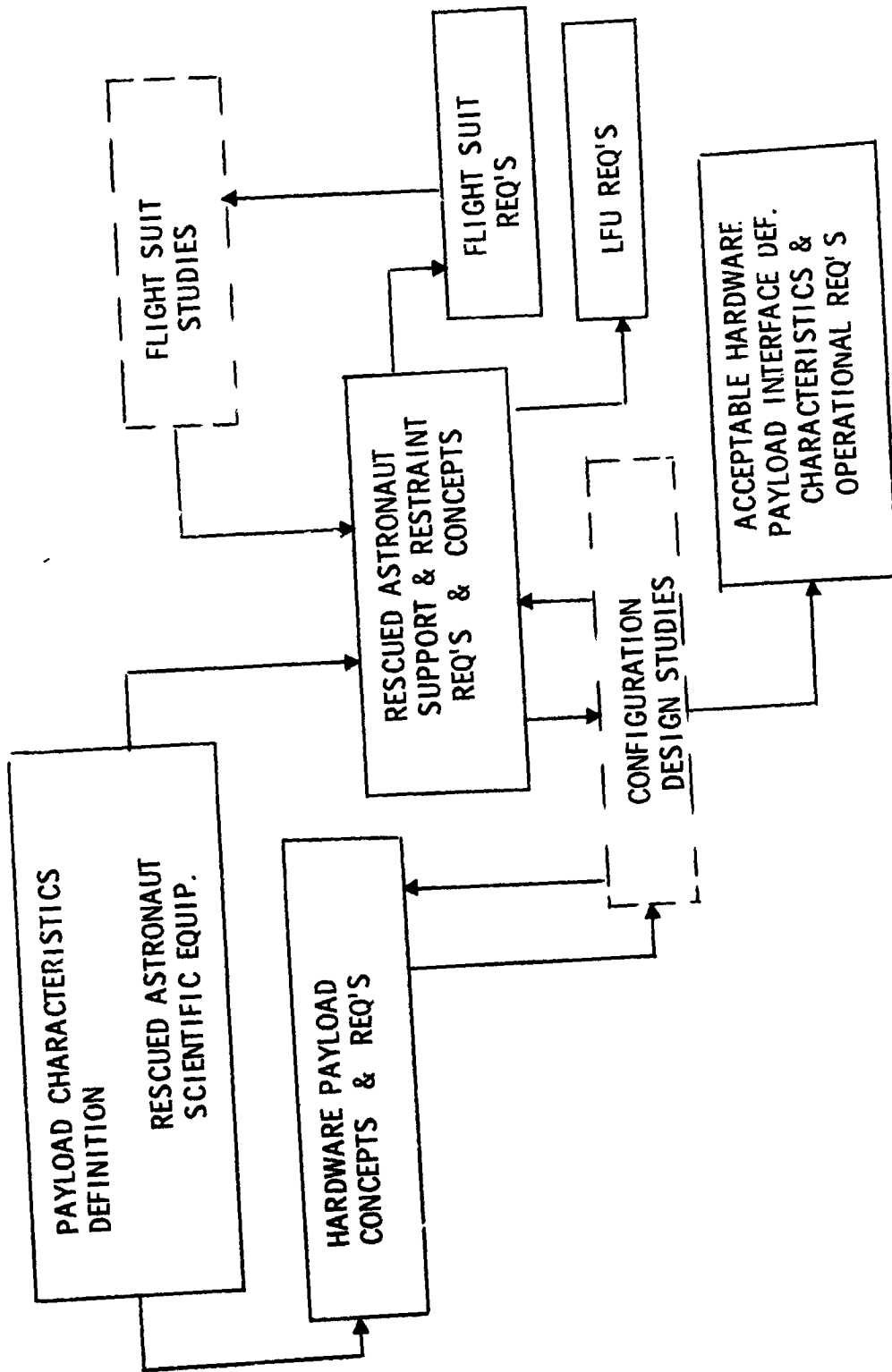
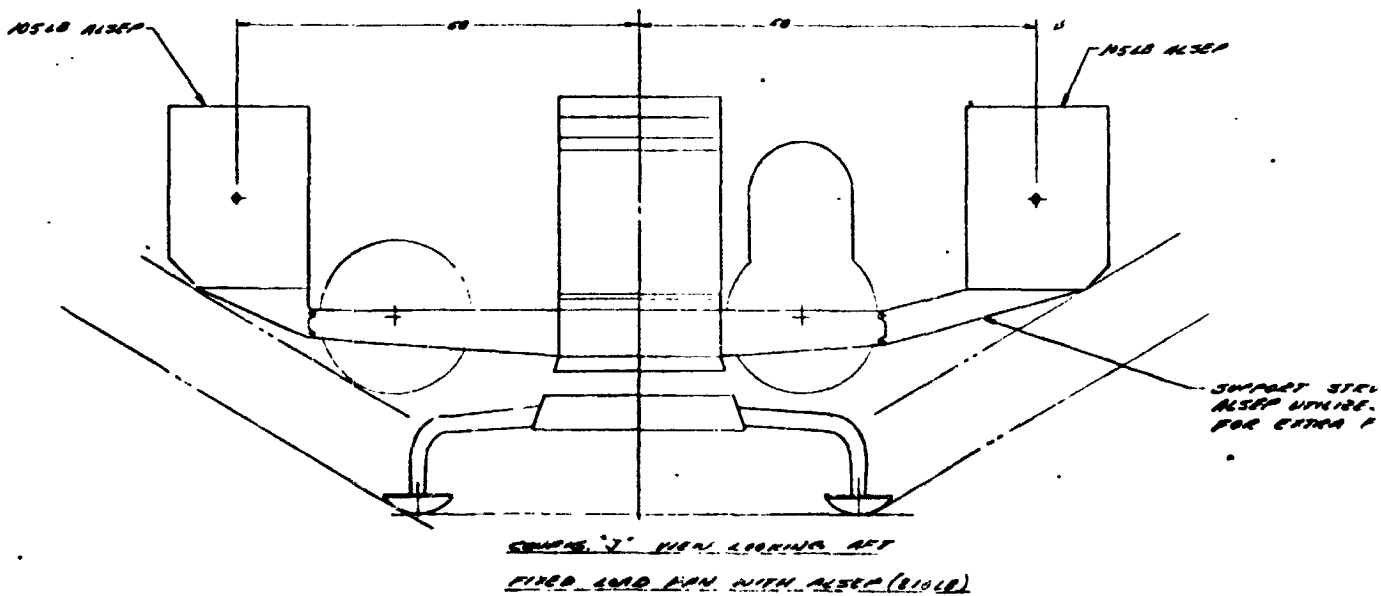


Figure 79. Payload Study Logic

NOTE: NO DISP. OF CENTER OF GRAVITY REQ'D  
 NO STABILITY PROBLEM ON FIXED PAN  
 INCREASES MASS MOMENT OF INERTIA IN ROLL MODE



FOLDOUT FRAME

FOLDOUT FRAME

NOTE: NO VISION LOSS FWD,  
SOME LOSS TO STARBOARD

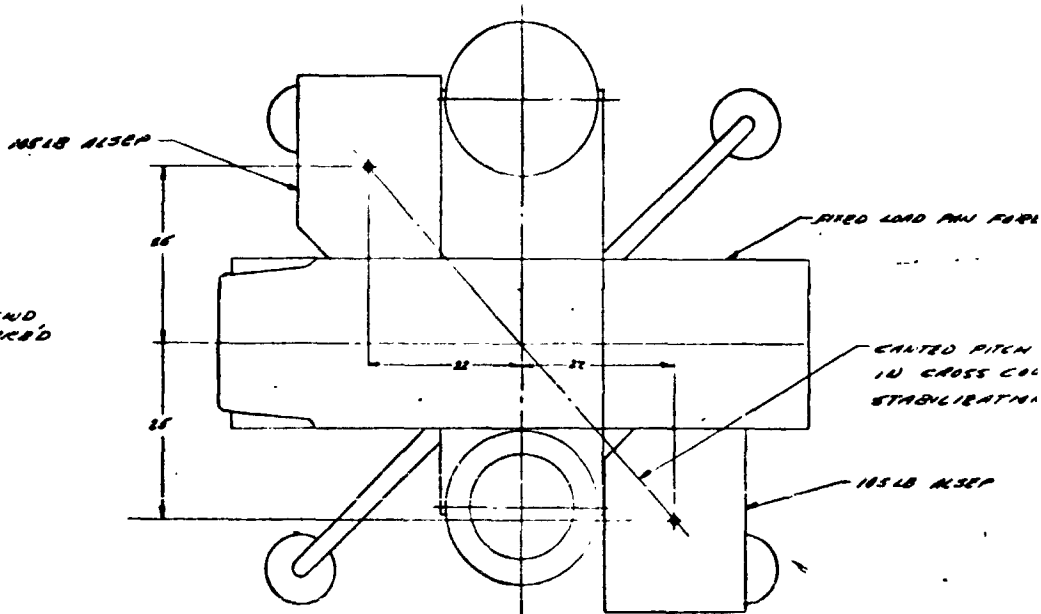
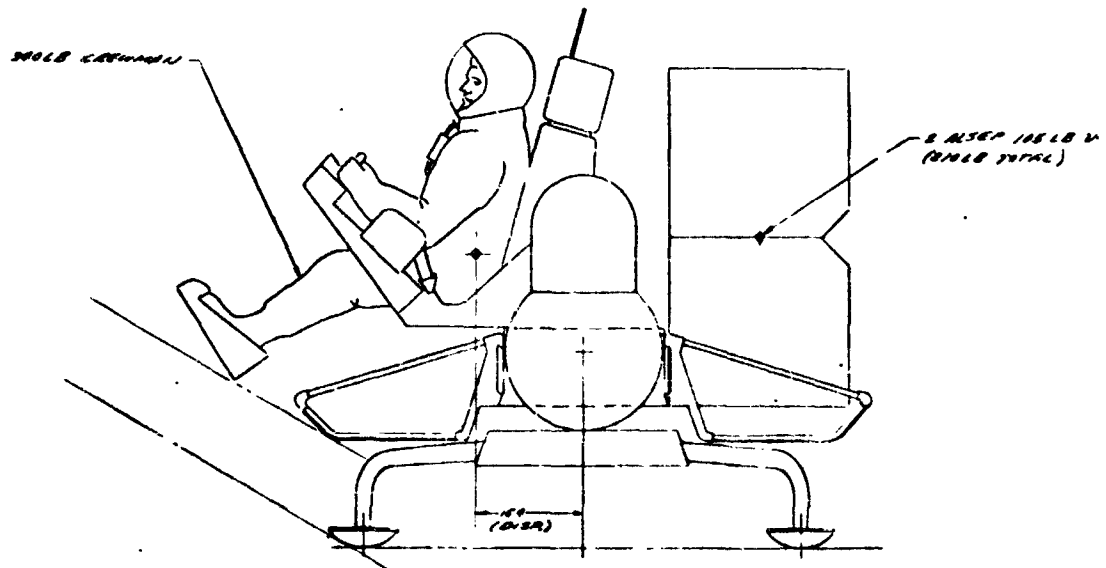
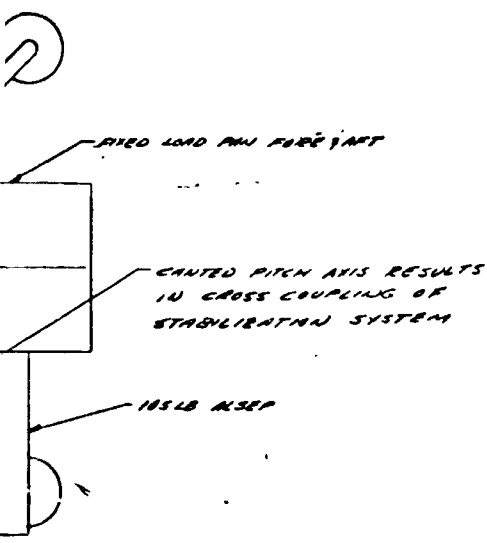


FIGURE I  
2 ALSEP UNITS CARRIED DIAGONALLY (210 LB)  
NOTE: NO BACK UP CUSHIONING REQ'D

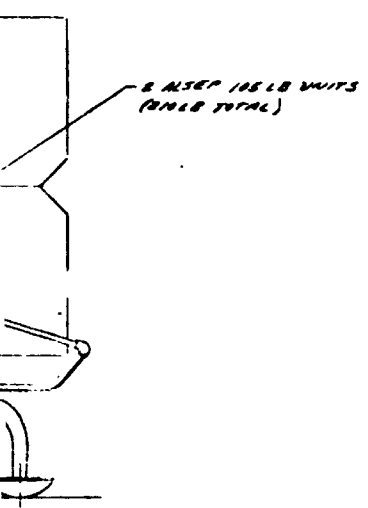


SMART STRUCTURE FOR  
ALSEP UNITS ATTACH POINTS  
FOR EXTRA FUEL TANK CONFIG

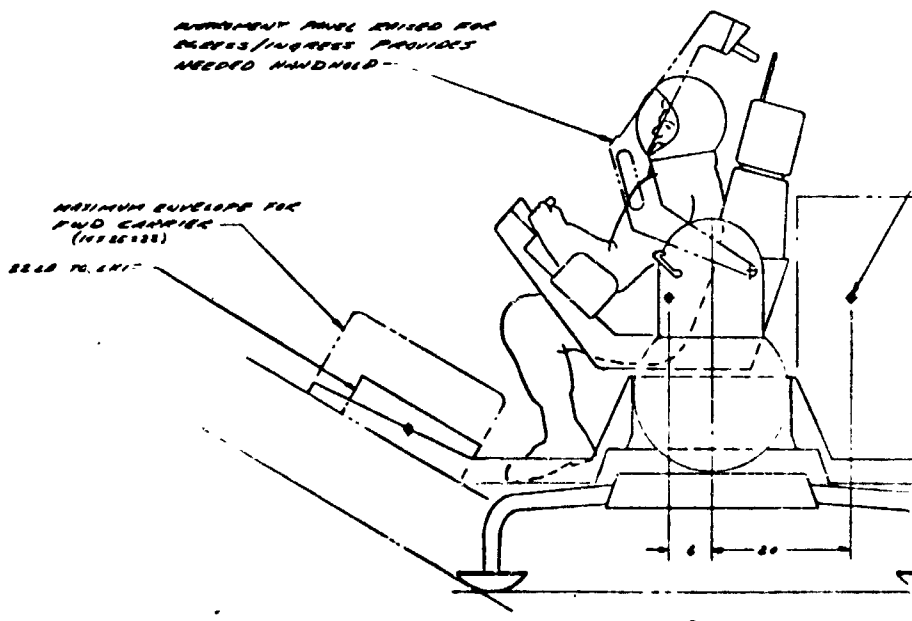
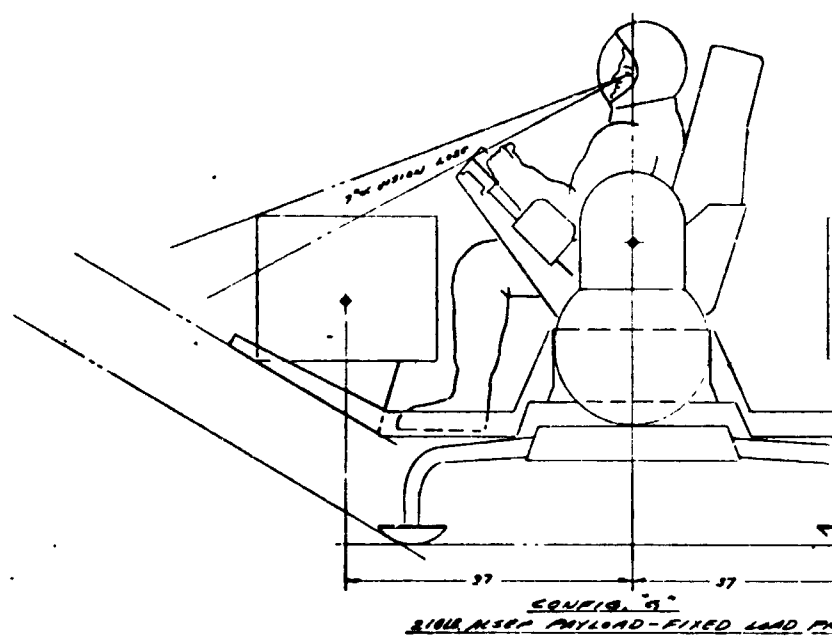
FIGURE N NOTE: FOR OTHER VARIATIONS OF THIS CO  
SEE DWG 0030-18  
FIXED LOAD PAN WITH ALSEP (210 LB)



INLET (G1012)  
292

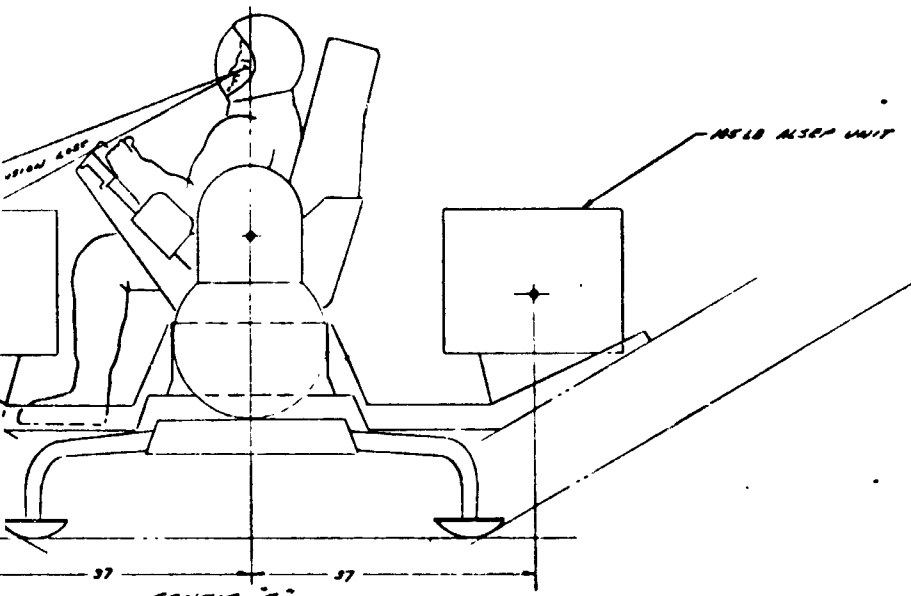


ON SE DIMENSIONS OF THIS CONFIG,  
DWG 8830-18

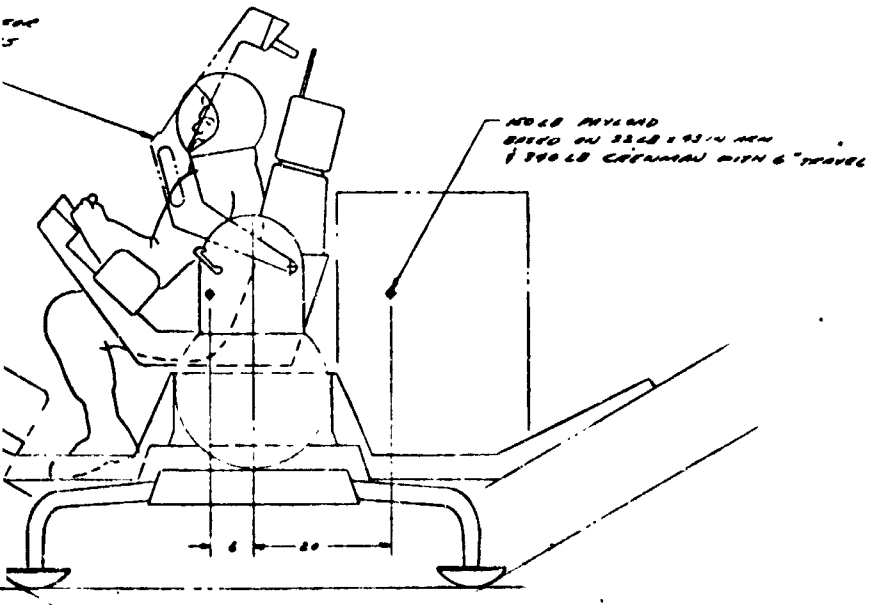


FOLDOUT FRAME

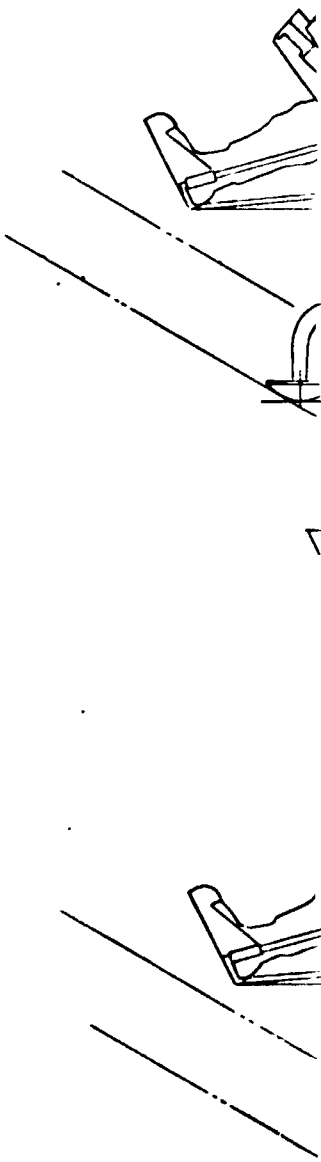
FOLDOUT FRAME

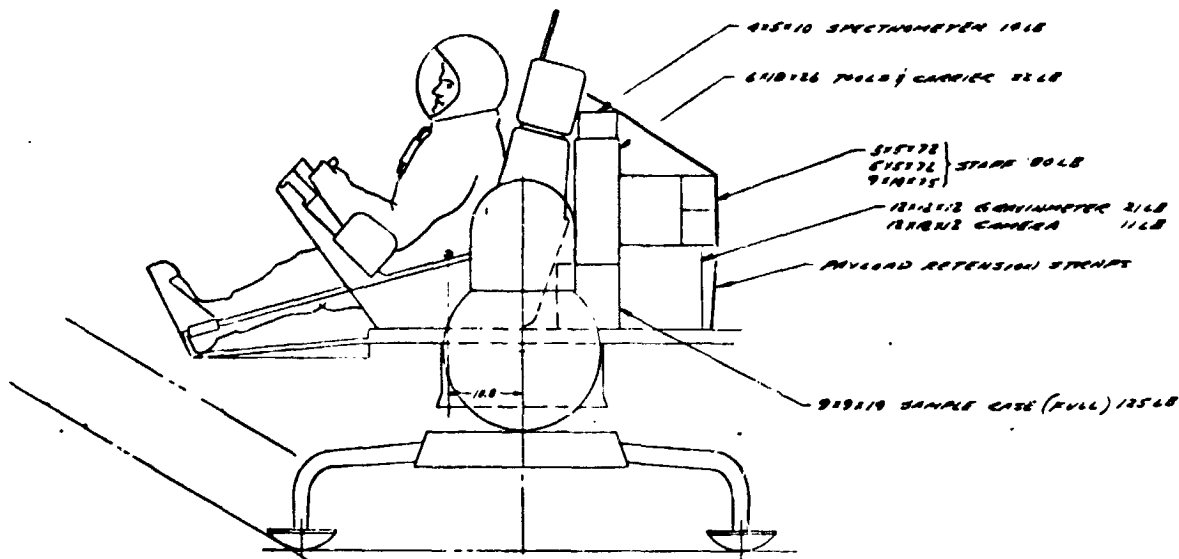


CONFIG. 9  
 210 LB ALSEP PAYLOAD - FIXED LOAD PHU



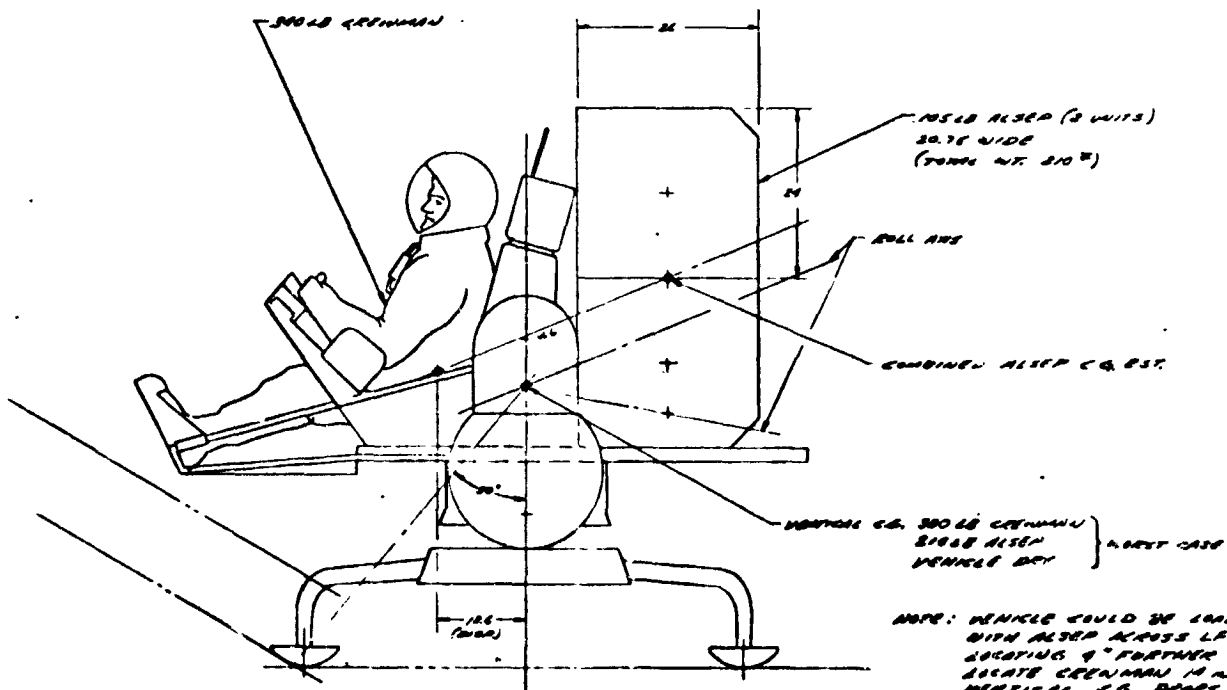
CONFIG. 7  
 FIXED LOAD PHU - 4 IN MAX CRYSTALLINE TRAVEL  
 178 LB PAYLOAD





**CONFIG. C**  
 275 LB REP REPRESENTATIVE PAYLOAD

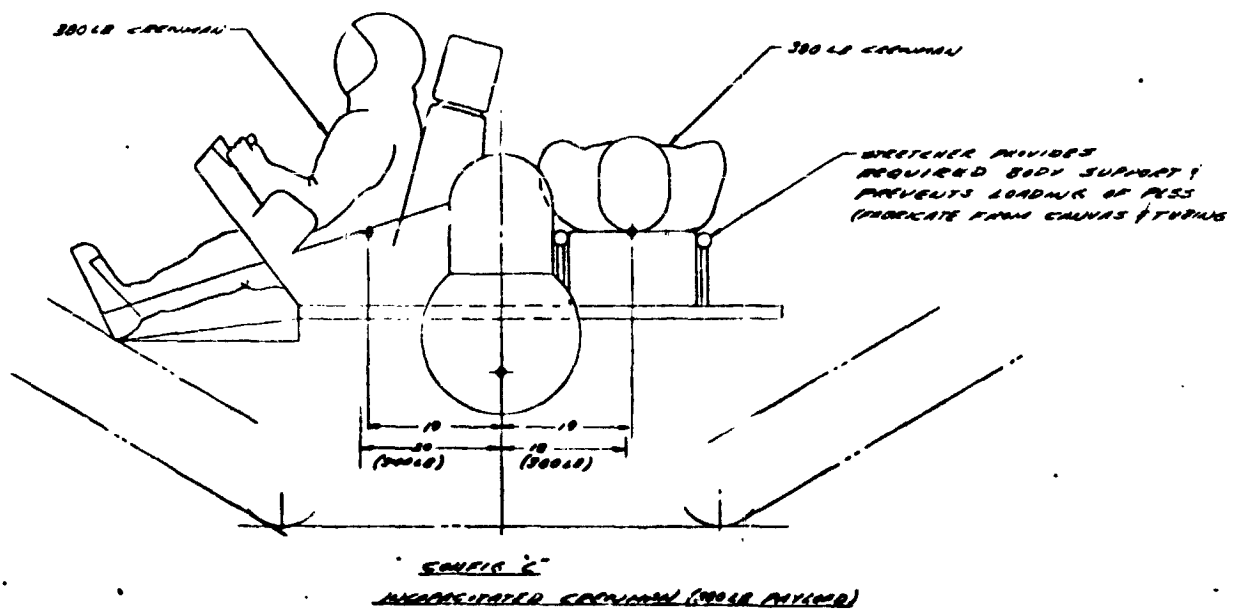
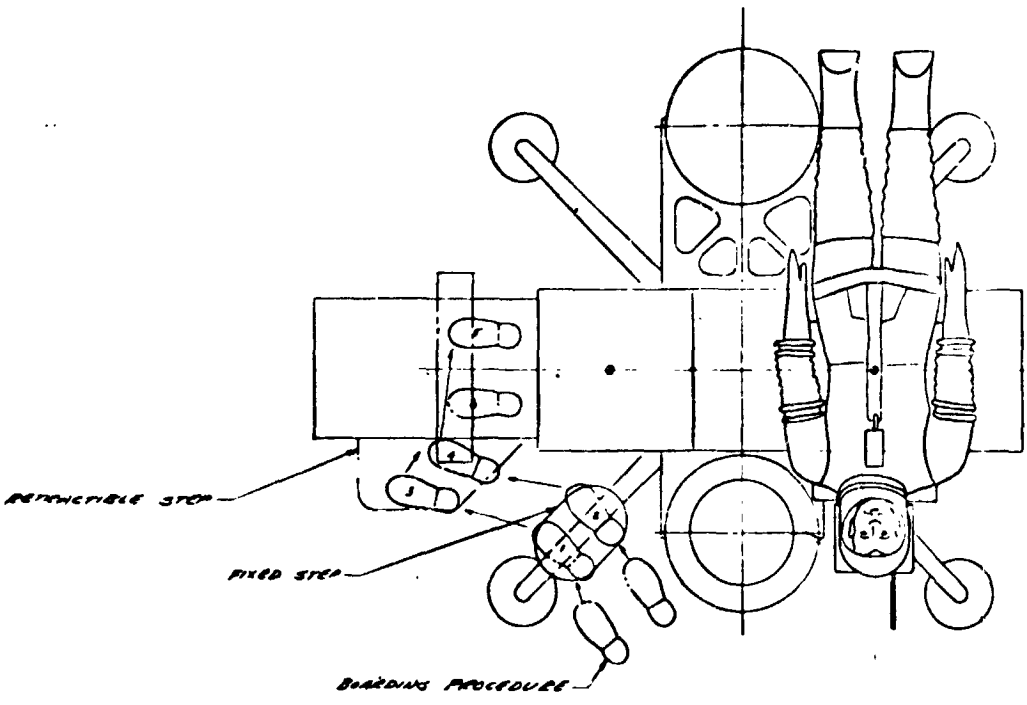
RETRACT



**CONFIG. D**  
 305 LB ALSEP

NOTE: VEHICLE COULD BE LOADED WITH ALSEP ACROSS LEV BY LOCATING 9\"/>





F

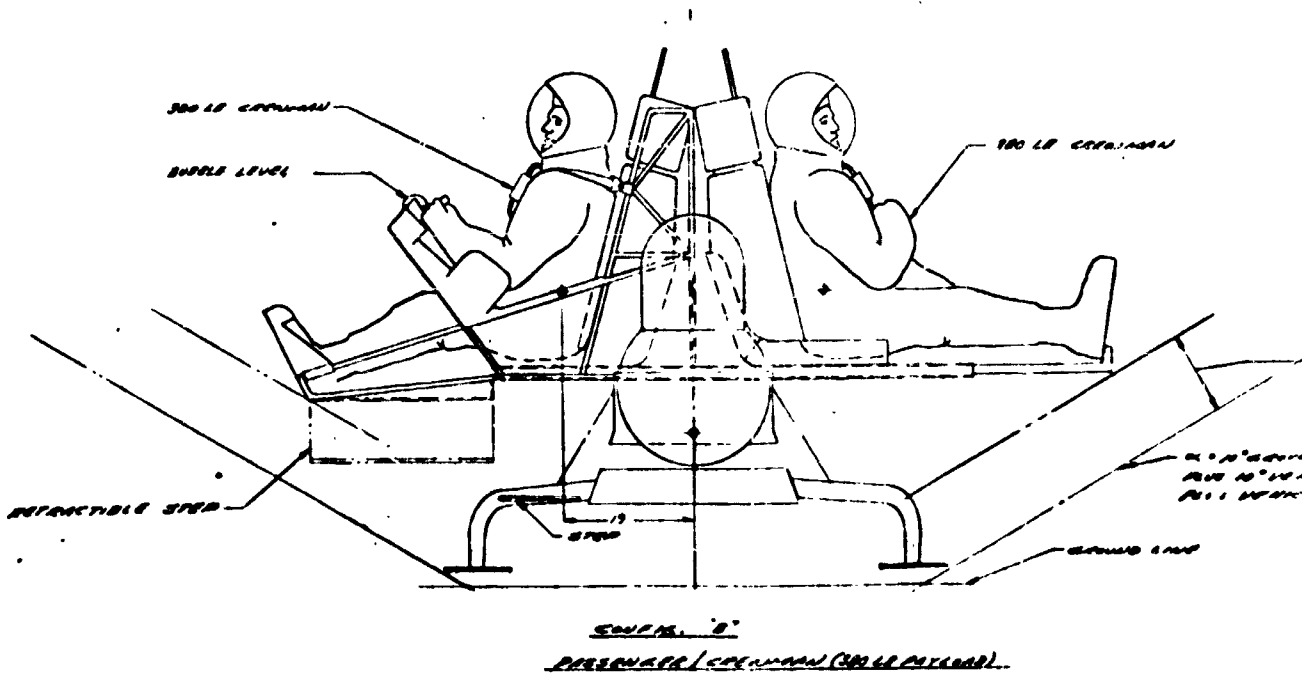
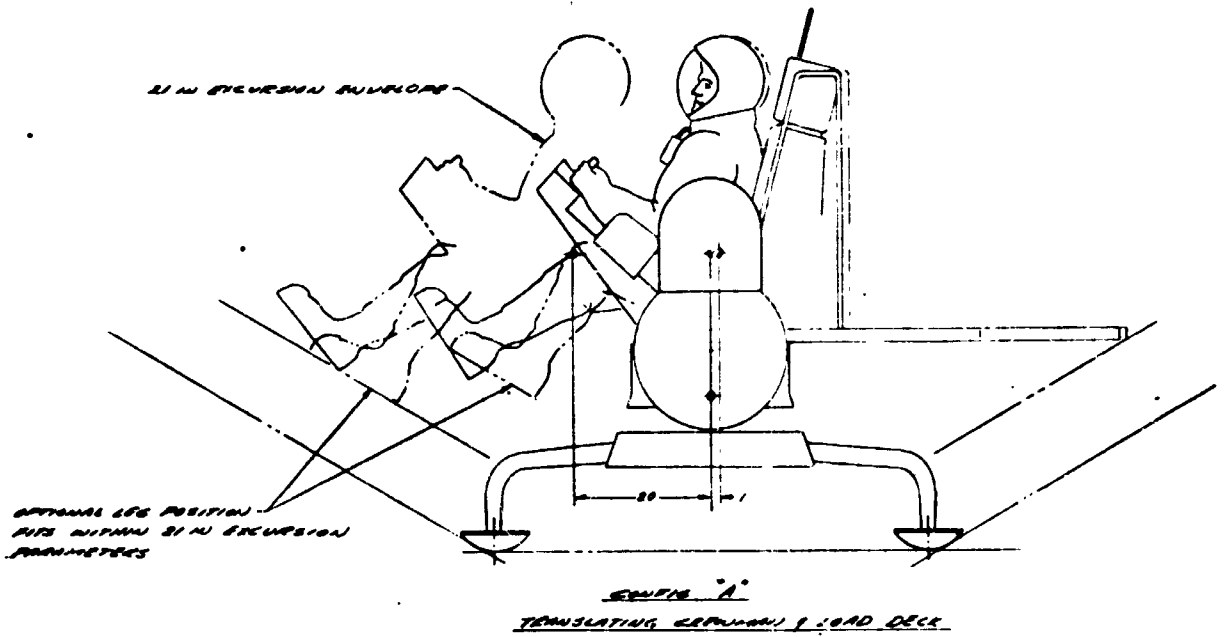
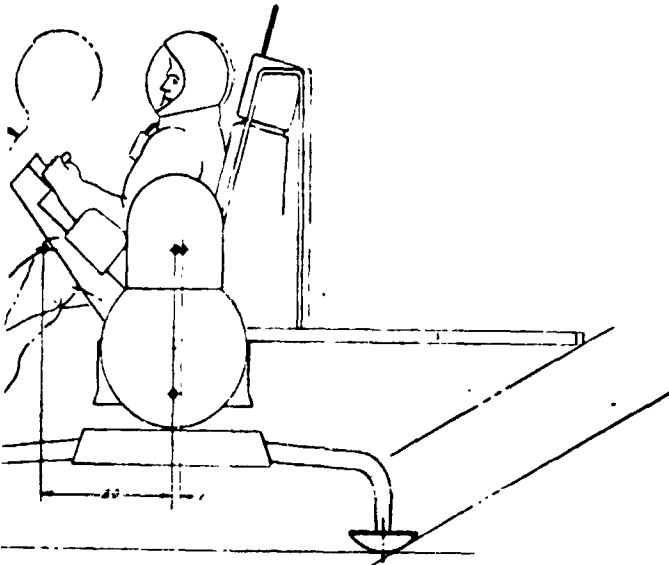


Figure 80. Pay

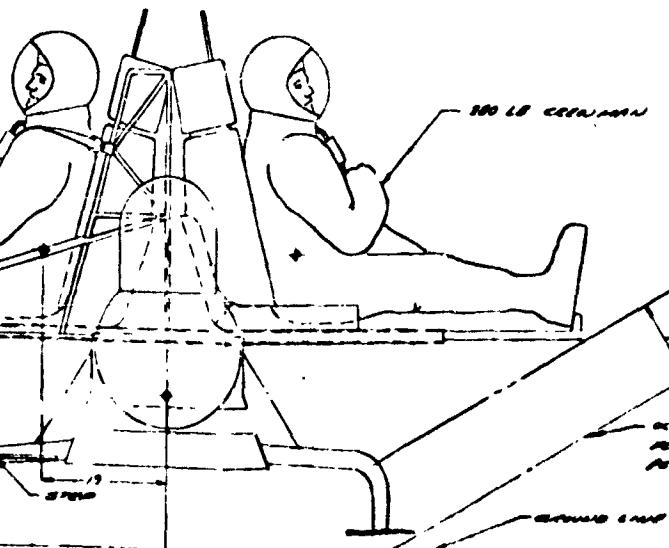
FOLDOUT FRAME

FOLDOUT FRAME



NOTE: CONFIG. A IS SUITABLE FOR PASSENGER / CREWMAN / DISABLED CREWMAN. OTHER PAYLOAD CONFIGURATIONS RESULT IN SPILLER CREWMAN DISPLACEMENT.

CONFIG. A  
INSULATING CREWMAN / LOAD DECK



100 LB CREWMAN  
10° CLEARANCE FROM DECK  
10° ATTITUDE  
10° ATTITUDE

CONFIG. B  
PASSENGER / CREWMAN (100 LB CREWMAN)

|  |          |           |         |
|--|----------|-----------|---------|
| REV  | DATE     | BY        | APP'D   |
| 1/0  | 11/11/69 | W. J. ... | ...     |
| SUB AREA: ...<br>PAYLOAD INVESTIGATION -<br>A/C. PAYLOAD |          |           | 2230-11 |

Figure 80. Payload Variations Studied (Drawing 2230-11)

Table 20. Representative LFV Payloads

| No. | Description                  | Weight (lb) | Volume (ft <sup>3</sup> ) |
|-----|------------------------------|-------------|---------------------------|
| 1   | Staff                        | 78.3        | 1.0                       |
| 2   | Closeup photography camera   | 3           | 0.04                      |
| 3   | Geology tools (drill)        | 25          | 0.4                       |
| 4   | Drill, 10-meter              | 100         | 2.0                       |
| 5   | Geophysical probe            | 11.2        | 1.2                       |
| 6   | Heatflow thermal probe       | 25.6        | 1.4                       |
| 7   | Penetrometer                 | 4           | 0.01                      |
| 8   | Fascimile camera             | 6           | 0.5                       |
| 9   | Mass spectrometer (portable) | 15          | 1.5                       |
| 10  | X-ray diffractometer         | 20          | 1.0                       |
| 11  | Water detector               | 6           | 0.4                       |
| 12  | Aseptec sampling device      | 4           | 0.2                       |
| 13  | Organic carbon analyzer      | 12          | 0.7                       |
| 14  | Active seismic (explosives)  | 8           | 0.2                       |
| 15  | RGM station                  | 100         |                           |
| 16  | Passive seismic              | 12          | 0.7                       |
| 17  | Active seismic (geophones)   | 14          | 0.8                       |
| 18  | Vector magnetometer          | 11.5        | 2.0                       |
| 19  | Laser reflector              | 25          | 1.0                       |
| 20  | ALSEP                        | 223         | 9.0                       |

pan which interfered with ingress and/or visibility were considered acceptable. The study included consideration of 300 pounds of fuel as extra payload, as well as scientific equipment and a rescued astronaut. As noted in Figure 80, one of the controlling conditions was ground clearance during landing at rotational angles resulting from horizontal kinetic energy and ground slope.

The parameters established for the investigation of Figure 81 consisted of miscellaneous loading the configuration depicted by Part H of Figure 79. All fore and aft vehicle trimming is accomplished by distributing the load as much as possible and limiting the crewman displacement from -1 to +6 inches.

Payload B utilizes the NASA-requested payload, consisting of a 22-pound tool kit, a 14-pound spectrometer, an 80-pound staff, a 21-pound gravimeter, an 11-pound camera, and a 5-pound empty sample case. A 340-pound astronaut is translated 3.5 inches in this configuration. Payload B with sample case full (125 pounds) can be balanced by rearranging the payload, thus leaving the crewman on the c. g. of the LFV.

Payload C involved only an empty sample case, a tool kit, and a 100-pound low-density payload carried on the aft load pan. A maximum width is established for this load, but the other two dimensions can be somewhat more flexible.

Payload D is a case involving a 22-pound tool kit and a full sample case weighing 125 pounds. A 5-inch seat translation is required.

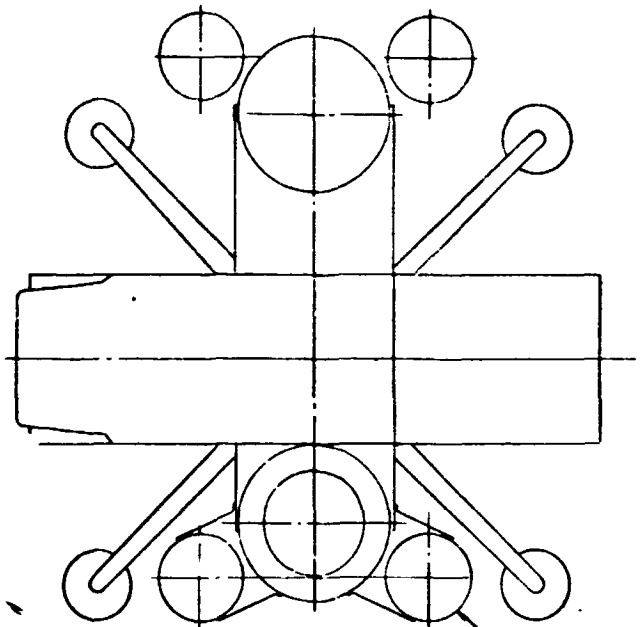
Payload E depicts an additional 300 pounds of fuel carried in four 12.2- by 17.4-inch Apollo-type reaction control system tanks. The tanks are arranged so that no translation of the crewman is required.

For the selected configuration (Figure 19), the payload concept was to accommodate miscellaneous payloads and individual (one-package) payloads up to 100 pounds. The individual payload case dictated the 6 inches of seat translation.

### Preliminary Design

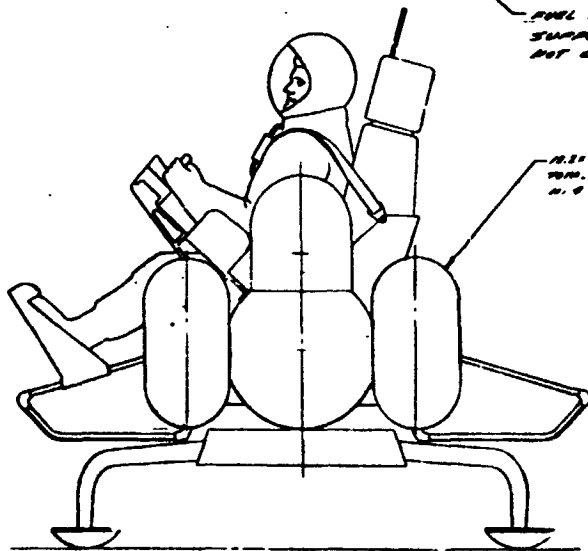
At the completion of the parametric phase, none of the concepts (described in the preceding) were entirely satisfactory. However, during the preliminary design phase, the visibility and ingress/egress disadvantages of the design of Figure 80 were eliminated while the advantages were retained. This was accomplished simply by rotating the pilot's seat alignment 45 degrees from the load pan axis, as shown in Figure 19. Seat adjustment is plus 6 inches or minus 1 inch along the load pan axis.

The vehicle must be balanced within about one-half inch prior to takeoff, as engine gimbal angle does not allow for a large offset c. g. correction. It is expected that on a given LFV flight the astronaut would know the required seat location from predetermined program data.

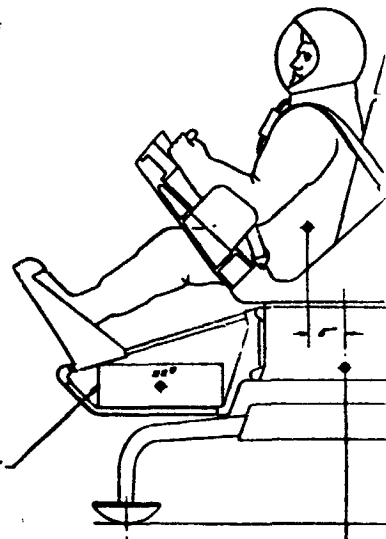


PLAN VIEW

FUEL TANKS PROVIDE  
SUPPORT STRUCTURE  
NOT CARRIED ON VEHICLE



15.5" 17.5" FUEL TANK  
FORM. OF 300" FUEL  
H. 8 TANKS



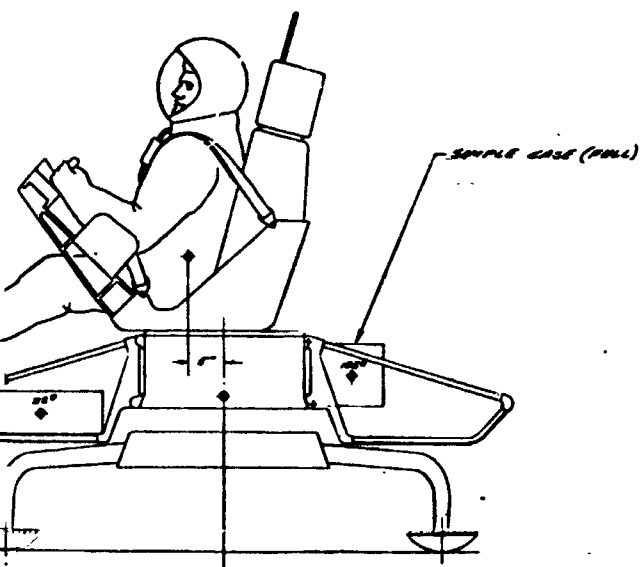
TOOL KIT

LOADING 'B'

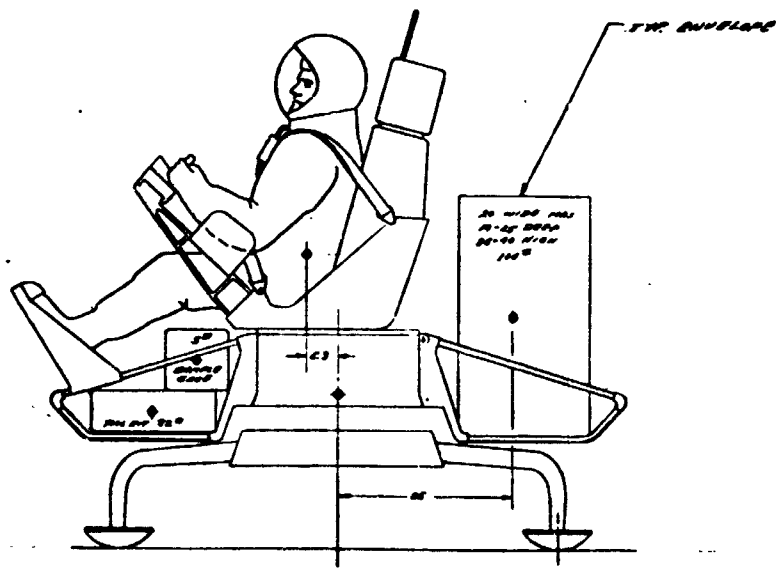
300 LBS FUEL (EXTRA)

LOADING 'D'

(TOOL KIT & FUEL)



FOLDOUT 'D'  
(TOOL KIT & FULL SAMPLE CASE) 197LB



FOLDOUT 'E'  
190 LB. 2000 BOUNDARY LOAD (TOTAL PA 197LB)  
SMALL BENCH BENCH: 2000 LB FULL-THROAT IN CASE BENCHING S.S. (2000LB)

FOLDOUT FRAME

FOLDOUT 1

FOR ENVELOPE

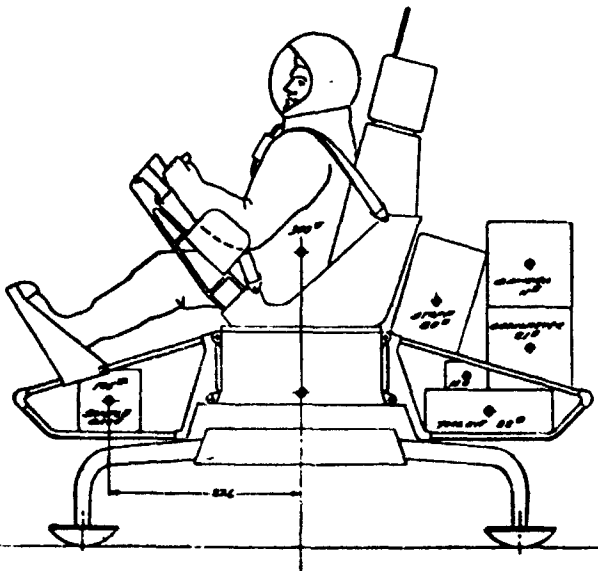


FIGURE 8

(SAMPLE CASE FILE)  
(REF REPRESENTATIVE FIGURE) 27342

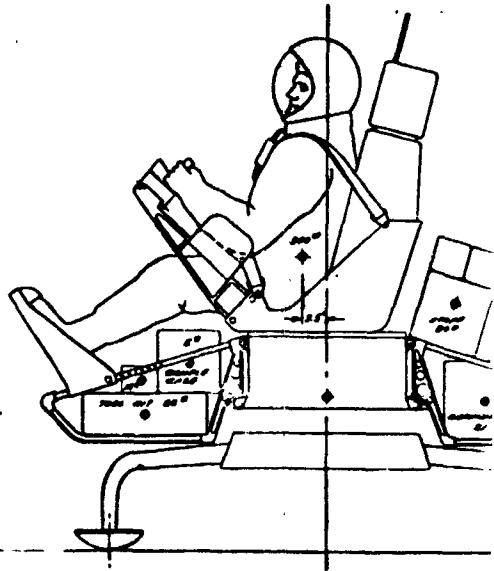


FIGURE 8 (AND FIG. 7)

(SAMPLE CASE FILE) 171

FOLDOUT FRAME



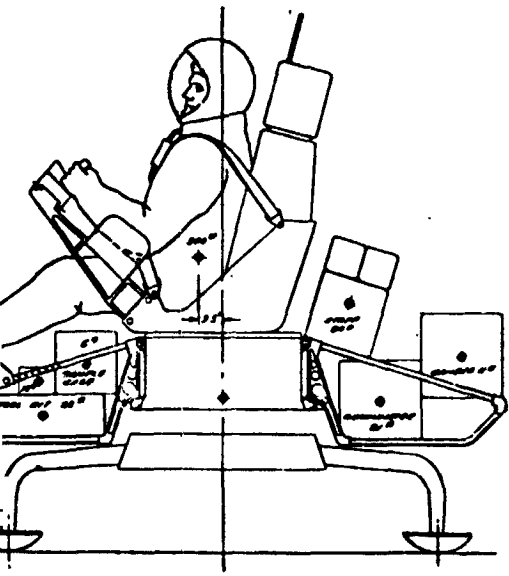
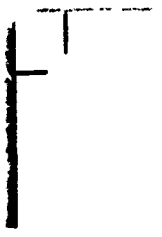
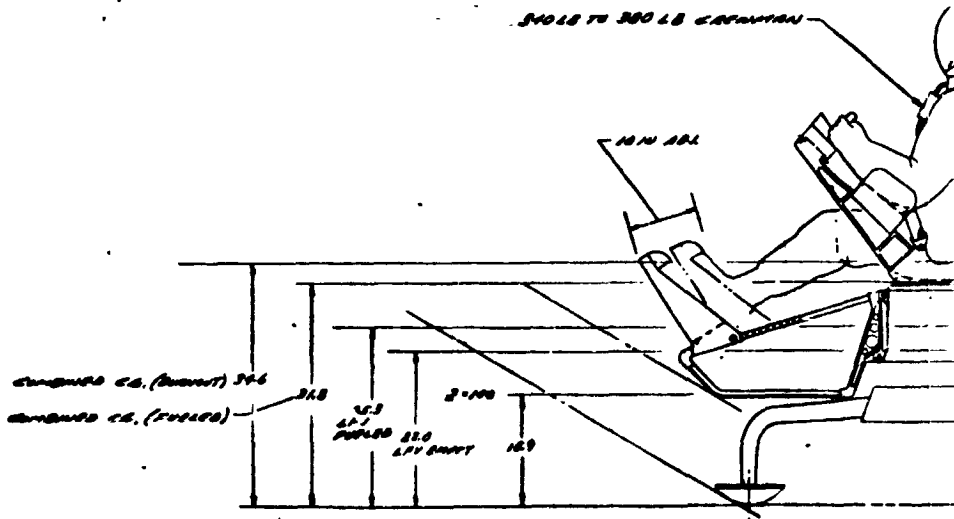


FIGURE 9 (SEE FOR FIGURES)  
SMALL SIZE PARTY 111A



RETRACTED CO. (DOWN) 31.6  
RETRACTED CO. (UP) 31.6

300 LB TO 350 LB CAPACITY

10 IN DIA

2' 000

12.0

12.0

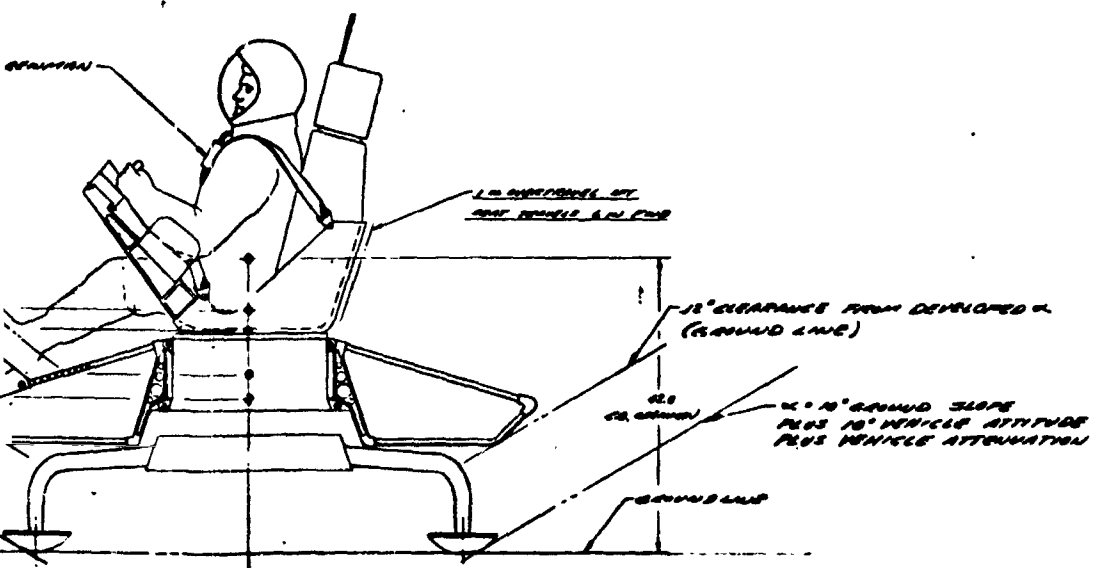
12.0

12.0

GENERAL VIEW  
SMALL SIZE PARTY  
111A

FOLDOUT FRAME





SEAT "X" (REF DWG 2230-4)  
FIXED LOAD PAN  
LEV IS SUPPORTED BY TRANSLATING PANOP  
& DISTRIBUTING LOAD

|   |                 |        |                     |
|---|-----------------|--------|---------------------|
| REV   | BY              | DATE   | DESCRIPTION         |
| 1   | W. J. [unclear] | 6-1-69 | ISSUE FOR [unclear] |
| ONE MAN LEV - PARAMETRIC<br>PAYLOAD INVESTIGATION -<br>FIXED LOAD PAN |                 |        | 2230-12             |

Figure 81. Fixed Load Pan Variations (Drawing 2230-12)

Therefore, the only problem would be deviations from this flight program and picking up unknown objects, such as rocks, etc. When the astronaut added unknown objects to the LFV, he would be required to weigh this payload and determine the seat and payload location. Alternates would be to provide a central jack and balancing level, deployable knife-edge jacks at each of the landing pads along with the balancing level, or in-flight seat adjustment to balance the vehicle.

### Payload Capability

The preliminary design arrangement of load pans has the capability defined in the curves of Figure 82, where the least payload density (bulkiest payload) is the parameter. The curves refer to the aft payload, the forward load being assumed as centered.

### LUNAR MODULE INTEGRATION

LFV stowing on the lunar module (LM) for transport to the lunar surface, removal of the LFV from the LM, and integration of propellant servicing are considered in this subsection.

As general requirements, the LFV should not compromise any LM functions or require any additional flight testing of the LM for qualification. Removal from the LM should be reliable and should be accomplished safely and quickly by one astronaut. If folding or disassembly is required for stowing, assembly should require minimum time and exertion and should be accomplished by one astronaut.

During the precontract activity, several areas were considered for stowage of the two LFV's, and a location on the upper aft area of the descent stage was selected. However, this location was rather high above the lunar surface, which complicated LFV removal. It also was unacceptable with respect to the LM because the location interfered with spacecraft/LM adapter (SLA) access and because no protrusions from the descent stage above the ascent stage separation plane were permitted by LM ground rule, since this would jeopardize ascent stage abort. At the inception of the contracted study, Reference 23 was forwarded by NASA as representing the accepted LM interface requirement. This document defines the corner compartments, as shown in Figure 83, as being available. Figure 84 illustrates stowage of the baseline configuration in these compartments. For this design, the LFV was constrained between Stations  $X = 133.6$  and  $X = 193.5$ ,  $Y = -30$ , and  $Z = +30$ , and was to have minimum protrusion into the reaction control system (RCS) engine plume area. As may be seen, the four truss struts were folded, and the fuel tank was telescoped as far as

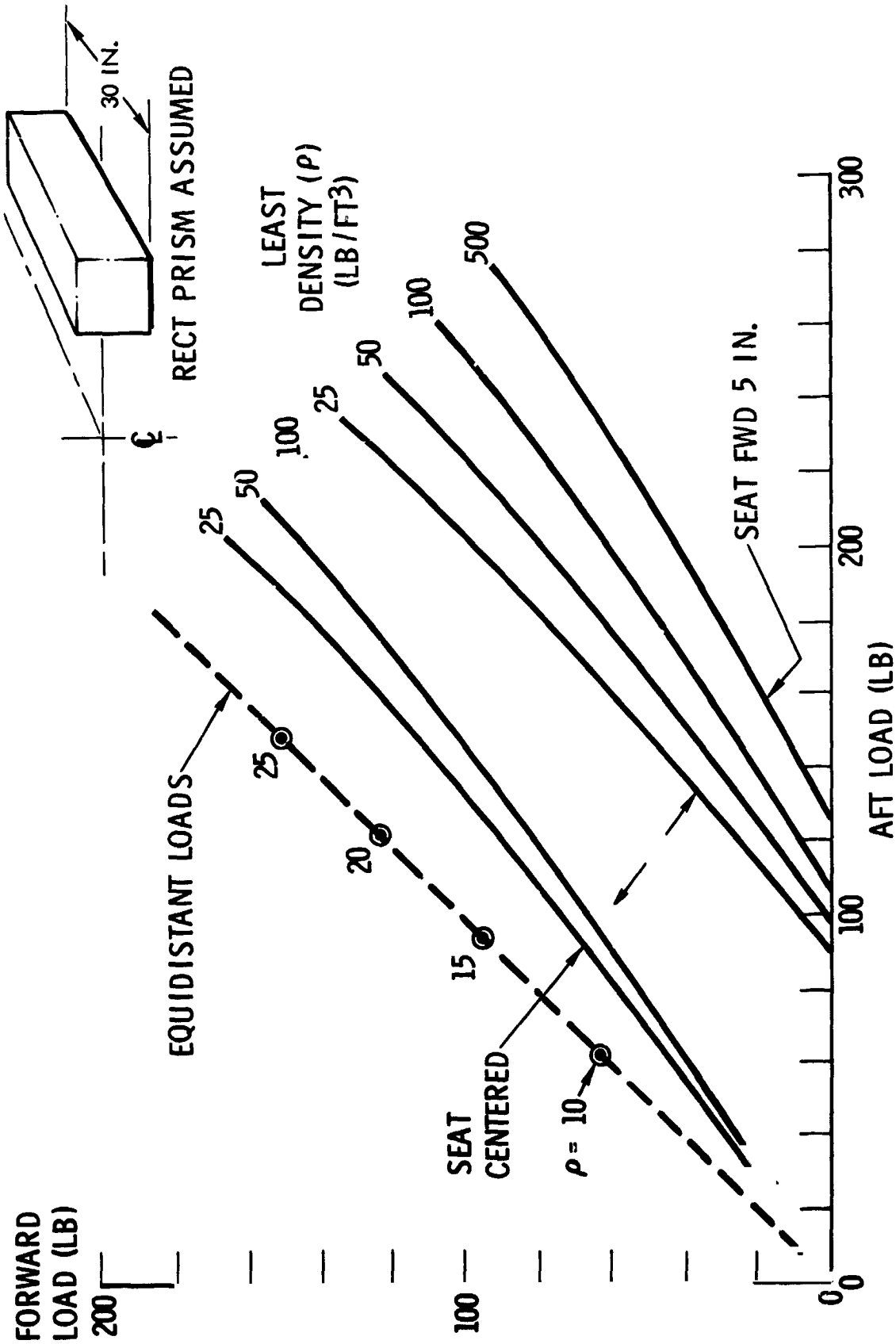


Figure 82 . Payload Capability Envelope

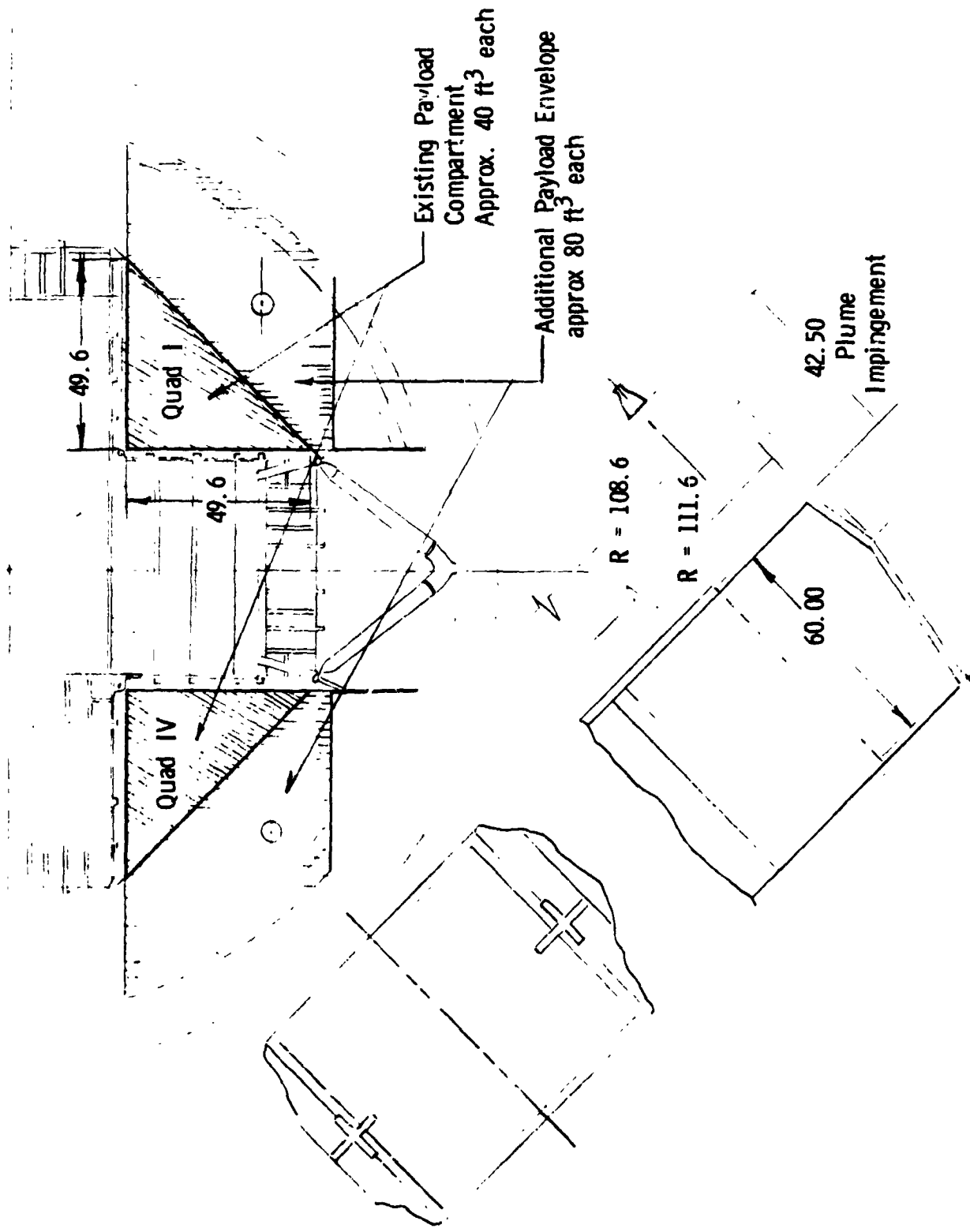
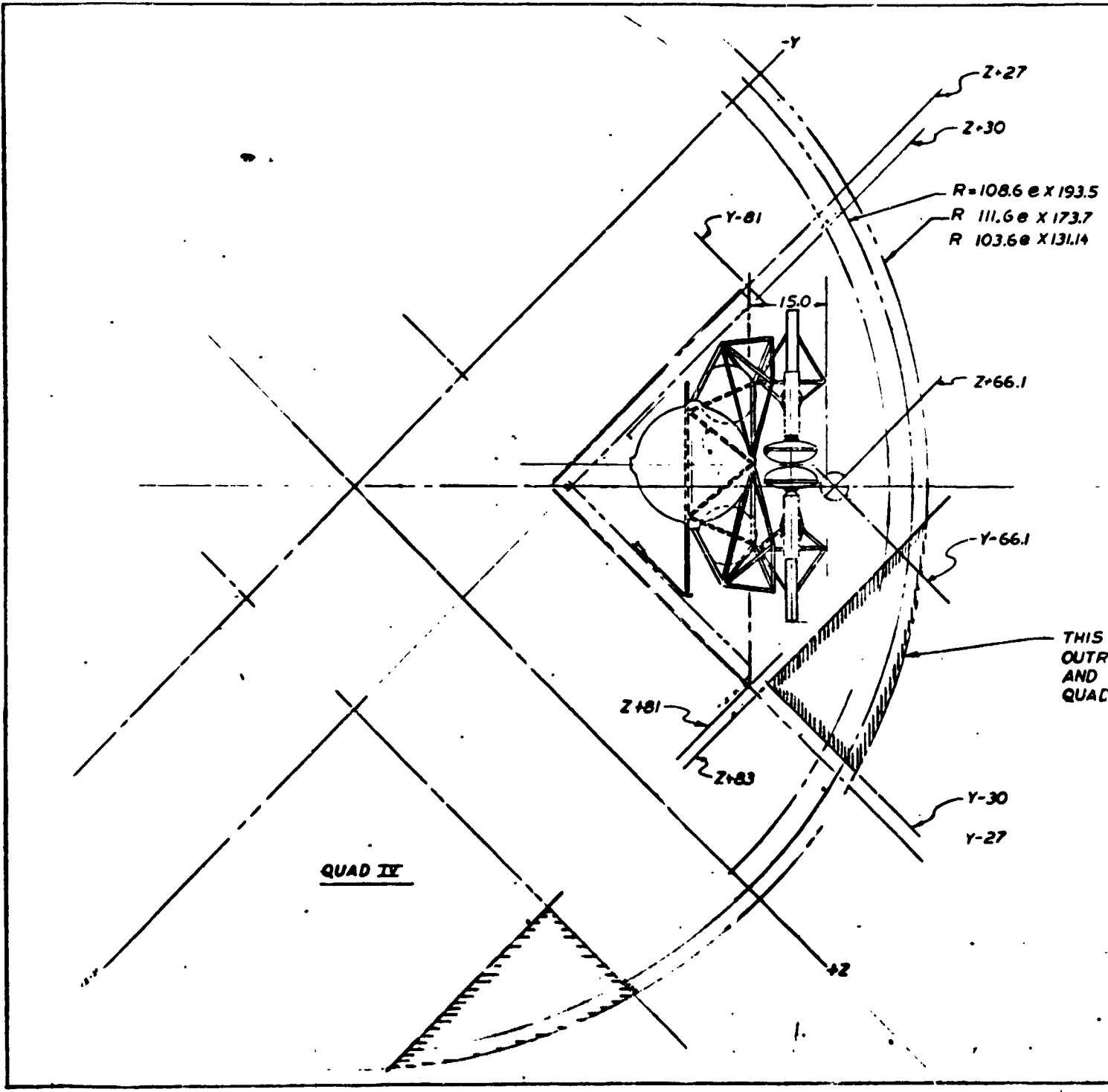


Figure 83. ELM, Roving Vehicle Interface Definition



QUAD IX

FOLD

-Z-27

-30

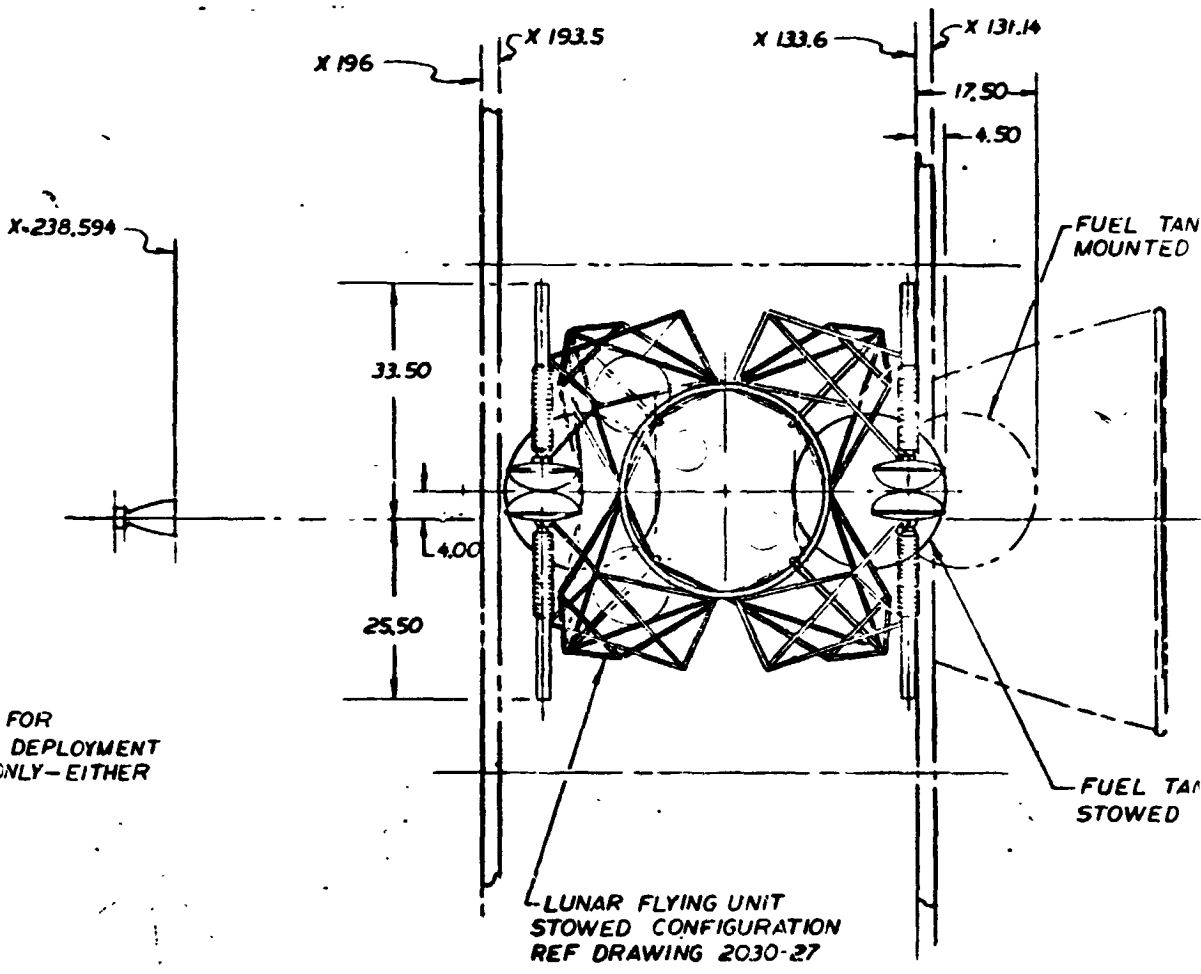
-108.6 e x 193.5  
111.6 e x 173.7  
103.6 e x 131.14

Z+66.1

-Y-66.1

-30

-27



THIS RESTRICTION IS FOR  
OUTRIGGER EQUIPMENT DEPLOYMENT  
AND IS ON ONE SIDE ONLY - EITHER  
QUAD I OR QUAD IV

|   |    |      |
|---|----|------|
| DATE  | BY | CHKD |
| 2-10-59   |    |      |
| STOWING ARRANGEMENT<br>(STUDY)<br>LUNAR FLYING UNIT |    |      |

Figure 84. Stowing Arrangement, Initial Control Vehi Configuration (Drawing 2230-3A)

FOLDOUT FRAME

FOLDOUT FRAME

PRECEDING PAGE BLANK NOT FILMED.

possible, but the LFV still protrudes beyond the lower allowable limit. This investigation, conducted early in the study, reaffirmed an important fact: the stowing envelope is a strong constraint on the LFV and must be considered early in configuration concept development.

The configuration illustrated in Figure 6 does not extend beyond the maximum allowable stowing envelope but requires excessive dismantling. The four pads, attenuators, and drag link assemblies must be removed (rather than hinged), and the console, seat, and footrest assemblies are removed. The excessive EVA time required to reassemble these items is a disadvantage.

Stowing of the concept shown in Figure 7 is similar to that of Figure 6. The stowing envelope is not violated, but extensive removal of LFV components is required. The four landing pads, lower frame, and cargo carrier are removed and stowed as separate items, and the console and foot support require folding.

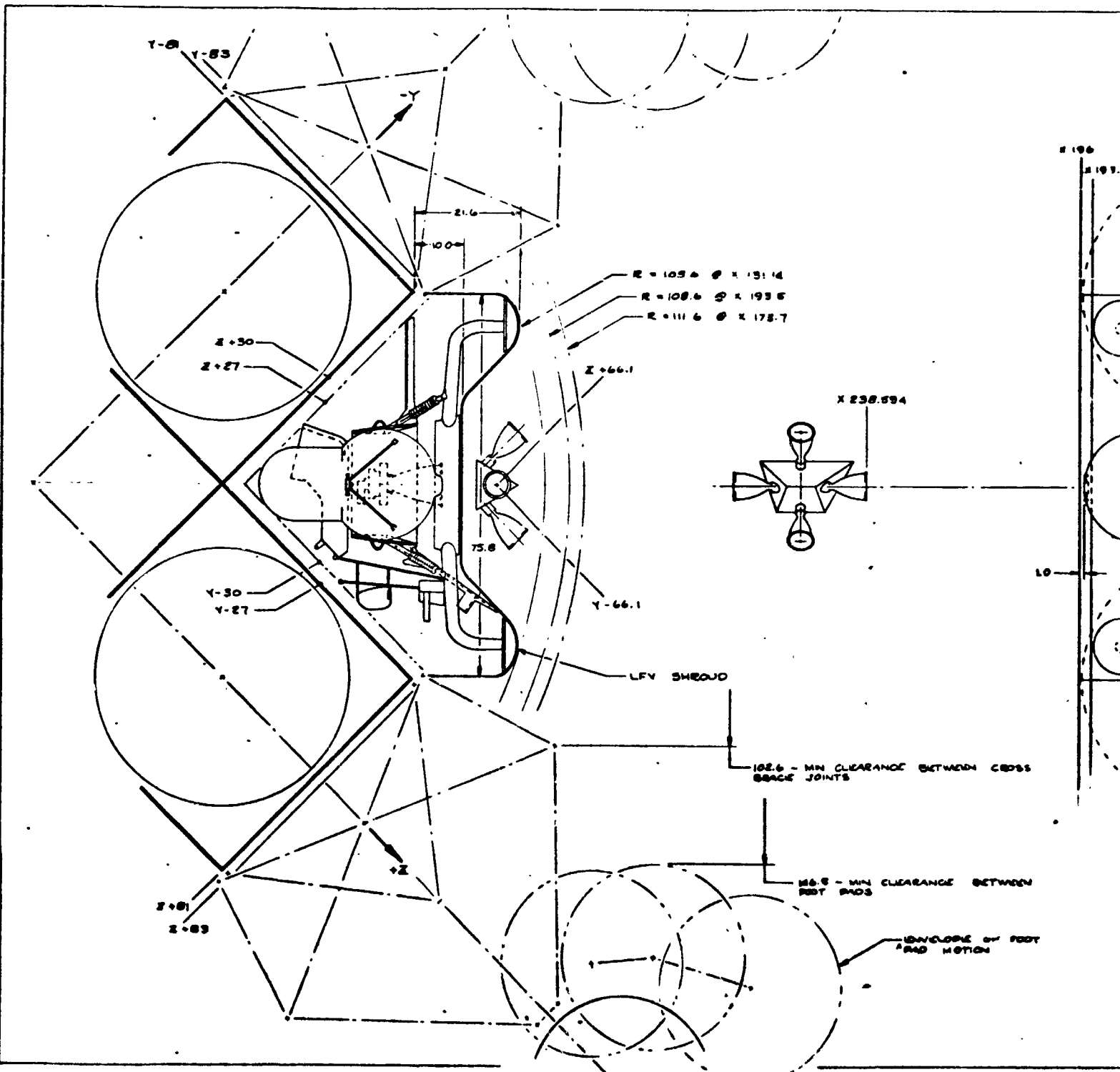
After inspecting a LM descent stage at MSC and after discussions with NASA, it was determined that the LM corner compartment aft bulkhead (located at station X = 131.14) could be penetrated without compromising the LM. The LM heat shield located at Station X = 116.34 now represents the lower envelope limit. This extension of the stowage envelope allowed the two-tank concepts to be stowed without telescoping the fuel tank.

The stowed configurations of Figures 12 and 85 are quite different due to the stowage philosophy considered, but the concepts are essentially interchangeable. In Figure 12, the stowed envelope was again minimized, which required additional dismantling of the LFV. The two cargo decks and one of the landing pad struts are removed and stowed as separate items. The three remaining struts are telescoped and rotated as shown. Finally, the console and yaw thruster truss must be rotated. By allowing local protrusions around the gear, but still within the overall envelope constraints, the LFV can be stowed intact except for hinging of the console and forward cargo deck (Figure 85). In this version, the LFV shroud would be removed, the LFV vehicle uncaged and removed from the ELM, and the LFV deployed with a minimum of EVA time and exertion of the astronaut.

The three-gear concept of Figure 86 was an attempt at simplification, but has stowage problems because the longer gear struts require a canted hinge line to stow as illustrated. The console is again folded, and the cargo decks would be telescoped inboard as shown.

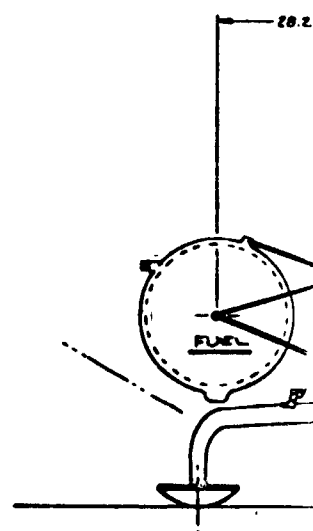
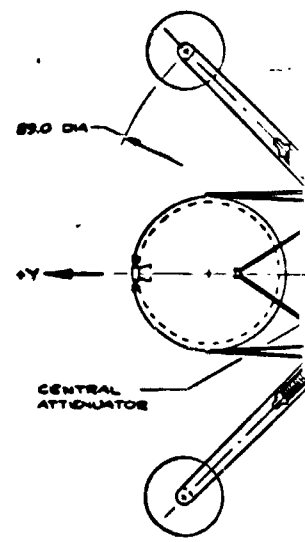
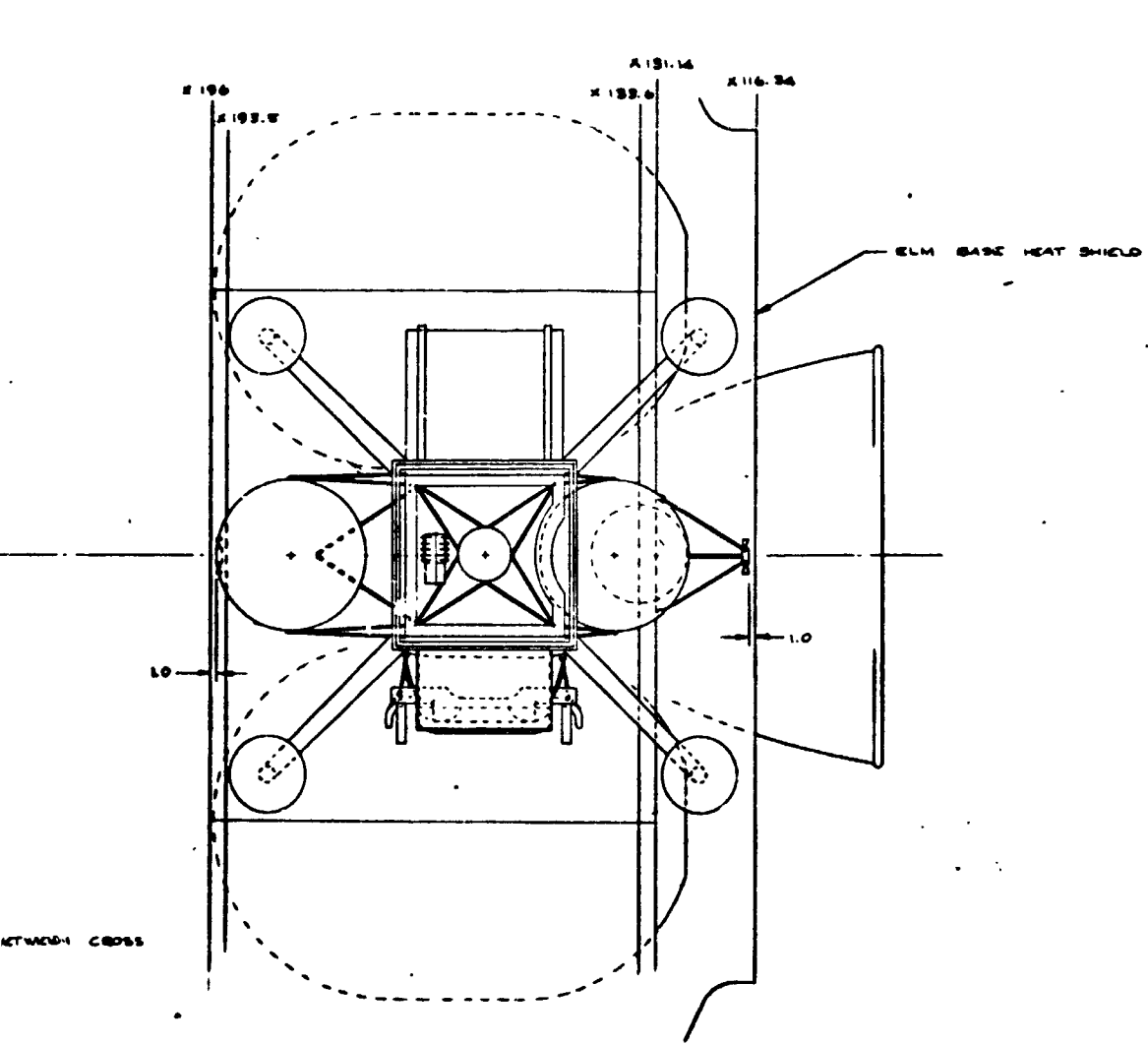
Due to the increased tank spread of the design of Figure 17, the stowing problem was magnified. The LFV was inverted within the ELM bay and tilted 6.25 degrees to best utilize the allowable stowage volume.





FOLDOUT FRAME

FOLDOUT FRAME

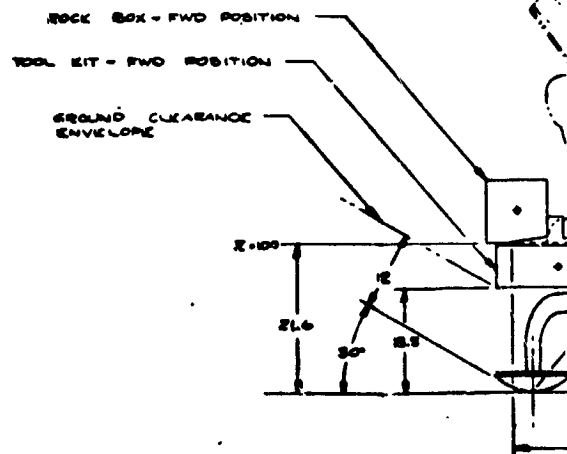
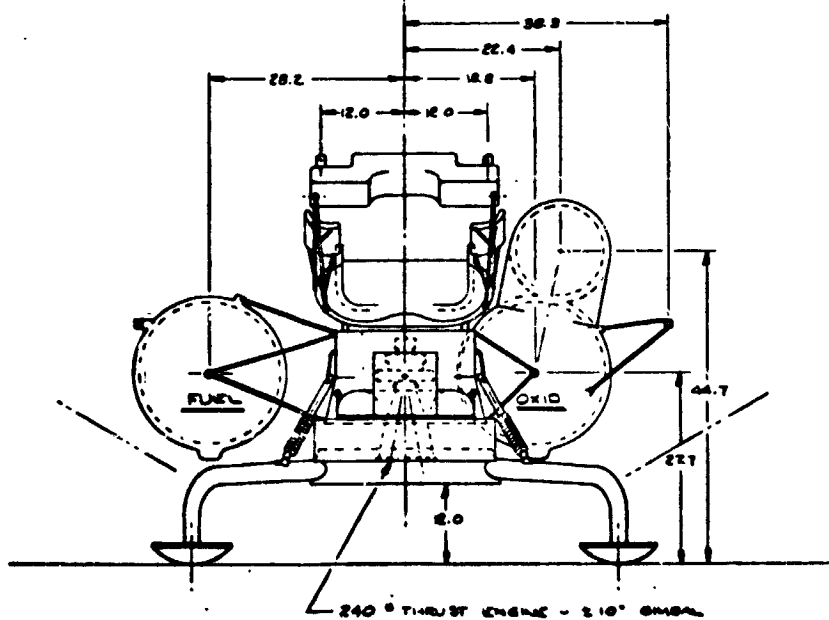
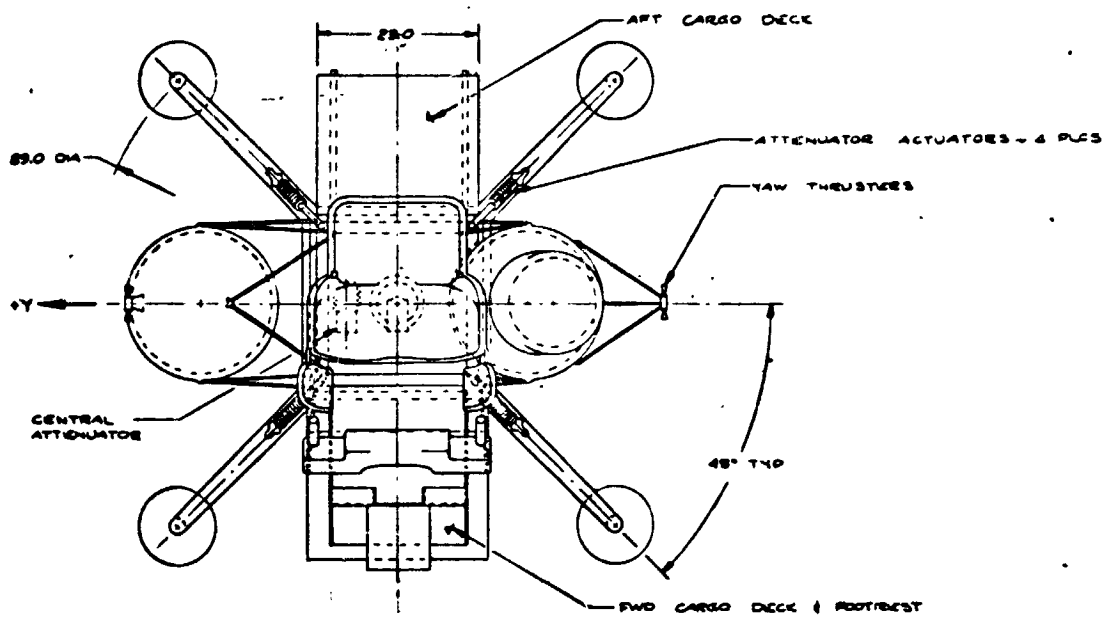


BETWEEN CROSS

ANGE BETWEEN

VELOPE OF FOOT  
 MOTION

MUT FRAME



FOLDOUT FRAME

4 PLS

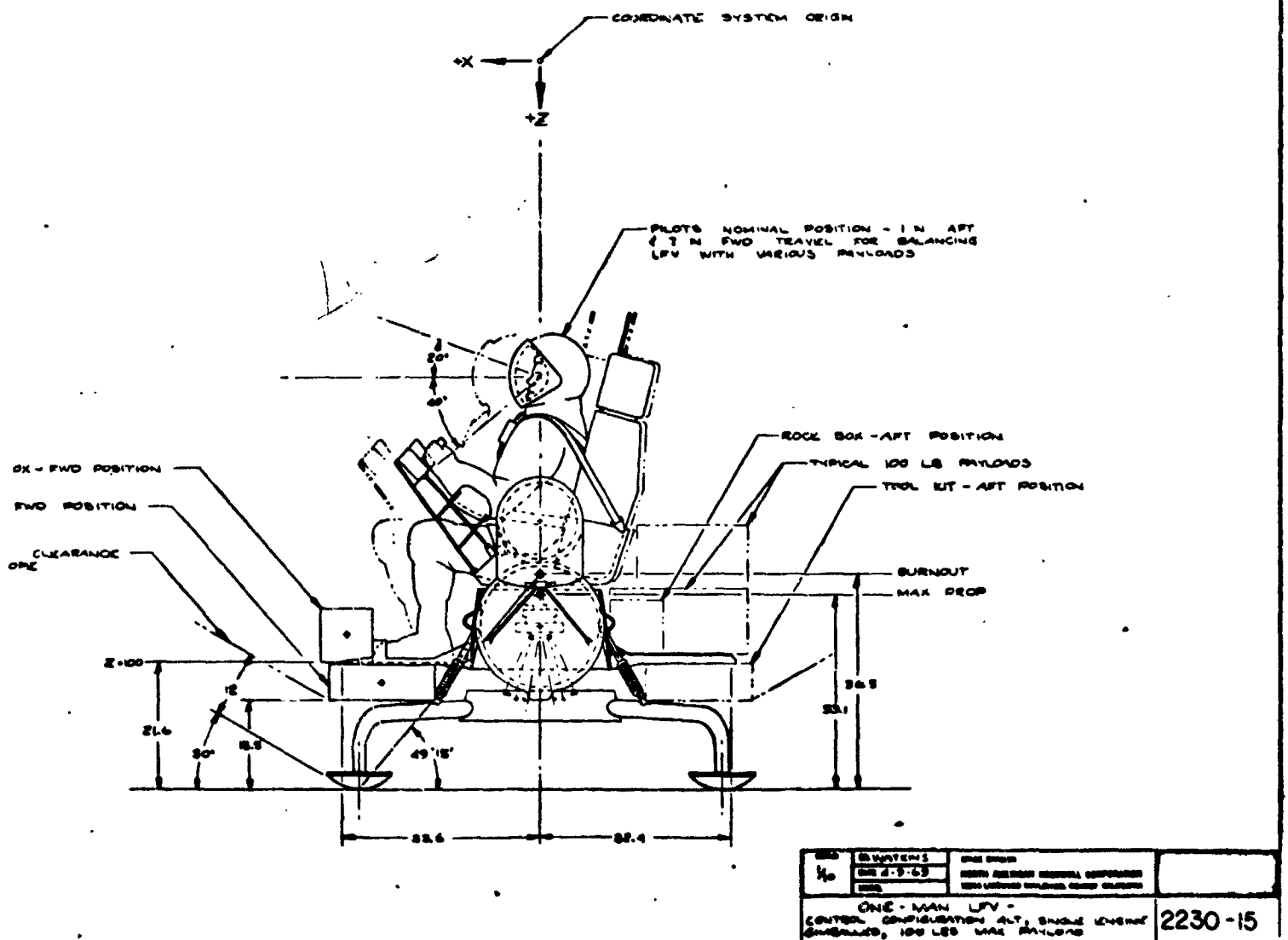


Figure 85. 100-Pound Maximum Payload Vehicle Configuration  
(Drawing 2230-15)

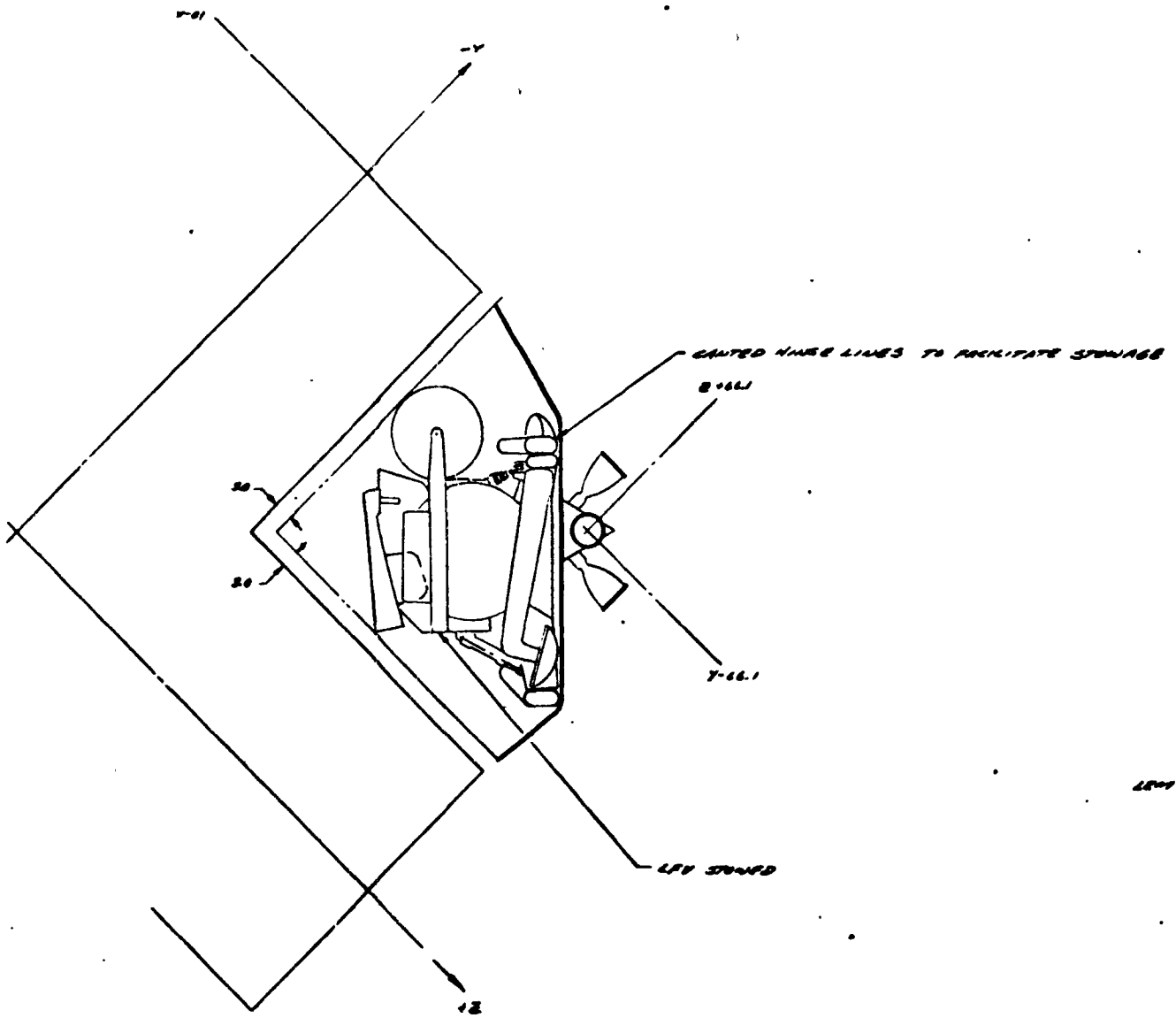
- 209, 210 -

SD 69-419-4

IT FRAME

FOLDOUT FRAME

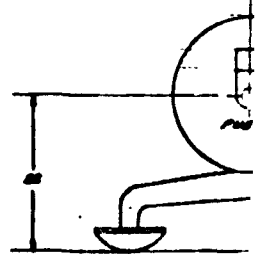
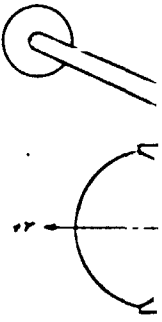
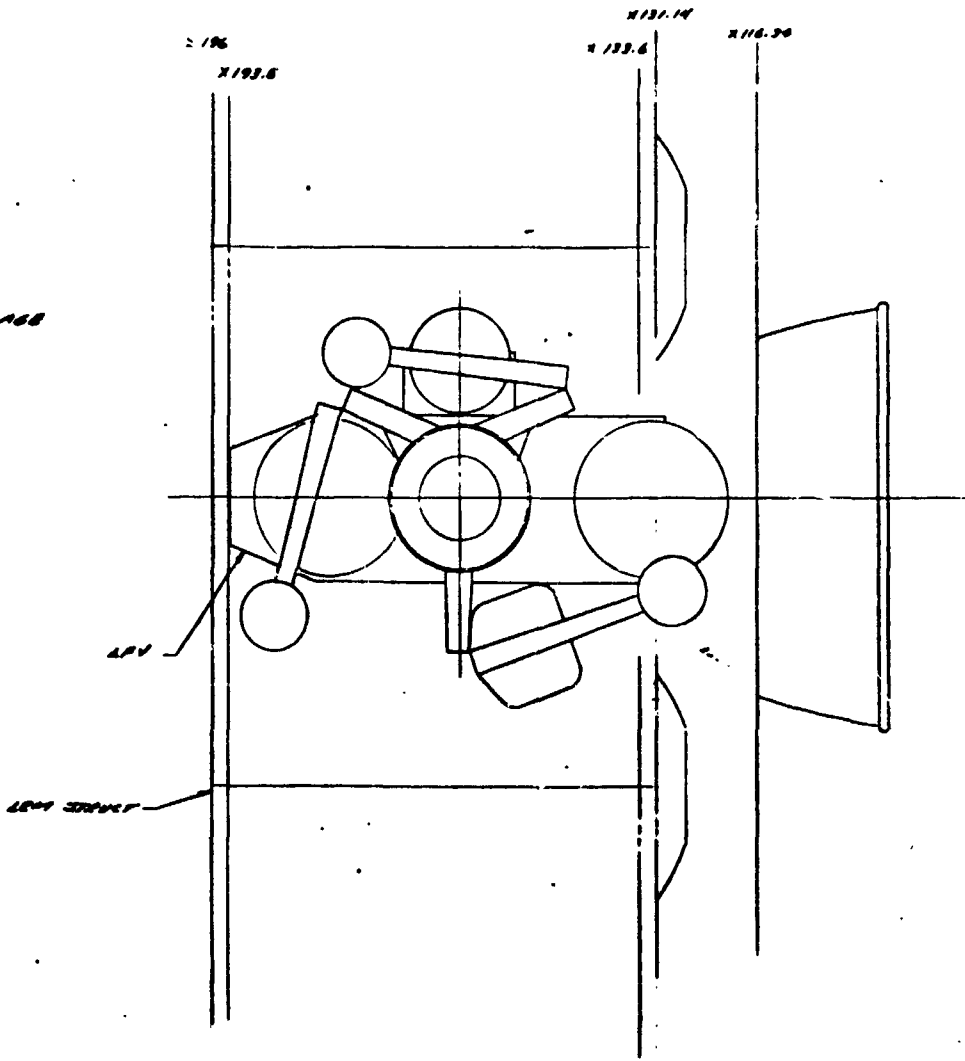
PRECEDING PAGE BLANK NOT FILMED.



LRY J

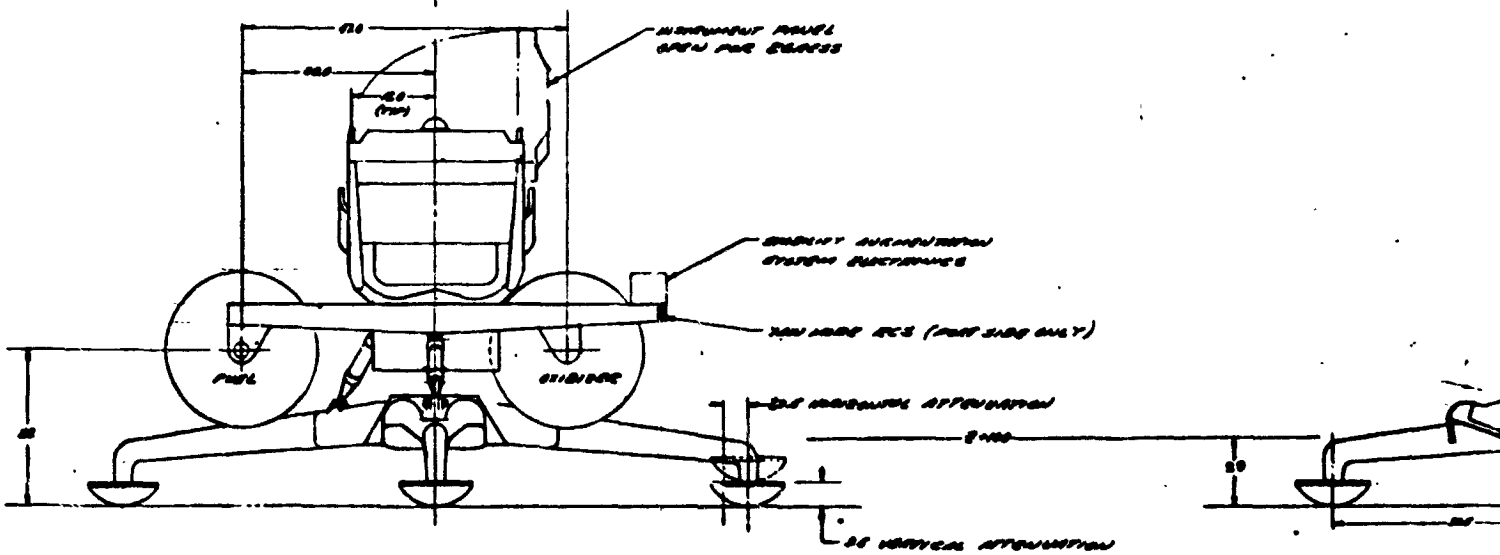
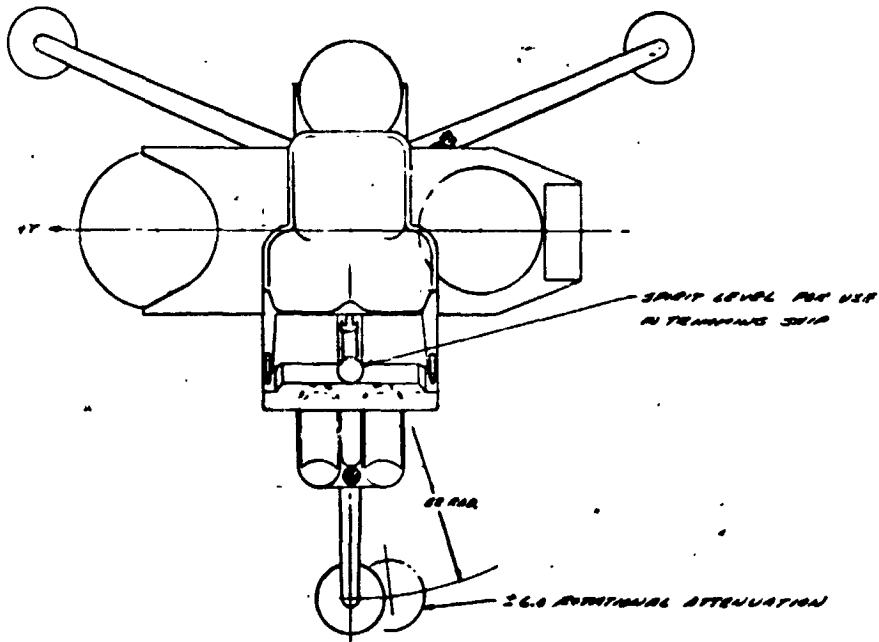
LRY STOWED

LRY STOWAGE IN LRY



FOLDOUT FRAME

FOLDOUT FRAME



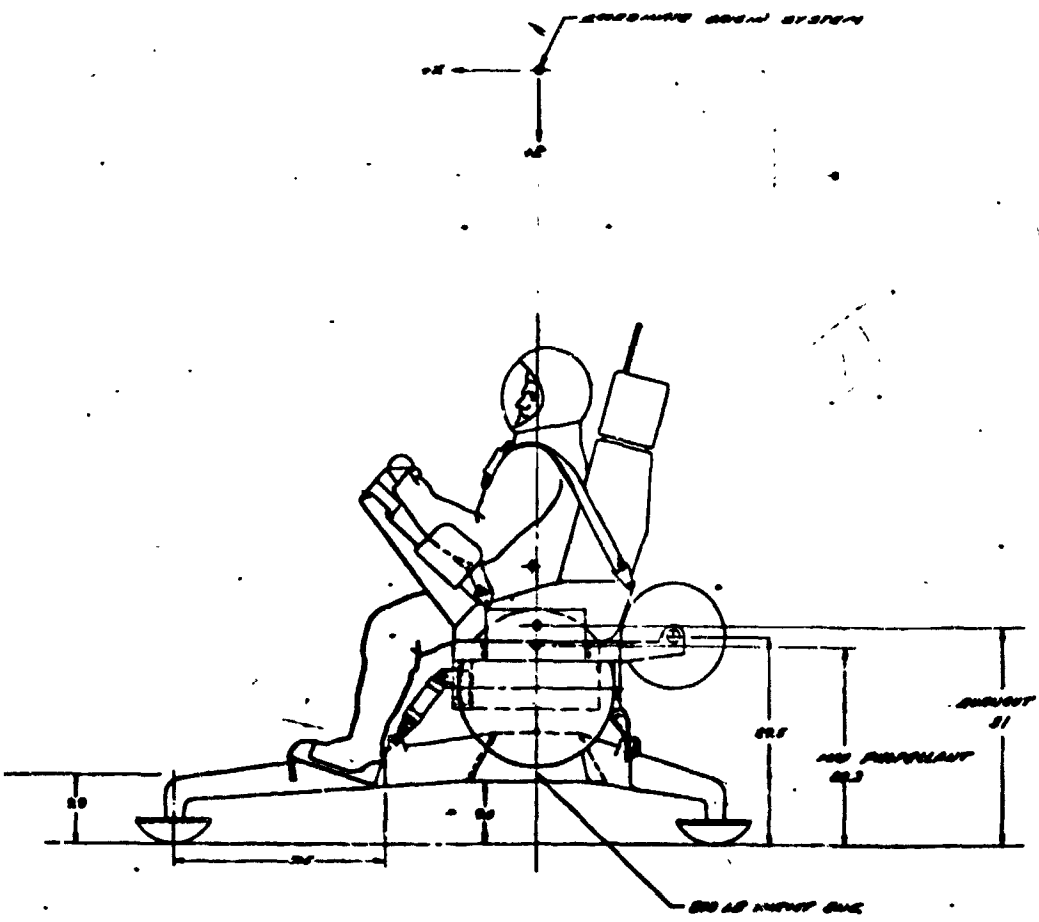
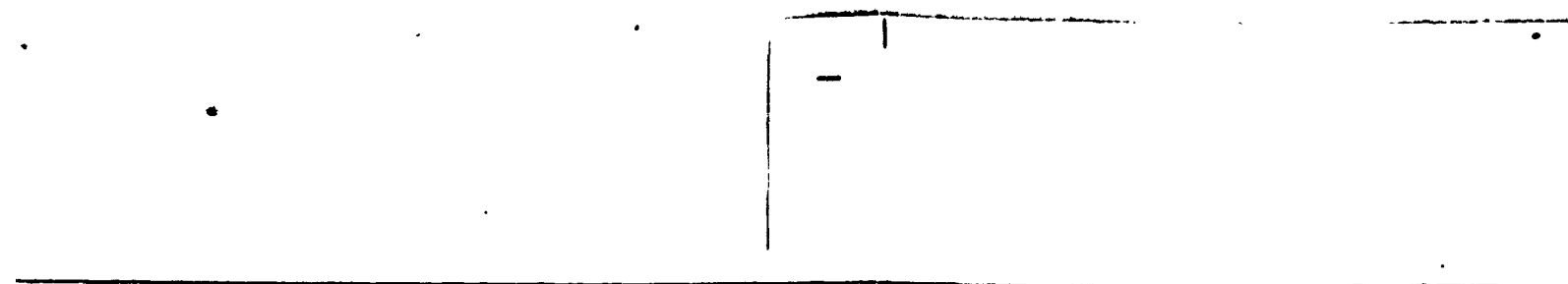


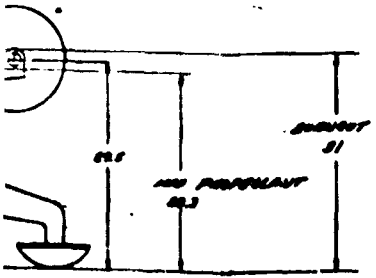
Figure 86. Simplified, Fixed  
(Drawin  
- 21

FOLDOUT FRAME

FOLDOUT FRAME



NO. 2030-17



NO. 2030-17

|  |         |         |  |
|--|---------|---------|--|
| NO.  | 2030-17 | DATE    |  |
| REV.   | 0-1-1   | BY      |  |
| LUNAR FLIGHT SERVICE<br>Simplified Version -<br>Fixed Components |         | 2230-17 |  |

Figure 86. Simplified, Fixed Component Vehicle Configuration  
(Drawing 2230-17)

- 211, 212 -

SD 69-419-4

FOLDOUT FRAME

As illustrated, minimum clearance is maintained at the four landing pads, oxidizer and helium tanks, pilot seat, console, and the two cargo decks. For stowing, the seat is translated forward, and the footrest, cargo decks, and console are rotated as shown.

Stowing of the selected concept (Figure 19) is illustrated in Figure 21. The arrangement is similar to that of Figure 17, although the vehicle is deeper. The vehicle extends past the corner compartment bulkhead and below the LMD aft heat shield line by 1.4 inches. The legs extend into the RCS plume area approximately 20 inches. The latter penetration is considered acceptable (see Reference 23), and the extent of plume protection required is subject to a heating analysis. The shroud shown in the figure is a maximum requirement, even with the cutout areas indicated, and could be reduced in all areas except the lower face, where ejecta protection is required. The basic design is a thermally open compartment (one of two choices described in the LM interface document, Reference 23) with LM insulation on the inner walls of the compartment.

The penetration of the aft bulkhead could be reduced if part of the thrust vector control (TVC) gimbal travel can be used to track a propellant c.g., excursion. For example, if the tanks are closed up 4 inches and only partially balanced, the gimbal angle required to track the c.g. is  $\pm 1.4$  degrees.

At present, the penetration of the aft bulkhead requires that the LM corner lower diagonal be removable both for LFV/LM mating and after lunar landing. Although this is an undesirable interface requirement, it is not a severe compromise. With proper design, the structural integrity of the LM can be maintained at a 2- to 4-lb weight penalty for the removability provision.

To stow, the seat is translated forward (utilizing the tracks available) and rotated 45 degrees, both cargo decks are rotated down 45 degrees, the right-hand attitude controller is rotated approximately 90 degrees upward across the oxidizer tank, the left-hand console is rotated approximately 90 degrees upward across the seat, and the footrest assembly rotates down and aft to an area under the fuel tank.

Propellant tank support beams are utilized to support and remove the LFV from the LM. To remove the LFV, it would be uncaged from the LM at each tank support, and the hoist cable would be released to permit outward and downward motion until the lower portion locks at a detent in the lower tracks. The cable assembly would then permit rotation of the LFV until the landing pads contacted the lunar surface. The unit would then be manually released from the lower track, and the cables would be disconnected. The deployable and replaceable items on the LFV would then be deployed and secured.

After the takeoff pad is deployed and secured, the LFV would be manually transported to the takeoff site, the propellant lines would be unreeled, propellant would be transferred from the LM to the LFV, and the vehicle would be checked out prior to flight.

The second available bay of the LM descent stage is utilized to stow the miscellaneous lunar support equipment, additional helium tanks, and scientific experiments. Ample volume is available for this stowage. The lunar support equipment includes the two propellant transfer hoses, the two propellant vent lines, portable checkout unit, remote takeoff pads, LM-site landing/takeoff pad, and tools.

#### LUNAR SUPPORT EQUIPMENT

Lunar Support Equipment (LSE) requirement areas requiring investigation were identified early in the study for support of the following operations:

1. LFV assembly and deployment
2. Checkout
3. Propellant servicing
4. Helium vessel replacement
5. LM site landing and takeoff
6. Remote site takeoff
7. Preflight weight and balance determination
8. Standby (fueled) storage
9. Dormant (long duration) storage

A description of these operations is contained in Volume 2, and servicing operations are discussed further under "Propulsion Subsystem" in Volume 3.

As operational and design concepts developed, the characteristics of the equipment were defined. In a few areas, special studies were needed, notably the servicing equipment (see Figure 87 and Volume 3) and the takeoff debris protection mats (see following paragraphs) defined as needed equipment for Items 5 and 6 above. Since weight minimization is the dominant

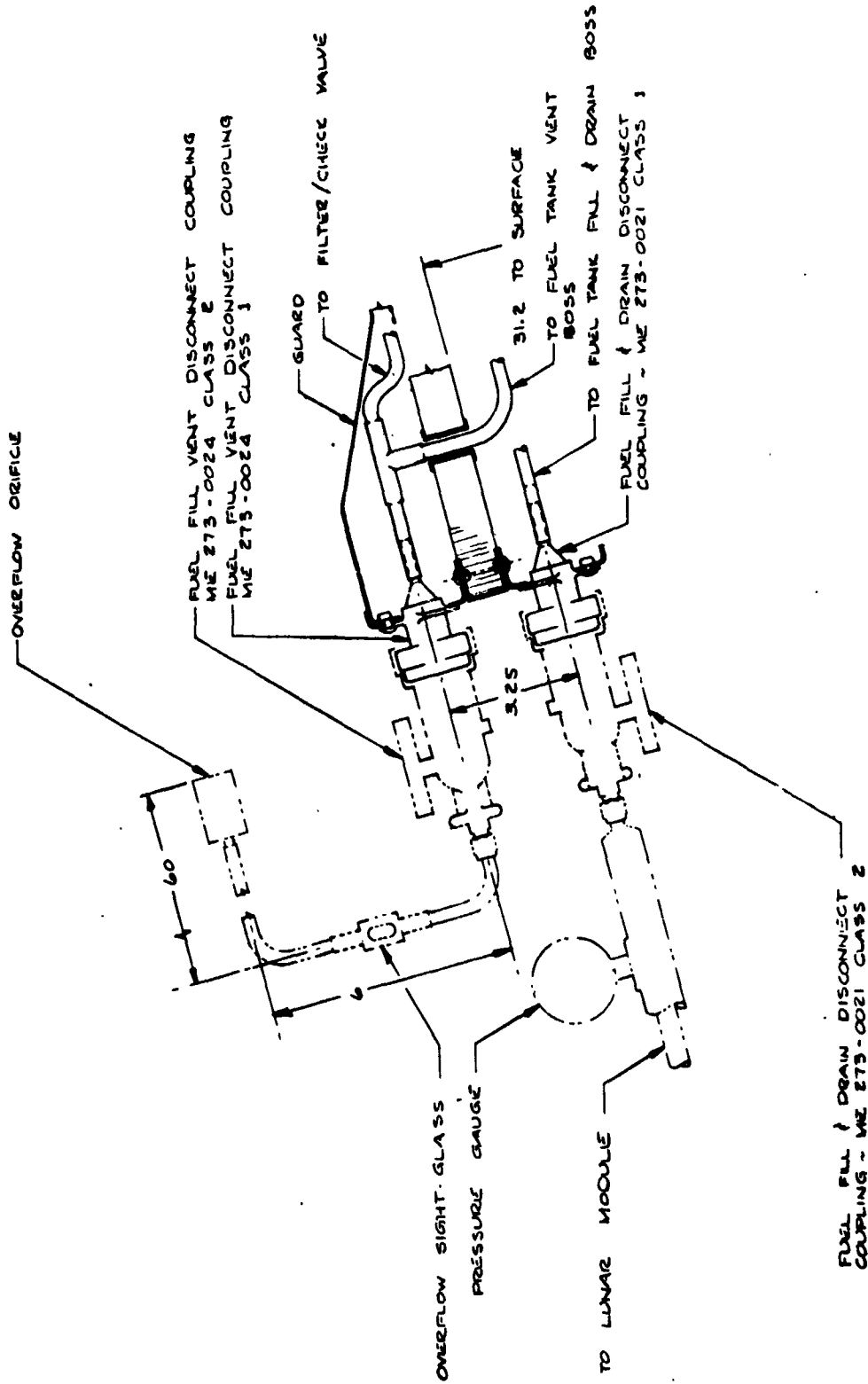


Figure 87. Propellant Servicing Configuration

criterion, equipment was eliminated wherever possible. Eliminations included: wheels, sleds, and other aids for transport from the LM to the takeoff site (Item 1); all except minor tools for Items 4 and 7; and thermal protective covers for Items 8 and 9.

### Lunar Debris Control

During the descent and ascent of the lunar flying vehicle from the surface of the moon, there exists a strong possibility that rocket exhaust gases will kickup and impart velocity to lunar debris. Debris with sufficient size and velocity could cause some damage to the lunar module structure, propellant tanks, plumbing controls, etc., if some precautions are not taken. The pilot and passenger astronaut are also in danger if lunar particles puncture protective space suits.

Helicopters encounter debris problems during landings and takeoffs from unprepared sandy or dry soil. In the Army and Air Force efforts to control dust and debris, various concepts from spraying fast-curing resin and foams on the proposed landing area to deploying portable landing mats were evaluated. The resin and foam techniques required a special on-board pressurized system which did not always function reliably and reduced payload capacity. The mat concept proved to be more feasible, although the final solution was development and installation of high-capacity dust filtering units for gas, oil, and air intake systems, and a layer of plastic tape applied to blade leading edges.

While the main problem for the helicopter is dust ingestion and not damage to structural members from flying debris, the reverse is true in the case of the lunar flight vehicle. The resin and foam concept that was considered for helicopter application was reviewed, but the same plumbing and resin weight, the even less predictable reliability of operation on the lunar surface (30 operations after one month storage in the thermal, radiation, and vacuum of space), and the added weight to the vehicle remain. In addition, calculation indicated that 5 to 10 pounds of resin per landing would be required to satisfactorily stabilize the lunar soil, particularly in the area immediately below the rocket engines, where gas velocities, impact energies, and thermal loads are high. The second method would require the astronaut to deploy a lightweight plastic or foil mat with augmented thermal protection in the projected plume impingement area.

For the LFV, a minimum-area, four-pointed star mat configuration was considered. The points of the mat are pinned to the lunar surface and afford debris protection to each landing gear. Kapton film and nickel foil were considered for the main mat material, and 7.6 lb/ft cork was evaluated for ablative thermal protection in the 4- by 4-foot projected plume impingement area. Weight predictions for the lunar mat were made from

the data contained in Figure 2, which shows a plot of material (Kapton, nickel, and cork) weight for various areas protected. Using the data in Figures 88 and 89, weight values per hop for reasonable mat designs appear to be 3.315 for 1-mil nickel with a 1/16-inch layer of cork, and a 3.30 pound for 5-mil Kapton with 1/8-inch cork.

A third concept involved integrating the debris impact protection system with the underbody thermal protection system which is required to reduce the effect of engine plume radiation.

Comparison of Concepts 2 and 3 showed that the mat was the only certain lightweight solution. Underbody protection is potentially lighter and more efficient operationally, but only if the plume ejecta model indicates that little or no protection is needed. The mat concept depends on prevention rather than protection, and a precise plane ejecta model is not needed for its design. At present, insufficient data on the ejecta model makes the mat choice the preferred one.

#### Weight and Balance Equipment

To accommodate changes in LFV payloads, pilot weight, and other variations, LSE weight and balance aids were considered. To perform this operation, balance points on the vehicle would be needed, along with a small portable spring-weight scale. A central ball pivot was considered, but it would necessarily be a telescopic type to allow retraction, since engines and pilot seat are in the center of the vehicle. Pivots located on the landing pads, which are deployable in pairs by the pilot's foot, were also considered.

A preprogrammed method requiring only a spring scale was selected as being simpler and substantially lighter. The method utilizes grid coordinates on the load pans, and mission plan book data to permit the crew to load any part or all of the payload properly. If lunar rock samples are to be loaded, they would be weighed first, and the data book would be used to indicate load placements. All other items are of known mass and dimensions.

#### Preliminary Design

With the exception of servicing equipment (described in Volume 3) no LSE preliminary designs were developed for this study phase. A list of the items required and an estimate of their weights is shown under "Mass Properties Summary."

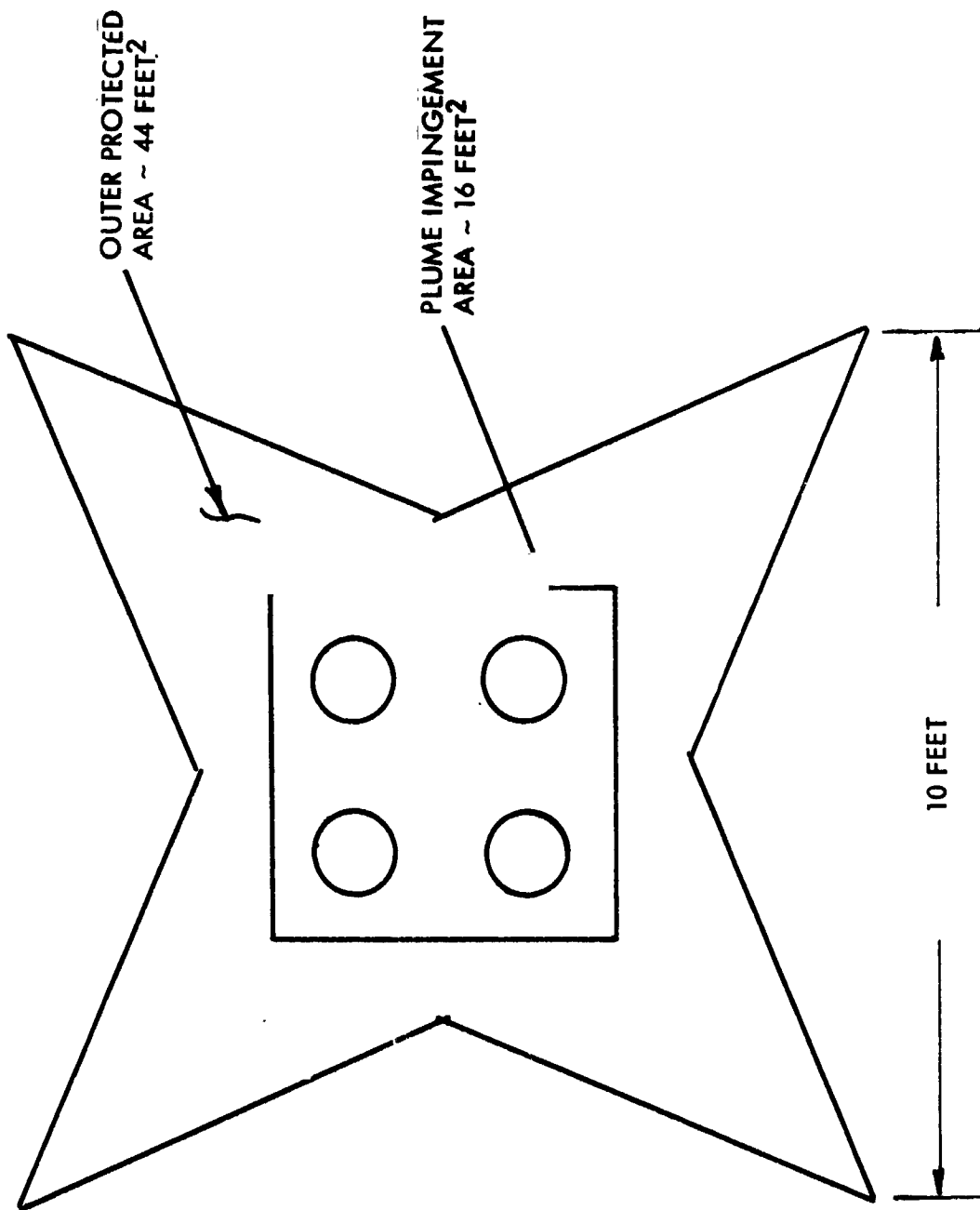


Figure 88. Takeoff Mat Coverage Pattern

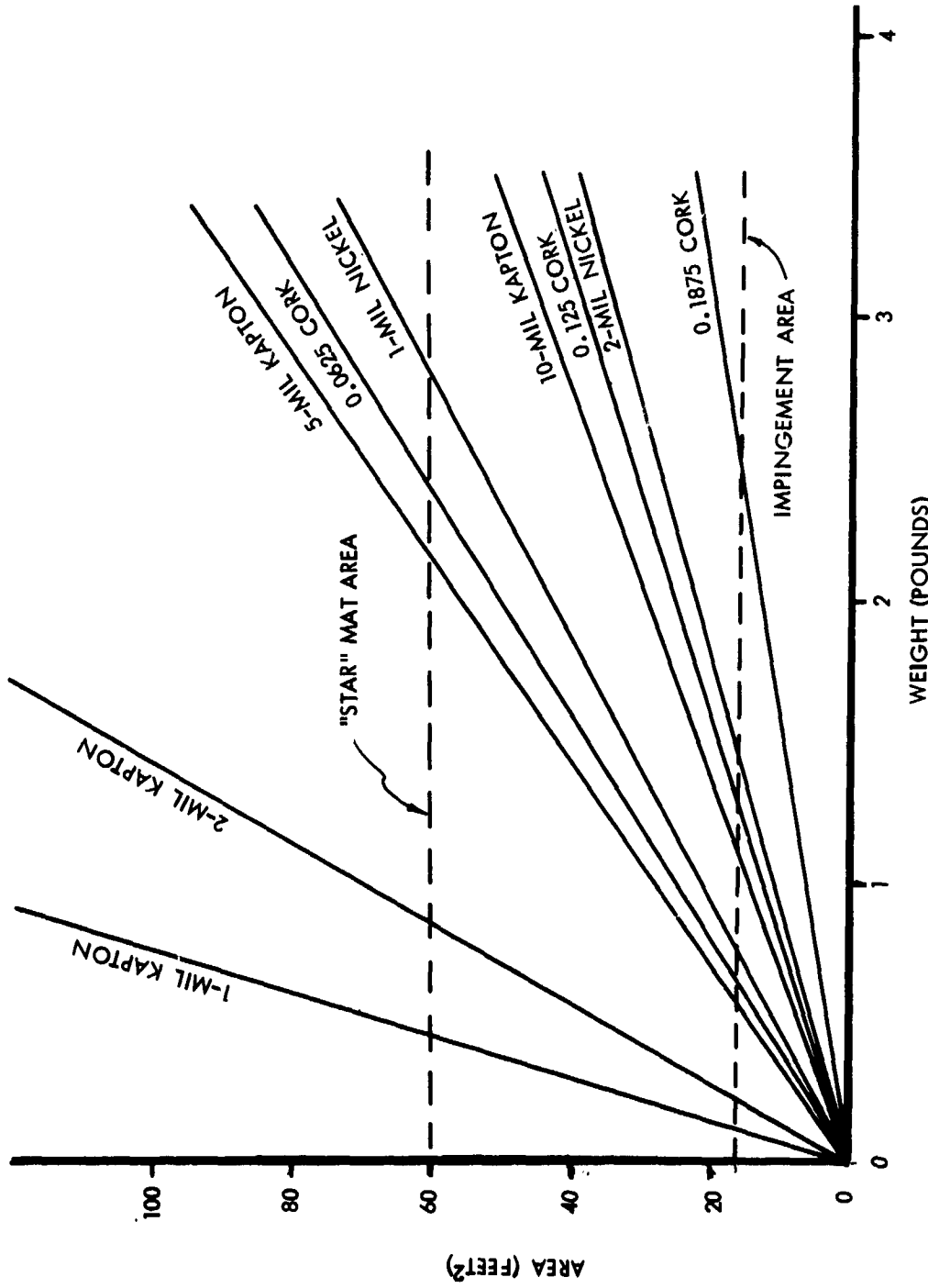


Figure 89. Weights of Candidate Mat Materials



**MASS PROPERTIES SUMMARY**

The weight data are presented in tabular form for the baseline configuration of the one-man lunar flying vehicle in the spacecraft summary weight statement. A configuration description has been included for clarification of the mass properties data. The primary distinguishing characteristics of the baseline configuration are one man seated for flight operation with four dual-axis gimballed engines, eight actuators, stability-augmented control, four landing gear legs with eight attenuators, and two spherical propellant tanks containing 300 pounds of usable propellant.

Summary and detail mass properties for the 100-pound and 370-pound payload cases are, respectively, on tabulated forms derived from MIL-M-38310A(USAF). Basically, mass properties data were developed from analysis of preliminary design drawings, mission and design requirements, and empirical data. The vehicle empty weight includes a 10-percent growth factor. The significant mass properties are given in Tables 21 through 24.

Table 21. Vehicle Weight and Balance

| Condition                            | Weight (lb) | Center of Gravity (In.) |      |       |
|--------------------------------------|-------------|-------------------------|------|-------|
|                                      |             | X                       | Y    | Z     |
| Empty                                | 303.6       | 2.5                     | -0.2 | 100.2 |
| Burnout with pilot only              | 692.6       | 1.1                     | -0.1 | 87.4  |
| Burnout with pilot + 100-lb payload  | 792.6       | 0.9                     | -0.1 | 88.4  |
| Burnout with pilot +370-lb payload   | 1062.6      | 0.7                     | -0.1 | 90.2  |
| Gross Weight pilot only              | 992.6       | 0.7                     | -0.1 | 91.1  |
| Gross weight - (100-lb payload)      | 1092.6      | 0.7                     | -0.1 | 91.5  |
| Gross weight - (370-lb payload)      | 1362.2      | 0.5                     | -0.0 | 92.3  |
| Lunar escape configuration - burnout | 1188.7      | -2.8                    | -2.2 | 79.4  |
| Lunar escape configuration - gross   | 2188.7      | -1.5                    | -1.2 | 84.9  |



Table 22. Vehicle Inertias (Slug Ft<sup>2</sup>)

| Inertia              | Burnout, Pilot Only               | Burnout, Pilot + 100-lb Payload | Burnout, Pilot + 100-lb Payload | Gross Weight, Pilot Only | Gross Weight, 100-lb Payload | Gross Weight, 370-lb Payload | Burnout, Lunar Escape | Gross Weight, Lunar Escape |
|----------------------|-----------------------------------|---------------------------------|---------------------------------|--------------------------|------------------------------|------------------------------|-----------------------|----------------------------|
| Pitch                | 58                                | 70                              | 100                             | 90                       | 100                          | 129                          | 165                   | 261                        |
| Roll                 | 50                                | 62                              | 92                              | 82                       | 93                           | 121                          | 148                   | 279                        |
| Yaw                  | 37                                | 57                              | 110                             | 87                       | 106                          | 160                          | 109                   | 289                        |
| Product              | XY - 0.65<br>XZ - 0.45<br>YZ 0.64 | -0.66<br>-0.62<br>0.65          | -0.66<br>-0.90<br>0.67          | -0.66<br>-1.05<br>0.68   | -0.66<br>-1.11<br>0.69       | -0.66<br>-1.24<br>0.70       | --<br>--<br>--        | 2.14<br>15.71<br>12.95     |
| Principal axis (deg) | YY 1.9<br>XX - 1.7<br>ZZ 4.6      | 7.0<br>-2.9<br>4.7              | -2.8<br>3.6<br>4.8              | -11.9<br>-12.0<br>4.9    | -4.5<br>6.4<br>5.0           | -1.8<br>1.3<br>5.0           | --<br>--<br>--        | 36.2<br>21.8<br>-28.1      |

Reference Axis System

Horizontal arms: inches measured from vertical centerline of the vehicle (X axis); + is forward and - is aft.

Lateral arms: inches measured from vertical centerline of the vehicle (Y axis); + is right-hand and - is left-hand.

Vertical arms: inches measured from 100 inches above foot level of payload platform (Z axis); + is down and - is up. Ground line is at +129.75.

Principal axis: angle of inclination (degrees) is XZ plane. Negative angle indicates nose up with respect to horizontal axis.

Table 23. Vehicle Summary Weight Statement, Baseline Configuration

| Code               | System                                | Pilot Only   | 100-lb Payload Case | 370-lb Payload Case | Lunar Escape  |
|--------------------|---------------------------------------|--------------|---------------------|---------------------|---------------|
| 2.0                | Body structure                        | 36.9         | 36.9                | 36.9                | 30.4          |
| 3.0                | Induced environment Protection        | 11.0         | 11.0                | 11.0                | 11.0          |
| 4.0                | Launch recovery and docking           | 62.1         | 62.1                | 62.1                | 62.1          |
| 5.0                | Main propulsion                       | 98.3         | 98.3                | 98.3                | 194.9         |
| 7.0                | Prime power source                    | 18.3         | 18.3                | 18.3                | 18.3          |
| 8.0                | Power conversion and Distribution     | 8.8          | 8.8                 | 8.8                 | 8.8           |
| 9.0                | Guidance and Navigation               | 32.9         | 32.9                | 32.9                | 32.9          |
| 14.0               | Personnel provisions                  | 9.3          | 9.3                 | 9.3                 | 14.4          |
| 15.0               | Crew Station control and panels       | 25.8         | 25.8                | 25.8                | 25.8          |
|                    | Program roundoff                      | 0.2          | 0.2                 | 0.2                 | 0.1           |
|                    | Subtotals                             | 303.6        | 303.6               | 303.6               | 398.7         |
| 17.0               | Personnel                             | 380.0        | 380.0               | 380.0               | 760.0         |
|                    | Subtotals                             | 683.6        | 683.6               | 683.6               | 1158.7        |
| 18.0               | Cargo                                 | --           | 100.0               | 370.0               | --            |
|                    | Subtotals                             | 683.6        | 783.6               | 1053.6              | 1158.7        |
| 21.0               | Residual propellant and service items | 9.0          | 9.0                 | 9.0                 | 30.0          |
|                    | Subtotals                             | 692.6        | 792.6               | 1062.6              | 1188.7        |
| 25.0               | Usable propellant                     | 300.0        | 300.0               | 300.0               | 1000.0        |
| <b>TOTALS (lb)</b> |                                       | <b>992.6</b> | <b>1092.6</b>       | <b>1362.6</b>       | <b>2188.7</b> |

**Table 24. Lunar Flying Vehicle Flight Elements  
 Summary Weight Statement**

| Item                                      | Item Weight (lb) | Total Weight (lb) |
|---|------------------|-------------------|
| Vehicle                                   |                  | 303.6             |
| Replacement items                         |                  |                   |
| Helium vessels (2)                        | 20.0             | 20.0              |
| Lunar support equipment*                  |                  |                   |
| Checkout equipment                        | 5.0              |                   |
| Landing mats (1 large, 4 small)           | 7.5              |                   |
| Tools, weighing scale, mat stakes         | 5.0              |                   |
| Propellant servicing hoses (2)            | 21.0             |                   |
|   | <hr/> 38.5       | 38.5              |
| LM modifications and stowing accessories* |                  |                   |
| LM lower corner diagonal modification     | 4.0              |                   |
| LFV protective shroud                     | 15.0             |                   |
| LM attach fittings                        | 6.0              |                   |
| LFV support braces                        | 2.0              |                   |
| Hoist rails                               | 6.0              |                   |
| Hoist                                     | 5.0              |                   |
|   | <hr/> 38.0       | 38.0              |
| <b>System Installed Weight</b>            |                  | <b>400.1</b>      |
| <b>*Estimated weights</b>                 |                  |                   |

## PULSE-MODULATED THRUSTER CONCEPT

Pulse modulation of the engine provides an alternate means of controlling the magnitude and the position of the thrust vector. In the pulse modulation mode, the impulse rate of the engine is altered by varying the amount of time that the engine is left on. The variation may be accomplished by use of an off-on valve operated by a solenoid. The primary reason for considering the pulsed concept was to determine the feasibility of using the Marquardt R4D 100-lb thrust engines which are used in pulse-mode to provide RCS thrust for the lunar module. Since the LFV engines are the longest-leadtime item, it is anticipated that the use of the R4D engines would lead to a reduction in development time.

Primary emphases in this Company-sponsored study were placed on assessment of the characteristics of the R4D engine, comparison of the ranging capability of pulsed-thruster and proportionately throttled concepts, determination of vibration-isolation requirements for pulse-mode operation, and the development of candidate design concepts. The following sections summarize the results of these studies.

### R4D Engine Characteristics

The characteristics of the Marquardt R4D engine are presented in Table 25. The "Specification" column presents the characteristics for which the engine is currently qualified; the "Demonstrated" column presents the regions where additional engine development has been accomplished.

In this study, emphasis was placed on the qualified capability in order to determine the feasibility of using the R4D engine without modification. This implied the following characteristics:

$$T_{\max} = 100 \text{ pound/engine}$$

Minimum on-time = 0.020 second (assumed to be twice the minimum pulse width)

Pulse frequency less than 5 cycles/second (allows 4 sorties at less than 10,000 pulses)

The specific impulse of the R4D engine is presented in Figure 90 as a function of percent of maximum thrust for operation at 6.7 cycles/second frequency and a mixture ratio of 2.0. These data were used in estimating flight-performance characteristics.

6.7 HERTZ  
2.0 M.R.

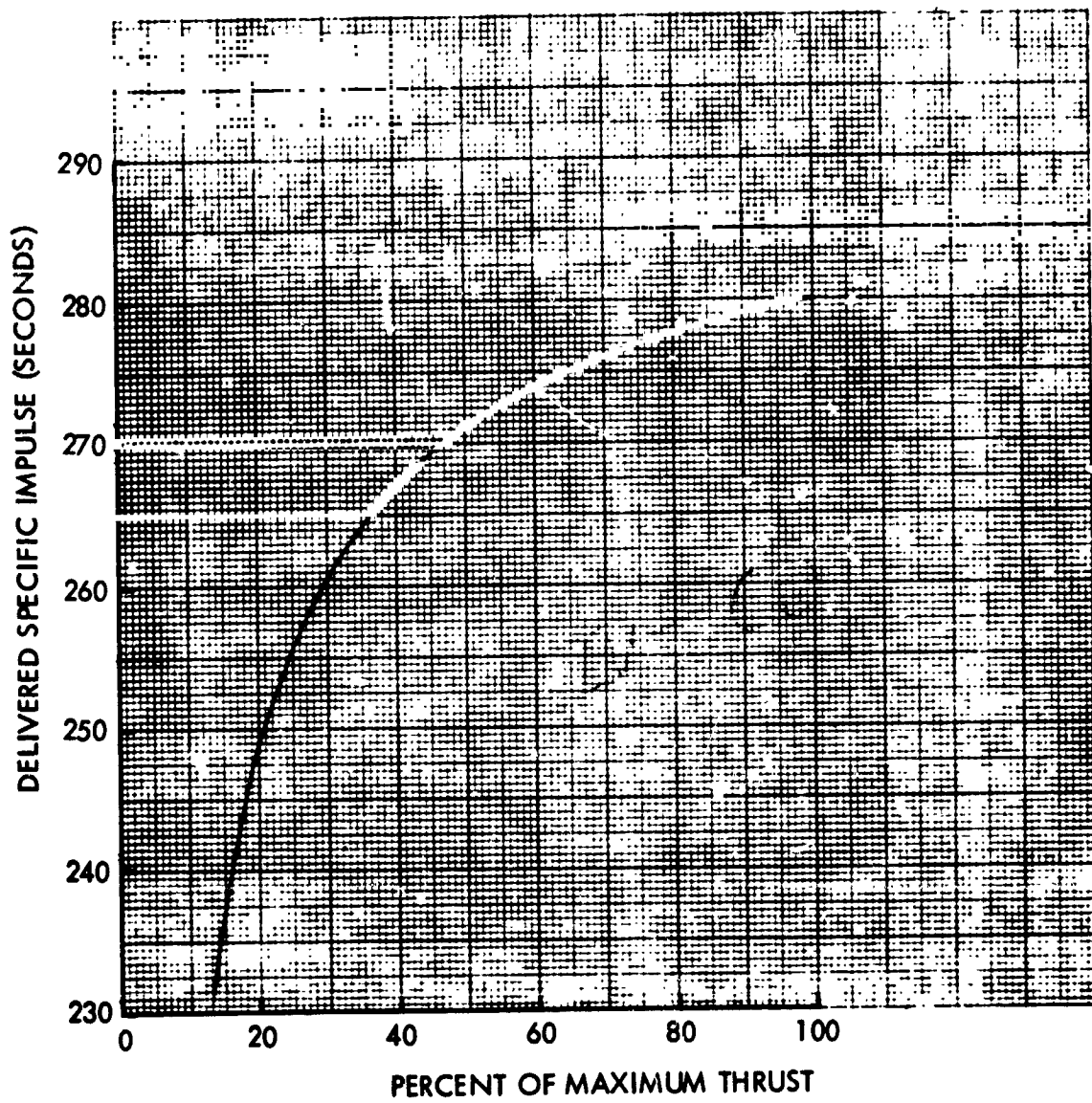


Figure 90. Pulse-Width Modulated Performance - R4D

Table 25. Marquardt R4D Engine Characteristics

| Parameter        | Specification           | Demonstrated    |
|------------------|-------------------------|-----------------|
| Thrust           | 100 lb                  | 25 lb to 170 lb |
| Propellants      | $N_2O_4$ /A-50 or MMH   | --              |
| Mixture ratio    | 2.0                     | 1.5 to 2.1      |
| Specific impulse | 276 sec                 | Up to 297       |
| Pulse width      | 0.010 sec to continuous | --              |
| Number of pulses | 10,000                  | 103,000         |
| Operating life   | 1,500 sec               | 31,000 sec      |
| Chamber pressure | 94 psia                 | --              |
| Area ratio       | 40 : 1                  | --              |
| Dry weight       | 4.9 lb                  | --              |
| Length           | 13.4                    | --              |
| Diameter         | 5.7                     | --              |

### Pulsed-Thruster Concepts

Two basic concepts were studied: (1) a concept which uses the pulsed thrusters to provide platform rotation for thrust-vector rotation; and (2) a concept which has thrusters canted both fore and aft which are pulsed to provide thrust-vector inclination and magnitude control while retaining a level platform.

Conceptual designs of these systems are shown in Figures 91 and 92 respectively. The tilting-platform concept has eight R4D thrusters located in a square platform (two per corner for engine-out redundancy). The level-platform concept also has eight R4D engines, four on each side of the vehicle. These are arranged in pairs pointing forward and aft at a 45 degree angle from the vertical.

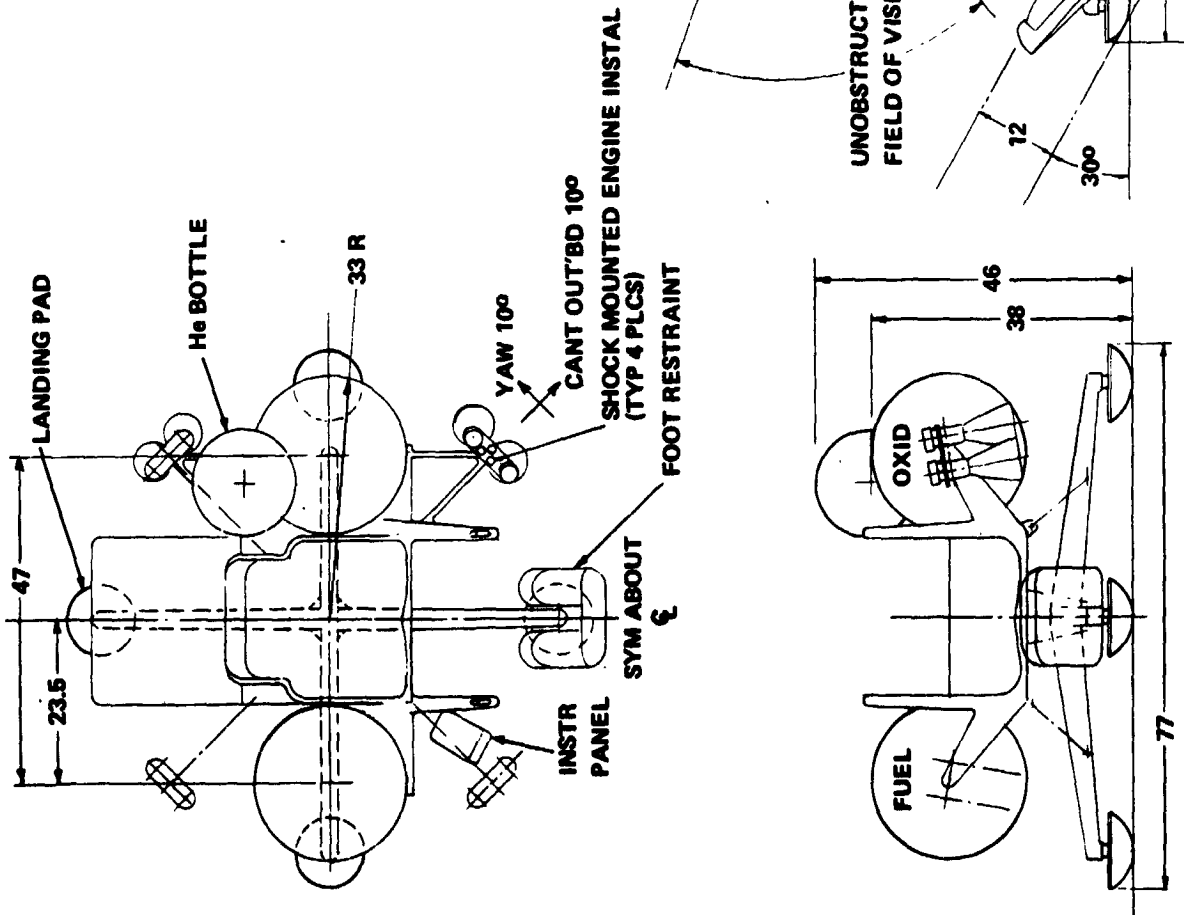
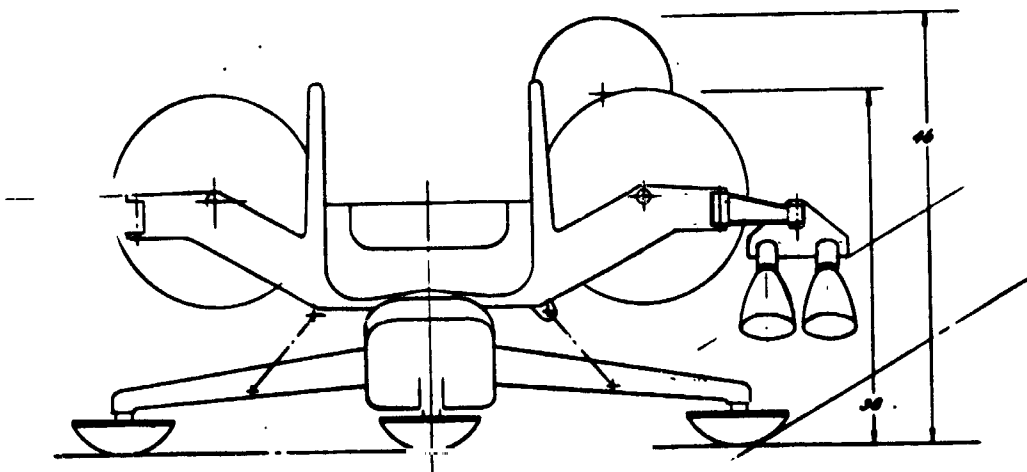
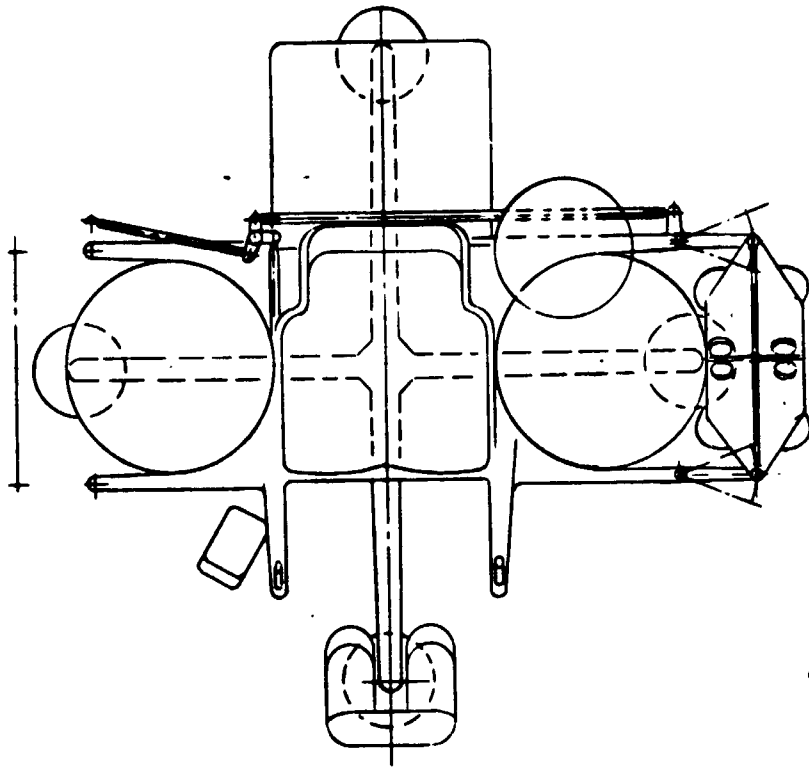
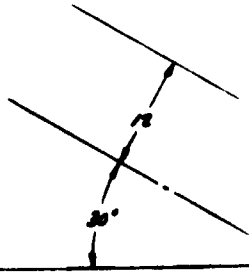


Figure 91. Tilting-Platform, Pulsed-Thruster Concept





WIDE VIEW  
FIELD OF



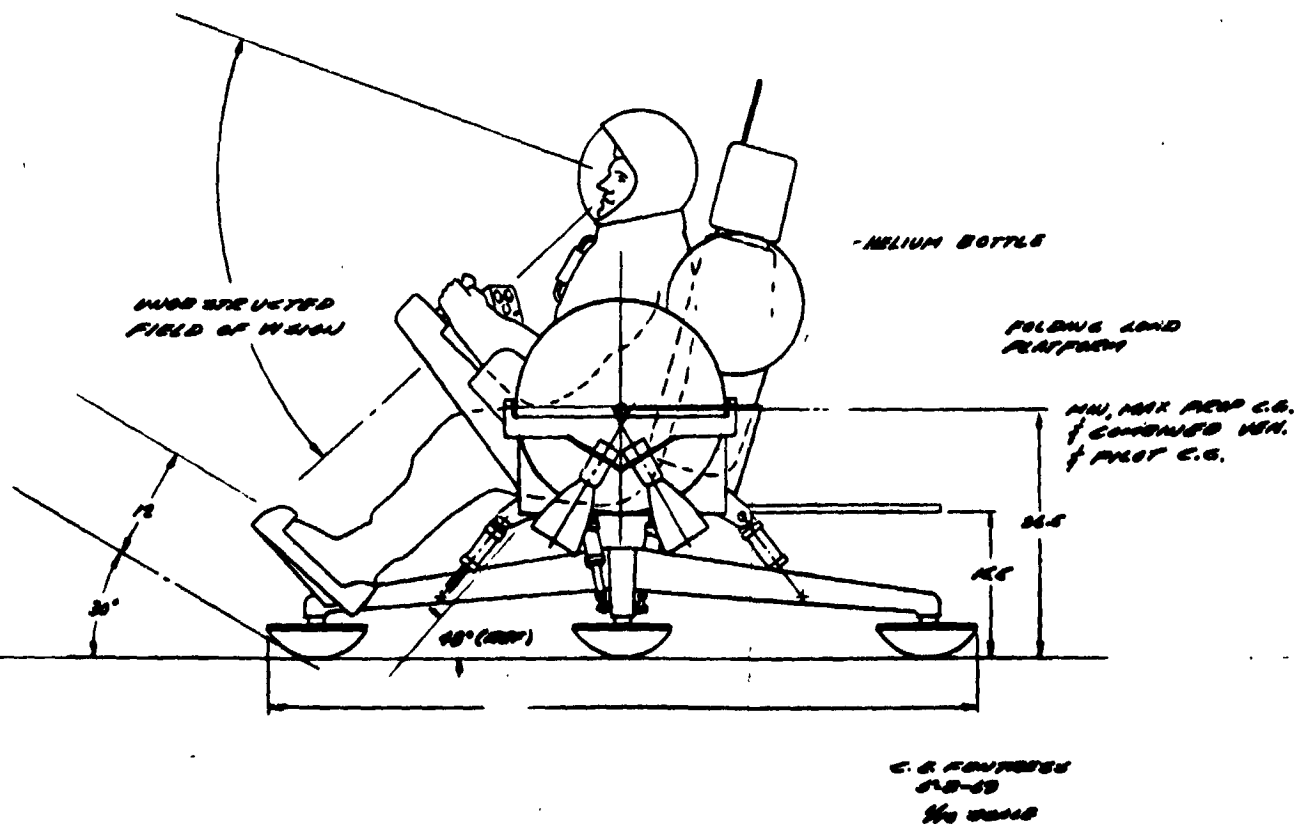


Figure 92. Level-Platform, Pulsed-Thruster Concept

Rotation of the tilting-platform concept in pitch and roll is achieved by differentially pulsing the forward and aft engines and the left and right engines, respectively. Yaw control is obtained (without pitch and roll coupling) by differential pulsing of the opposing-corner engines. The engines are canted at a 10-degree angle normal to the corner axis to provide a side component of thrust for yaw control. Control of thrust-vector magnitude is obtained by the pulsing of all engines.

Pitch-plane thrust-vector control of the level-platform concept is obtained by either moving the astronaut forward and aft or moving the engines forward and aft. The requirement to maintain a level platform results in an increase in the aft thrust level and a decrease in the forward thrust level as the c. g. is moved forward. This results in a component of thrust in the forward direction. Out-of-plane maneuvering can be accomplished by either yawing or by introducing small roll angles. Platform trim control is required to assure that platform attitude is maintained during flight. Both the level and tilting platform concepts are assumed to have stability-augmented systems with attitude-hold capability.

Both designs result in compact arrangements. As shown in Figures 91 and 92, with the tanks symmetrically located on the pitch axis, the center of gravity would not lie in the center with full fuel tanks, and differential throttling of the roll engine pairs would be required to achieve trim. Further study of the tank arrangement is required to determine arrangements which result in trim control boundaries. The payload is also located off center, behind the seated astronaut, causing a similar pitch imbalance. The resulting concept has a very low center of gravity and a low seat for easy ingress and egress.

#### Engine-Induced Vibration

A study was conducted to determine the effects of engine-induced vibration on the LFV structure and pilot. It was found that vibration isolation will be required in most cases to reduce the levels to those stipulated as tolerable for the pilot (Reference 24). If the engines are operated in such a manner that the vibration-excitation frequency is always at least twice the basic engine-pulse rate, the vibration forces can be reduced to tolerable levels by simple spring isolation on each engine or on the pilot seat.

The configuration used in this study included a structural frame holding a pilot seat at the center, a propellant tank on either side of the seat, an engine cluster (4 engines each) outboard of each tank and a cargo platform behind the seat. Subsystem components were considered to be distributed to achieve mass balance, and the main frame was shock isolated from the landing gear assembly.

For the purposes of the study, the structural main frame was sized to withstand an 8-g landing. A schematic of the frame and structure stiffness in each section is shown in Figure 93. Based on these data, the structure will have a vertical resonance (approximately a free-free beam mode) at 35 hertz and a horizontal resonance at 20 hertz. A schematic of the assumed engine configuration is shown in Figure 94 along with engine thrust and overall LFV weights used in the study.

An evaluation of several possible engine-firing sequences, which would provide the lift thrust required for maximum and minimum vehicle weights, was made to estimate the amplitude and frequency characteristics of the vibratory forces from the pulsing thrusters. It was determined that the basic vibration-excitation frequency in the vertical direction was  $nR$ , where  $R$  is the basic engine pulse rate and  $n$  is the number of separate engine firing lag times contained within one period at the basic pulse rate ( $n$  varies from 1 to 8). That is, with simultaneous ignition and termination of all engines,  $n = 1$ ; if the eight engines were individually ignited at equally spaced intervals within one basic firing period,  $n = 8$ . The frequency of horizontal vibration and pitch, roll, and yaw forces will be some integral fraction of  $nR$ , dependent on the engine firing sequence. Table 26 summarizes the results of the study.

The amplitude of vibration forces will depend on the time phasing of engine ignition and the overlapping of engine-firing time to accumulate the desired overall lift thrust. For example, with lunar gravitational acceleration on a full-weight vehicle, a time-averaged lift thrust of 217 pounds is required for hovering ( $T/W = 1.0$ ). If all eight engines were simultaneously ignited, the total lift thrust would be 640 pounds, and the required engine on-off time ratio would be 0.34. Total thrust decay would occur prior to engine reignition. This results in a peak-to-peak excitation force in the vertical direction on the vehicle of 640 pounds at the basic engine pulse rate ( $R$ ).

If the vehicle structure is structurally stiff at the frequency of engine ignition (i. e., the first structural resonance is greater than three times the engine pulse rate), a peak-to-peak excitation force of 640 pounds would cause a vibration level of 0.25 g (peak) in a full-weight vehicle and 0.48 g (peak) in a minimum-weight vehicle at the engine pulse rate of possibly 3.5 to 5 hertz. While these vibration levels are easily accommodated structurally, data (Reference 24) indicate that levels in excess of 0.07 g, in the frequency range from 3 to 25 hertz, will impede pilot performance.

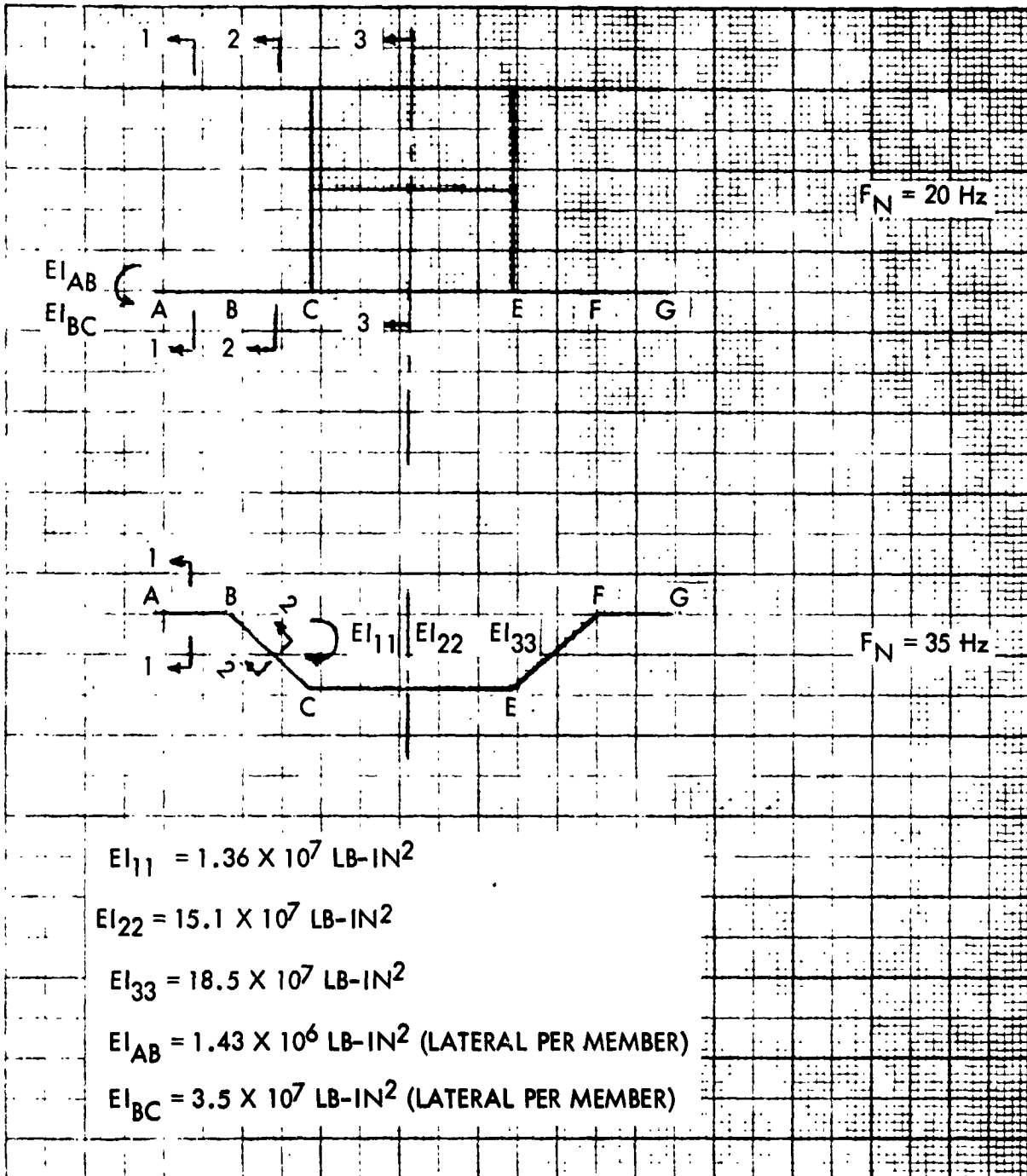
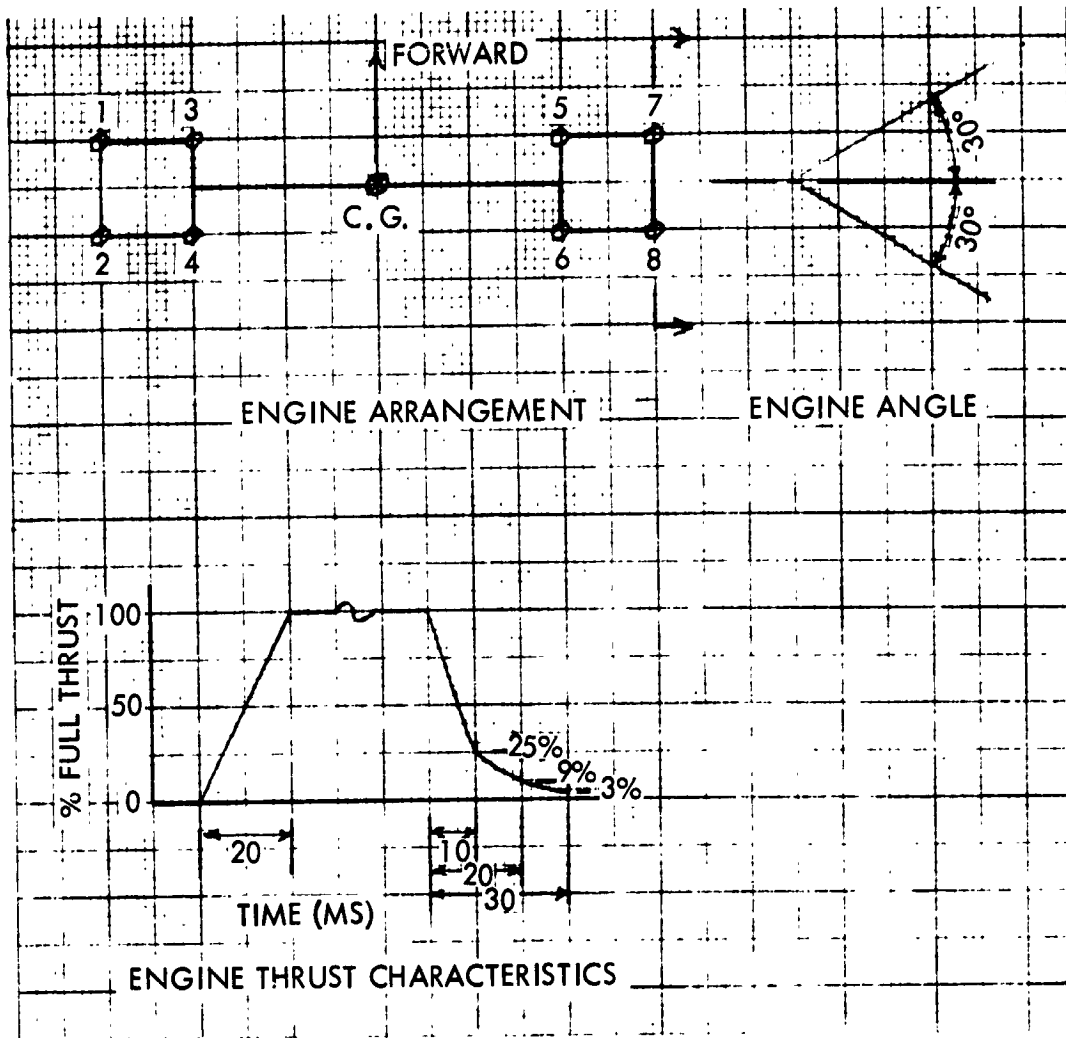


Figure 93. LFV Pulsed Thruster, Body Frame Schematic



ENGINE: 92-LB THRUST (80-LB LIFT, 46-LB HORIZONTAL THRUST)

|           |              | EARTH   | MOON   | SLUGS |
|-----------|--------------|---------|--------|-------|
| LFV MASS: | MAX          | 1300 LB | 217 LB | 40.4  |
|           | MIN          | 670 LB  | 112 LB | 20.8  |
|           | PILOT & SUIT | 380 LB  | 63 LB  | 11.8  |

(MAX & MIN INCLUDE PILOT & SUIT)

| TOTAL LIFT REQMT'S     | MAX WT | MIN WT | T/W |
|------------------------|--------|--------|-----|
| LIFT-OFF               | 304 LB | 156 LB | 1.4 |
| HOVER & FORWARD MOTION | 217 LB | 112 LB | 1.0 |

Figure 94. Engine and Mass Data for LFV Pulsed Thruster

**Table 26. Vibration Isolation Versus Engine-Operation Mode.**

| Engine Sequence                        | Maximum Oscillating Force (p-p) (lb) | Oscillating Frequency | Max Osc Accel <sup>1</sup> (p-p) (ft/sec <sup>2</sup> ) | Isolation System Requirements |              |                             |         |             |         |
|--|--------------------------------------|-----------------------|---|-------------------------------|--------------|-----------------------------|---------|-------------|---------|
|  |                                      |                       |   | Seat                          |              | Engine Cluster <sup>3</sup> |         | Each Engine |         |
|  |                                      |                       |   | K (lb/in.)                    | D (p-p)(in.) | K (lb/in.)                  | D (in.) | K (lb/in.)  | D (in.) |
| All                                    | 640                                  | R                     | 30.8  | 30                            | 21           | 50                          | 6.2     | 13          | 7       |
| 1, 2, 7, 8-2, 3, 4, 5, 6<br>No overlap | 320 (Lift)                           | 2R                    | 15.4  | 210                           | 1.5          | 291                         | 0.55    | 173         | 0.53    |
| 2, 8-1, 7-4, 6-3, 5<br>Overlap         | 148 Vector                           | 4R                    | 7.1   | 1575                          | 0.094        | 2630                        | 0.05    | 656         | 0.14    |
| 2-8-1-7-4-6-3-5<br>Overlap             | 80 (Eng)<br>40 (Seat)<br>Vector      | 4R<br>8R              | 1.92  |                               |              | None required               |         |             |         |
| 2, 8-4, 6<br>Overlap                   | 184 Vector                           | 2R                    | 8.85  | 328                           | 0.056        | 1100                        | 0.085   | 550         | 0.167   |

**Notes:**

- 1 Pilot tolerance 4.5 foot/second<sup>2</sup>, 2.8 - 25 hertz
- 2 R = 3.5 hertz, M = 20.8 slugs (minimum weight - structure = 9 slugs; pilot = 11.8 slugs)
- 3 Isolation of engine cluster rejected because of attitude instability.

For an engine pulse rate (R) of 3.5 hertz and a minimum-weight vehicle, the vehicle vibration must be attenuated by a factor of 0.073. This would require a lightly damped isolation system ( $c/cc \leq 0.02$ ) with a natural frequency of 1.25 hertz. If the system were used to isolate the engine clusters from the main frame, the spring rate for the system would have to be 50 pound/inch and permit a total vertical displacement in excess of 6 inches. Such a system would permit large rotation of the engine mounting plate, and resultant thrust vector, whenever the burn times of fore and aft engines of a cluster are different. If the engine mounting plate were rigidly attached to the main frame and each engine independently isolated by a spring-guide system, the spring rate for each system would have to be 13 pound/inch with a free displacement length of 7 inches. Isolation of the pilot seat, instead of the engines would require a system with a spring rate of 30 pound/inch and 21 inches displacement. None of these isolation systems is considered practical.

While the spring rates and displacement requirements for lightly damped isolation systems are linearly related to the amplitude of applied forces, they are dependent on the square of the frequency. Therefore, a review was made of engine operational modes that would satisfy thrust requirements for various conditions but would effectively increase the frequency of vibration excitation to the LFV structure. Since only 320 pounds of lift thrust is required for a  $T/W = 1.4$  on a full-weight vehicle, the combined lift thrust from four engines is all that is required at any time. This will permit an engine-firing sequence of four engines firing alternately. For hovering a minimum-weight vehicle, the maximum oscillatory force will be 320 pounds (p-p) at a frequency of  $2R$  as shown in Figure 95. The amplitude of oscillatory forces can be further reduced and the resultant excitation frequency increased by staggered ignition of engine pairs (Figure 96) or individual engines (Figure 97). The data on Figure 97 indicate that staggered ignition of individual engines results in roll and yaw forces which will have to be counteracted by the control system.

The fluctuation of lift and forward thrust forces for a maximum-weight vehicle is shown in Figure 98. While four engines are used to attain the maximum average lift thrust of 217 pounds, the ignition of engines 2 and 8 are staggered with that of engines 4 and 6 so that the excitation frequency is  $2R$ . The maximum-vector force (30 degrees to vertical) for this condition is 160 pounds (p-p).

Of the probable operating modes, the staggered four-engine operation of Figure 95 will give the most severe oscillatory forces (384-pound vector, peak-to-peak) at the lowest effective frequency ( $2R$ ). The isolation of the engine cluster is not considered feasible because of stability problems; however, the isolation of the seat or of individual engines is reasonable.



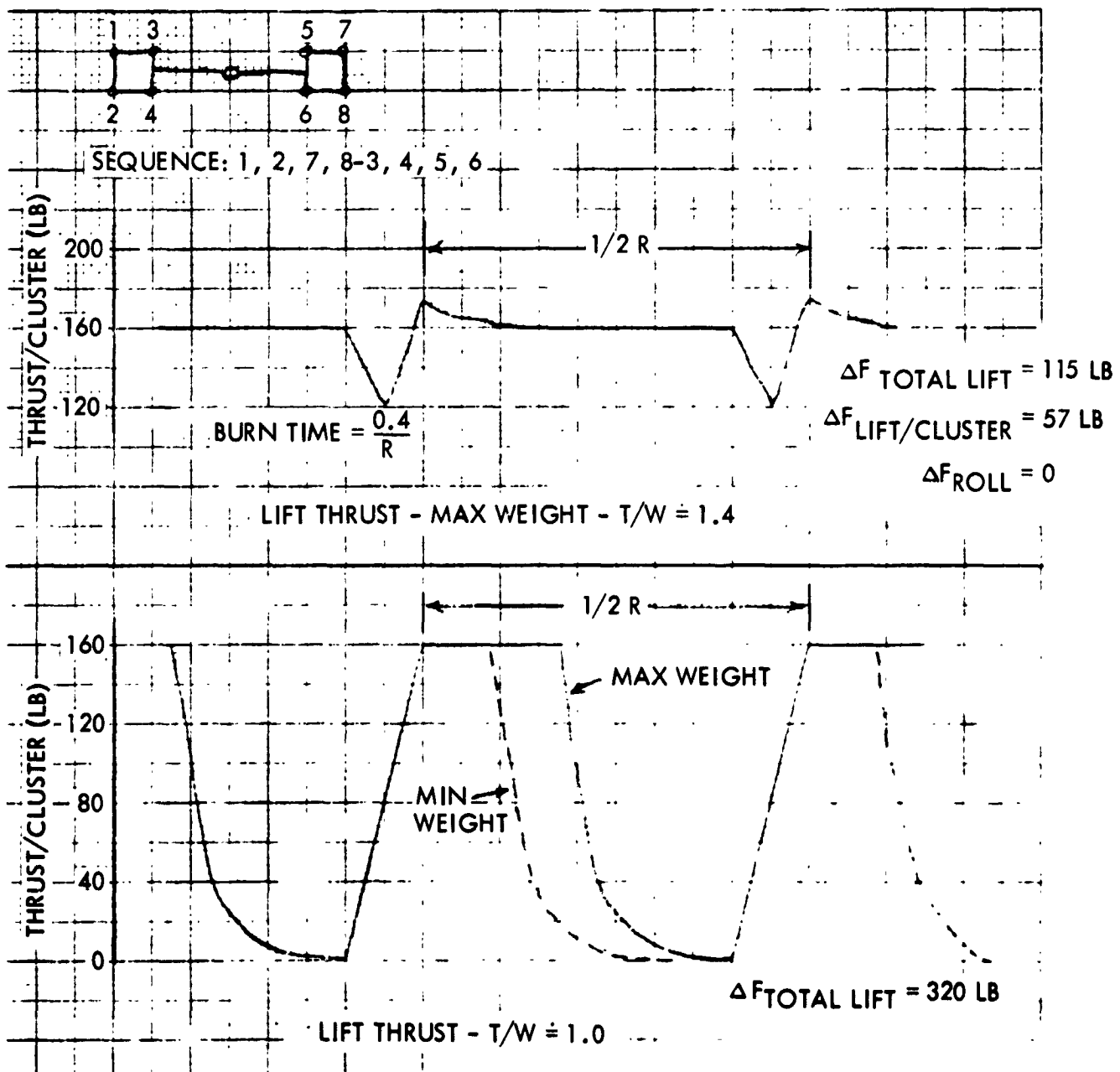


Figure 95. LFV Pulsed Thruster, Fluctuation of Lift Forces With Staggered Ignition of Four Engines

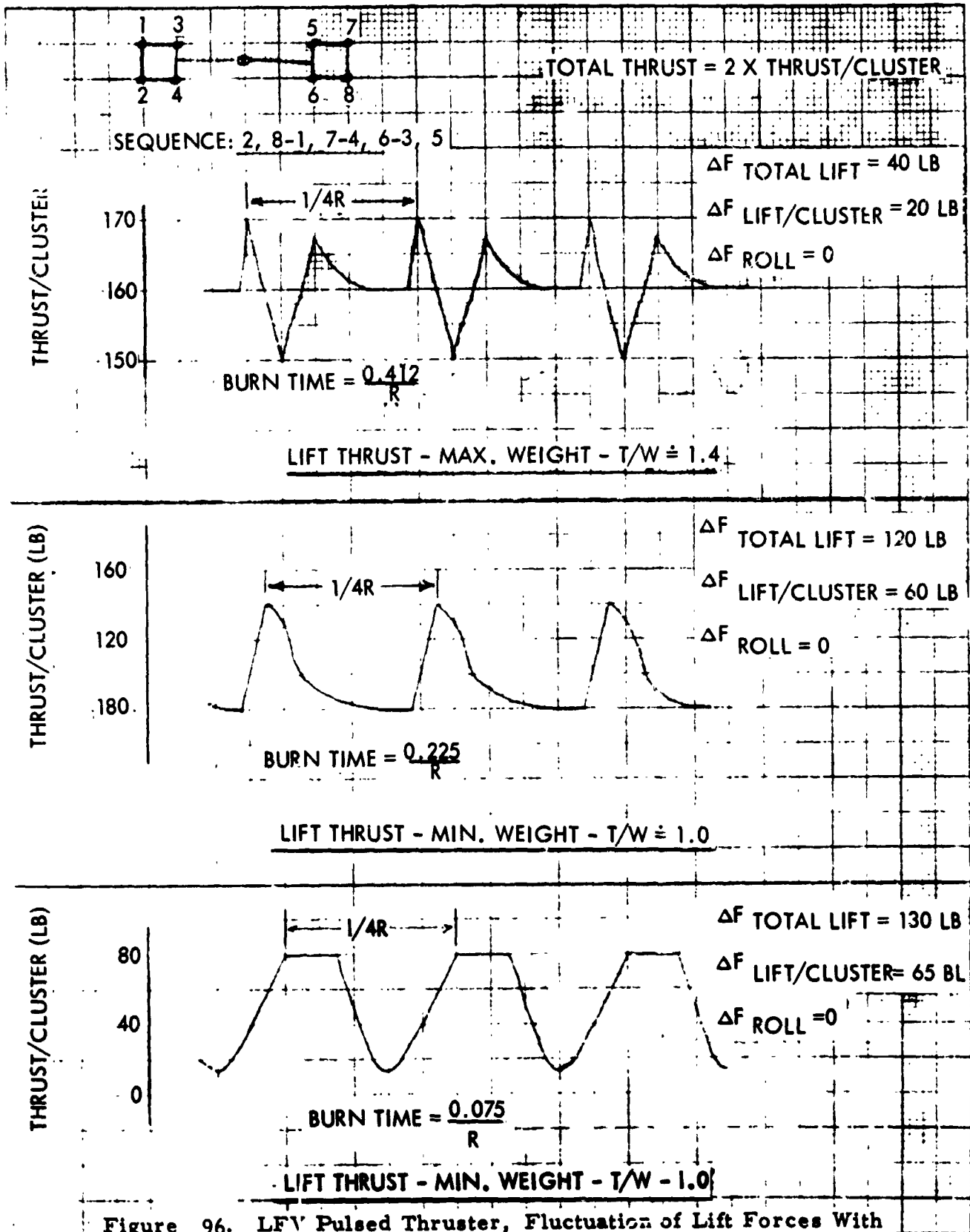


Figure 96. LFV Pulsed Thruster, Fluctuation of Lift Forces With Staggered Ignition of Paired Engines

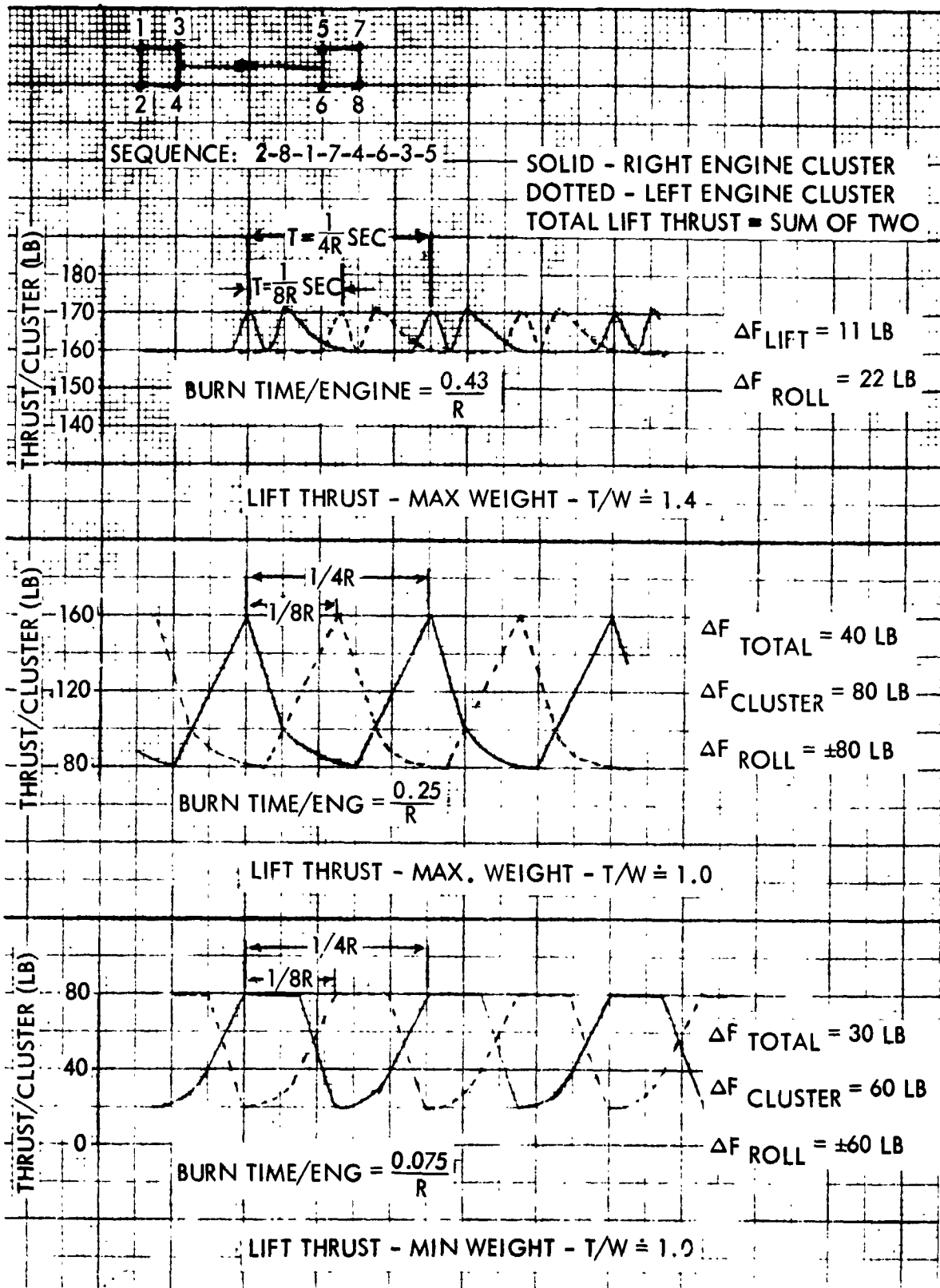


Figure 97. FV Pulsed Thruster, Fluctuation of Lift Forces With Staggered Ignition of Individual Engines

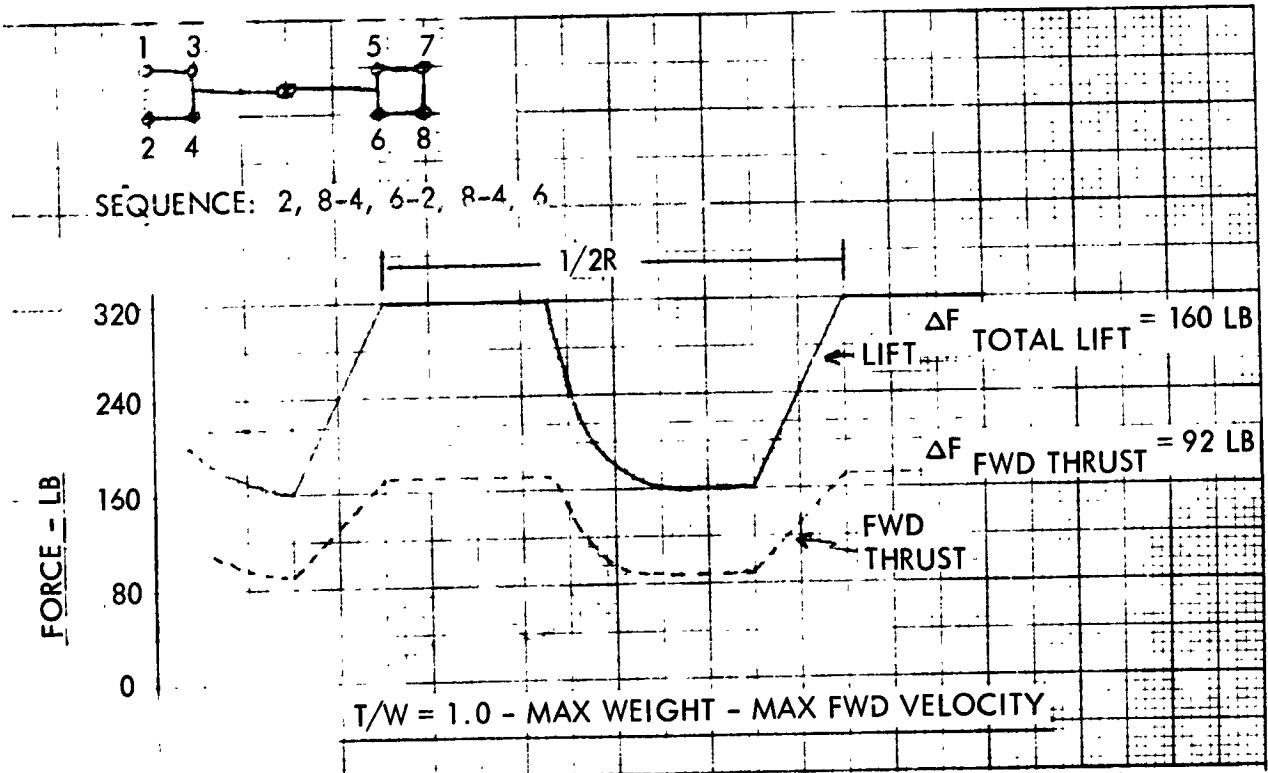


Figure 98. LFV Pulsed Thruster, Fluctuation of Lift and Forward Thrust Forces With Staggered Ignition of Paired Engines

The seat-isolator system would require a spring rate of 210 pounds/inch and allowable displacement of 1.5 inches (p-p). The engine isolators would require guided, in-line coil springs with a stiffness of 173 pounds/inch and allowable displacement of 0.53 inches (p-p).

With either of these isolator systems, the vibration experienced by the pilot would be equal to, or less than, the tolerable 0.07 g for most operating modes. If, for emergency cases, it were necessary to operate engines so that the vibration frequency was R, the vibration experienced by the pilot would increase to 0.28 g. This level is the published intolerable, or stressed limit, and pilot performance will be degraded after short periods of exposure.

Based on available engine operating data and estimated structural characteristics, it has been assumed during this study that there would be no coupling between the pulsating engines and structural vibration modes. This assumption is logical when only the fundamental excitation and response frequencies are considered. Inspection of the force-time histories in Figures 95 through 98 indicates that the oscillatory forces have considerable harmonic content which will excite resonances in either, or both, primary and secondary structure. These higher frequency vibrations, like the

structural response to landing shocks, were not considered critical to the pilot and have not been evaluated. Higher frequency vibration of this type is critical to subsystem performance and will have to be analyzed if the pulsed engine concept for the LFV is adopted.

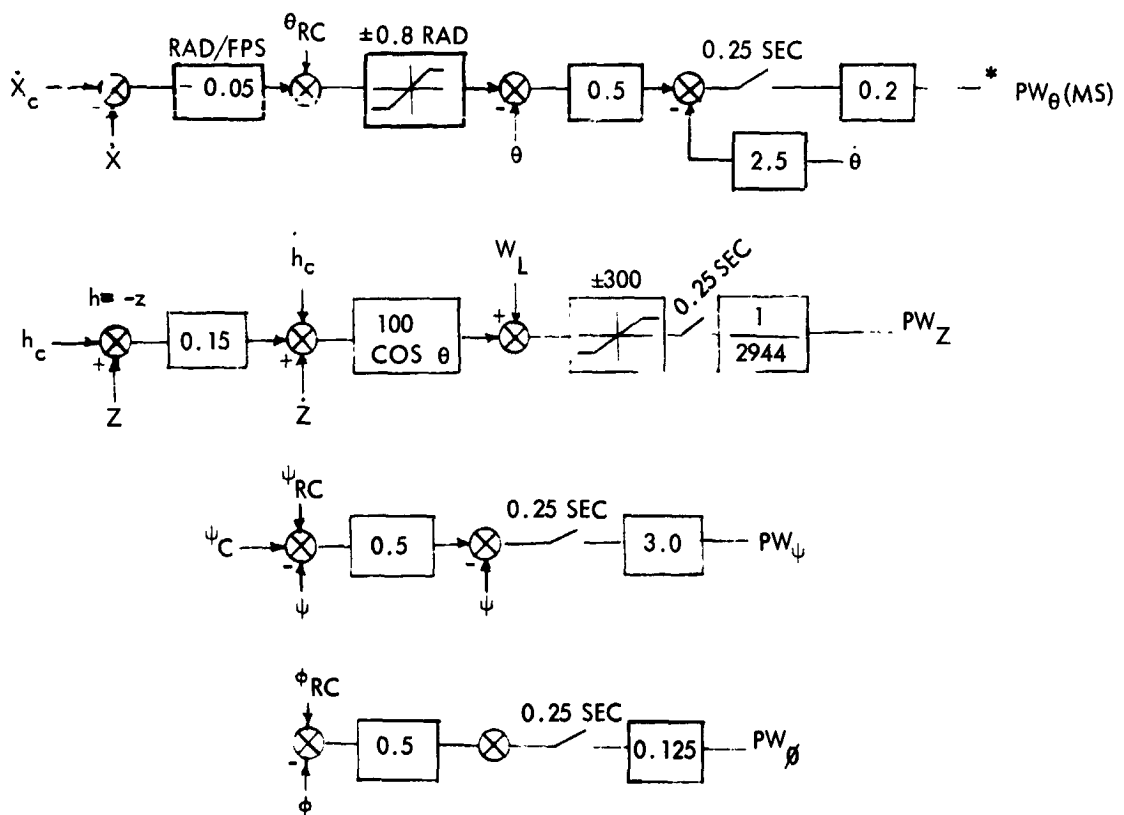
### Control System Characteristics

In addition to the control-system studies presented in this report, NASA/MSD personnel conducted studies which are not contained in this report. Space Division studies were concentrated on the dynamics of tilting-platform flight; the NASA studies concentrated on the dynamics of level-platform flight.

A fully augmented control system was developed and mechanized in a 6-degree-of-freedom digital program to demonstrate the feasibility of a pulsed-jet tilting-platform lunar flying vehicle. Duty cycles, attitude-limit cycle amplitudes, vertical-trajectory oscillation amplitudes, and typical ranging-performance data were obtained. The closed-loop control systems are depicted in Figure 99. Pulse-width commands were computed at 0.25-second intervals to insure that no engine exceeded 10,000 cycles, the present specification on the Marquardt R4D engines. Even though this control frequency (4 cycles per second) may seem low for attitude control, good results were obtained even with a large center-of-gravity uncertainty. Also of concern was the vertical steady-state oscillation produced by pulsed jets. This effect was reduced to less than 0.7 inch by staggering the firing times. Each jet was delayed 10 milliseconds in the following order: A<sub>1</sub>, C<sub>1</sub>, B<sub>1</sub>, D<sub>1</sub>, A<sub>2</sub>, C<sub>2</sub>, B<sub>2</sub>, D<sub>2</sub> (Figure 100). The total delay between the first jet, A<sub>1</sub>, and the last, D<sub>2</sub>, was 70 milliseconds. Total firing times were constrained to 160 milliseconds out of each 250-millisecond interval. This was necessary to obtain proper operation of a jet-delay simulation subroutine and is not considered a necessary design feature. No doubt, some performance penalty was introduced; however, this restriction would be eliminated in any future simulation work and, of course, in the design of the airborne-computer logic.

The altitude and downrange-velocity commands were programed as functions of time. Those used to generate the trajectory data of Figures 101 through 104 are superimposed on the altitude and velocity timelines. Rate and attitude-time histories for zero center-of-gravity error are shown in Figure 105. The effect on limit-cycle amplitude of a 0.05-foot center-of-gravity error in x, y, and z axes may be seen by comparing Figures 105 and 106 through 108.

PULSED LFV CONTROL SYSTEM



- \*
  - PW's ARE PULSE WIDTH COMMANDS WHICH ARE SUMMED FOR EACH JET
  - $\theta_{RC}$ ,  $\psi_{RC}$ ,  $\phi_{RC}$  ARE MANUAL ROTATION COMMANDS USED FOR RETRIMMING ONLY IN A FULLY AUGMENTED SYSTEM
  - $W_2$  IS THE VEHICLE LUNAR WEIGHT

Figure 99. Control System for Pulsed LFV.

PULSED LFV ENGINE GEOMETRY  
8 ENGINES

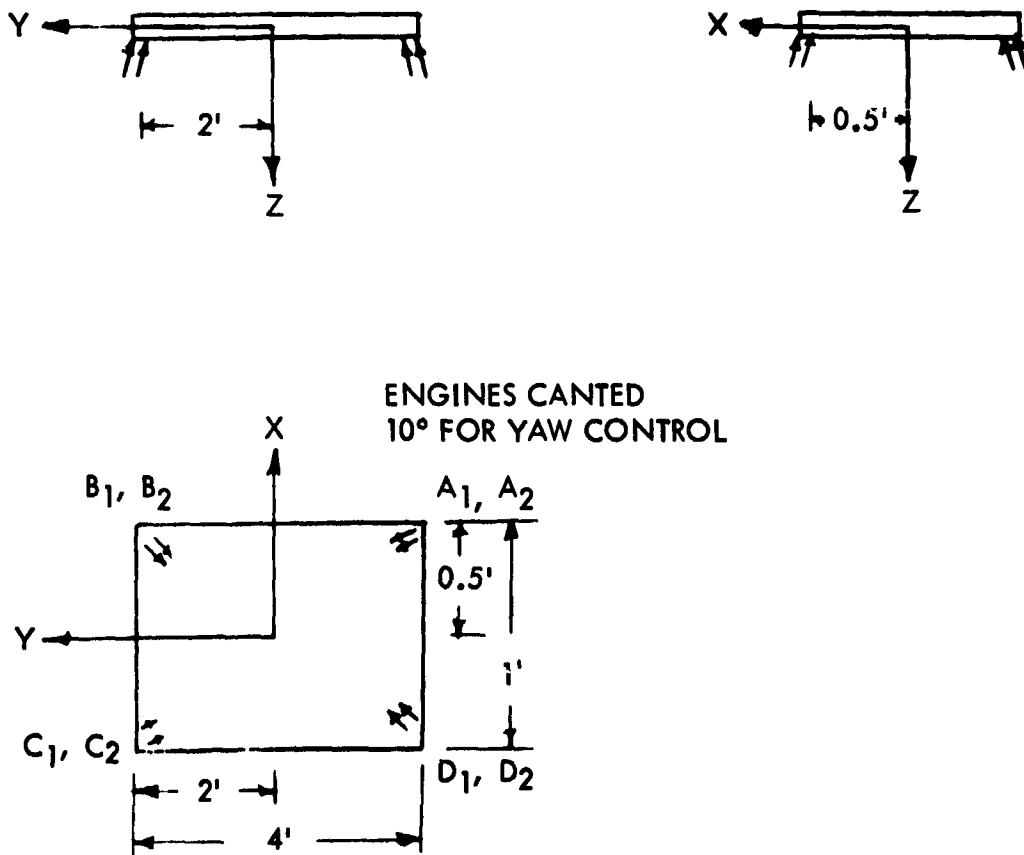


Figure 100. Engine Geometry for Pulsed LFV, Eight Engines

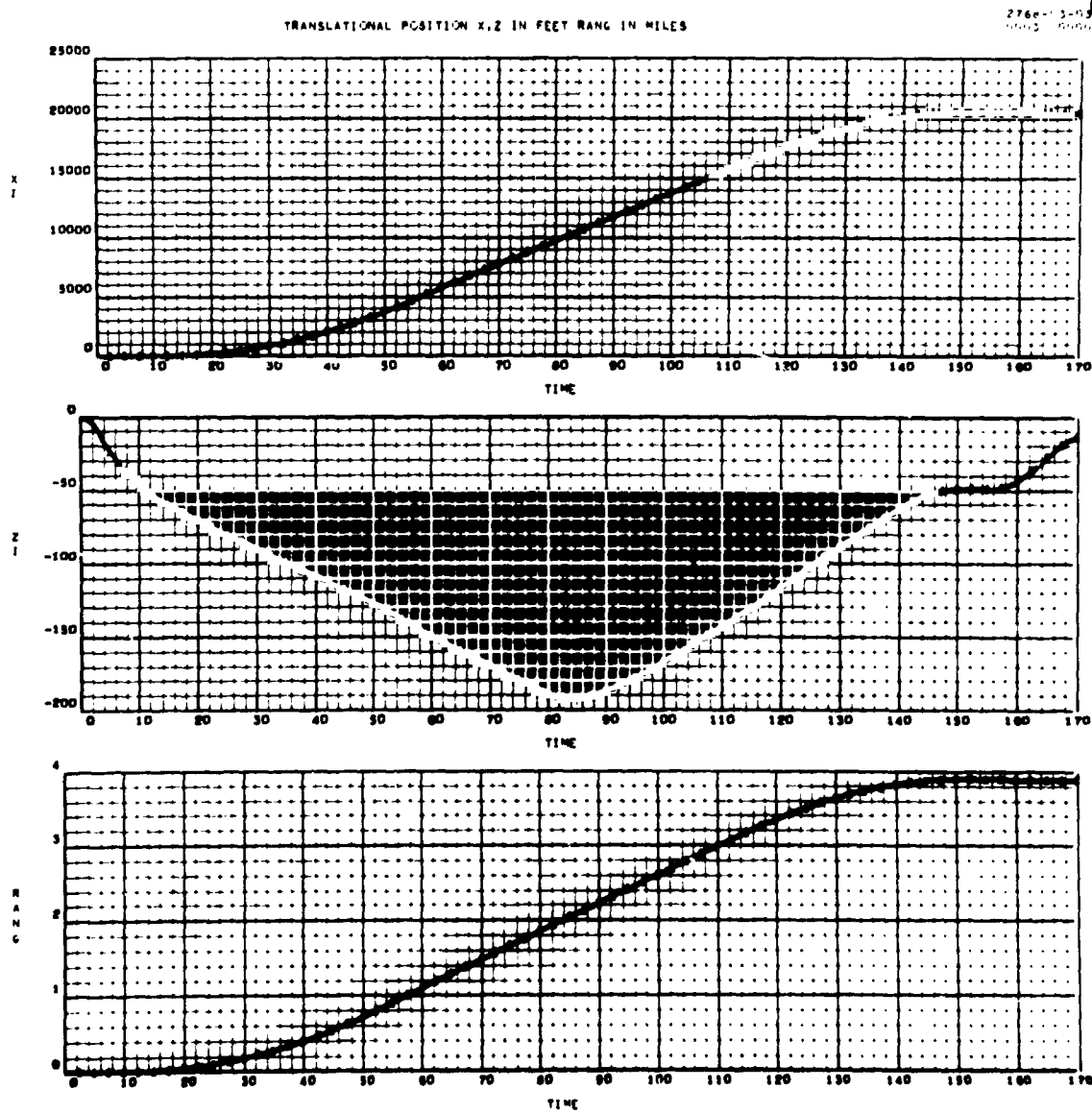


Figure 101. Translational Dynamics



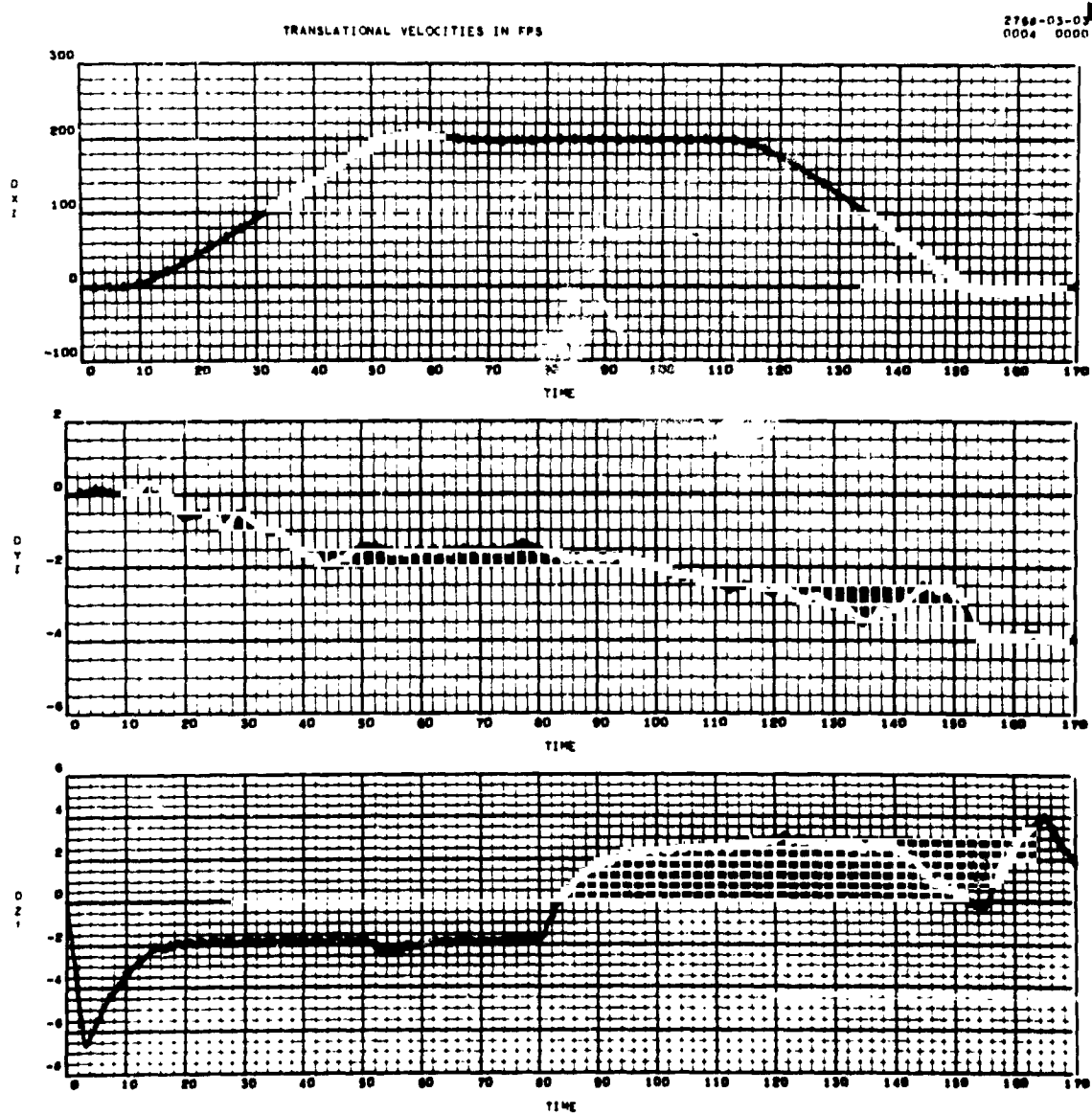


Figure 102. Translational Dynamics and Propellant Consumption

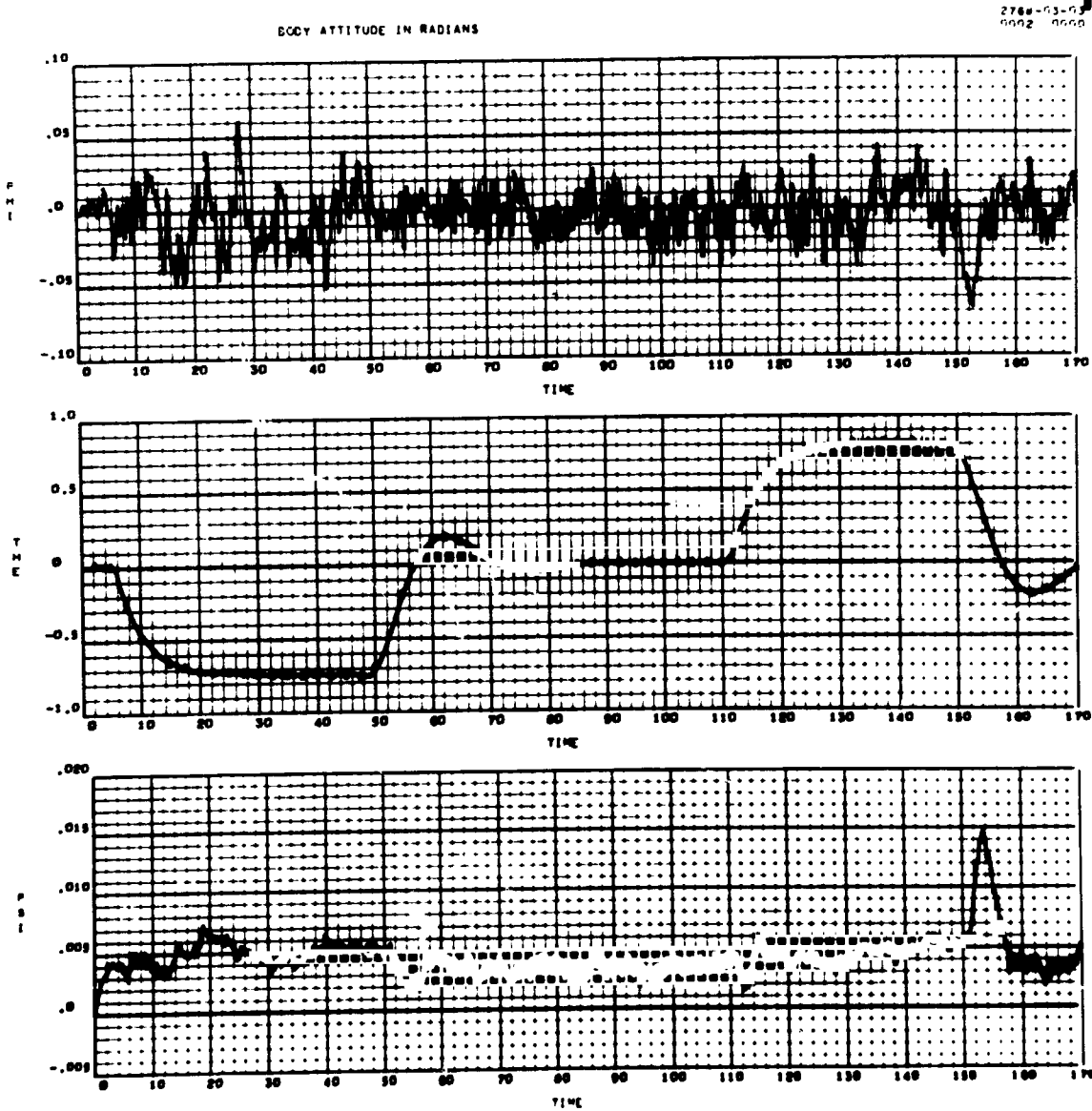


Figure 103. Rotational Dynamics, Body Attitude in Radians

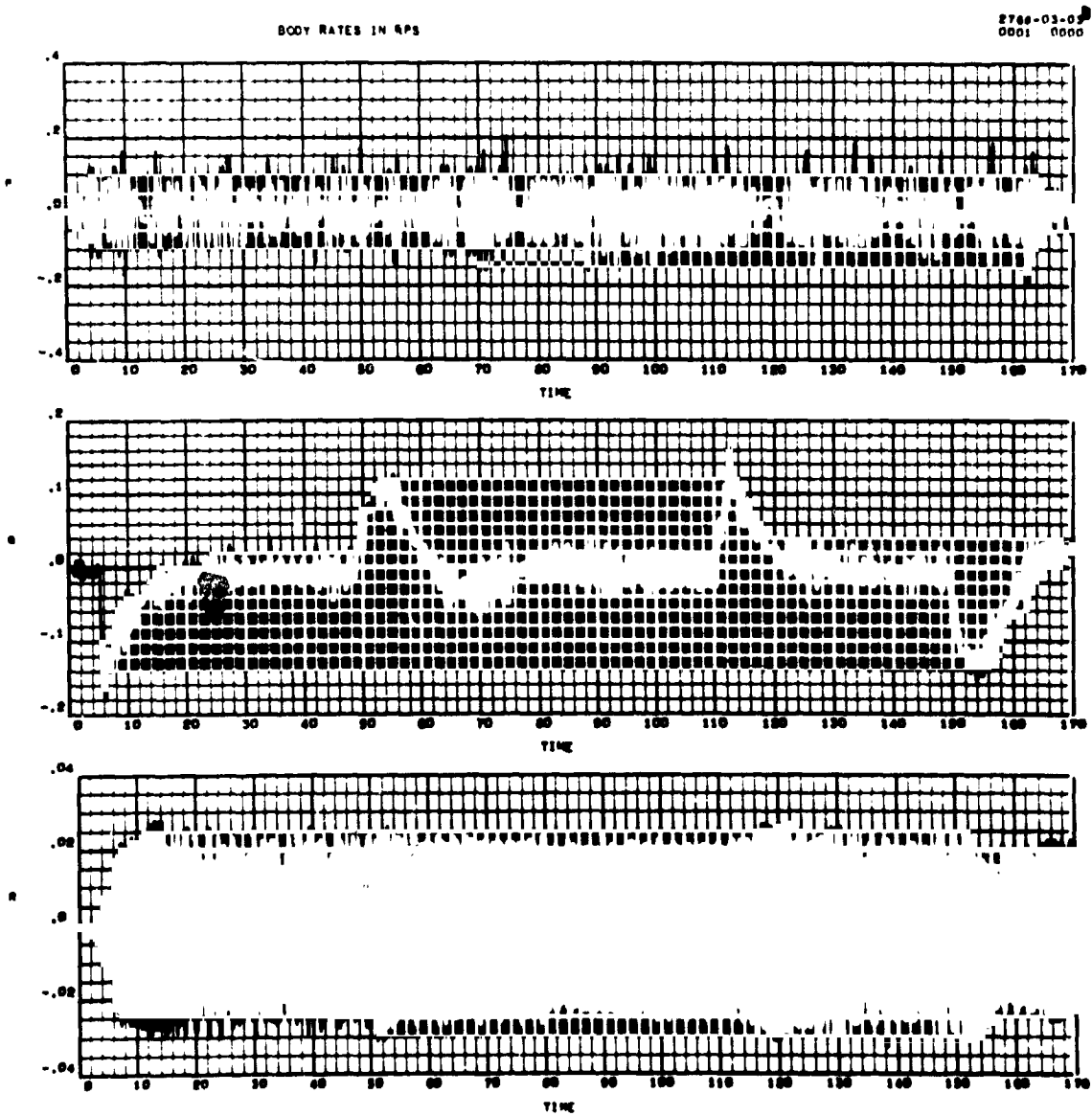


Figure 104. Rotational Dynamics, Body Rates in RPS

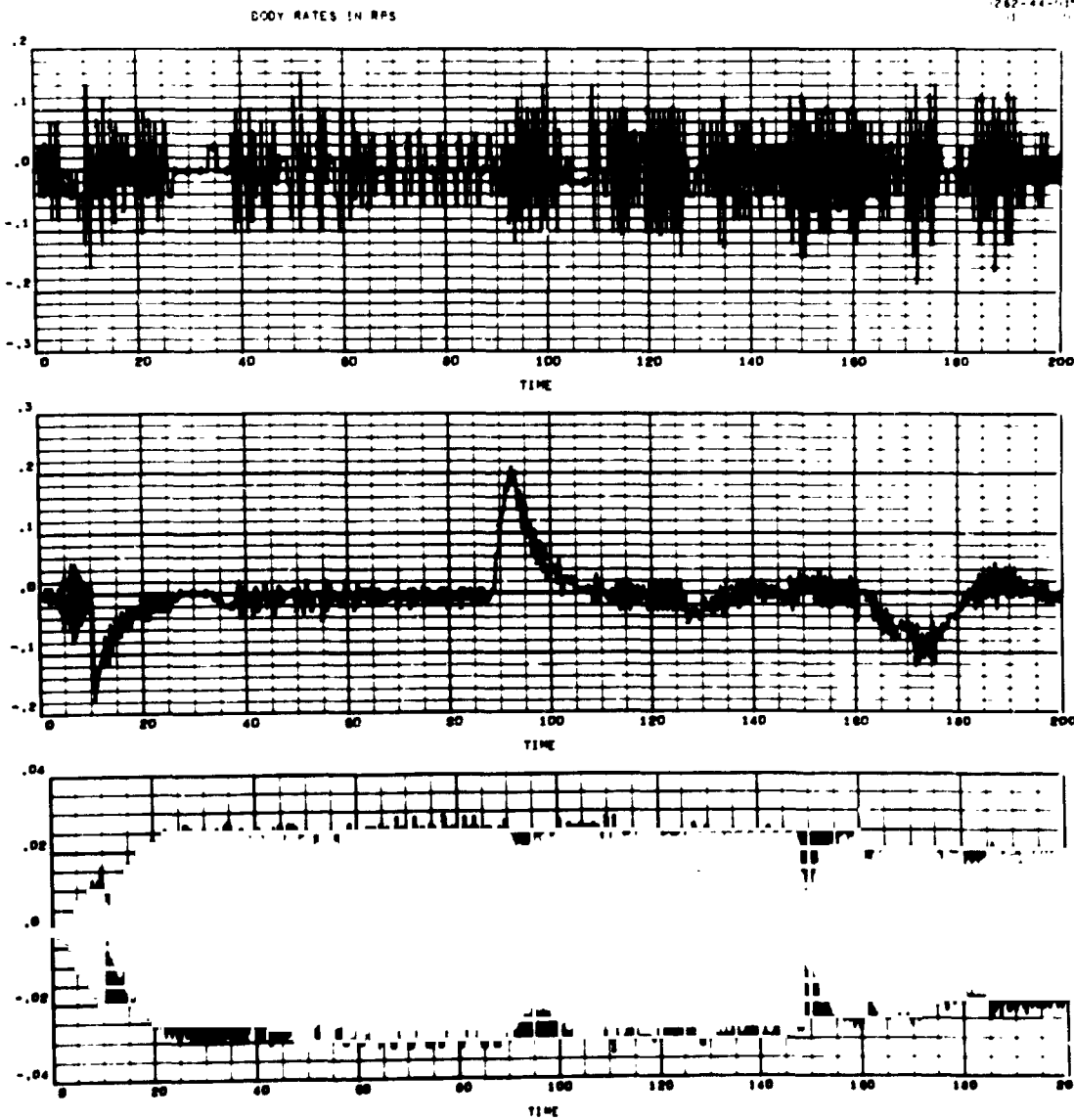


Figure 105. Limit Cycle Amplitudes, Body Rates in RPS

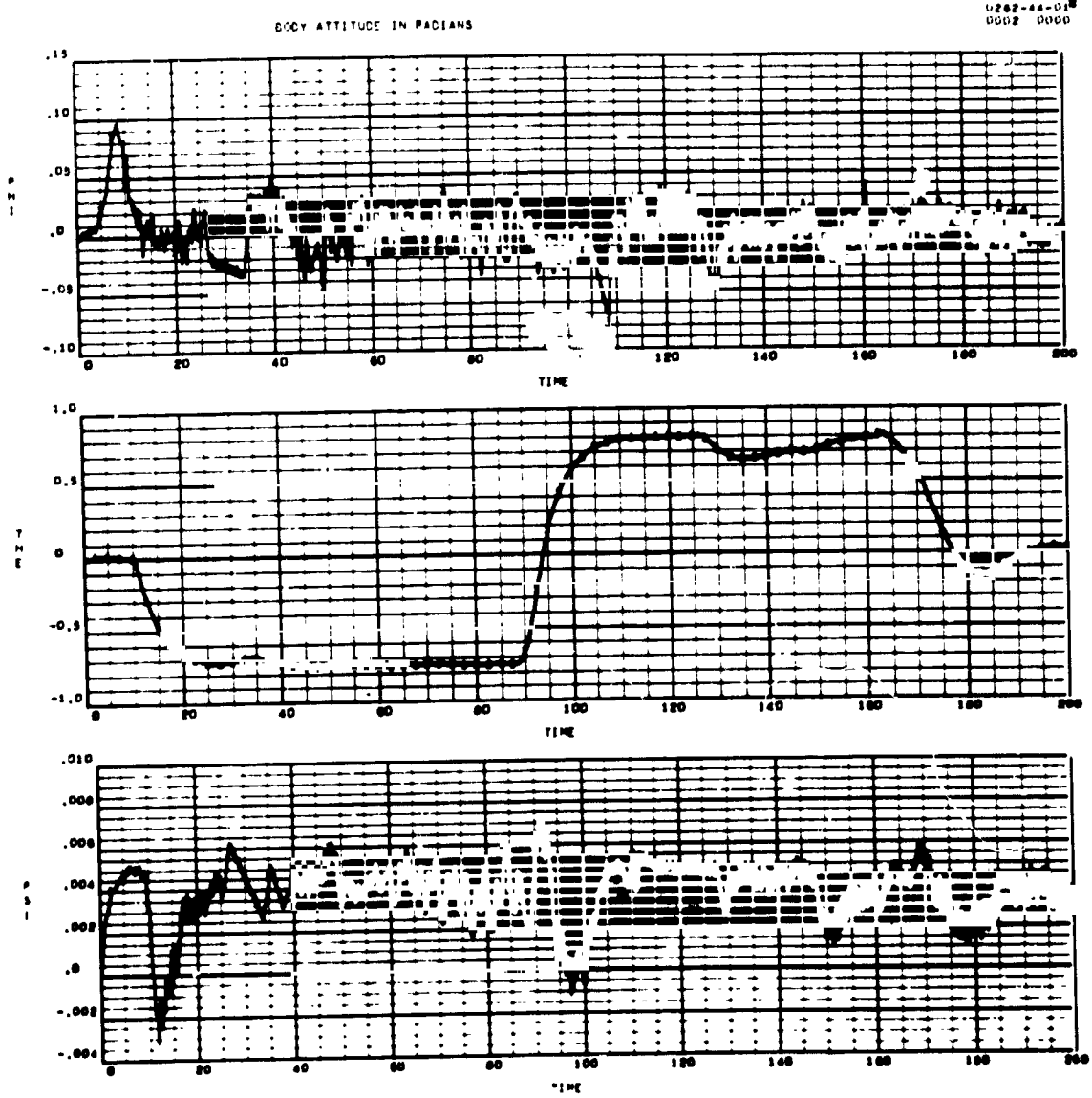


Figure 106. Limit Cycle Amplitudes, Body Attitude in Radians

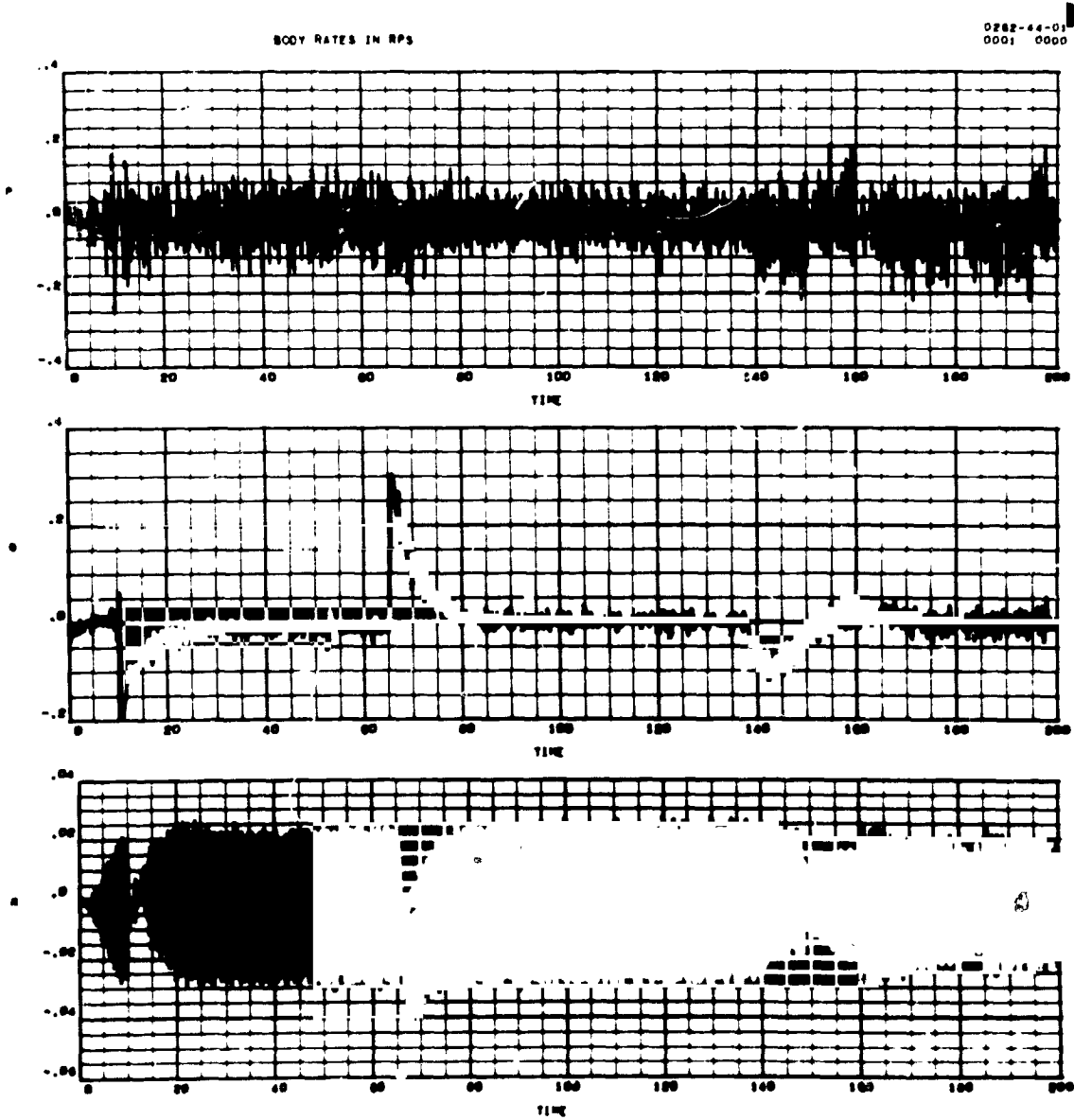


Figure 107. Effect of C. G. Error on Limit Cycle Amplitudes, Body Rates in RPS

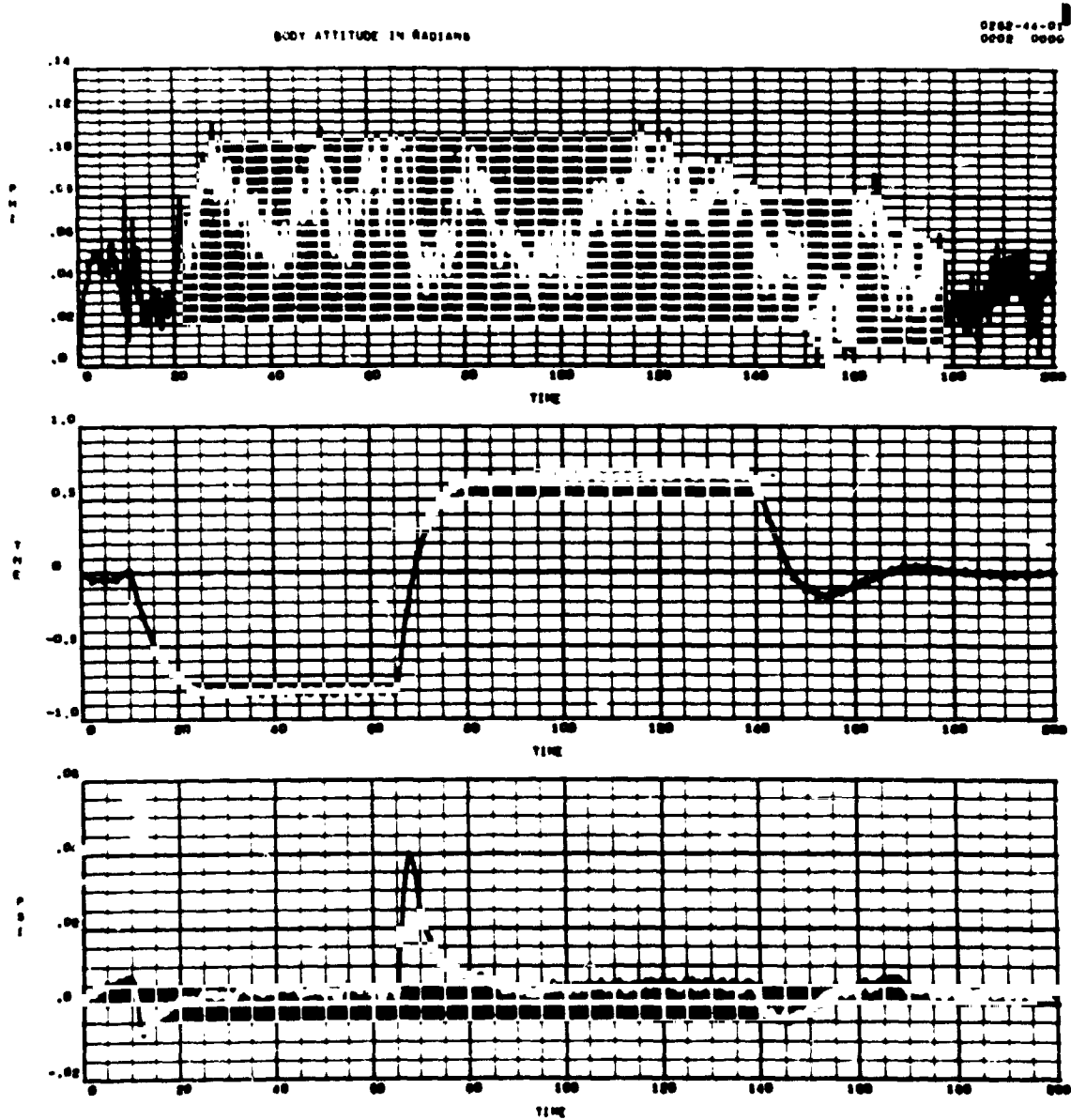


Figure 108. Effect of C. G. Error on Limit Cycle Amplitudes, Body Attitude in Radians

Several conceptual levels of sophistication for an augmented flyer appear feasible. Some possibilities are as follows:

1. Attitude rate would require rate gyros and some electronics (possibly an airborne computer) for generating reaction-jet inputs.
2. Adding body attitude to 1 would add some complexity to the electronics.
3. In addition to attitude augmentation, a control loop would be added for horizontal velocity. This capability would require three accelerometers and an airborne computer.
4. Finally, altitude and altitude-rate control loops could be included with essentially no additional hardware required over that required for 3.

The fourth concept listed is the one which was simulated. Man-in-the-loop simulation is required to evaluate concepts 1, 2, and 3 and is required to investigate failure modes for all augmented concepts.

As a result of the analyses and simulation, it was determined that control of both the attitude and translation of a tilting platform is feasible. Further investigation will require man-in-the-loop visual simulation and refinements in control-system logic.

A brief study of contingency modes indicated that sufficient thrust was available for the 8-engine tilting-platform concept to recover from an engine failure and continue the nominal mission profile. The eight-engine level-platform design did not have sufficient thrust to continue the mission profile unless platform tilting is used for thrust-vector control. This result may be unique to the assumed engine arrangement.

### Flight Performance

The ranging capability of pulsed-thruster concepts was compared with the capability of the proportionately throttled concepts. Visual simulation results were employed in determining propellant use during flight.



Table 27 summarizes the results of this study for three cases: (1) a tilting-platform case with  $I_{sp} = 280$  seconds (which corresponds to a proportionately throttled engine), (2) a tilting-platform case with  $I_{sp} = 250$  seconds (which corresponds to a pulse-throttled engine), and (3) a level-platform case with  $I_{sp} = 250$  seconds (pulse-throttled engine).

The level-platform configuration is the design previously shown with engines tilted 45 degrees fore and aft in the pitch plane. The pilot-influence propellant requirements obtained from visual simulation was based on a proportionately throttled engine that was not canted at the large angle associated with the level platform. The pilot-influence propellants were determined in two segments, (1) landing-propellant requirements (66 pounds for remote and homesite landings) and (2) trajectory-variation propellants (35 pounds). Because of the effect of the lower  $I_{sp}$  and the losses related to canted engines during a landing maneuver, the landing-propellant requirements are increased significantly for the level-platform case. The results are shown in Table 27. The operational radius for the concepts are compared in Table 27, which assumes a total loaded propellant of 300 pounds. Constant-altitude trajectories are assumed for all cases. The tilting-platform concepts follow "optimum cruise velocity" trajectories, described in Volume 2 (Mission Analysis) which have a cruise portion at zero attitude angle between an acceleration and deceleration phase. The level-platform trajectory is also a constant-altitude trajectory, but it does not have a cruise portion. This trajectory assumes acceleration at maximum thrust-vector inclination to the trajectory midpoint and deceleration during the second half of the trajectory. This results in better performance for the level platform (as compared to the "optimum cruise velocity" trajectory) because of the high  $I_{sp}$  losses at zero thrust-vector attitude caused by thruster inclination. Table 27 indicates that the level-platform concept has a considerably reduced operational radius as compared to the  $I_{sp} = 280$  seconds, tilting-platform concept. Because of its reduced  $I_{sp}$ , the tilting-platform, pulse-throttled concept ( $I_{sp} = 250$  seconds) has an operational radius of about 1.1 nautical miles less than the proportionately throttled ( $I_{sp} = 280$  seconds) tilting-platform concept.

Based on the above results, it was concluded that the large degradation in range related to the level-platform concept did not justify the potential gain in handling qualities. Even though the pulse-modulated, tilting-platform concept has a somewhat degraded range, the possibility of using existing engines may justify this concept. Further studies of this concept to establish a preliminary design are recommended.

Table 27. Flight Performance Comparisons

| System                                     | Radius (N. M.)*                             |                   |
|--|---|-------------------|
|  | No Payload                                  | 100-pound Payload |
| Tilting platform                           |   |                   |
| $I_{sp}$ = 280 seconds                     | 4.8   | 4.0               |
| $I_{sp}$ = 250 seconds                     | 3.7   | 3.1               |
| Level Platform                             |   |                   |
| $I_{sp}$ = 250<br>$\delta T$ = 45 degrees  | 1.6   | 1.4               |
| *Radius calculations assume the following: |   |                   |
| System                                     | WPROP for Trajectory Variations and Landing | WPROP for Ranging |
| Tilting platform                           |   |                   |
| $I_{sp}$ = 280 seconds                     | 101   | 199               |
| $I_{sp}$ = 250 seconds                     | 106   | 194               |
| Level platform                             | 130   | 170               |
| No propellant for reserve and residual     |   |                   |

## MODIFIED VEHICLE OPTIONS

### 100-POUND MAXIMUM PAYLOAD VEHICLE

As part of the parametric phase, a study was made to establish the gains that could be obtained by limiting the LFV payload design requirement to 100 pounds as opposed to 370 pounds for the baseline version. The design developed is shown in Figure 85. The general arrangement is effectively the same as the Phase 2 control configuration (Figure 17) except for the load pans. The forward load pan may be omitted, and seat travel of 6 inches forward permits all of the load to be placed on the aft load pan.

These differences also apply to the preliminary design, Figure 19. The maximum gross weight of the vehicle is reduced, permitting a reduction of engine thrust from 105 to 85 pounds. Since the maximum weight is relatively unchanged, the required throttle ratio is reduced only 18 percent. A dry weight reduction is obtained by reducing the size of payload racks, body structure, landing gear, engines, and, for constant range, propellant and pressurant tanks. As shown in Table 28, the reduction was estimated on two bases, constant propellant and constant range. The constant-propellant basis is more realistic, since it involves no change to the propellant tank diameter, which is fixed by available hardware tooling. It permits a range increase of 2.6 percent (at the same payload) and a dry weight reduction of 14.4 pounds.

### EARTHSHINE OPERATIONS VEHICLE

The baseline vehicle is designed for a nominal dawn (daylight) mission. In Volume 3, Part III, "Thermal Studies," the requirements for a design suitable for earthshine operations were also developed. A summary of those results is shown in Table 29. The additional insulation, heaters, and batteries indicate a weight increase of 25 pounds over the baseline vehicle.

It is not yet clear whether the baseline vehicle could be readily retrofitted for earthshine operations after manufacturing, since detailed thermal design provisions such as heat shorts, thermal standoffs, and thermal coatings are not yet defined. At this time, however, it appears that fundamental differences would exist at final assembly, and retrofit would not be possible unless one or both vehicles were severely compromised. In any case, substantial differences in thermal and detailed design engineering and tests are involved for the two vehicles.

Table 28. Weight Reduction, 100-Pound Maximum Payload Vehicle

| Item                           | Dry Weight (lb) |
|--------------------------------|-----------------|
| <b>CONSTANT PROPELLANT</b>     |                 |
| Payload racks                  | 2.0             |
| Body structure                 | 2.3             |
| Landing gear                   | 5.2             |
| Engine                         | 2.0             |
| Growth                         | 2.9             |
| Total                          | 14.4            |
| Range increase: 2.6%           |                 |
| <b>CONSTANT RANGE</b>          |                 |
| Payload racks                  | 2.0             |
| Body structure                 | 2.3             |
| Landing gear                   | 5.3             |
| Engine                         | 2.0             |
| Propellants and<br>pressurants | 1.2             |
| Growth                         | 3.2             |
| Total                          | 16.0            |
| Propellant decrease: 5.8 lb    |                 |

Table 29. Earthshine Vehicle Differences

| Item                     | Estimated<br>Dry Weight Increase<br>(lb) |
|--------------------------|--|
| Tank insulation (0.5 in) | 2  |
| Heater and Batteries     | —  |
| Tanks                    | 13                                       |
| Engines and lines        | 6  |
| Subtotal                 | 21                                       |
| Growth allowance         | 4  |
| Total                    | 25                                       |

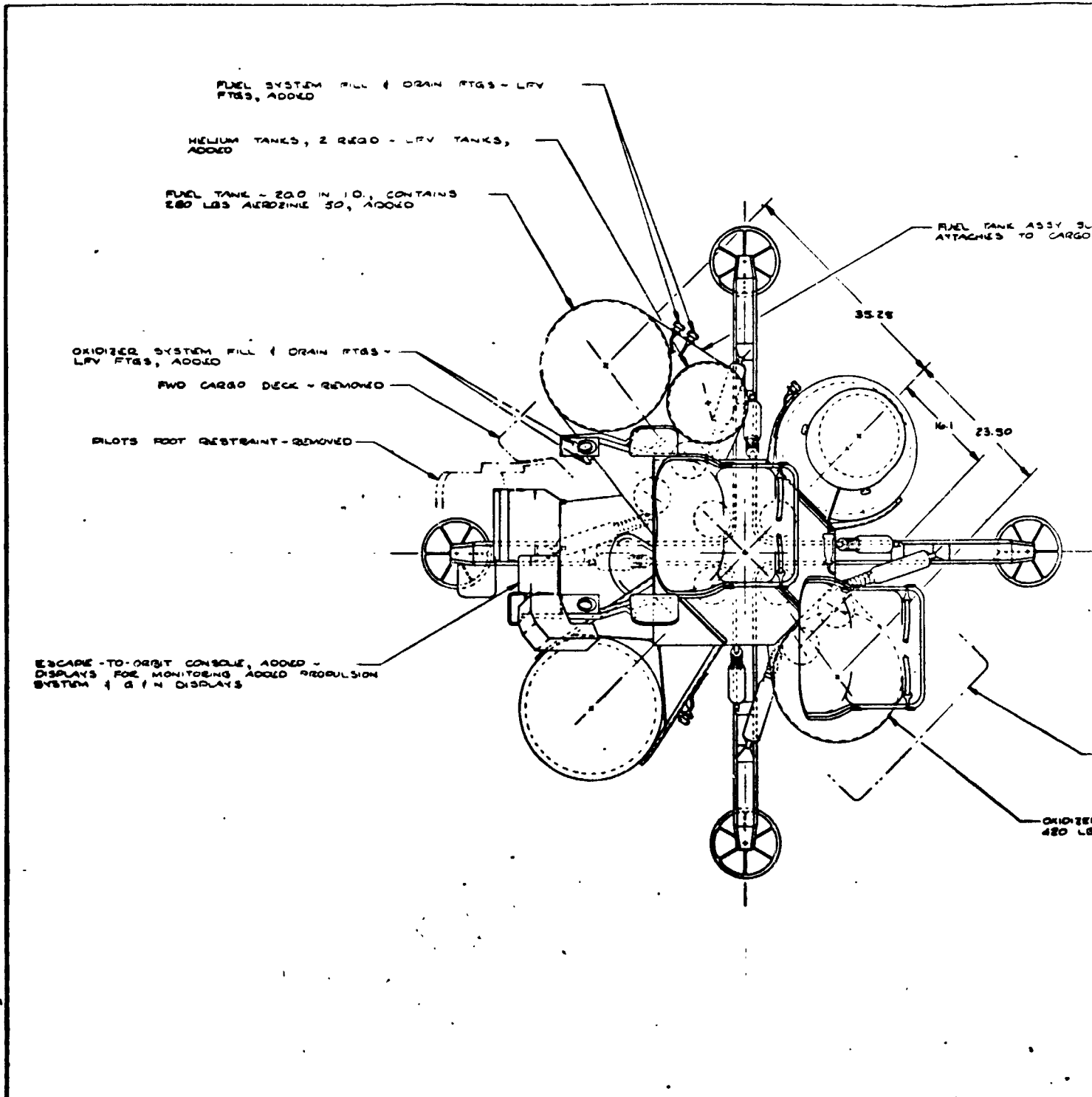
## ESCAPE-TO-ORBIT VEHICLE

A configuration showing modifications to the baseline vehicle for an escape-to-lunar-orbit capability is shown in Figure 109, and the corresponding weight statement is shown in Table 23. The design requirement is to reach a lunar orbit altitude of 50,000 feet carrying the two crew members. This requires additional propellant (a propellant fraction of 0.5) to achieve the ideal velocity requirement of about 6,500 fps. The thrust-to-weight ratio required is from 0.3 to 0.5 and results in the requirement for at least three additional engines. The design shown is capable of retrofit on the lunar surface, but not without some complicated operations. These complications were kept to a minimum to hold the modification time to a value that might be required under emergency conditions. For this reason, the landing gear is not removed, although a reduction in propellant could be obtained in that manner. As shown in the figure, the two payload decks are removed, and the following major assemblies are added:

1. Two helium vessel assemblies (LFV type)
2. Two propellant tanks and engine cluster assemblies (20-inch cylindrical tanks with two engines each, LFV type modified for constant thrust and ungimbaled)
3. One escape mission console (additional guidance and navigation, and displays)
4. One passenger support assembly

The added propulsion system is independent of the basic LFV system, rather than being integrated. After initial boost, the LFV system would be throttled back while still providing thrust vector control. The fixed thrust supplemental system reaches depletion first, and the remainder of the profile is completed by the LFV system.

It is probable that the modifications involve some design compromises to the LFV, primarily with respect to secondary structure, where lunar surface assembly fittings are involved.



FOLD-OUT FRAME

ASSY SUPPORT STRUCTURE, ADDED.  
CARGO DECK SUPPORT RTA'S

PILOT POSITION - PILOT TRANSLATES FWD MAX,  
60 IN ( ROTATES FWD 15°

AFT CARGO DECK, REMOVED

OXIDIZER TANK - 2000 IN I.O., CONTAINS  
420 LBS  $N_2O_4$ , ADDED

PILOTS FOOT RESTRAINT, ADDED

FWD ENGINE ASSY - 2 LPV ENGINES WITHOUT GASOLINE  
OR THROTTLE (PART OF FUEL TANK ASSY)

PASSENGER

AFT 1  
OR TH

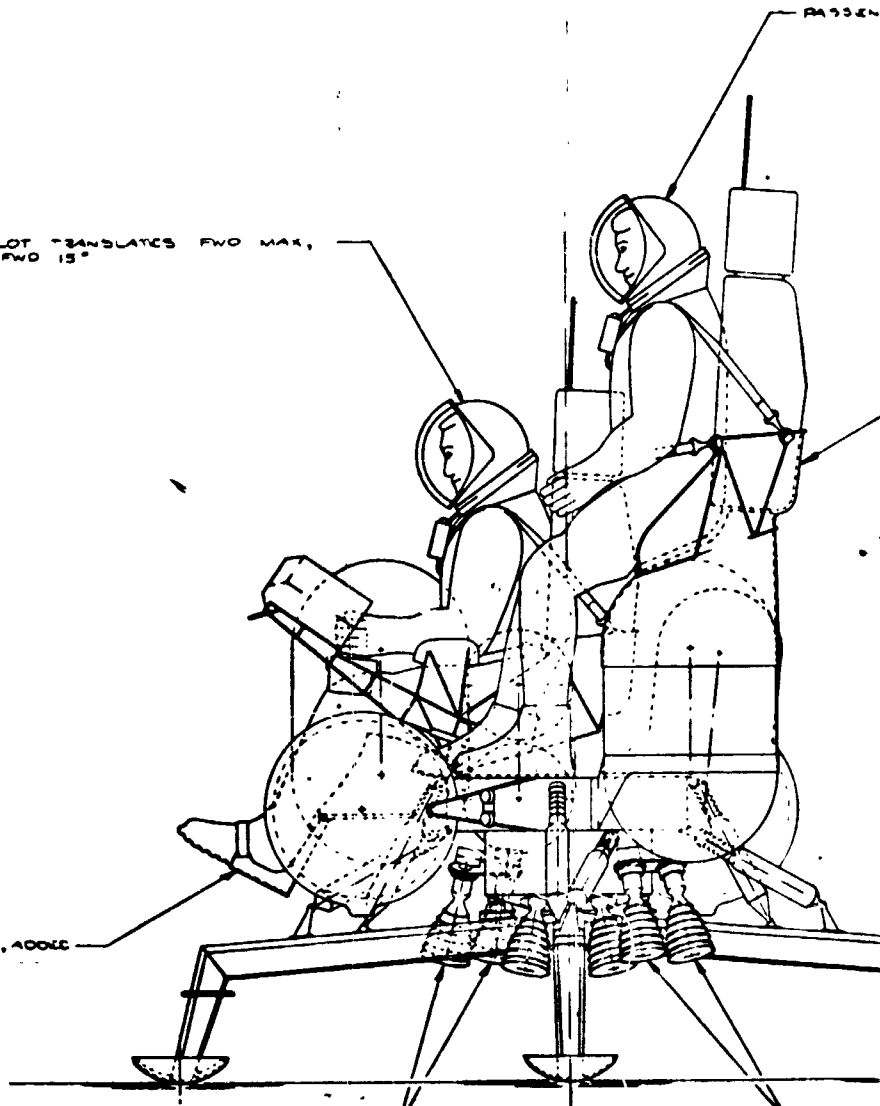
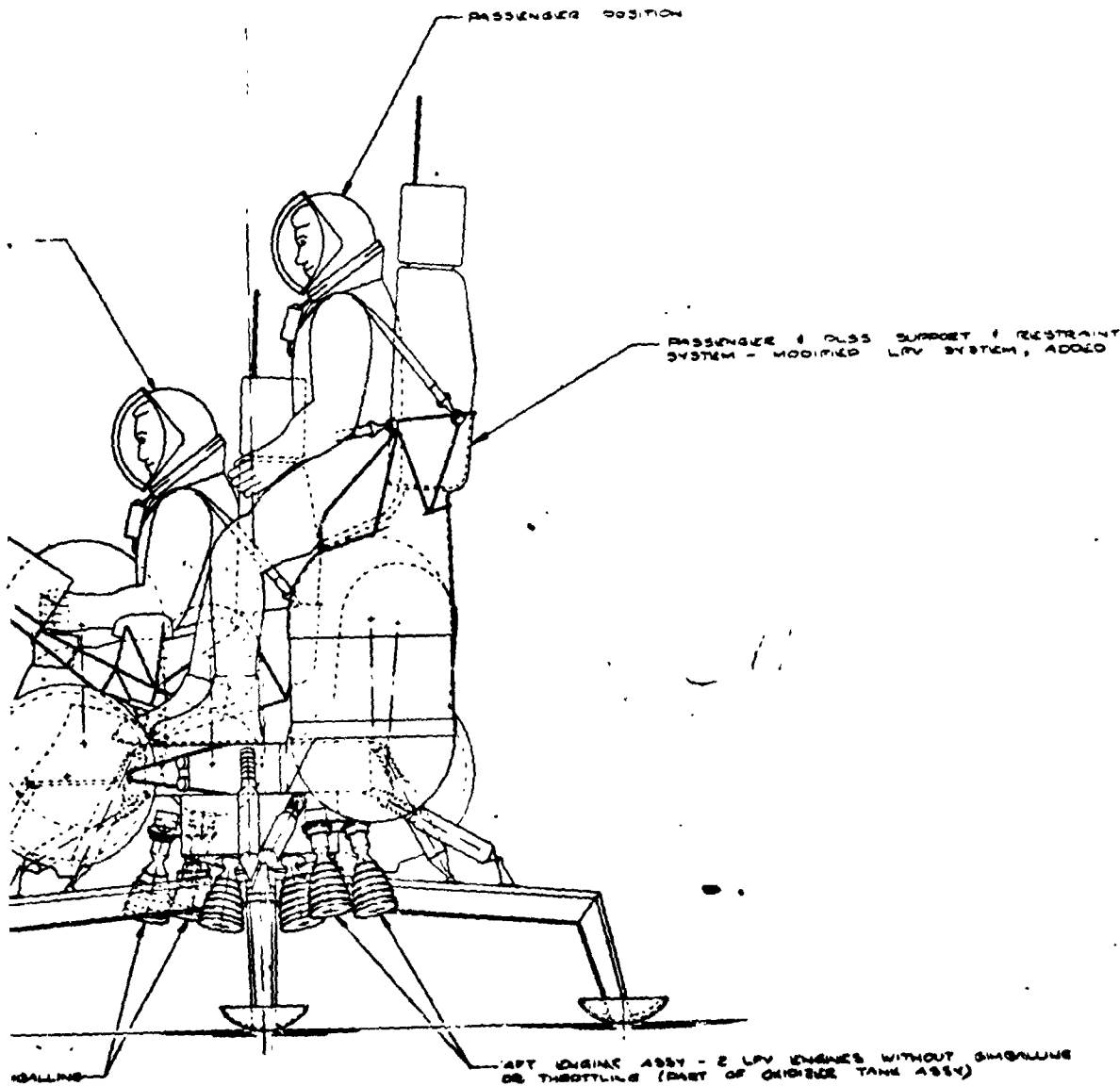


Figure 100

FOLDOUT FRAME

FOLDOUT FRAME

UPSIZE PAGEMAT - 120% KEYLINE IMAGE  
BLOW UP CALCOUTS 120% - REDUCE TO 83% OF



|     |          |    |     |  |
|-----|----------|----|-----|--|
| REV | DATE     | BY | APP | DESCRIPTION  |
| V8  | 02-13-69 |    |     | ONE-MAN LUNAR FLYING VEHICLE - MODIFICATIONS FOR ESCAPE TO ORBIT MISSION |
|     |          |    |     | 2230-28  |

Figure 109. Escape-to-Orbit Vehicle Configuration

- 259,260 -

PRECEDING PAGE BLANK NOT FILMED  
SD 69-417-4

FOLDOUT FRAME

UPRIZE PAGEMAT - 120% KEYLINE IMAGE AREA  
BLOW UP CALLOUTS 120% - REDUCE TO 83% OF ORIGINAL

PLEASE MAKE CORRECTIONS ON TISSUE OVERLAYS,  
OR READING COPY IF AVAILABLE

REDUCE TO 11 INCHES